

---

# Continuum Mechanics

---

GUILLAUME PUEL  
ANDREA BARBARULO

CENTRALESUPÉLEC  
2020–2021  
1EL5000

---

**Image and photo credits:** **32.** Wikimedia Commons / McSush / CC-BY-SA-3.0 and Wikimedia Commons / Kaboldy / CC-BY-SA-3.0 – **44.** Wikimedia Commons / Cdang / CC-BY-SA-3.0 – **45.** Wikimedia Commons / Cdang / CC-BY-SA-3.0 and [https://www.samhs.org.au/Virtual%20Museum/Medicine/Apothecary\\_scales/Apothecary\\_scales.html](https://www.samhs.org.au/Virtual%20Museum/Medicine/Apothecary_scales/Apothecary_scales.html) – **55.** Wikimedia Commons / Nordelch / CC-BY-SA-3.0 – **71.** Université Numérique des Sciences Odontologiques Francophones – **73.** Wikimedia Commons / Sigmund / CC-BY-SA-3.0 – **73.** Wikimedia Commons / Sigmund / CC-BY-SA-3.0 and Wikimedia Commons / CTho / CC-BY-SA-3.0 – **74.** Wikimedia Commons / Cdang / CC-BY-SA-3.0 – **75.** Wikimedia Commons / Aboalbiss / CC-BY-SA-3.0 and Wikimedia Commons / Sigmund / CC-BY-SA-3.0 – **83.** École des Mines d'Albi-Carmaux / CC-BY-NC-SA-4.0 – **84.** École des Mines d'Albi-Carmaux / CC-BY-NC-SA-4.0 – **84.** [https://www.researchgate.net/publication/257920095\\_Platine\\_de\\_traction\\_in-situ\\_l'\\_emergence\\_des\\_bandes\\_de\\_glisserment\\_dans\\_le\\_nickel](https://www.researchgate.net/publication/257920095_Platine_de_traction_in-situ_l'_emergence_des_bandes_de_glisserment_dans_le_nickel) – **85.** Wikimedia Commons / Betienne / CC-BY-SA-3.0 – **85.** Wikimedia Commons / Betienne / CC-BY-SA-3.0 – **90.** [http://www.si.ens-cachan.fr/accueil\\_V2.php?page=affiche\\_ressource&id=178](http://www.si.ens-cachan.fr/accueil_V2.php?page=affiche_ressource&id=178) – **91.** <http://classes.mst.edu/civeng2211/index.html> – **93.** M. Taroni, Snecma Moteurs, 2001 – **95.** J. Salençon, *Mécanique des milieux continus*, Éditions de l'École Polytechnique, 2007 – **151, 157** and **158.** [https://eduscol.education.fr/sti/si-ens-cachan/ressources\\_pedagogiques/mise-en-evidence-du-domaine-de-validite-de-la-theorie-des-poutres](https://eduscol.education.fr/sti/si-ens-cachan/ressources_pedagogiques/mise-en-evidence-du-domaine-de-validite-de-la-theorie-des-poutres) – **191.** <http://www.tboake.com/SSEF1/pin.shtml> – **192.** Wikimedia Commons / Roulex45 / CC-BY-SA-3.0 and Wikimedia Commons / K800i / CC-BY-SA-3.0 – **193.** Wikimedia Commons / Roulex45 / CC-BY-SA-3.0 – **202.** Wikimedia Commons / Volpe National Transportation Systems Center (USA) – **206.** Wikimedia Commons / Saint Martin / CC-BY-SA-3.0

© 2020 – G. PUEL AND A. BARBARULO

LATEX style inspired from <http://www.latextemplates.com>

*August 2020*

This textbook is structured to prioritize the concepts and illustrations covered in the Continuum Mechanics course; the formatting of these various constitutive elements is detailed below. In addition, a table of contents and an index provide direct access to the information.

---

### HOW TO USE THIS TEXTBOOK?

The body of the text allows a reasoned and logical presentation of the different concepts covered in the Continuum Mechanics course, as well as the basic reasoning to solve the problems encountered: it is then the recommended reading level for the comprehension of the course.

**Definition.** The definitions describe the concepts that make it possible to pose a problem in Continuum Mechanics, while introducing the vocabulary adapted to this field.

**Summary 0.1 — Principle and disclaimer.** The summaries synthesize the basic elements necessary for understanding and solving the problems encountered in Continuum Mechanics; alone, these basics are insufficient for comprehensive knowledge on the concepts covered this year.

■ **Example 0.1 — Illustrations and applications.** The examples serve as practical support for understanding the concepts and information presented in the course, and illustrate the use of Continuum Mechanics tools in various fields of application; they can be skipped in the first reading. ■

 The exclamation marks indicate the classic mistakes or confusions to be avoided at all costs; they contribute to a more detailed understanding of the concepts covered.

 *The remarks allow us to give further references and to go into greater depth into the framework set out in this document, and give*

We have chosen to use, in this textbook, a unified formalism based on the intrinsic representation of vectors and matrices, which is reflected in the following notations.

---

### WHICH NOTATIONS?

#### Vectors

The space vectors are noted in boldface:  $\mathbf{a}$ , of scalar components  $a_n$  in a space vector basis  $(\mathbf{i}_1, \mathbf{i}_2, \mathbf{i}_3)$ . Among the main notations, we will then use:

- for the scalar product of two vectors  $\mathbf{a}$  and  $\mathbf{b}$  :  $\langle \mathbf{a}, \mathbf{b} \rangle$ ;
- for the norm of a vector  $\mathbf{a}$  :  $\|\mathbf{a}\|$ ;
- for the vector product of two vectors  $\mathbf{a}$  and  $\mathbf{b}$  :  $\mathbf{a} \wedge \mathbf{b}$ .

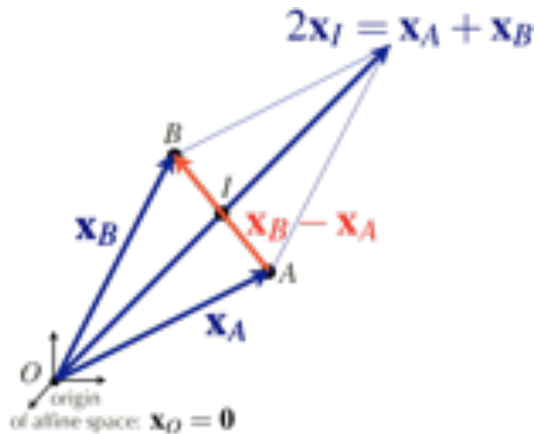
More details on the mathematical definitions of these concepts can be found in Appendix A.1.1.

#### Points

The points in space are considered through their position vectors: the associated position vector  $\mathbf{x}_A$  is thus associated with point  $A$ . This implies, for example, that:

- the vector that connects a point  $A$  to a point  $B$  is written as  $\mathbf{x}_B - \mathbf{x}_A$ ;
- the origin  $O$  of the space verifies  $\mathbf{x}_O = \mathbf{0}$ ;
- the middle point  $I$  of the segment  $[AB]$  is such that  $\mathbf{x}_I = (\mathbf{x}_A + \mathbf{x}_B)/2$ .

For simplicity, we will note  $\mathbf{x}$  the position vector associated with the current point  $M$ .

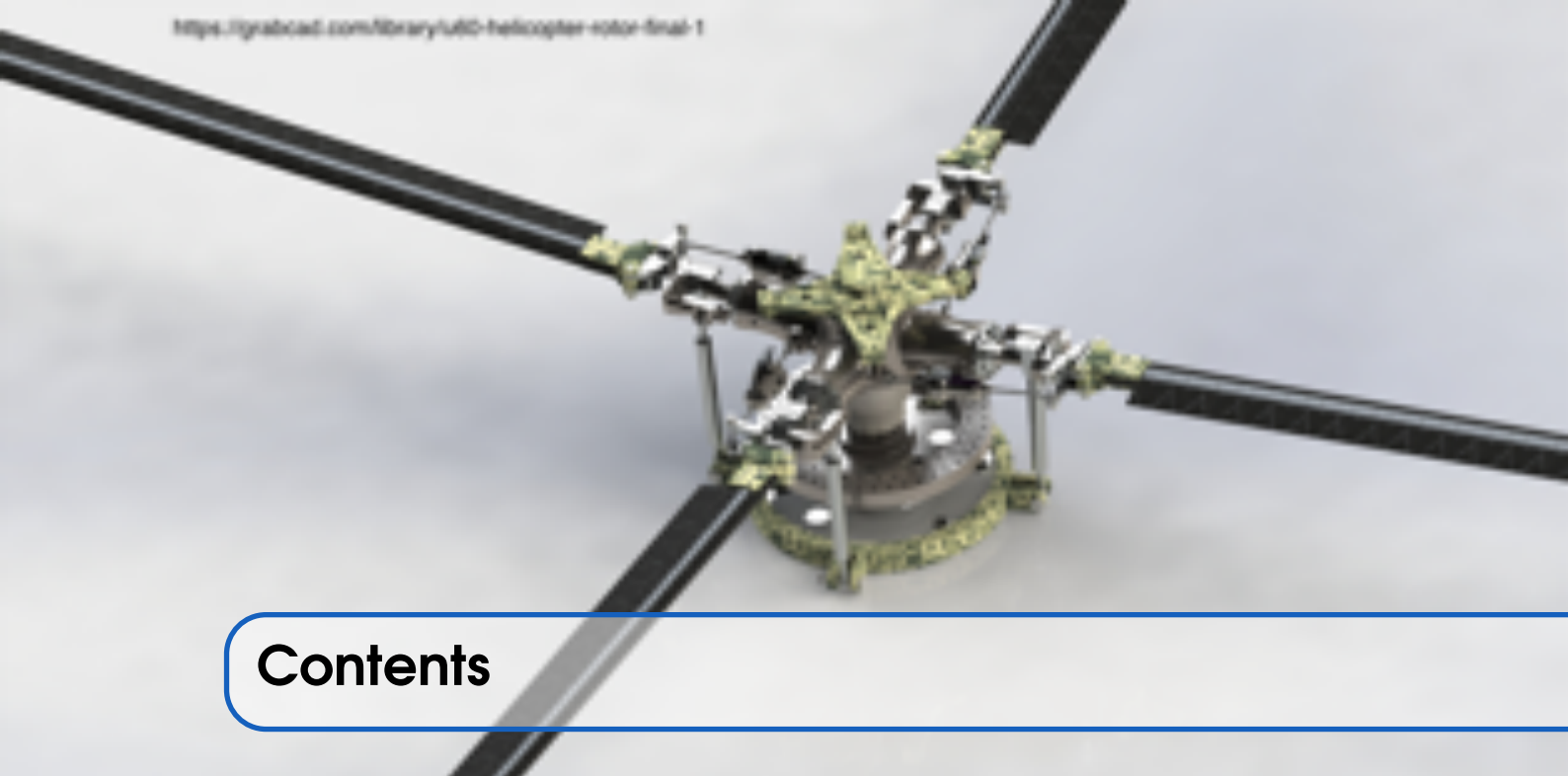


#### Matrices (or second-order tensors)

The matrices are noted with blackboard bold letters:  $\mathbb{A}$ , of scalar components  $A_{mn}$  in a space vector basis  $(\mathbf{i}_1, \mathbf{i}_2, \mathbf{i}_3)$ . We then note:

- the product  $\mathbf{b}$  of a matrix  $\mathbb{A}$  by a vector  $\mathbf{a}$ :  $\mathbf{b} = \mathbb{A}\mathbf{a}$ ;
- the product  $\mathbb{C}$  of two matrices  $\mathbb{A}$  and  $\mathbb{B}$ :  $\mathbb{C} = \mathbb{A}\mathbb{B}$ ;
- the transpose of a matrix  $\mathbb{A}$ :  $\mathbb{A}^T$ ;
- the inverse of a matrix  $\mathbb{A}$ :  $\mathbb{A}^{-1}$ .

More details on the mathematical definitions of these concepts can be found in Appendix A.2.1.



## Contents

<b>1</b>	<b>Deformations</b>	<b>3</b>
1.1	<b>Lagrangian description of movement</b>	<b>3</b>
1.1.1	<i>Generic formulation</i>	3
1.1.2	<i>Material velocity and acceleration</i>	7
1.2	<b>Deformation of a continuous medium</b>	<b>9</b>
1.2.1	<i>Deformation gradient tensor</i>	9
	<i>Tensor expressions</i>	12
1.2.2	<i>Green-Lagrange strain tensor</i>	15
	<i>Length variation in the neighbourhood of a material point</i>	15
	<i>Angle variation in the neighbourhood of a material point</i>	17
	<i>Interpretation</i>	19
1.3	<b>Infinitesimal strain tensor</b>	<b>22</b>
1.3.1	<i>Infinitesimal deformation hypothesis</i>	22
1.3.2	<i>Definition and properties</i>	23
	<i>Tensor expressions</i>	24
	<i>Interpretation</i>	25
1.3.3	<i>Study of infinitesimal local perturbations</i>	28
	<i>Transformation of the neighbourhood of a point</i>	28
	<i>Local analysis of strains</i>	29
	<i>Strain measurement</i>	31
1.4	<b>Volume change and mass conservation</b>	<b>32</b>
1.4.1	<i>Volume change</i>	32
1.4.2	<i>Mass conservation</i>	35
	<i>Material expression</i>	35
	<i>Incompressibility</i>	36
1.5	<b>Summary of important formulas</b>	<b>36</b>

<b>2</b>	<b>Stresses</b>	<b>39</b>
<b>2.1</b>	<b>Fundamental principles of dynamics for a material domain</b>	<b>39</b>
2.1.1	<i>Conservation of momentum and angular momentum</i> . . . . .	39
	Conservation of momentum . . . . .	40
	Conservation of the angular momentum . . . . .	41
2.1.2	<i>Actions</i> . . . . .	42
2.1.3	<i>Static equilibrium</i> . . . . .	43
	Equilibrium of a material domain subjected to two pure forces . . . . .	44
	Equilibrium of a material domain subjected to three pure forces . . . . .	44
<b>2.2</b>	<b>Concept of stress</b>	<b>46</b>
2.2.1	<i>Internal forces</i> . . . . .	46
	Modeling . . . . .	46
	Consideration . . . . .	47
2.2.2	<i>Stress tensor</i> . . . . .	48
	Action-reaction principle . . . . .	48
	Linearity of the stress vector . . . . .	49
	Mathematical representation . . . . .	50
	Symmetry property . . . . .	53
<b>2.3</b>	<b>Local equilibrium equation</b>	<b>56</b>
2.3.1	<i>Obtaining the equation</i> . . . . .	56
	Tensor expressions of the divergence of the stress tensor . . . . .	60
2.3.2	<i>Solving the equation</i> . . . . .	62
	Conditions on the external boundary . . . . .	62
	Conditions on an internal interface . . . . .	64
<b>2.4</b>	<b>Summary of important formulas</b>	<b>66</b>
<b>3</b>	<b>Strength criteria</b> . . . . .	<b>67</b>
<b>3.1</b>	<b>Mechanical testing of materials</b>	<b>67</b>
3.1.1	<i>Tensile test</i> . . . . .	68
	Determination of the stress state . . . . .	68
	Tensile curves . . . . .	70
	Orders of magnitude . . . . .	72
3.1.2	<i>Types of material failure</i> . . . . .	72
	Brittle failure . . . . .	73
	Ductile failure . . . . .	74
<b>3.2</b>	<b>Criteria</b>	<b>75</b>
3.2.1	<i>Local study of stresses</i> . . . . .	75
	Quantities related to the choice of the facet . . . . .	75
	Principal stresses . . . . .	77
	Mohr's circles . . . . .	78
3.2.2	<i>Cleavage failure criteria</i> . . . . .	80
3.2.3	<i>Shear failure criteria</i> . . . . .	83
	Criterion based on the maximum shear . . . . .	84
	'Alternative' criterion . . . . .	86
3.2.4	<i>Other criteria</i> . . . . .	89
	Tsai-Hill criterion . . . . .	89
	Mohr-Coulomb criterion . . . . .	89

<b>3.3</b>	<b>Stress concentrations</b>	<b>90</b>
3.3.1	<i>Influence of a hole</i> . . . . .	91
	Plate with a circular hole in tension . . . . .	91
	From the hole to the crack . . . . .	92
3.3.2	<i>Influence of geometry</i> . . . . .	94
<b>3.4</b>	<b>Summary of important formulas</b>	<b>95</b>
<b>4</b>	<b>Material behaviour</b> . . . . .	<b>97</b>
<b>4.1</b>	<b>Mechanical behaviour of deformable solids</b>	<b>97</b>
4.1.1	<i>Review of the unknowns and equations of the problem</i> . . . . .	97
4.1.2	<i>Diversity of material behaviours</i> . . . . .	98
4.1.3	<i>Linear elastic material for infinitesimal deformations</i> . . . . .	101
	Mathematical representation of the constitutive relation . . . . .	101
	Voigt notation . . . . .	102
<b>4.2</b>	<b>Isotropic linear elastic material for infinitesimal deformations</b>	<b>103</b>
4.2.1	<i>Isotropy hypothesis</i> . . . . .	103
4.2.2	<i>Link with the tensile test</i> . . . . .	105
	Practical construction of the constitutive relation . . . . .	105
	Common parameter values . . . . .	107
<b>4.3</b>	<b>Thermoelastic behaviour for infinitesimal deformations</b>	<b>110</b>
4.3.1	<i>Linear thermoelasticity framework</i> . . . . .	110
4.3.2	<i>Dealing with a thermoelasticity problem</i> . . . . .	111
<b>4.4</b>	<b>Summary of important formulas</b>	<b>115</b>
<b>5</b>	<b>Infinitesimal elasticity</b> . . . . .	<b>117</b>
<b>5.1</b>	<b>Posing an elasticity problem</b>	<b>117</b>
5.1.1	<i>Equations to be solved</i> . . . . .	117
5.1.2	<i>Boundary conditions</i> . . . . .	119
	Conditions on the external boundary . . . . .	119
	Conditions on an internal interface . . . . .	120
5.1.3	<i>Solution properties</i> . . . . .	122
	Unicity in the static framework . . . . .	122
	Unicity in the dynamic framework . . . . .	124
<b>5.2</b>	<b>Methods for solving an elasticity problem</b>	<b>125</b>
5.2.1	<i>Displacement approach</i> . . . . .	125
	Displacement solution strategy . . . . .	125
	Navier's equation . . . . .	128
5.2.2	<i>Stress approach</i> . . . . .	129
	Stress solution strategy . . . . .	129
	Compatibility equations . . . . .	132
5.2.3	<i>Approximate solutions</i> . . . . .	135
	Saint-Venant's principle . . . . .	135
	Towards numerical solutions . . . . .	137
<b>5.3</b>	<b>Simplification of an elasticity problem</b>	<b>139</b>
5.3.1	<i>Principle of superposition</i> . . . . .	139
5.3.2	<i>Plane elasticity</i> . . . . .	141
	Plane strain . . . . .	141
	Plane stress . . . . .	142

5.3.3	<i>Axisymmetry</i> . . . . .	144
	<i>Taking into account symmetry planes</i> . . . . .	145
<b>5.4</b>	<b>Summary of important formulas</b>	<b>147</b>
<b>6</b>	<b>Beam approximation</b> . . . . .	<b>149</b>
<b>6.1</b>	<b>Kinematics of a beam</b>	<b>149</b>
6.1.1	<i>Geometry and parameterization</i> . . . . .	149
6.1.2	<i>Perfectly rigid cross-section hypothesis</i> . . . . .	150
	Displacement expression . . . . .	150
	Infinitesimal strain tensor . . . . .	152
6.1.3	<i>Euler-Bernoulli hypothesis</i> . . . . .	157
	Displacement expression . . . . .	157
	Infinitesimal strain tensor . . . . .	158
<b>6.2</b>	<b>Internal loads in a beam</b>	<b>161</b>
6.2.1	<i>Assumption on the stresses</i> . . . . .	161
6.2.2	<i>Resultant force of the internal loads and associated equilibrium equation</i> . . . . .	162
	Equilibrium equation for the resultant force: global approach . . . . .	163
	Equilibrium equation for the resultant force: local approach . . . . .	167
6.2.3	<i>Moment of the internal loads and associated equilibrium equation</i> . . . . .	169
	Equilibrium equation for the moment: global approach . . . . .	170
	Equilibrium equation for the moment: local approach . . . . .	173
<b>6.3</b>	<b>Beam constitutive relations</b>	<b>176</b>
6.3.1	<i>Stress-strain relations</i> . . . . .	176
6.3.2	<i>Constitutive relation for the resultant force of the internal loads</i> . . . . .	177
6.3.3	<i>Constitutive relation for the moment of the internal loads</i> . . . . .	178
	Tensor $\mathbb{J}$ : properties and practical calculation . . . . .	179
6.3.4	<i>Stresses within a cross-section</i> . . . . .	186
<b>6.4</b>	<b>Connections between beams</b>	<b>188</b>
6.4.1	<i>Kinematics associated with a connection</i> . . . . .	188
	Rigid connection . . . . .	189
	Spherical joint . . . . .	191
	Pin joint . . . . .	191
	Roller support . . . . .	192
6.4.2	<i>Connection actions</i> . . . . .	193
6.4.3	<i>Complete solution of a beam problem</i> . . . . .	195
	Statically determinate beams . . . . .	195
	Statically indeterminate problems . . . . .	197
<b>6.5</b>	<b>Buckling of straight beams</b>	<b>202</b>
6.5.1	<i>Local moment equilibrium equation in the deformed configuration</i> . . . . .	203
6.5.2	<i>Linear buckling</i> . . . . .	203
<b>6.6</b>	<b>Summary of important formulas</b>	<b>207</b>
<b>A</b>	<b>Tensor algebra</b> . . . . .	<b>211</b>
<b>A.1</b>	<b>Vectors</b>	<b>211</b>
A.1.1	<i>Definitions and notations</i> . . . . .	211
A.1.2	<i>Classical vector bases</i> . . . . .	212
	Cartesian vector basis . . . . .	212
	Cylindrical vector basis . . . . .	213

Spherical vector basis . . . . .	213
<b>A.2 Second-order tensors</b>	<b>214</b>
A.2.1 Definitions and properties . . . . .	214
Tensor product of two vectors . . . . .	215
Symmetrical and antisymmetrical parts . . . . .	215
A.2.2 Scalar product and tensor norm . . . . .	216
Trace of a tensor . . . . .	216
Properties . . . . .	217
A.2.3 Determinant of a tensor and remarkable relations . . . . .	217
Definition and properties . . . . .	217
Piola's formula . . . . .	218
A.2.4 Invariants of a tensor . . . . .	218
Spectral decomposition of a tensor . . . . .	218
Invariants . . . . .	218
A.2.5 Square root of a tensor . . . . .	219
Definition and properties . . . . .	219
Polar decomposition of a tensor . . . . .	219
A.2.6 Rotation tensors . . . . .	219
Definition and properties . . . . .	219
Axis and angle of a rotation . . . . .	220
Case of an infinitesimal rotation . . . . .	221
<b>A.3 Fourth-order tensors</b>	<b>222</b>
A.3.1 Definition and properties . . . . .	222
A.3.2 Particular forms . . . . .	222
Orthotropy . . . . .	222
Cubic symmetry . . . . .	223
Transverse isotropy . . . . .	223
Isotropy . . . . .	223
<b>B Tensor analysis</b>	<b>225</b>
<b>B.1 Differentiation</b>	<b>225</b>
B.1.1 Conventional space operators . . . . .	225
Gradient . . . . .	225
Divergence . . . . .	226
Curl . . . . .	226
Laplacian . . . . .	227
B.1.2 Useful formulas . . . . .	227
Vector relations . . . . .	227
Tensor relations . . . . .	227
B.1.3 Time differentiation . . . . .	228
General principle . . . . .	228
Angular velocity vector . . . . .	228
<b>B.2 Transformations of integrals</b>	<b>229</b>
B.2.1 Substitutions . . . . .	229
Volume integration . . . . .	229
Surface Integral . . . . .	230
B.2.2 Stokes formulas . . . . .	230
Gradient formula . . . . .	230
Divergence formula . . . . .	231
Derived formulas . . . . .	231

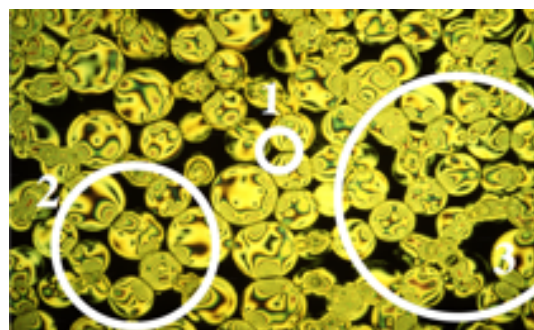
<b>B.3</b>	<b>Formulas</b>	<b>232</b>
B.3.1	<i>Change of coordinates</i>	232
B.3.2	<i>Cylindrical coordinates</i>	232
	Expressions of the conventional operators	233
	Mechanical equations	233
B.3.3	<i>Spherical coordinates</i>	234
	Expressions of the conventional operators	235
	Mechanical equations	235
	<b>Index</b>	<b>237</b>

## Foreword

The purpose of Continuum Mechanics is to predict the movements of a material medium, be it solid or fluid, and to relate these movements to the origins that cause them; it is, therefore, necessary to understand in depth the deformation mechanisms of these media and to understand the stresses that are developing within them. In this end, the approach is at the **macroscopic** scale, without necessarily establishing a quantitative link with the nature of atomic or molecular forces: we then define an equivalent **continuous medium**, the “form” of which is mathematical, allowing the use of mathematical analysis tools such as differential and integral calculation, which enable partial derivative equations to be solved exactly or approximately.

The question then arises as to how this equivalent continuous medium can be defined; if we take the example of a physical quantity such as density, in the case of a medium consisting of a set of beads in contact with each other (as in the image below), we notice that this quantity typically evolves according to the medium’s observation scale:

- below a certain specimen size (i.e., at the “microscopic” scale), the organisation of matter is heterogeneous (or even discrete, as in the example considered), hence we observe a strong variation of the average density from one sample to another, as if at random;
- from a certain specimen size larger than the order of magnitude of the heterogeneities’ size, the average density no longer changes much over short distances; we are then at the “mesoscopic” scale;
- over longer distances (typically the order of magnitude of the size of the domain in question), the average density can again vary significantly, as in the case of a heterogeneous material. However, this time they are fluctuations at the “macroscopic” scale.



In order to define an equivalent continuous medium, the analysed sample should be large in comparison to local heterogeneities, and of small size compared to the domain under study. In the example above, we note that sample 1 is too small, and that sample 3 has a size allowing to overlook details of the contact behaviour of the beads rubbing against each other, thus being a “representative volume element” allowing to model this medium as continuous. Thus, we end up modelling the density of the medium as a continuous function of the coordinates of the point under study; a common (but incorrect, strictly speaking) way of referring to this point is to use the term of “**particle**” or “material point”. This means we consider a physical quantity defined as an average over a subdomain (corresponding to the particle’s volume), and that the subdomain’s size implies that, at the studied domain’s scale, we can assume this quantity as being a function of the point under study.





# 1. Deformations

All bodies deform. Modelling the material shaping (such as stamping), on the one hand, or analysing the flow of polymers, on the other hand, requires quantifying large deformations. On the contrary, in order to avoid failure, most materials used in industry or construction to withstand or transmit loads need to endure small deformation. In all cases, this deformation can vary from one point to another within the bodies under study, and its description depends on the directions.

---

## WHY STUDY DEFORMATIONS?

### 1.1 Lagrangian description of movement

In the case of a deformable material domain, a relevant framework is to highlight a preferred configuration, which serves as a reference in the context of a description known as the “Lagrangian” description of movement: it is usually the state of the domain when it is not subjected to any external stress. This configuration is often referred to as “undeformed” (in the intuitive meaning of the word), or “initial” (by associating a time  $t = 0$ ), as opposed to what we describe later, which corresponds to a “deformed” or “current” configuration (i.e. at the current time  $t$ ).

#### 1.1.1 Generic formulation

We consider a domain  $\Omega$  whose particles are tracked over time, as shown in Figure 1.1 :

- at the initial time  $t = 0$ , the domain is undeformed, and we locate each particle of  $\Omega$  with its position vector  $\mathbf{p}$ , of coordinates  $(p_1, p_2, p_3)$  given in a determined Cartesian vector basis  $(\mathbf{i}_1, \mathbf{i}_2, \mathbf{i}_3)$ ; the spatial domain occupied by all the particles of  $\Omega$  is then noted as  $\Omega_0$  ;
- at the given time  $t$ , the particles may have changed positions with respect to the initial configuration; we then assume that we can define the current position of each particle of  $\Omega$ , noted  $\mathbf{x}$ , as a known vector function  $\mathbf{f}$ , called “placement” vector ; the latter depends on time, but also on the vector  $\mathbf{p}$  allowing to “identify” the particle we are tracking over time:

$$\mathbf{x} = \mathbf{f}(\mathbf{p}, t), \forall \mathbf{p} \in \Omega_0$$

The particles of  $\Omega$  now occupy a spatial domain noted  $\Omega_t$ , defined as:

$$\Omega_t = \{\mathbf{x} = \mathbf{f}(\mathbf{p}, t) | \forall \mathbf{p} \in \Omega_0\}$$

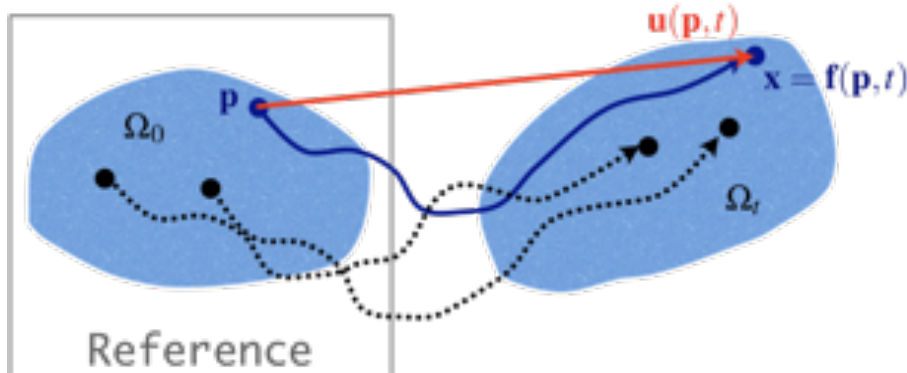


Figure 1.1: Placement vector and movement of particles of a material domain  $\Omega$ .

The knowledge of the placement vector  $\mathbf{f}$  over time therefore allows for describing the transformation of the domain  $\Omega$ : we define trajectories of the different material points of  $\Omega$ , for which we can specify the components in a given Cartesian vector basis  $(\mathbf{i}_1, \mathbf{i}_2, \mathbf{i}_3)$ :

$$\begin{aligned}x_1 &= f_1(p_1, p_2, p_3, t) = \langle \mathbf{f}(\mathbf{p}, t), \mathbf{i}_1 \rangle \\x_2 &= f_2(p_1, p_2, p_3, t) = \langle \mathbf{f}(\mathbf{p}, t), \mathbf{i}_2 \rangle \\x_3 &= f_3(p_1, p_2, p_3, t) = \langle \mathbf{f}(\mathbf{p}, t), \mathbf{i}_3 \rangle\end{aligned}$$

noting that we necessarily have the compatibility condition  $\mathbf{f}(\mathbf{p}, 0) = \mathbf{p}$ , such that:

$$\begin{aligned}f_1(p_1, p_2, p_3, 0) &= p_1 \\f_2(p_1, p_2, p_3, 0) &= p_2 \\f_3(p_1, p_2, p_3, 0) &= p_3\end{aligned}$$



Thus, it is necessary to distinguish the quantity  $\mathbf{x} = \mathbf{f}(\mathbf{p}, t)$ , which gives the position, at the current time, of a given particle, from the quantity simply noted as  $\mathbf{x}$ , which indicates a point in space, regardless of the particle that could be found there (and therefore of time).

In practice, we will often note  $\mathbf{x}$  only, when there is no risk of confusion.

**Displacement field.** The vector  $\mathbf{u}$  that joins the initial position of a particle to its current position is called displacement:

$$\mathbf{u}(\mathbf{p}, t) = \mathbf{f}(\mathbf{p}, t) - \mathbf{p}$$

The displacements of all the particles of a material domain  $\Omega$  constitute, at a given time  $t$ , a displacement field, defined on the initial configuration  $\Omega_0$ . The knowledge of this field is equivalent to that of the placement vector  $\mathbf{x} = \mathbf{f}(\mathbf{p}, t)$  on the entire domain.

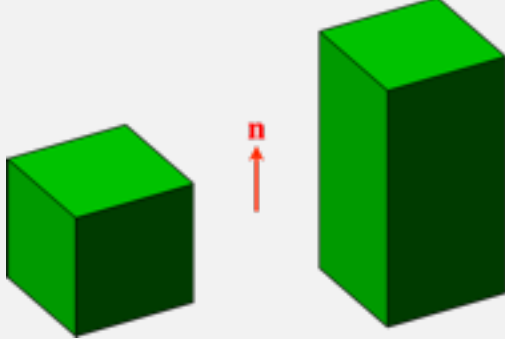
■ **Example 1.1 — Uniform elongation.** We consider a material domain  $\Omega$  undergoing a transformation of the form:

$$\mathbf{x} = \mathbf{f}(\mathbf{p}, t) = \mathbf{p} + a(t) \langle \mathbf{p}, \mathbf{n} \rangle \mathbf{n}, \forall \mathbf{p} \in \Omega_0$$

where  $a$  is an arbitrary dimensionless scalar function of time, and  $\mathbf{n}$  is a fixed unit vector.

The surface consisting of all the points such that  $\langle \mathbf{p}, \mathbf{n} \rangle = C$ , where  $C$  is a given constant, is a portion of a plane

moving according to an overall displacement  $\mathbf{u} = a(t)C\mathbf{n}$ , with  $\mathbf{n}$  the unit normal vector to this plane, and therefore does not deform. This overall displacement is all the more important as the “coordinate”  $C$  of this surface with respect to a given origin (associated with  $\mathbf{p} = \mathbf{0}$ ) is large: we then speak of elongation according to the direction  $\mathbf{n}$ , since all the segments connecting two material points, which are initially oriented along this direction, see their length evolve over time.



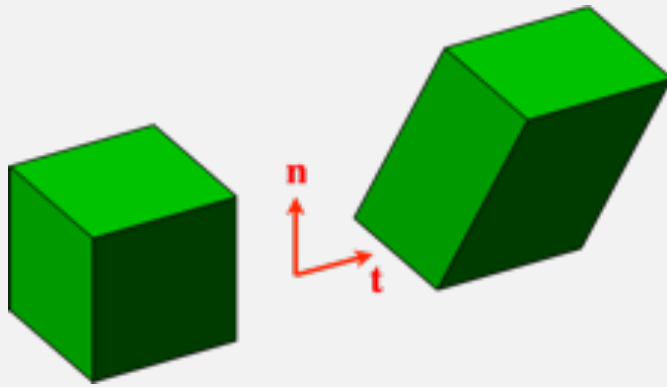
The fact that this elongation is said to be uniform will be justified in Example 1.11. ■

■ **Example 1.2 — Uniform shear strain.** We consider a material domain  $\Omega$  undergoing a transformation of the form:

$$\mathbf{x} = \mathbf{f}(\mathbf{p}, t) = \mathbf{p} + b(t)\langle \mathbf{p}, \mathbf{n} \rangle \mathbf{t}, \forall \mathbf{p} \in \Omega_0$$

where  $b$  is an arbitrary dimensionless scalar function of time, and  $\mathbf{n}$  and  $\mathbf{t}$  two fixed unit vectors, perpendicular to each other.

The surface consisting of all the points such that  $\langle \mathbf{p}, \mathbf{n} \rangle = C$ , where  $C$  is a given constant, is a portion of a plane moving according to an overall displacement  $\mathbf{u} = b(t)\mathbf{C}\mathbf{t}$  contained in the plane of this surface and thus does not deform. This overall displacement is the more important as the “coordinate”  $C$  of this surface with respect to a given origin (associated with  $\mathbf{p} = \mathbf{0}$ ) is large: we then speak of shear on a plane of normal  $\mathbf{n}$  according to the direction  $\mathbf{t}$ . The angle between two segments, each connecting two material points, and initially from directions  $\mathbf{t}$  and  $\mathbf{n}$ , therefore changes over time.



The fact that this shear strain is called uniform will be justified in Example 1.13. ■

■ **Example 1.3 — Movement of rigid bodies.** We consider a material domain  $\Omega$  undergoing a transformation of the form:

$$\mathbf{x} = \mathbf{f}(\mathbf{p}, t) = \mathbf{x}_A(t) + \mathbb{R}(t)(\mathbf{p} - \mathbf{p}_A), \forall \mathbf{p} \in \Omega_0$$

where  $\mathbf{x}_A(t) = \mathbf{f}(\mathbf{p}_A, t)$  is the placement of a given material point  $A$  of  $\Omega$ , and  $\mathbb{R}(t)$  is a rotation matrix, i.e. a matrix verifying  $\mathbb{R}^T \mathbb{R} = \mathbb{I}$  (orthogonality property, detailed in Appendix A.2.6).

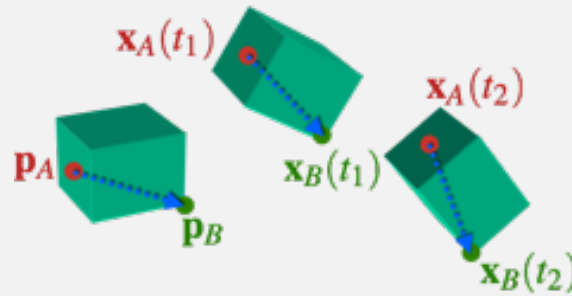
Thus, if we follow over time the vector linking the point  $A$  to a given point  $B$  of  $\Omega$ , we find that:

$$\mathbf{x}_B(t) = \mathbf{f}(\mathbf{p}_B, t) = \mathbf{x}_A(t) + \mathbb{R}(t)(\mathbf{p}_B - \mathbf{p}_A)$$

which establishes that:

$$\|\mathbf{x}_B(t) - \mathbf{x}_A(t)\|^2 = \langle \mathbb{R}(t)(\mathbf{p}_B - \mathbf{p}_A), \mathbb{R}(t)(\mathbf{p}_B - \mathbf{p}_A) \rangle = \langle \mathbb{R}(t)^T \mathbb{R}(t)(\mathbf{p}_B - \mathbf{p}_A), \mathbf{p}_B - \mathbf{p}_A \rangle = \|\mathbf{p}_B - \mathbf{p}_A\|^2$$

considering the orthogonality property of the rotation matrices. Any segment connecting two points of the solid  $\Omega$  is therefore of constant length over time, but its direction can evolve in any way in space.



Finally, it can be seen that, for such a movement, six parameters are necessary and sufficient to describe the position at a given time of all the particles in the domain: physically, they consist of:

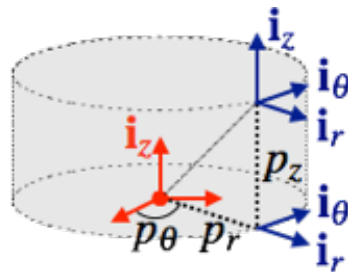
- three translation parameters, allowing to place spatially for example the point  $A$  used above;
- and three rotation parameters, allowing to orient in space the vector connecting point  $A$  to a given point of the solid.

It is then said that an undeformable solid, or “rigid body”, (without any linkage, i.e. free in space) has six degrees of freedom. ■



Naturally, in the case of a curved domain, a curvilinear coordinate system associated with the geometry can be used to describe the placement vector of the material domain. For example, in the case of a domain  $\Omega$  with a cylindrical shape of axis  $\mathbf{i}_z$ , we can use a cylindrical vector basis  $(\mathbf{i}_r(p_\theta), \mathbf{i}_\theta(p_\theta), \mathbf{i}_z)$ , with associated coordinates  $(p_r, p_\theta, p_z)$ , to define the initial positions of the particles of  $\Omega$ :

$$\mathbf{p} = p_r \mathbf{i}_r(p_\theta) + p_z \mathbf{i}_z$$



as well as, for the current placement vector, using the coordinates  $(r, \theta, z)$  and the associated cylindrical vector basis:

$$\mathbf{x} = r \mathbf{i}_r(\theta) + z \mathbf{i}_z$$

■ **Example 1.4 — Torsion of a cylindrical shaft.** We consider a material domain  $\Omega$  with a cylindrical shape of axis  $\mathbf{i}_z$ , of circular cross-section of radius  $R$  and length  $L$ , undergoing a transformation of the form:

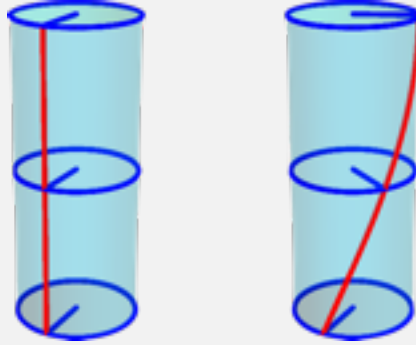
$$\boxed{\mathbf{x} = \mathbf{f}(\mathbf{p}, t) = \mathbf{p} + p_r (\mathbf{i}_r(p_\theta + c(t)p_z/L) - \mathbf{i}_r(p_\theta)), \forall \mathbf{p} \in \Omega_0}$$

where  $\mathbf{p} = p_r \mathbf{i}_r(p_\theta) + p_z \mathbf{i}_z$  is the initial placement vector, and  $c$  is an arbitrary dimensionless scalar function of time.

This transformation is expressed in terms of cylindrical coordinates as:

$$\begin{aligned} r &= p_r, \forall p_r \in [0, R] \\ \theta &= p_\theta + \frac{c(t)p_z}{L}, \forall (p_\theta, p_z) \in [0, 2\pi] \times [0, L] \\ z &= p_z, \forall p_z \in [0, L] \end{aligned}$$

Thus, any cross-section of fixed altitude  $p_z$  undergoes a rigid body rotation, of axis  $\mathbf{i}_z$  and angle  $c(t)p_z/L$ :  $c(t)$  represents the angular offset (in radians) imposed between the two cylinder end sections.



In addition, an initially straight line parallel to the  $\mathbf{i}_z$  axis of the cylinder (in red in the figure above) verifies  $p_r = C_1$  and  $p_\theta = C_2$ , where  $C_1$  and  $C_2$  are given constants. It is therefore transformed at time  $t$  as:

$$\begin{aligned} r &= C_1 \\ \theta &= C_2 + \frac{c(t)p_z}{L}, \forall p_z \in [0, L] \\ z &= p_z, \forall p_z \in [0, L] \end{aligned}$$

i.e. as a helix with an axis  $\mathbf{i}_z$ , same radius  $C_1$  and pitch  $2\pi L/c(t)$ . ■

### 1.1.2 Material velocity and acceleration

Since the placement vector  $\mathbf{x} = \mathbf{f}(\mathbf{p}, t)$  allows for locating the position of each particle at any given time, it is natural to define the material velocity  $\dot{\mathbf{x}}$  (or Lagrangian velocity) as the variation of the placement vector between two very close instants  $t$  and  $t + \Delta t$ , or, using the limit ( $\Delta t \rightarrow 0$ ):

$$\dot{\mathbf{x}} = \frac{\partial \mathbf{f}}{\partial t}(\mathbf{p}, t), \forall \mathbf{p} \in \Omega_0$$

Similarly, the material acceleration  $\ddot{\mathbf{x}}$  (or Lagrangian acceleration) is then defined as the second derivative with respect to time of the placement vector:

$$\ddot{\mathbf{x}} = \frac{\partial^2 \mathbf{f}}{\partial t^2}(\mathbf{p}, t), \forall \mathbf{p} \in \Omega_0$$



*For the time being, we have deliberately avoided the question of the “reference frame”, which defines the reference relative to which we will express the variations of the placement vector, and, consequently the expression of its temporal derivative. We, therefore, assume here that the movements are described with respect to a “fixed observer” without further details.*

■ **Example 1.5 — Uniform elongation: material velocities and accelerations.** By deriving with respect to time the placement vector field studied in Example 1.1:

$$\mathbf{x} = \mathbf{f}(\mathbf{p}, t) = \mathbf{p} + a(t) \langle \mathbf{p}, \mathbf{n} \rangle \mathbf{n}, \forall \mathbf{p} \in \Omega_0$$

where  $a$  is an arbitrary scalar function of time, and  $\mathbf{n}$  a fixed unit vector, we obtain the following material velocity field:

$$\dot{\mathbf{x}} = \frac{\partial \mathbf{f}}{\partial t}(\mathbf{p}, t) = \dot{a}(t) \langle \mathbf{p}, \mathbf{n} \rangle \mathbf{n}, \forall \mathbf{p} \in \Omega_0$$

as well as the material acceleration field:

$$\ddot{\mathbf{x}} = \frac{\partial^2 \mathbf{f}}{\partial t^2}(\mathbf{p}, t) = \ddot{a}(t) \langle \mathbf{p}, \mathbf{n} \rangle \mathbf{n}, \forall \mathbf{p} \in \Omega_0$$

Each plane of equation  $\langle \mathbf{p}, \mathbf{n} \rangle = C$  consists of particles that all have the same velocity  $\dot{a}(t)C\mathbf{n}$  and the same acceleration  $\ddot{a}(t)C\mathbf{n}$ , which is logical since this plane does not deform over time. ■



*It is possible to adopt another point of view: instead of considering the velocities and accelerations specific to each particle, we can privilege the fact that, at a given time, we have a spatial map of velocity and acceleration vectors, without worrying about the particles associated with each point of space; in this description, the space variables  $\mathbf{x}$  and time variables  $t$  are therefore independent of each other.*

*This point of view, where the velocities and accelerations are called “spatial” (or “Eulerian”), is commonly adopted when describing the kinematics of fluid media, for which it is neither relevant nor easy to identify an initial configuration. However, the following example also illustrates this point of view in the case of a solid deformable medium.*

■ **Example 1.6 — Torsion of a cylindrical shaft: material velocities and accelerations.** By deriving with respect to time the placement vector studied in Example 1.4 (where  $\mathbf{p} = p_r \mathbf{i}_r(p_\theta) + p_z \mathbf{i}_z$ , and  $c$  is an arbitrary scalar function of time):

$$\mathbf{x} = \mathbf{f}(\mathbf{p}, t) = \mathbf{p} + p_r (\mathbf{i}_r(p_\theta + c(t)p_z/L) - \mathbf{i}_r(p_\theta)), \forall \mathbf{p} \in \Omega_0$$

we obtain the following material velocity field:

$$\dot{\mathbf{x}} = \frac{\partial \mathbf{f}}{\partial t}(\mathbf{p}, t) = p_r \frac{\dot{c}(t)p_z}{L} \mathbf{i}_\theta \left( p_\theta + \frac{c(t)p_z}{L} \right)$$

since  $\frac{d\mathbf{i}_r}{dt}(p_\theta(t)) = \dot{p}_\theta \mathbf{i}_\theta(p_\theta(t))$ , or, finally:

$$\dot{\mathbf{x}} = \frac{\dot{c}(t)p_z}{L} \mathbf{i}_z \wedge \mathbf{f}(\mathbf{p}, t), \forall \mathbf{p} \in \Omega_0$$

for which we recognize the classical expression, for each particle, of the velocity of a point  $\mathbf{x} = \mathbf{f}(\mathbf{p}, t)$  rotating about the axis  $\mathbf{i}_z$ , with angular velocity  $\dot{c}(t)p_z/L$ .

In the same way, the material acceleration field is expressed as:

$$\ddot{\mathbf{x}} = \frac{\partial^2 \mathbf{f}}{\partial t^2}(\mathbf{p}, t) = p_r \frac{\ddot{c}(t)p_z}{L} \mathbf{i}_\theta \left( p_\theta + \frac{c(t)p_z}{L} \right) - p_r \left( \frac{\dot{c}(t)p_z}{L} \right)^2 \mathbf{i}_r \left( p_\theta + \frac{c(t)p_z}{L} \right)$$

since  $\frac{d\mathbf{i}_\theta}{dt}(p_\theta(t)) = -\dot{p}_\theta \mathbf{i}_r(p_\theta(t))$ , or, finally:

$$\ddot{\mathbf{x}} = \frac{\ddot{c}(t)p_z}{L} \mathbf{i}_z \wedge \mathbf{f}(\mathbf{p}, t) - \left( \frac{\dot{c}(t)p_z}{L} \right)^2 (\mathbf{f}(\mathbf{p}, t) - p_z \mathbf{i}_z), \forall \mathbf{p} \in \Omega_0$$

for which we recognize the classical expression, for each particle, of the acceleration of a point  $\mathbf{x} = \mathbf{f}(\mathbf{p}, t)$  in rotation about the axis  $\mathbf{i}_z$ , with angular velocity  $\dot{c}(t)p_z/L$  and angular acceleration  $\ddot{c}(t)p_z/L$ .

It is remarkable that these two fields only depend on the positions at time  $t$  of the particles under study: it is indeed possible to adopt a spatial representation (or “Eulerian”) of this movement, by writing the velocity :

$$\mathbf{v}(\mathbf{x}, t) = \frac{\dot{c}(t)p_z}{L} \mathbf{i}_z \wedge \mathbf{x}, \forall \mathbf{x} \in \Omega_t$$

and, likewise, the acceleration:

$$\mathbf{a}(\mathbf{x}, t) = \frac{\ddot{c}(t)z}{L}\mathbf{i}_z \wedge \mathbf{x} - \left(\frac{\dot{c}(t)z}{L}\right)^2 (\mathbf{x} - z\mathbf{i}_z), \forall \mathbf{x} \in \Omega_t$$

as functions of space (where  $\mathbf{x}(r, \theta, z) = r\mathbf{i}_r(\theta) + z\mathbf{i}_z$  using cylindrical coordinates) and time, which are independent of each other. ■

## 1.2 Deformation of a continuous medium

The purpose of this part is to define the notion of deformation, which will allow for describing locally (i.e. in the vicinity of any particle) variations both in length and angle. To do this, quantitatively determining how the neighbourhood of a given particle evolves over time is necessary.

### 1.2.1 Deformation gradient tensor

We have already mentioned that the notion of a continuous medium must be interpreted both physically and mathematically: in the latter, this is equivalent to say that the placement vector  $\mathbf{f}$  is a continuous function of space, represented by the initial position  $\mathbf{p}$  of each particle.

In order to describe the movement of particles being very close to a given particle  $\mathbf{p}$ , we then wish to write the series expansion of the placement vector  $\mathbf{f}$  in  $\mathbf{p}$ . In typical cases, a first-order expansion is sufficient and allows for building a linear theory, called “first gradient” theory; we then assume that the placement vector is differentiable to write:

$$f_m(\mathbf{q}, t) = f_m(\mathbf{p}, t) + \sum_{n=1}^3 (q_n - p_n) \frac{\partial f_m}{\partial p_n}(\mathbf{p}, t) + o(\|\mathbf{q} - \mathbf{p}\|), \quad 1 \leq m \leq 3$$

for any point  $\mathbf{q}$  of coordinates  $(q_1, q_2, q_3)$  in a Cartesian vector basis  $(\mathbf{i}_1, \mathbf{i}_2, \mathbf{i}_3)$ , located near a given point  $\mathbf{p}$ , of coordinates  $(p_1, p_2, p_3)$  in the same basis, as represented in Figure 1.2. Then we define  $d\mathbf{p} = \mathbf{q} - \mathbf{p}$  and  $d\mathbf{x} = \mathbf{y} - \mathbf{x}$ , which are infinitesimal vectors that characterize the neighbourhood of  $\mathbf{p}$  (at  $t = 0$ ) and  $\mathbf{x}$  (at  $t$ ) respectively.

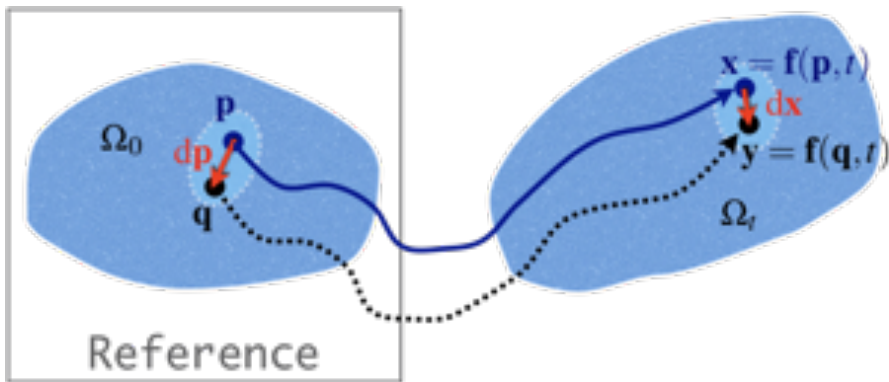


Figure 1.2: Transformation of the neighbourhood of a material point.

**Deformation gradient tensor.** The deformation gradient tensor (or transformation tensor)  $\mathbb{F}(\mathbf{p}, t)$  is the linear application associated with the Jacobian matrix of the placement vector  $\mathbf{x} = \mathbf{f}(\mathbf{p}, t)$ , as defined in Appendix B.1.1:

$$\mathbb{F}(\mathbf{p}, t) = \mathbb{D}_{\mathbf{p}} \mathbf{x}(\mathbf{p}, t)$$

allowing to relate the neighbourhoods of a point in the initial and current configurations:

$$\mathrm{d}\mathbf{x} = \mathbb{F}(\mathbf{p}, t) \mathrm{d}\mathbf{p}$$

and whose components in a Cartesian vector basis  $(\mathbf{i}_1, \mathbf{i}_2, \mathbf{i}_3)$  are expressed as:

$$F_{mn}(\mathbf{p}, t) = \frac{\partial x_m}{\partial p_n}(\mathbf{p}, t)$$

where  $(p_1, p_2, p_3)$  and  $(x_1, x_2, x_3)$  are the respective coordinates of  $\mathbf{p}$  and  $\mathbf{x} = \mathbf{f}(\mathbf{p}, t)$  in this same vector basis.

Appendix A.2 gives an overview of the manipulation of a second-order tensor, either in its matrix form when expressed in a vector basis, or in a more “intrinsic” form using the tensor product:

$$\mathbb{F} = \sum_{m=1}^3 \sum_{n=1}^3 \frac{\partial x_m}{\partial p_n} \mathbf{i}_m \otimes \mathbf{i}_n$$

**R** It is also possible to express the deformation gradient tensor using the displacement field  $\mathbf{u}(\mathbf{p}, t)$ : indeed, since:

$$\mathbf{x} = \mathbf{f}(\mathbf{p}, t) = \mathbf{p} + \mathbf{u}(\mathbf{p}, t)$$

it can be directly established that:

$$\mathbb{F}(\mathbf{p}, t) = \mathbb{I} + \mathbb{D}_{\mathbf{p}}\mathbf{u}(\mathbf{p}, t)$$

where  $\mathbb{I}$  refers to the identity tensor, and  $\mathbb{D}_{\mathbf{p}}\mathbf{u}$  is the displacement gradient tensor.

■ **Example 1.7 — Uniform elongation: deformation gradient tensor.** Let us consider the transformation studied in Example 1.1:

$$\mathbf{x} = \mathbf{f}(\mathbf{p}, t) = \mathbf{p} + a(t) \langle \mathbf{p}, \mathbf{n} \rangle \mathbf{n}, \forall \mathbf{p} \in \Omega_0$$

which can be rewritten, by virtue of the properties of the tensor product (presented in Appendix A.2.1), as:

$$\mathbf{x} = (\mathbb{I} + a(t) \mathbf{n} \otimes \mathbf{n}) \mathbf{p}, \forall \mathbf{p} \in \Omega_0$$

which makes it possible to immediately express the deformation gradient tensor as:

$$\mathbb{F}(\mathbf{p}, t) = \mathbb{D}_{\mathbf{p}}\mathbf{x}(\mathbf{p}, t) = \mathbb{I} + a(t) \mathbf{n} \otimes \mathbf{n}, \forall \mathbf{p} \in \Omega_0$$

or, in a Cartesian vector basis  $(\mathbf{i}_1, \mathbf{i}_2 = \mathbf{n}, \mathbf{i}_3)$  including the vector  $\mathbf{n}$ :

$$\boxed{\mathbb{F}(\mathbf{p}, t) = \begin{pmatrix} 1 & 0 & 0 \\ 0 & 1 + a(t) & 0 \\ 0 & 0 & 1 \end{pmatrix}_{(\mathbf{i}_1, \mathbf{i}_2 = \mathbf{n}, \mathbf{i}_3)}}$$

where  $\mathbf{i}_1$  and  $\mathbf{i}_3$  are two unit vectors perpendicular to  $\mathbf{n}$ , and to each other. We then verify that:

$$F_{mn} = \frac{\partial x_m}{\partial p_n}$$

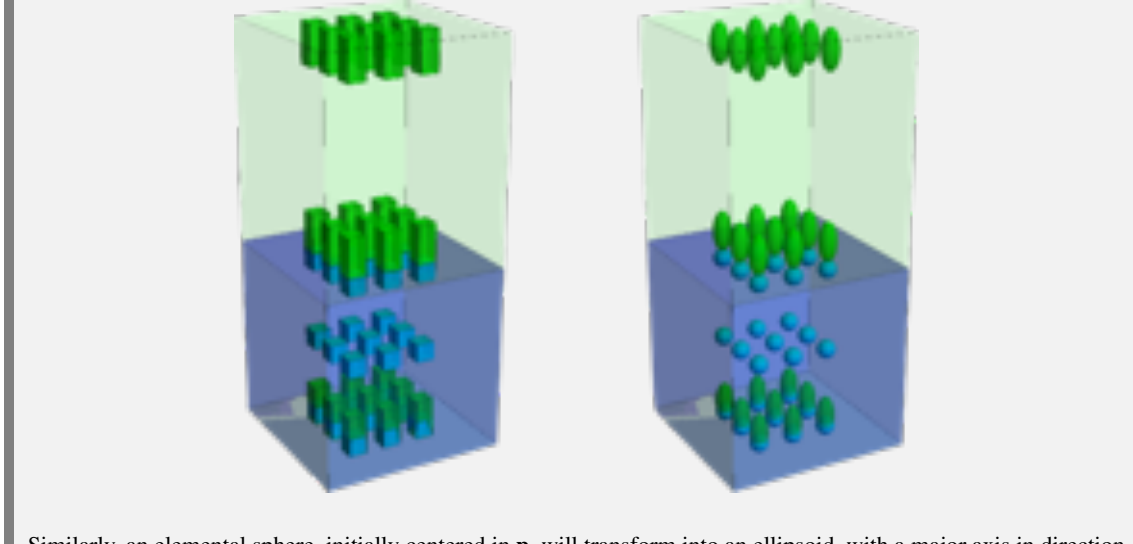
considering that, in our vector basis,  $x_1 = p_1$ ,  $x_2 = p_2 + a(t)p_2$  and  $x_3 = p_3$ .

The neighbourhood of a point  $\mathbf{p}$ , characterized by the infinitesimal vector  $\mathrm{d}\mathbf{p}$ , is therefore transformed as :

$$\mathrm{d}\mathbf{x} = (\mathbb{I} + a(t) \mathbf{n} \otimes \mathbf{n}) \mathrm{d}\mathbf{p} = \mathrm{d}\mathbf{p} + a(t) \langle \mathrm{d}\mathbf{p}, \mathbf{n} \rangle \mathbf{n}$$

for any  $\mathbf{p}$ . In the vector basis  $(\mathbf{i}_1, \mathbf{i}_2 = \mathbf{n}, \mathbf{i}_3)$ , we then have  $\mathrm{d}x_1 = \mathrm{d}p_1$ ,  $\mathrm{d}x_2 = (1 + a(t)) \mathrm{d}p_2$  and  $\mathrm{d}x_3 = \mathrm{d}p_3$ .

Thus, an elemental cube, of center the particle initially located in  $\mathbf{p}$ , and with one of its edges along  $\mathbf{n}$ , will elongate in this latter direction, while the sections perpendicular to  $\mathbf{n}$  will not deform.



Similarly, an elemental sphere, initially centered in  $\mathbf{p}$ , will transform into an ellipsoid, with a major axis in direction  $\mathbf{n}$ . ■

■ **Example 1.8 — Uniform shear strain: deformation gradient tensor.** Let us consider the transformation studied in Example 1.2:

$$\mathbf{x} = \mathbf{f}(\mathbf{p}, t) = \mathbf{p} + b(t)\langle \mathbf{p}, \mathbf{n} \rangle \mathbf{t}, \forall \mathbf{p} \in \Omega_0$$

that, similarly to Example 1.7, can be rewritten as:

$$\mathbf{x} = (\mathbb{I} + b(t)\mathbf{t} \otimes \mathbf{n})\mathbf{p}, \forall \mathbf{p} \in \Omega_0$$

which makes it possible to immediately express the deformation gradient tensor as:

$$\mathbb{F}(\mathbf{p}, t) = \mathbb{D}_{\mathbf{p}}\mathbf{x}(\mathbf{p}, t) = \mathbb{I} + b(t)\mathbf{t} \otimes \mathbf{n}, \forall \mathbf{p} \in \Omega_0$$

or, in a Cartesian vector basis ( $\mathbf{i}_1 = \mathbf{t}, \mathbf{i}_2 = \mathbf{n}, \mathbf{i}_3$ ) including vectors  $\mathbf{t}$  and  $\mathbf{n}$ :

$$\mathbb{F}(\mathbf{p}, t) = \begin{pmatrix} 1 & b(t) & 0 \\ 0 & 1 & 0 \\ 0 & 0 & 1 \end{pmatrix}_{(\mathbf{i}_1=\mathbf{t}, \mathbf{i}_2=\mathbf{n}, \mathbf{i}_3)}$$

where  $\mathbf{i}_3 = \mathbf{t} \wedge \mathbf{n}$ . We then verify that:

$$F_{mn} = \frac{\partial x_m}{\partial p_n}$$

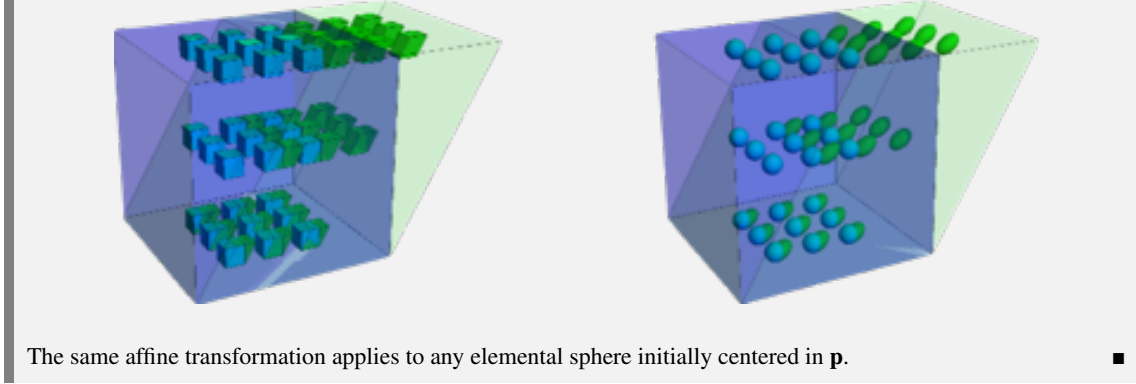
since in our vector basis,  $x_1 = p_1 + b(t)p_2$ ,  $x_2 = p_2$  and  $x_3 = p_3$ .

The neighbourhood of a point  $\mathbf{p}$ , characterized by the infinitesimal vector  $d\mathbf{p}$ , is therefore transformed as:

$$d\mathbf{x} = (\mathbb{I} + b(t)\mathbf{t} \otimes \mathbf{n})d\mathbf{p} = d\mathbf{p} + b(t)\langle d\mathbf{p}, \mathbf{n} \rangle \mathbf{t}$$

for any  $\mathbf{p}$ . In the vector basis ( $\mathbf{i}_1 = \mathbf{t}, \mathbf{i}_2 = \mathbf{n}, \mathbf{i}_3$ ), we then have  $dx_1 = dp_1 + b(t)dp_2$ ,  $dx_2 = dp_2$  and  $dx_3 = dp_3$ .

Thus, an elemental cube, whose center is the particle initially located in  $\mathbf{p}$ , and one of whose faces has edges along  $\mathbf{n}$  and  $\mathbf{t}$ , will deform into a non-rectangular parallelepiped..



■ **Example 1.9 — Movement of rigid bodies: deformation gradient tensor.** Let us consider the transformation studied in Example 1.3:

$$\mathbf{x} = \mathbf{f}(\mathbf{p}, t) = \mathbf{x}_A(t) + \mathbb{R}(t)(\mathbf{p} - \mathbf{p}_A), \forall \mathbf{p} \in \Omega_0$$

We immediately establish that the deformation gradient tensor is:

$$\mathbb{F}(\mathbf{p}, t) = \mathbb{D}_{\mathbf{p}} \mathbf{x}(\mathbf{p}, t) = \mathbb{R}(t)$$

which means that the neighbourhood of the point  $\mathbf{p}$ , characterized by the infinitesimal vector  $d\mathbf{p}$ , undergoes a simple rotation:

$$d\mathbf{x} = \mathbb{R}(t) d\mathbf{p}$$

and does not deform, since  $\|d\mathbf{x}\|^2 = \langle \mathbb{R}(t) d\mathbf{p}, \mathbb{R}(t) d\mathbf{p} \rangle = \langle \mathbb{R}(t)^T \mathbb{R}(t) d\mathbf{p}, d\mathbf{p} \rangle = \|d\mathbf{p}\|^2$ . ■

### Tensor expressions

We have seen that the components of the tensor  $\mathbb{F}$  in a Cartesian vector basis  $(\mathbf{i}_1, \mathbf{i}_2, \mathbf{i}_3)$  can be expressed as:

$$F_{mn}(\mathbf{p}, t) = \frac{\partial x_m}{\partial p_n}(\mathbf{p}, t)$$

This makes it possible to obtain a synthetic expression of the tensor  $\mathbb{F}$ ; by using the expression of a tensor on the basis of tensor products, given in Appendix A.2.1, we obtain indeed:

$$\mathbb{F} = \sum_{m=1}^3 \sum_{n=1}^3 F_{mn} \mathbf{i}_m \otimes \mathbf{i}_n = \sum_{m=1}^3 \sum_{n=1}^3 \frac{\partial x_m}{\partial p_n} \mathbf{i}_m \otimes \mathbf{i}_n$$

that can be transformed as:

$$\mathbb{F} = \sum_{n=1}^3 \left( \sum_{m=1}^3 \frac{\partial x_m}{\partial p_n} \mathbf{i}_m \right) \otimes \mathbf{i}_n = \sum_{n=1}^3 \frac{\partial}{\partial p_n} \left( \sum_{m=1}^3 x_m \mathbf{i}_m \right) \otimes \mathbf{i}_n$$

hence, finally, the intrinsic expression:

$$\mathbb{F} = \sum_{n=1}^3 \frac{\partial \mathbf{x}}{\partial p_n} \otimes \mathbf{i}_n$$

for which, in practice, it is possible to express  $\mathbf{x}$  in a vector basis other than  $(\mathbf{i}_1, \mathbf{i}_2, \mathbf{i}_3)$ .

Also, if it is more convenient to use cylindrical coordinates  $(p_r, p_\theta, p_z)$  to express the placement vector of points of  $\Omega$ , it is possible to intrinsically express the tensor  $\mathbb{F}$  in a cylindrical vector basis  $(\mathbf{i}_r(p_\theta), \mathbf{i}_\theta(p_\theta), \mathbf{i}_z)$ , using the chain rule:

$$\mathbb{F} = \sum_{n=1}^3 \left( \frac{\partial \mathbf{x}}{\partial p_r} \frac{\partial p_r}{\partial p_n} + \frac{\partial \mathbf{x}}{\partial p_\theta} \frac{\partial p_\theta}{\partial p_n} + \frac{\partial \mathbf{x}}{\partial p_z} \frac{\partial p_z}{\partial p_n} \right) \otimes \mathbf{i}_n$$

where we can group together:

$$\sum_{n=1}^3 \frac{\partial p_r}{\partial p_n} \mathbf{i}_n = \nabla_{\mathbf{p}} p_r, \quad \sum_{n=1}^3 \frac{\partial p_\theta}{\partial p_n} \mathbf{i}_n = \nabla_{\mathbf{p}} p_\theta, \quad \sum_{n=1}^3 \frac{\partial p_z}{\partial p_n} \mathbf{i}_n = \nabla_{\mathbf{p}} p_z$$

with  $\nabla_{\mathbf{p}}$  referring to the gradient in the initial configuration. As established in Appendix B.3.2, we have  $\nabla_{\mathbf{p}} p_r = \mathbf{i}_r$ ,  $\nabla_{\mathbf{p}} p_\theta = \mathbf{i}_\theta / p_r$  and  $\nabla_{\mathbf{p}} p_z = \mathbf{i}_z$ , resulting in:

$$\mathbb{F} = \frac{\partial \mathbf{x}}{\partial p_r} \otimes \mathbf{i}_r + \frac{\partial \mathbf{x}}{\partial p_\theta} \otimes \frac{\mathbf{i}_\theta}{p_r} + \frac{\partial \mathbf{x}}{\partial p_z} \otimes \mathbf{i}_z$$



The latter approach for expressing  $\mathbb{F}$  can of course be generalized to any arbitrary system of curvilinear coordinates  $(p_\xi, p_\eta, p_\zeta)$ :

$$\mathbb{F} = \frac{\partial \mathbf{x}}{\partial p_\xi} \otimes \nabla_{\mathbf{p}} p_\xi + \frac{\partial \mathbf{x}}{\partial p_\eta} \otimes \nabla_{\mathbf{p}} p_\eta + \frac{\partial \mathbf{x}}{\partial p_\zeta} \otimes \nabla_{\mathbf{p}} p_\zeta$$

where it is then sufficient to calculate the gradients of these coordinates in the initial configuration. More details can be found in Appendix B.3.1.

**Summary 1.1 — Deformation gradient tensor.** The deformation gradient tensor  $\mathbb{F} = \mathbb{D}_{\mathbf{p}} \mathbf{x}$  allows the infinitesimal vector  $d\mathbf{x} = \mathbf{y} - \mathbf{x}$  connecting two particles considered in the current configuration, to be expressed relative to the corresponding vector  $d\mathbf{p} = \mathbf{q} - \mathbf{p}$  in the initial configuration as:

$$d\mathbf{x}(\mathbf{p}, t) = \mathbb{F}(\mathbf{p}, t) d\mathbf{p}, \quad \forall \mathbf{p} \in \Omega_0, \quad \forall t$$

In a Cartesian vector basis  $(\mathbf{i}_1, \mathbf{i}_2, \mathbf{i}_3)$  associated with coordinates  $(p_1, p_2, p_3)$ , this tensor is expressed as:

$$\mathbb{F}(p_1, p_2, p_3, t) = \frac{\partial \mathbf{x}}{\partial p_1}(p_1, p_2, p_3, t) \otimes \mathbf{i}_1 + \frac{\partial \mathbf{x}}{\partial p_2}(p_1, p_2, p_3, t) \otimes \mathbf{i}_2 + \frac{\partial \mathbf{x}}{\partial p_3}(p_1, p_2, p_3, t) \otimes \mathbf{i}_3$$

In a cylindrical vector basis  $(\mathbf{i}_r(p_\theta), \mathbf{i}_\theta(p_\theta), \mathbf{i}_z)$  associated with coordinates  $(p_r, p_\theta, p_z)$ , this tensor is expressed as:

$$\mathbb{F}(p_r, p_\theta, p_z, t) = \frac{\partial \mathbf{x}}{\partial p_r}(p_r, p_\theta, p_z, t) \otimes \mathbf{i}_r + \frac{\partial \mathbf{x}}{\partial p_\theta}(p_r, p_\theta, p_z, t) \otimes \frac{\mathbf{i}_\theta}{p_r} + \frac{\partial \mathbf{x}}{\partial p_z}(p_r, p_\theta, p_z, t) \otimes \mathbf{i}_z$$

■ **Example 1.10 — Torsion of a cylindrical shaft: deformation gradient tensor.** Let us consider the transformation studied in Example 1.4:

$$\mathbf{x} = \mathbf{f}(\mathbf{p}, t) = \mathbf{p} + p_r (\mathbf{i}_r(p_\theta + c(t)p_z/L) - \mathbf{i}_r(p_\theta)) = p_r \mathbf{i}_r(p_\theta + c(t)p_z/L) + p_z \mathbf{i}_z, \quad \forall \mathbf{p} \in \Omega_0$$

The deformation gradient tensor is then calculated as:

$$\mathbb{F}(p_r, p_\theta, p_z, t) = \frac{\partial \mathbf{x}}{\partial p_r} \otimes \mathbf{i}_r(p_\theta) + \frac{\partial \mathbf{x}}{\partial p_\theta} \otimes \frac{\mathbf{i}_\theta(p_\theta)}{p_r} + \frac{\partial \mathbf{x}}{\partial p_z} \otimes \mathbf{i}_z$$

with:

$$\begin{aligned} \frac{\partial \mathbf{x}}{\partial p_r} &= \mathbf{i}_r \left( p_\theta + \frac{c(t)p_z}{L} \right) \\ \frac{\partial \mathbf{x}}{\partial p_\theta} &= p_r \mathbf{i}_\theta \left( p_\theta + \frac{c(t)p_z}{L} \right) \\ \frac{\partial \mathbf{x}}{\partial p_z} &= p_r \frac{c(t)}{L} \mathbf{i}_\theta \left( p_\theta + \frac{c(t)p_z}{L} \right) + \mathbf{i}_z \end{aligned}$$

or, finally:

$$\begin{aligned}\mathbb{F} = & \mathbf{i}_r(p_\theta + c(t)p_z/L) \otimes \mathbf{i}_r(p_\theta) + \mathbf{i}_\theta(p_\theta + c(t)p_z/L) \otimes \mathbf{i}_\theta(p_\theta) \\ & + \left( p_r \frac{c(t)}{L} \mathbf{i}_\theta(p_\theta + c(t)p_z/L) + \mathbf{i}_z \right) \otimes \mathbf{i}_z\end{aligned}$$

We immediately notice the advantages of a tensor expression: the latter is very compact because it allows for mixing vectors from different vector bases. Indeed, if one wishes to express the associated matrix, it is necessary to choose a particular vector basis, which implies projections, and therefore additional terms, for example:

$$\mathbb{F} = \begin{pmatrix} \cos\left(\frac{c(t)p_z}{L}\right) & -\sin\left(\frac{c(t)p_z}{L}\right) & -p_r \frac{c(t)}{L} \sin\left(\frac{c(t)p_z}{L}\right) \\ \sin\left(\frac{c(t)p_z}{L}\right) & \cos\left(\frac{c(t)p_z}{L}\right) & p_r \frac{c(t)}{L} \cos\left(\frac{c(t)p_z}{L}\right) \\ 0 & 0 & 1 \end{pmatrix}_{(\mathbf{i}_r(p_\theta), \mathbf{i}_\theta(p_\theta), \mathbf{i}_z)}$$

if you choose the cylindrical vector basis  $(\mathbf{i}_r(p_\theta), \mathbf{i}_\theta(p_\theta), \mathbf{i}_z)$  associated with the initial configuration.

In addition, the obtained tensor  $\mathbb{F}$  can be expressed as the product of two particular tensors:

$$\boxed{\mathbb{F}(p_r, p_\theta, p_z, t) = \mathbb{R}(p_\theta, p_z, t) \mathbb{G}(p_r, p_\theta, p_z, t)}$$

with

$$\mathbb{R}(p_\theta, p_z, t) = \mathbf{i}_r(p_\theta + c(t)p_z/L) \otimes \mathbf{i}_r(p_\theta) + \mathbf{i}_\theta(p_\theta + c(t)p_z/L) \otimes \mathbf{i}_\theta(p_\theta) + \mathbf{i}_z \otimes \mathbf{i}_z$$

$$\mathbb{G}(p_r, p_\theta, p_z, t) = \mathbb{I} + p_r \frac{c(t)}{L} \mathbf{i}_\theta(p_\theta) \otimes \mathbf{i}_z$$

or, in the vector basis  $(\mathbf{i}_r(p_\theta), \mathbf{i}_\theta(p_\theta), \mathbf{i}_z)$  associated with the initial configuration:

$$\begin{aligned}\mathbb{R} = & \begin{pmatrix} \cos\left(\frac{c(t)p_z}{L}\right) & -\sin\left(\frac{c(t)p_z}{L}\right) & 0 \\ \sin\left(\frac{c(t)p_z}{L}\right) & \cos\left(\frac{c(t)p_z}{L}\right) & 0 \\ 0 & 0 & 1 \end{pmatrix}_{(\mathbf{i}_r(p_\theta), \mathbf{i}_\theta(p_\theta), \mathbf{i}_z)} \\ \mathbb{G} = & \begin{pmatrix} 1 & 0 & 0 \\ 0 & 1 & \frac{p_r c(t)}{L} \\ 0 & 0 & 1 \end{pmatrix}_{(\mathbf{i}_r(p_\theta), \mathbf{i}_\theta(p_\theta), \mathbf{i}_z)}\end{aligned}$$

While  $\mathbb{R}$  is the tensor associated with the rotation around axis  $\mathbf{i}_z$ , with angle  $c(t)p_z/L$ ,  $\mathbb{G}$  is a tensor, which is characteristic of a uniform shear strain state (as detailed in Example 1.8). Physically, the neighbourhood of a point  $\mathbf{p}$ , characterized by the infinitesimal vector  $d\mathbf{p}$ , undergoes a transformation:

$$d\mathbf{x} = \mathbb{F} d\mathbf{p} = \mathbb{R} \mathbb{G} d\mathbf{p}$$

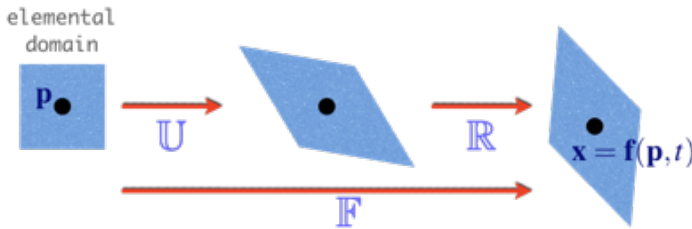
which is the composition of a simple shear strain transformation and a rotation. ■



*In general, it is demonstrably always possible to decompose the deformation gradient tensor as the composition of a tensor  $\mathbb{U}$ , expressing how the neighbourhood of the material point under study is deformed, with a tensor  $\mathbb{R}$  associated with a rotation, which allows us to obtain the “polar decomposition” of  $\mathbb{F}$  as:*

$$\boxed{\mathbb{F}(\mathbf{p}, t) = \mathbb{R}(\mathbf{p}, t) \mathbb{U}(\mathbf{p}, t), \forall \mathbf{p} \in \Omega_0, \forall t}$$

where  $\mathbb{U}$  is the square root of the tensor  $\mathbb{C} = \mathbb{F}^T \mathbb{F}$ , which is a symmetrical and positive tensor. More details are given in Appendix A.2.5.



*It is important to note that this relation is local and depends a priori on the point  $\mathbf{p}$  that one considers.*

### 1.2.2 Green-Lagrange strain tensor

Now that we can mathematically describe how the vicinity of a material point evolves within a continuous medium, we can define the deformation at each point of such a medium. We have seen in the previous examples that we can express it in two ways:

- a variation in the length of the segments oriented along a given direction, as in Example 1.7;
- an angle variation (or “distortion”) between pairs of segments oriented into two given directions, as in Example 1.8;

which can possibly be mixed, as in Example 1.10. To describe all these variations in a unified manner, we introduce the following tensor.

**Green-Lagrange strain tensor.** The Green-Lagrange strain tensor is the tensor defined at any point in the initial configuration of the continuous medium  $\Omega$  as:

$$\mathbb{E}(\mathbf{p}, t) = \frac{1}{2} (\mathbb{F}(\mathbf{p}, t)^T \mathbb{F}(\mathbf{p}, t) - \mathbb{I}), \quad \forall \mathbf{p} \in \Omega_0$$

where  $\mathbb{F}(\mathbf{p}, t)$  is the deformation gradient tensor, and  $\mathbb{I}$  the identity tensor.

#### Length variation in the neighbourhood of a material point

We consider the infinitesimal vector  $d\mathbf{x}$  connecting two infinitely close particles  $\mathbf{x}$  and  $\mathbf{y}$ ; as we have seen above, this vector evolves over time as:

$$d\mathbf{x} = \mathbb{F} d\mathbf{p}$$

where  $d\mathbf{p}$  is the infinitesimal vector linking these same two particles located in  $\mathbf{p}$  and  $\mathbf{q}$  in the initial configuration, as shown in Figure 1.3.

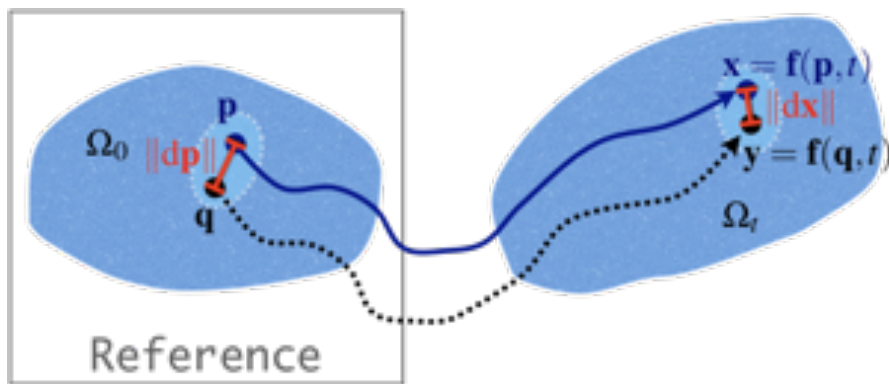


Figure 1.3: Length variation in the neighbourhood of a material point.

We can then focus on the variation over time of the length of this infinitesimal vector, or, in an equivalent way, of the square of its length, which is expressed as:

$$\|d\mathbf{x}\|^2 = \langle d\mathbf{x}, d\mathbf{x} \rangle = \langle \mathbb{F} d\mathbf{p}, \mathbb{F} d\mathbf{p} \rangle = \langle \mathbb{F}^T \mathbb{F} d\mathbf{p}, d\mathbf{p} \rangle$$

using the transpose of the deformation gradient tensor. By comparing with the square of the length of the initial infinitesimal vector, we then obtain:

$$\|d\mathbf{x}\|^2 - \|d\mathbf{p}\|^2 = \langle (\mathbb{F}^T \mathbb{F} - \mathbb{I}) d\mathbf{p}, d\mathbf{p} \rangle$$

or, by using the expression of the Green-Lagrange strain tensor:

$$\|d\mathbf{x}\|^2 - \|d\mathbf{p}\|^2 = 2 \langle \mathbb{E} d\mathbf{p}, d\mathbf{p} \rangle$$

If we express, in the initial configuration, the infinitesimal vector as  $d\mathbf{p} = l_{1p}\mathbf{i}_1$ , where  $\mathbf{i}_1$  is unitary, and by noting  $l_{1x} = \|d\mathbf{x}\|$ , the previous relation can be rewritten as:

$$l_{1x}^2 - l_{1p}^2 = 2l_{1p}^2 \langle \mathbb{E}\mathbf{i}_1, \mathbf{i}_1 \rangle = 2l_{1p}^2 E_{11}$$

by noting  $E_{mn}$  the components of  $\mathbb{E}$  in a Cartesian vector basis  $(\mathbf{i}_1, \mathbf{i}_2, \mathbf{i}_3)$ . The diagonal terms  $E_{nn}$  of the Green-Lagrange strain tensor can, therefore, be interpreted as the relative variations of the squares of the lengths of infinitesimal vectors along respective directions  $\mathbf{i}_n$ , which are vectors of the Cartesian basis associated with the expression of the components  $E_{nn}$ .

**R** Given the definition, since  $l_{1x}^2 > 0$ , we note that  $E_{11} > -1/2$ . In addition, the relation established above can still be rewritten as:

$$\frac{l_{1x}}{l_{1p}} = \sqrt{1 + 2E_{11}} = \sqrt{C_{11}} = U_{11} > 0$$

where terms  $C_{mn}$  are the components in a Cartesian vector basis  $(\mathbf{i}_1, \mathbf{i}_2, \mathbf{i}_3)$  of tensor  $\mathbb{C} = \mathbb{F}^T \mathbb{F}$ , called the right Cauchy-Green deformation tensor, and  $U$  is the square root of  $\mathbb{C}$ , of components  $U_{mn}$  in  $(\mathbf{i}_1, \mathbf{i}_2, \mathbf{i}_3)$ , as defined in Appendix A.2.5.

■ **Example 1.11 — Uniform elongation: length variations.** Let us consider the transformation studied in Example 1.1, whose deformation gradient tensor has been calculated in Example 1.7 as:

$$\mathbb{F}(\mathbf{p}, t) = \mathbb{I} + a(t)\mathbf{n} \otimes \mathbf{n}, \forall \mathbf{p} \in \Omega_0$$

The Green-Lagrange strain tensor is then written as:

$$\mathbb{E}(\mathbf{p}, t) = \frac{1}{2} (\mathbb{F}(\mathbf{p}, t)^T \mathbb{F}(\mathbf{p}, t) - \mathbb{I}) = \frac{1}{2} (\mathbb{I} + 2a(t)\mathbf{n} \otimes \mathbf{n} + a(t)^2 (\mathbf{n} \otimes \mathbf{n})(\mathbf{n} \otimes \mathbf{n}) - \mathbb{I})$$

since  $\mathbb{F}^T = (\mathbb{I} + a(t)\mathbf{n} \otimes \mathbf{n})^T = \mathbb{I} + a(t)\mathbf{n} \otimes \mathbf{n} = \mathbb{F}$ . Finally, as  $(\mathbf{n} \otimes \mathbf{n})(\mathbf{n} \otimes \mathbf{n}) = \langle \mathbf{n}, \mathbf{n} \rangle \mathbf{n} \otimes \mathbf{n} = \mathbf{n} \otimes \mathbf{n}$ , we get:

$$\boxed{\mathbb{E}(\mathbf{p}, t) = \left( a(t) + \frac{a(t)^2}{2} \right) \mathbf{n} \otimes \mathbf{n}, \forall \mathbf{p} \in \Omega_0}$$

which shows that the strain tensor is the same whatever the point under study, hence the term “uniform” for this transformation.

In a Cartesian vector basis  $(\mathbf{i}_1, \mathbf{i}_2 = \mathbf{n}, \mathbf{i}_3)$  including the vector  $\mathbf{n}$ , the tensor  $\mathbb{E}$  can be written as:

$$\mathbb{E}(\mathbf{p}, t) = \left( a(t) + \frac{a(t)^2}{2} \right) \begin{pmatrix} 0 & 0 & 0 \\ 0 & 1 & 0 \\ 0 & 0 & 0 \end{pmatrix}_{(\mathbf{i}_1, \mathbf{i}_2 = \mathbf{n}, \mathbf{i}_3)}$$

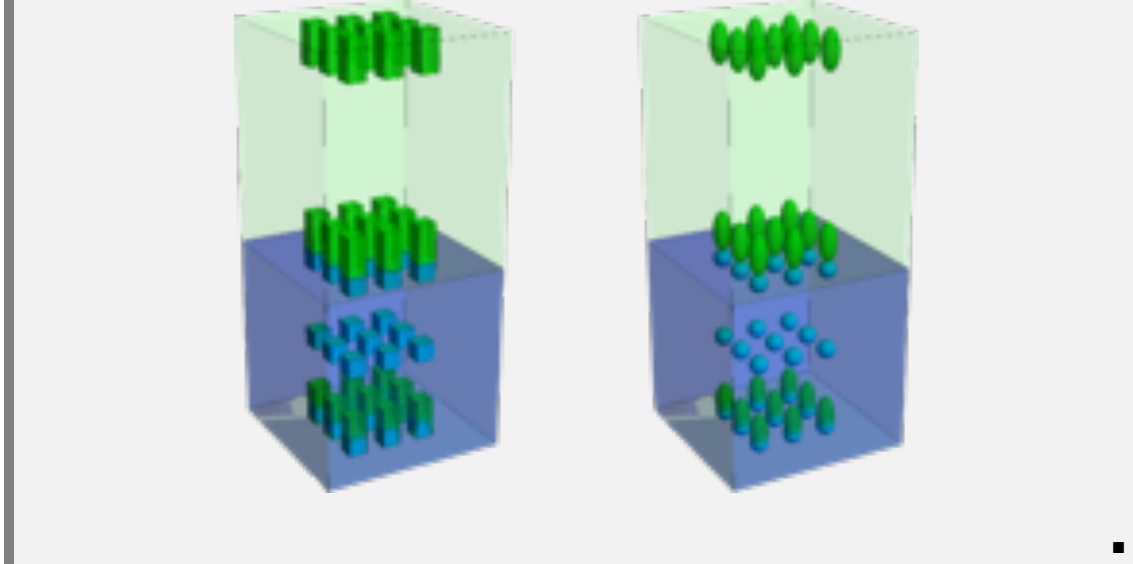
where  $\mathbf{i}_1$  and  $\mathbf{i}_3$  are two unit vectors perpendicular to  $\mathbf{n}$ , and to each other. It is then easy to express the length variations of infinitesimal vectors oriented along the different directions of this vector basis:

- for an infinitesimal vector oriented along  $\mathbf{n} = \mathbf{i}_2$ , and of initial length  $l_{2p}$ , the current length is expressed as  $l_{2x} = (1 + a(t))l_{2p}$ , hence a relative variation of the square of the length equal to:

$$\boxed{\frac{l_{2x}^2 - l_{2p}^2}{l_{2p}^2} = (1 + a(t))^2 - 1 = 2a(t) + a(t)^2 = 2E_{22}}$$

- for an infinitesimal vector oriented along  $\mathbf{i}_1$  or  $\mathbf{i}_3$ , the length remains unchanged, hence a relative variation of the square of the length equal to zero, which is consistent with the fact that  $E_{11} = 0 = E_{33}$ .

These results are directly observed in the figures below.



### Angle variation in the neighbourhood of a material point

We now consider two infinitesimal vectors  $dx_1$  and  $dx_2$  connecting the particles  $x$  and  $y_1$  on the one hand,  $x$  and  $y_2$  on the other hand, knowing that  $y_1$  and  $y_2$  are very close to  $x$ ; these two infinitesimal vectors then evolve over time as:

$$dx_1 = F dp_1, \text{ and } dx_2 = F dp_2$$

where  $dp_1$  and  $dp_2$  are the infinitesimal vectors connecting these same two pairs of particles in the initial configuration, as shown in Figure 1.4.

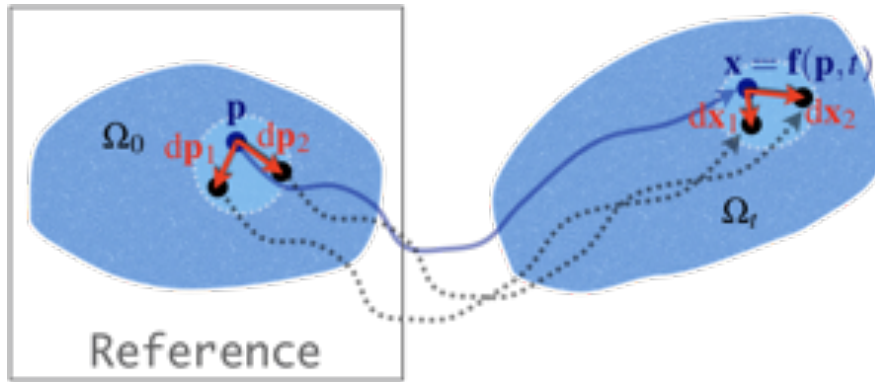


Figure 1.4: Angle variation in the neighbourhood of a material point.

We can then focus on the variation over time of the angle formed by these two infinitesimal vectors, or, in an equivalent way, on the evolution of the scalar product of these two vectors, which is then expressed as:

$$\langle dx_1, dx_2 \rangle = \langle F dp_1, F dp_2 \rangle = \langle F^T F dp_1, dp_2 \rangle$$

By calling  $\alpha_{12x}$  the angle formed by the two vectors  $dx_1$  and  $dx_2$ , and by using the expression of the Green-Lagrange strain tensor, we finally obtain:

$$\|dx_1\| \|dx_2\| \cos \alpha_{12x} = \langle (2E + I) dp_1, dp_2 \rangle$$

If we express, in the initial configuration, the two infinitesimal vectors as  $d\mathbf{p}_1 = l_{1p}\mathbf{i}_1$  and  $d\mathbf{p}_2 = l_{2p}\mathbf{i}_2$ , where  $\mathbf{i}_1$  and  $\mathbf{i}_2$  are unit vectors, and by noting  $l_{1x} = \|d\mathbf{x}_1\| = \|\mathbb{F}d\mathbf{p}_1\|$  and  $l_{2x} = \|d\mathbf{x}_2\| = \|\mathbb{F}d\mathbf{p}_2\|$ , the previous relation can be rewritten as:

$$l_{1x}l_{2x}\cos\alpha_{12x} = l_{1p}l_{2p}\langle(2\mathbb{E} + \mathbb{I})\mathbf{i}_1, \mathbf{i}_2\rangle = l_{1p}l_{2p}(2\langle\mathbb{E}\mathbf{i}_1, \mathbf{i}_2\rangle + \cos\alpha_{12p})$$

where  $\alpha_{12p}$  refers to the angle formed by the two vectors  $d\mathbf{p}_1$  et  $d\mathbf{p}_2$ . Taking as a special case the situation where  $\mathbf{i}_1$  and  $\mathbf{i}_2$  are perpendicular to each other, and noting  $E_{mn}$  the components of  $\mathbb{E}$  in the resulting Cartesian vector basis  $(\mathbf{i}_1, \mathbf{i}_2, \mathbf{i}_3 = \mathbf{i}_1 \wedge \mathbf{i}_2)$ , we finally get:

$$\frac{l_{1x}}{l_{1p}} \frac{l_{2x}}{l_{2p}} \cos\alpha_{12x} = 2E_{21}$$

The off-diagonal terms  $E_{mn}$  ( $m \neq n$ ) of the Green-Lagrange strain tensor are therefore related to the variation in the angle (or “distortion”) between two vectors of the basis allowing to express the tensor: indeed, if  $E_{mn} = 0$ , then the angle between two vectors of respective initial directions  $\mathbf{i}_m$  and  $\mathbf{i}_n$  is still right in the current configuration.

■ **Example 1.12 — Uniform elongation: angle variations.** Let us consider the transformation studied in Example 1.1, for which the Green-Lagrange strain tensor has been calculated in Example 1.11 as:

$$\mathbb{E}(\mathbf{p}, t) = \left(a(t) + \frac{a(t)^2}{2}\right) \mathbf{n} \otimes \mathbf{n}, \forall \mathbf{p} \in \Omega_0$$

or, in a Cartesian vector basis  $(\mathbf{i}_1, \mathbf{i}_2 = \mathbf{n}, \mathbf{i}_3)$ :

$$\mathbb{E}(\mathbf{p}, t) = \left(a(t) + \frac{a(t)^2}{2}\right) \begin{pmatrix} 0 & 0 & 0 \\ 0 & 1 & 0 \\ 0 & 0 & 0 \end{pmatrix}_{(\mathbf{i}_1, \mathbf{i}_2 = \mathbf{n}, \mathbf{i}_3)}$$

All off-diagonal terms of  $\mathbb{E}$  in this basis being equal to zero, the initially right angles between the three vectors of the basis remain right over time: there is no distortion of the basis, as can be seen in the figures of Example 1.11.

However, if we choose two orthogonal vectors that are not collinear with the basis vectors, there may be distortion: indeed, with  $d\mathbf{p}_i = \mathbf{n} + \mathbf{i}_1 = \mathbf{i}_2 + \mathbf{i}_1$  and  $d\mathbf{p}_j = \mathbf{n} - \mathbf{i}_1 = \mathbf{i}_2 - \mathbf{i}_1$  which are perpendicular to each other, we get:

$$\|d\mathbf{x}_i\| \|d\mathbf{x}_j\| \cos\alpha_{ij} = \langle(2\mathbb{E} + \mathbb{I})d\mathbf{p}_i, d\mathbf{p}_j\rangle = 2\langle\mathbb{E}d\mathbf{p}_i, d\mathbf{p}_j\rangle = (2a(t) + a(t)^2)\langle\mathbf{i}_2, \mathbf{i}_2 - \mathbf{i}_1\rangle$$

or, by specifying:

$$\|d\mathbf{x}_i\|^2 = \langle(2\mathbb{E} + \mathbb{I})d\mathbf{p}_i, d\mathbf{p}_i\rangle = \langle(1 + 2a(t) + a(t)^2)\mathbf{i}_2 + \mathbf{i}_1, \mathbf{i}_2 + \mathbf{i}_1\rangle = 2 + 2a(t) + a(t)^2$$

$$\|d\mathbf{x}_j\|^2 = \langle(2\mathbb{E} + \mathbb{I})d\mathbf{p}_j, d\mathbf{p}_j\rangle = \langle(1 + 2a(t) + a(t)^2)\mathbf{i}_2 - \mathbf{i}_1, \mathbf{i}_2 - \mathbf{i}_1\rangle = 2 + 2a(t) + a(t)^2$$

it is established that:

$$\boxed{\cos\alpha_{ij} = \frac{2a(t) + a(t)^2}{2 + 2a(t) + a(t)^2}}$$

meaning that the angle  $\alpha_{ij}$  changes over time. ■

■ **Example 1.13 — Uniform shear strain: angle variations.** Let us consider the transformation studied in Example 1.2, whose deformation gradient tensor has been calculated in Example 1.8 as:

$$\mathbb{F}(\mathbf{p}, t) = \mathbb{I} + b(t)\mathbf{t} \otimes \mathbf{n}, \forall \mathbf{p} \in \Omega_0$$

The Green-Lagrange strain tensor is then expressed as:

$$\mathbb{E}(\mathbf{p}, t) = \frac{1}{2} (\mathbb{F}(\mathbf{p}, t)^T \mathbb{F}(\mathbf{p}, t) - \mathbb{I}) = \frac{1}{2} (\mathbb{I} + b(t)\mathbf{t} \otimes \mathbf{n} + b(t)\mathbf{n} \otimes \mathbf{t} + b(t)^2(\mathbf{n} \otimes \mathbf{t})(\mathbf{t} \otimes \mathbf{n}) - \mathbb{I})$$

since  $\mathbb{F}^T = (\mathbb{I} + b(t)\mathbf{t} \otimes \mathbf{n})^T = \mathbb{I} + b(t)\mathbf{n} \otimes \mathbf{t}$ . In the end we obtain:

$$\mathbb{E}(\mathbf{p}, t) = b(t)\mathbf{t} \otimes_S \mathbf{n} + \frac{b(t)^2}{2}\mathbf{n} \otimes \mathbf{n}, \forall \mathbf{p} \in \Omega_0$$

by noting  $\mathbf{t} \otimes_S \mathbf{n} = \frac{1}{2}(\mathbf{t} \otimes \mathbf{n} + \mathbf{n} \otimes \mathbf{t})$  the symmetrical part of the tensor product  $\mathbf{t} \otimes \mathbf{n}$ . It can then be seen that the strain tensor is the same regardless the point under study, hence the term “uniform” for this transformation.

In a Cartesian vector basis  $(\mathbf{i}_1 = \mathbf{t}, \mathbf{i}_2 = \mathbf{n}, \mathbf{i}_3)$  including vectors  $\mathbf{t}$  and  $\mathbf{n}$ , the tensor  $\mathbb{E}$  can be written as:

$$\mathbb{E}(\mathbf{p}, t) = \frac{b(t)}{2} \begin{pmatrix} 0 & 1 & 0 \\ 1 & b(t) & 0 \\ 0 & 0 & 0 \end{pmatrix}_{(\mathbf{i}_1=\mathbf{t}, \mathbf{i}_2=\mathbf{n}, \mathbf{i}_3)}$$

where  $\mathbf{i}_3 = \mathbf{t} \wedge \mathbf{n}$ . Some off-diagonal terms are non-zero, so there is distortion of the vector basis  $(\mathbf{t}, \mathbf{n}, \mathbf{n}, \mathbf{i}_3)$ . Indeed:

$$\|\mathbb{F}\mathbf{t}\| \|\mathbb{F}\mathbf{n}\| \cos \alpha_{tn} = 2\langle \mathbb{E}\mathbf{t}, \mathbf{n} \rangle = b(t)$$

where  $\alpha_{tn}$  is the angle formed by the two infinitesimal vectors initially oriented along  $\mathbf{t}$  and  $\mathbf{n}$  respectively. By specifying the length variations of these two infinitesimal vectors:

$$\|\mathbb{F}\mathbf{t}\|^2 = \langle (2\mathbb{E} + \mathbb{I})\mathbf{t}, \mathbf{t} \rangle = \langle \mathbf{t}, \mathbf{t} \rangle = 1$$

$$\|\mathbb{F}\mathbf{n}\|^2 = \langle (2\mathbb{E} + \mathbb{I})\mathbf{n}, \mathbf{n} \rangle = (1 + b(t)^2) \langle \mathbf{n}, \mathbf{n} \rangle = 1 + b(t)^2$$

we finally establish that:

$$\cos \alpha_{tn} = \frac{b(t)}{\sqrt{1 + b(t)^2}}$$

Besides, since  $\langle \mathbb{E}\mathbf{t}, \mathbf{i}_3 \rangle = 0 = \langle \mathbb{E}\mathbf{n}, \mathbf{i}_3 \rangle$ , we establish that the directions initially oriented along  $\mathbf{t}$  and  $\mathbf{i}_3$  on the one hand, and along  $\mathbf{n}$  and  $\mathbf{i}_3$  on the other hand, remain perpendicular to each other at all times. ■

### Interpretation

Considering the results of the previous paragraphs, we can, therefore, establish that the Green-Lagrange strain tensor  $\mathbb{E}$  allows for expressing the two ways that a three-dimensional continuous medium can deform:

- a variation in the length of the segments oriented along a given direction;
- a variation in angle (or distortion) between pairs of segments oriented along two given directions.

Since the tensor  $\mathbb{E}$  is symmetrical by definition ( $\mathbb{E}^T = \mathbb{E}$ ), only six of the nine components of this tensor in a given vector basis are independent:

- three diagonal terms, each one corresponding to the variation of the square of the length of the segments initially oriented along the three vectors of the basis used to express the components;
- three off-diagonal terms (e.g. superior), each one corresponding to the variation in the initial right angles between each pair of vectors of the used vector basis.

Of course, in the general case, these six components may depend on the point  $\mathbf{p}$  under study in the initial configuration.

■ **Example 1.14 — Movement of rigid bodies: Green-Lagrange strain tensor.** Let us consider the transformation studied in Example 1.3 as:

$$\mathbf{x} = \mathbf{f}(\mathbf{p}, t) = \mathbf{x}_A(t) + \mathbb{R}(t)(\mathbf{p} - \mathbf{p}_A), \forall \mathbf{p} \in \Omega_0$$

where  $\mathbf{x}_A(t)$  is the placement vector of a given point  $A$  of  $\Omega$ , and  $\mathbb{R}(t)$  is a rotation tensor. The deformation gradient tensor is then expressed directly as:

$$\mathbb{F}(\mathbf{p}, t) = \mathbb{D}_{\mathbf{p}} \mathbf{x}(\mathbf{p}, t) = \mathbb{R}(t), \forall \mathbf{p} \in \Omega_0$$

and the Green-Lagrange strain tensor is then given by:

$$\mathbb{E}(\mathbf{p}, t) = \frac{1}{2} (\mathbb{R}(t)^T \mathbb{R}(t) - \mathbb{I}) = \mathbb{0}, \forall \mathbf{p} \in \Omega_0$$

considering the orthogonality property of  $\mathbb{R}$ .

We therefore rigorously verify that the solid is non-deformable: the tensor  $\mathbb{E}$  being equal to zero at all points, there is no variation in length or angle within the domain. ■

■ **Example 1.15 — Torsion of a cylindrical shaft: interpretation of the components of the Green-Lagrange strain tensor.** Let us consider the transformation studied in Example 1.4, whose deformation gradient tensor has been calculated in Example 1.10 as:

$$\begin{aligned} \mathbb{F} = & \mathbf{i}_r(p_\theta + c(t)p_z/L) \otimes \mathbf{i}_r(p_\theta) + \mathbf{i}_\theta(p_\theta + c(t)p_z/L) \otimes \mathbf{i}_\theta(p_\theta) \\ & + \left( p_r \frac{c(t)}{L} \mathbf{i}_\theta(p_\theta + c(t)p_z/L) + \mathbf{i}_z \right) \otimes \mathbf{i}_z \end{aligned}$$

Since its transpose can be expressed as:

$$\begin{aligned} \mathbb{F}^T = & \mathbf{i}_r(p_\theta) \otimes \mathbf{i}_r(p_\theta + c(t)p_z/L) + \mathbf{i}_\theta(p_\theta) \otimes \mathbf{i}_\theta(p_\theta + c(t)p_z/L) \\ & + \mathbf{i}_z \otimes \left( p_r \frac{c(t)}{L} \mathbf{i}_\theta(p_\theta + c(t)p_z/L) + \mathbf{i}_z \right) \end{aligned}$$

the right Cauchy-Green deformation tensor  $\mathbb{C} = \mathbb{F}^T \mathbb{F}$  is such that:

$$\begin{aligned} \mathbb{C} = & \langle \mathbf{i}_r(p_\theta + c(t)p_z/L), \mathbf{i}_r(p_\theta + c(t)p_z/L) \rangle \mathbf{i}_r(p_\theta) \otimes \mathbf{i}_r(p_\theta) \\ & + \langle \mathbf{i}_\theta(p_\theta + c(t)p_z/L), \mathbf{i}_\theta(p_\theta + c(t)p_z/L) \rangle \mathbf{i}_\theta(p_\theta) \otimes \mathbf{i}_\theta(p_\theta) \\ & + \left\langle p_r \frac{c(t)}{L} \mathbf{i}_\theta(p_\theta + c(t)p_z/L) + \mathbf{i}_z, p_r \frac{c(t)}{L} \mathbf{i}_\theta(p_\theta + c(t)p_z/L) + \mathbf{i}_z \right\rangle \mathbf{i}_z \otimes \mathbf{i}_z \\ & + \langle \mathbf{i}_r(p_\theta + c(t)p_z/L), \mathbf{i}_\theta(p_\theta + c(t)p_z/L) \rangle (\mathbf{i}_r(p_\theta) \otimes \mathbf{i}_\theta(p_\theta) + \mathbf{i}_\theta(p_\theta) \otimes \mathbf{i}_r(p_\theta)) \\ & + \left\langle \mathbf{i}_r(p_\theta + c(t)p_z/L), p_r \frac{c(t)}{L} \mathbf{i}_\theta(p_\theta + c(t)p_z/L) + \mathbf{i}_z \right\rangle (\mathbf{i}_r(p_\theta) \otimes \mathbf{i}_z + \mathbf{i}_z \otimes \mathbf{i}_r(p_\theta)) \\ & + \left\langle \mathbf{i}_\theta(p_\theta + c(t)p_z/L), p_r \frac{c(t)}{L} \mathbf{i}_\theta(p_\theta + c(t)p_z/L) + \mathbf{i}_z \right\rangle (\mathbf{i}_\theta(p_\theta) \otimes \mathbf{i}_z + \mathbf{i}_z \otimes \mathbf{i}_\theta(p_\theta)) \\ = & \mathbf{i}_r(p_\theta) \otimes \mathbf{i}_r(p_\theta) + \mathbf{i}_\theta(p_\theta) \otimes \mathbf{i}_\theta(p_\theta) + \left( 1 + \left( p_r \frac{c(t)}{L} \right)^2 \right) \mathbf{i}_z \otimes \mathbf{i}_z \\ & + p_r \frac{c(t)}{L} (\mathbf{i}_\theta(p_\theta) \otimes \mathbf{i}_z + \mathbf{i}_z \otimes \mathbf{i}_\theta(p_\theta)) \end{aligned}$$

which means that the Green-Lagrange strain tensor is written simply as:

$$\boxed{\mathbb{E}(\mathbf{p}, t) = p_r \frac{c(t)}{L} \mathbf{i}_\theta(p_\theta) \otimes_S \mathbf{i}_z + \frac{p_r^2 c(t)^2}{2L^2} \mathbf{i}_z \otimes \mathbf{i}_z, \forall \mathbf{p} \in \Omega_0}$$

by noting  $\mathbf{a} \otimes_S \mathbf{b} = (\mathbf{a} \otimes \mathbf{b} + \mathbf{b} \otimes \mathbf{a})/2$  the symmetrical part of the tensor product  $\mathbf{a} \otimes \mathbf{b}$ , or, in the vector basis  $(\mathbf{i}_r(p_\theta), \mathbf{i}_\theta(p_\theta), \mathbf{i}_z)$ :

$$\mathbb{E}(\mathbf{p}, t) = \frac{p_r c(t)}{2L} \begin{pmatrix} 0 & 0 & 0 \\ 0 & 0 & 1 \\ 0 & 1 & p_r \frac{c(t)}{L} \end{pmatrix}_{(\mathbf{i}_r(p_\theta), \mathbf{i}_\theta(p_\theta), \mathbf{i}_z)}$$

This corresponds to the case of the shear strain studied in Example 1.13, with the difference that, here, the expression of the tensor  $\mathbb{E}$  depends on the point under study.

We can then express the angle variations as in Example 1.13, with  $b(t) = p_r c(t)/L$ , to obtain that:

$$\boxed{\cos \alpha_{\theta z} = \frac{p_r c(t)}{L \sqrt{1 + p_r^2 c(t)^2 / L^2}}}$$

where  $\alpha_{\theta_z}$  is the angle formed in the current configuration by the initial vectors along  $\mathbf{i}_\theta$  and  $\mathbf{i}_z$ .

Besides, we obtain the length variations for infinitesimal vectors oriented along the different directions of the cylindrical vector basis as:

- for an infinitesimal vector initially radial or orthoradial, there is no variation in length because each cross-section undergoes a rigid body rotation, which is consistent with  $E_{rr} = 0 = E_{\theta\theta}$ ;
- for an infinitesimal vector parallel to the axis of the shaft, and of initial length  $l_{zp}$ , the Pythagorean theorem allows us to write that its current length verifies  $l_{zx}^2 = l_{zp}^2 + (c(t)p_r l_{zp}/L)^2$ , which corresponds to a variation:

$$\frac{l_{zx}^2 - l_{zp}^2}{l_{zp}^2} = \left( \frac{c(t)}{L} p_r \right)^2 = 2E_{zz}$$

We also verify in this right triangle that  $\cos \alpha_{\theta_z} = \frac{p_r c(t)}{L \sqrt{1 + p_r^2 c(t)^2 / L^2}}$ . ■

The previous results allow us to conclude that if we know, at any point  $\mathbf{p}$ :

- the elongations along three independent directions in the initial configuration;
- the angle variations of three independent couples of orthogonal directions in the initial configuration;

then the elongation along any direction and the angle variations of any couple of directions can be determined at this point  $\mathbf{p}$ .

**Summary 1.2 — Green-Lagrange strain tensor.** The deformation of a continuous medium at any point in the initial configuration is given by the Green-Lagrange strain tensor:

$$\mathbb{E}(\mathbf{p}, t) = \frac{1}{2} \left( \mathbb{F}(\mathbf{p}, t)^T \mathbb{F}(\mathbf{p}, t) - \mathbb{I} \right), \quad \forall \mathbf{p} \in \Omega_0$$

which is a symmetrical tensor.

The variation of the square of the length in the current configuration of an infinitesimal vector initially equal to  $d\mathbf{p} = \|d\mathbf{p}\| \mathbf{e}_p$  (with  $\mathbf{e}_p$  a unit vector) is then expressed as:

$$\frac{\|\mathbf{dx}\|^2 - \|d\mathbf{p}\|^2}{\|d\mathbf{p}\|^2} = 2\langle \mathbb{E}\mathbf{e}_p, \mathbf{e}_p \rangle$$

where  $\mathbf{dx} = \mathbb{F} d\mathbf{p}$  is the vector corresponding to  $d\mathbf{p}$  in the current configuration.

The angle  $\alpha_{12x}$  in the current configuration between two infinitesimal vectors initially equal to  $d\mathbf{p}_1 = \|d\mathbf{p}_1\| \mathbf{e}_{p1}$  and  $d\mathbf{p}_2 = \|d\mathbf{p}_2\| \mathbf{e}_{p2}$  (with  $\mathbf{e}_{p1}$  and  $\mathbf{e}_{p2}$  two unit vectors) is then expressed as:

$$\cos \alpha_{12x} = \frac{\langle \mathbb{F}\mathbf{e}_{p1}, \mathbb{F}\mathbf{e}_{p2} \rangle}{\|\mathbb{F}\mathbf{e}_{p1}\| \|\mathbb{F}\mathbf{e}_{p2}\|} = \frac{\cos \alpha_{12p} + 2\langle \mathbb{E}\mathbf{e}_{p1}, \mathbf{e}_{p2} \rangle}{\sqrt{\langle (2\mathbb{E} + \mathbb{I})\mathbf{e}_{p1}, \mathbf{e}_{p1} \rangle \langle (2\mathbb{E} + \mathbb{I})\mathbf{e}_{p2}, \mathbf{e}_{p2} \rangle}}$$

knowing that the initial angle  $\alpha_{12p}$  verifies  $\cos \alpha_{12p} = \langle \mathbf{e}_{p1}, \mathbf{e}_{p2} \rangle$ .



As before, it is also possible to use the displacement field  $\mathbf{u}(\mathbf{p}, t)$  of the studied domain. It had been established that:

$$\mathbb{F} = \mathbb{I} + \mathbb{D}_{\mathbf{p}} \mathbf{u}$$

This then allows the Green-Lagrange strain tensor to be easily expressed as:

$$\mathbb{E} = \frac{1}{2} (\mathbb{D}_{\mathbf{p}} \mathbf{u} + (\mathbb{D}_{\mathbf{p}} \mathbf{u})^T + (\mathbb{D}_{\mathbf{p}} \mathbf{u})^T \mathbb{D}_{\mathbf{p}} \mathbf{u})$$

It can then be seen that this tensor is non-linearly dependent on the displacement field.

Given the definition of the tensor  $\mathbb{E}$ , the different components of the tensor are dimensionless

numbers. The typical orders of magnitude that can be encountered before failure for several conventional materials are presented in Table 1.1. In practice, we can see that, except for certain classes of materials such as elastomers (rubber being a member of this family), deformations remain very small (often in the order of a few per cent): it is, therefore, possible to focus on an approximate expression of these deformations, developed in the following part.

Materials	Orders of magnitude
Steel (reversible deformations)	$10^{-4} \text{ à } 10^{-2}$ (0.01 % à 1 %)
Steel (irreversible deformations)	$10^{-2} \text{ à } 10^{-1}$ (1 % à 10 %)
Concrete	$10^{-3}$ (0.1 %)
Soil	$10^{-2}$ (1 %)
Rubber	superior to 1 (100 %)

Table 1.1: Typical values of admissible deformations for different materials.

### 1.3 Infinitesimal strain tensor

Most deformable solids used in industry or construction to support or transmit loads generally require small levels of deformation to avoid failure. Such an observation then allows for introducing a linearized description framework that simplifies the expressions obtained in the previous paragraphs, and that we will use throughout the rest of this textbook.

#### 1.3.1 Infinitesimal deformation hypothesis

The so-called framework of the “infinitesimal deformation hypothesis” is in fact based on two distinct but complementary assumptions:

1. an infinitesimal transformation hypothesis, ensuring that the two configurations, initial and current, can be considered as similar:

$$\mathbf{x} = \mathbf{f}(\mathbf{p}, t) = \mathbf{p} + \mathbf{u}(\mathbf{p}, t) \approx \mathbf{p}, \forall \mathbf{p} \in \Omega_0$$

hypothesis equivalent to assuming that the displacement at any point is very small compared to the characteristic dimension  $\mathcal{L}$  of the domain under study:

$$\|\mathbf{u}(\mathbf{p}, t)\| \ll \mathcal{L}, \forall \mathbf{p} \in \Omega_0$$

2. an infinitesimal strain hypothesis, equivalent to assuming that the norm of the gradient tensor of the displacement field at any point is very small:

$$\|\mathbb{D}_{\mathbf{p}} \mathbf{u}(\mathbf{p}, t)\| \ll 1, \forall \mathbf{p} \in \Omega_0$$

where the tensor norm  $\|\mathbb{D}_{\mathbf{p}} \mathbf{u}\|^2 = \text{tr}((\mathbb{D}_{\mathbf{p}} \mathbf{u})^T \mathbb{D}_{\mathbf{p}} \mathbf{u})$  is used as explained in Appendix A.2.2; this allows us to linearize the expression of the Green-Lagrange strain tensor as a function of the displacement field:

$$\mathbb{E}(\mathbf{p}, t) = \frac{1}{2} (\mathbb{D}_{\mathbf{p}} \mathbf{u} + (\mathbb{D}_{\mathbf{p}} \mathbf{u})^T + (\mathbb{D}_{\mathbf{p}} \mathbf{u})^T \mathbb{D}_{\mathbf{p}} \mathbf{u}) \approx \frac{1}{2} (\mathbb{D}_{\mathbf{p}} \mathbf{u} + (\mathbb{D}_{\mathbf{p}} \mathbf{u})^T)$$

**R** The previous hypothesis also allows us to consider as similar the gradient expressions in the initial and current configurations; indeed, for any vector field  $\mathbf{w}_p(\mathbf{p}, t)$  in the initial configuration, which is transformed as  $\mathbf{w}_x(\mathbf{x}, t) = \mathbf{w}_x(\mathbf{f}(\mathbf{p}, t), t) = \mathbf{w}_p(\mathbf{p}, t)$  in the current configuration, the chain rule allows for establishing that:

$$\mathbb{D}_{\mathbf{p}} \mathbf{w}_p = (\mathbb{D}_{\mathbf{x}} \mathbf{w}_x) \mathbb{F} = \mathbb{D}_{\mathbf{x}} \mathbf{w}_x (\mathbb{I} + \mathbb{D}_{\mathbf{p}} \mathbf{u}) \approx \mathbb{D}_{\mathbf{x}} \mathbf{w}_x$$

assuming that  $\|\mathbb{D}_{\mathbf{p}} \mathbf{u}(\mathbf{p}, t)\| \ll 1$ .

Given the infinitesimal deformation hypothesis, in what follows, we arbitrarily choose to keep the notation  $\mathbf{x}$  to designate the placement vector of a particle, regardless of the configuration that we consider.

### 1.3.2 Definition and properties

In what follows, a new description of the deformations of the studied medium is introduced in the framework of the infinitesimal deformation hypothesis.

**Infinitesimal strain tensor.** The symmetrical part of the displacement gradient tensor is called the infinitesimal strain tensor:

$$\boldsymbol{\varepsilon}(\mathbf{x}, t) = \frac{1}{2} \left( \mathbb{D}_{\mathbf{x}} \mathbf{u}(\mathbf{x}, t) + (\mathbb{D}_{\mathbf{x}} \mathbf{u}(\mathbf{x}, t))^T \right), \quad \forall \mathbf{x} \in \Omega, \quad \forall t$$

in the framework of the infinitesimal deformation hypothesis, where the initial and current configurations have been merged into a single one denoted  $\Omega$ .

This tensor corresponds to the linearization of the Green-Lagrange strain tensor when we assume that the displacement gradient tensor is “small enough”; indeed, as mentioned above, this is equivalent, in practice, to writing, with  $\mathbf{x} \approx \mathbf{p}$ :

$$\mathbb{E}(\mathbf{p}, t) = \frac{1}{2} (\mathbb{D}_{\mathbf{p}} \mathbf{u} + (\mathbb{D}_{\mathbf{p}} \mathbf{u})^T + (\mathbb{D}_{\mathbf{p}} \mathbf{u})^T \mathbb{D}_{\mathbf{p}} \mathbf{u}) \approx \frac{1}{2} (\mathbb{D}_{\mathbf{x}} \mathbf{u} + (\mathbb{D}_{\mathbf{x}} \mathbf{u})^T)$$

■ **Example 1.16 — Torsion of a cylindrical shaft: infinitesimal strain tensor.** Let us consider the transformation studied in Example 1.4, for which the displacement field is written as:

$$\mathbf{u}(\mathbf{p}, t) = p_r (\mathbf{i}_r(p_\theta + c(t)p_z/L) - \mathbf{i}_r(p_\theta)), \quad \forall \mathbf{p} \in \Omega_0$$

As defined above, the infinitesimal deformation hypothesis is equivalent to assume:

1. that  $\|\mathbf{u}(\mathbf{p}, t)\| \ll \min(R, L)$ ,  $\forall \mathbf{p} \in \Omega_0$ , which is equivalent to consider  $\mathbf{u}(\mathbf{x}, t) = rzc(t)/L \mathbf{i}_\theta(\theta)$ , when you assume  $|c(t)| \ll 1$ ,  $\forall t$ , and in the usual case where  $R < L$ ;
2. that  $\|\mathbb{D}_{\mathbf{p}} \mathbf{u}(\mathbf{p}, t)\| = \|\mathbb{F}(\mathbf{p}, t) - \mathbb{I}\| \ll 1$ , which is the same here as assuming that  $R|c(t)| \ll L$ ,  $\forall t$ .

These two hypotheses are not necessarily equivalent: indeed, in the case of a very slender cylinder ( $R \ll L$ ), it is possible to have  $R|c(t)| \ll L$  without  $|c(t)|$  being small.

In this context, the infinitesimal strain tensor can be expressed as the symmetrical part of the displacement gradient tensor (expressed in the current coordinate system):

$$\boldsymbol{\varepsilon} = \frac{1}{2} (\mathbb{D}_{\mathbf{x}} \mathbf{u} + (\mathbb{D}_{\mathbf{x}} \mathbf{u})^T)$$

where the displacement gradient tensor is equal to:

$$\begin{aligned} \mathbb{D}_{\mathbf{x}} \mathbf{u}(\mathbf{x}, t) &= \frac{\partial \mathbf{u}}{\partial r}(\mathbf{x}, t) \otimes \mathbf{i}_r(\theta) + \frac{\partial \mathbf{u}}{\partial \theta}(\mathbf{x}, t) \otimes \frac{\mathbf{i}_\theta(\theta)}{r} + \frac{\partial \mathbf{u}}{\partial z}(\mathbf{x}, t) \otimes \mathbf{i}_z \\ &= \frac{zc(t)}{L} \mathbf{i}_\theta(\theta) \otimes \mathbf{i}_r(\theta) - \frac{zc(t)}{L} \mathbf{i}_r(\theta) \otimes \mathbf{i}_\theta(\theta) + \frac{rc(t)}{L} \mathbf{i}_\theta(\theta) \otimes \mathbf{i}_z \end{aligned}$$

hence, finally:

$$\boxed{\boldsymbol{\varepsilon}(\mathbf{x}, t) = \frac{rc(t)}{L} \mathbf{i}_\theta(\theta) \otimes_S \mathbf{i}_z}$$

This result can also be found by linearizing the Green-Lagrange strain tensor (determined in Example 1.15),

when we assume that  $R|c(t)| \ll L, \forall t$ :

$$\mathbb{E}(\mathbf{p}, t) = p_r \frac{c(t)}{L} \left( \mathbf{i}_\theta(p_\theta) \otimes_S \mathbf{i}_z + \frac{p_r c(t)}{2L} \mathbf{i}_z \otimes \mathbf{i}_z \right) \approx p_r \frac{c(t)}{L} \mathbf{i}_\theta(p_\theta) \otimes_S \mathbf{i}_z$$

after considering the two configurations as one when it is assumed that  $|c(t)| \ll 1, \forall t$ . ■



It is, of course, essential to adopt the infinitesimal deformation hypothesis in order to correctly use the infinitesimal strain tensor to describe the deformation of the medium.

Thus, if we take the case of the movement of a rigid body, we had determined in Example 1.14 that the Green-Lagrange strain tensor  $\mathbb{E}$  was equal to zero. Therefore, we can write that the infinitesimal strain tensor is:

$$\boldsymbol{\varepsilon} = \frac{1}{2} (\mathbb{D}_{\mathbf{x}} \mathbf{u} + (\mathbb{D}_{\mathbf{x}} \mathbf{u})^T) = \mathbb{E} - \frac{1}{2} (\mathbb{D}_{\mathbf{x}} \mathbf{u})^T \mathbb{D}_{\mathbf{x}} \mathbf{u} = -\frac{1}{2} (\mathbb{D}_{\mathbf{x}} \mathbf{u})^T \mathbb{D}_{\mathbf{x}} \mathbf{u}$$

with  $\mathbb{D}_{\mathbf{x}} \mathbf{u} = \mathbb{R} - \mathbb{I} = \mathbb{R} - \mathbb{I}$  in this case (see Example 1.14), where  $\mathbb{R}$  is a rotation tensor, which verifies the orthogonality property:  $\mathbb{R}^T \mathbb{R} = \mathbb{I}$  (as detailed in Appendix A.2.6). We then find that:

$$\boldsymbol{\varepsilon} = -\frac{1}{2} (\mathbb{R} - \mathbb{I})^T (\mathbb{R} - \mathbb{I}) = \frac{1}{2} (\mathbb{R} + \mathbb{R}^T - 2\mathbb{I})$$

which is not equal to zero in the case of an arbitrary rotation: this is logical, since, in the general case, it is not possible to consider the initial and current configurations as one.

The infinitesimal strain tensor is equal to zero only if  $\mathbb{R} + \mathbb{R}^T = 2\mathbb{I}$ , which corresponds to the case when the rotation tensor can be written as:

$$\mathbb{R} = \mathbb{I} + \mathbf{r}, \text{ with } \mathbf{r}^T = -\mathbf{r}$$

which in fact corresponds, as detailed in Appendix A.2.6, to an infinitesimal rotation of angle  $\varphi = \|\mathbf{r}\|$  around the direction  $\mathbf{e} = \mathbf{r}/\|\mathbf{r}\|$ , where  $\mathbf{r}$  is the vector associated with the antisymmetric tensor  $\mathbf{r}$  (see Appendix A.2.1). This result confirms that the infinitesimal strain tensor is able to represent the non-deformability of the solid, provided that one is actually within the framework of the infinitesimal deformation hypothesis.

### Tensor expressions

The tensor expression of the infinitesimal strain tensor is derived directly from the one obtained for the displacement gradient tensor, which, formally, is very similar to that set for the deformation gradient tensor.

In the case of a Cartesian vector basis  $(\mathbf{i}_1, \mathbf{i}_2, \mathbf{i}_3)$ , we can write this displacement gradient tensor, at any point  $\mathbf{x} = x_1 \mathbf{i}_1 + x_2 \mathbf{i}_2 + x_3 \mathbf{i}_3$ , as:

$$\mathbb{D}_{\mathbf{x}} \mathbf{u} = \sum_{n=1}^3 \frac{\partial \mathbf{u}}{\partial x_n} \otimes \mathbf{i}_n$$

hence, for the infinitesimal strain tensor:

$$\boldsymbol{\varepsilon} = \sum_{n=1}^3 \frac{\partial \mathbf{u}}{\partial x_n} \otimes_S \mathbf{i}_n = \sum_{n=1}^3 \frac{1}{2} \left( \frac{\partial \mathbf{u}}{\partial x_n} \otimes \mathbf{i}_n + \mathbf{i}_n \otimes \frac{\partial \mathbf{u}}{\partial x_n} \right)$$

or, in matrix form in the same vector basis:

$$\boldsymbol{\varepsilon}(\mathbf{x}, t) = \begin{pmatrix} \frac{\partial u_1}{\partial x_1} & \frac{1}{2} \left( \frac{\partial u_1}{\partial x_2} + \frac{\partial u_2}{\partial x_1} \right) & \frac{1}{2} \left( \frac{\partial u_1}{\partial x_3} + \frac{\partial u_3}{\partial x_1} \right) \\ \frac{1}{2} \left( \frac{\partial u_1}{\partial x_2} + \frac{\partial u_2}{\partial x_1} \right) & \frac{\partial u_2}{\partial x_2} & \frac{1}{2} \left( \frac{\partial u_2}{\partial x_3} + \frac{\partial u_3}{\partial x_2} \right) \\ \frac{1}{2} \left( \frac{\partial u_1}{\partial x_3} + \frac{\partial u_3}{\partial x_1} \right) & \frac{1}{2} \left( \frac{\partial u_2}{\partial x_3} + \frac{\partial u_3}{\partial x_2} \right) & \frac{\partial u_3}{\partial x_3} \end{pmatrix}_{(\mathbf{i}_1, \mathbf{i}_2, \mathbf{i}_3)}$$

where  $\mathbf{u} = u_1 \mathbf{i}_1 + u_2 \mathbf{i}_2 + u_3 \mathbf{i}_3$ .

In addition, it is possible to obtain a similar tensor expression for another coordinate system; in the case of cylindrical coordinates  $(r, \theta, z)$  associated with the vector basis  $(\mathbf{i}_r(\theta), \mathbf{i}_\theta(\theta), \mathbf{i}_z)$ , we obtain, as in the case of the deformation gradient tensor:

$$\mathbb{D}_{\mathbf{x}} \mathbf{u} = \frac{\partial \mathbf{u}}{\partial r} \otimes \mathbf{i}_r + \frac{\partial \mathbf{u}}{\partial \theta} \otimes \frac{\mathbf{i}_\theta}{r} + \frac{\partial \mathbf{u}}{\partial z} \otimes \mathbf{i}_z$$

which implies the following expression for the infinitesimal strain tensor:

$$\boldsymbol{\epsilon} = \frac{\partial \mathbf{u}}{\partial r} \otimes_S \mathbf{i}_r + \frac{\partial \mathbf{u}}{\partial \theta} \otimes_S \frac{\mathbf{i}_\theta}{r} + \frac{\partial \mathbf{u}}{\partial z} \otimes_S \mathbf{i}_z$$

Calculating the tensor using this expression must take into account the fact that two of the three basis vectors depend on the angle  $\theta$ , and that the derivatives with respect to the latter must be included in the term:

$$\frac{\partial \mathbf{u}}{\partial \theta} = \frac{\partial u_r}{\partial \theta} \mathbf{i}_r + u_r \frac{\partial \mathbf{i}_r}{\partial \theta} + \frac{\partial u_\theta}{\partial \theta} \mathbf{i}_\theta + u_\theta \frac{\partial \mathbf{i}_\theta}{\partial \theta} + \frac{\partial u_z}{\partial \theta} \mathbf{i}_z$$

with  $\mathbf{u} = u_r \mathbf{i}_r + u_\theta \mathbf{i}_\theta + u_z \mathbf{i}_z$ . Since:

$$\frac{\partial \mathbf{i}_r}{\partial \theta}(\theta) = \mathbf{i}_\theta(\theta), \text{ and } \frac{\partial \mathbf{i}_\theta}{\partial \theta}(\theta) = -\mathbf{i}_r(\theta)$$

we finally obtain the following matrix expression:

$$\boldsymbol{\epsilon}(\mathbf{x}, t) = \begin{pmatrix} \frac{\partial u_r}{\partial r} & \frac{1}{2} \left( \frac{1}{r} \frac{\partial u_r}{\partial \theta} + \frac{\partial u_\theta}{\partial r} - \frac{u_\theta}{r} \right) & \frac{1}{2} \left( \frac{\partial u_r}{\partial z} + \frac{\partial u_z}{\partial r} \right) \\ \frac{1}{2} \left( \frac{1}{r} \frac{\partial u_r}{\partial \theta} + \frac{\partial u_\theta}{\partial r} - \frac{u_\theta}{r} \right) & \frac{1}{r} \frac{\partial u_\theta}{\partial \theta} + \frac{u_r}{r} & \frac{1}{2} \left( \frac{\partial u_\theta}{\partial z} + \frac{1}{r} \frac{\partial u_z}{\partial \theta} \right) \\ \frac{1}{2} \left( \frac{\partial u_r}{\partial z} + \frac{\partial u_z}{\partial r} \right) & \frac{1}{2} \left( \frac{\partial u_\theta}{\partial z} + \frac{1}{r} \frac{\partial u_z}{\partial \theta} \right) & \frac{\partial u_z}{\partial z} \end{pmatrix}_{(\mathbf{i}_r, \mathbf{i}_\theta, \mathbf{i}_z)}$$

### Interpretation

As with the Green-Lagrange strain tensor, the infinitesimal strain tensor is symmetrical, and therefore only six of the nine components of the latter are independent in a given vector basis.

Concerning the diagonal terms, we can see that, starting from the interpretation defined above for the Green-Lagrange strain tensor, we can establish that for an infinitesimal vector  $l_0 \mathbf{e}$ , with  $l_0 \ll 1$  and  $\mathbf{e}$  a unit vector, and whose length varies by  $\Delta l$ :

$$2\langle \mathbb{E}\mathbf{e}, \mathbf{e} \rangle = \frac{l^2 - l_0^2}{l_0^2} = \frac{(l_0 + \Delta l)^2 - l_0^2}{l_0^2} \approx 2 \frac{\Delta l}{l_0} = 2\langle \boldsymbol{\epsilon}\mathbf{e}, \mathbf{e} \rangle$$

up to order one in  $\Delta l$ , assuming, in the context of the infinitesimal deformation hypothesis, that  $\Delta l \ll l_0$ .

Similarly, we can write for the off-diagonal terms, with infinitesimal vectors  $l_{10} \mathbf{e}_1$  and  $l_{20} \mathbf{e}_2$  (where  $l_{10} \ll 1$ ,  $l_{20} \ll 1$ , and  $\mathbf{e}_1, \mathbf{e}_2$  unit vectors and perpendicular to each other) that:

$$2\langle \mathbb{E}\mathbf{e}_2, \mathbf{e}_1 \rangle = \frac{l_1 l_2}{l_{10} l_{20}} \cos \alpha_{12} = \frac{(l_{10} + \Delta l_1)(l_{20} + \Delta l_2)}{l_{10} l_{20}} \cos \left( \frac{\pi}{2} - \Delta \alpha_{12} \right) \approx \Delta \alpha_{12}$$

up to order zero in  $\Delta l_1 \ll l_{10}$  and  $\Delta l_2 \ll l_{20}$ , and up to order one in  $\Delta \alpha_{12}$ , which represents distortion, i.e. the variation in angle with respect to the right initial angle, using the infinitesimal deformation hypothesis ( $\Delta \alpha_{12} \ll 1$ ).

■ **Example 1.17 — Uniform elongation: infinitesimal strain tensor.** We consider the transformation described in Example 1.1, for which we can express the displacement as:

$$\mathbf{u}(\mathbf{p}, t) = a(t) \langle \mathbf{p}, \mathbf{n} \rangle \mathbf{n} = a(t) (\mathbf{n} \otimes \mathbf{n}) \mathbf{p}, \forall \mathbf{p} \in \Omega_0$$

In the case where  $|a(t)| \ll 1, \forall t$ , we can assume that  $\mathbf{p} \approx \mathbf{x}$  and place ourselves in the framework of the infinitesimal deformation hypothesis, thus calculating the infinitesimal strain tensor as the symmetrical part of the displacement gradient tensor. This latter is expressed as:

$$\mathbb{D}_{\mathbf{x}} \mathbf{u}(\mathbf{x}, t) = a(t) \mathbf{n} \otimes \mathbf{n}, \forall \mathbf{x} \in \Omega$$

which indeed verifies that  $\|\mathbb{D}_{\mathbf{x}} \mathbf{u}(\mathbf{x}, t)\| \ll 1, \forall \mathbf{x} \in \Omega$ . Since this gradient tensor is symmetrical, we finally get:

$$\boldsymbol{\varepsilon}(\mathbf{x}, t) = a(t) \mathbf{n} \otimes \mathbf{n}, \forall \mathbf{x} \in \Omega$$

which corresponds exactly to the approximate expression, up to order one in  $a(t)$ , of the Green-Lagrange strain tensor obtained in Example 1.11:

$$\mathbb{E} = \left( a(t) + \frac{a(t)^2}{2} \right) \mathbf{n} \otimes \mathbf{n} \approx a(t) \mathbf{n} \otimes \mathbf{n}$$

In a Cartesian vector basis ( $\mathbf{i}_1, \mathbf{i}_2 = \mathbf{n}, \mathbf{i}_3$ ) including the vector  $\mathbf{n}$ , the infinitesimal strain tensor can be written as:

$$\boldsymbol{\varepsilon}(\mathbf{x}, t) = \begin{pmatrix} 0 & 0 & 0 \\ 0 & a(t) & 0 \\ 0 & 0 & 0 \end{pmatrix}_{(\mathbf{i}_1, \mathbf{i}_2 = \mathbf{n}, \mathbf{i}_3)}$$

where  $\mathbf{i}_1$  et  $\mathbf{i}_3$  are two unit vectors perpendicular to  $\mathbf{n}$ , and to each other. It is then easy to express the length variations of infinitesimal vectors oriented along the different directions of this vector basis:

- for an infinitesimal vector oriented along  $\mathbf{n} = \mathbf{i}_2$  and of initial length  $l_0$ , the current length is expressed as  $l = (1 + a(t))l_0$ , meaning a variation in length  $\Delta l$  verifying:

$$\frac{\Delta l}{l_0} = a(t) = \varepsilon_{22}(t)$$

- for an infinitesimal vector oriented along  $\mathbf{i}_1$  or  $\mathbf{i}_3$ , the current length remains unchanged, meaning no change in length, which is consistent with the fact that  $\varepsilon_{11} = 0 = \varepsilon_{33}$ .

■

■ **Example 1.18 — Uniform shear strain: infinitesimal strain tensor.** We consider the transformation described in Example 1.2, for which we can express the displacement as:

$$\mathbf{u}(\mathbf{p}, t) = b(t) \langle \mathbf{p}, \mathbf{n} \rangle \mathbf{t} = b(t) (\mathbf{t} \otimes \mathbf{n}) \mathbf{p}, \forall \mathbf{p} \in \Omega_0$$

In the case where  $|b(t)| \ll 1, \forall t$ , we can assume that  $\mathbf{p} \approx \mathbf{x}$  and place ourselves in the framework of the infinitesimal deformation hypothesis. The displacement gradient tensor is then written as:

$$\mathbb{D}_{\mathbf{x}} \mathbf{u}(\mathbf{x}, t) = b(t) \mathbf{t} \otimes \mathbf{n}, \forall \mathbf{x} \in \Omega$$

and we finally obtain the infinitesimal strain tensor as the symmetrical part of this displacement gradient tensor:

$$\boldsymbol{\varepsilon}(\mathbf{x}, t) = b(t) \mathbf{t} \otimes_S \mathbf{n}, \forall \mathbf{x} \in \Omega$$

which corresponds exactly to the approximate expression, up to order one in  $b(t)$ , of the Green-Lagrange strain tensor obtained in Example 1.13:

$$\mathbb{E} = b(t) \mathbf{t} \otimes_S \mathbf{n} + \frac{b(t)^2}{2} \mathbf{n} \otimes \mathbf{n} \approx b(t) \mathbf{t} \otimes_S \mathbf{n}$$

In a Cartesian vector basis ( $\mathbf{i}_1 = \mathbf{t}, \mathbf{i}_2 = \mathbf{n}, \mathbf{i}_3$ ) including the vectors  $\mathbf{t}$  and  $\mathbf{n}$ , the infinitesimal strain tensor can be

written as:

$$\boldsymbol{\varepsilon}(\mathbf{x}, t) = \frac{b(t)}{2} \begin{pmatrix} 0 & 1 & 0 \\ 1 & 0 & 0 \\ 0 & 0 & 0 \end{pmatrix}_{(\mathbf{i}_3 = \mathbf{t}, \mathbf{i}_2 = \mathbf{n}, \mathbf{i}_3)}$$

where  $\mathbf{i}_3 = \mathbf{t} \wedge \mathbf{n}$ . All diagonal terms are equal to zero, so it can be deduced that there is no variation in length (adopting the infinitesimal deformation hypothesis).

Besides, some of the off-diagonal terms are non-zero, so there is distortion of the vector basis  $(\mathbf{t}, \mathbf{n}, \mathbf{i}_3)$ . Indeed:

$$b(t) = 2\langle \boldsymbol{\varepsilon}\mathbf{t}, \mathbf{n} \rangle \approx \cos\left(\frac{\pi}{2} - \Delta\alpha_{tn}\right) \approx \Delta\alpha_{tn}$$

where  $\Delta\alpha_{tn} \ll 1$  is the variation of the initially right angle, formed by the two infinitesimal vectors initially oriented along  $\mathbf{t}$  and  $\mathbf{n}$  respectively.

Conversely, since  $\langle \boldsymbol{\varepsilon}\mathbf{t}, \mathbf{i}_3 \rangle = 0 = \langle \boldsymbol{\varepsilon}\mathbf{n}, \mathbf{i}_3 \rangle$ , we establish that the directions initially oriented along  $\mathbf{t}$  and  $\mathbf{i}_3$  on the one hand, and along  $\mathbf{n}$  and  $\mathbf{i}_3$  on the other hand, remain perpendicular to each other at all times. ■

**Summary 1.3 — Infinitesimal strain tensor.** In the infinitesimal deformation hypothesis, the infinitesimal strain tensor corresponds to the symmetrical part of the displacement gradient tensor:

$$\boldsymbol{\varepsilon} = \frac{1}{2} (\mathbb{D}_{\mathbf{x}}\mathbf{u} + (\mathbb{D}_{\mathbf{x}}\mathbf{u})^T)$$

In a Cartesian vector basis  $(\mathbf{i}_1, \mathbf{i}_2, \mathbf{i}_3)$ , with associated coordinates  $(x_1, x_2, x_3)$ , this tensor can be expressed as:

$$\boldsymbol{\varepsilon}(x_1, x_2, x_3) = \frac{\partial \mathbf{u}}{\partial x_1}(x_1, x_2, x_3) \otimes_S \mathbf{i}_1 + \frac{\partial \mathbf{u}}{\partial x_2}(x_1, x_2, x_3) \otimes_S \mathbf{i}_2 + \frac{\partial \mathbf{u}}{\partial x_3}(x_1, x_2, x_3) \otimes_S \mathbf{i}_3$$

where, by definition,  $\mathbf{a} \otimes_S \mathbf{b} = (\mathbf{a} \otimes \mathbf{b} + \mathbf{b} \otimes \mathbf{a})/2$ .

In a cylindrical vector basis  $(\mathbf{i}_r(\theta), \mathbf{i}_\theta(\theta), \mathbf{i}_z)$ , with associated coordinates  $(r, \theta, z)$ , this tensor can be expressed as:

$$\boldsymbol{\varepsilon}(r, \theta, z) = \frac{\partial \mathbf{u}}{\partial r}(r, \theta, z) \otimes_S \mathbf{i}_r(\theta) + \frac{\partial \mathbf{u}}{\partial \theta}(r, \theta, z) \otimes_S \frac{\mathbf{i}_\theta(\theta)}{r} + \frac{\partial \mathbf{u}}{\partial z}(r, \theta, z) \otimes_S \mathbf{i}_z$$

The variation in length  $\Delta l$  of an infinitesimal vector of length  $l_0$  and direction  $\mathbf{e}$  can be expressed as :

$$\frac{\Delta l}{l_0} = \langle \boldsymbol{\varepsilon}\mathbf{e}, \mathbf{e} \rangle$$

The angle variation  $\Delta\alpha_{12}$  between two infinitesimal vectors of respective lengths  $l_{10}$  and  $l_{20}$ , and directions  $\mathbf{e}_1$  and  $\mathbf{e}_2$  perpendicular to each other, verifies:

$$\frac{\Delta\alpha_{12}}{2} = \langle \boldsymbol{\varepsilon}\mathbf{e}_2, \mathbf{e}_1 \rangle$$

■ **Example 1.19 — Radial expansion of a cylinder.** We consider a cylinder of revolution of axis  $\mathbf{i}_z$ , whose radius increases over time; by choosing the cylindrical vector basis  $(\mathbf{i}_r(\theta), \mathbf{i}_\theta(\theta), \mathbf{i}_z)$  associated with this latter, the displacement of a given point of the cylinder, of coordinates  $(r, \theta, z)$ , can then be written, at each instant, as:

$$\mathbf{u}(r, \theta, z, t) = u_r(r, t)\mathbf{i}_r(\theta)$$

where it is assumed that the radial displacement  $u_r$  is invariant by rotation around the cylinder axis, and does not depend on the altitude of the point along the axis.

The infinitesimal strain tensor is then obtained using the intrinsic expression established above in cylindrical

coordinates:

$$\boldsymbol{\varepsilon} = \frac{\partial \mathbf{u}}{\partial r} \otimes_S \mathbf{i}_r + \frac{\partial \mathbf{u}}{\partial \theta} \otimes_S \frac{\mathbf{i}_\theta}{r} + \frac{\partial \mathbf{u}}{\partial z} \otimes_S \mathbf{i}_z$$

where:

$$\begin{aligned}\frac{\partial \mathbf{u}}{\partial r} &= u'_r \mathbf{i}_r \\ \frac{\partial \mathbf{u}}{\partial \theta} &= u_r \mathbf{i}_\theta \\ \frac{\partial \mathbf{u}}{\partial z} &= 0\end{aligned}$$

with  $\bullet' = \frac{\partial \bullet}{\partial r}$ , which results in the following expression:

$$\boxed{\boldsymbol{\varepsilon}(r, \theta, z) = u'_r(r, t) \mathbf{i}_r(\theta) \otimes \mathbf{i}_r(\theta) + \frac{u_r(r, t)}{r} \mathbf{i}_\theta(\theta) \otimes \mathbf{i}_\theta(\theta)}$$

This example illustrates the curvature effects that play an extremely important role in the mechanical study of structures; indeed, the cylindrical geometry of the domain links the radial and circumferential dimensions since, if the radius of the cylinder increases, its circumference also increases. This is reflected in the infinitesimal strain tensor, which allows us to find locally that:

$$\frac{\Delta l_\theta}{l_{\theta 0}} = \varepsilon_{\theta \theta} = \frac{u_r}{r}$$

for any infinitesimal segment of direction  $\mathbf{i}_\theta$  and length  $l_{\theta 0}$ . ■



The previous example shows that it is essential to be aware that, even if the studied displacement is invariant by rotation around the cylinder axis, the infinitesimal strain tensor has a circumferential component; indeed, the circumference of the cylinder can only change if the cylinder radius is modified.

### 1.3.3 Study of infinitesimal local perturbations

Here we illustrate different aspects related to the analysis and measurement of deformations, within the framework of the infinitesimal deformation hypothesis.

#### Transformation of the neighbourhood of a point

In Paragraph 1.2.1, we have defined the deformation gradient tensor, which allows us to characterize the transformation of the neighbourhood of a point, by specifying the evolution over time of an infinitesimal vector  $d\mathbf{p}$  given in the initial configuration, and we have seen how to express it using the displacement gradient tensor:

$$d\mathbf{x} = \mathbb{F}(\mathbf{p}, t) d\mathbf{p} = (\mathbb{I} + \mathbb{D}_{\mathbf{p}} \mathbf{u}(\mathbf{p}, t)) d\mathbf{p}, \forall \mathbf{p} \in \Omega_0, \forall t$$

In the framework of the infinitesimal deformation hypothesis, it is then possible to consider the initial and current configurations as one, and, by choosing  $\mathbf{x}$  as the space variable, to simply write that:

$$d\mathbf{x} = (\mathbb{I} + \mathbb{D}_{\mathbf{x}} \mathbf{u}(\mathbf{x}, t)) d\mathbf{p} = (\mathbb{I} + \boldsymbol{\varepsilon}(\mathbf{x}, t) + \mathbf{r}(\mathbf{x}, t)) d\mathbf{p}, \forall \mathbf{x} \in \Omega, \forall t$$

where  $\mathbf{r}$  is the antisymmetrical part of the displacement gradient tensor, defined as:

$$\mathbf{r}(\mathbf{x}, t) = \frac{1}{2} \left( \mathbb{D}_{\mathbf{x}} \mathbf{u}(\mathbf{x}, t) - (\mathbb{D}_{\mathbf{x}} \mathbf{u}(\mathbf{x}, t))^T \right), \forall \mathbf{x} \in \Omega, \forall t$$

We can then show that we can associate to this antisymmetrical tensor a vector  $\mathbf{r}$  such that, for any arbitrary vector  $\mathbf{c}$ , we have :

$$\mathbf{r}(\mathbf{x}, t) \mathbf{c} = \mathbf{r}(\mathbf{x}, t) \wedge \mathbf{c}, \forall \mathbf{x} \in \Omega, \forall t$$

(see Appendix A.2.1 for more details), and that the tensor  $\mathbb{I} + \mathbf{r}$  actually corresponds to an infinitesimal rotation with angle  $\varphi = \|\mathbf{r}\|$  and direction  $\mathbf{e} = \mathbf{r}/\|\mathbf{r}\|$ , as detailed in Appendix A.2.6.

Thus, the neighbourhood of a point, undergoes, in the framework of the infinitesimal deformation hypothesis, a transformation that can be decomposed as the sum of a pure deformation, represented by the infinitesimal strain tensor  $\mathbf{\epsilon}$ , and a (infinitesimal) rigid body rotation, represented by the tensor  $\mathbb{I} + \mathbf{r}$ .

**R** This result can also be obtained from the polar decomposition of the deformation gradient tensor, which was mentioned as a remark at the end of Paragraph 1.2.1:

$$\mathbf{F} = \mathbb{R}\mathbb{U}$$

where  $\mathbb{R}$  is a rotation tensor, and  $\mathbb{U}$  is the square root of the right Cauchy-Green deformation tensor  $\mathbb{C} = \mathbb{I} + 2\mathbb{E}$ , which is symmetrical. Indeed, by placing oneself within the framework of the infinitesimal deformation hypothesis, one can approximate the rotation as:

$$\mathbb{R} \approx \mathbb{I} + \mathbf{r}, \text{ with } \mathbf{r}^T = -\mathbf{r}$$

considering what is described in Appendix A.2.6, and the square root, using a series expansion similar to what can be written on scalar functions:

$$\mathbb{U} = (\mathbb{I} + 2\mathbb{E})^{\frac{1}{2}} \approx \mathbb{I} + \frac{2\mathbb{E}}{2}$$

implying finally, up to order one:

$$\mathbf{F} = \mathbb{R}\mathbb{U} \approx (\mathbb{I} + \mathbf{r})(\mathbb{I} + \mathbb{E}) \approx \mathbb{I} + \mathbb{E} + \mathbf{r}$$

### ■ Example 1.20 — Torsion of a cylindrical shaft: transformation of the neighbourhood of a point.

We consider the transformation described in Example 1.4, for which we saw in Example 1.16 that the displacement field, in the context of the infinitesimal deformation hypothesis, was written as:

$$\boxed{\mathbf{u}(\mathbf{x}, t) = \frac{zc(t)}{L} \mathbf{i}_\theta(\theta), \forall \mathbf{x} \in \Omega}$$

and that, in the same context, the displacement gradient tensor was expressed as:

$$\mathbb{D}_{\mathbf{x}} \mathbf{u}(\mathbf{x}, t) = \frac{zc(t)}{L} \mathbf{i}_\theta(\theta) \otimes \mathbf{i}_r(\theta) - \frac{zc(t)}{L} \mathbf{i}_r(\theta) \otimes \mathbf{i}_\theta(\theta) + \frac{rc(t)}{L} \mathbf{i}_\theta(\theta) \otimes \mathbf{i}_z$$

which allowed to determine the infinitesimal strain tensor as follows:

$$\boxed{\mathbf{\epsilon}(\mathbf{x}, t) = \frac{rc(t)}{L} \mathbf{i}_\theta(\theta) \otimes_S \mathbf{i}_z}$$

From these results, it is easy to obtain that the antisymmetrical part of the displacement gradient tensor is written as:

$$\boxed{\mathbf{r}(\mathbf{x}, t) = 2 \frac{zc(t)}{L} \mathbf{i}_\theta(\theta) \otimes_A \mathbf{i}_r(\theta) + \frac{rc(t)}{L} \mathbf{i}_\theta(\theta) \otimes_A \mathbf{i}_z}$$

where  $\mathbf{a} \otimes_A \mathbf{b} = (\mathbf{a} \otimes \mathbf{b} - \mathbf{b} \otimes \mathbf{a})/2$  is the antisymmetrical part of the tensor  $\mathbf{a} \otimes \mathbf{b}$ . The first term can be interpreted as an infinitesimal rotation around the axis  $\mathbf{i}_z$  and with angle  $zc(t)/L$ , which corresponds to the rotation tensor  $\mathbb{R}$  that was highlighted in Example 1.10. ■

### Local analysis of strains

We have seen earlier that, in general, the infinitesimal strain tensor is not diagonal when expressed in a given vector basis  $(\mathbf{i}_1, \mathbf{i}_2, \mathbf{i}_3)$ : this physically means that an elemental subdomain, with cubic shape and edges along these three directions, is distorted. We can then wonder if it is possible to find orientations such that these elemental cubes remain effectively parallelepiped in shape, with right angles.

The answer to this question can be mathematical: indeed, we have seen that, by definition, the infinitesimal strain tensor is, at any point and at any time, symmetrical. It is thus possible to find an

orthonormal basis of eigenvectors  $\phi_k^\varepsilon$  such that we can write:

$$\varepsilon \phi_k^\varepsilon = \lambda_k^\varepsilon \phi_k^\varepsilon$$

The eigenvalues  $\lambda_k^\varepsilon$  are called “principal strains”, and the eigenvectors  $\phi_k^\varepsilon$  associated with the latter “principal strain directions”. In the general case, these quantities depend on the point and time that one considers

Thus, physically, any elemental sub-domain of cubic shape and oriented along these three directions  $\phi_k^\varepsilon$  undergoes only elongations or shortenings along these axes, without any distortion. From a graphical point of view, it is then possible to represent, at each point of the domain, three vectors oriented according to the principal directions  $\phi_k^\varepsilon$  and with amplitudes the values of the principal strains  $\lambda_k^\varepsilon$ , which can facilitate the understanding of the strain tensor field of a complicated mechanical part.

■ **Example 1.21 — Torsion of a cylindrical shaft: principal strains.** We consider the transformation described in Example 1.4, for which we saw in Example 1.16 that the displacement field, in the context of the infinitesimal deformation hypothesis, was written as:

$$\mathbf{u}(\mathbf{x}, t) = \frac{rc(t)}{L} \mathbf{i}_\theta(\theta), \forall \mathbf{x} \in \Omega$$

and that, in the same context, the infinitesimal strain tensor was expressed as:

$$\varepsilon(\mathbf{x}, t) = \frac{rc(t)}{L} \mathbf{i}_\theta(\theta) \otimes_S \mathbf{i}_z$$

Since the principal strains  $\lambda_k^\varepsilon$  are defined as the eigenvalues of the infinitesimal strain tensor, it is possible, for example, to determine them as the roots of the characteristic polynomial (as specified in Appendix A.2.4):

$$0 = \det(\varepsilon - \lambda_k^\varepsilon \mathbb{I}) = -\lambda_k^{\varepsilon 3} + \left( \frac{rc(t)}{2L} \right)^2 \lambda_k^\varepsilon$$

which therefore allows for obtaining as principal strains:

$$\boxed{\lambda_1^\varepsilon = \frac{rc(t)}{2L}, \lambda_2^\varepsilon = 0, \lambda_3^\varepsilon = -\frac{rc(t)}{2L}}$$

of associated principal directions:

$$\boxed{\phi_1^\varepsilon = (\mathbf{i}_\theta + \mathbf{i}_z)/\sqrt{2}, \phi_2^\varepsilon = \mathbf{i}_r, \phi_3^\varepsilon = (\mathbf{i}_\theta - \mathbf{i}_z)/\sqrt{2}}$$

The figure below shows these principal directions for various points on the lateral surface of the cylinder.



Thus, any elemental domain of cubic shape and oriented according to  $\mathbf{i}_r$  and according to the bisector of the angle formed by  $\mathbf{i}_\theta$  and  $\mathbf{i}_z$  is not distorted: it extends of  $(\mathbf{i}_\theta + \mathbf{i}_z)/\sqrt{2}$ , and shortens of  $(\mathbf{i}_\theta - \mathbf{i}_z)/\sqrt{2}$ . ■

**R** It is, of course, possible to define in a similar way the principal strains and directions of the Green Lagrange strain tensor, since the latter is symmetrical. The physical interpretation is then identical to the case of infinitesimal strain.

### Strain measurement

From an experimental point of view, strain measurement is part of what is called “extensometry”; among the most common techniques, we can mention:

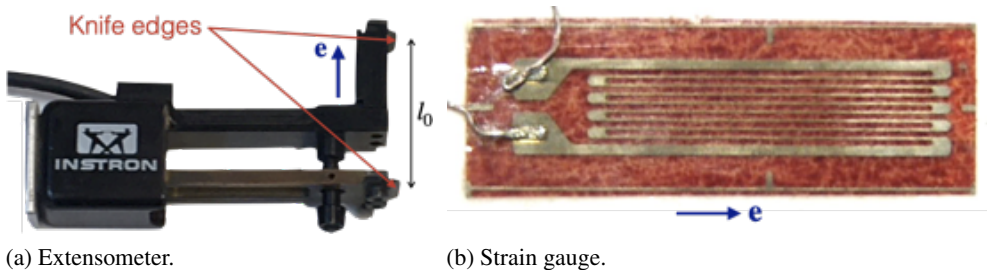
- extensometers, which are devices fixed to the surface of the object under study using two “knife edges” aligned perpendicularly to the measurement axis  $\mathbf{e}$  (as shown in Figure 1.5a), and which thus allow for measuring the variation in length  $\Delta l$  between the two zones in contact with the extensometer; we then assume that the strain is homogeneous between the two knife edges (initially spaced  $l_0$  apart), in order to determine:

$$\varepsilon_{ee} = \langle \boldsymbol{\varepsilon} \mathbf{e}, \mathbf{e} \rangle = \frac{\Delta l}{l_0}$$

- strain gauges, which consist of a conductor wire whose variation in electrical resistance is measured using a Wheatstone bridge; as shown in Figure 1.5b, this wire is arranged in a zig-zag pattern of parallel lines oriented along a specific  $\mathbf{e}$  direction, along which the strain is measured since the variation in length of an electrical conductor is directly proportional to the variation in electrical resistance  $R$ :

$$\varepsilon_{ee} = \langle \boldsymbol{\varepsilon} \mathbf{e}, \mathbf{e} \rangle \propto \frac{\Delta R}{R}$$

the dimensions of the gauge being usually small, we can consider that the measurement is punctual; besides, by associating gauges of different orientations at the same point, it is possible to determine the three strain components in the plane of the surface on which the gauges are glued, as we will see in Example 1.22;



(a) Extensometer.

(b) Strain gauge.

Figure 1.5: Strain measurement.

- image correlation techniques, which make it possible, using successive images (photographs, electron microscopy images, ...), to determine by computer processing the displacements of the various points of the image from one image to another, and thus to calculate the strain field in the plane ( $\mathbf{i}_1, \mathbf{i}_2$ ) of the observed surface:

$$\boldsymbol{\varepsilon} = \varepsilon_{11} \mathbf{i}_1 \otimes \mathbf{i}_1 + \varepsilon_{22} \mathbf{i}_2 \otimes \mathbf{i}_2 + 2\varepsilon_{12} \mathbf{i}_1 \otimes_S \mathbf{i}_2$$

in the case where it is possible to have two acquisition devices, it is then possible, by stereocorrelation, to obtain information concerning the out-of-plane displacement of the points of the observed surface (which, moreover, can then be of any arbitrary shape).

■ **Example 1.22 — Strain gauge rosettes.** Around the same point, on the flat surface of a structure, three strain gauges with different orientations  $\mathbf{e}_k$  are placed, each of which measures the longitudinal strain  $\varepsilon_{e_k}$  along the direction  $\mathbf{e}_k$ . We then try to link these three measurements to the components of the infinitesimal strain tensor at the point under study, in a vector basis  $(\mathbf{i}_1, \mathbf{i}_2)$  of the studied surface:

$$\boldsymbol{\varepsilon} = \varepsilon_{11}\mathbf{i}_1 \otimes \mathbf{i}_1 + \varepsilon_{22}\mathbf{i}_2 \otimes \mathbf{i}_2 + 2\varepsilon_{12}\mathbf{i}_1 \otimes_S \mathbf{i}_2$$

Considering that  $\theta_k$  is the angle formed by the direction  $\mathbf{i}_1$  and the direction  $\mathbf{e}_k$  of the  $k$ -th gauge, we can write that:

$$\begin{aligned} \varepsilon_{e_k} &= \langle \mathbf{e}_k, \boldsymbol{\varepsilon} \mathbf{e}_k \rangle \\ &= \langle \cos \theta_k \mathbf{i}_1 + \sin \theta_k \mathbf{i}_2, \boldsymbol{\varepsilon} (\cos \theta_k \mathbf{i}_1 + \sin \theta_k \mathbf{i}_2) \rangle \\ &= \langle \cos \theta_k \mathbf{i}_1 + \sin \theta_k \mathbf{i}_2, \cos \theta_k (\varepsilon_{11}\mathbf{i}_1 + \varepsilon_{12}\mathbf{i}_2) + \sin \theta_k (\varepsilon_{12}\mathbf{i}_1 + \varepsilon_{22}\mathbf{i}_2) \rangle \\ &= \cos^2 \theta_k \varepsilon_{11} + \sin^2 \theta_k \varepsilon_{22} + 2 \cos \theta_k \sin \theta_k \varepsilon_{12} \end{aligned}$$

The components of the infinitesimal strain tensor are then determined by inverting the following matrix system:

$$\begin{pmatrix} \cos^2 \theta_1 & \sin^2 \theta_1 & 2 \cos \theta_1 \sin \theta_1 \\ \cos^2 \theta_2 & \sin^2 \theta_2 & 2 \cos \theta_2 \sin \theta_2 \\ \cos^2 \theta_3 & \sin^2 \theta_3 & 2 \cos \theta_3 \sin \theta_3 \end{pmatrix} \begin{pmatrix} \varepsilon_{11} \\ \varepsilon_{22} \\ \varepsilon_{12} \end{pmatrix} = \begin{pmatrix} \varepsilon_{e_1} \\ \varepsilon_{e_2} \\ \varepsilon_{e_3} \end{pmatrix}$$

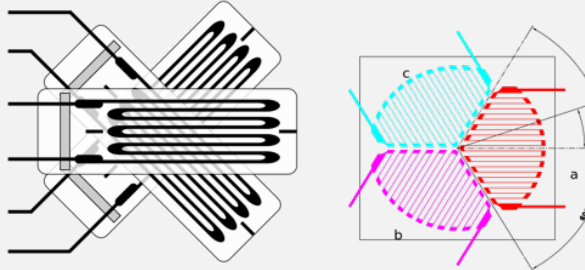
In practice, it is possible to use gauge “rosettes”, using gauges oriented at particular angles:

- rectangular rosettes, where the gauges are then separated by angles of  $45^\circ$  ( $\theta_1 = 0^\circ$ ,  $\theta_2 = 45^\circ$ ,  $\theta_3 = 90^\circ$  for example), which establishes that :

$$\varepsilon_{11} = \varepsilon_{e_1}, \quad \varepsilon_{22} = \varepsilon_{e_3}, \quad \varepsilon_{12} = \varepsilon_{e_2} - \frac{\varepsilon_{e_1} + \varepsilon_{e_3}}{2}$$

- equiangular rosettes, where the gauges are separated by angles of  $60^\circ$  ( $\theta_1 = -60^\circ$ ,  $\theta_2 = 0^\circ$ ,  $\theta_3 = 60^\circ$  for example), which allows us to obtain:

$$\varepsilon_{11} = \varepsilon_{e_2}, \quad \varepsilon_{22} = \frac{2\varepsilon_{e_1} + 2\varepsilon_{e_3} - \varepsilon_{e_2}}{3}, \quad \varepsilon_{12} = \frac{\varepsilon_{e_3} - \varepsilon_{e_1}}{\sqrt{3}}$$



■

## 1.4 Volume change and mass conservation

In addition to studying local variations in length and angle, it may be interesting to determine whether or not the volume of the studied domain remains constant when transformed. Since mass is assumed to be an invariant property of matter, local volume change then provides information on the evolution of density over time.

### 1.4.1 Volume change

On a global scale, it is possible to link estimates of the volume occupied by the material domain between the initial and current configurations; by definition, we can write that:

$$\mathcal{V}_0 = \mathcal{V}(0) = \int_{\Omega_0} dV_p$$

is the initial volume of the domain, while the volume at the current time is:

$$\mathcal{V}(t) = \int_{\Omega_t} dV_x$$

By using the substitution  $\mathbf{x} = \mathbf{f}(\mathbf{p}, t)$  in this latter integral, we establish, using the result of Appendix B.2.1, that:

$$\mathcal{V}(t) = \int_{\Omega_t} dV_x = \int_{\Omega_0} \det \mathbb{F}(\mathbf{p}, t) dV_p$$

or, locally, as shown in Figure 1.6, that the volume element  $dV_p = |\langle dp_1, dp_2 \wedge dp_3 \rangle|$  in the initial configuration is transformed as  $dV_x = |\langle dx_1, dx_2 \wedge dx_3 \rangle|$  such that:

$$dV_x = \det \mathbb{F}(\mathbf{p}, t) dV_p$$

which allows us to affirm that the local volume change is expressed using the determinant of the deformation gradient tensor.

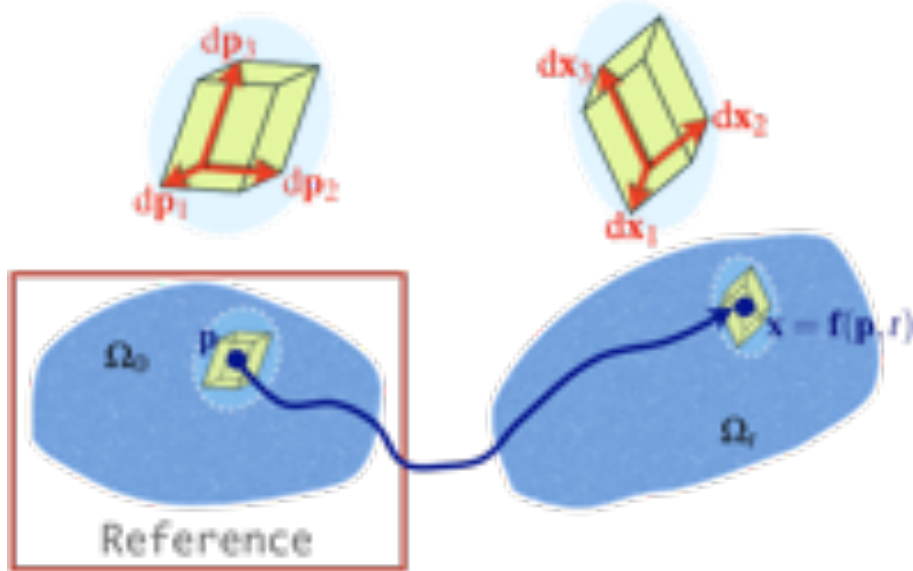


Figure 1.6: Elemental volume change.

If we consider the infinitesimal deformation hypothesis, we then write that  $\mathbb{F} = \mathbb{I} + \mathbb{D}_x \mathbf{u}$  with  $\|\mathbb{D}_x \mathbf{u}\| \ll 1$ , which allows us to establish, using a series expansion up to order one of the determinant, that:

$$\det \mathbb{F} = \det(\mathbb{I} + \mathbb{D}_x \mathbf{u}) \approx 1 + \text{tr } \mathbb{D}_x \mathbf{u}$$

Rewriting this expression using Cartesian coordinates  $(x_1, x_2, x_3)$ , we notice that:

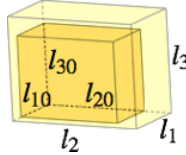
$$\text{tr } \mathbb{D}_x \mathbf{u} = \text{tr } \boldsymbol{\epsilon} = \sum_{k=1}^3 \frac{\partial u_k}{\partial x_k} = \text{div}_x \mathbf{u}$$

where  $\text{div}_x \mathbf{u}$  is the divergence of the displacement field (defined in Appendix B.1.1), which finally establishes that the relative local volume change can be written, for any volume element  $\mathcal{V}$  located in  $\mathbf{x}$ , as:

$$\frac{d\mathcal{V}}{\mathcal{V}} = \text{div}_x \mathbf{u}$$

where  $d\mathcal{V}$  is the variation in volume  $\mathcal{V}$  between the two configurations.

**R** This last result can be physically interpreted using a volume element of rectangular parallelepipedic shape, initially of dimensions  $l_{10}$ ,  $l_{20}$  and  $l_{30}$  along the directions  $(\mathbf{i}_1, \mathbf{i}_2, \mathbf{i}_3)$  of the infinitesimal strain tensor at that point.



At the current time, these dimensions then become  $l_1 = l_{10} + \Delta l_1$ ,  $l_2 = l_{20} + \Delta l_2$  and  $l_3 = l_{30} + \Delta l_3$  respectively, so that it can be written that:

$$\frac{d\mathcal{V}}{\mathcal{V}} \approx \frac{\Delta l_1}{l_{10}} + \frac{\Delta l_2}{l_{20}} + \frac{\Delta l_3}{l_{30}} = \varepsilon_1 + \varepsilon_2 + \varepsilon_3 = \text{tr} \boldsymbol{\varepsilon} = \text{div}_{\mathbf{x}} \mathbf{u}$$

since  $|\Delta l_k| \ll l_{k0}$ ,  $1 \leq k \leq 3$ .

■ **Example 1.23 — Uniform elongation: volume change.** The transformation described in Example 1.1 is considered:

$$\mathbf{x} = \mathbf{f}(\mathbf{p}, t) = \mathbf{p} + a(t) \langle \mathbf{p}, \mathbf{n} \rangle \mathbf{n}, \forall \mathbf{p} \in \Omega_0$$

for which we expressed in Example 1.7 the deformation gradient tensor in a vector basis  $(\mathbf{i}_1, \mathbf{i}_2 = \mathbf{n}, \mathbf{i}_3)$  as:

$$\mathbb{F}(\mathbf{p}, t) = \begin{pmatrix} 1 & 0 & 0 \\ 0 & 1 + a(t) & 0 \\ 0 & 0 & 1 \end{pmatrix}_{(\mathbf{i}_1, \mathbf{i}_2 = \mathbf{n}, \mathbf{i}_3)}$$

where  $\mathbf{i}_1$  and  $\mathbf{i}_3$  are two unit vectors perpendicular to  $\mathbf{n}$ , and to each other.

It is then easy to determine that  $\det \mathbb{F} = 1 + a(t)$ ,  $\forall \mathbf{p} \in \Omega_0$ , and therefore that the relative local volume change is uniform, and is expressed as the overall volume change:

$$\boxed{\frac{\mathcal{V}(t) - \mathcal{V}_0}{\mathcal{V}_0} = a(t)}$$

In the context of the infinitesimal deformation hypothesis ( $|a(t)| \ll 1$ ,  $\forall t$ ), we find on this specific example a similar result:

$$\boxed{\frac{d\mathcal{V}}{\mathcal{V}} = \text{div}_{\mathbf{x}} \mathbf{u} = \text{tr} \mathbb{D}_{\mathbf{x}} \mathbf{u} = \text{tr}(a(t) \mathbf{n} \otimes \mathbf{n}) = a(t)}$$

which is uniform, and allows us to find the same global volume change as before. ■

The previous relations then allow to introduce and characterize the notion of incompressibility.

**Incompressibility.** A material domain will be qualified as incompressible if the transformation it undergoes is carried out locally, at any point, at a constant volume, i.e. if:

$$\det \mathbb{F}(\mathbf{p}, t) = 1, \forall \mathbf{p} \in \Omega_0, \forall t$$

This condition becomes, in the context of the infinitesimal deformation hypothesis:

$$\boxed{\text{div}_{\mathbf{x}} \mathbf{u}(\mathbf{x}, t) = 0, \forall \mathbf{x} \in \Omega, \forall t}$$

■ **Example 1.24 — Torsion of a cylindrical shaft: volume change.** The transformation described in Example 1.4 is considered:

$$\mathbf{x} = \mathbf{f}(\mathbf{p}, t) = \mathbf{p} + p_r (\mathbf{i}_r(p_\theta + c(t)p_z/L) - \mathbf{i}_r(p_\theta)) = p_r \mathbf{i}_r(p_\theta + c(t)p_z/L) + p_z \mathbf{i}_z, \forall \mathbf{p} \in \Omega_0$$

and for which the deformation gradient tensor has been expressed in Example 1.10 as:

$$\mathbb{F} = \mathbb{R} \mathbb{G}$$

where  $\mathbb{R}$  is a rotation tensor, which verifies that  $\det \mathbb{R} = 1$ , and :

$$\mathbb{G} = \begin{pmatrix} 1 & 0 & 0 \\ 0 & 1 & \frac{p_r c(t)}{L} \\ 0 & 0 & 1 \end{pmatrix}_{(\mathbf{i}_r(p_\theta), \mathbf{i}_\theta(p_\theta), \mathbf{i}_z)}$$

It is then easy to determine that  $\det \mathbb{F} = (\det \mathbb{R})(\det \mathbb{G}) = 1$ ,  $\forall \mathbf{p} \in \Omega_0$ , which means that there is no relative local volume change, and therefore that :

$$\mathcal{V}(t) = \mathcal{V}_0, \forall t$$

Indeed, the cylinder, even in torsion, always has the same volume since its different cross-sections only rotate rigidly around the axis  $\mathbf{i}_z$ .

In the context of the infinitesimal deformation hypothesis, we find on this specific example a similar result:

$$\frac{d\mathcal{V}}{\mathcal{V}} = \operatorname{div}_{\mathbf{x}} \mathbf{u} = \frac{c(t)}{L} \operatorname{div}_{\mathbf{x}} (rz \mathbf{i}_\theta(\theta)) = 0$$

which allows us to find that the volume of the domain remains constant over time. ■

**Summary 1.4 — Local volume change.** The variation over time of the volume of an elemental sub-domain  $d\Omega_0$ , around  $\mathbf{p}$  in the initial configuration, is expressed as:

$$dV_x = \det \mathbb{F}(\mathbf{p}, t) dV_p, \forall \mathbf{p} \in \Omega_0, \forall t$$

In the infinitesimal deformation hypothesis, the relative volume change for an elemental volume  $\mathcal{V}$  is:

$$\frac{d\mathcal{V}}{\mathcal{V}} = \operatorname{tr} \mathbb{D}_{\mathbf{x}} \mathbf{u}(\mathbf{x}, t) = \operatorname{div}_{\mathbf{x}} \mathbf{u}(\mathbf{x}, t), \forall \mathbf{x} \in \Omega, \forall t$$



*It is possible to evaluate, in the same way as for volumes, the evolution of the area of a surface; Appendix B.2.1 allows for establishing that an elemental surface  $dS_p = \|d\mathbf{p}_1 \wedge d\mathbf{p}_2\|$  in the initial configuration changes to  $dS_x = \|\mathbf{dx}_1 \wedge \mathbf{dx}_2\|$  such that:*

$$dS_x = \det \mathbb{F} \left\| \mathbb{F}^{-T} (d\mathbf{p}_1 \wedge d\mathbf{p}_2) \right\| = \det \mathbb{F} \left\| \mathbb{F}^{-T} \mathbf{n}_p \right\| dS_p$$

*by noting  $\mathbf{n}_p$  the unit normal vector to the initial surface (such that  $d\mathbf{p}_1 \wedge d\mathbf{p}_2 = dS_p \mathbf{n}_p$ ).*

*In particular, even in the case of an incompressible transformation ( $\det \mathbb{F} = 1$ ), it is possible, for specific surfaces, to have variations in area ( $\|\mathbb{F}^{-T} \mathbf{n}_p\| \neq 1$ ).*

### 1.4.2 Mass conservation

A corollary to the expression of volume change is the evolution of density, which we defined as a local quantity, attached to the particles constituting the medium under consideration, assuming the continuity of this latter.

#### Material expression

Thus, we can consider an arbitrary sub-domain  $\omega_t$ , contained in the domain  $\Omega_t$ ; since the mass is a property that is assumed to be invariant, it is possible to affirm that:

$$\mathcal{M} = \int_{\omega_t} \rho(\mathbf{x}, t) dV_x = \int_{\omega_0} \rho_0(\mathbf{p}) dV_p, \forall t$$

by associating the initial configuration with the density  $\rho_0$ , and the current configuration with the density  $\rho$ . By transforming, as in the case of volume change, the first integral using the substitution  $\mathbf{x} = \mathbf{f}(\mathbf{p}, t)$ , we can thus affirm that:

$$\int_{\omega_0} (\rho(\mathbf{f}(\mathbf{p}, t), t) \det \mathbb{F}(\mathbf{p}, t) - \rho_0(\mathbf{p})) dV_p = 0, \forall t, \forall \omega_t \subset \Omega_t$$

Since this relation is valid regardless of the sub-domain  $\omega_t$  included in  $\Omega_t$ , we can deduce that the integrand is equal to zero, and therefore that:

$$\rho(\mathbf{f}(\mathbf{p}, t), t) = \frac{\rho_0(\mathbf{p})}{\det \mathbb{F}(\mathbf{p}, t)}, \forall \mathbf{p} \in \Omega_0, \forall t$$

knowing that we always have  $\det \mathbb{F} > 0$ .

Moreover, if we place ourselves within the framework of the infinitesimal deformation hypothesis, we can, as before, write up to order one that :

$$(\det \mathbb{F})^{-1} \approx 1 - \text{tr} \mathbb{D}_{\mathbf{x}} \mathbf{u} = 1 - \text{div}_{\mathbf{x}} \mathbf{u}$$

and thus obtain, always up to order one, that:

$$\rho(\mathbf{x}, t) = \rho_0(\mathbf{x})(1 - \text{div}_{\mathbf{x}} \mathbf{u}(\mathbf{x}, t)), \forall \mathbf{x} \in \Omega, \forall t$$

by assuming  $\mathbf{p} \approx \mathbf{x}$ .

**R** *These two terms are rarely used in practice; in the case of fluid media where mass conservation is often used, a spatial version of this principle, which is more appropriate, is preferred.*

### Incompressibility

Incompressibility is directly expressed in terms of density as:

$$\rho(\mathbf{f}(\mathbf{p}, t), t) = \rho_0(\mathbf{p}), \forall \mathbf{p} \in \Omega_0, \forall t$$

whether or not we are in the infinitesimal deformation hypothesis. Physically, each particle has its density unchanged over time.

**Summary 1.5 — Mass conservation.** The local density  $\rho$  evolves over time as:

$$\rho(\mathbf{f}(\mathbf{p}, t), t) = \frac{\rho_0(\mathbf{p}_0)}{\det \mathbb{F}(\mathbf{p}, t)}, \forall \mathbf{p} \in \Omega_0, \forall t$$

where  $\rho_0$  is the local density in the reference configuration.

## 1.5 Summary of important formulas

**Deformation gradient tensor** – Summary 1.1 page 13

$$d\mathbf{x} = \mathbb{F} d\mathbf{p}$$

$$\mathbb{F} = \sum_{n=1}^3 \frac{\partial \mathbf{x}}{\partial p_n} \otimes \mathbf{i}_n$$

$$\mathbb{F} = \frac{\partial \mathbf{x}}{\partial p_r} \otimes \mathbf{i}_r + \frac{\partial \mathbf{x}}{\partial p_\theta} \otimes \frac{\mathbf{i}_\theta}{p_r} + \frac{\partial \mathbf{x}}{\partial p_z} \otimes \mathbf{i}_z$$

**Green-Lagrange strain tensor** – Summary 1.2 page 21

$$\mathbb{E} = \frac{1}{2} (\mathbb{F}^T \mathbb{F} - \mathbb{I})$$

$$\frac{\|\mathbf{dx}\|^2 - \|\mathbf{dp}\|^2}{\|\mathbf{dp}\|^2} = 2\langle \mathbb{E}\mathbf{e}_p, \mathbf{e}_p \rangle$$

$$\cos \alpha_{12x} = \frac{\langle \mathbb{F}\mathbf{e}_{p1}, \mathbb{F}\mathbf{e}_{p2} \rangle}{\|\mathbb{F}\mathbf{e}_{p1}\| \|\mathbb{F}\mathbf{e}_{p2}\|} = \frac{\cos \alpha_{12p} + 2\langle \mathbb{E}\mathbf{e}_{p1}, \mathbf{e}_{p2} \rangle}{\sqrt{\langle (2\mathbb{E} + \mathbb{I})\mathbf{e}_{p1}, \mathbf{e}_{p1} \rangle \langle (2\mathbb{E} + \mathbb{I})\mathbf{e}_{p2}, \mathbf{e}_{p2} \rangle}}$$

**Infinitesimal strain tensor – Summary 1.3 page 27**

$$\boldsymbol{\varepsilon} = \frac{1}{2} \left( \mathbb{D}_{\mathbf{x}} \mathbf{u} + (\mathbb{D}_{\mathbf{x}} \mathbf{u})^T \right)$$

$$\boldsymbol{\varepsilon} = \sum_{n=1}^3 \frac{\partial \mathbf{u}}{\partial x_n} \otimes_S \mathbf{i}_n$$

$$\boldsymbol{\varepsilon} = \frac{\partial \mathbf{u}}{\partial r} \otimes_S \mathbf{i}_r + \frac{\partial \mathbf{u}}{\partial \theta} \otimes_S \frac{\mathbf{i}_\theta}{r} + \frac{\partial \mathbf{u}}{\partial z} \otimes_S \mathbf{i}_z$$

$$\frac{\Delta l}{l_0} = \langle \boldsymbol{\varepsilon} \mathbf{e}, \mathbf{e} \rangle$$

$$\frac{\Delta \alpha_{12}}{2} = \langle \boldsymbol{\varepsilon} \mathbf{e}_2, \mathbf{e}_1 \rangle$$

**Local volume change – Summary 1.4 page 35**

$$d\Omega_t = \det \mathbb{F} d\Omega_0$$

$$\frac{d\mathcal{V}}{\mathcal{V}} = \text{tr } \mathbb{D}_{\mathbf{x}} \mathbf{u} = \text{div}_{\mathbf{x}} \mathbf{u}$$

**Mass conservation – Summary 1.5 page 36**

$$\rho = \frac{\rho_0}{\det \mathbb{F}}$$



## 2. Stresses

Stresses reflect the internal forces within the deformable media, by replacing the mechanical action exerted by a volume of matter, which would then be removed (virtually) from the domain, on the remaining part of the domain. These stresses depend on the point under study and the orientation of the cut surface. The calculation and optimization of stresses are essential in any design study of an object that must resist mechanical stresses.

---

### WHY STUDY STRESSES?

#### 2.1 Fundamental principles of dynamics for a material domain

As in the previous chapter, we consider a material domain that we follow over time; we assume that it currently occupies the domain  $\Omega_t$ , whose position and shape depend on the forces applied to the domain, namely, as shown in Figure 2.1:

- a volume force density (or body force density)  $\mathbf{f}_V(\mathbf{x}, t)$ , which is applied at any point  $\mathbf{x}$  within the domain  $\Omega_t$ , and which is expressed in  $\text{N/m}^3$ ; these are typically forces that are exerted at a distance (gravity force, Laplace force, ...);
- a surface force density  $\mathbf{f}_S(\mathbf{x}, t)$ , which is applied at any point  $\mathbf{x}$  of the boundary  $\partial\Omega_t$  of the domain  $\Omega_t$ , and is expressed in  $\text{N/m}^2$ ; this time these are forces that are exerted by contact (pressure force of a fluid on a wall, force at the contact surface between two solids, ...).

In both cases, it is indeed the current configuration  $\Omega_t$  that must be taken into account to apply the fundamental principles of dynamics.

##### 2.1.1 Conservation of momentum and angular momentum

At any given time, we consider all the particles constituting the domain  $\Omega_t$ , and for which we can apply Newton's laws.

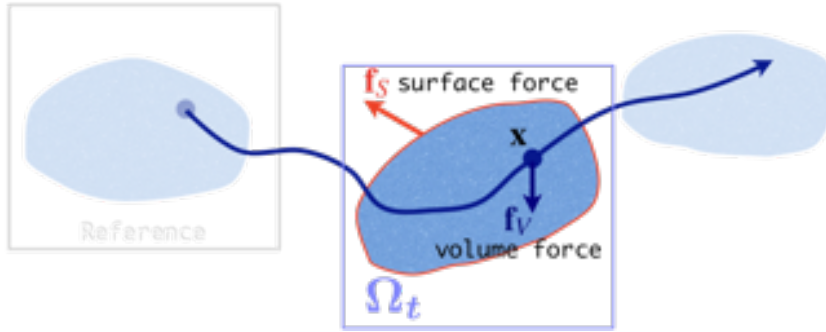


Figure 2.1: Force densities applied to a material domain.

### Conservation of momentum

The (linear) momentum  $\mathbf{q}_k$  of a point particle  $k$  of mass  $m_k$  and velocity  $\mathbf{v}_k$  is conventionally defined as the product of one by the other:  $\mathbf{q}_k(t) = m_k \mathbf{v}_k(t)$ ,  $\forall t$ . Newton's second law then consists in expressing that this quantity evolves at any given time as the sum of the forces  $\mathbf{F}_k$  that are exerted on the particle:

$$\dot{\mathbf{q}}_k(t) = \mathbf{F}_k(t), \forall t$$

with  $\dot{\mathbf{q}}_k(t) = m_k \mathbf{a}_k(t)$ , where  $\mathbf{a}_k$  is the acceleration of the particle in question.

If we now consider a set  $\mathcal{S}$  of  $N$  point particles of respective masses and velocities  $m_k$  and  $\mathbf{v}_k$ , the sum of the different equations allows us to establish that:

$$\sum_{k=1}^N \dot{\mathbf{q}}_k(t) = \sum_{k=1}^N \mathbf{F}_k(t), \forall t$$

Among the total forces  $\mathbf{F}_k$  exerted on the particles, we can consider in particular the forces  $\mathbf{F}_{i \rightarrow j}$  and  $\mathbf{F}_{j \rightarrow i}$  which are exerted between two given particles  $i$  and  $j$ ; under Newton's third law (or the "action-reaction" principle), we can write that these two forces compensate each other:  $\mathbf{F}_{i \rightarrow j} = -\mathbf{F}_{j \rightarrow i}$ . This allows us to eliminate in the previous sum all the forces that are exerted between two particles of the set  $\mathcal{S}$ , which makes it possible to write that:

$$\sum_{k=1}^N \dot{\mathbf{q}}_k(t) = \sum_{k=1}^N \mathbf{F}_{\bar{\mathcal{S}} \rightarrow k}(t) = \mathbf{F}_{\bar{\mathcal{S}} \rightarrow \mathcal{S}}(t), \forall t$$

by noting  $\mathbf{F}_{\bar{\mathcal{S}} \rightarrow \mathcal{S}}$  the sum of the forces exerted by the "outside" on the considered set. Finally, by assuming that the momentum  $\mathbf{q}_{\mathcal{S}}$  of the set  $\mathcal{S}$  is the sum of the momentums of the particles that constitute it, we then get:

$$\dot{\mathbf{q}}_{\mathcal{S}}(t) = \mathbf{F}_{\bar{\mathcal{S}} \rightarrow \mathcal{S}}(t), \forall t$$

Considering now that the particles are the elemental particles of the domain  $\Omega_t$ , we can go so far as replacing the discrete sum by an integral, by defining the momentum of the material domain as:

$$\mathbf{q}_{\Omega}(t) = \int_{\Omega_t} \rho(\mathbf{x}, t) \mathbf{v}(\mathbf{x}, t) dV_x, \forall t$$

where  $\mathbf{v}(\mathbf{x}, t)$  is the velocity of the particle located in  $\mathbf{x}$  at time  $t$ , and  $\rho(\mathbf{x}, t)$  is its density. Similarly, the forces exerted on  $\Omega$  do correspond to the surface and volume densities mentioned above, which must, therefore, be integrated respectively on the boundaries and in the interior of the domain  $\Omega_t$ . The conservation of momentum is therefore written for the material domain as:

$$\dot{\mathbf{q}}_{\Omega}(t) = \overbrace{\int_{\Omega_t} \rho(\mathbf{x}, t) \mathbf{v}(\mathbf{x}, t) dV_x}^{\cdot} = \int_{\Omega_t} \mathbf{f}_V(\mathbf{x}, t) dV_x + \int_{\partial\Omega_t} \mathbf{f}_S(\mathbf{x}, t) dS_x, \forall t$$

At first glance, the left-hand side seems difficult to calculate, since it is a question of differentiating with respect to time an integral whose integration domain ( $\Omega_t$ ) itself depends on time; but by using results which are not detailed here, it is possible to transform the derivative of the momentum to obtain finally:

$$\int_{\Omega_t} \rho(\mathbf{x}, t) \mathbf{a}(\mathbf{x}, t) dV_x = \int_{\Omega_t} \mathbf{f}_V(\mathbf{x}, t) dV_x + \int_{\partial\Omega_t} \mathbf{f}_S(\mathbf{x}, t) dS_x, \forall t$$

where  $\mathbf{a}(\mathbf{x}, t)$  is the acceleration of the particle located in  $\mathbf{x}$  at time  $t$ .

### Conservation of the angular momentum

A conservation equation similar to the previous one concerns the angular momentum, which plays a similar role with respect to rotations to that played by the (amount of motion)linear momentum for translations; for a point particle of mass  $m_k$ , velocity  $\mathbf{v}_k$ , and located in  $\mathbf{x}_k$ , we define the angular momentum as the moment with respect to a fixed point  $O$  (in the considered reference frame) of the momentum, namely:  $\mathbf{s}_{\mathbf{x}_O}^k(t) = (\mathbf{x}_k - \mathbf{x}_O) \wedge \mathbf{q}_k(t)$ ,  $\forall t$ . Its derivative is then written as:

$$\dot{\mathbf{s}}_{\mathbf{x}_O}^k(t) = \overline{(\mathbf{x}_k - \mathbf{x}_O)} \wedge (m_k \mathbf{v}_k(t)) + (\mathbf{x}_k - \mathbf{x}_O) \wedge \dot{\mathbf{q}}_k(t)$$

Since  $O$  is fixed, we have  $\overline{(\mathbf{x}_k - \mathbf{x}_O)} = \dot{\mathbf{x}}_k$ , which is the time derivative of the position of the particle under study, namely  $\mathbf{v}_k(t)$ . So we have:

$$\dot{\mathbf{s}}_{\mathbf{x}_O}^k(t) = \mathbf{v}_k(t) \wedge m_k \mathbf{v}_k(t) + (\mathbf{x}_k - \mathbf{x}_O) \wedge \dot{\mathbf{q}}_k(t) = (\mathbf{x}_k - \mathbf{x}_O) \wedge m_k \mathbf{a}_k(t)$$

By using the conservation of momentum, we finally end up with:

$$\dot{\mathbf{s}}_{\mathbf{x}_O}^k(t) = (\mathbf{x}_k - \mathbf{x}_O) \wedge \mathbf{F}_k(t), \forall t$$

where  $\mathbf{F}_k$  is the sum of the forces exerted on the particle.

As in the case of the conservation of the momentum, the previous expression can be transposed to the case of a material domain, consisting of elemental particles of density  $\rho(\mathbf{x}, t)$ , for which we write that:

$$\dot{\mathbf{s}}_{\mathbf{x}_O}^\Omega(t) = \overline{(\mathbf{x} - \mathbf{x}_O) \wedge \rho(\mathbf{x}, t) \mathbf{v}(\mathbf{x}, t) dV_x} = \int_{\Omega_t} (\mathbf{x} - \mathbf{x}_O) \wedge \mathbf{f}_V(\mathbf{x}, t) dV_x + \int_{\partial\Omega_t} (\mathbf{x} - \mathbf{x}_O) \wedge \mathbf{f}_S(\mathbf{x}, t) dS_x, \forall t$$

where  $\mathbf{s}_{\mathbf{x}_O}^\Omega$  is the angular momentum of  $\Omega$  at point  $O$ . Once again, it is possible to transform the previous expression as:

$$\int_{\Omega_t} (\mathbf{x} - \mathbf{x}_O) \wedge \rho(\mathbf{x}, t) \mathbf{a}(\mathbf{x}, t) dV_x = \int_{\Omega_t} (\mathbf{x} - \mathbf{x}_O) \wedge \mathbf{f}_V(\mathbf{x}, t) dV_x + \int_{\partial\Omega_t} (\mathbf{x} - \mathbf{x}_O) \wedge \mathbf{f}_S(\mathbf{x}, t) dS_x, \forall t$$

 As in the previous chapter, we deliberately avoided the question of the reference frame, assuming therefore for now that the movements are described in relation to a fixed observer without further detail.

**Summary 2.1 — Fundamental principles of dynamics.** Any set of particles, currently occupying at time  $t$  the domain  $\Omega_t$ , and subjected to:

- volume force densities  $\mathbf{f}_V(\mathbf{x}, t)$ ,  $\forall \mathbf{x} \in \Omega_t$ ;
- surface force densities  $\mathbf{f}_S(\mathbf{x}, t)$ ,  $\forall \mathbf{x} \in \partial\Omega_t$ ;

satisfies the principle of conservation of momentum:

$$\int_{\Omega_t} \rho(\mathbf{x}, t) \mathbf{a}(\mathbf{x}, t) dV_x = \int_{\Omega_t} \mathbf{f}_V(\mathbf{x}, t) dV_x + \int_{\partial\Omega_t} \mathbf{f}_S(\mathbf{x}, t) dS_x, \forall t$$

(also called fundamental principle of dynamics for forces), and the principle of conservation of angular momentum, at any fixed point  $O$ :

$$\int_{\Omega_t} (\mathbf{x} - \mathbf{x}_O) \wedge \rho(\mathbf{x}, t) \mathbf{a}(\mathbf{x}, t) dV_x = \int_{\Omega_t} (\mathbf{x} - \mathbf{x}_O) \wedge \mathbf{f}_V(\mathbf{x}, t) dV_x + \int_{\partial\Omega_t} (\mathbf{x} - \mathbf{x}_O) \wedge \mathbf{f}_S(\mathbf{x}, t) dS_x, \forall t$$

(also called fundamental principle of dynamics for moments). In addition,  $\rho(\mathbf{x}, t)$  and  $\mathbf{a}(\mathbf{x}, t)$  refer respectively to the density and acceleration, defined at any point  $\mathbf{x} \in \Omega_t$  of the continuous medium.

## 2.1.2 Actions

These two equations for the conservation of (linear) momentum and angular momentum allow for highlighting what an action is in mechanics; it is derived from the volume and surface force densities applied to the material domain.

**Actions.** An action is a cause acting on the movement or deformation of a material domain. To describe all the actions applied to a material domain, we define classically:

- the resultant force of all the forces applied to the domain, which is given by the integral, respectively on the boundary and in the interior of the domain, of the surface and volume force densities taken into account:

$$\mathbf{R}^{ext}(t) = \int_{\Omega_t} \mathbf{f}_V(\mathbf{x}, t) dV_x + \int_{\partial\Omega_t} \mathbf{f}_S(\mathbf{x}, t) dS_x, \forall t$$

- the moment at a given point  $O$  of all the forces applied to the domain, which is expressed as the integral, respectively on the boundary and in the interior of the domain, of the moments in  $O$  of these surface and volume force densities:

$$\mathbf{M}_{\mathbf{x}_O}^{ext}(t) = \int_{\Omega_t} (\mathbf{x} - \mathbf{x}_O) \wedge \mathbf{f}_V(\mathbf{x}, t) dV_x + \int_{\partial\Omega_t} (\mathbf{x} - \mathbf{x}_O) \wedge \mathbf{f}_S(\mathbf{x}, t) dS_x, \forall t$$

Similarly, an action is therefore characterized by a resultant force and a moment, which is expressed at a point.

The expression of the moment naturally changes according to the chosen point: if we take the example of a surface force density  $\mathbf{f}_S$  (contact force on a surface  $\Sigma_c$  for example), the moment  $\mathbf{M}_{\mathbf{x}_A}^c$  at an arbitrary point  $A$  can be expressed as:

$$\mathbf{M}_{\mathbf{x}_A}^c = \int_{\Sigma_c} (\mathbf{x} - \mathbf{x}_A) \wedge \mathbf{f}_S dS_x$$

and, if we bring in another arbitrary point  $B$ , we get:

$$\mathbf{M}_{\mathbf{x}_A}^c = \int_{\Sigma_c} (\mathbf{x} - \mathbf{x}_B + \mathbf{x}_B - \mathbf{x}_A) \wedge \mathbf{f}_S dS_x = \int_{\Sigma_c} (\mathbf{x} - \mathbf{x}_B) \wedge \mathbf{f}_S dS_x + (\mathbf{x}_B - \mathbf{x}_A) \wedge \left( \int_{\Sigma_c} \mathbf{f}_S dS_x \right)$$

which allows us to introduce the resultant force  $\mathbf{R}^c$  associated with this contact action, and to obtain the classical relation to change the point of expression of the moment of an action:

$$\mathbf{M}_{\mathbf{x}_A}^c = \mathbf{M}_{\mathbf{x}_B}^c + (\mathbf{x}_B - \mathbf{x}_A) \wedge \mathbf{R}^c$$

**R** We deduce from the previous relation that it is very easy to express the conservation of angular momentum at a point other than  $O$ ; indeed, we can write using a point  $A$  that:

$$\int_{\Omega_t} (\mathbf{x} - \mathbf{x}_A + \mathbf{x}_A - \mathbf{x}_O) \wedge \rho \mathbf{a} dV_x = \int_{\Omega_t} (\mathbf{x} - \mathbf{x}_A + \mathbf{x}_A - \mathbf{x}_O) \wedge \mathbf{f}_V dV_x + \int_{\partial\Omega_t} (\mathbf{x} - \mathbf{x}_A + \mathbf{x}_A - \mathbf{x}_O) \wedge \mathbf{f}_S dS_x$$

then, by using the conservation of momentum:

$$\int_{\Omega_t} (\mathbf{x}_A - \mathbf{x}_O) \wedge \rho \mathbf{a} dV_x = (\mathbf{x}_A - \mathbf{x}_O) \wedge \int_{\Omega_t} \rho \mathbf{a} dV_x = (\mathbf{x}_A - \mathbf{x}_O) \wedge \left( \int_{\Omega_t} \mathbf{f}_V(\mathbf{x}, t) dV_x + \int_{\partial\Omega_t} \mathbf{f}_S(\mathbf{x}, t) dS_x \right)$$

we can simplify it like:

$$\int_{\Omega_t} (\mathbf{x} - \mathbf{x}_A) \wedge \rho \mathbf{a} dV_x = \int_{\Omega_t} (\mathbf{x} - \mathbf{x}_A) \wedge \mathbf{f}_V dV_x + \int_{\partial\Omega_t} (\mathbf{x} - \mathbf{x}_A) \wedge \mathbf{f}_S dS_x$$

which corresponds to the expression of the conservation of angular momentum at point  $A$ .

**Special actions.** Two particular actions can be defined:

- **Couple:** an action whose resultant force is zero is called “couple”, or “pure moment”; because of the relation to change its point of expression, the associated moment is then independent of the point at which it is expressed, and is also called a couple.
- **Pure force:** an action for which there is at least one point where the moment is zero is called a “pure force”; in this case, the moment is zero at all the points of the line passing through this particular point, and of direction that of the resultant force. However incorrectly, we often simply speak of force to designate a pure force.

■ **Example 2.1 — Action of gravity.** For example, the action of gravity is characterized by a volume force density  $\mathbf{f}_V(\mathbf{x}, t) = -\rho(\mathbf{x}, t)g\mathbf{i}_3$ ,  $\forall \mathbf{x} \in \Omega_t$ , where  $\mathbf{i}_3$  is a vertical (upward) unit vector. The associated resultant force is:

$$\mathbf{R}^g = \int_{\Omega_t} -\rho(\mathbf{x}, t)g\mathbf{i}_3 dV_x = -\left( \int_{\Omega_t} \rho(\mathbf{x}, t) dV_x \right) g\mathbf{i}_3$$

considering that the acceleration of gravity  $g$  is uniform, hence finally:

$$\boxed{\mathbf{R}^g = -m_\Omega g\mathbf{i}_3}$$

The mass  $m_\Omega$  has thus been defined naturally as the integral on the volume of  $\Omega$  of the density  $\rho(\mathbf{x}, t)$ : we notice that according to the conservation principle set out in Paragraph 1.4.2, the mass does not depend on time, whereas the density can evolve spatially over time within the material domain. Besides, the moment expressed at an arbitrary point  $A$  is written as:

$$\mathbf{M}_{\mathbf{x}_A}^g = \int_{\Omega_t} (\mathbf{x} - \mathbf{x}_A) \wedge (-\rho(\mathbf{x}, t)g\mathbf{i}_3) dV_x = \left( \int_{\Omega_t} \rho(\mathbf{x}, t)\mathbf{x} dV_x - m_\Omega \mathbf{x}_A \right) \wedge (-g\mathbf{i}_3)$$

By introducing the barycenter  $C(t)$  of the spatial distribution of mass within  $\Omega_t$ , also classically known as the “center of mass”, we find that:

$$\boxed{\mathbf{M}_{\mathbf{x}_A}^g = (\mathbf{x}_C(t) - \mathbf{x}_A) \wedge (-m_\Omega g\mathbf{i}_3) = (\mathbf{x}_C(t) - \mathbf{x}_A) \wedge \mathbf{R}^g}$$

which leads to the conclusion that the moment of the action of gravity, expressed at the center of mass  $\mathbf{x}_C(t)$  of the domain  $\Omega_t$ , is zero, and therefore that the action of gravity is a pure force. ■

### 2.1.3 Static equilibrium

A domain is in static equilibrium if the positions of its different particles do not change over time: we therefore have a zero acceleration ( $\mathbf{a}(\mathbf{x}, t) = 0$ ,  $\forall \mathbf{x} \in \Omega_t$ ,  $\forall t$ ), which allows us to write:

$$\mathbf{R}^{ext}(t) = \int_{\Omega_t} \mathbf{f}_V(\mathbf{x}, t) dV_x + \int_{\partial\Omega_t} \mathbf{f}_S(\mathbf{x}, t) dS_x = \mathbf{0}, \forall t$$

$$\mathbf{M}_{\mathbf{x}_O}^{ext}(t) = \int_{\Omega_t} (\mathbf{x} - \mathbf{x}_O) \wedge \mathbf{f}_V(\mathbf{x}, t) dV_x + \int_{\partial\Omega_t} (\mathbf{x} - \mathbf{x}_O) \wedge \mathbf{f}_S(\mathbf{x}, t) dS_x = \mathbf{0}, \forall t$$

In what follows we mention some particular classic cases of static equilibrium, detailing what this implies for the actions exerted on the material domain.

### Equilibrium of a material domain subjected to two pure forces

The simplest case that can be studied is that of a material domain subjected to two pure forces, namely two actions of respective resultant forces  $\mathbf{R}_1$  and  $\mathbf{R}_2$  and of zero associated moments, at points  $A_1$  and  $A_2$  respectively. In this case, the equilibrium equation allows for establishing that:

$$\mathbf{R}_1 + \mathbf{R}_2 = \mathbf{R}^{ext} = \mathbf{0}$$

with regard to the resultant forces, and, if we write the static equilibrium equation for the moments at point  $A_1$ :

$$(\mathbf{x}_{A_2} - \mathbf{x}_{A_1}) \wedge \mathbf{R}_2 = \mathbf{M}_{\mathbf{x}_{A_1}}^{ext} = \mathbf{0}$$

This last relation then makes it possible to affirm that  $\mathbf{R}_2$  (and consequently  $\mathbf{R}_1$ , which is opposed to it) is collinear to the vector that connects the two points  $A_1$  and  $A_2$  (as depicted in Figure 2.2), regardless the shape of the material domain.

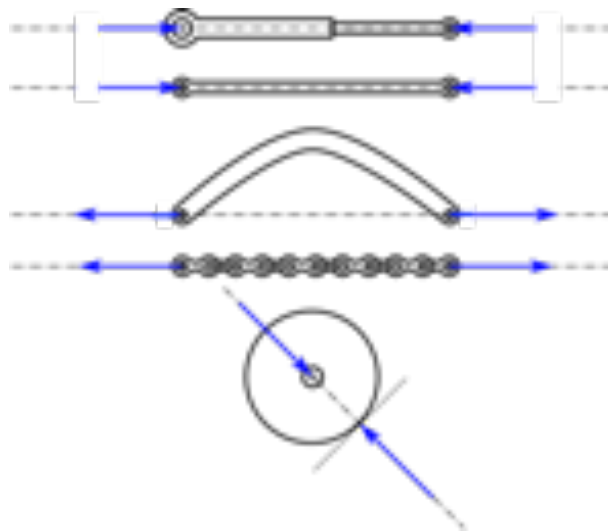


Figure 2.2: Equilibrium of a material domain subjected to two pure forces.

#### **Summary 2.2 — Static equilibrium of a material domain subjected to two pure forces.**

We consider a domain  $\Omega$  subjected to two pure forces, i.e. two actions of respective resultant forces  $\mathbf{R}_1$  and  $\mathbf{R}_2$ , and zero associated moments at points  $A_1$  and  $A_2$  respectively.

If  $\Omega$  is in static equilibrium, then necessarily the two resultant forces  $\mathbf{R}_1$  and  $\mathbf{R}_2$  are opposed and collinear to the vector connecting points  $A_1$  and  $A_2$ .

### Equilibrium of a material domain subjected to three pure forces

Another typical case is that of a material domain subjected to three pure forces, namely three actions of respective resultant forces  $\mathbf{R}_1$ ,  $\mathbf{R}_2$  and  $\mathbf{R}_3$  and zero associated moments, at points  $A_1$ ,  $A_2$  and  $A_3$  respectively. As in the case of two pure forces, the equilibrium equation concerning the resultant forces merely allows for affirming that:

$$\mathbf{R}_1 + \mathbf{R}_2 + \mathbf{R}_3 = \mathbf{R}^{ext} = \mathbf{0}$$

which implies that the three resultant forces are coplanar. In addition, the equilibrium equations for the moments expressed at point  $A_1$  gives:

$$(\mathbf{x}_{A_2} - \mathbf{x}_{A_1}) \wedge \mathbf{R}_2 + (\mathbf{x}_{A_3} - \mathbf{x}_{A_1}) \wedge \mathbf{R}_3 = \mathbf{M}_{\mathbf{x}_{A_1}}^{ext} = \mathbf{0}$$

which makes it possible to affirm that the plane containing the three resultant forces is actually the plane defined by the three points  $A_1, A_2$  and  $A_3$ .

Several situations are then possible:

- if the two resultant forces  $\mathbf{R}_2$  and  $\mathbf{R}_3$  (when they are placed at  $A_2$  and  $A_3$  respectively) intersect at a point  $I$ , the moments at that point of these two actions are then zero, and the equilibrium equation in terms of moments at that point can be written as:

$$(\mathbf{x}_{A_1} - \mathbf{x}_I) \wedge \mathbf{R}_1 = \mathbf{M}_{\mathbf{x}_I}^{ext} = \mathbf{0}$$

which implies that  $\mathbf{R}_1$  is collinear to the vector connecting the points  $A_1$  and  $I$ , or, in other words, that the three resultant forces are concurrent; moreover, the sum of the three resultant forces is equal to zero, indicating that these latter form a triangle, often called “triangle of forces”;

- if the two resultant forces  $\mathbf{R}_2$  and  $\mathbf{R}_3$  are parallel, but on different lines (when they are placed respectively at  $A_2$  and  $A_3$ ), in this case, we can only say that the resultant force  $\mathbf{R}_3$  is in the same plane as the other two (and equal to the opposite of the sum of the two others);
- if the two resultant forces  $\mathbf{R}_2$  and  $\mathbf{R}_3$  are on the same line (when they are placed respectively at  $A_2$  and  $A_3$ ), in this case, the moments at a point on this line of these two actions are equal to zero, and we can, for example, write the equilibrium equation for the moments at  $A_2$  as:

$$(\mathbf{x}_{A_1} - \mathbf{x}_{A_2}) \wedge \mathbf{R}_1 = \mathbf{M}_{\mathbf{x}_{A_2}}^{ext} = \mathbf{0}$$

which means that the resultant force  $\mathbf{R}_1$  is also on the line in question, since  $\mathbf{R}_1$  is, because of the equilibrium equation for the forces, necessarily parallel to the other two (and equal to the opposite of the sum of the other two).

The two first situations are depicted on Figure 2.3.

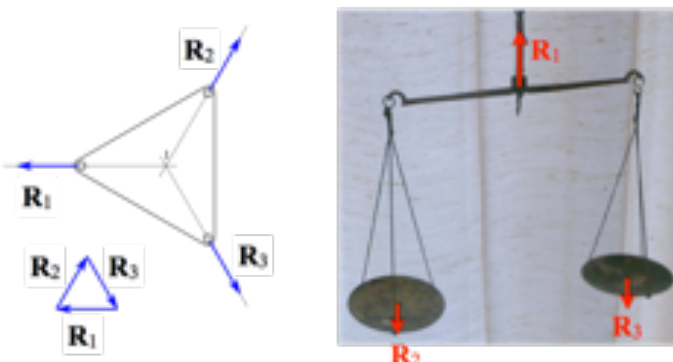


Figure 2.3: Equilibrium of a material domain subjected to three pure forces: case of three concurrent forces (left) and case of three parallel forces (right).

### Summary 2.3 — Static equilibrium of a material domain subjected to three pure forces.

We consider a domain  $\Omega$  subjected to three pure forces, i.e. three actions of respective resultant forces  $\mathbf{R}_1, \mathbf{R}_2$  and  $\mathbf{R}_3$ , and zero associated moments at points  $A_1, A_2$  and  $A_3$  respectively.

If  $\Omega$  is in static equilibrium, then necessarily the three resultant forces  $\mathbf{R}_1, \mathbf{R}_2$  and  $\mathbf{R}_3$  have their sum equal to zero, and can be (when placed respectively at  $A_1, A_2$  and  $A_3$ ):

- concurrent;
- parallel, and, in this case, either coplanar or on the same line.

## 2.2 Concept of stress

In the previous paragraph, we only took into account the actions exerted by the external environment on the material domain  $\Omega$ . In order for the latter to be able to withstand these loadings, there are cohesion forces within the material, which are the interatomic binding forces, which depend on the physicochemical composition of the material and its structure.

Of course, given the continuous medium that we are considering, we do not wish to go as far as this level of detail here, but only to reflect the fact that these forces are very short-range, which means that two particles far from each other in the domain exert negligible actions on each other. It is, therefore, these forces exerted from one particle to the next, between the different particles that constitute the domain under study, that we will model in the following.

### 2.2.1 Internal forces

We consider a material domain in its current configuration  $\Omega_t$ , and, within it, a sub-domain  $\omega_t$  that we also follow over time, so that it occupies the volume  $\omega_t$  at the current time, as shown in Figure 2.4. This sub-domain  $\omega_t$  can be of any shape or size; moreover, it can have a common part with the boundary  $\partial\Omega_t$  of the domain  $\Omega_t$ , or even split this latter into two separate parts.

#### Modeling

This sub-domain  $\omega_t$  is then subjected to the actions defined above (which are external to the domain  $\Omega_t$ ), but also to the action of the complementary sub-domain of  $\omega_t$  in  $\Omega_t$ , noted  $\omega_t^* = \Omega_t \setminus \omega_t$ , since we assumed that the cohesion forces were exerted from close to close. It seems natural to assume that these forces are exerted on the cut surface  $\Sigma_t$  that has been created by (mentally) isolating the sub-domain  $\omega_t$ : since these are, so to speak, contact forces between two material domains, it is assumed that they can be represented by a surface force density, hence the following definition.

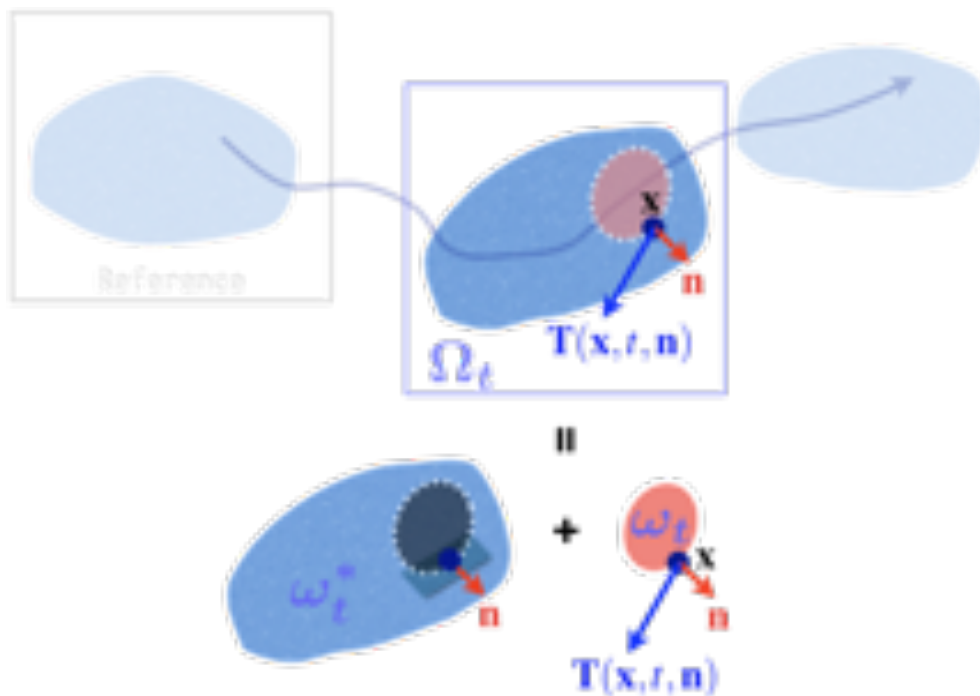


Figure 2.4: Internal forces within a material domain.

**Stress vector.** The surface force density  $\mathbf{T}$  exerted on the isolated subdomain  $\omega_t$ , at any point on the virtual cut surface  $\Sigma_t$ , by the complementary part  $\omega_t^*$ , is called “stress vector” (or “surface traction”):

$$\mathbf{T}(\mathbf{x}, t, \mathbf{n}) = \mathbf{f}_\Sigma(\mathbf{x}, t), \quad \forall \mathbf{x} \in \Sigma_t, \text{ and } \mathbf{n} \perp \Sigma_t \text{ in } \mathbf{x}$$

In the general case, this density depends on the point  $\mathbf{x}$  and time, but also on the local orientation of the surface at the point  $\mathbf{x}$ , represented by the outer unit normal vector  $\mathbf{n}$  in  $\mathbf{x}$ , which is perpendicular to the local tangent plane (also called “facet”).



*Assuming a priori that the stress vector depends on the local orientation of the cut surface reflects the fact that, at a given point, the material is not loaded in the same way depending on the direction considered.*

*On the other hand, one considers that the local curvature of the cut surface has no influence on the description of the internal forces and that we can, therefore, be satisfied with the orientation of the facet, given by the direction of the outer normal vector  $\mathbf{n}$  of the domain, at the point under study.*

### Consideration

To determine the internal forces that have just been modelled, it is sufficient to use them in the fundamental principles of dynamics which have been given in Paragraph 2.1: instead of considering all the particles constituting the material domain  $\Omega_t$ , we limit ourselves to those defining the particular subdomain  $\omega_t$  that we follow during its movement. For any sub-domain  $\omega_t$  strictly contained in  $\Omega_t$ , we then simply obtain that:

$$\int_{\omega_t} \rho(\mathbf{x}, t) \mathbf{a}(\mathbf{x}, t) dV_x = \int_{\omega_t} \mathbf{f}_V(\mathbf{x}, t) dV_x + \int_{\partial \omega_t} \mathbf{T}(\mathbf{x}, t, \mathbf{n}) dS_x, \quad \forall t$$

for the conservation of momentum, and:

$$\int_{\omega_t} (\mathbf{x} - \mathbf{x}_O) \wedge \rho(\mathbf{x}, t) \mathbf{a}(\mathbf{x}, t) dV_x = \int_{\omega_t} (\mathbf{x} - \mathbf{x}_O) \wedge \mathbf{f}_V(\mathbf{x}, t) dV_x + \int_{\partial \omega_t} (\mathbf{x} - \mathbf{x}_O) \wedge \mathbf{T}(\mathbf{x}, t, \mathbf{n}) dS_x, \quad \forall t$$

for the conservation of angular momentum.

These relations highlight the fact that, if we know the stress vector  $\mathbf{T}(\mathbf{x}, t, \mathbf{n})$  at any point of the cut surface  $\Sigma_t$ , we know the dynamics of the sub-domain  $\omega_t$ , which means that everything happens as if we had cut  $\Omega_t$  and removed the complementary part  $\omega_t^*$  without affecting the movement of  $\omega_t$ . Of course, if, on the other hand, we choose to keep  $\omega_t^*$  and remove  $\omega_t$ , we can apply the same relations, this time taking the opposite normal vector on the facet, and thus taking the stress vector  $\mathbf{T}(\mathbf{x}, t, -\mathbf{n})$ .

Besides, we see that we defined internal forces which are, by nature, local since they depend on the point under study, as can be the volume force densities exerted within the material domain. Thus, whereas the two conservation principles applied to the complete material domain allow for obtaining only six scalar equations, applying them to an arbitrary sub-domain underlines that the distribution of internal forces plays an essential role in the evolution of the deformable medium under study. This is indeed the approach adopted in the following to specify the properties of the stress vector  $\mathbf{T}(\mathbf{x}, t, \mathbf{n})$ .



*As seen in Example 1.3 (on page 5), the movement in space of a perfectly rigid body is characterized by six parameters. We have just mentioned that the application of the two conservation principles to the complete material domain allows for obtaining six independent scalar equations, which are therefore sufficient to determine the evolution of the six parameters describing the motion of the solid over time. It is therefore not necessary to focus on internal forces in the case of a perfectly rigid body since the spatial distribution of these forces plays no role in the motion of this latter.*

## 2.2.2 Stress tensor

We will focus here on specifying the dependence of the stress vector  $\mathbf{T}(\mathbf{x}, t, \mathbf{n})$  on the orientation of the normal vector  $\mathbf{n}$  to the cut surface in  $\mathbf{x}$ . To do this, we will apply the principle of conservation of momentum to two sub-domains of very particular shapes.

### Action-reaction principle

First, elemental sub-domains  $\omega_t^h$ , cylindrical in shape, are considered in the vicinity of a given point  $\mathbf{x}_O$ , as shown in Figure 2.5.

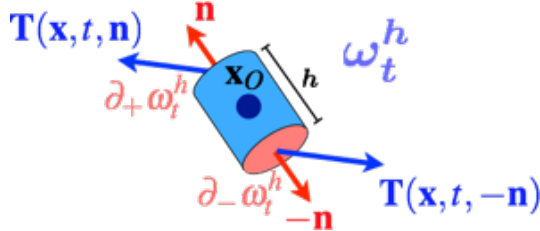


Figure 2.5: Dynamic equilibrium of an elemental cylinder.

The conservation of momentum is naturally written as:

$$\int_{\omega_t^h} (\rho(\mathbf{x}, t) \mathbf{a}(\mathbf{x}, t) - \mathbf{f}_V(\mathbf{x}, t)) dV_x = \int_{\partial \omega_t^h} \mathbf{T}(\mathbf{x}, t, \mathbf{n}) dS_x, \forall t$$

Since the two integrands are continuous functions of space, the mean value theorem then allows us to affirm that there is for each integral a point in the integration domain such that the value of the integrand at this point is equal to the integral divided by the area or volume of the integration domain. Thus, for the left-hand side, there is  $\mathbf{x}_V \in \omega_t^h$  such that:

$$\int_{\omega_t^h} (\rho(\mathbf{x}, t) \mathbf{a}(\mathbf{x}, t) - \mathbf{f}_V(\mathbf{x}, t)) dV_x = \pi R^2 h (\rho(\mathbf{x}_V, t) \mathbf{a}(\mathbf{x}_V, t) - \mathbf{f}_V(\mathbf{x}_V, t))$$

where  $R$  and  $h$  are the radius and height of the cylindrical domain respectively. In addition, the right-hand side can be split into three surface integrals corresponding to the three sides of the cylinder:

$$\int_{\partial \omega_t^h} \mathbf{T}(\mathbf{x}, t, \mathbf{n}) dS_x = \int_{\partial_L \omega_t^h} \mathbf{T}(\mathbf{x}, t, \mathbf{n}) dS_x + \int_{\partial_+ \omega_t^h} \mathbf{T}(\mathbf{x}, t, \mathbf{n}) dS_x + \int_{\partial_- \omega_t^h} \mathbf{T}(\mathbf{x}, t, \mathbf{n}) dS_x$$

where  $\partial_L \omega_t^h$ ,  $\partial_+ \omega_t^h$  and  $\partial_- \omega_t^h$  are the lateral, upper and lower surfaces of the cylinder respectively. Applying the mean value theorem to each of these integrals, we conclude that there are  $\mathbf{x}_L \in \partial_L \omega_t^h$ ,  $\mathbf{x}_+ \in \partial_+ \omega_t^h$  and  $\mathbf{x}_- \in \partial_- \omega_t^h$  such that:

$$\begin{aligned} \int_{\partial_L \omega_t^h} \mathbf{T}(\mathbf{x}, t, \mathbf{n}) dS_x + \int_{\partial_+ \omega_t^h} \mathbf{T}(\mathbf{x}, t, \mathbf{n}) dS_x + \int_{\partial_- \omega_t^h} \mathbf{T}(\mathbf{x}, t, \mathbf{n}) dS_x &= 2\pi Rh \mathbf{T}(\mathbf{x}_L, t, \mathbf{n}_L) \\ &\quad + \pi R^2 (\mathbf{T}(\mathbf{x}_+, t, \mathbf{n}) + \mathbf{T}(\mathbf{x}_-, t, -\mathbf{n})) \end{aligned}$$

where  $\mathbf{n}_L$ ,  $\mathbf{n}$  et  $-\mathbf{n}$  are the outer unit normal vectors on the surface of the cylinder, in  $\mathbf{x}_L$ ,  $\mathbf{x}_+$  and  $\mathbf{x}_-$  respectively. If we use cylindrical coordinates to express that  $\mathbf{x}_+ = \mathbf{x}_O + (h/2)\mathbf{n} + r_+ \mathbf{i}_r(\theta_+)$  and  $\mathbf{x}_- = \mathbf{x}_O - (h/2)\mathbf{n} + r_- \mathbf{i}_r(\theta_-)$ , then if the height  $h$  of the cylinder approaches zero, we finally obtain that:

$$\mathbf{T}(\mathbf{x}_O + r_+ \mathbf{i}_r(\theta_+), t, \mathbf{n}) + \mathbf{T}(\mathbf{x}_O + r_- \mathbf{i}_r(\theta_-), t, -\mathbf{n}) = \mathbf{0}$$

Finally, assuming that the cylinder has a radius small enough to be able to consider at a last step that  $\mathbf{x}_O + r_+ \mathbf{i}_r(\theta_+) \approx \mathbf{x}_O \approx \mathbf{x}_O + r_- \mathbf{i}_r(\theta_-)$ , we finally get:

$$\mathbf{T}(\mathbf{x}_O, t, -\mathbf{n}) = -\mathbf{T}(\mathbf{x}_O, t, \mathbf{n}), \forall \mathbf{x}_O \in \Omega_t, \forall t$$

which constitutes the action-reaction principle.

Physically, this result can also be interpreted as a consequence of Newton's third law: indeed, on the cut surface which allows the sub-domain  $\omega_t$  to be isolated (mentally) from its complementary part  $\omega_t^*$ , the particles that interact exert forces on each other that are directly opposed. This allows us to conclude that the stress vector is antisymmetric relatively to the normal vector  $\mathbf{n}$ .

### Linearity of the stress vector

In a second step, we consider elemental subdomains  $\omega_t^h$ , of tetrahedral shape, in the vicinity of a given point  $\mathbf{x}_O$ ; each of these tetrahedrons is right-angled, with three of its edges oriented along the vectors of a basis  $(\mathbf{i}_1, \mathbf{i}_2, \mathbf{i}_3)$ , as represented in Figure 2.6. By defining  $(n_1, n_2, n_3)$  the components in this basis of the outer normal vector  $\mathbf{n}$  to the oblique face, and  $h$  the height of the tetrahedron along this normal, we deduce the following geometric characteristics:

- the three edges parallel to the basis vectors have the following lengths:  $\frac{h}{n_k}$ ;
- the lateral faces  $\partial_k \omega_t^h$ , generated in particular by these edges, have as outer normal vectors  $-\mathbf{i}_k$ , and respective areas:  $\frac{h^2}{2n_i n_j}$ ,  $i \neq j \neq k$ ;
- the oblique face  $\partial_n \omega_t^h$ , of outer normal vector  $\mathbf{n}$ , has an area:  $\frac{h^2}{2n_1 n_2 n_3}$ ;
- the tetrahedron has a volume:  $\frac{h^3}{2n_1 n_2 n_3}$ .

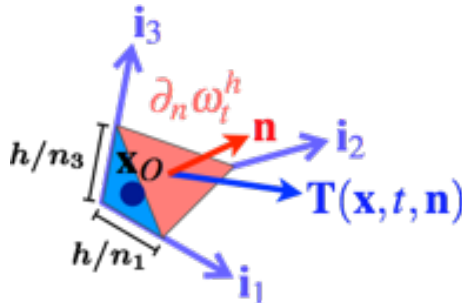


Figure 2.6: Dynamic equilibrium of an elemental tetrahedron (“Cauchy tetrahedron”).

As in the previous paragraph, the mean value theorem is applied to each integral present in the expression of the conservation of momentum:

$$\int_{\omega_t^h} (\rho(\mathbf{x}, t) \mathbf{a}(\mathbf{x}, t) - \mathbf{f}_V(\mathbf{x}, t)) dV_x = \int_{\partial_n \omega_t^h} \mathbf{T}(\mathbf{x}, t, \mathbf{n}) dS_x + \sum_{k=1}^3 \int_{\partial_k \omega_t^h} \mathbf{T}(\mathbf{x}, t, -\mathbf{i}_k) dS_x, \forall t$$

Thus, for the left-hand side, there is  $\mathbf{x}_V \in \omega_t^h$  such that:

$$\int_{\omega_t^h} (\rho(\mathbf{x}, t) \mathbf{a}(\mathbf{x}, t) - \mathbf{f}_V(\mathbf{x}, t)) dV_x = \frac{h^3}{2n_1 n_2 n_3} (\rho(\mathbf{x}_V, t) \mathbf{a}(\mathbf{x}_V, t) - \mathbf{f}_V(\mathbf{x}_V, t))$$

while, for each integral of the right-hand side, there is  $\mathbf{x}_k \in \partial_k \omega_t^h$  ( $1 \leq k \leq 3$ ) and  $\mathbf{x}_n \in \partial_n \omega_t^h$  such

that:

$$\int_{\partial_n \omega_t^h} \mathbf{T}(\mathbf{x}, t, \mathbf{n}) dS_x = \frac{h^2}{2n_1 n_2 n_3} \mathbf{T}(\mathbf{x}_n, t, \mathbf{n})$$

$$\int_{\partial_k \omega_t^h} \mathbf{T}(\mathbf{x}, t, -\mathbf{i}_k) dS_x = \frac{h^2}{2n_i n_j} \mathbf{T}(\mathbf{x}_k, t, -\mathbf{i}_k), i \neq j \neq k$$

When the height  $h$  approaches zero, we can see that the volume integral, in  $h^3$ , becomes negligible relatively to the sum of the surface integrals, which are all in  $h^2$ . In addition, by approximating  $\mathbf{x}_n \approx \mathbf{x}_O \approx \mathbf{x}_k$  (for  $1 \leq k \leq 3$ ), it is then determined that:

$$\mathbf{T}(\mathbf{x}_O, t, \mathbf{n}) + \sum_{k=1}^3 n_k \mathbf{T}(\mathbf{x}_O, t, -\mathbf{i}_k) = \mathbf{0}, \forall \mathbf{x}_O \in \Omega_t$$

or, by using the action-reaction principle:

$$\mathbf{T}(\mathbf{x}_O, t, \mathbf{n}) = \sum_{k=1}^3 n_k \mathbf{T}(\mathbf{x}_O, t, \mathbf{i}_k), \forall \mathbf{x}_O \in \Omega_t, \forall t$$

which means that the stress vector depends linearly on the outer unit normal vector  $\mathbf{n}$  to the facet, for the cut surface under study.

**R** The reasoning previously carried out on the elemental tetrahedron is, strictly speaking, not sufficient to conclude, since, with such a geometry, it is not possible to have a normal vector  $\mathbf{n}$  parallel to one of the basis vectors  $\mathbf{i}_k$ . In this case, however, the established relation is still valid because we have  $n_j = \pm 1$  and  $n_k = 0$  for  $k \neq j$ .

### Mathematical representation

In order to take advantage of the previous results, the following tensor is introduced.

**Cauchy stress tensor.** The Cauchy stress tensor is the tensor  $\sigma$  defined as, using the vector basis  $(\mathbf{i}_1, \mathbf{i}_2, \mathbf{i}_3)$ :

$$\sigma(\mathbf{x}, t) = \sum_{k=1}^3 \mathbf{T}(\mathbf{x}, t, \mathbf{i}_k) \otimes \mathbf{i}_k, \forall \mathbf{x} \in \Omega_t, \forall t$$

where  $\mathbf{T}(\mathbf{x}, t, \mathbf{i}_k)$  is the stress vector at the same point and at the same time, for a facet of outer unit normal vector  $\mathbf{i}_k$ . The stress vector along a given normal vector  $\mathbf{n}$  is then expressed as the image of the vector  $\mathbf{n}$  by the linear application represented by  $\sigma$ :

$$\mathbf{T}(\mathbf{x}, t, \mathbf{n}) = \sigma(\mathbf{x}, t) \mathbf{n} = \sum_{k=1}^3 \langle \mathbf{n}, \mathbf{i}_k \rangle \mathbf{T}(\mathbf{x}, t, \mathbf{i}_k), \forall \mathbf{x} \in \Omega_t, \forall t, \forall \mathbf{n}$$

Therefore, in this same vector basis, the components of the stress tensor are expressed simply as:

$$\sigma_{mn} = \langle \mathbf{T}(\mathbf{x}, t, \mathbf{i}_n), \mathbf{i}_m \rangle, 1 \leq m, n \leq 3$$

Physically, this means that it is sufficient to know at point  $\mathbf{x}$  and at time  $t$  the stress vectors on three facets of linearly independent normal vectors to completely know the stress tensor, and, consequently, the stress vector (at the same point and at the same time) relative to a facet of any arbitrary normal vector  $\mathbf{n}$ . Figure 2.7 summarizes this in the case where we choose the three facets as three faces of an elemental cube centred in  $\mathbf{x}$ . When there is no ambiguity, we simply talk about stress tensor, without being more precise.

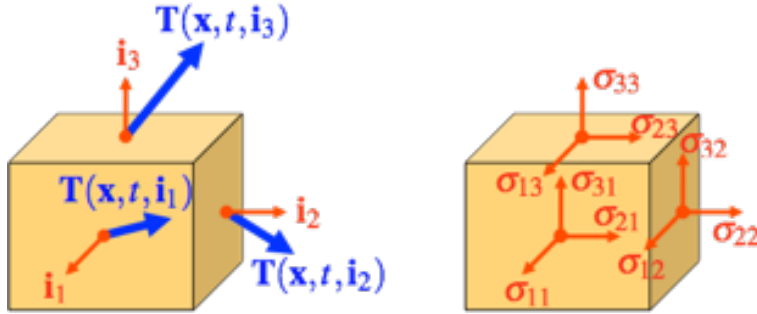
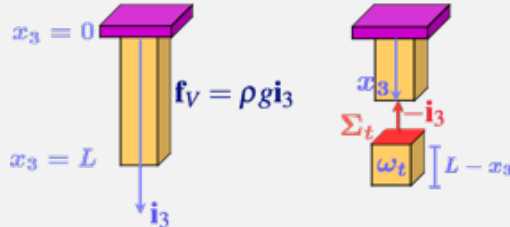


Figure 2.7: Stress vector and components of the stress tensor on an elemental cube.

Given the above definition, and the proposed modelling for internal forces, the stresses are similar to surface force densities, and are therefore expressed in N/m<sup>2</sup> or Pa. In practice, since the atmospheric pressure within a gas is in the order of one bar, or 0.1 MPa, for most deformable media that can be studied, we typically use the MPa (or N/mm<sup>2</sup>), with stresses that can evolve up to several hundreds (or even thousands) of MPa without failure for the most resistant materials. The following chapter will be devoted to the criteria used to assess this resistance.

**■ Example 2.2 — Bar under the action of gravity: global approach.** We consider the case of a rectangular parallelepiped, the upper face of which is attached to a perfectly rigid and fixed support. This bar is in static equilibrium when subjected to the action of gravity, as well as to the action of the support.

We define  $\mathbf{i}_3$  as the unit vertical vector (which is oriented downwards for simplicity) so that the upper face is in  $x_3 = 0$ , and the lower face is in  $x_3 = L$ , as shown in the figure below. We also assume that the density is uniform throughout the beam.



This beam can then be virtually cut at a given cross-section  $\Sigma_t$  of altitude  $x_3$ , so that the part  $\omega_t$  with altitudes between  $x_3$  and  $L$  can be studied. This part is in static equilibrium thanks to the action of the complementary part  $\omega_t^*$  expressed on the plane  $\Sigma_t$ , which compensates the action of gravity. We then have, in terms of resultant forces:

$$\int_{\Sigma_t} \sigma(-\mathbf{i}_3) dS_x + \int_{\omega_t} \rho g \mathbf{i}_3 dV_x = \mathbf{0}$$

where the stress vector on  $\Sigma_t$  is expressed using the outer unit normal vector  $-\mathbf{i}_3$  at the cut plane.

If we make the simplifying assumption that the stress vector  $\sigma(-\mathbf{i}_3)$  depends only on the altitude  $x_3$ , and is therefore uniform over the entire cut surface  $\Sigma_t$  (this will be justified in Example 2.9), we then arrive at:

$$\sigma(-\mathbf{i}_3)A + \rho g(L - x_3)A\mathbf{i}_3 = \mathbf{0}$$

where  $A$  is the area of the cross-section; thus, the resultant force of the internal forces is, as expected, exactly compensating for the weight of the isolated part, of height  $L - x_3$ . We finally deduce from this that:

$$\sigma(x_3)\mathbf{i}_3 = \rho g(L - x_3)\mathbf{i}_3, \forall x_3 \in (0, L)$$

or, in terms of components expressed in the vector basis  $(\mathbf{i}_1, \mathbf{i}_2, \mathbf{i}_3)$  shown below:

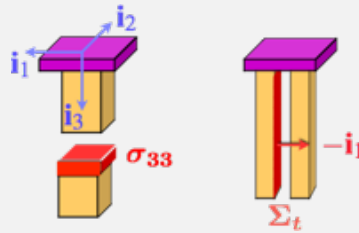
$$\sigma_{13}(x_3) = 0 = \sigma_{23}(x_3), \text{ and } \sigma_{33}(x_3) = \rho g(L - x_3), \forall x_3 \in (0, L)$$

The component  $\sigma_{33}$  being positive, this is referred to as a “tensile” stress, indicating that the stress tends to stretch the material locally. This stress is maximum in  $x_3 = 0$ , and corresponds to the surface force that the fixed support must exert locally to maintain the beam in static equilibrium.

In addition, other cuts can be considered, for example, along a vertical plane of normal vector  $\mathbf{i}_1$ . Thus, for the isolated part represented below, on the right, the outer unit normal vector is  $-\mathbf{i}_1$ , and the equilibrium of the subdomain  $\omega_t$  establishes that:

$$\int_{\Sigma_t} \boldsymbol{\sigma}(-\mathbf{i}_1) dS_x = \mathbf{0}$$

since the action of the support in  $x_3 = 0$  exactly compensates for the action of gravity. Then, by isolating subdomains similar to the previous one, but located between the planes of altitudes  $x_3$  and  $L$ , we can deduce that  $\boldsymbol{\sigma}(x_3)\mathbf{i}_1 = \mathbf{0}$ ,  $\forall x_3 \in (0, L)$ . Physically, we realize on the figure below (right) that everything happens as if we had two half-bars suspended side by side: for each of them, it is the action of the support in  $x_3 = 0$  that compensates for the action of gravity, and it is therefore not necessary for the two half-bars to exert an effort on each other. We will rigorously find this result in Example 2.9.



In terms of components in the vector basis  $(\mathbf{i}_1, \mathbf{i}_2, \mathbf{i}_3)$ , we then obtain that:

$$\boxed{\sigma_{11}(x_3) = \sigma_{21}(x_3) = \sigma_{31}(x_3) = 0, \forall x_3 \in (0, L)}$$

Similarly, by considering cut planes of normal vector  $\mathbf{i}_2$ , we can establish that:

$$\boxed{\sigma_{12}(x_3) = \sigma_{22}(x_3) = \sigma_{32}(x_3) = 0, \forall x_3 \in (0, L)}$$

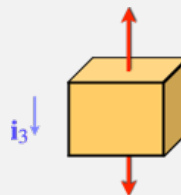
The stress tensor is therefore finally expressed as:

$$\boxed{\boldsymbol{\sigma}(x_3) = \rho g(L - x_3) \mathbf{i}_3 \otimes \mathbf{i}_3}$$

or, in a vector basis  $(\mathbf{i}_1, \mathbf{i}_2, \mathbf{i}_3)$ :

$$\boldsymbol{\sigma}(x_3) = \rho g(L - x_3) \begin{pmatrix} 0 & 0 & 0 \\ 0 & 0 & 0 \\ 0 & 0 & 1 \end{pmatrix}_{(\mathbf{i}_1, \mathbf{i}_2, \mathbf{i}_3)}$$

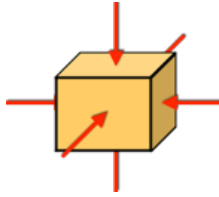
which can also be represented using the elemental cube, defined in Figure 2.7, as below:



representation that justifies the qualification of this stress field as uniaxial. ■



Figure 2.7 has shown that, on a facet, the direction of the stress vector is a priori arbitrary, and therefore is not necessarily normal to that facet. In this respect, the concept of stress generalizes the concept of pressure as it is found in a fluid at rest: indeed, in this latter case, the stress vector is normal to the facet, taking the form  $\mathbf{T} = -p\mathbf{n}$  (where  $p$  is the pressure of the fluid, which depends on space and time a priori), hence the following representation using the elemental cube. The stress tensor is then written simply as  $\boldsymbol{\sigma} = -p\mathbb{I}$ ; given its proportionality to the identity tensor  $\mathbb{I}$ , the stress tensor is then called “isotropic”, or “spherical”.



■ **Example 2.3 — Archimedes' principle: global approach.** We will determine here the expression of the “buoyancy” (or “buoyant force”) that a fluid exerts on a submerged solid. To do this, let us start by isolating in the fluid a sub-domain  $\omega_t$  of arbitrary shape; the resulting (static) equilibrium equation is then written as:

$$\int_{\omega_t} \rho_f g \mathbf{i}_3 dV_x + \int_{\partial \omega_t} \sigma \mathbf{n} dS_x = \mathbf{0}$$

where  $\mathbf{i}_3$  is the vertical unit vector (oriented downwards), and  $\rho_f$  the density of the fluid; since  $\sigma = -p\mathbb{I}$ , with  $p$  the pressure of the fluid, we then have:

$$-\int_{\partial \omega_t} p \mathbf{n} dS_x = -\left( \int_{\omega_t} \rho_f dV_x \right) g \mathbf{i}_3 = -m_f g \mathbf{i}_3$$

where  $m_f$  is the mass of the fluid subdomain  $\omega_t$ . The action of the complementary part  $\omega_t^*$  of  $\omega_t$  within  $\Omega_t$  then allows for compensating for the action of gravity on the subdomain  $\omega_t$ , so that this latter could be in static equilibrium.

If we consider now a submerged solid, whose domain corresponds precisely to the fluid subdomain  $\omega_t$  under study, we can assume, since the complementary part  $\omega_t^*$  is still at rest, that the submerged solid exerts on  $\omega_t^*$  the same action as that exerted by  $\omega_t$ . Using the action-reaction principle, we can then conclude that the action of the fluid subdomain  $\omega_t^*$ , consisting of pressure forces, on the solid has a resultant force  $\mathbf{R}^f$  such that:

$$\boxed{\mathbf{R}^f = -\int_{\partial \omega_t} p \mathbf{n} dS_x = -m_f g \mathbf{i}_3}$$

showing that the buoyant force exerted on the submerged solid is equal to the weight of the “displaced” fluid volume, i.e. the weight corresponding to a volume  $|\omega_t|$  of fluid. ■

### Symmetry property

So far, we have only used the conservation of momentum as a means of determining the stress tensor. It is, of course, possible to obtain additional information from the application of the conservation of angular momentum to any sub-domain  $\omega_t$  contained in the domain  $\Omega_t$ .

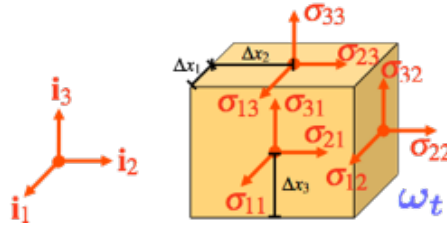


Figure 2.8: Equilibrium in terms of moments of an elemental rectangular parallelepiped.

Thus, if we consider an elemental sub-domain  $\omega_t$  in the form of a rectangular parallelepiped, centered on a point  $\mathbf{x}_O$ , the conservation of angular momentum at point  $O$  allows us to write:

$$\int_{\omega_t} (\mathbf{x} - \mathbf{x}_O) \wedge (\rho \mathbf{a} - \mathbf{f}_V) dV_x = \int_{\partial \omega_t} (\mathbf{x} - \mathbf{x}_O) \wedge \sigma \mathbf{n} dS_x$$

As in the case of the dynamic equilibrium of the Cauchy tetrahedron, studied above, it can be established that the volume integral can be neglected in the previous expression when compared to

the surface integral, and that this latter can be approximated as:

$$\mathbf{0} = \int_{\partial\Omega_t} (\mathbf{x} - \mathbf{x}_O) \wedge \boldsymbol{\sigma} \mathbf{n} dS_x \approx \sum_{k=1}^3 \Delta x_{i \neq k} \Delta x_{j \neq k} \Delta x_k \mathbf{i}_k \wedge \boldsymbol{\sigma}(\mathbf{x}_O, t) \mathbf{i}_k$$

with the notations of Figure 2.8. By specifying in this equilibrium equation in terms of moments the stress vectors using the components of  $\boldsymbol{\sigma}$  on the basis  $(\mathbf{i}_1, \mathbf{i}_2, \mathbf{i}_3)$ , we find that:

$$\sum_{k=1}^3 \mathbf{i}_k \wedge (\sigma_{1k} \mathbf{i}_1 + \sigma_{2k} \mathbf{i}_2 + \sigma_{3k} \mathbf{i}_3) = \mathbf{0}$$

or, by expanding:

$$(\sigma_{32} - \sigma_{23}) \mathbf{i}_1 + (\sigma_{13} - \sigma_{31}) \mathbf{i}_2 + (\sigma_{21} - \sigma_{12}) \mathbf{i}_3 = \mathbf{0}$$

which shows the symmetry of the stress tensor:

$$\boldsymbol{\sigma}(\mathbf{x}_O, t) = \boldsymbol{\sigma}(\mathbf{x}_O, t)^T, \forall \mathbf{x}_O \in \Omega_t, \forall t$$

Consequently, the existence of a tangential component (along a direction  $\mathbf{t}$ ) of the stress vector on a facet of given orientation  $\mathbf{n}$  necessarily implies, at the same point, a tangential component of direction  $\mathbf{n}$  and of the same intensity on a facet of orientation  $\mathbf{t}$ . This stress field, referred to as “pure shear”, is shown in Figure 2.9.

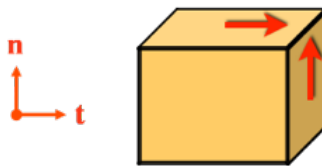


Figure 2.9: Pure shear.



*This result is a direct consequence of having modelled the actions within the domain as volume force densities only. In some cases, this may be insufficient: in magneto-hydrodynamics, for example, where ionized gas flows are coupled with magnetic effects, it is necessary to introduce volume torque densities  $\mathbf{c}_V$  at each point of the domain, which results in the following relations between the components of  $\boldsymbol{\sigma}$ :*

$$\sum_{k=1}^3 \mathbf{i}_k \wedge (\sigma_{1k} \mathbf{i}_1 + \sigma_{2k} \mathbf{i}_2 + \sigma_{3k} \mathbf{i}_3) + \mathbf{c}_V = \mathbf{0}$$

*at any point of the domain. The stress tensor is then not symmetrical.*

**Summary 2.4 — Cauchy stress tensor.** The Cauchy stress tensor is a tensor  $\boldsymbol{\sigma}$  allowing us to express, at any point of a material domain  $\Omega_t$ , and at any time, the internal forces on a facet of unit normal vector  $\mathbf{n}$  as the following stress vector:

$$\mathbf{T}(\mathbf{x}, t, \mathbf{n}) = \boldsymbol{\sigma}(\mathbf{x}, t) \mathbf{n}, \forall \mathbf{x} \in \Omega_t, \forall t$$

Using an orthonormal vector basis  $(\mathbf{i}_1, \mathbf{i}_2, \mathbf{i}_3)$  and the knowledge of these internal forces on three facets of respective normal vectors  $\mathbf{i}_k$ , we can express this tensor as:

$$\boldsymbol{\sigma}(\mathbf{x}, t) = \sum_{k=1}^3 \mathbf{T}(\mathbf{x}, t, \mathbf{i}_k) \otimes \mathbf{i}_k, \forall \mathbf{x} \in \Omega_t, \forall t$$

In addition, in the framework proposed in the course, the stress tensor is symmetrical:

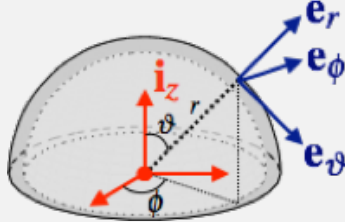
$$\boldsymbol{\sigma}(\mathbf{x}, t) = \boldsymbol{\sigma}(\mathbf{x}, t)^T, \forall \mathbf{x} \in \Omega_t, \forall t$$

■ **Example 2.4 — Spherical pressure tank: global approach.** We consider here the case of a spherical tank, with an inner radius  $R$  and a thickness  $e$ , similar to the illustration below, and whose function is to contain gas under pressure. We try to estimate the stresses within the wall of this tank, in the typical case where its thickness is much smaller than its radius ( $e \ll R$ ) and assuming that we can consider the gas pressure  $p$  as uniform.



We also assume that the action of gravity is negligible when compared to the action of internal pressure  $p$  so that this latter can be considered to be the only action exerted on the tank (the action of the support on the tank being, in fact, also neglected).

We propose to isolate the upper half-tank, obtained after cutting the structure along a horizontal plane passing through its center; we then use the spherical vector basis  $(\mathbf{e}_r, \mathbf{e}_\vartheta, \mathbf{e}_\phi)$  associated with the coordinates  $(r, \vartheta, \phi)$ .



Given the spherical symmetry of the geometry and stresses (the fluid pressure is uniform and is normally exerted on the inner surface of the tank), it can be assumed that the stress tensor components are independent of the angles  $\vartheta$  and  $\phi$ , and that the vectors  $\mathbf{e}_\vartheta$  and  $\mathbf{e}_\phi$  play similar roles. We can thus write the stress tensor as:

$$\begin{aligned} \boldsymbol{\sigma}(r, \vartheta, \phi) = & \sigma_{rr}(r)\mathbf{e}_r(\vartheta, \phi) \otimes \mathbf{e}_r(\vartheta, \phi) + \sigma_{\vartheta\vartheta}(r)\mathbf{e}_\vartheta(\vartheta, \phi) \otimes \mathbf{e}_\vartheta(\vartheta, \phi) + \sigma_{\phi\phi}(r)\mathbf{e}_\phi(\phi) \otimes \mathbf{e}_\phi(\phi) \\ & + 2\sigma_{r\vartheta}(r)\mathbf{e}_r(\vartheta, \phi) \otimes_S \mathbf{e}_\vartheta(\vartheta, \phi) + 2\sigma_{r\phi}(r)\mathbf{e}_r(\vartheta, \phi) \otimes_S \mathbf{e}_\phi(\phi) \\ & + 2\sigma_{\vartheta\phi}(r)\mathbf{e}_\vartheta(\vartheta, \phi) \otimes_S \mathbf{e}_\phi(\phi) \end{aligned}$$

with  $\sigma_{\vartheta\vartheta}(r) = \sigma_{\phi\phi}(r)$  and  $\sigma_{r\vartheta}(r) = \sigma_{r\phi}(r)$ ,  $\forall r$ , and where  $\mathbf{a} \otimes_S \mathbf{b} = (\mathbf{a} \otimes \mathbf{b} + \mathbf{b} \otimes \mathbf{a})/2$ ,  $\forall \mathbf{a}, \mathbf{b}$ .

Since the cut plane is  $(\mathbf{e}_r, \mathbf{e}_\phi)$ , the static equilibrium of the half tank is then written as:

$$\mathbf{0} = \int_{\Sigma_i \cup \Sigma_e \cup \Sigma_0} \boldsymbol{\sigma} \mathbf{n} dS_x = \int_{\Sigma_i} \boldsymbol{\sigma}(-\mathbf{e}_r) dS_x + \int_{\Sigma_e} \boldsymbol{\sigma} \mathbf{e}_r dS_x + \int_{\Sigma_0} \boldsymbol{\sigma} \mathbf{e}_\vartheta dS_x$$

where  $\Sigma_i$  denotes the inner surface in contact with the pressurized fluid,  $\Sigma_e$  the outer surface under atmospheric pressure (considered equal to zero), and  $\Sigma_0$  the cut surface, of outer unit normal vector  $\mathbf{e}_\vartheta$ . By approximating that the stress vector on this latter is uniform given the very thin thickness of the wall of the tank, we can then establish that:

$$\mathbf{0} = p \int_{\Sigma_i} \mathbf{e}_r dS_x + A_0 \boldsymbol{\sigma} \mathbf{e}_\vartheta$$

where  $A_0 \approx 2\pi Re$  is the area of the cut surface when assuming  $e \ll R$ . Considering the symmetries, and the fact that, on  $\Sigma_0$ ,  $\mathbf{e}_\vartheta = -\mathbf{i}_z$  (with  $\mathbf{i}_z$  the vertical unit vector, oriented upward), it is easy to show that:

$$\int_{\Sigma_i} \mathbf{e}_r dS_x = \pi R^2 \mathbf{i}_z$$

where  $\pi R^2$  corresponds to what is called the projected area of  $\Sigma_i$  perpendicular to  $\mathbf{i}_z$ . We then find for  $e \ll R$  that:

$$\sigma_{\vartheta\vartheta} \approx \frac{pR}{2e}$$

and that the shear stresses  $\sigma_{r\vartheta}$  are  $\sigma_{\vartheta\phi}$  are equal to zero in the wall.

In order to determine the radial stress, this time a circumferential part of the half tank can be isolated:  $\omega_t^\rho = \{\mathbf{x} = r\mathbf{e}_r(\vartheta, \phi) | R + \rho \leq r \leq R + e, 0 \leq \vartheta \leq \pi/2\}$ , with  $0 < \rho < e$ . The resulting static equilibrium equation gives us:

$$\mathbf{0} = \int_{\Sigma_\rho \cup \Sigma_e \cup \Sigma_0} \boldsymbol{\sigma} \mathbf{n} dS_x = \int_{\Sigma_\rho} \boldsymbol{\sigma}(-\mathbf{e}_r) dS_x + \int_{\Sigma_e} \boldsymbol{\sigma} \mathbf{e}_r dS_x + \int_{\Sigma_0^*} \boldsymbol{\sigma} \mathbf{e}_\vartheta dS_x$$

where  $\Sigma_\rho$  is the circumferential cut surface ( $r = R + \rho$ ), and  $\Sigma_0^*$  the diametrical cut surface. We then find that:

$$0 = \pi(R + \rho)^2 \sigma_{rr}(R + \rho) + A_0^* \sigma_{\vartheta\vartheta}$$

with  $A_0^* \approx 2\pi R(e - \rho)$  when  $e \ll R$ . We then get:

$$\sigma_{rr}(R + \rho) \approx -p \frac{R^2(e - \rho)}{e(R + \rho)^2} \approx p \frac{\rho - e}{e}$$

i.e. a linear evolution of the radial stress in the thickness of the wall, when  $e \ll R$ .

Finally, with some simplifying hypotheses, the following stress tensor is obtained in the case of a thin-walled tank:

$$\boldsymbol{\sigma}(r, \vartheta, \phi) = p \frac{r - R - e}{e} \mathbf{e}_r(\vartheta, \phi) \otimes \mathbf{e}_r(\vartheta, \phi) + \frac{pR}{2e} (\mathbf{e}_\vartheta(\vartheta, \phi) \otimes \mathbf{e}_\vartheta(\vartheta, \phi) + \mathbf{e}_\phi(\phi) \otimes \mathbf{e}_\phi(\phi))$$

It can also be seen that the circumferential stresses are predominant in the wall, since  $p = |\sigma_{rr}|_{max} \ll \sigma_{\vartheta\vartheta} = \sigma_{\phi\phi} = \frac{pR}{2e}$  when  $e \ll R$ . ■

## 2.3 Local equilibrium equation

We have seen earlier how to model internal forces within a material domain, and that it was possible to estimate them by applying the conservation of momentum to specific isolated sub-domains. However, this estimation is complex in use when it comes to the global application of the fundamental principles of dynamics because it requires choosing sub-domains to be isolated in a relevant manner; this is why in practice we prefer to use as an alternative a local equilibrium equation, verified at every point within the material domain.

### 2.3.1 Obtaining the equation

The starting point is, as before, to write the conservation of momentum for a sub-domain  $\omega_t$  of  $\Omega_t$ :

$$\int_{\omega_t} (\rho \mathbf{a} - \mathbf{f}_V) dV_x = \int_{\partial \omega_t} \boldsymbol{\sigma} \mathbf{n} dS_x$$

where we have replaced the stress vector by its expression using the stress tensor  $\boldsymbol{\sigma}$  and the outer unit normal vector  $\mathbf{n}$  at any point on the boundary. In order to establish a local formulation, formally, we would like to consider a sub-domain  $\omega_t$  around a point  $\mathbf{x}_O$ , whose size we would reduce in order to be able to assimilate the volume integral to the value of the integrand at point  $\mathbf{x}_O$ . This requires first transforming the surface integral on the boundary of  $\omega_t$  to a volume integral. To do this, we

consider the scalar product of the previous equation by a constant and arbitrary vector  $\mathbf{c}$ :

$$\int_{\omega_t} \langle \rho \mathbf{a} - \mathbf{f}_V, \mathbf{c} \rangle dV_x = \int_{\partial \omega_t} \langle \boldsymbol{\sigma} \mathbf{n}, \mathbf{c} \rangle dS_x$$

hence, by using the transposition property for the scalar product:

$$\int_{\omega_t} \langle \rho \mathbf{a} - \mathbf{f}_V, \mathbf{c} \rangle dV_x = \int_{\partial \omega_t} \langle \boldsymbol{\sigma}^T \mathbf{c}, \mathbf{n} \rangle dS_x$$

Using the divergence theorem, given in Appendix B.2.2, we can then transform the surface integral on the boundary of  $\omega_t$  into a volume integral on the subdomain:

$$\int_{\omega_t} \langle \rho \mathbf{a} - \mathbf{f}_V, \mathbf{c} \rangle dV_x = \int_{\omega_t} \operatorname{div}_{\mathbf{x}}(\boldsymbol{\sigma}^T \mathbf{c}) dV_x$$

where  $\operatorname{div}_{\mathbf{x}}$  is the divergence operator for a vector expressed in the current configuration. Since the integrand of the right-hand side is linear with respect to  $\mathbf{c}$ , the following definition is then introduced to pursue the reasoning.

**Divergence of the stress tensor.** The divergence of the stress tensor (expressed in the current configuration) is the vector, noted  $\operatorname{div}_{\mathbf{x}} \boldsymbol{\sigma}$ , defined as:

$$\langle \operatorname{div}_{\mathbf{x}} \boldsymbol{\sigma}, \mathbf{c} \rangle = \operatorname{div}_{\mathbf{x}}(\boldsymbol{\sigma}^T \mathbf{c}), \forall \mathbf{c} \text{ constant}$$

By successively choosing for  $\mathbf{c}$  the vectors of a Cartesian basis  $(\mathbf{i}_1, \mathbf{i}_2, \mathbf{i}_3)$ , we then obtain the associated components of the divergence vector, using the well-known expression of the divergence of a vector (recalled in Appendix B.1.1):

$$\langle \operatorname{div}_{\mathbf{x}} \boldsymbol{\sigma}, \mathbf{i}_m \rangle = \operatorname{div}_{\mathbf{x}}(\boldsymbol{\sigma}^T \mathbf{i}_m) = \sum_{n=1}^3 \frac{\partial \langle \boldsymbol{\sigma}^T \mathbf{i}_m, \mathbf{i}_n \rangle}{\partial x_n} = \sum_{n=1}^3 \frac{\partial \sigma_{mn}}{\partial x_n}, 1 \leq m \leq 3$$

where  $(x_1, x_2, x_3)$  are the Cartesian coordinates, and  $\sigma_{mn}$  are the components of  $\boldsymbol{\sigma}$ , associated with the vector basis  $(\mathbf{i}_1, \mathbf{i}_2, \mathbf{i}_3)$ . Thus, in a Cartesian coordinate system, the components of the divergence of the stress tensor are formally calculated as the (scalar) divergence of the row vectors of the associated matrix.

In addition, this definition allows for defining what is known as the generalized divergence theorem:

$$\int_{\partial \omega_t} \boldsymbol{\sigma}(\mathbf{x}, t) \mathbf{n}(\mathbf{x}) dS_t = \int_{\omega_t} \operatorname{div}_{\mathbf{x}} \boldsymbol{\sigma}(\mathbf{x}, t) dV_t$$

where  $\mathbf{n}(\mathbf{x})$  is the outer unit normal vector at any point on the boundary.

By substituting the previous definition in the dynamic equilibrium equation, we obtain:

$$\int_{\omega_t} \langle \rho \mathbf{a} - \mathbf{f}_V - \operatorname{div}_{\mathbf{x}} \boldsymbol{\sigma}, \mathbf{c} \rangle dV_x = 0$$

which is valid regardless of the sub-domain  $\omega_t$  isolated within the domain  $\Omega_t$ . We can then deduce that the integrand then vanishes, and this, regardless the point under study:

$$\rho(\mathbf{x}, t) \mathbf{a}(\mathbf{x}, t) = \mathbf{f}_V(\mathbf{x}, t) + \operatorname{div}_{\mathbf{x}} \boldsymbol{\sigma}(\mathbf{x}, t), \forall \mathbf{x} \in \Omega_t, \forall t$$

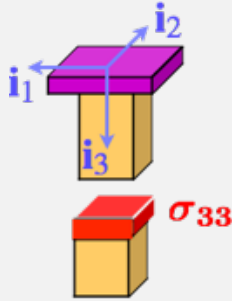
which is the local equilibrium equation verified by the stress tensor within the material domain.

■ **Example 2.5 — Bar under the action of gravity: verification of the local equilibrium equation.**

Let us consider once again Example 2.2 for which we had determined, with some assumptions of common sense, the stress tensor inside a bar suspended from a fixed support, and subjected to the action of gravity:

$$\sigma(x_3) = \rho g(L - x_3) \mathbf{i}_3 \otimes \mathbf{i}_3$$

with the conventions in the figure below.



Now let us see if the local equilibrium equation is actually satisfied; for that, we calculate the divergence of the tensor  $\sigma$  in the Cartesian vector basis  $(\mathbf{i}_1, \mathbf{i}_2, \mathbf{i}_3)$ , as the divergence of the row vectors of the matrix  $\sigma$ :

$$\begin{aligned}\langle \operatorname{div}_{\mathbf{x}} \sigma, \mathbf{i}_1 \rangle &= \frac{\partial \sigma_{11}}{\partial x_1} + \frac{\partial \sigma_{12}}{\partial x_2} + \frac{\partial \sigma_{13}}{\partial x_3} = 0 \\ \langle \operatorname{div}_{\mathbf{x}} \sigma, \mathbf{i}_2 \rangle &= \frac{\partial \sigma_{21}}{\partial x_1} + \frac{\partial \sigma_{22}}{\partial x_2} + \frac{\partial \sigma_{23}}{\partial x_3} = 0 \\ \langle \operatorname{div}_{\mathbf{x}} \sigma, \mathbf{i}_3 \rangle &= \frac{\partial \sigma_{31}}{\partial x_1} + \frac{\partial \sigma_{32}}{\partial x_2} + \frac{\partial \sigma_{33}}{\partial x_3} = -\rho g\end{aligned}$$

We have thus:

$$\operatorname{div}_{\mathbf{x}} \sigma + \mathbf{f}_V = -\rho g \mathbf{i}_3 + \rho g \mathbf{i}_3 = \mathbf{0}, \forall \mathbf{x}$$

which effectively corresponds to a state of static equilibrium ( $\mathbf{a} = \mathbf{0}$ ). ■



A physical interpretation of the divergence of the stress tensor is as follows. If we consider an elemental rectangular parallelepiped  $\omega_t$  centered on a point  $\mathbf{x}$  of coordinates  $(x_1, x_2, x_3)$  in a Cartesian vector basis  $(\mathbf{i}_1, \mathbf{i}_2, \mathbf{i}_3)$ , the application of the generalized divergence theorem allows us to write that:

$$\int_{\omega_t} \operatorname{div}_{\mathbf{x}} \sigma dV_t = \int_{\partial \omega_t} \sigma \mathbf{n} dS_t$$

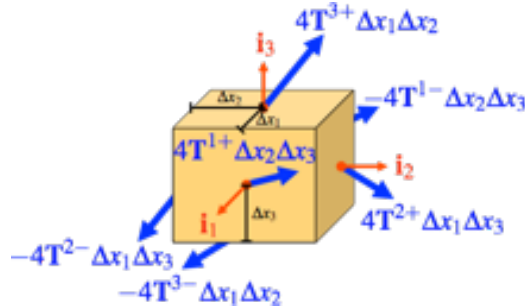
or, for a rectangular parallelepiped whose dimensions  $2\Delta x_k$  along the respective directions  $\mathbf{i}_k$  become very small:

$$8\Delta x_1 \Delta x_2 \Delta x_3 \operatorname{div}_{\mathbf{x}} \sigma(\mathbf{x}, t) \approx \sum_{k=1}^3 4\Delta x_{i \neq k} \Delta x_{j \neq k} (\sigma(\mathbf{x} + \Delta x_k \mathbf{i}_k, t) \mathbf{i}_k + \sigma(\mathbf{x} - \Delta x_k \mathbf{i}_k, t) (-\mathbf{i}_k))$$

which makes it possible to obtain, by defining, for  $1 \leq k \leq 3$ ,  $\mathbf{T}^{k\pm} = \sigma(\mathbf{x} \pm \Delta x_k \mathbf{i}_k, t) \mathbf{i}_k$  as the stress vector according to each vector of the basis:

$$\operatorname{div}_{\mathbf{x}} \sigma \approx \sum_{k=1}^3 \frac{1}{2\Delta x_k} (\mathbf{T}^{k+} - \mathbf{T}^{k-})$$

as shown in the figure below; this shows the balance of the resultant forces of the surface force densities on the faces of the parallelepiped.



The divergence of the stress tensor thus represents the local balance of the internal surface forces applied within the material to the faces of the elemental parallelepiped: this balance is expressed as the variation of the stress vector according to the three directions associated with the Cartesian basis.

**■ Example 2.6 — Archimedes' principle: local approach.** We can establish here, using the local equilibrium equation, the result about the buoyancy force, which we had established in a global and intuitive way in Example 2.3. Considering the form of the stress tensor for a fluid at rest, of density  $\rho_f$  ( $\mathfrak{G} = -p\mathbb{I}$ , where  $p$  is the fluid pressure), the local equilibrium equation allows us to establish that:

$$\mathbf{0} = \mathbf{f}_v + \operatorname{div}_{\mathbf{x}}(-p\mathbb{I}) = \rho_f g \mathbf{i}_3 - \sum_{k=1}^3 \frac{\partial p}{\partial x_k} \mathbf{i}_k$$

in the case of a Cartesian vector basis  $(\mathbf{i}_1, \mathbf{i}_2, \mathbf{i}_3)$ , where  $\mathbf{i}_3$  is a vertical (downward) unit vector. Noting  $\nabla_{\mathbf{x}} p$  as the gradient of  $p$ , we thus obtain:

$$\boxed{\nabla_{\mathbf{x}} p = \rho_f g \mathbf{i}_3}$$

This result reflects the well-known fact that pressure increases linearly with depth (provided the density  $\rho_f$  is uniform).

If we now consider a solid whose domain  $\omega_t$  is totally immersed in the fluid, the action exerted by this latter on the solid is given by all the pressure forces on its boundary  $\partial\omega_t$ , of resultant force:

$$\mathbf{R}^f = - \int_{\partial\omega_t} p \mathbf{n} dS_x$$

where  $\mathbf{n}$  is the outer normal vector at any point on the boundary of the solid. We then use Stokes' theorem, obtained in Appendix B.2.2, which allows us to write that:

$$\int_{\partial\omega_t} p \mathbf{n} dS_x = \int_{\omega_t} \nabla_{\mathbf{x}} p dV_x$$

The resultant force of the pressure forces applied to a closed surface is thus linked to the resultant force of the gradient of these latter in the volume contained in the surface under study. Since the pressure evolution within the fluid is not influenced by the presence of the solid, and therefore verifies the gradient vector established above, we can simply write that:

$$\mathbf{R}^f = - \int_{\omega_t} \nabla_{\mathbf{x}} p dV_x = - \int_{\omega_t} \rho_f g \mathbf{i}_3 dV_x = -m_f g \mathbf{i}_3$$

where  $m_f g$  is the weight corresponding to a volume  $|\omega_t|$  of fluid.

Besides, it is easy to generalize this result for a partially immersed solid; in this case, the emerged part is subjected to the pressure of the surrounding air, which, according to the local equilibrium equation, also verifies a gradient vector of similar shape. The previous approach then allows us to obtain in the same way that, in this case, the buoyancy is equal to:

$$\boxed{\mathbf{R}^f = -(m_f + m_a)g \mathbf{i}_3}$$

where  $m_f g$  is the weight corresponding to a volume of fluid equal to the volume of submerged solid, and  $m_a g$  is the weight corresponding to an air volume equal to the volume of emerged solid. As, in practice for a liquid,  $m_a g \ll m_f g$ , the buoyancy is finally expressed as:

$$\mathbf{R}^f \approx -m_f g \mathbf{i}_3$$

hence the usual statement that the buoyancy is equal to the weight of displaced liquid. ■

**R** As in the case of the conservation of (linear) momentum, it is possible to consider locally the principle of conservation of angular momentum; for any sub-domain  $\omega_t$  contained in the domain  $\Omega_t$ , we can write that, at a fixed point  $O$ :

$$\int_{\omega_t} (\mathbf{x} - \mathbf{x}_O) \wedge (\rho \mathbf{a} - \mathbf{f}_V) dV_x = \int_{\partial \omega_t} (\mathbf{x} - \mathbf{x}_O) \wedge \sigma \mathbf{n} dS_x$$

To transform the surface integral on the boundary, a variant of the divergence theorem, obtained in Appendix B.2.2, is then used, in a Cartesian vector basis  $(\mathbf{i}_1, \mathbf{i}_2, \mathbf{i}_3)$ :

$$\int_{\partial \omega_t} (\mathbf{x} - \mathbf{x}_O) \wedge \sigma \mathbf{n} dS_x = \int_{\omega_t} \left( (\mathbf{x} - \mathbf{x}_O) \wedge \operatorname{div}_{\mathbf{x}} \sigma + \sum_{n=1}^3 \mathbf{i}_n \wedge \sigma \mathbf{i}_n \right) dV_x$$

where we verify, according to the local equilibrium equation, that:

$$\operatorname{div}_{\mathbf{x}} \sigma = \rho \mathbf{a} - \mathbf{f}_V$$

After simplification, we then obtain:

$$\int_{\partial \omega_t} \sum_{n=1}^3 \mathbf{i}_n \wedge \sigma \mathbf{i}_n dS_x = \mathbf{0}$$

Knowing that this relationship is true regardless of the isolated material sub-domain  $\omega_t$ , the integrand is actually equal to zero at any point in the domain  $\Omega_t$ . By developing the expressions of the stress vectors using the components of  $\sigma$  in the vector basis  $(\mathbf{i}_1, \mathbf{i}_2, \mathbf{i}_3)$ , we get:

$$\mathbf{0} = \sum_{n=1}^3 \mathbf{i}_n \wedge \left( \sum_{m=1}^3 \sigma_{mn} \mathbf{i}_m \right) = \sum_{1 \leq m < n \leq 3} (\sigma_{nm} - \sigma_{mn}) \mathbf{i}_m \wedge \mathbf{i}_n$$

which allows us to recover, as expected, the symmetry property of the stress tensor.

### Tensor expressions of the divergence of the stress tensor

As with kinematics in the previous chapter, it is often more interesting to perform calculations directly in a tensor way, rather than using tensor components in a given vector basis.

Thus, we have seen that the components of the divergence of the stress tensor in a Cartesian vector basis  $(\mathbf{i}_1, \mathbf{i}_2, \mathbf{i}_3)$  can be expressed as:

$$\langle \operatorname{div}_{\mathbf{x}} \sigma, \mathbf{i}_m \rangle = \sum_{n=1}^3 \frac{\partial \sigma_{mn}}{\partial x_n}, \quad 1 \leq m \leq 3$$

where  $(x_1, x_2, x_3)$  are the Cartesian coordinates associated with this basis. We deduce from this that, since  $\mathbf{i}_n$  is constant:

$$\operatorname{div}_{\mathbf{x}} \sigma = \sum_{m=1}^3 \sum_{n=1}^3 \frac{\partial \sigma_{mn}}{\partial x_n} \mathbf{i}_m = \sum_{n=1}^3 \frac{\partial (\sum_{m=1}^3 \sigma_{mn} \mathbf{i}_m)}{\partial x_n} = \sum_{n=1}^3 \frac{\partial \sigma \mathbf{i}_n}{\partial x_n}$$

hence, finally, the intrinsic expression:

$$\operatorname{div}_{\mathbf{x}} \sigma = \sum_{n=1}^3 \frac{\partial \sigma}{\partial x_n} \mathbf{i}_n$$

where  $\sigma$  is expressed using tensor products, which may not involve the vectors of the basis  $(\mathbf{i}_1, \mathbf{i}_2, \mathbf{i}_3)$ .

Besides, in the case of curved parts, it may be more interesting to use curvilinear coordinates with an associated vector basis. In the case of a cylindrical geometry with an axis  $\mathbf{i}_z$ , we then express the stress tensor as:

$$\begin{aligned} \sigma(\mathbf{x}, t) = & \sigma_{rr}(r, \theta, z, t) \mathbf{i}_r(\theta) \otimes \mathbf{i}_r(\theta) + \sigma_{\theta\theta}(r, \theta, z, t) \mathbf{i}_\theta(\theta) \otimes \mathbf{i}_\theta(\theta) + \sigma_{zz}(r, \theta, z, t) \mathbf{i}_z \otimes \mathbf{i}_z \\ & + 2\sigma_{r\theta}(r, \theta, z, t) \mathbf{i}_r(\theta) \otimes_S \mathbf{i}_\theta(\theta) + 2\sigma_{rz}(r, \theta, z, t) \mathbf{i}_r(\theta) \otimes_S \mathbf{i}_z + 2\sigma_{\theta z}(r, \theta, z, t) \mathbf{i}_\theta(\theta) \otimes_S \mathbf{i}_z \end{aligned}$$

considering its symmetry property. By applying the chain rule in the expression of the divergence obtained above, we obtain:

$$\mathbf{div}_x \boldsymbol{\sigma} = \sum_{n=1}^3 \left( \frac{\partial \boldsymbol{\sigma}}{\partial r} \frac{\partial r}{\partial x_n} + \frac{\partial \boldsymbol{\sigma}}{\partial \theta} \frac{\partial \theta}{\partial x_n} + \frac{\partial \boldsymbol{\sigma}}{\partial z} \frac{\partial z}{\partial x_n} \right) \mathbf{i}_n$$

where we can group together:

$$\sum_{n=1}^3 \frac{\partial r}{\partial x_n} \mathbf{i}_n = \nabla_x r, \quad \sum_{n=1}^3 \frac{\partial \theta}{\partial x_n} \mathbf{i}_n = \nabla_x \theta, \quad \sum_{n=1}^3 \frac{\partial z}{\partial x_n} \mathbf{i}_n = \nabla_x z$$

where  $\nabla_x$  refers to the gradient in the current configuration. As set out in Appendix B.3.2:  $\nabla_x r = \mathbf{i}_r$ ,  $\nabla_x \theta = \mathbf{i}_\theta / r$  and  $\nabla_x z = \mathbf{i}_z$ , so we finally end up with:

$$\mathbf{div}_x \boldsymbol{\sigma} = \frac{\partial \boldsymbol{\sigma}}{\partial r} \mathbf{i}_r + \frac{\partial \boldsymbol{\sigma}}{\partial \theta} \frac{\mathbf{i}_\theta}{r} + \frac{\partial \boldsymbol{\sigma}}{\partial z} \mathbf{i}_z$$

which can be clarified in the form of the following vector expression:

$$\begin{aligned} \mathbf{div}_x \boldsymbol{\sigma} &= \left( \frac{\partial \sigma_{rr}}{\partial r} + \frac{1}{r} \frac{\partial \sigma_{r\theta}}{\partial \theta} + \frac{\partial \sigma_{rz}}{\partial z} + \frac{\sigma_{rr} - \sigma_{\theta\theta}}{r} \right) \mathbf{i}_r \\ &\quad + \left( \frac{\partial \sigma_{r\theta}}{\partial r} + \frac{1}{r} \frac{\partial \sigma_{\theta\theta}}{\partial \theta} + \frac{\partial \sigma_{\theta z}}{\partial z} + 2 \frac{\sigma_{r\theta}}{r} \right) \mathbf{i}_\theta \\ &\quad + \left( \frac{\partial \sigma_{rz}}{\partial r} + \frac{1}{r} \frac{\partial \sigma_{\theta z}}{\partial \theta} + \frac{\partial \sigma_{zz}}{\partial z} + \frac{\sigma_{rz}}{r} \right) \mathbf{i}_z \end{aligned}$$

since:

$$\frac{\partial \mathbf{i}_r}{\partial \theta}(\theta) = \mathbf{i}_\theta(\theta), \text{ and } \frac{\partial \mathbf{i}_\theta}{\partial \theta}(\theta) = -\mathbf{i}_r(\theta)$$

and since the derivative of a tensor product is similar to the derivative of a product:

$$\frac{\partial(\mathbf{a} \otimes \mathbf{b})}{\partial x_k} = \left( \frac{\partial \mathbf{a}}{\partial x_k} \right) \otimes \mathbf{b} + \mathbf{a} \otimes \left( \frac{\partial \mathbf{b}}{\partial x_k} \right), \forall \mathbf{a}, \mathbf{b}$$

In addition, the following example illustrates the calculation of the stress tensor divergence when using a spherical vector basis.

**■ Example 2.7 — Spherical pressure tank: verification of the local equilibrium equation.** Here we consider the case of a spherical tank under internal pressure: Example 2.4 had made it possible to determine the stress tensor in the case of a thin-walled tank ( $e \ll R$ ):

$$\boxed{\boldsymbol{\sigma} = p \frac{r - R - e}{e} \mathbf{e}_r \otimes \mathbf{e}_r + \frac{pR}{2e} (\mathbf{e}_\vartheta \otimes \mathbf{e}_\vartheta + \mathbf{e}_\phi \otimes \mathbf{e}_\phi)}$$

Using the results of Appendix B.3.3, we can establish that the divergence of the stress tensor is written, in spherical coordinates, as:

$$\mathbf{div}_x \boldsymbol{\sigma} = \frac{\partial \boldsymbol{\sigma}}{\partial r} \mathbf{e}_r + \frac{\partial \boldsymbol{\sigma}}{\partial \vartheta} \frac{\mathbf{e}_\vartheta}{r} + \frac{\partial \boldsymbol{\sigma}}{\partial \phi} \frac{\mathbf{e}_\phi}{r \sin \vartheta}$$

or, in terms of components:

$$\begin{aligned} \mathbf{div}_x \boldsymbol{\sigma} &= \left( \frac{\partial \sigma_{rr}}{\partial r} + \frac{1}{r} \frac{\partial \sigma_{r\vartheta}}{\partial \vartheta} + \frac{1}{r \sin \vartheta} \frac{\partial \sigma_{r\phi}}{\partial \phi} + \frac{2\sigma_{rr} - \sigma_{\vartheta\vartheta} - \sigma_{\phi\phi} + \sigma_{r\vartheta} \cot \vartheta}{r} \right) \mathbf{e}_r \\ &\quad + \left( \frac{\partial \sigma_{r\vartheta}}{\partial r} + \frac{1}{r} \frac{\partial \sigma_{\vartheta\vartheta}}{\partial \vartheta} + \frac{1}{r \sin \vartheta} \frac{\partial \sigma_{\vartheta\phi}}{\partial \phi} + \frac{(\sigma_{\vartheta\vartheta} - \sigma_{\phi\phi}) \cot \vartheta + 3\sigma_{r\vartheta}}{r} \right) \mathbf{e}_\vartheta \\ &\quad + \left( \frac{\partial \sigma_{r\phi}}{\partial r} + \frac{1}{r} \frac{\partial \sigma_{\vartheta\phi}}{\partial \vartheta} + \frac{1}{r \sin \vartheta} \frac{\partial \sigma_{\phi\phi}}{\partial \phi} + \frac{3\sigma_{r\phi} + 2\sigma_{\vartheta\phi} \cot \vartheta}{r} \right) \mathbf{e}_\phi \end{aligned}$$

In this specific case, we establish that:

$$\mathbf{div}_x \boldsymbol{\sigma} \approx \left( \frac{p}{e} + 2p \frac{r-R-e}{er} - p \frac{R}{er} \right) \mathbf{e}_r \approx \frac{p}{eR} (3(r-R) - 2e) \mathbf{e}_r$$

which is a result that can be considered negligible, since it is in the order of  $p/R$ .

The exact solution to this problem is naturally more complex; by designating  $R_i$  and  $R_e$  as the inner and outer radii respectively, it is actually possible to establish that:

$$\boldsymbol{\sigma} = \frac{pR_i^3}{R_e^3 - R_i^3} \left( 1 - \left( \frac{R_e}{r} \right)^3 \right) \mathbf{e}_r \otimes \mathbf{e}_r + \frac{pR_i^3}{R_e^3 - R_i^3} \left( 1 + \frac{1}{2} \left( \frac{R_e}{r} \right)^3 \right) (\mathbf{e}_\theta \otimes \mathbf{e}_\theta + \mathbf{e}_\phi \otimes \mathbf{e}_\phi)$$

and we can easily see that this expression satisfies  $\mathbf{div}_x \boldsymbol{\sigma} = \mathbf{0}$  exactly. ■

**R** From above, we can make two practical observations:

- deformable bodies resist forces by developing stress gradients if they are straight, as in the case of Example 2.5 dealing with the bar subjected to the action of gravity;
- when their geometry is curved, deformable bodies can resist forces by arching, simply from the stresses themselves; Example 2.7 of the spherical tank under internal pressure shows, in the case where the wall thickness is very small, that the circumferential, constant stresses are predominant over the radial stress in the thickness:  $|\sigma_{rr}|_{max} \ll \sigma_{\vartheta\vartheta} = \sigma_{\phi\phi}$ .

**Summary 2.5 — Local equilibrium equation.** The stress tensor  $\boldsymbol{\sigma}$  satisfies, at any point within a material domain  $\Omega_t$ , and at any time  $t$ , the following local equilibrium equation:

$$\rho(\mathbf{x}, t) \mathbf{a}(\mathbf{x}, t) = \mathbf{f}_V(\mathbf{x}, t) + \mathbf{div}_x \boldsymbol{\sigma}(\mathbf{x}, t), \quad \forall \mathbf{x} \in \Omega_t, \quad \forall t$$

where  $\mathbf{a}$  is the acceleration of the particle located in  $\mathbf{x}$ , of density  $\rho$ .

In a Cartesian vector basis  $(\mathbf{i}_1, \mathbf{i}_2, \mathbf{i}_3)$  associated with the coordinates  $(x_1, x_2, x_3)$ , this equation is expressed as:

$$\rho(x_1, x_2, x_3, t) \mathbf{a}(x_1, x_2, x_3, t) = \mathbf{f}_V(x_1, x_2, x_3, t) + \sum_{k=1}^3 \frac{\partial \boldsymbol{\sigma}}{\partial x_k}(x_1, x_2, x_3, t) \mathbf{i}_k$$

while, in a cylindrical vector basis  $(\mathbf{i}_r(\theta), \mathbf{i}_\theta(\theta), \mathbf{i}_z)$  associated with the coordinates  $(r, \theta, z)$ , it is possible to write that:

$$\rho(r, \theta, z, t) \mathbf{a}(r, \theta, z, t) = \mathbf{f}_V(r, \theta, z, t) + \frac{\partial \boldsymbol{\sigma}}{\partial r}(r, \theta, z, t) \mathbf{i}_r(\theta) + \frac{\partial \boldsymbol{\sigma}}{\partial \theta}(r, \theta, z, t) \frac{\mathbf{i}_\theta(\theta)}{r} + \frac{\partial \boldsymbol{\sigma}}{\partial z}(r, \theta, z, t) \mathbf{i}_z$$

### 2.3.2 Solving the equation

The local equilibrium equation that has just been established is a first-order partial differential equation; integration constants are then required to solve it.

#### Conditions on the external boundary

In general, the only information available and consistent with the stress tensor are the surface force densities  $\mathbf{f}_S$  that can be applied on the external boundary of the domain  $\Omega_t$ . By isolating a sub-domain  $\omega_t$  whose part of the boundary is the same as the boundary of the domain (as shown in Figure 2.10), we can express that the stress vector on this common boundary must be equal to the imposed surface force density: this is equivalent to extend (by continuity) to the external boundary the stress tensor by writing that:

$$\boldsymbol{\sigma}(\mathbf{x}, t) \mathbf{n}(\mathbf{x}) = \mathbf{f}_S(\mathbf{x}, t), \quad \forall \mathbf{x} \in \partial \Omega_t, \quad \forall t$$

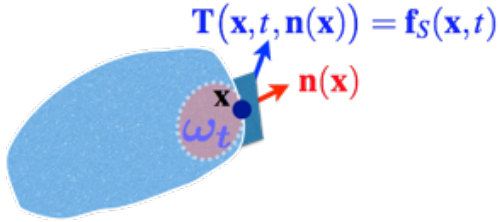


Figure 2.10: Imposed surface force density on the external boundary.

where  $\mathbf{n}(\mathbf{x})$  is the outer unit normal vector at point  $\mathbf{x}$  of the external boundary.

When we are in the presence of a solid material domain, whose surface  $\Sigma$  is in contact with air at atmospheric pressure, it is usual to write a so-called “free surface” condition, since we write that:

$$\boldsymbol{\sigma}(\mathbf{x}, t)\mathbf{n}(\mathbf{x}) = \mathbf{0}, \forall \mathbf{x} \in \Sigma, \forall t$$

Indeed, the material domain in its initial configuration  $\Omega_0$  is already subjected to the atmospheric pressure of surrounding air. In this configuration, it is usual to consider that the stress field within the domain is equal to zero since it will be negligible when compared to the other mechanical loadings to which the domain will be subjected (remember that an atmospheric pressure of one bar corresponds to a surface stress of 0.1 MPa).

However, when we are interested in stresses within a fluid domain, in contact with air, we need to effectively take atmospheric pressure into account since the previous reasoning has no reason to be valid.

■ **Example 2.8 — Pressure in a fluid at rest.** A direct and trivial application of above is the determination of the pressure within a fluid at rest (or “hydrostatic” pressure). Indeed, as established in Example 2.6, the local equilibrium equation, into which the form of the stress tensor for a fluid at rest ( $\boldsymbol{\sigma} = -p\mathbb{I}$ ) is injected, allows us to write directly that:

$$\mathbf{0} = \mathbf{f}_V + \mathbf{div}_{\mathbf{x}}(-p\mathbb{I}) = \rho_f g \mathbf{i}_3 - \nabla_{\mathbf{x}} p$$

where  $\mathbf{i}_3$  is a vertical (downward) unit vector, and  $\rho_f$  refers to the density of the fluid.

Considering that the boundary  $x_3 = 0$  corresponds to the free surface in contact with air, whose pressure is assumed to be constant and equal to  $p_a$ , we find that the pressure is a function of the depth  $x_3$ :

$$p(x_3) = p_a + g \int_0^{x_3} \rho_f(\zeta) d\zeta$$

which, in the case of a uniform density fluid  $\rho_f$ , leads to :

$$p(x_3) = p_a + \rho_f g x_3$$

which is the well-known expression of hydrostatic pressure that changes linearly with depth. ■



*Even if the surface force boundary conditions allow for solving the local equilibrium equation, its solution only provides three scalar relations for the six components of the stress tensor. Additional relations will be required to fully solve the problem under study unless some simplifying assumptions can be made (e.g. symmetry properties, as in Example 2.4), which will be the subject of Chapter 4.*

■ **Example 2.9 — Bar under the action of gravity: local approach.** Here we consider once again the case of the bar suspended from a fixed support, and subjected to the action of gravity. Example 2.5 had allowed us to verify that the following stress tensor:

$$\boldsymbol{\sigma}(x_3) = \rho g(L - x_3) \mathbf{i}_3 \otimes \mathbf{i}_3$$

satisfied the local equilibrium equation. We will now consider the boundary conditions. The surface force densities are known on the four lateral faces and on the lower side (in  $x_3 = L$ ): in fact, they are equal to zero since these faces

are free surfaces, and we verify on the one hand that:

$$\sigma(\pm \mathbf{i}_1) = \pm \rho g(L - x_3) \langle \mathbf{i}_3, \mathbf{i}_1 \rangle \mathbf{i}_3 = \mathbf{0} = \pm \rho g(L - x_3) \langle \mathbf{i}_3, \mathbf{i}_2 \rangle \mathbf{i}_3 = \sigma(\pm \mathbf{i}_2)$$

at any point on the lateral surfaces, and, on the other hand, that:

$$\sigma_{(x_3=L)} \mathbf{i}_3 = \rho g(L - L) \mathbf{i}_3 = \mathbf{0}$$

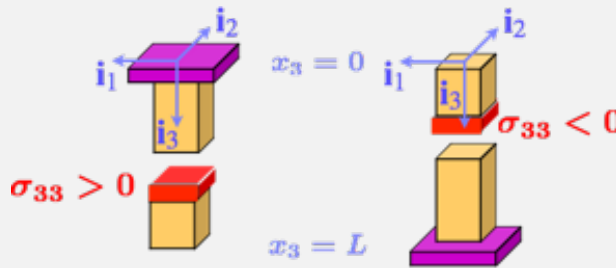
The solution proposed in Example 2.2 therefore satisfies all the equations of the problem.

Describing the boundary conditions correctly is of course essential to get the solution; thus, if we consider that the bar is now placed on a fixed support, rather than being suspended, the condition on the upper surface (in  $x_3 = 0$ ) becomes a free surface condition:

$$\sigma_{(x_3=0)}(-\mathbf{i}_3) = \mathbf{0}$$

while there are no more known surface force conditions on the lower surface (in  $x_3 = L$ ). Since the local equilibrium equation remains unchanged, the associated solution is found as:

$$\boxed{\sigma(x_3) = -\rho g x_3 \mathbf{i}_3 \otimes \mathbf{i}_3}$$



Thus, if formally, the two solutions have the same gradient (due to the same local equilibrium equation), in the case of the suspended bar, we have a tensile state ( $\sigma_{33} > 0$ ), while the laid bar is in compression ( $\sigma_{33} < 0$ ), as shown above. ■

### Conditions on an internal interface

When several material domains are studied, the local equilibrium equation is to be written separately within each domain. Moreover, the surface force densities are not known on the boundaries which are common to the two domains; on these interfaces, it is, therefore, necessary to be able to establish relations of another nature.

To do this, it is sufficient to express the reciprocity of the stress vector (i.e. action-reaction principle) at each point of the interface  $\Sigma_i$  between the two domains  $\Omega_k$  and  $\Omega_l$ :

$$\sigma^k(\mathbf{x}, t) \mathbf{n}_k(\mathbf{x}) + \sigma^l(\mathbf{x}, t) \mathbf{n}_l(\mathbf{x}) = \mathbf{0}, \forall \mathbf{x} \in \Sigma_i, \forall t$$

where  $\sigma^k$  and  $\sigma^l$  refer to the stress tensor defined in  $\Omega_k$  and  $\Omega_l$  respectively. Since  $\mathbf{n}_k(\mathbf{x})$  and  $\mathbf{n}_l(\mathbf{x})$  are, in  $\mathbf{x} \in \Sigma_i$ , the outer normal vectors of  $\Omega_k$  and  $\Omega_l$  respectively (as represented in Figure 2.11), they are necessarily opposed since they are defined on the common tangent plane at the point under study, which allows us to write:

$$\sigma^k(\mathbf{x}, t) \mathbf{n}(\mathbf{x}) = \sigma^l(\mathbf{x}, t) \mathbf{n}(\mathbf{x}), \forall \mathbf{x} \in \Sigma_i, \forall t$$

where  $\mathbf{n}(\mathbf{x})$  refers to either of the two normal vectors defined above. For obvious reasons, we then speak of “continuity of the stress vector” at the interface between the two domains.

**⚠** The previous result only reflects the continuity of the stress vector at the interface and not that of the complete stress tensor: only three of the six components are thus concerned. The following example highlights this important point.

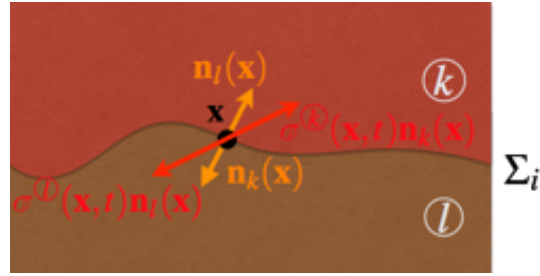


Figure 2.11: Surface force conditions on an internal interface.

■ **Example 2.10 — Spherical pressure tank: local approach.** We consider here the case of a spherical internal pressure tank, for which we had observed in Example 2.7 that the solution proposed in Example 2.4:

$$\sigma = p \frac{r - R - e}{e} \mathbf{e}_r \otimes \mathbf{e}_r + \frac{pR}{2e} (\mathbf{e}_\theta \otimes \mathbf{e}_\theta + \mathbf{e}_\phi \otimes \mathbf{e}_\phi)$$

in case the thickness was very small ( $e \ll R$ ), satisfied the local equilibrium equation.

With respect to boundary conditions, the tank is subjected to the fluid pressure  $p$  on its inner surface, and to atmospheric pressure (considered to be equal to zero) on its outer surface. We can then see that the stress vectors on these two surfaces are respectively:

$$\sigma_{(r=R)}(-\mathbf{e}_r) = -p \frac{R - R - e}{e} \mathbf{e}_r = p\mathbf{e}_r$$

and

$$\sigma_{(r=R+e)}\mathbf{e}_r = p \frac{R + e - R - e}{e} \mathbf{e}_r = \mathbf{0}$$

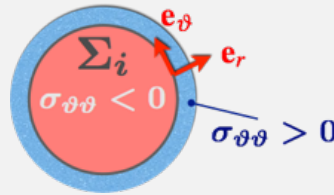
the last condition effectively reflecting the fact that the outer surface is free of forces, since it is only subjected to atmospheric pressure.

In addition, the condition on the inner surface (in  $r = R$ ) can be analyzed a little more precisely. The fluid being a continuous medium, the associated stress tensor is  $\sigma^f = -p\mathbb{I}$ . The condition in  $r = R$  can thus be interpreted as a continuity condition of the stress vector at the interface between the two material domains: it is indeed verified that, on this interface:

$$\sigma_{(r=R)}\mathbf{e}_r = -p\mathbf{e}_r = \sigma_{(r=R)}^f\mathbf{e}_r$$

This example also illustrates well the fact that there is no reason for all the stress tensor components to be continuous through the interface; indeed, we have:

$$\sigma_{(r=R)}\mathbf{e}_\theta = \frac{pR}{2e}\mathbf{e}_\theta \neq -p\mathbf{e}_\theta = \sigma_{(r=R)}^f\mathbf{e}_\theta$$



The tank thus presents circumferential tensile stresses, while the fluid is compressed. ■

**Summary 2.6 — Boundary conditions for the stress vector.** At any point on the external boundary of a material domain  $\Omega_t$ , the stress vector is equal to the applied surface force density  $\mathbf{f}_S$ :

$$\sigma(\mathbf{x}, t)\mathbf{n}(\mathbf{x}) = \mathbf{f}_S(\mathbf{x}, t), \forall \mathbf{x} \in \partial\Omega_t, \forall t$$

where  $\mathbf{n}(\mathbf{x})$  is the outer unit normal vector at point  $\mathbf{x}$ .

In the case of a boundary between two different material domains  $k$  and  $l$ , we express the continuity of the stress vector at this interface as:

$$\boldsymbol{\sigma}^{(k)}(\mathbf{x}, t)\mathbf{n}(\mathbf{x}) = \boldsymbol{\sigma}^{(l)}(\mathbf{x}, t)\mathbf{n}(\mathbf{x}), \forall \mathbf{x} \in \Sigma_i, \forall t$$

where  $\mathbf{n}(\mathbf{x})$  is the unit normal vector (whatever the sense) at point  $\mathbf{x}$ .

## 2.4 Summary of important formulas

**Fundamental principles of dynamics** – Summary 2.1 page 41

$$\int_{\Omega_t} \rho \mathbf{a} dV_x = \int_{\Omega_t} \mathbf{f}_V dV_x + \int_{\partial\Omega_t} \mathbf{f}_S dS_x$$

$$\int_{\Omega_t} (\mathbf{x} - \mathbf{x}_O) \wedge \rho \mathbf{a} dV_x = \int_{\Omega_t} (\mathbf{x} - \mathbf{x}_O) \wedge \mathbf{f}_V dV_x + \int_{\partial\Omega_t} (\mathbf{x} - \mathbf{x}_O) \wedge \mathbf{f}_S dS_x$$

**Cauchy stress tensor** – Summary 2.4 page 54

$$\mathbf{T}(\mathbf{n}) = \boldsymbol{\sigma}\mathbf{n}$$

$$\boldsymbol{\sigma} = \sum_{k=1}^3 \mathbf{T}(\mathbf{i}_k) \otimes \mathbf{i}_k$$

$$\boldsymbol{\sigma} = \boldsymbol{\sigma}^T$$

**Local equilibrium equation** – Summary 2.5 page 62

$$\rho \mathbf{a} = \mathbf{f}_V + \mathbf{div}_x \boldsymbol{\sigma}$$

$$\mathbf{div}_x \boldsymbol{\sigma} = \sum_{k=1}^3 \frac{\partial \boldsymbol{\sigma}}{\partial x_k} \mathbf{i}_k$$

$$\mathbf{div}_x \boldsymbol{\sigma} = \frac{\partial \boldsymbol{\sigma}}{\partial r} \mathbf{i}_r + \frac{\partial \boldsymbol{\sigma}}{\partial \theta} \frac{\mathbf{i}_\theta}{r} + \frac{\partial \boldsymbol{\sigma}}{\partial z} \mathbf{i}_z$$

**Boundary conditions for the stress vector** – Summary 2.6 page 65

$$\boldsymbol{\sigma}\mathbf{n} = \mathbf{f}_S$$

$$\boldsymbol{\sigma}^{(k)}\mathbf{n} = \boldsymbol{\sigma}^{(l)}\mathbf{n}$$



## 3. Strength criteria

The internal forces within matter can be modelled as a stress tensor which, being symmetrical, has six independent scalar components varying *a priori* at each point of the studied domain and at any given time. To know if, locally, the material can resist these stresses, one has to be able to deduce from this tensor a scalar “indicator”, which can be compared to a threshold value characteristic of the material’s strength. This indicator should be linked in particular to the nature and physical structure of this material.

---

### WHY STUDY STRENGTH CRITERIA?

#### 3.1 Mechanical testing of materials

The simplest way to study the behaviour of a material, and in particular its mechanical strength, is to set up experimental tests, thus allowing them to be tested under specific stress fields. Given the notion of stress introduced in the previous chapter, it is easy to understand that it is difficult to experimentally measure a stress field within a mechanical part, unlike strains whose measurement is straightforward and benefits from recent advances in imaging equipment and associated image processing software. Thus, the aim is generally to impose a state of uniaxial stress (i.e. having a single scalar component) and, if possible, even homogeneous stress in the area of interest of the tested part, in order to be able to determine this stress state with the only measure of the forces globally exerted on the part, i.e., generally a resultant force and/or a moment characterizing the action of the test machine on the part.

From this point of view, the most traditional uniaxial test is the simple “tensile test”, which we will describe in detail in the following paragraph, and which makes it possible to obtain a homogeneous stress state in the area of interest of the tested part. A multitude of other tests can of course be considered: for example, the “torsion test” (mentioned in Example 5.1, on page 120), or the “bending test” (detailed in Example 6.14, on page 200), for which the stress field changes linearly within the part. Finally, in some cases, it may be necessary to set up multiaxial tests to highlight certain phenomena or behaviours that uniaxial tests do not allow to observe.

### 3.1.1 Tensile test

The principle of the tensile test is to obtain a homogeneous uniaxial stress state in a specific area of the tested part:  $\sigma = \sigma_{ee} \mathbf{e} \otimes \mathbf{e}$ . For this purpose, the parts, which are called “specimens”, are elongated in shape and have three distinct parts, visible in Figure 3.1:

- a thin, elongated central part, called “reduced section” or “gauge section” because it is there that the assumption of homogeneity of the stress state will be adopted;
- two parts at the ends, called “shoulders” or “grip section”, which are wider than the gauge section, and which are intended for being readily gripped in the test machine;
- a “fillet” connecting these sections, which serve as transition zones for geometry, and whose importance will be justified in Paragraph 3.3.2.

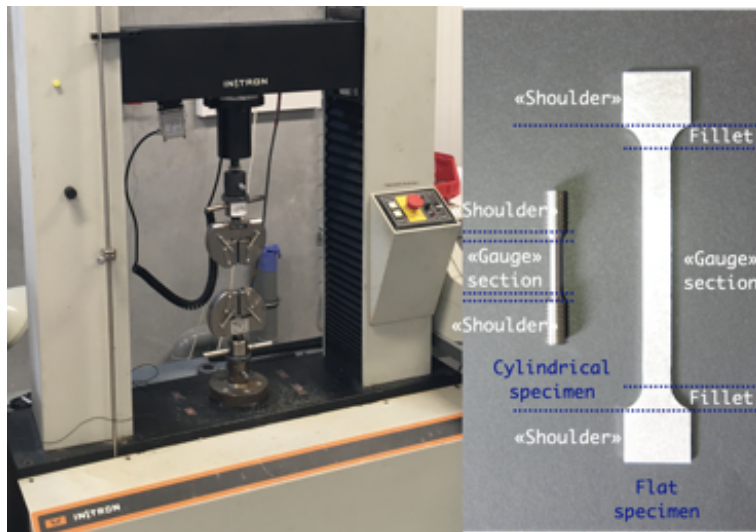


Figure 3.1: Test machine (left) and typical tensile specimens (right).

#### Determination of the stress state

This stress state is obtained using a test machine, represented in Figure 3.1, whose role is to apply to both ends of the specimen (at the level of the shoulders) two actions characterized by two resultant forces  $\mathbf{R}^0 = -\mathbf{R}^L$ , opposite and in the direction of the longitudinal axis  $\mathbf{e}$  of the specimen, assumed vertical and oriented upward.

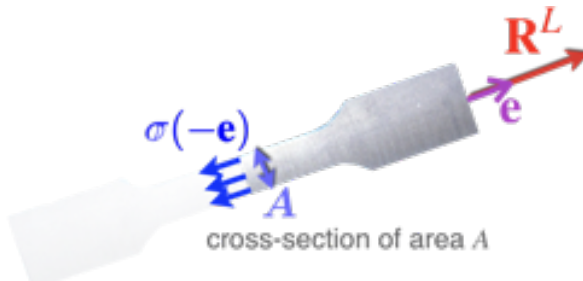


Figure 3.2: Isolation of a half specimen

If we virtually cut the specimen into two symmetrical halves (as shown in Figure 3.2), and if we neglect the action of gravity, the upper half is in static equilibrium, being subjected to the action

of the machine, of resultant force  $\mathbf{R}^L$ , and to the action of the lower half, of resultant force:

$$\mathbf{R} = \int_{\Sigma} \sigma(-\mathbf{e}) dS_x = - \int_{\Sigma} \sigma_{ee} \mathbf{e} dS_x$$

where  $\Sigma$  is the horizontal median cut plane of the specimen. Assuming that the stress state is homogeneous in the gauge section of the specimen, it is so at any point in the cross-section  $\Sigma$  of area  $A$ , and we can directly write using the static equilibrium of the upper half that:

$$\mathbf{R}^L = \sigma_{ee} A \mathbf{e}$$

which therefore allows us to obtain the longitudinal stress from the measurement of the force exerted on the specimen, and the area of its cross-section:  $\sigma_{ee} = \|\mathbf{R}^L\|/A$ .

In practice, the specimen is fixed on one side to a fixed part of the test machine, and on the other side to a moving part called the “cross head”, whose displacement is measured. It is then possible to control the test in terms of stress (via the measurement of the resultant force exerted) or in terms of strain (by controlling the movement of the cross head).

One way to justify *a posteriori* the homogeneity of the longitudinal stress in the gauge section may be to use numerical simulation to evaluate the stress field within the specimen. To do this, we need to question the precise nature of the forces applied locally to the specimen, since we saw in Paragraph 2.3.2 that the problem required the knowledge of the stress vectors on the mechanically loaded parts of the boundary. We then propose to test three different boundary conditions, but all three of which have the same resultant force:

1. surface force densities normally applied to the end surfaces of the two specimen shoulders, and assumed to be uniform;
2. surface force densities applied tangentially to the lateral surfaces of the two specimen shoulders, and assumed to be uniform;
3. an “extreme” case where the force application area is reduced to a point at each end (which is actually possible in the case of a numerical simulation).

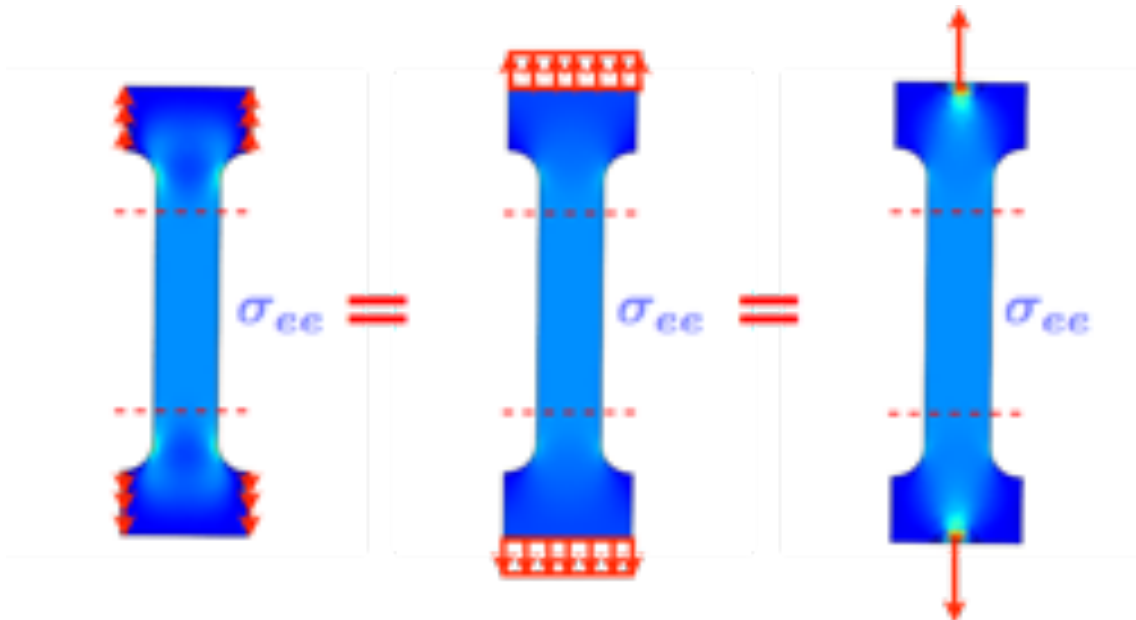


Figure 3.3: Uniaxial stress states  $\sigma_{ee}$  obtained by numerical simulation for the three studied loading cases: case 1 (centre), case 2 (left), and case 3 (right).

The uniaxial stress state associated with each of these cases is represented in Figure 3.3, in the case of a material behaviour called “elastic”: this stress state is homogeneous within the gauge section for each case, and the associated values are the same, despite the diversity of the forces applied locally. On the other hand, we see that the stress fields are potentially very different in the shoulders of the specimen, which justifies the interest of having chosen an elongated shape for the latter; indeed, what one calls “Saint-Venant’s principle” allows for justifying that the local distribution of the applied forces has only little influence at “high” distance, provided that these forces have identical overall characteristics, namely the same resultant forces and same moments (equal to zero here in the case of a simple tensile test). This principle will be explained in more detail in Paragraph 5.2.3.

### Tensile curves

In addition to the longitudinal stress  $\sigma_{ee}$ , the longitudinal strain  $\varepsilon_{ee} = \langle \mathbf{e}, \mathbf{e} \rangle$  is also measured on the gauge section, and is also homogeneous in the case of the simple tensile test. This then makes it possible to draw a so-called “tensile curve”, characteristic of the material’s behaviour until its final failure.

For most materials, two regions are corresponding to very different behaviours, visible in Figure 3.4 (left curve):

1. a reversible behaviour, insofar as, as soon as the forces applied to the specimen are removed, it returns to its original, undeformed shape: this corresponds to a behaviour known as “elasticity”, which is observed for moderate deformations and is very often characterized by a linear evolution of the uniaxial stress as a function of the longitudinal strain;
2. above a certain stress threshold (called “yield strength”), a “plastic” behaviour, which results in irreversible deformations: after removal of the applied forces, the specimen does not return to its original shape, which means that some deformation remains at zero stress: we speak of “plasticity”.

Materials presenting these two regions are called “ductile”; on the other hand, some materials have a very limited or even non-existent plastic region, as shown on the right-hand curve of Figure 3.4: they are “fragile” or “brittle” materials.

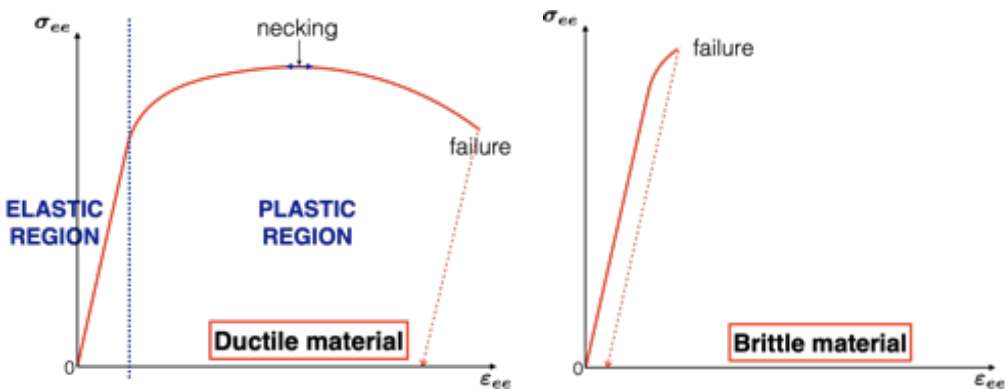


Figure 3.4: Tensile curves for ductile materials (left) and brittle materials (right).

These two regions (elasticity and plasticity) correspond to very different phenomena at the atomic scale, which can be summarized very briefly as follows:

- the elastic region corresponds to a deformation of the network of atoms, in which they leave their equilibrium position corresponding to the minimum of the atomic interaction potential, and are then subjected to a restoring force that tends to make them return to this optimal position; this explains the reversibility of elasticity;

- above a certain threshold, locally the bonds between atoms may break, but some of these atoms recreate bonds with neighbouring atoms, creating a deformation that is then irreversible, because (unless a contrary effort is exerted exceeding the threshold again) the suppression of stresses leaves the atoms with their new neighbours.

Figure 3.5 (top) summarizes the description of these two phenomena, in the case of a network of atoms subjected to shear.

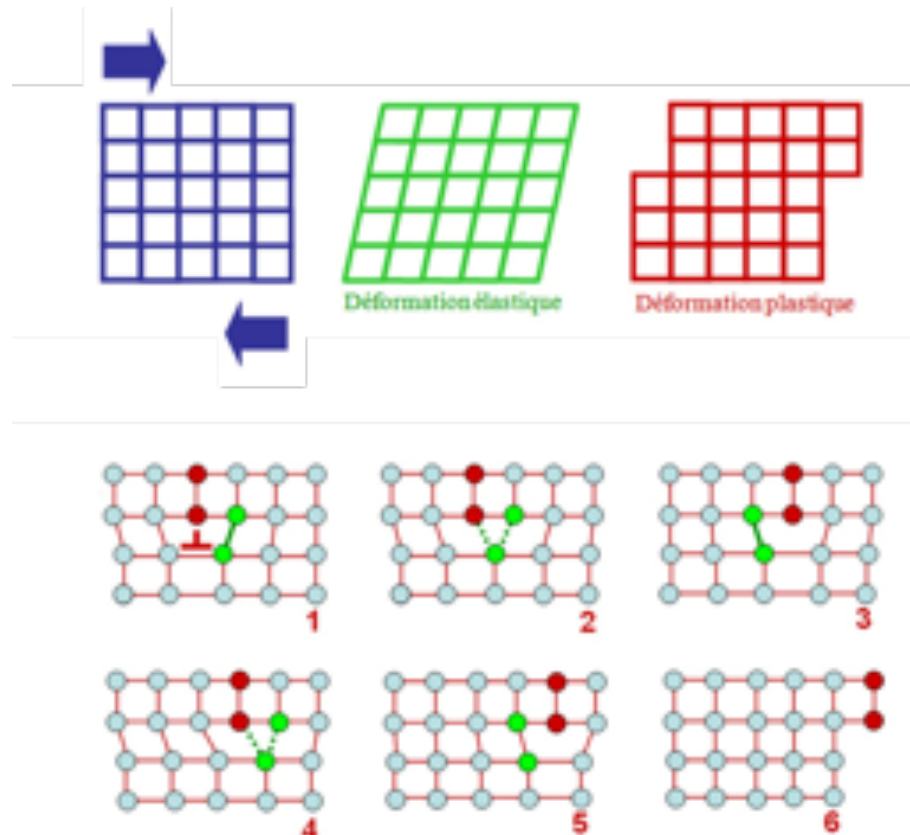
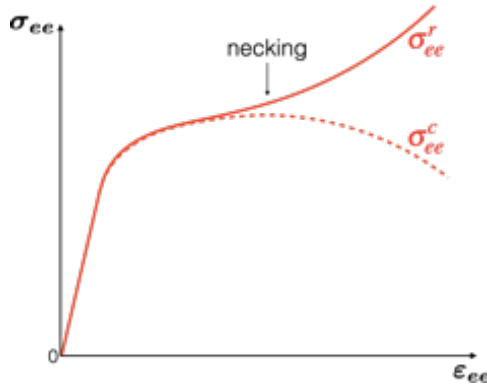


Figure 3.5: Principle of elastic and plastic deformations (top) and movement of a dislocation (bottom).

In practice, however, it is not possible to have the slip of atomic planes by simultaneous rupture of all the interatomic bonds separating the two planes concerned, because this would require much higher levels of stress than what is observed experimentally. This slip is in fact obtained by the “propagation” of defects, generally linear discontinuities of the atomic structure, called “dislocations”: Figure 3.5 (below) illustrates how the slip between two atomic planes occurs gradually, by successive breaks in the bonds between the atoms surrounding the defect.

**R** We did not insist above, when determining the longitudinal stress as a function of the force applied by the test machine, on measuring the area of the section. Indeed, during the tensile test, it is observed that this area evolves significantly, especially in the case of a ductile material: a phenomenon known as “necking” (whose apparition is identified on the left curve of Figure 3.4) corresponds to the localized and rapid reduction of the cross-section area of the specimen, finally leading to the failure at this zone.

As the curve drawn in Figure 3.4 does not take into account the reduction of this area (we speak then of “engineering” curve), there is an increase in strain for a stress  $\sigma_{ee}^c$  that appears to decrease until failure; in fact, if the actual area is taken into account, the actual stress  $\sigma_{ee}^r$  (or “true” stress) increases until failure, as illustrated in the figure below.



*In practice, it is often sufficient to consider the engineering stress, bearing in mind that the actual failure stress is underestimated, which is a safety factor.*

### Orders of magnitude

Material	Yield strength (MPa)	Tensile strength (MPa)
wood ( $\perp$ fibres)		0.5–1.5
concrete		2–5
rubber		15
high density polyethylene	26–33	35–40
wood ( $\parallel$ fibres)		10–40
composites ( $\perp$ fibres)		30–50
glass		30–60
nylon	45	75
bone	104–121	130
copper	70	220
aluminum alloy	240–400	300–500
brass	200	550
tungsten	940	1500
composites ( $\parallel$ fibres)		1000–1800
sapphire	400	1900
steel	130–2500	200–2500
diamond	1600	2800

Table 3.1: Typical values for various materials of yield strength and tensile strength.

Table 3.1 lists, for various common materials, the typical values of their tensile strength, as well as their yield strength in the case of ductile materials. For some material families, such as metal alloys, orders of magnitude have wide variation ranges, as the properties can be modulated in various ways during material elaboration (addition elements, heat treatments, ...). Besides, some materials, such as long-fibre composites, do not have the same characteristics depending on whether they are loaded parallel or perpendicular to the fibres. Finally, parameters such as temperature can influence the observed values.

#### 3.1.2 Types of material failure

Characterization tests, such as the tensile test just analyzed, therefore provide a threshold value associated with material failure. However, the question now arises as to how to use this threshold value in the case of an actual structure, of potentially complex shape, and subjected to an arbitrary

loading. Besides, the multiplicity of failure modalities that can be observed in the case of the tensile test shows that there is a multitude of local mechanisms at the microscopic level that must be understood before this transposition can be carried out.

In a deliberately simplistic manner, we consider here only two types of material failure, related to the two generic behaviours shown in Figure 3.4, and whose microscopic mechanisms are very different (this, however, does not exclude the possibility of coexistence of these two types). The associated fracture surfaces, obtained during a tensile test, are represented schematically in Figure 3.4, and are briefly justified in what follows.

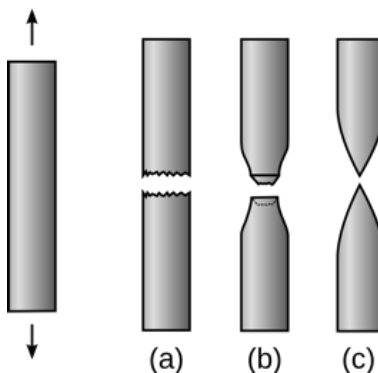


Figure 3.6: Typical fracture surfaces for a brittle material (a) and a ductile material (b)-(c).

### Brittle failure

This type of failure occurs for materials in which it is not possible to have significant plastic deformation levels, such as ceramics, or, at low temperatures, metals and some polymers. Once a crack has been initiated, it does not require much energy to propagate, resulting in a sudden failure, as in the case of glass, for example, without necessarily significantly increasing the applied stresses.

In the case of materials with a so-called crystalline structure (characterized by highly ordered stacks of atoms), the creation of the crack results from a failure of the atomic bonds between two weakly bound crystalline planes, which are thus separated by forces applied perpendicularly to them: we speak then of “cleavage” failure. As the latter creates a multitude of small, perfectly faceted surfaces, the fracture surface can have a shiny appearance, as in the case of cast iron shown in Figure 3.7.



Figure 3.7: Fracture surfaces in the case of cast iron (left) and glass (right).

For amorphous materials (i.e. with no crystalline structure), the absence of characteristic

separation planes results in the failure being carried out according to a curved and smooth breakage surface, as in the case of glass shown in Figure 3.7, propagating perpendicular to the applied force. We call this a “conchoidal” fracture.

### Ductile failure

Unlike the previous case, this type of failure occurs with the presence of a significant amount of plastic deformation, visible in particular in the necking phenomenon that was observed during the tensile test. For particularly pure metals, this deformation can go as far as separating the specimen into two halves with sharpened ends (case (c) shown in Figure 3.6).

However, most metals used in the industry contain particles (such as addition elements in the case of alloys), and at the heart of plastically deformed areas, microcracks form at the interface between these particles and the surrounding metal. The movement of the dislocations, obtained by the slip of certain crystalline planes as described above, tends to transform these microcracks into small cavities of increasing sizes which finally coalesce in the necking zone to form the cracks that will cause the material to break. All these steps are summarized in Figure 3.8.

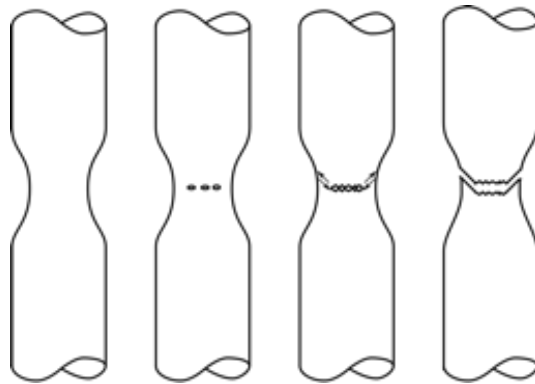


Figure 3.8: Steps of the ductile failure: necking, then creation, and coalescence of the micro-cavities, and finally cup-and-cone shaped cracking of the specimen.

The propagation of cracks is, therefore, less abrupt than in the brittle case, because there is a need for energy (and therefore an increasing force) to increase the crack length (the energy dissipated during a tensile test, directly estimable as the area under the tensile curve, is very different for the two behaviours presented in Figure 3.4). The propagation of these cracks tends to occur in the slip directions of the crystalline planes involved in the movement of the dislocations, especially as one approaches the boundaries of the specimen, which explains the generally observed “cup-and-cone” shape of the fracture surface, as in the case of the two metallic materials in Figure 3.9. Besides, the “dark” appearance of the fracture surface still bears traces of the cavities that formed during the rupture, which appear in the form of “cupules”, mainly in the central zone of the specimen.



*Rather than precisely characterizing the instant of failure, the purpose of the strength criteria presented below is to provide dimensional information regarding the structure to be designed.*

*Thus, in the case of ductile materials, it is often considered that the threshold corresponding to the plastic region (i.e. the yield strength) is the criterion that should be used, rather than the extreme value for which the failure occurs: indeed, on the one hand, the failure threshold is generally not so far from the yield strength, even in the case of very ductile materials, and, on the other hand, the appearance of irreversible deformations may, in any case, be detrimental to the function that the structure in service must perform.*

*For brittle materials, on the other hand, this distinction does not apply, since, with an extremely small plasticity region, failure occurs at the moment of leaving the pure elasticity region.*



Figure 3.9: Fracture surface in the case of steel (left) and aluminum alloy (right).

## 3.2 Criteria

In order to be able to introduce relevant strength criteria for the different types of materials that can be studied, it is first essential to define new quantities related to the stress tensor that has been calculated. Indeed, one understands well that the values taken by the components of the latter are directly related to the vector basis chosen: it is, therefore, necessary either to choose a relevant basis taking into account the nature of the local phenomena in play or to define invariant quantities, independent of the chosen vector basis used to express the stresses.

### 3.2.1 Local study of stresses

This paragraph is devoted to the presentation of the different local representations of stresses, which can be used in the different strength criteria that will be presented below.

#### Quantities related to the choice of the facet

A first way is to consider the characteristic elements associated with the cleavage surface that is introduced (mentally) when defining the stress vector, namely the plane tangent to this surface at the point under study, and the outer unit normal vector  $\mathbf{n}$ , which is orthogonal to this facet.

**Normal and tangential stresses.** The quantities defined here are shown in Figure 3.10.

The normal stress, noted  $\sigma_{nn}$ , is defined as the component of the stress vector along the outer normal vector at the cut surface at the point under study:

$$\sigma_{nn}(\mathbf{x}, t) = \langle \boldsymbol{\sigma}(\mathbf{x}, t) \mathbf{n}, \mathbf{n} \rangle, \forall \mathbf{x} \in \Omega_t, \forall t$$

The tangential stress, or “shear stress”, noted  $\tau_\Sigma$ , is defined as the projection of the stress vector in the plane of the facet  $\Sigma$ ; it can therefore be obtained as:

$$\tau_\Sigma(\mathbf{x}, t) = \boldsymbol{\sigma}(\mathbf{x}, t) \mathbf{n} - \sigma_{nn}(\mathbf{x}, t) \mathbf{n}, \forall \mathbf{x} \in \Omega_t, \forall t$$

This vector can then be decomposed on a vector basis of the plane of the facet; thus, if  $\mathbf{m}$  is a unit vector of this plane (therefore  $\mathbf{m} \perp \mathbf{n}$ ), we note:

$$\tau_{mn}(\mathbf{x}, t) = \langle \boldsymbol{\sigma}(\mathbf{x}, t) \mathbf{n}, \mathbf{m} \rangle = \langle \tau_\Sigma(\mathbf{x}, t), \mathbf{m} \rangle, \forall \mathbf{x} \in \Omega_t, \forall t$$

which is called “shear” along the direction  $\mathbf{m}$  for a plane of normal vector  $\mathbf{n}$ .

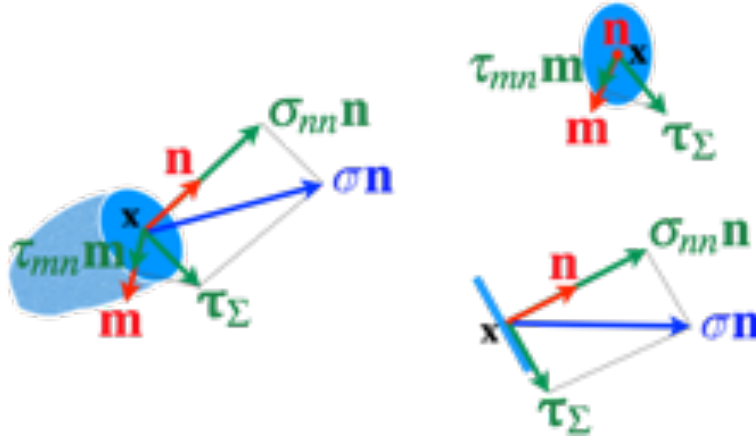


Figure 3.10: Normal stress, tangential stress, shear.

■ **Example 3.1 — Simple tensile test: quantities related to the facet.** The definition of local quantities in the case of a simple tensile test in the direction  $\mathbf{e}$  is straightforward; indeed, since the stress tensor is expressed simply as  $\boldsymbol{\sigma} = \sigma_{ee}\mathbf{e} \otimes \mathbf{e}$  with  $\sigma_{ee} > 0$ , we obtain:

- for the normal stress:

$$\sigma_{nn} = \langle \boldsymbol{\sigma}\mathbf{n}, \mathbf{n} \rangle = \langle \sigma_{ee}\langle \mathbf{e}, \mathbf{n} \rangle \mathbf{e}, \mathbf{n} \rangle = \sigma_{ee}\langle \mathbf{e}, \mathbf{n} \rangle^2$$

hence, by defining  $\alpha$  as the angle between the direction  $\mathbf{e}$  of tension and the normal vector  $\mathbf{n}$  on the facet:

$$\boxed{\sigma_{nn} = \sigma_{ee} \cos^2 \alpha}$$

- for the tangential stress:

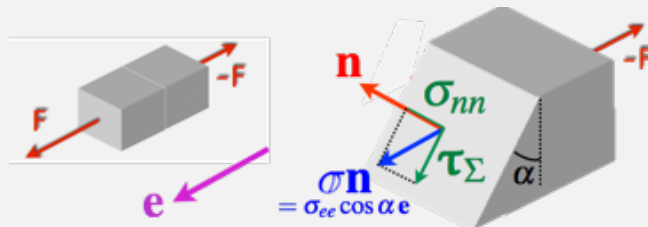
$$\tau_\Sigma = \boldsymbol{\sigma}\mathbf{n} - \sigma_{nn}\mathbf{n} = \sigma_{ee}\langle \mathbf{e}, \mathbf{n} \rangle (\mathbf{e} - \langle \mathbf{e}, \mathbf{n} \rangle \mathbf{n}) = \sigma_{ee} \cos \alpha (\mathbf{e} - \cos \alpha \mathbf{n})$$

whose norm is:

$$\begin{aligned} \|\tau_\Sigma\| &= \sigma_{ee} |\cos \alpha| \|\mathbf{e} - \cos \alpha \mathbf{n}\| = \sigma_{ee} |\cos \alpha| \sqrt{\langle \mathbf{e}, \mathbf{e} \rangle - 2 \cos \alpha \langle \mathbf{e}, \mathbf{n} \rangle + \cos^2 \alpha \langle \mathbf{n}, \mathbf{n} \rangle} \\ &= \sigma_{ee} |\cos \alpha| \sqrt{1 - 2 \cos \alpha \cos \alpha + \cos^2 \alpha} = \sigma_{ee} |\cos \alpha \sin \alpha| \end{aligned}$$

or, finally:

$$\boxed{\|\tau_\Sigma\| = \frac{\sigma_{ee} |\sin(2\alpha)|}{2}}$$



- for the shear along the direction  $\mathbf{m}$  perpendicular to  $\mathbf{n}$ :

$$\boxed{\tau_{mn} = \langle \boldsymbol{\sigma}\mathbf{n}, \mathbf{m} \rangle = \sigma_{ee}\langle \mathbf{e}, \mathbf{n} \rangle \langle \mathbf{e}, \mathbf{m} \rangle}$$

which allows for finding, for a unit vector  $\mathbf{m}$  collinear to  $\tau_\Sigma$ , a shear equal to the norm of the tangential stress:  $\tau_{mn} = \sigma_{ee} |\sin(2\alpha)|/2$ . ■

### Principal stresses

We know that the stress tensor  $\sigma$  is symmetrical: it is therefore diagonalizable, and admits real eigenvalues, associated with eigenvectors forming an orthonormal basis.

**Principal stresses and principal directions of stress.** The eigenvalues  $\lambda_k^\sigma$  of the stress tensor, called principal stresses, and the associated eigenvectors  $\phi_k^\sigma$ , called principal directions, verify the following relation:

$$\sigma \phi_k^\sigma = \lambda_k^\sigma \phi_k^\sigma$$

Physically, the principal directions correspond to facet orientations (defined by their normal vector) such that the stress vector is along the normal itself, which means that there is no tangential stress on these facets; since these principal directions are perpendicular to each other, we find ourselves in the situation represented in Figure 3.11.

When there is no possible ambiguity with the components of the stress tensor, the principal stresses are often noted  $\sigma_k$ , ranking them from the largest to the smallest. If one of the principal stresses is equal to zero, the stress state is said to be “biaxial”, or “plane”. If all three are the same, it is referred to as a “spherical” stress state, as seen in the case of a fluid at rest. In the case of multiple eigenvalues, it is still possible to determine an orthonormal basis of principal directions.

The principal stresses, as well as their associated principal directions, are invariant in the sense that their expressions are not related to the choice of the vector basis since they are calculated as the roots of the characteristic polynomial:

$$\det(\sigma - \sigma_k \mathbb{I}) = -\sigma_k^3 + i_1(\sigma)\sigma_k^2 - i_2(\sigma)\sigma_k + i_3(\sigma) = 0, \quad 1 \leq k \leq 3$$

where the terms  $i_k(\sigma)$  are the invariants of the stress tensor, defined in Appendix A.2.4.

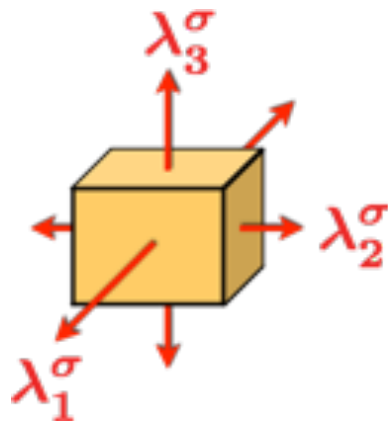


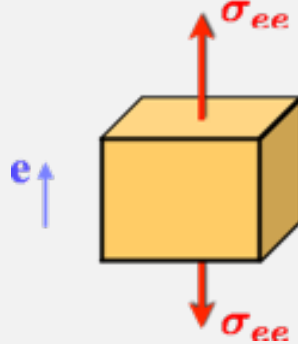
Figure 3.11: Stress state in the basis of the principal directions of stress.



Although the principal stresses and their associated principal directions are indeed independent of the choice of a basis, they still *a priori* depend on the point  $x \in \Omega_t$ , as well as on time.

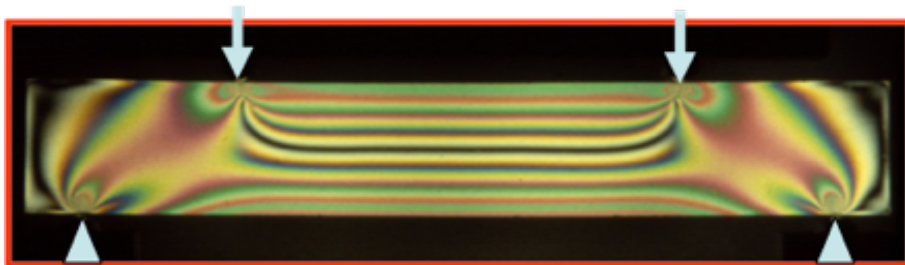
■ **Example 3.2 — Simple tensile test: principal stresses and associated principal directions.** Since, in the case of a simple tensile test in a direction  $e$ , the stress tensor is uniaxial ( $\sigma = \sigma_{ee}e \otimes e$ ), the determination of the principal stresses is straightforward. Indeed, the stress vector on a facet of normal  $n$  is  $\sigma n = \sigma_{ee}\langle e, n \rangle e$ , hence, in particular :

1.  $\sigma\mathbf{e} = \sigma_{ee}\mathbf{e}$ , which means that  $\sigma_{ee}$  is a principal stress, associated with the direction  $\mathbf{e}$  which corresponds to the direction of the tensile test;
2.  $\sigma\mathbf{m} = \mathbf{0}$ ,  $\forall \mathbf{m} \perp \mathbf{e}$ , which shows that any unit vector  $\mathbf{m}$  perpendicular to  $\mathbf{e}$  is a principal direction, associated with a principal stress equal to zero; this latter corresponds to a double eigenvalue of the tensor  $\sigma$ , and any vector basis of the normal plane  $\mathbf{e}$  is principal.



**R** Experimentally, some transparent materials, called “photoelastic”, have the property of presenting coloured fringes when they are placed between two filters that polarize light in directions perpendicular to each other. This cross-polarized light allows for directly visualizing the differences between the principal stresses within the material. Thus, the stress gradients are all the stronger as the fringes, called “isochromatic”, are tightened.

The example of a “four-point bending” test, presented below, shows a linear evolution of the longitudinal stress as a function of the transverse dimension in the central area of the specimen.



### Mohr's circles

In parallel with the previous definitions, there is a need for a graphical representation that allows the information contained in the six components of the stress tensor (at each point of the material domain) to be condensed pragmatically. In particular, by anticipating a little on the nature of the criteria presented below, it is generally a question of being able to determine the extreme values of the local quantities that have just been previously introduced, without necessarily linking them to the orientation of the facet under study.

This is the purpose of Mohr's circles, which carry in a system of two orthonormal axes, the normal stress  $\sigma_{nn}$  on the abscissa and the norm  $\tau = \|\boldsymbol{\tau}_\Sigma\|$  of the tangential stress on the ordinate, for different orientations of the normal vector  $\mathbf{n}$  at the point  $\mathbf{x} \in \Omega_t$  under study. We can then show that, in this planar representation, the end of the stress vector is constrained to move in the area between three circles whose centres are located on the abscissa axis, and whose intersection points with this axis have as respective coordinates the principal stresses associated with the tensor  $\sigma$  at the point  $\mathbf{x} \in \Omega_t$  under study. Logically, this representation, visible in Figure 3.12 is called “Mohr's circles”; given that it is the norm of tangential stress that is plotted on the ordinate, it is usual to represent only the semicircles located above the abscissa axis.

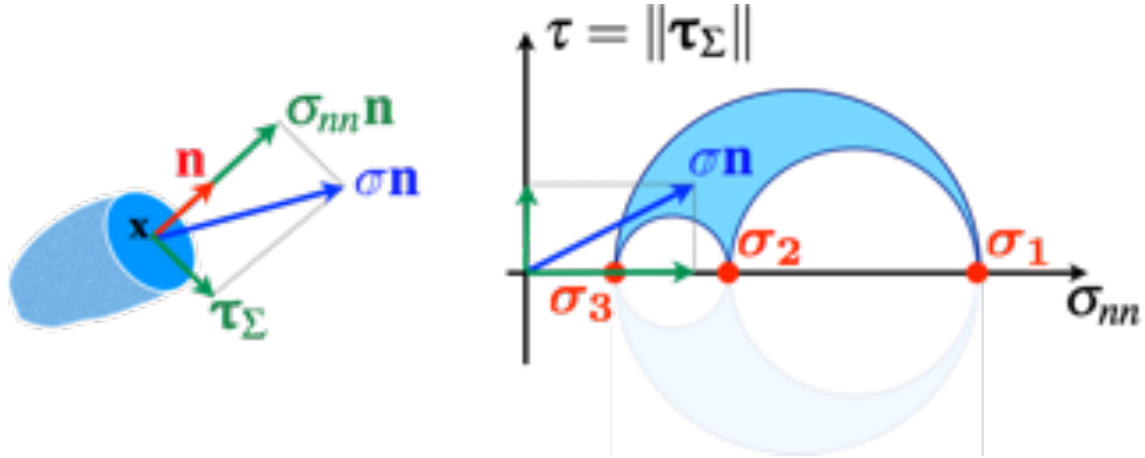


Figure 3.12: Mohr's circles.

**R** This remarkable result is obtained by using the basis  $(\phi_1^\sigma, \phi_2^\sigma, \phi_3^\sigma)$  of the stress tensor's principal directions at the point under study; by noting  $(n_1, n_2, n_3)$  the components in this basis of the normal vector  $\mathbf{n}$ , we can write that the normal and tangential components of the stress vector are expressed as:

$$\begin{aligned}\sigma_{nn} &= \sigma_1 n_1^2 + \sigma_2 n_2^2 + \sigma_3 n_3^2 \\ \tau^2 &= \sigma_1^2 n_1^2 + \sigma_2^2 n_2^2 + \sigma_3^2 n_3^2 - \sigma_{nn}^2\end{aligned}$$

Knowing that  $\|\mathbf{n}\|^2 = n_1^2 + n_2^2 + n_3^2 = 1$ , we can express the squares of the components of the normal vector  $\mathbf{n}$  as functions of the normal and tangential stresses:

$$\begin{aligned}n_1^2 &= \frac{\tau^2 + (\sigma_{nn} - \sigma_2)(\sigma_{nn} - \sigma_3)}{(\sigma_1 - \sigma_2)(\sigma_1 - \sigma_3)} \\ n_2^2 &= \frac{\tau^2 + (\sigma_{nn} - \sigma_3)(\sigma_{nn} - \sigma_1)}{(\sigma_2 - \sigma_3)(\sigma_2 - \sigma_1)} \\ n_3^2 &= \frac{\tau^2 + (\sigma_{nn} - \sigma_1)(\sigma_{nn} - \sigma_2)}{(\sigma_3 - \sigma_1)(\sigma_3 - \sigma_2)}\end{aligned}$$

Recalling that the principal stresses are classified in descending order ( $\sigma_1 \geq \sigma_2 \geq \sigma_3$ ), making it clear that, necessarily,  $n_k^2 \geq 0$  (for  $1 \leq k \leq 3$ ) allows us to obtain the following conditions for the location of the vector end  $\sigma\mathbf{n}$  in the Mohr's plane:

$$\begin{aligned}\tau^2 + (\sigma_{nn} - \sigma_2)(\sigma_{nn} - \sigma_3) &\geq 0 \\ \tau^2 + (\sigma_{nn} - \sigma_3)(\sigma_{nn} - \sigma_1) &\leq 0 \\ \tau^2 + (\sigma_{nn} - \sigma_1)(\sigma_{nn} - \sigma_2) &\geq 0\end{aligned}$$

hence:

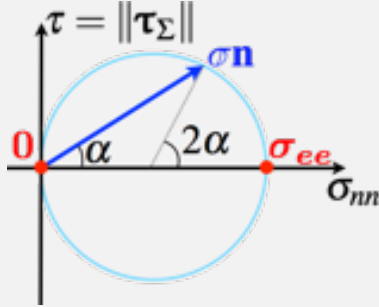
$$\begin{aligned}\left(\sigma_{nn} - \frac{\sigma_2 + \sigma_3}{2}\right)^2 + \tau^2 &\geq \left(\frac{\sigma_2 - \sigma_3}{2}\right)^2 \\ \left(\sigma_{nn} - \frac{\sigma_1 + \sigma_3}{2}\right)^2 + \tau^2 &\leq \left(\frac{\sigma_1 - \sigma_3}{2}\right)^2 \\ \left(\sigma_{nn} - \frac{\sigma_1 + \sigma_2}{2}\right)^2 + \tau^2 &\geq \left(\frac{\sigma_1 - \sigma_2}{2}\right)^2\end{aligned}$$

which effectively corresponds to the area between three circles, tangent to each other, and intersecting the abscissa axis in  $\sigma_1$ ,  $\sigma_2$  and  $\sigma_3$ .

In the case where two principal stresses are equal, the three circles are reduced to only one circle, on which the end of the stress vector is constrained to move, as shown in the example below.

The above developments apply of course to the case of any symmetrical tensor, and therefore, in particular, to the Green-Lagrange strain tensor  $\mathbb{E}$ , and to the infinitesimal strain tensor  $\mathbf{e}$ . Mohr's circles are widely used, for example, for the graphical analysis of strain rosettes.

■ **Example 3.3 — Simple tensile test: Mohr's circle.** In the case of the simple tensile test, we saw in Example 3.2 that the associated principal stresses were  $\sigma_{ee}$  and 0 (double eigenvalue). The Mohr's circles are therefore reduced to a single circle, represented below, on which the end of the stress vector moves.



More precisely, by defining  $\alpha$  as the angle between the direction  $\mathbf{e}$  of tension and the normal vector  $\mathbf{n}$  on the facet, we find as in Example 3.1 that:

$$\begin{aligned}\sigma_{nn} &= \sigma_{ee} \cos^2 \alpha = \frac{\sigma_{ee}}{2} (1 + \cos(2\alpha)) \\ \tau &= \frac{\sigma_{ee}}{2} |\sin(2\alpha)|\end{aligned}$$

which, in this case, allows us to directly visualize the angle  $\alpha$  on Mohr's circle. ■

### 3.2.2 Cleavage failure criteria

The first criterion presented here concerns the case of brittle fracture, referred to in Paragraph 3.1.2; the associated microscopic phenomena correspond to the separation of atomic planes following the application of normal forces to them, which we call “cleavage”. In the case of a monocrystalline material occupying the domain  $\Omega_t$  at the instant  $t$ , the cleavage planes, which are the ones likely to break first, are perfectly known, and are characterized by the orientations  $\mathbf{n}_k$  ( $1 \leq k \leq N$ ) of their respective normal vectors. In this case, the material resists if the normal stresses  $\sigma_{n_k n_k}$  according to these planes, at any given point and at the studied time, are below the cleavage threshold:

$$\max_{1 \leq k \leq N} \sigma_{n_k n_k}(\mathbf{x}, t) = \max_{1 \leq k \leq N} \langle \boldsymbol{\sigma}(\mathbf{x}, t) \mathbf{n}_k, \mathbf{n}_k \rangle < \sigma_c, \quad \forall \mathbf{x} \in \Omega_t, \quad \forall t$$

where  $\sigma_c$  refers to the cleavage threshold stress of the studied material. Conversely, there is cleavage as soon as, at least at one point  $\mathbf{x}_O$  of the domain, there is a direction  $\mathbf{n}_l$  of the crystal such that we have:

$$\sigma_{n_l n_l}(\mathbf{x}_O, t) = \langle \boldsymbol{\sigma}(\mathbf{x}_O, t) \mathbf{n}_l, \mathbf{n}_l \rangle = \sigma_c$$

In the case of a polycrystalline material, composed of a multitude of crystals (or “grains”) of any orientation, or in the case of amorphous materials, which are without crystal structure, the most straightforward generalization of the previous criterion is to assume that all facets play a similar role with respect to cleavage, hence the following criterion.

**Maximum normal stress criterion.** For brittle materials subjected to cleavage, the maximum normal stress criterion specifies that cleavage failure will occur as soon as, at a specific point in the material domain, the normal stress on a facet reaches a threshold value  $\sigma_r$ , independent of the orientation of the facet, and which can be determined by a macroscopic characterization test (such as a tensile test, for example). Thus, there is no failure if:

$$\max_{\|\mathbf{n}\|=1} \sigma_{nn}(\mathbf{x}, t) < \sigma_r, \quad \forall \mathbf{x} \in \Omega_t, \quad \forall t$$

and, conversely, failure occurs as soon as there is  $\mathbf{x}_O \in \Omega_t$  such that:

$$\max_{\|\mathbf{n}\|=1} \sigma_{nn}(\mathbf{x}_O, t) = \sigma_r$$

The facet that breaks is therefore the facet that has suffered the greatest normal stress, all facets combined; the Mohr's circles, visible in Figure 3.13, allow to immediately establish that it is actually the major principal stress ( $\sigma_1$ ) at the point under study:

$$\max_{\|\mathbf{n}\|=1} \sigma_{nn}(\mathbf{x}, t) = \sigma_1(\mathbf{x}, t), \forall \mathbf{x} \in \Omega_t, \forall t$$

and that the compliance with the criterion therefore consists of the situation described in the figure.

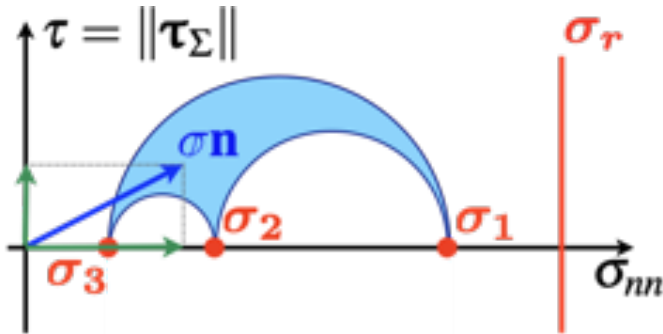


Figure 3.13: Mohr's circles: compliance with the maximum normal stress criterion.

■ **Example 3.4 — Tensile strength of concrete.** Concrete is a good example of a brittle material that breaks by cleavage; it is actually a ceramic (cement), reinforced by particles (grains of sand and stones), and has extremely low resistance to cleavage, namely a few MPa at most. This implies that we often prefer to consider that this material can not withstand tension, and say that there is a failure as soon as:

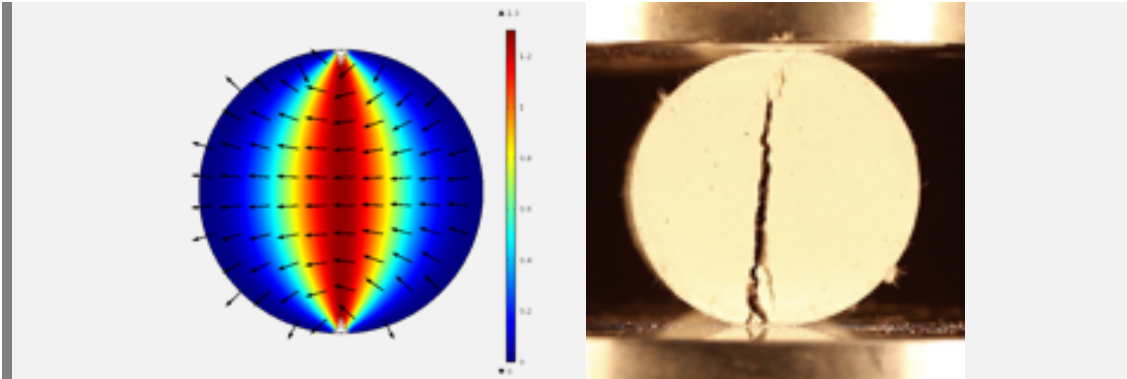
$$\max_{\|\mathbf{n}\|=1} \sigma_{nn} > 0$$

at a point in the structure under study.

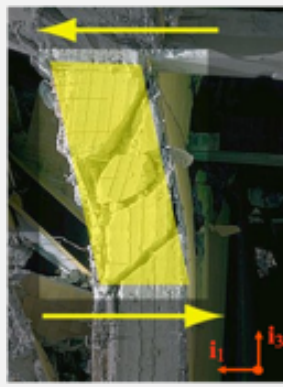
In practice, this explains why the determination of this tensile strength cannot be carried out using a conventional tensile test, as the failure would occur far too quickly to be able to deduce a reliable value. The tensile strength is then determined by a “Brazilian test”, which consists of a diametral compression test of a cylindrical specimen of concrete. It can then be shown that the major principal stress is maximum at any point along this diameter, and is:

$$\max_{\mathbf{x} \in \Omega_t} \sigma_1(\mathbf{x}) = \frac{2P}{\pi DH}$$

where  $P$  is the compression force, and  $D$  and  $H$  are the diameter and height of the cylindrical specimen, respectively. For conventional specimen sizes ( $D \approx H \approx 10\text{cm}$ ), the compression failure force is then about ten kN, which guarantees good experimental precision. The figure below compares the result of a numerical simulation (where the colours are associated with the major principal stress, expressed in MPa, and the arrows represent the associated principal direction, at each point) with the cracking during an experimental test.



This criterion also makes it possible to interpret the mode of failure of concrete pillars subjected to seismic loading, as shown below.



This loading can, as a first approximation, be modelled as a uniform shear stress in the pillar:

$$\sigma = t(\mathbf{i}_1 \otimes \mathbf{i}_3 + \mathbf{i}_3 \otimes \mathbf{i}_1)$$

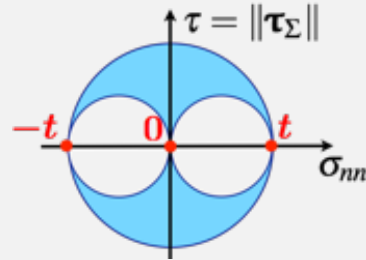
with  $t > 0$ , and where  $\mathbf{i}_3$  is vertical, upwards, and  $\mathbf{i}_1$  is the shear direction on the lower and upper surfaces of the pillar. The principal stresses are then solutions of:

$$\det(\sigma - \sigma_k \mathbb{I}) = -\sigma_k^3 + t^2 \sigma_k = 0$$

or, at any point (since the shear is uniform):

$$\sigma_1 = t, \sigma_2 = 0, \sigma_3 = -t$$

which can be seen in Mohr's plane below. The major principal stress  $\sigma_1$  is therefore strictly positive, of associated principal direction  $\Phi_1^\sigma = (\mathbf{i}_1 + \mathbf{i}_3)/\sqrt{2}$ . This allows us to justify *a posteriori* why the cracks form an angle of approximately  $45^\circ$  with respect to the vertical: this angle corresponds to the orientation of the facets which are subjected to pure tension.



**Summary 3.1 — Design according to a cleavage failure criterion.** A material domain  $\Omega_t$ , whose material is brittle, with a cleavage strength  $\sigma_r$ , maintains its integrity if:

$$\sigma_1(\mathbf{x}, t) = \max_{\|\mathbf{n}\|=1} \sigma_{nn}(\mathbf{x}, t) < \sigma_r, \forall \mathbf{x} \in \Omega_t, \forall t$$

where  $\sigma_1$  and  $\sigma_{nn}$  are respectively the first principal stress, and the normal stress associated with a facet of normal  $\mathbf{n}$ . Failure then occurs at the first point  $\mathbf{x}_O$  such that, at time  $t$ :

$$\sigma_1(\mathbf{x}_O, t) = \max_{\|\mathbf{n}\|=1} \sigma_{nn}(\mathbf{x}_O, t) = \sigma_r$$

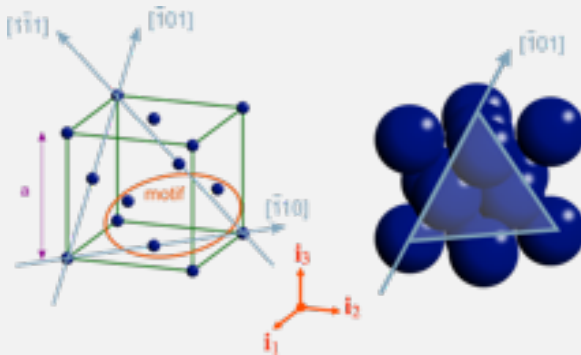
### 3.2.3 Shear failure criteria

In the case of ductile materials, which have a predominantly crystalline structure, we have seen in Paragraph 3.1.1 that slips could occur according to certain privileged atomic planes, creating irreversible movements that cause the specimen to undergo plastic deformation. Thus, in the case of a monocrystalline material occupying the domain  $\Omega_t$  at the instant  $t$ , we can establish a criterion similar to the one we had established for cleavage failure: it is Schmid's law which, for slip directions  $\mathbf{m}_k$  ( $1 \leq k \leq N$ ) associated with respective slip planes of normal vectors  $\mathbf{n}_k$ , establishes that there is no plastic slip if the shear stress  $\tau_{m_k n_k}$  according to these directions, at any given point and at the studied time, are below the slip threshold:

$$\max_{1 \leq k \leq N} \tau_{m_k n_k}(\mathbf{x}, t) = \max_{1 \leq k \leq N} \langle \boldsymbol{\sigma}(\mathbf{x}, t) \mathbf{n}_k, \mathbf{m}_k \rangle < \tau_c, \forall \mathbf{x} \in \Omega_t, \forall t$$

where  $\tau_c$  is the critical shear stress.

#### ■ Example 3.5 — Tensile test on a single crystal.

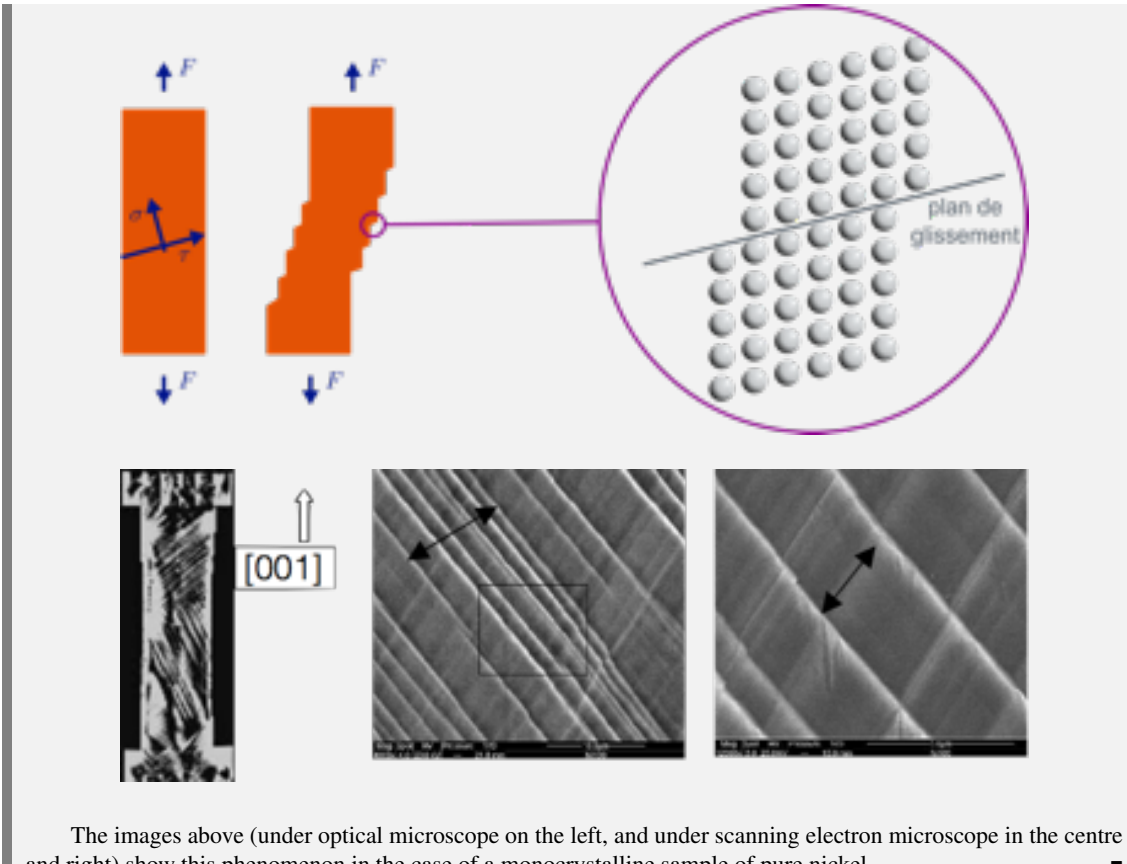


We consider a faced-centred cubic single crystal, subjected to pure tension of axis  $\mathbf{e} = \mathbf{i}_3$  parallel to the vertical axis of the cube represented above:  $\boldsymbol{\sigma} = \sigma_{ee} \mathbf{i}_3 \otimes \mathbf{i}_3$ . The first activated slip system has as characteristics the slip planes of normal vectors  $\mathbf{n}_1 = (\mathbf{i}_1 + \mathbf{i}_2 + \mathbf{i}_3)/\sqrt{3}$  (whose trace on the cube is shown above) and slip directions  $\mathbf{m}_1 = (-\mathbf{i}_1 + \mathbf{i}_3)/\sqrt{2}$  (corresponding to the line  $\bar{[101]}$  above).

Since the stress tensor is assumed to be uniform, Schmid's law then makes it possible to establish that there is no slip if:

$$\tau_{m_1 n_1} = \langle \boldsymbol{\sigma} \mathbf{n}_1, \mathbf{m}_1 \rangle = \sigma_{ee} \langle \mathbf{i}_3, \mathbf{n}_1 \rangle \langle \mathbf{i}_3, \mathbf{m}_1 \rangle = \frac{\sigma_{ee}}{\sqrt{6}} < \tau_c$$

Otherwise, the affected planes may slip, causing "steps" to appear on the surface of the sample, as shown below.



### Criterion based on the maximum shear

In the case of polycrystalline materials (composed of a multitude of grains of any orientation), it can be assumed, as in the case of the cleavage criterion presented above, that all facets play a similar role with respect to slip, thus allowing the following criterion to be proposed.

**Tresca Criterion.** The Tresca criterion for a ductile material specifies that yielding (i.e. exit of the pure elastic region) will occur as soon as, at a point in the material domain, the tangential stress on a facet is higher than a threshold value  $\tau_0$  independent of the orientation of the facet, and which can be determined by a macroscopic characterization test (such as a tensile test for example). Thus, we can say that we remain in the elastic region if:

$$\max_{\|\mathbf{n}\|=1} \|\boldsymbol{\tau}_\Sigma(\mathbf{x}, t)\| < \tau_0, \forall \mathbf{x} \in \Omega_t, \forall t$$

and, conversely, yield occurs as soon as there is  $\mathbf{x}_O \in \Omega_t$  such that:

$$\max_{\|\mathbf{n}\|=1} \|\boldsymbol{\tau}_\Sigma(\mathbf{x}_O, t)\| = \tau_0$$

Mohr's circles, visible in Figure 3.14, show that the greatest tangential stress (as a norm) is equal to the radius of the largest circle, which corresponds to the half difference between the major and minor principal stresses at the point under study:

$$\max_{\|\mathbf{n}\|=1} \|\boldsymbol{\tau}_\Sigma(\mathbf{x}, t)\| = \frac{\sigma_1(\mathbf{x}, t) - \sigma_3(\mathbf{x}, t)}{2}$$

and that it is obtained for facets whose normal vectors are the bisectors of the angles formed by the principal directions  $\phi_1^\sigma$  and  $\phi_3^\sigma$ , hence:

$$\mathbf{n} = \frac{1}{\sqrt{2}}(\phi_1^\sigma \pm \phi_3^\sigma)$$

In addition, the following example shows that the shear threshold value is directly related to the tensile yield strength  $\sigma_0$ :  $\tau_0 = \sigma_0/2$ .

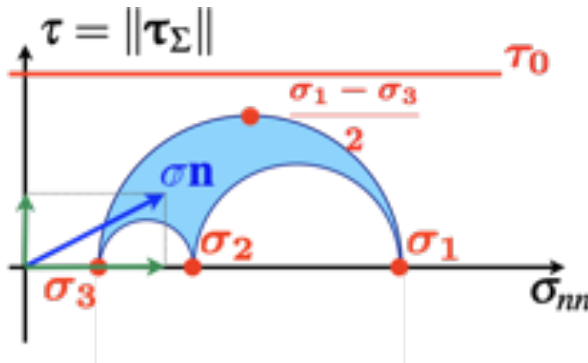


Figure 3.14: Mohr's circles: compliance with the Tresca criterion.

■ **Example 3.6 — Tensile test on a polycrystal: Tresca criterion.** A polycrystal is subjected to a simple tensile test of direction  $\mathbf{e}$ :  $\boldsymbol{\sigma} = \sigma_{ee}\mathbf{e} \otimes \mathbf{e}$ . The Tresca criterion makes it possible to affirm that one remains in the elastic region as long as:

$$\frac{\sigma_1 - \sigma_3}{2} = \frac{\sigma_{ee}}{2} < \tau_0$$

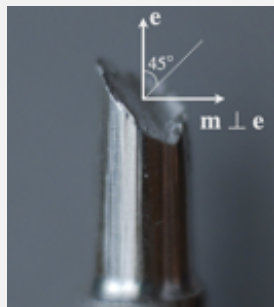
where the principal stresses  $\sigma_1 = \sigma_{ee}$  and  $\sigma_3 = 0$  were determined in Example 3.2. This shows that the threshold value  $\tau_0$  is easily determined with a tensile test, taking  $\tau_0 = \sigma_0/2$ , where  $\sigma_0$  is the tensile yield strength of the studied material.

This result is of course consistent with the expression of the norm of the tangential stress obtained in Example 3.1:

$$\|\boldsymbol{\tau}_\Sigma\| = \frac{\sigma_{ee} |\sin(2\alpha)|}{2}$$

where  $\alpha$  refers to the angle between the direction  $\mathbf{e}$  of tension and the normal vector  $\mathbf{n}$  to the facet. Indeed, this norm is maximum for  $\alpha = 45^\circ$  and is  $\|\boldsymbol{\tau}_\Sigma\|_{max} = \sigma_{ee}/2$ .

Besides, the concerned facets are inclined at  $45^\circ$  with respect to the axis of tension, which effectively corresponds to normal vectors equal to the bisectors of the angles formed by the direction of tension  $\mathbf{e}$  and any direction perpendicular to  $\mathbf{e}$ . This can be confirmed by experiments: for some materials and specific loading conditions, instead of the cup-and-cone shaped fracture surfaces visible in Figure 3.9, it is possible to observe an approximately flat fracture surface, inclined at  $45^\circ$ , as shown in the illustration below, for the failure of an aluminium test specimen.



**R** Given its definition, the stress assessed in the Tresca criterion, commonly referred to as the Tresca stress, is an invariant of the stress tensor, since it does not depend on the choice of the vector basis for expressing this latter, and is written in a simple way using the principal stresses.

### 'Alternative' criterion

Since the Tresca criterion that has just been established does not always agree with experiments, and also requires the calculation of the principal stresses, another proposal is to define a criterion directly related to the stress tensor, or at least to the part of it that is characteristic of shear. For this purpose, the following decomposition is introduced.

**Orthogonal decomposition of the stress tensor.** We can write at any point of the domain the stress tensor as the sum of two tensors:

$$\boldsymbol{\sigma} = \sigma_m \mathbb{I} + \boldsymbol{\sigma}_D = \frac{\text{tr } \boldsymbol{\sigma}}{3} \mathbb{I} + \boldsymbol{\sigma}_D$$

where  $\sigma_m \mathbb{I}$  is the "spherical part" of  $\boldsymbol{\sigma}$ , which represents the average normal stress in the domain, and  $\boldsymbol{\sigma}_D$  is called the "deviatoric part" of  $\boldsymbol{\sigma}$ , which by construction has a trace equal to zero because:

$$\text{tr } \boldsymbol{\sigma}_D = \text{tr}(\boldsymbol{\sigma} - \sigma_m \mathbb{I}) = \text{tr } \boldsymbol{\sigma} - \sigma_m \text{tr } \mathbb{I} = \text{tr } \boldsymbol{\sigma} - \frac{\text{tr } \boldsymbol{\sigma}}{3} \cdot 3 = 0$$

A schematic representation of this decomposition is given in Figure 3.15.

This decomposition is referred to as orthogonal because we have, in the sense of the tensor scalar product, as defined in Appendix A.2.2:

$$\langle \boldsymbol{\sigma}_D, \sigma_m \mathbb{I} \rangle = \text{tr}(\sigma_m \mathbb{I}^T \boldsymbol{\sigma}_D) = \sigma_m \text{tr } \boldsymbol{\sigma}_D = 0$$

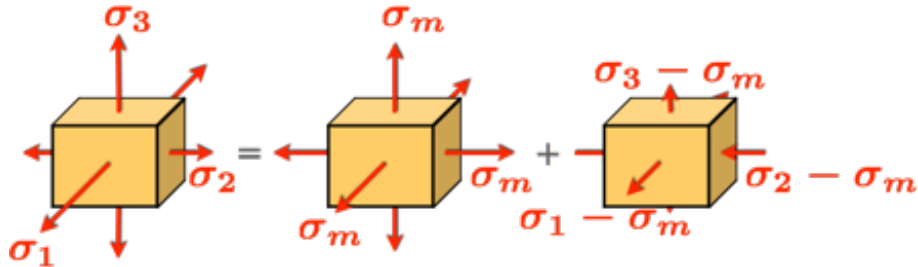


Figure 3.15: Orthogonal decomposition of the stress tensor (in the basis of the principal directions).

The deviatoric part  $\boldsymbol{\sigma}_D$  defined in this manner is an indicator of shear: if it is zero, we necessarily have  $\boldsymbol{\sigma} = \sigma_m \mathbb{I}$  which is isotropic, in other words, which has no shear, regardless of the facet under study. A new shear failure criterion is then defined using  $\boldsymbol{\sigma}_D$ .

**von Mises Criterion.** The von Mises criterion for a ductile material specifies that yield will occur as soon as, at a material point, the equivalent von Mises stress  $\sigma_{\text{eq}}$  is greater than the tensile yield stress  $\sigma_0$ . We therefore remain in the elastic region if:

$$\sigma_{\text{eq}}(\mathbf{x}, t) < \sigma_0, \forall \mathbf{x} \in \Omega_t, \forall t$$

where the definition of von Mises stress, at any point and at any time, is associated with the

tensor norm (as defined in Appendix : A.2.2) of the deviatoric part of  $\sigma$ :

$$\sigma_{\text{eq}}(\mathbf{x}, t) = \sqrt{\frac{3}{2} \|\sigma_D(\mathbf{x}, t)\|^2} = \sqrt{\frac{3}{2} \text{tr}(\sigma_D(\mathbf{x}, t)^2)}$$

since  $\sigma_D$  is symmetrical. Conversely, yield occurs as soon as there is  $\mathbf{x}_O \in \Omega_t$  such that:

$$\sigma_{\text{eq}}(\mathbf{x}_O, t) = \sigma_0$$



*The previous criterion can also have an energetic interpretation: indeed, we can show that the von Mises stress is related to what is defined as the elastic shear strain energy, implying that the criterion can express the fact that one enters plasticity as soon as this energy reaches a given threshold.*

*Moreover, whatever the interpretation adopted, we find that the von Mises stress is an invariant of the stress tensor, which can be expressed as a function of the principal stresses:*

$$\sigma_{\text{eq}} = \sqrt{\frac{(\sigma_1 - \sigma_2)^2 + (\sigma_2 - \sigma_3)^2 + (\sigma_3 - \sigma_1)^2}{2}}$$

■ **Example 3.7 — Tensile test on a polycrystal: von Mises criterion.** We consider a polycrystal subjected to a simple tensile test of direction  $\mathbf{e} = \mathbf{i}_3$ :  $\sigma = \sigma_{ee}\mathbf{i}_3 \otimes \mathbf{i}_3$ , with  $\sigma_{ee} > 0$ . The von Mises criterion makes it possible to affirm that one remains in the elastic region as long as:

$$\sigma_{\text{eq}} < \sigma_0$$

where  $\sigma_0$  is the tensile yield strength of the studied material. In this case, the equivalent von Mises stress is expressed as:

$$\sigma_{\text{eq}} = \sqrt{\frac{3}{2} \text{tr} \sigma_D^2} = \sqrt{\frac{3}{2} \text{tr} \left( \left( \sigma - \frac{\sigma_{ee}}{3} \mathbb{I} \right)^2 \right)}$$

taking into account the definition of the deviator part of  $\sigma$ :  $\sigma_D = \sigma - (\text{tr } \sigma) \mathbb{I}/3$ . We then obtain :

$$\sigma_{\text{eq}} = \sqrt{\frac{3}{2} \text{tr} \left( \left( -\frac{\sigma_{ee}}{3} (\mathbf{i}_1 \otimes \mathbf{i}_1 + \mathbf{i}_2 \otimes \mathbf{i}_2) + \frac{2\sigma_{ee}}{3} \mathbf{i}_3 \otimes \mathbf{i}_3 \right)^2 \right)} = \sqrt{\frac{3}{2} \left( \frac{\sigma_{ee}^2}{9} + \frac{\sigma_{ee}^2}{9} + \frac{4\sigma_{ee}^2}{9} \right)} = \sigma_{ee}$$

since  $\text{tr}(\mathbb{A}^2) = A_{11}^2 + A_{22}^2 + A_{33}^2 + 2A_{12}^2 + 2A_{13}^2 + 2A_{23}^2$  for a symmetrical tensor  $\mathbb{A}$ , of components  $A_{mn}$  in the vector basis  $(\mathbf{i}_1, \mathbf{i}_2, \mathbf{i}_3)$ .

In the case of a tensile test, the equivalent von Mises stress  $\sigma_{\text{eq}}$  is therefore directly equal to the value of the uniaxial stress, which justifies *a posteriori* the 3/2 coefficient in the definition of  $\sigma_{\text{eq}}$ . The von Mises criterion is therefore reduced in this case to:

$$\sigma_{ee} < \sigma_0$$

to ensure that we stay in the elastic region. ■

**Summary 3.2 — Design according to a shear failure criterion.** A material domain  $\Omega_t$ , whose material is ductile and has a yield strength  $\sigma_0$ , remains in the elastic region if it meets one of the following two criteria, to be chosen according to the material studied:

- Tresca criterion:

$$\frac{\sigma_1(\mathbf{x}, t) - \sigma_3(\mathbf{x}, t)}{2} = \max_{\|\mathbf{n}\|=1} \|\boldsymbol{\tau}_\Sigma(\mathbf{x}, t)\| < \frac{\sigma_0}{2}, \quad \forall \mathbf{x} \in \Omega_t, \quad \forall t$$

where  $\sigma_1$  and  $\sigma_3$  are the major and minor principal stresses respectively, and  $\boldsymbol{\tau}_\Sigma$  is the shear stress associated with a facet of normal vector  $\mathbf{n}$ ;

- von Mises criterion:

$$\sigma_{\text{eq}}(\mathbf{x}, t) = \sqrt{\frac{3}{2} \operatorname{tr}(\boldsymbol{\sigma}_D(\mathbf{x}, t)^2)} < \sigma_0, \forall \mathbf{x} \in \Omega_t, \forall t$$

where  $\boldsymbol{\sigma}_D(\mathbf{x}, t) = \boldsymbol{\sigma}(\mathbf{x}, t) - (\operatorname{tr} \boldsymbol{\sigma}(\mathbf{x}, t)) / 3 \mathbb{I}$  is the deviatoric part of the stress tensor.

Yield then occurs locally at the first point  $\mathbf{x}_O$  such that, at time  $t$ , the selected criterion for the material is no longer verified, i.e. respectively when:

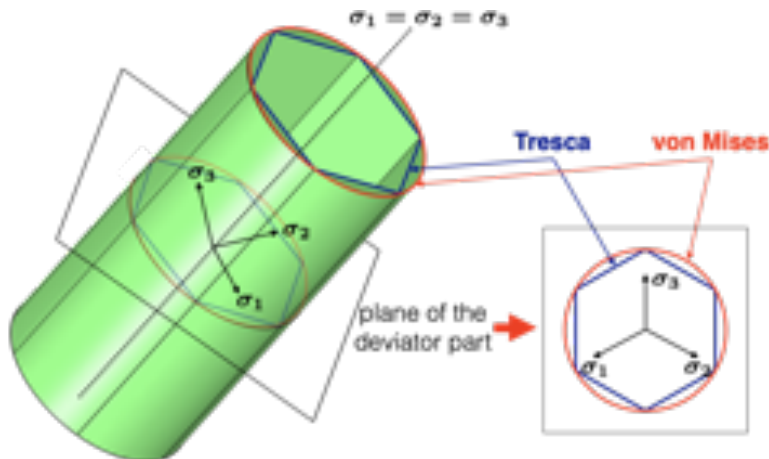
$$\frac{\sigma_1(\mathbf{x}_O, t) - \sigma_3(\mathbf{x}_O, t)}{2} = \max_{\|\mathbf{n}\|=1} \|\boldsymbol{\tau}_{\Sigma}(\mathbf{x}_O, t)\| = \frac{\sigma_0}{2}$$

$$\sigma_{\text{eq}}(\mathbf{x}_O, t) = \sqrt{\frac{3}{2} \operatorname{tr}(\boldsymbol{\sigma}_D(\mathbf{x}_O, t)^2)} = \sigma_0$$

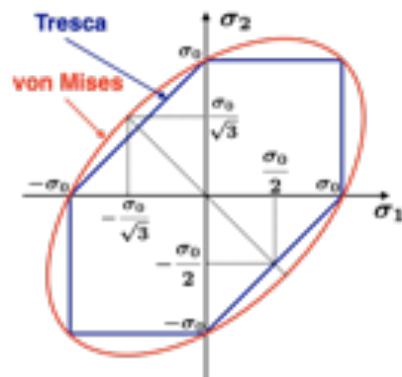


*It is interesting to compare the Tresca and von Mises criteria, for the same yield strength  $\sigma_0$ . First of all, the two criteria, of course, have the common property of being insensitive to pressure: indeed, if the stress state  $\boldsymbol{\sigma}$  is admissible,  $\boldsymbol{\sigma} + p\mathbb{I}$  is also admissible, regardless of the pressure  $p$ .*

*Besides, both criteria can easily be represented in the three-dimensional basis of principal stresses. By definition, the von Mises criterion can be represented as a cylinder of revolution, of radius  $\sigma_0$ , and of axis the line corresponding to the identity tensor (of components  $(1, 1, 1, 1)$  in this basis); similarly, we can show that the Tresca criterion takes the form of a hexagonal base cylinder of side  $\sigma_0$  and axis of the same direction. Both criteria are shown in the figures below.*



*A projection of these criteria, interesting to analyze, corresponds to the case where one of the principal stresses ( $\sigma_3$  for example) is equal to zero. In this case, the curves obtained for the von Mises and Tresca criteria are shown below.*



### 3.2.4 Other criteria

In the above, we have deliberately limited ourselves to presenting the most commonly used criteria for the design of parts or structures based on metallic or ceramic materials. There is a multitude of others, some of which may focus on the strain tensor rather than the stress tensor. In any case, all have in common the ability to represent, at a macroscopic scale, phenomena that occur at a microscopic scale. Without being exhaustive, here are two criteria that allow us to see the diversity of possible forms.

#### Tsai-Hill criterion

In the case of materials with a highly anisotropic microstructure, it is necessary to have a criterion that is associated with the different directions characteristic of the medium. This is the case, for example, of long-fibre composite materials, the structure of which is shown in Figure 3.16, and for which the tensile strength may be ten times higher for a tensile test along the fibre direction than in a perpendicular direction, as shown in Table 3.1. These materials are generally manufactured in the form of layers (or “plies”) for which the directions of the fibres are all identical.

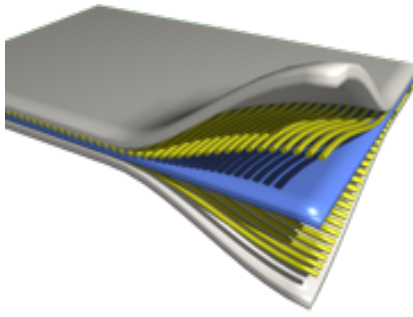


Figure 3.16: Example of a long-fibre composite material (two plies shown).

In the case of a thin plate (of plane  $(\mathbf{i}_1, \mathbf{i}_2)$ ), for which only one direction of fibres is present, a strength criterion can be written (assuming that the stress along the third direction  $\mathbf{i}_1 \wedge \mathbf{i}_2$  is negligible) as:

$$\left(\frac{\sigma_L}{X}\right)^2 - \frac{\sigma_L \sigma_T}{X^2} + \left(\frac{\sigma_T}{Y}\right)^2 + \left(\frac{\tau_{LT}}{S}\right)^2 < 1$$

where we have considered a local vector basis associated with the direction of the fibres in the plate ( $\mathbf{e}_L$ : direction of the fibres,  $\mathbf{e}_T$ : direction, which is perpendicular to that of the fibres):

$$\sigma_L = \langle \boldsymbol{\sigma} \mathbf{e}_L, \mathbf{e}_L \rangle, \quad \sigma_T = \langle \boldsymbol{\sigma} \mathbf{e}_T, \mathbf{e}_T \rangle, \quad \tau_{LT} = \langle \boldsymbol{\sigma} \mathbf{e}_L, \mathbf{e}_T \rangle = \langle \boldsymbol{\sigma} \mathbf{e}_T, \mathbf{e}_L \rangle$$

and the associated strength values, measured using specific tests, are noted  $X$ ,  $Y$  and  $S$  respectively. Figure 3.17 allows us to visualize the domain where the criterion is verified, for different values of the local shear stress  $\tau_{LT}$ .

#### Mohr-Coulomb criterion

Another criterion, widely used in the case of granular or porous media, is the Mohr-Coulomb criterion, which allows for taking into account the increase in the shear strength of the medium when the applied pressure increases (which justifies *a posteriori* the interest of compacting a soil). This criterion can be used in particular in the case of concrete, although there are other specific and more precise criteria for this material. To avoid failure, one has to verify:

$$\|\boldsymbol{\tau}_\Sigma\| + \sigma_{nn} \tan \phi < c$$

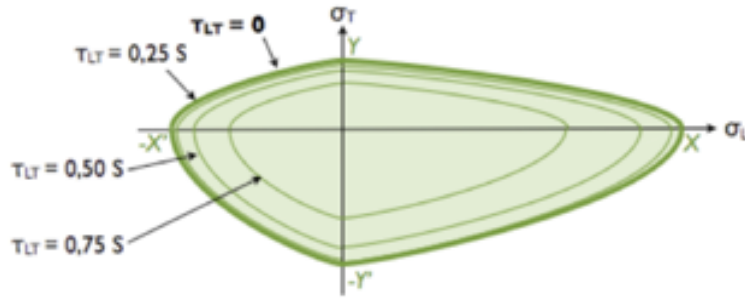


Figure 3.17: Visualization of the Tsai-Hill criterion in the stress plane  $(\sigma_L, \sigma_T)$ .

where  $c$  represents the “cohesion” of the medium, which refers to the shear strength of the medium at zero pressure, and  $\phi$  is the “angle of internal friction” characterizing the strength of the medium due to friction forces between its grains. The visualization of this criterion is straightforward using the Mohr’s circles: it consists in saying that the Mohr’s circles must remain below the line of equation  $\tau = c - \sigma_{nn} \tan \phi$  to avoid failure. Figure 3.18 depicts two different stress states verifying this criterion and shows the improved strength of the medium when the pressure increases, i.e. when the Mohr’s circles move to the left.

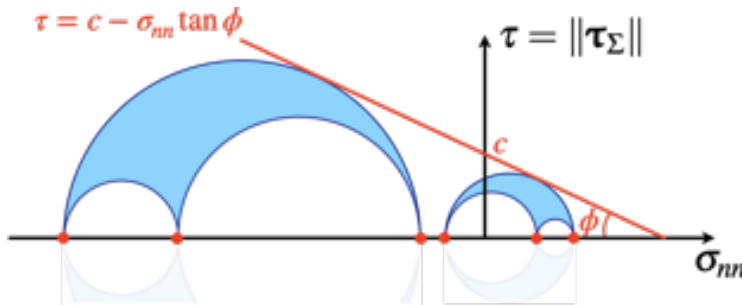


Figure 3.18: Visualization of the Mohr-Coulomb criterion in the Mohr plane.



In all this part, we have limited ourselves to the case of monotonous stresses that are applied until fracture. Another important class of loadings to take into account is cyclic loadings, which can lead to material failure after a more or less significant number of cycles, and for load amplitudes that are much smaller than in the monotonous case. This is referred to as “fatigue failure” of the material.

Besides, to be exhaustive, it would also be necessary to mention all causes other than mechanical that can lead to failure: thermal, chemical, ...

### 3.3 Stress concentrations

An essential point to take into account in the parts or structures being designed is that the presence of defects, such as holes, tends to increase the expected stress level significantly, and can quickly lead to failure. In the same way, specific shapes are to be avoided for the geometry of the part, otherwise, the stresses may locally increase. Figure 3.19 shows this phenomenon for compression specimens where the stress field is visualized by photoelasticity. Of course, these variations are related to the elastic behaviour of the material and would be different for another kind of behaviour.



Figure 3.19: Influence of defects on the stress field in compression specimens: visualization of isochromatic fringes obtained by photoelasticity.

### 3.3.1 Influence of a hole

A first typical example of the nature of the phenomenon is to study the influence of a hole on an otherwise uniform stress field. This scenario will show that the resulting local increase in stress is not related to the reduction in the area of the cross-section actually able to withstand internal forces; we will then speak of “stress concentration” to designate this phenomenon. The estimation of this latter can be obtained by solving the associated elasticity problem, as defined in Chapter 5. In what follows, we show how numerical simulation can be an efficient way of evaluating this phenomenon.

#### Plate with a circular hole in tension

One case that can be treated analytically is that of a plate, subjected to a simple tensile stress along one of its edges ( $\sigma = \sigma_\infty \mathbf{i}_1 \otimes \mathbf{i}_1$ ), and which has a circular hole in its centre with dimensions significantly smaller than the lateral dimensions of the plate, so that there is no influence of the free boundary conditions (on the sides of the plate) on the stress field near the hole.

Figure 3.20 shows the two components  $\sigma_{11}$  (bottom right) and  $\sigma_{22}$  (bottom left) of the stress tensor, obtained by numerical simulation for the upper right quarter of the geometry (the solution being symmetrical with respect to the two median planes of the plate). We see:

- on the one hand, that there is a compression area, “before” and “after” the hole along the longitudinal direction of the specimen; this zone is thus dominated by negative transverse stresses ( $\sigma_{22}$ ), the minimum being directly the opposite of the tensile stress  $\sigma_\infty$  applied to the plate;
- on the other hand, that there is a high-tension area at the hole, along a direction perpendicular to the direction of tension; the longitudinal stresses ( $\sigma_{11}$ ), just at the edge of the hole, amount

to three times the tensile stress  $\sigma_\infty$  applied to the plate.

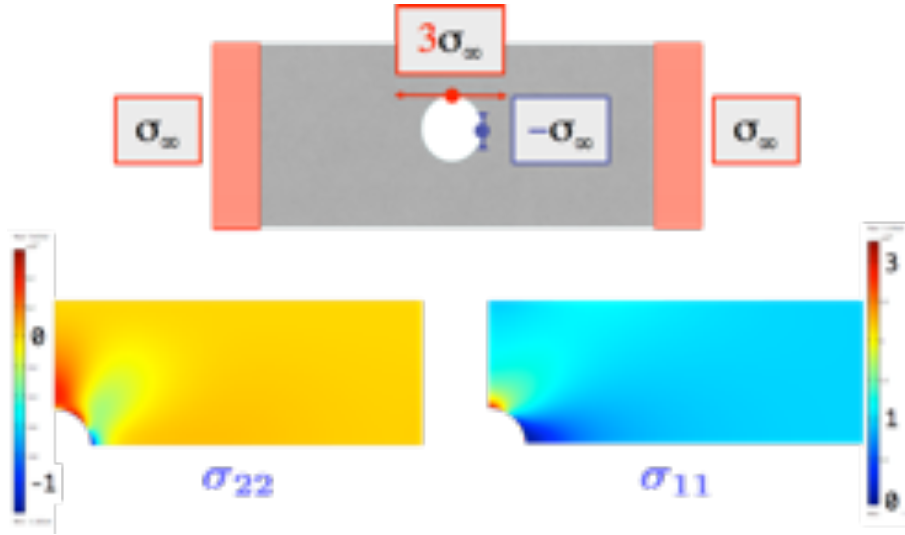


Figure 3.20: Stress field in a plate with a circular hole.

The stress concentration coefficient, noted  $K_t$ , is then defined as the ratio between the maximum stress obtained because of the defect and the nominal stress that would have been observed in the absence of the defect, i.e. here:  $K_t = 3$ .

In particular, it can be seen that this coefficient does not depend on the radius of the hole, but only on the geometry of the defect, as confirmed below.

#### From the hole to the crack

If we now study a hole of elliptical shape, of half axes  $a$  and  $b$  respectively according to  $\mathbf{i}_2$  and  $\mathbf{i}_1$ , a tensile stress identical to the previous case ( $\boldsymbol{\sigma} = \sigma_\infty \mathbf{i}_1 \otimes \mathbf{i}_1$ ) allows us to obtain, by numerical simulation, a component  $\sigma_{11}$  represented on Figure 3.21 (on a quarter of the geometry).

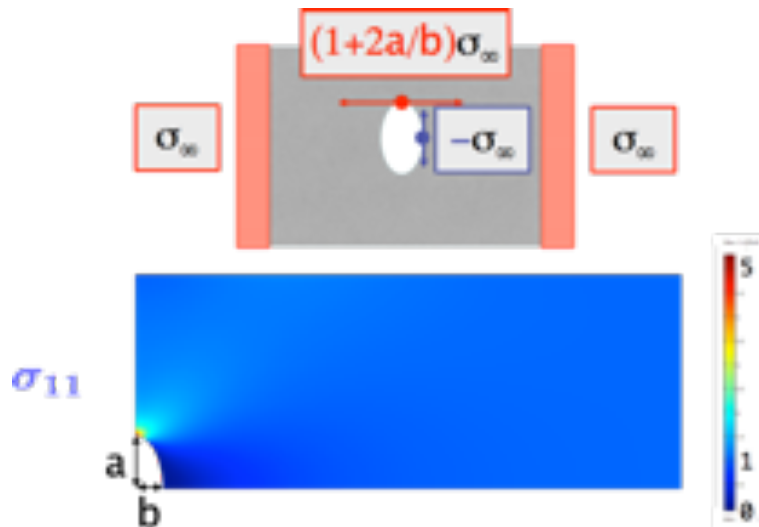


Figure 3.21: Stress field in a plate with an elliptical hole.

We then see that, even if stress concentrations are much more confined near the hole, the

maximum value of the longitudinal stress ( $\sigma_{11}$ ) now implies a stress concentration coefficient:

$$K_t = 1 + 2 \frac{a}{b}$$

or a maximum longitudinal stress, located at  $90^\circ$  at the edge of the hole, equal to five times the nominal stress  $\sigma_\infty$  in the case of a hole twice as wide as long.

In the extreme case where the hole is thin enough to be perceived as a crack, it is possible to establish that it is the minimum radius of curvature  $\rho$  of the hole that is dimensioning, with a resulting stress concentration factor:

$$K_t = 1 + 2 \sqrt{\frac{a}{\rho}}$$

Figure 3.22 allows us to observe the evolution of the longitudinal stress ( $\sigma_{11}$ ), obtained by numerical simulation on a quarter of geometry. It can thus be concluded that the more “angular” the shape of the defect is (in the sense of the more or less rapid variation of its boundary), the more intense the stress concentrations are. This is confirmed by Figure 3.23, which shows the isochromatic fringes of the stress field obtained by photoelasticity.

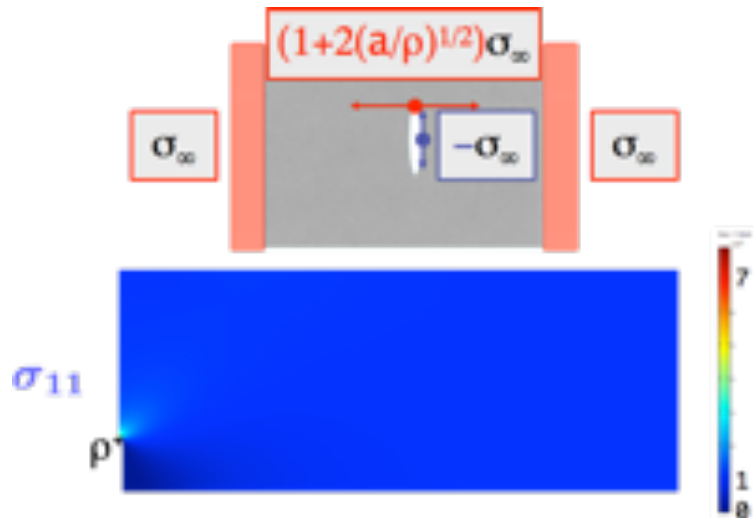


Figure 3.22: Stress field in a plate with a crack.

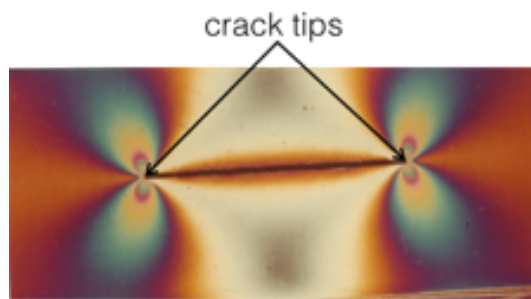


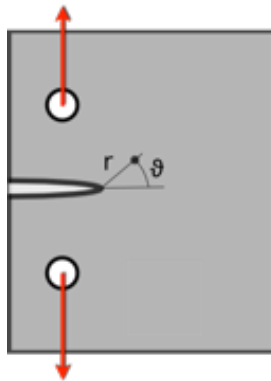
Figure 3.23: Stress field around a crack, observed by photoelasticity (isochromatic fringes).

**R** In the limit case where the radius of curvature  $\rho$  is zero, we find an infinite stress at the crack tip. The framework of fracture mechanics (in the planar case) then allows us to specify the asymptotic form of the stress field in the vicinity of this singular point:

$$\begin{aligned}\sigma_{rr} &\sim \frac{K_I}{4\sqrt{2\pi r}} \left[ 5 \cos\left(\frac{\theta}{2}\right) - \cos\left(\frac{3\theta}{2}\right) \right] \\ \sigma_{\theta\theta} &\sim \frac{K_I}{4\sqrt{2\pi r}} \left[ 3 \cos\left(\frac{\theta}{2}\right) + \cos\left(\frac{3\theta}{2}\right) \right] \\ \sigma_{r\theta} &\sim \frac{K_I}{4\sqrt{2\pi r}} \left[ \sin\left(\frac{\theta}{2}\right) + \sin\left(\frac{3\theta}{2}\right) \right]\end{aligned}$$

where  $(r, \theta)$  are the polar coordinates taking as origin the crack tip. It is then the coefficient  $K_I$ , called "stress intensity factor", that characterizes the field intensity in the vicinity of the crack tip, and therefore the ability of the material to more or less resist crack propagation.

This coefficient can be measured experimentally using specific tests such as tensile tests on notched specimens, called "Compact Tension" (or "CT") specimens, whose geometry is represented schematically below.



In reality, the stress field cannot, of course, be singular at the crack tip: there is a confined plasticity zone that limits the extreme stress values, without significantly influencing the experimental estimation of the stress intensity factor.

### 3.3.2 Influence of geometry

Similarly, variations in the geometry of the structure can have a strong influence on the evolution of the stress field. Figure 3.24 shows in photo-elasticity that, for a fixed overall shape and loading, the presence of concave corners has a significant local influence on the spatial variation of the stress field, but also on the extreme values of this latter.

These findings justify the form adopted for the tensile test specimens, and more precisely, the presence of connection fillets between the shoulders and the gauge section of the test specimen, as mentioned in Paragraph 3.1.1. These fillets make it possible to limit the influence of a sudden variation in geometry, such as a change in section; indeed, Figure 3.25 allows us to compare, on a tensile specimen made of photoelastic material, the evolution of the stress field for a sudden variation in section (left) and for a variation "softened" by the presence of the fillet (right): in the latter case, the coloured fringes are closer than in the immediate vicinity of the right angle on the left side of the specimen.

In order to effectively design such specimens, abacus such as the one in Figure 3.26 can be used to estimate the stress concentration coefficient for a shaft under tensile stress, whose cross-sectional variation is done using a connecting fillet. At fixed diameter ratio  $D/d$ , the coefficient  $K_I$  increases when the radius  $r$  of the fillet decreases, and this increase is all the greater when this radius decreases.

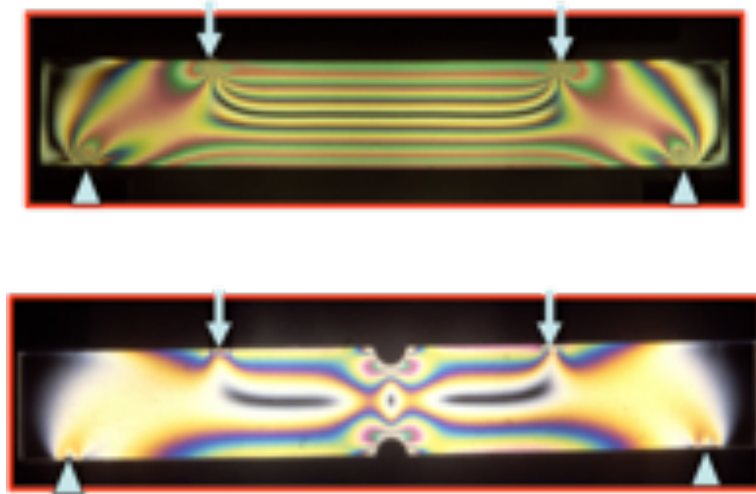


Figure 3.24: Influence of the presence of concave corners: observations in photoelasticity (isochromatic fringes).



Figure 3.25: Influence of a connecting fillet on a tensile specimen: photoelastic observations (isochromatic fringes).

### 3.4 Summary of important formulas

**Design according to a cleavage failure criterion – Summary 3.1 page 83**

$$\text{no failure if } \sigma_1 = \max_{\|\mathbf{n}\|=1} \sigma_{nn} < \sigma_r$$

**Design according to a shear failure criterion – Summary 3.2 page 87**

$$\text{no yield according to the Tresca criterion if } \frac{\sigma_1 - \sigma_3}{2} = \max_{\|\mathbf{n}\|=1} \|\boldsymbol{\tau}_\Sigma\| < \frac{\sigma_0}{2}$$

$$\text{no yield according to the von Mises criterion if } \sigma_{eq} = \sqrt{\frac{3}{2} \text{tr}(\boldsymbol{\sigma}_D^2)} < \sigma_0$$

$$\boldsymbol{\sigma}_D = \boldsymbol{\sigma} - \frac{\text{tr} \boldsymbol{\sigma}}{3} \mathbb{I}$$

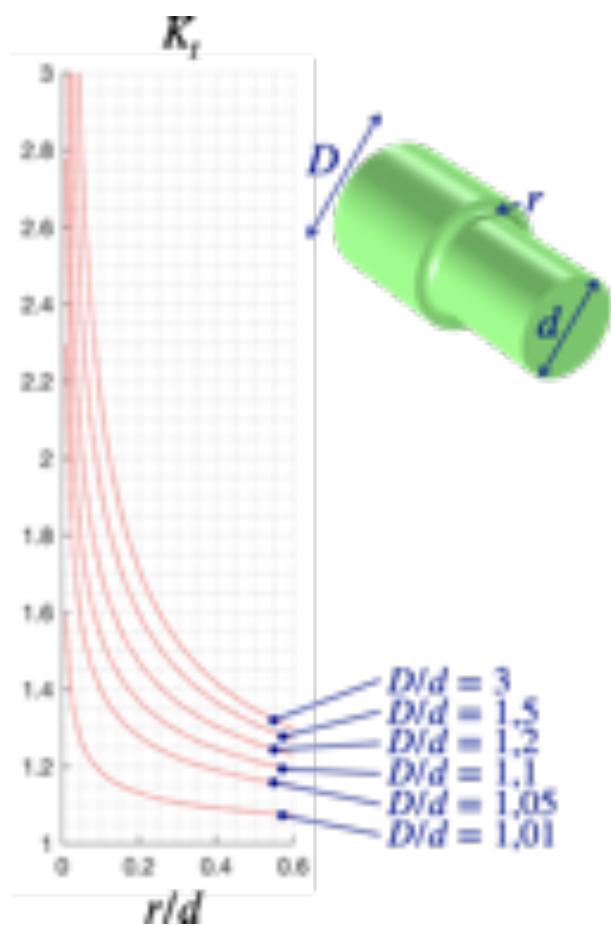


Figure 3.26: Abacus to estimate the stress concentration coefficient in the case of a shaft with shoulders in tension.



## 4. Material behaviour

The previous chapters have allowed us to define the strains and stresses separately within a given material domain. However, it is clear that, for fixed geometry and loading, two bodies made of different materials will deform differently *a priori*. It is, therefore, necessary to establish mathematical relations between the strain and stress tensors in order to solve a mechanical problem in its entirety.

---

### WHY STUDY MATERIAL BEHAVIOUR?

#### 4.1 Mechanical behaviour of deformable solids

Here we summarize the concepts of the previous chapters, which will allow us to solve a complete problem. We limit ourselves to the framework of the infinitesimal deformation hypothesis, which allows us to consider as one the initial and current configurations: we will then note  $\mathbf{x}$  the spatial variable.

##### 4.1.1 Review of the unknowns and equations of the problem

To solve a continuum mechanics problem is to be able to determine, at each point  $\mathbf{x}$  of a material domain  $\Omega$ , and at any time  $t$ :

- the displacement field  $\mathbf{u}(\mathbf{x}, t)$ , consisting of three scalar functions of space and time;
- the strain field  $\boldsymbol{\epsilon}(\mathbf{x}, t)$  (represented by the infinitesimal strain tensor because of the adopted framework), consisting, because of its symmetry, of six scalar functions of space and time;
- the stress field  $\boldsymbol{\sigma}(\mathbf{x}, t)$ , consisting, because of its symmetry, of six scalar functions of space and time.

In all, there are, therefore, fifteen scalar functions of space and time that must be determined to solve the problem under study.

For this purpose, several partial differential equations are currently available, which are valid at any point within the domain, and at any time:

- an equation linking displacement and strains:

$$\boldsymbol{\varepsilon}(\mathbf{x}, t) = \frac{1}{2} \left( \mathbb{D}_{\mathbf{x}} \mathbf{u}(\mathbf{x}, t) + (\mathbb{D}_{\mathbf{x}} \mathbf{u}(\mathbf{x}, t))^T \right)$$

consisting, after projection in a vector basis, of six scalar partial differential equations;

- a local equilibrium equation:

$$\rho(\mathbf{x}, t) \mathbf{a}(\mathbf{x}, t) = \mathbf{f}_V(\mathbf{x}, t) + \operatorname{div}_{\mathbf{x}} \boldsymbol{\sigma}(\mathbf{x}, t)$$

where  $\rho$  and  $\mathbf{a}$  can be expressed as functions of the displacement (the precise details will be recalled in Paragraph 5.1.1); three scalar partial differential equations are then obtained.

We then have nine scalar equations, at any point in the domain and at any time, for which we can write as many boundary conditions as needed:

- known components of the displacement field at certain points on the boundary of the domain;
- known components of the stress vector at other points on the domain boundary;
- initial conditions in displacement and velocity at any point within the domain.

From this list, we can deduce that six scalar equations are missing at each point of the domain at any given time. It is quite instinctive to assume that these missing relations are to be established between stresses and strains, which we have studied separately until now. Indeed, with fixed geometry and loads, it is logical to anticipate that different deformations occur according to the material chosen for the part or structure studied, in particular, if we consider stiffness properties, which we will define later in this chapter.

#### 4.1.2 Diversity of material behaviours

The “constitutive relations” that we seek to establish between stress and strain can be of very different natures depending on the materials studied, and the loadings they undergo (mechanical, thermal, hygrometric, chemical, ...). Ideally, these relations could be determined by describing local phenomena at very small scales within matter, using the results of statistical physics or molecular dynamics, for example. In practice, even if the advances in these fields are significant, it is still challenging to use the results directly to determine the form of constitutive relations (or merely the parameters that govern them) at the macroscopic scale, which is the scale taken into account in the context of continuum mechanics.

Thus, as in the previous chapter, characterization tests such as the tensile test are preferred to determine laws of a phenomenological type (Figure 4.1 allows us to see the diversity of tensile curves that can be obtained for different materials). The working hypothesis is to assume that the mechanical properties that are measured on a sample of material are representative of the properties throughout the medium. Behind this hypothesis, at least one property of macroscopic homogeneity is hidden. Thus, we must take into account as many constitutive relations as there are macroscopically distinct media. For example, if a mechanical structure is obtained by welding, or glueing, of two parts made of different steels, it is necessary to know the respective properties of these two components (and possibly of the weld or glue if it is assumed that the assembly is not perfect) in order to be able to set the equations in each of these media.

Besides, it is also essential to have a certain homogeneity at the microscopic level: different areas must have similar behaviours when considering a volume of sufficient size (but much smaller of course than the size of the test specimen studied). This hypothesis of defining what is called a “representative volume element” (or “RVE”) is what allows us to consider concrete as a homogeneous material on a macroscopic scale despite its different components on the microscopic scale, or steel as an isotropic material despite the multiple orientations of the “grains” which compose it.

Thus, the various characterization tests that can be carried out allow for highlighting a multiplicity of generic classes of behaviours, of which here are some brief elements.

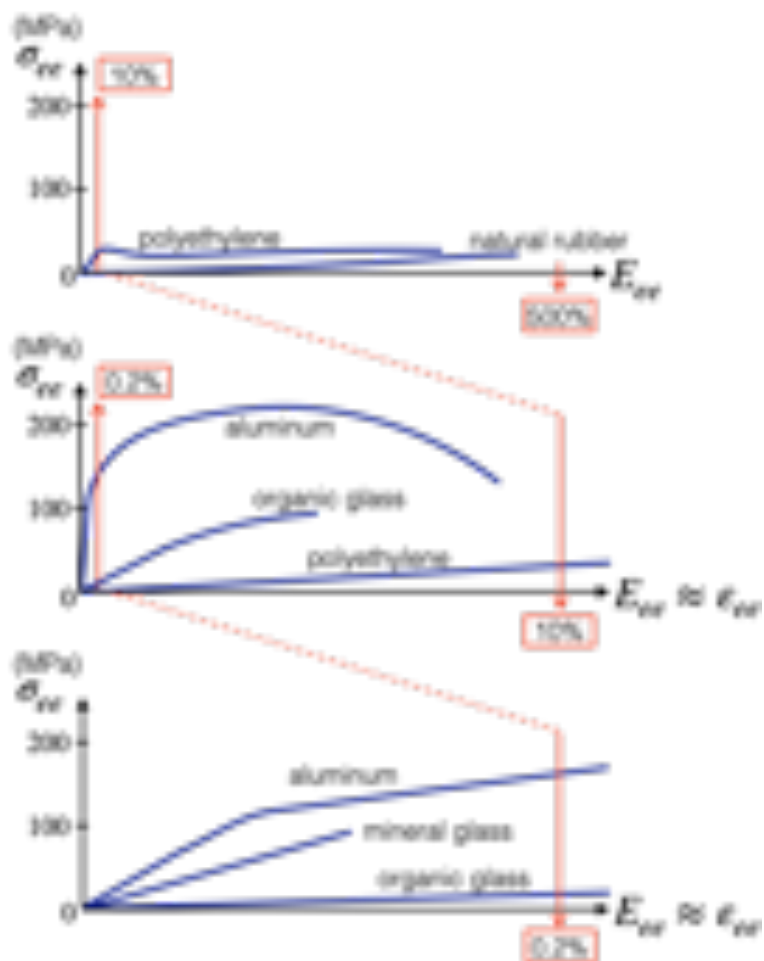


Figure 4.1: Typical tensile curves for different materials.

**Elasticity (linear and non-linear) –** For a low load level, the behaviour is often linear and reversible: during the tensile test, the specimen can be loaded and then discharged several times, each time returning at the origin of the tensile curve, as already mentioned in Paragraph 3.1.1. Depending on the materials, the elastic behaviour may remain when the deformation increases, but with significant non-linearity, as in the case of elastomers for example, as shown in Figure 4.3 (left).

**Yield strength and irreversible deformations –** For ductile materials, beyond a certain threshold called “yield strength”, irreversible deformations appear, which means that after discharge and return to zero stress, we do not return at the origin of the tensile curve. In the case of metallic materials, microscopic mechanisms related to plasticity were quickly mentioned in Paragraph 3.1.1; for polymers, irreversible deformations are mainly due to the sliding of molecular macro-chains between them. When the yield strength does not change as a function of plastic deformation, the material is called “perfectly” plastic; if it changes (as in Figure 4.2), we talk about “hardening”, which can be “isotropic” or “kinematic” depending on the nature of the elastic region evolution.

**Time-dependent behaviour –** For most materials, we can observe a more or less significant evolution of the state of stress or strain while the external loading no longer evolves with time; we then speak of “creep”, when the material gradually deforms under constant loading, or “relaxation”, when the stresses decrease while the specimen shoulders are held still in

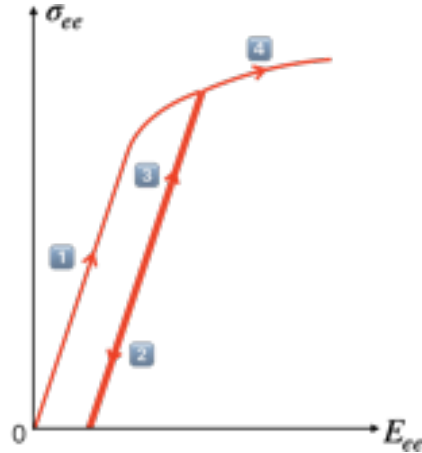
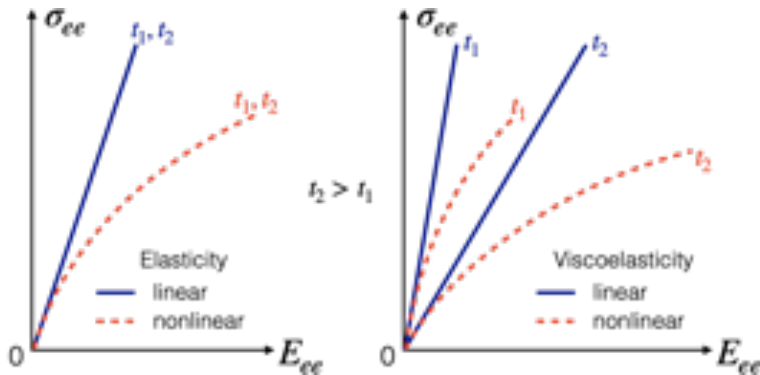


Figure 4.2: Material with hardening.

the machine. These phenomena may be related to “viscoelasticity”, where the stiffness characteristics of the material depend on the stress or strain rates applied, as in the case of polymers in the glass transition zone for example. Figure 4.3 (right) shows the associated behaviour in the case of “isochronous” tests, for which we plot, for different levels of the applied stress, the value of the strain at different times  $t_k$ .

Figure 4.3: Elastic and viscoelastic behaviour for isochronous tests ( $t_2 > t_1$ ).

**Damage** – Mechanical properties can be modified by the evolution of the structure’s “health”: indeed, as we have seen in Paragraph 3.1.2, materials degrade over time under the effect of the loadings they undergo; the defects they contain (voids, inclusions, microcracks) increase due to the underlying stress concentrations, and weaken in particular the overall stiffness. Figure 4.4 shows the typical evolution of the compression behaviour of concrete for several successive loading and unloading operations.

**Cyclic loading and fatigue** – During cyclic loadings, the material may, depending on the case, see its deformations stabilise, or, on the contrary, amplify until failure: we then distinguish “elastic shakedown” (or “adaptation”), “plastic shakedown” (or “accommodation”), and “ratcheting”, depending on whether, on the stress-strain curve, there is stabilisation according to a segment, a loop, or no stabilisation at all (the different cases are shown in Figure 4.5). In the case of fatigue with a large number of cycles, negligible permanent deformations or damage at the beginning can develop and lead to material failure, even at stress levels well below the yield strength.

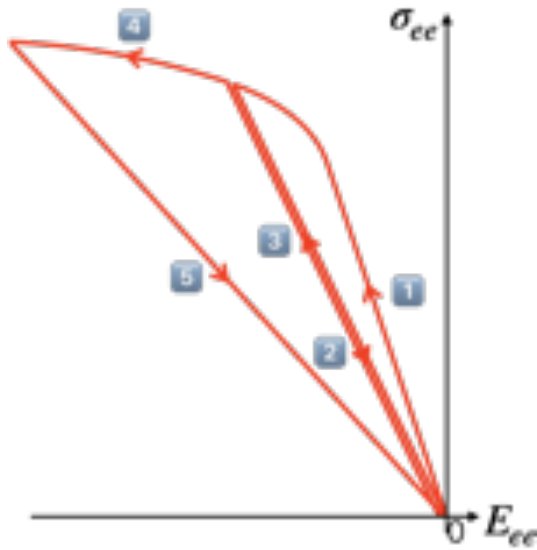


Figure 4.4: Elastic behaviour of concrete with damage (in compression).

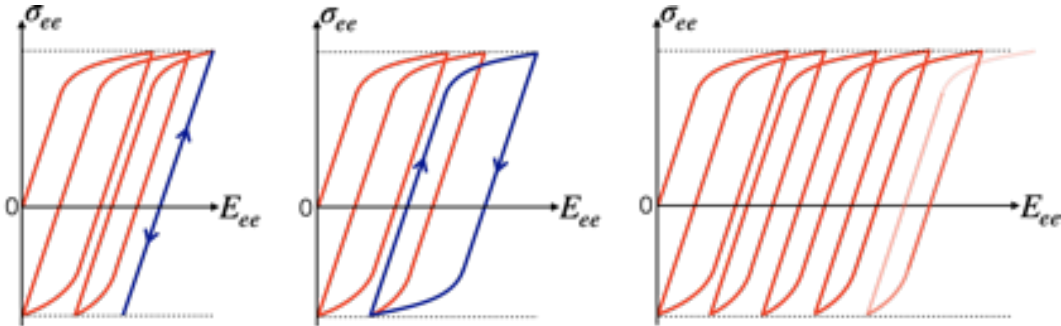


Figure 4.5: Fatigue behaviours: elastic shakedown, plastic shakedown and ratcheting (from left to right).

#### 4.1.3 Linear elastic material for infinitesimal deformations

The previous paragraph allowed us to consider the extreme diversity of the behaviours that can be observed. We will limit ourselves here to the most elementary behaviour to be described, and which is present in all materials: linear elasticity. Elasticity is characterized by reversible behaviour, which means that the relations between stress and strain to be defined is instantaneous: regardless of the history of previous loadings, they have (ideally) no influence on the described behaviour. Besides, the tensile curves presented in Figure 4.1 systematically show a proportionality relationship between uniaxial stress and strain, at least at the beginning of the test.

Of course, this does not allow us to conclude that the stress and strain tensors are proportional: indeed, we have seen in Paragraph 3.1.1 that the transverse dimensions of the specimen decreased when the specimen lengthened; for a tensile test along the axis  $\mathbf{i}_3$ , when we look at the components of the two tensors in a vector basis  $(\mathbf{i}_1, \mathbf{i}_2, \mathbf{i}_3)$ , we have  $\varepsilon_{11} \neq 0$  and  $\varepsilon_{22} \neq 0$ , while the corresponding components of the stress tensor are zero ( $\sigma_{11} = 0 = \sigma_{22}$ ), since the only non-zero component of  $\sigma$  is  $\sigma_{33}$ .

##### Mathematical representation of the constitutive relation

Mathematically, we have seen in the previous chapters that second-order tensors represent linear applications of the vector space in itself: thus, the stress tensor, defined in Paragraph 2.2.2, implies that the stress vector depends linearly on the normal vector at the facet under study.

To obtain a linear dependence of the stress tensor with respect to the infinitesimal strain tensor (or vice versa), we can, therefore, focus on the linear applications of the space of second-order tensors in itself: these applications consist of fourth-order tensors, of which we give some theoretical elements in Appendix A.3. A specific fourth-order tensor is then defined in what follows.

**Elasticity tensor.** The “elasticity tensor” (or “stiffness tensor”) is defined as the fourth-order tensor  $\mathbf{C}$  relating the infinitesimal strain tensor to the stress tensor, at any point of the domain  $\Omega$  and at any time:

$$\boldsymbol{\sigma}(\mathbf{x}, t) = \mathbf{C}(\mathbf{x})\boldsymbol{\varepsilon}(\mathbf{x}, t), \forall \mathbf{x} \in \Omega, \forall t$$

This is equivalent to writing in terms of components in a vector basis  $(\mathbf{i}_1, \mathbf{i}_2, \mathbf{i}_3)$  that:

$$\sigma_{mn} = \sum_{p=1}^3 \sum_{q=1}^3 C_{mnpq} \varepsilon_{pq}, \quad 1 \leq m, n \leq 3$$

It is therefore possible to interpret the elasticity tensor as a four-dimensional table, whose components satisfy:

$$C_{mnpq} = \text{tr}((\mathbf{i}_m \otimes \mathbf{i}_n)^T \mathbf{C}(\mathbf{i}_p \otimes \mathbf{i}_q)), \quad 1 \leq m, n, p, q \leq 3$$

Taking into account the symmetry of the stress and strain tensors, we get the number of independent components of the elasticity tensor reduced, initially, to 36, since:

$$C_{mnpq} = C_{nmpq}, \text{ and } C_{mnpq} = C_{mnqp}, \quad 1 \leq m, n, p, q \leq 3$$

Besides, one can show, using thermodynamic considerations, that the elasticity tensor can be obtained as the second-order derivative of an elastic internal energy, which implies another symmetry condition, namely the “major” symmetry condition:

$$C_{mnpq} = C_{pqmn}, \quad 1 \leq m, n, p, q \leq 3$$

Therefore, the elasticity tensor eventually has 21 independent components *a priori*, which, if they are arbitrary, are therefore able to represent the linear elastic behaviour of every anisotropic material. Of course, this number can be reduced as soon as we can highlight specific material symmetries of behaviour, which implies additional relations between the different components of the elasticity tensor, as we will see in Paragraph 4.2.



In the general case, these components may depend on the point under study (if the material is heterogeneous), but also on other environmental factors, such as temperature or humidity, for example.



*It is of course possible to mathematically invert the constitutive relation, by expressing the infinitesimal strain tensor as a function of the stress tensor:*

$$\boldsymbol{\varepsilon}(\mathbf{x}, t) = \mathbf{S}(\mathbf{x})\boldsymbol{\sigma}(\mathbf{x}, t)$$

where  $\mathbf{S}$  is the “compliance” tensor, such that  $\mathbf{S} = \mathbf{C}^{-1}$ .

### Voigt notation

It may be convenient, in order to simplify calculations when manipulating the components of the different tensors, to use Voigt notation, the principle of which is to reorganize the component indices in order to obtain a more accessible representation. To do this, we “contract” each pair of indices into a single one, to transform the symmetrical second-order tensors into six-component vectors, and the symmetrical fourth-order tensors into six  $\times$  six matrices, as shown in the following.

**Voigt notation in linear elasticity.** The constitutive relation  $\sigma = \mathbf{C}\epsilon$  becomes, using Voigt notation and a vector basis  $(\mathbf{i}_1, \mathbf{i}_2, \mathbf{i}_3)$ :

$$\underbrace{\begin{pmatrix} \tilde{\sigma}_1 = \sigma_{11} \\ \tilde{\sigma}_2 = \sigma_{22} \\ \tilde{\sigma}_3 = \sigma_{33} \\ \tilde{\sigma}_4 = \sigma_{23} \\ \tilde{\sigma}_5 = \sigma_{13} \\ \tilde{\sigma}_6 = \sigma_{12} \end{pmatrix}}_{\tilde{\sigma}} = \underbrace{\begin{pmatrix} \tilde{C}_{11} & \tilde{C}_{12} & \tilde{C}_{13} & \tilde{C}_{14} & \tilde{C}_{15} & \tilde{C}_{16} \\ \tilde{C}_{12} & \tilde{C}_{22} & \tilde{C}_{23} & \tilde{C}_{24} & \tilde{C}_{25} & \tilde{C}_{26} \\ \tilde{C}_{13} & \tilde{C}_{23} & \tilde{C}_{33} & \tilde{C}_{34} & \tilde{C}_{35} & \tilde{C}_{36} \\ \tilde{C}_{14} & \tilde{C}_{24} & \tilde{C}_{34} & \tilde{C}_{44} & \tilde{C}_{45} & \tilde{C}_{46} \\ \tilde{C}_{15} & \tilde{C}_{25} & \tilde{C}_{35} & \tilde{C}_{45} & \tilde{C}_{55} & \tilde{C}_{56} \\ \tilde{C}_{16} & \tilde{C}_{26} & \tilde{C}_{36} & \tilde{C}_{46} & \tilde{C}_{56} & \tilde{C}_{66} \end{pmatrix}}_{\tilde{\mathbf{C}}} \underbrace{\begin{pmatrix} \tilde{\epsilon}_1 = \epsilon_{11} \\ \tilde{\epsilon}_2 = \epsilon_{22} \\ \tilde{\epsilon}_3 = \epsilon_{33} \\ \tilde{\epsilon}_4 = 2\epsilon_{23} \\ \tilde{\epsilon}_5 = 2\epsilon_{13} \\ \tilde{\epsilon}_6 = 2\epsilon_{12} \end{pmatrix}}_{\tilde{\epsilon}}$$

which means that, for the different tensors, the indices were contracted in pairs according to the convention:

$$nn \rightarrow n, \text{ and } mn \rightarrow 9 - m - n, \quad m \neq n$$

taking care to apply a multiplier factor of 2 to the last three components of  $\tilde{\epsilon}$ , which is necessary to be able to write that  $\tilde{\sigma} = \tilde{\mathbf{C}}\tilde{\epsilon}$ .

Besides, the major symmetry condition of the elasticity tensor ( $C_{mnpq} = C_{pqmn}$ ,  $1 \leq m, n, p, q \leq 3$ ) implies that the matrix  $\tilde{\mathbf{C}}$  is symmetrical ( $\tilde{C}_{ij} = \tilde{C}_{ji}$ ,  $1 \leq i, j \leq 6$ ).



Thanks to the introduced factor 2, we can directly write what represents a volume density of elastic strain energy as:

$$\text{tr}(\tilde{\sigma}\tilde{\epsilon}) = \langle \tilde{\sigma}, \tilde{\epsilon} \rangle$$

in the sense of the scalar product between two vectors (with six components here).

## 4.2 Isotropic linear elastic material for infinitesimal deformations

We will describe here the most common constitutive relation used in continuum mechanics, which allows us to take into account a minimum number of material parameters.

### 4.2.1 Isotropy hypothesis

As already mentioned above, while almost all materials are inherently anisotropic, at least locally, most of them behave isotropically at the macroscopic scale: for example, polycrystalline materials such as metals are composed of a large number of anisotropic “grains”, but the random nature of the distribution of crystallographic orientations of the different grains makes these materials have an overall isotropy, of a statistical nature.

From a practical point of view, to say that a material exhibits an isotropic behaviour at a point is to assume that the relation between the stress and strain tensors at this point will be the same, regardless of the prior change in orientation that may have been caused to the material domain. Mathematically, this change in orientation can be described by applying a rotation matrix  $\mathbb{R}_0$  (as defined in Appendix A.2.6) to the reference configuration  $\Omega_0$ . This implies that a point  $\mathbf{q}$  in the neighbourhood of  $\mathbf{p}$  is represented in the new initial configuration  $\Omega_0^*$  by:

$$\mathbf{q}^* = \mathbf{p} + \mathbb{R}_0(\mathbf{q} - \mathbf{p})$$

We then consider the same deformation of the neighbourhood of  $\mathbf{p}$  for the two initial configurations, which means that we apply displacements  $\mathbf{u}(\mathbf{q})$  et  $\mathbf{u}^*(\mathbf{q}^*)$  verifying:

$$\mathbf{u}^*(\mathbf{q}^*) = \mathbb{R}_0\mathbf{u}(\mathbf{q})$$

hence, considering the associated displacement gradient tensors, expressed at point  $\mathbf{p}$ :

$$\mathbb{D}_{\mathbf{p}^*}\mathbf{u}^* = \mathbb{R}_0(\mathbb{D}_{\mathbf{p}}\mathbf{u})(\mathbb{D}_{\mathbf{p}^*}\mathbf{p}) = \mathbb{R}_0(\mathbb{D}_{\mathbf{p}}\mathbf{u})\mathbb{R}_0^T$$

since the rotation matrix verifies  $\mathbb{R}_0^{-1} = \mathbb{R}_0^T$ . We then deduce that the infinitesimal strain tensor  $\boldsymbol{\varepsilon}^*$ , as described by an observer linked to the configuration  $\Omega_0^*$ , is expressed as:

$$\boldsymbol{\varepsilon}^* = \mathbb{R}_0\boldsymbol{\varepsilon}\mathbb{R}_0^T$$

Since the isotropy assumption implies that the constitutive relation has to remain unchanged whatever the considered reference configuration ( $\mathbf{C}^* = \mathbf{C}$ ), one then has:

$$\boldsymbol{\sigma}^* = \mathbf{C}^*\boldsymbol{\varepsilon}^* = \mathbf{C}\boldsymbol{\varepsilon}^*$$

where  $\boldsymbol{\sigma}^*$  is the stress tensor in the current configuration, as described by an observer linked to the reference configuration  $\Omega_0^*$ . This tensor is then expressed using  $\boldsymbol{\sigma} = \mathbf{C}\boldsymbol{\varepsilon}$ , as described by an observer linked to  $\Omega_0$ . For this, we use the “material frame-indifference” principle, which states that the stress vector should not depend on the vector basis used to express it, or, equivalently, that the stress vector should rotate if we keep the vector basis unchanged and if we rotate the current configuration. In this situation, if the observer linked to  $\Omega_0$  describes at  $\mathbf{x}$ , and for a vector  $\mathbf{n}$  normal to the facet, a stress vector  $\mathbf{T} = \boldsymbol{\sigma}\mathbf{n}$ , the one linked to  $\Omega_0^*$  describes at the same point a stress vector  $\mathbf{T}^* = \boldsymbol{\sigma}^*(\mathbb{R}_0\mathbf{n})$  such that:

$$\boldsymbol{\sigma}^*(\mathbb{R}_0\mathbf{n}) = \mathbb{R}_0(\boldsymbol{\sigma}\mathbf{n})$$

which allows for writing that:

$$\boldsymbol{\sigma}^* = \mathbb{R}_0\boldsymbol{\sigma}\mathbb{R}_0^T$$

Therefore, the isotropy hypothesis finally implies that:

$$\mathbb{R}_0(\mathbf{C}\boldsymbol{\varepsilon})\mathbb{R}_0^T = \mathbb{R}_0\boldsymbol{\sigma}\mathbb{R}_0^T = \boldsymbol{\sigma}^* = \mathbf{C}^*\boldsymbol{\varepsilon}^* = \mathbf{C}\boldsymbol{\varepsilon}^* = \mathbf{C}(\mathbb{R}_0\boldsymbol{\varepsilon}\mathbb{R}_0^T)$$

whatever the infinitesimal strain tensor  $\boldsymbol{\varepsilon}$  and the rotation matrix  $\mathbb{R}_0$ . We then conclude with the following theorem.

**Rivlin-Ericksen theorem (linear case).** A fourth-order tensor  $\mathbf{T}$ , acting from the space of symmetrical second-order tensors in itself, is said to be isotropic if and only if it satisfies:

$$\mathbb{R}(\mathbf{T}\mathbb{A})\mathbb{R}^T = \mathbf{T}(\mathbb{R}\mathbb{A}\mathbb{R}^T), \forall \mathbb{A} \text{ symmetrical}, \forall \mathbb{R} \text{ such that } \mathbb{R}\mathbb{R}^T = \mathbb{I}$$

Then there are two scalars  $\alpha$  and  $\beta$  such that the tensor  $\mathbf{T}$  can be expressed as:

$$\mathbf{T}\mathbb{A} = \alpha\mathbb{A} + \beta(\operatorname{tr}\mathbb{A})\mathbb{I}, \forall \mathbb{A} \text{ symmetrical}$$

The proof of this result is detailed in Appendix A.3.2.

The application of this result is straightforward in the case of the elasticity tensor, leading to the following definition.

**Hooke's law.** The isotropy hypothesis allows the linear elastic constitutive relation to be written as:

$$\boldsymbol{\sigma}(\mathbf{x}, t) = \mathbf{C}(\mathbf{x})\boldsymbol{\varepsilon}(\mathbf{x}, t) = \lambda(\mathbf{x})(\operatorname{tr}\boldsymbol{\varepsilon}(\mathbf{x}, t))\mathbb{I} + 2\mu(\mathbf{x})\boldsymbol{\varepsilon}(\mathbf{x}, t)$$

where  $\lambda(\mathbf{x})$  and  $\mu(\mathbf{x})$  are called “Lamé parameters”, associated with the isotropic material under study, and which are generally expressed in GPa. If, in addition, the material is homogeneous, these two parameters  $\lambda$  and  $\mu$  are constant, which means that only two scalars are needed to describe the linear elastic behaviour of the material.

To invert this relation, we begin by expressing the trace of the stress tensor as a function of the infinitesimal strain tensor:

$$\text{tr}\sigma = \lambda(\text{tr}\epsilon)(\text{tr}\mathbb{I}) + 2\mu \text{tr}\epsilon = (3\lambda + 2\mu) \text{tr}\epsilon$$

which allows for writing:

$$\epsilon(\mathbf{x}, t) = -\frac{\lambda(\mathbf{x})}{2\mu(\mathbf{x})(3\lambda(\mathbf{x}) + 2\mu(\mathbf{x}))} (\text{tr}\sigma(\mathbf{x}, t))\mathbb{I} + \frac{1}{2\mu(\mathbf{x})}\sigma(\mathbf{x}, t)$$

in the general case of a heterogeneous material.



*The form of the isotropic linear elastic constitutive relation makes it possible to establish that the principal strains and stresses share the same associated principal directions; indeed, if we use, at a given point  $\mathbf{x}$ , the vector basis  $(\phi_1^\sigma, \phi_2^\sigma, \phi_3^\sigma)$  of the principal directions associated with principal stresses  $(\sigma_1, \sigma_2, \sigma_3)$ , we find that the infinitesimal strain tensor is written, using the same basis vectors, as:*

$$\epsilon = -\frac{\lambda}{2\mu(3\lambda + 2\mu)} \left( \sum_{k=1}^3 \sigma_k \right) \mathbb{I} + \frac{1}{2\mu} \sum_{k=1}^3 \sigma_k \phi_k^\sigma \otimes \phi_k^\sigma$$

hence, finally:

$$\epsilon = \sum_{k=1}^3 \epsilon_k \phi_k^\sigma \otimes \phi_k^\sigma, \text{ with } \epsilon_k = \frac{(\lambda + \mu)\sigma_k}{\mu(3\lambda + 2\mu)} - \frac{\lambda}{2\mu(3\lambda + 2\mu)} \sum_{l \neq k} \sigma_l$$

These strains are principal since there is no shear strain term in the basis  $(\phi_1^\sigma, \phi_2^\sigma, \phi_3^\sigma)$ .

#### 4.2.2 Link with the tensile test

While the previous paragraph highlighted the two Lamé parameters in the expression of the isotropic constitutive relation, a second set of parameters is traditionally proposed, whose origin comes from the analysis of the tensile test, allowing for building the constitutive relation practically.

##### Practical construction of the constitutive relation

If we consider a tensile test along the direction  $\mathbf{e}$ , and the associated stress tensor ( $\sigma = \sigma_{ee}\mathbf{e} \otimes \mathbf{e}$  with  $\sigma_{ee} > 0$ ), we can then determine the infinitesimal strain tensor as:

$$\epsilon = -\frac{\lambda\sigma_{ee}}{2\mu(3\lambda + 2\mu)} \mathbb{I} + \frac{\sigma_{ee}}{2\mu} \mathbf{e} \otimes \mathbf{e}$$

in the case of a homogeneous material, i.e. with constant Lamé parameters. If we consider a vector basis  $(\mathbf{i}_1, \mathbf{i}_2, \mathbf{i}_3 = \mathbf{e})$ , we finally find:

$$\epsilon = -\frac{\lambda\sigma_{ee}}{2\mu(3\lambda + 2\mu)} (\mathbf{i}_1 \otimes \mathbf{i}_1 + \mathbf{i}_2 \otimes \mathbf{i}_2) + \frac{(\lambda + \mu)\sigma_{ee}}{\mu(3\lambda + 2\mu)} \mathbf{i}_3 \otimes \mathbf{i}_3$$

As expected, we find that the longitudinal strain  $\epsilon_{33}$  is proportional to the longitudinal stress  $\sigma_{ee}$ , but also that the cross-section narrows, given the negative transverse deformations  $\epsilon_{11}$  and  $\epsilon_{22}$ . With regard to these observations, the following two parameters are then defined.

**Young's modulus and Poisson's ratio.** Based on the analysis of a tensile test of a material in its elastic region, we define classically:

- the Young's modulus, noted  $E$ , as the coefficient of proportionality between longitudinal stress and strain:

$$E = \frac{\sigma_{33}}{\epsilon_{33}} = \frac{\sigma_{ee}}{\epsilon_{33}} = \frac{\mu(3\lambda + 2\mu)}{(\lambda + \mu)}$$

- the Poisson's ratio, noted  $\nu$ , as the opposite of the coefficient of proportionality between transverse and longitudinal strains:

$$\nu = -\frac{\varepsilon_{11}}{\varepsilon_{33}} = -\frac{\varepsilon_{22}}{\varepsilon_{33}} = \frac{\lambda}{2(\lambda + \mu)}$$

Given these definitions, it is easy to see that Young's modulus is similar to a stress (and is usually expressed in GPa), while Poisson's ratio is dimensionless.

In order to build the constitutive relation from these definitions, it is sufficient to use the basis of the principal directions associated with the principal stresses and to consider the strains in these same directions. Thus, the strain  $\varepsilon_1$  associated with the first principal direction is obtained by expressing the "superposition" of three tensile tests, each in a different direction, and with intensity the value of the associated principal stress, as shown in Figure 4.6. For this direction, the strain  $\varepsilon_1$  corresponds to a longitudinal strain for the first test, and a transverse strain for the other two, which implies, given the definitions of  $E$  and  $\nu$ , that:

$$\varepsilon_1 = \frac{\sigma_1}{E} - \nu \frac{\sigma_2}{E} - \nu \frac{\sigma_3}{E}$$

Indeed, as we will discuss more precisely in Paragraph 5.3.1, all the equations of the problem are linear, and it is thus possible to decompose the problem into a sum of simpler problems, whose solutions are added to give the final solution of the problem under study.

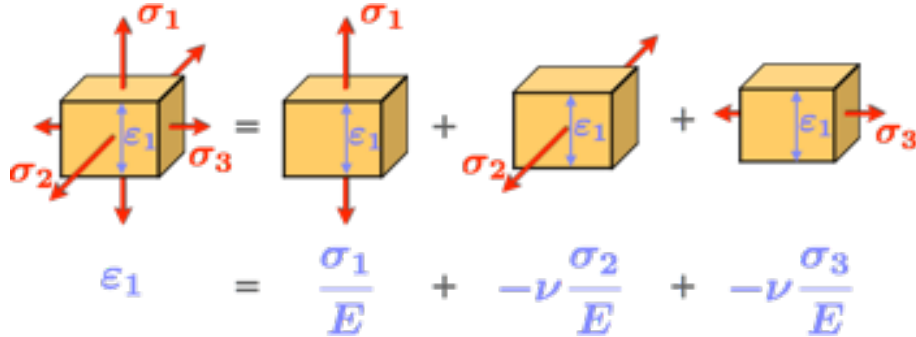


Figure 4.6: Construction of the constitutive relation by superimposing three tensile tests.

By doing the same in the other two principal directions (knowing that there is no shear strain), the constitutive relation is constructed as follows;

$$\boldsymbol{\varepsilon} = \left( \frac{\sigma_1}{E} - \frac{\nu}{E}(\sigma_2 + \sigma_3) \right) \mathbf{i}_1 \otimes \mathbf{i}_1 + \left( \frac{\sigma_2}{E} - \frac{\nu}{E}(\sigma_1 + \sigma_3) \right) \mathbf{i}_2 \otimes \mathbf{i}_2 + \left( \frac{\sigma_3}{E} - \frac{\nu}{E}(\sigma_1 + \sigma_2) \right) \mathbf{i}_3 \otimes \mathbf{i}_3$$

or by explicitly using the trace of the stress tensor:

$$\begin{aligned} \boldsymbol{\varepsilon} = & \left( \frac{1+\nu}{E} \sigma_1 - \frac{\nu}{E} (\sigma_1 + \sigma_2 + \sigma_3) \right) \mathbf{i}_1 \otimes \mathbf{i}_1 + \left( \frac{1+\nu}{E} \sigma_2 - \frac{\nu}{E} (\sigma_1 + \sigma_2 + \sigma_3) \right) \mathbf{i}_2 \otimes \mathbf{i}_2 \\ & + \left( \frac{1+\nu}{E} \sigma_3 - \frac{\nu}{E} (\sigma_1 + \sigma_2 + \sigma_3) \right) \mathbf{i}_3 \otimes \mathbf{i}_3 \end{aligned}$$

hence, in condensed form:

$$\boldsymbol{\varepsilon} = \frac{1+\nu}{E} \boldsymbol{\sigma} - \frac{\nu}{E} (\text{tr } \boldsymbol{\sigma}) \mathbb{I}$$

This also allows us to give a second set of relationships between Lamé parameters and Young's modulus – Poisson's ratio, namely:

$$\lambda = \frac{\nu E}{(1+\nu)(1-2\nu)}, \quad \mu = \frac{E}{2(1+\nu)}$$

### Common parameter values

The physical interpretation that can be given to Young's modulus and Poisson's ratio allows for setting bounds, which are also physical, for these latter. First of all, considering that a specimen stretches when a tensile force is exerted on it, we can affirm that Young's modulus is positive:

$$E > 0$$

In addition, in a shear test, the shear strain is along the shear direction; as these two quantities are linked by the Lamé parameter  $\mu$  (which is actually also called the "shear modulus"), this latter is also positive, therefore:

$$\mu = \frac{E}{2(1+\nu)} > 0, \text{ hence: } \nu > -1$$

Finally, if we consider the case of an isotropic compression test, where we impose  $\sigma = -p\mathbb{I}$  with a pressure  $p > 0$  (obtained for example by the action of a fluid), we can write that the associated infinitesimal strain tensor is:

$$\varepsilon = \frac{1+\nu}{E}(-p\mathbb{I}) - \frac{\nu}{E}(-3p)\mathbb{I} = -\frac{1-2\nu}{E}p\mathbb{I}$$

This tensor is constant, and we then deduce the volume change of the specimen using the expression developed in Paragraph 1.4.1 within the infinitesimal deformation hypothesis, which gives:

$$\frac{dV}{V} = \text{tr}\varepsilon = -\frac{3(1-2\nu)}{E}p$$

which is therefore uniform. Since, in practice, all materials subjected to isotropic compression have their volume reduced, it can be deduced that:

$$\frac{3(1-2\nu)}{E} > 0, \text{ hence } \nu < \frac{1}{2}$$

Therefore, it is concluded that Poisson's ratio necessarily verifies:

$$-1 < \nu < \frac{1}{2}$$

Table 4.1 gives some typical values of Young's moduli and Poisson's ratios for several commonly used materials, some at different temperatures.

**Summary 4.1 — Isotropic linear elastic material (Hooke's law).** The relation that connects the stress and infinitesimal strain tensors is written, in the case of an isotropic linear elastic material, as:

$$\sigma(\mathbf{x}, t) = \mathbf{C}(\mathbf{x})\varepsilon(\mathbf{x}, t) = \lambda(\mathbf{x})(\text{tr}\varepsilon(\mathbf{x}, t))\mathbb{I} + 2\mu(\mathbf{x})\varepsilon(\mathbf{x}, t), \forall \mathbf{x} \in \Omega_t, \forall t$$

when expressed in stiffness, where  $\lambda(\mathbf{x})$  and  $\mu(\mathbf{x})$  are the Lamé parameters, which are characteristic of the material under study, or else:

$$\varepsilon(\mathbf{x}, t) = \mathbf{C}^{-1}\sigma(\mathbf{x}, t) = \frac{1+\nu(\mathbf{x})}{E(\mathbf{x})}\sigma(\mathbf{x}, t) - \frac{\nu(\mathbf{x})}{E(\mathbf{x})}(\text{tr}\sigma(\mathbf{x}, t))\mathbb{I}, \forall \mathbf{x} \in \Omega_t, \forall t$$

when expressed in compliance, where  $E(\mathbf{x})$  and  $\nu(\mathbf{x})$  are respectively the Young's modulus and Poisson's ratio of the material under study.

In the case where the material is homogeneous, the different coefficients become constants, which are characteristic of the material. In addition, the two pairs of material coefficients satisfy

Material	Young's modulus (GPa)	Poisson's ratio
rubber	$10^{-3}$ – $10^{-1}$	0.4999
plexiglas	2.4–2.9	0.40–0.43
epoxy resin	3–3.5	0.40
concrete	20–50	0.10–0.20
glass	50–90	0.18–0.30
aluminum	68–69	0.33–0.35
aluminum alloys	72–75	0.32
" (at 200°C)	66	0.325
" (at 500°C)	55	0.35
brass	100–130	0.37
bronze	125–130	0.34
" (at 180°C)	120	0.34
cast irons	80–170	0.21–0.29
titanium alloys	115–200	0.34
" (at 200°C)	103	0.34
" (at 315°C)	95	0.34
stainless steel	195–205	0.30–0.31
" (at 200°C)	170	0.30
" (at 700°C)	131	0.30
structural steels	210–220	0.27–0.30
" (at 200°C)	205	0.30
" (at 600°C)	170	0.315
silicon carbide	450	0.17
diamond	1050–1200	0.10

Table 4.1: Typical values of Young's modulus and Poisson's ratio for various materials (at room temperature, unless otherwise stated).

the following relations:

$$\lambda = \frac{vE}{(1+v)(1-2v)}, \mu = \frac{E}{2(1+v)}$$

$$E = \frac{\mu(3\lambda + 2\mu)}{(\lambda + \mu)}, v = \frac{\lambda}{2(\lambda + \mu)}$$

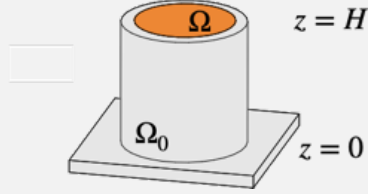
**R** In the case of the isotropic compression test described above, we define the “bulk modulus”  $\kappa$  as the opposite of the ratio between the applied pressure and the volume change obtained, i.e.:

$$\kappa = -\frac{p}{\text{tr}\epsilon} = \frac{E}{3(1-2v)}$$

The limit case  $v = 1/2$  corresponds to perfectly incompressible materials, for which the bulk modulus is therefore infinite. If, strictly speaking, there is no such material, elastomers are the closest materials to this limit situation: for example, natural rubber, whose Poisson's ratio is 0.4999.

■ **Example 4.1 — Cylindrical bar subjected to a pressure.** We consider a cylindrical bar  $\Omega$  with a vertical axis  $\mathbf{i}_z$ , circular cross-section of radius  $R$ , and height  $H$ . We also assume that the bar is in static equilibrium under the action of a uniform pressure applied on the upper surface, and the reaction of the support. Finally, the material is considered homogeneous and isotropic, and remains, with the infinitesimal deformation hypothesis, within the linear

elasticity region, characterized by a Young's modulus  $E$  and a Poisson's ratio  $\nu$ .



The list of equations and boundary conditions to be taken into account is as follows; by using the cylindrical vector basis  $(\mathbf{i}_r(\theta), \mathbf{i}_\theta(\theta), \mathbf{i}_z)$  associated with the cylinder (with  $z = 0$  corresponding to the lower surface of the bar), we want to determine a displacement field  $\mathbf{u}$  and a stress field  $\boldsymbol{\sigma}$  satisfying:

- the local equilibrium equation at every point of the domain:

$$\operatorname{div}_{\mathbf{x}} \boldsymbol{\sigma} = 0$$

- the contact condition with the support in terms of displacement (sliding contact):

$$\langle \mathbf{u}_{(z=0)}, \mathbf{i}_z \rangle = 0$$

- the contact condition with the support in terms of local forces (which are normal to the boundary because of frictionless contact):

$$\langle \boldsymbol{\sigma}_{(z=0)}(-\mathbf{i}_z), \mathbf{i}_r(\theta) \rangle = 0 = \langle \boldsymbol{\sigma}_{(z=0)}(-\mathbf{i}_z), \mathbf{i}_\theta(\theta) \rangle$$

- the free boundary condition on the lateral surface of the bar:

$$\boldsymbol{\sigma}_{(r=R)} \mathbf{i}_r = 0$$

- the applied (uniform) pressure  $p_0$  condition on the upper surface of the bar:

$$\boldsymbol{\sigma}_{(z=H)} \mathbf{i}_z = -p_0 \mathbf{i}_z$$

- the linear elastic, homogeneous and isotropic, constitutive relation of the material at each point of the domain, expressed in compliance for example:

$$\boldsymbol{\varepsilon} = \frac{1+\nu}{E} \boldsymbol{\sigma} - \frac{\nu}{E} (\operatorname{tr} \boldsymbol{\sigma}) \mathbb{I}$$

where the infinitesimal strain tensor is defined at each point as the symmetrical part of the displacement gradient tensor:

$$\boldsymbol{\varepsilon} = \frac{1}{2} (\mathbb{D}_{\mathbf{x}} \mathbf{u} + (\mathbb{D}_{\mathbf{x}} \mathbf{u})^T)$$

We then see that a uniform and uniaxial stress tensor  $\boldsymbol{\sigma} = \sigma_0 \mathbf{i}_z \otimes \mathbf{i}_z$  verifies all the equations related to forces:

$$\operatorname{div}_{\mathbf{x}} (\sigma_0 \mathbf{i}_z \otimes \mathbf{i}_z) = 0, (\sigma_0 \mathbf{i}_z \otimes \mathbf{i}_z) \mathbf{i}_r = 0, \text{ and } (\sigma_0 \mathbf{i}_z \otimes \mathbf{i}_z) \mathbf{i}_z = -p_0 \mathbf{i}_z$$

provided that  $\sigma_0 = -p_0$ .

There remains to verify that it is possible to associate to this stress state a displacement field respecting the condition at  $z = 0$ . To do this, the constitutive relation expressed in compliance allows us to establish that the infinitesimal strain tensor is written as:

$$\boldsymbol{\varepsilon}(\mathbf{x}) = -\frac{1+\nu}{E} p_0 \mathbf{i}_z \otimes \mathbf{i}_z + \frac{\nu}{E} (\operatorname{tr} \boldsymbol{\sigma}) \mathbb{I}$$

with  $\operatorname{tr} \boldsymbol{\sigma} = -p_0$ , hence:

$$\boldsymbol{\varepsilon}(\mathbf{x}) = -\frac{p_0}{E} \mathbf{i}_z \otimes \mathbf{i}_z + \frac{\nu p_0}{E} (\mathbf{i}_r(\theta) \otimes \mathbf{i}_r(\theta) + \mathbf{i}_\theta(\theta) \otimes \mathbf{i}_\theta(\theta))$$

which shows the vertical settlement of the bar, along with a radial expansion related to Poisson's effect.

Considering the axisymmetry of the problem, we will see in paragraph 5.3.2 that the displacement field can then be expressed as:

$$\mathbf{u}(\mathbf{x}) = u_r(r, z) \mathbf{i}_r(\theta) + u_z(r, z) \mathbf{i}_z$$

and must then satisfy:

$$\begin{aligned}\frac{\partial u_r}{\partial r} &= \varepsilon_{rr} = \frac{vp_0}{E} \\ \frac{u_r}{r} &= \varepsilon_{\theta\theta} = \frac{vp_0}{E} \\ \frac{\partial u_z}{\partial z} &= \varepsilon_{zz} = -\frac{p_0}{E} \\ \frac{\partial u_r}{\partial z} + \frac{\partial u_z}{\partial r} &= 2\varepsilon_{rz} = 0\end{aligned}$$

The second equation allows us to directly determine that the radial displacement  $u_r$  depends on  $r$  only:

$$u_r(r, z) = \frac{vp_0}{E} r = u_r(r)$$

which implies, using the fourth equation, that the vertical displacement  $u_z$  depends on  $z$  only. Finally, the third equation allows us to establish that:

$$u_z(z) = -\frac{p_0}{E} z$$

considering the contact condition with the support:  $u_z(0) = 0$ . The displacement field therefore represents the vertical settlement, along with a radial expansion, of the bar under the action of the upper pressure  $p_0$ :

$$\boxed{\mathbf{u}(\mathbf{x}) = -\frac{p_0}{E} z \mathbf{i}_z + \frac{vp_0}{E} r \mathbf{i}_r(\theta)}$$

■



It is essential to be able to satisfy all the equations and boundary conditions in order to state that the displacement field – stress field pair is the solution to the problem. In particular, it is essential to be able to determine a displacement field whose gradient tensor's symmetrical part corresponds to the infinitesimal strain tensor associated with the stress tensor through the constitutive relation.

Thus, the stress field determined in the case of Example ?? (on page ??), which deals with a bar subjected to the action of gravity, is not the mere solution to the problem, because it is not possible to associate a displacement field satisfying all the kinematic equations.

### 4.3 Thermoelastic behaviour for infinitesimal deformations

We have seen above how to describe the mechanical behaviour of a material in the linear elastic region; the parameters that describe it (at a given point when the material is heterogeneous, otherwise globally) are generally not intrinsic constants but may depend on factors related to the environment, such as temperature for example. These latter factors can also have a direct influence on the form of the constitutive relation: the most striking example is the account for temperature variations, which we will detail in the following.

#### 4.3.1 Linear thermoelasticity framework

The principle is to take into account in the constitutive relation what is called “thermal expansion”. From a thermodynamic point of view, temperature represents the average kinetic energy of atoms in matter, and thus influences interatomic bonds. Indeed, a temperature increase tends to increase the energy of atoms, which begin to oscillate around their respective equilibrium positions: the amplitude of these oscillations is as in Figure 4.7 where we add to the energy corresponding to the minimum of potential (associated with the reference equilibrium position, of interatomic distance  $r_0$ ) the energy of thermal origin. Since the potential curve is not symmetrical with respect to this minimum, the oscillation is made around a new equilibrium position that is at a greater distance ( $r_1 > r_0$ ), and this all the more so as the temperature increase is significant. This allows for explaining the phenomenon of thermal expansion which becomes visible on a macroscopic scale.

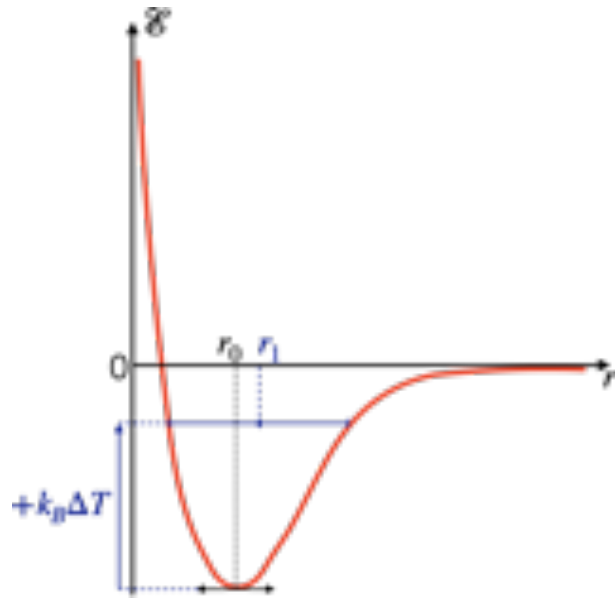


Figure 4.7: Interatomic potential: effect of the increase in energy due to an increase in temperature.

To take this phenomenon into account, it can be assumed that the infinitesimal “total” strain tensor  $\boldsymbol{\varepsilon}^t$  (which is related to the displacement field) is calculated as the sum of the infinitesimal elastic strain tensor (noted  $\boldsymbol{\varepsilon}^e$ , and associated with the stress tensor) and an infinitesimal thermal strain tensor  $\boldsymbol{\varepsilon}^{th}$ :

$$\frac{1}{2}(\mathbb{D}_{\mathbf{x}}\mathbf{u} + (\mathbb{D}_{\mathbf{x}}\mathbf{u})^T) = \boldsymbol{\varepsilon}^t = \boldsymbol{\varepsilon}^e + \boldsymbol{\varepsilon}^{th} = \mathbf{C}^{-1}\boldsymbol{\sigma} + \boldsymbol{\varepsilon}^{th}$$

**Infinitesimal thermal strain tensor.** For most solids, we can see that, for a given temperature range, thermal expansion is proportional to the temperature increase; if, moreover, this expansion is the same in all directions, we can therefore propose an isotropic tensor, defined as:

$$\boldsymbol{\varepsilon}^{th} = \alpha \Delta T \mathbb{I}$$

where  $\Delta T = T - T_{ref}$  is the temperature variation with respect to a reference temperature  $T_{ref}$ , and  $\alpha$  is called the “coefficient of thermal expansion”, which is expressed in  $K^{-1}$ .

Table 4.2 gives some typical values of the coefficients of thermal expansion for several commonly used materials; these are given at room temperature, knowing that temperature can have a strong influence on the value of these coefficients.

**R** Some materials, such as long-fiber composites shown in Figure 3.16, may have different coefficients of thermal expansion depending on the directions considered; in this case, the infinitesimal thermal strain tensor is written in terms of a symmetrical second-order tensor  $\alpha$ :

$$\boldsymbol{\varepsilon}^{th} = (\Delta T)\alpha$$

### 4.3.2 Dealing with a thermoelasticity problem

A thermoelasticity problem is solved in the same way as a problem purely based on mechanics. For this purpose, we assume that we know the temperature field  $T(\mathbf{x}, t)$  at all points  $\mathbf{x}$  of the domain and each instant  $t$ , and we replace the purely mechanical constitutive relation by the following relation.

Material	Coefficient of thermal expansion ( $\text{K}^{-1}$ )
diamond	$10^{-6}$
silicon carbide	$2.8 \times 10^{-6}$
glass (pyrex)	$3.2 \times 10^{-6} - 4 \times 10^{-6}$
tungsten	$4.5 \times 10^{-6}$
glass	$8.5 \times 10^{-6}$
titanium	$8.6 \times 10^{-6}$
cast iron	$1.1 \times 10^{-5}$
concrete	$1.2 \times 10^{-5}$
structural steels	$1.1 \times 10^{-5} - 1.3 \times 10^{-5}$
stainless steel	$1 \times 10^{-5} - 1.7 \times 10^{-5}$
copper	$1.7 \times 10^{-5}$
bronze	$1.8 \times 10^{-5}$
brass	$1.9 \times 10^{-5}$
aluminum	$2.3 \times 10^{-5}$

Table 4.2: Typical values for various materials of the coefficient of thermal expansion (at room temperature).

**Summary 4.2 — Isotropic linear thermoelastic material.** In the case of an anisothermal evolution, the constitutive relation between the stress and infinitesimal strain tensors is written, in the case of an isotropic linear thermoelastic material:

$$\begin{aligned} \frac{1}{2} \left( \mathbb{D}_{\mathbf{x}} \mathbf{u}(\mathbf{x}, t) + (\mathbb{D}_{\mathbf{x}} \mathbf{u}(\mathbf{x}, t))^T \right) &= \boldsymbol{\varepsilon}'(\mathbf{x}, t) = \mathbf{C}^{-1}(\mathbf{x}) \boldsymbol{\sigma}(\mathbf{x}, t) + \alpha(\mathbf{x}) \Delta T(\mathbf{x}, t) \mathbb{I} \\ &= \frac{1 + v(\mathbf{x})}{E(\mathbf{x})} \boldsymbol{\sigma}(\mathbf{x}, t) + \left( \alpha(\mathbf{x}) \Delta T(\mathbf{x}, t) - \frac{v(\mathbf{x})}{E(\mathbf{x})} \operatorname{tr} \boldsymbol{\sigma}(\mathbf{x}, t) \right) \mathbb{I} \end{aligned}$$

when expressed in compliance, or:

$$\begin{aligned} \boldsymbol{\sigma}(\mathbf{x}, t) &= \mathbf{C}(\mathbf{x}) (\boldsymbol{\varepsilon}'(\mathbf{x}, t) - \boldsymbol{\varepsilon}^{th}(\mathbf{x}, t)) = \mathbf{C}(\mathbf{x}) \left( \frac{1}{2} \left( \mathbb{D}_{\mathbf{x}} \mathbf{u}(\mathbf{x}, t) + (\mathbb{D}_{\mathbf{x}} \mathbf{u}(\mathbf{x}, t))^T \right) - \alpha(\mathbf{x}) \Delta T(\mathbf{x}, t) \mathbb{I} \right) \\ &= (\lambda(\mathbf{x}) \operatorname{tr} \boldsymbol{\varepsilon}'(\mathbf{x}, t) - (3\lambda(\mathbf{x}) + 2\mu(\mathbf{x})) \alpha(\mathbf{x}) \Delta T(\mathbf{x}, t)) \mathbb{I} + 2\mu(\mathbf{x}) \boldsymbol{\varepsilon}'(\mathbf{x}, t) \end{aligned}$$

when expressed in stiffness, with  $\mathbf{C}$  the elasticity tensor.  $\alpha(\mathbf{x})$  is the coefficient of thermal expansion of the studied material.

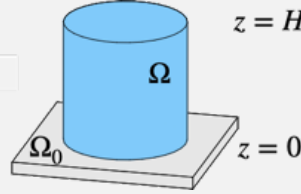


As seen in Table 4.1, Young's modulus and Poisson's ratio, and therefore the elasticity tensor  $\mathbf{C}$ , depend on temperature; if the variation  $\Delta T$  is large, then it is not possible to neglect, in all rigour, this dependence.

The same remark applies to the coefficient of thermal expansion  $\alpha$ .

**■ Example 4.2 — Thermal loading of a cylindrical bar.** We consider a cylindrical bar  $\Omega$  with a vertical axis  $\mathbf{i}_z$ , circular cross-section of radius  $R$  and height  $H$ , placed on a perfectly rigid and fixed support  $\Omega_0$ , on which it can slide without friction. Compared to a uniform reference temperature  $T_0$ , the entire bar is raised to a uniform temperature  $T_f = T_0 + \Delta T$ . We assume that the action of gravity can be neglected and that the bar is in static equilibrium. The material is considered homogeneous and isotropic, and remains within the linear elasticity region, characterized by a Young's modulus  $E$ , a Poisson's ratio  $v$  and a coefficient of thermal expansion  $\alpha$ , all three assumed

to be temperature independent.



The equation to be solved at every point of the domain is therefore:

$$\mathbf{div}_x \boldsymbol{\sigma} = \mathbf{0}$$

knowing that the constitutive relation expressed in compliance is written at any point as:

$$\frac{1}{2} (\mathbb{D}_x \mathbf{u} + (\mathbb{D}_x \mathbf{u})^T) = \mathbf{C}^{-1} \boldsymbol{\sigma} + \alpha \Delta T \mathbb{I}$$

As in Example 4.1, introducing the cylindrical vector basis  $(\mathbf{i}_r(\theta), \mathbf{i}_\theta(\theta), \mathbf{i}_z)$  associated with the cylinder, we assume that the displacement field can be written as:

$$\boxed{\mathbf{u}(\mathbf{x}) = u_r(r, z)\mathbf{i}_r + u_z(r, z)\mathbf{i}_z}$$

which implies that the infinitesimal total strain tensor takes the following form:

$$\begin{aligned} \boldsymbol{\varepsilon}^t(\mathbf{x}) = \boldsymbol{\varepsilon} &= \frac{\partial \mathbf{u}}{\partial r}(\mathbf{x}) \otimes_S \mathbf{i}_r(\theta) + \frac{\partial \mathbf{u}}{\partial \theta}(\mathbf{x}) \otimes_S \frac{\mathbf{i}_\theta(\theta)}{r} + \frac{\partial \mathbf{u}}{\partial z}(\mathbf{x}) \otimes_S \mathbf{i}_z \\ &\quad \frac{\partial u_r}{\partial r}(r, z)\mathbf{i}_r(\theta) \otimes \mathbf{i}_r(\theta) + \frac{u_r(r, z)}{r}\mathbf{i}_\theta(\theta) \otimes \mathbf{i}_\theta(\theta) + \frac{\partial u_z}{\partial z}(r, z)\mathbf{i}_z \otimes \mathbf{i}_z \\ &\quad + \left( \frac{\partial u_r}{\partial z}(r, z) + \frac{\partial u_z}{\partial r}(r, z) \right) \mathbf{i}_r(\theta) \otimes_S \mathbf{i}_z \end{aligned}$$

With regard to boundary conditions, the assumption of sliding contact with the support allows for writing that the vertical component of the displacement is equal to zero (maintained contact):

$$\langle \mathbf{u}_{(z=0)}, \mathbf{i}_z \rangle = 0$$

while the contact forces are purely normal (frictionless contact):

$$\langle \boldsymbol{\sigma}_{(z=0)}(-\mathbf{i}_z), \mathbf{i}_r \rangle = 0 = \langle \boldsymbol{\sigma}_{(z=0)}(-\mathbf{i}_z), \mathbf{i}_\theta \rangle$$

In addition, the lateral and upper surfaces are free of forces:

$$\boldsymbol{\sigma}_{(r=R)} \mathbf{i}_r = \mathbf{0} = \boldsymbol{\sigma}_{(z=H)} \mathbf{i}_z$$

It is then easily verified that a zero stress tensor satisfies all the equations related to stresses; this implies that:

$$\frac{1}{2} (\mathbb{D}_x \mathbf{u} + (\mathbb{D}_x \mathbf{u})^T) = \alpha \Delta T \mathbb{I}$$

or, in terms of scalar equations:

$$\begin{aligned} \frac{\partial u_r}{\partial r}(r, z) &= \alpha \Delta T \\ \frac{u_r(r, z)}{r} &= \alpha \Delta T \\ \frac{\partial u_z}{\partial z}(r, z) &= \alpha \Delta T \\ \frac{\partial u_r}{\partial z}(r, z) + \frac{\partial u_z}{\partial r}(r, z) &= 0 \end{aligned}$$

whose solution is:

$$\boxed{\begin{aligned} u_r(r, z) &= (\alpha \Delta T)r \\ u_z(r, z) &= (\alpha \Delta T)z \end{aligned}}$$

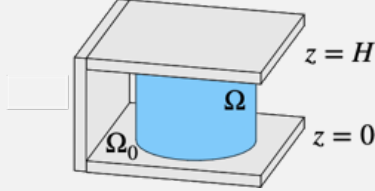
considering the boundary condition in  $z = 0$ :  $u_z(r, 0) = 0, \forall r$ . As expected, we find a uniform thermal expansion of the cylinder.

If, now, we imagine that, instead of being free, the upper surface of the cylinder is in frictionless contact with the same fixed support  $\Omega_0$ , the free boundary condition in  $z = H$  is replaced by a condition concerning the vertical component of the displacement:

$$\langle \mathbf{u}_{(z=H)}, \mathbf{i}_z \rangle = 0$$

and the nullity of the horizontal components of the stress vector:

$$\langle \boldsymbol{\sigma}_{(z=H)} \mathbf{i}_z, \mathbf{i}_r \rangle = 0 = \langle \boldsymbol{\sigma}_{(z=H)} \mathbf{i}_z, \mathbf{i}_\theta \rangle$$



It is then proposed to seek the solution in displacement in a form similar to that found in the previous situation:

$$\boxed{\mathbf{u}(\mathbf{x}) = ar\mathbf{i}_r + bz\mathbf{i}_z}$$

where  $a$  and  $b$  are two constants to be determined. This displacement automatically satisfies the boundary condition in  $z = 0$ , since  $\langle \mathbf{u}_{(z=0)}, \mathbf{i}_z \rangle = 0$ ; for it to satisfy the condition in  $z = H$  as well, we must have  $bH = 0$ , i.e.:

$$b = 0$$

Therefore, the infinitesimal total strain tensor is written, at every point, as:

$$\boldsymbol{\epsilon}^t = \frac{1}{2} (\mathbb{D}_{\mathbf{x}} \mathbf{u} + (\mathbb{D}_{\mathbf{x}} \mathbf{u})^\top) = a(\mathbf{i}_r \otimes \mathbf{i}_r + \mathbf{i}_\theta \otimes \mathbf{i}_\theta)$$

which makes it possible to obtain the stress tensor using the constitutive relation:

$$\boldsymbol{\sigma} = \mathbf{C}(\boldsymbol{\epsilon}^t - \alpha \Delta T \mathbb{I}) = \frac{\nu E}{(1+\nu)(1-2\nu)} (\text{tr}(\boldsymbol{\epsilon}^t - \alpha \Delta T \mathbb{I})) \mathbb{I} + \frac{E}{1+\nu} (\boldsymbol{\epsilon}^t - \alpha \Delta T \mathbb{I})$$

hence, considering  $\text{tr}(\boldsymbol{\epsilon}^t - \alpha \Delta T \mathbb{I}) = 2a - 3\alpha \Delta T$ :

$$\boldsymbol{\sigma} = \frac{E}{1-2\nu} \left( \left( \frac{a}{1+\nu} - \alpha \Delta T \right) (\mathbf{i}_r \otimes \mathbf{i}_r + \mathbf{i}_\theta \otimes \mathbf{i}_\theta) + \left( \frac{2\nu a}{1+\nu} - \alpha \Delta T \right) \mathbf{i}_z \otimes \mathbf{i}_z \right)$$

It is then easily verified that this stress tensor satisfies the local equilibrium equation:

$$\begin{aligned} \mathbf{div}_{\mathbf{x}} \boldsymbol{\sigma} &= \frac{\partial \boldsymbol{\sigma}}{\partial r} \mathbf{i}_r + \frac{\partial \boldsymbol{\sigma}}{\partial \theta} \frac{\mathbf{i}_\theta}{r} + \frac{\partial \boldsymbol{\sigma}}{\partial z} \mathbf{i}_z \\ &= \frac{E}{1-2\nu} \left( \frac{a}{1+\nu} - \alpha \Delta T \right) (\mathbf{i}_\theta \otimes \mathbf{i}_r + \mathbf{i}_r \otimes \mathbf{i}_\theta - \mathbf{i}_r \otimes \mathbf{i}_\theta - \mathbf{i}_\theta \otimes \mathbf{i}_r) \frac{\mathbf{i}_\theta}{r} = \mathbf{0} \end{aligned}$$

In addition, the stress vector on the upper and lower surfaces is collinear to  $\mathbf{i}_z$ :

$$\boldsymbol{\sigma}_{(z=H)} \mathbf{i}_z = \frac{E}{1-2\nu} \left( \frac{2\nu a}{1+\nu} - \alpha \Delta T \right) \mathbf{i}_z = -\boldsymbol{\sigma}_{(z=0)} (-\mathbf{i}_z)$$

Finally, the free boundary condition on the lateral surface allows us to determine the constant  $a$ :

$$\mathbf{0} = \boldsymbol{\sigma}_{(r=R)} \mathbf{i}_r = \frac{E}{1-2\nu} \left( \frac{a}{1+\nu} - \alpha \Delta T \right) \mathbf{i}_r$$

hence:

$$a = (1+\nu)\alpha \Delta T$$

which leads to the conclusion that the stress tensor is homogeneous, and is:

$$\boldsymbol{\sigma} = -E\alpha\Delta T \mathbf{i}_z \otimes \mathbf{i}_z$$

This allows us to observe that, since thermal expansion is hindered along the cylinder axis, a uniaxial compressive stress of thermal origin develops, proportional to Young's modulus and to the product of the coefficient of thermal expansion by the temperature variation. Conversely, expansion can occur freely in the radial direction:

$$\mathbf{u}(\mathbf{x}) = (1 + \nu)\alpha\Delta T r \mathbf{i}_r(\theta)$$

$$\boldsymbol{\epsilon} = (1 + \nu)\alpha\Delta T (\mathbf{i}_r(\theta) \otimes \mathbf{i}_r(\theta) + \mathbf{i}_\theta(\theta) \otimes \mathbf{i}_\theta(\theta))$$

which implies that there is no radial (or circumferential) stress.

Indeed, if we study a last situation, where, this time, the entire surface of the cylinder is constrained (by placing it for example in a perfectly rigid, hollow mass of cylindrical shape with the same radius  $R$ ), we find that there is no movement within the bar:

$$\mathbf{u}(\mathbf{x}) = \mathbf{0}, \forall \mathbf{x}$$

which implies that the stress tensor is of thermal origin only (since  $\boldsymbol{\epsilon}^t = \mathbf{0}$ ):

$$\boldsymbol{\sigma} = \mathbf{C}(-\alpha\Delta T \mathbb{I}) = -\frac{E\alpha\Delta T}{1-2\nu} \mathbb{I}$$

and corresponds to a uniform and isotropic compression state. ■

## 4.4 Summary of important formulas

### Isotropic linear elastic material – Summary 4.1 page 107

$$\boldsymbol{\sigma} = \mathbf{C}\boldsymbol{\epsilon} = \lambda(\text{tr}\boldsymbol{\epsilon})\mathbb{I} + 2\mu\boldsymbol{\epsilon}$$

$$\boldsymbol{\epsilon} = \mathbf{C}^{-1}\boldsymbol{\sigma} = \frac{1+\nu}{E}\boldsymbol{\sigma} - \frac{\nu}{E}(\text{tr}\boldsymbol{\sigma})\mathbb{I}$$

$$\lambda = \frac{\nu E}{(1+\nu)(1-2\nu)}, \quad \mu = \frac{E}{2(1+\nu)}$$

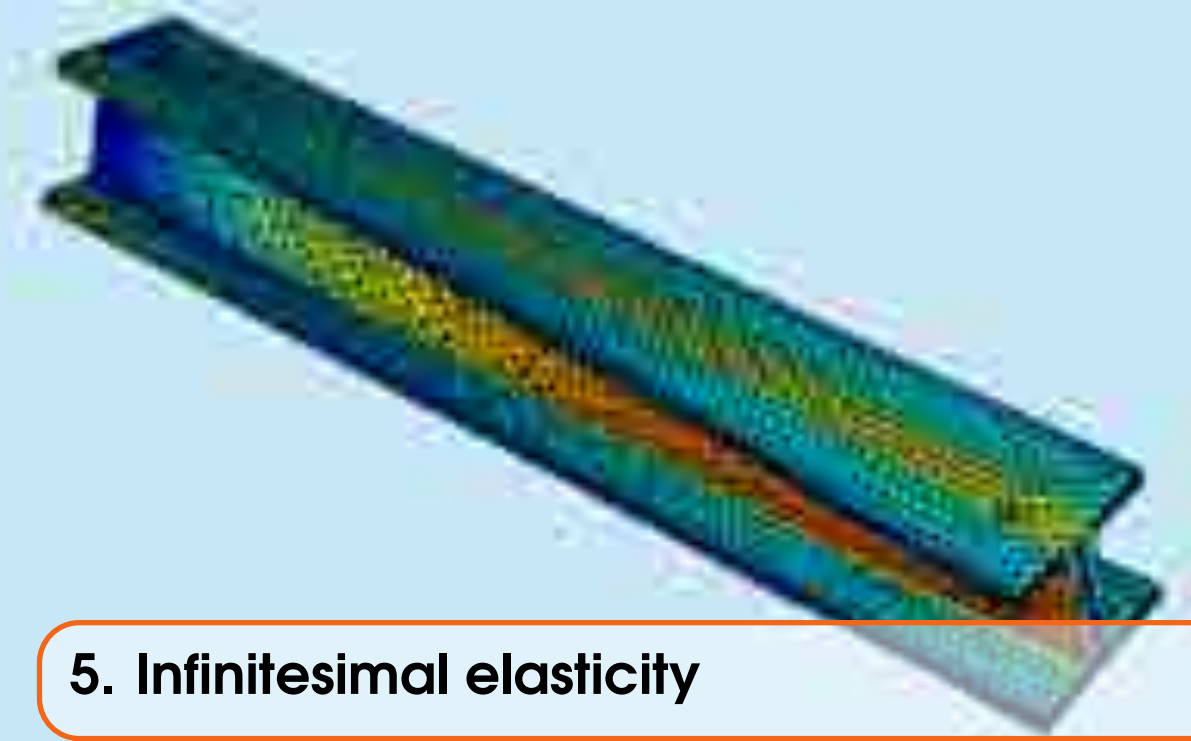
$$E = \frac{\mu(3\lambda+2\mu)}{(\lambda+\mu)}, \quad \nu = \frac{\lambda}{2(\lambda+\mu)}$$

### Isotropic linear thermoelastic material – Summary 4.2 page 112

$$\frac{1}{2}(\mathbb{D}_{\mathbf{x}}\mathbf{u} + (\mathbb{D}_{\mathbf{x}}\mathbf{u})^T) = \boldsymbol{\epsilon}^t = \mathbf{C}^{-1}\boldsymbol{\sigma} + \alpha\Delta T \mathbb{I} = \frac{1+\nu}{E}\boldsymbol{\sigma} + \left(\alpha\Delta T - \frac{\nu}{E}\text{tr}\boldsymbol{\sigma}\right)\mathbb{I}$$

$$\boldsymbol{\sigma} = \mathbf{C}(\boldsymbol{\epsilon}^t - \boldsymbol{\epsilon}^{th}) = \mathbf{C}\left(\frac{1}{2}(\mathbb{D}_{\mathbf{x}}\mathbf{u} + (\mathbb{D}_{\mathbf{x}}\mathbf{u})^T) - \alpha\Delta T \mathbb{I}\right) = (\lambda \text{tr}\boldsymbol{\epsilon}^t - (3\lambda+2\mu)\alpha\Delta T)\mathbb{I} + 2\mu\boldsymbol{\epsilon}^t$$





## 5. Infinitesimal elasticity

The previous chapters have allowed us to set all the equations and conditions necessary to solve a mechanical problem within the framework of isotropic linear elasticity; this is essential for an engineer since many structures are designed to operate in the elastic region. The task now is to study the properties of the solutions to these problems, and to propose analytical (useful for preliminary design projects) or numerical solution strategies.

---

### WHY STUDY ELASTICITY?

#### 5.1 Posing an elasticity problem

The objective is to review the equations and boundary conditions necessary and sufficient to determine the solution of a linear elasticity problem under the infinitesimal deformation hypothesis and for isothermal evolution. We remind that this solution, whose main mathematical properties we will describe, consists of a displacement vector  $\mathbf{u}$ , a (symmetrical) infinitesimal strain tensor  $\boldsymbol{\epsilon}$  and a (symmetrical as well) stress tensor  $\boldsymbol{\sigma}$ , which are *a priori* all functions of space and time. A specific example, dealing with the case of a gravity dam subjected to the hydrostatic pressure of water, and illustrated in Figure 5.1, summarizes all the equations and conditions to be taken into account to solve the (static) problem.

##### 5.1.1 Equations to be solved

These equations are those defined within the material domain  $\Omega$  under study. The first one, which could be described as fundamental, is the one resulting from the conservation of momentum, obtained in Paragraph 2.3.1, which involves the volume force density  $\mathbf{f}_V$  assumed known at any point within  $\Omega$ :

$$\rho(\mathbf{x}, t)\mathbf{a}(\mathbf{x}, t) = \mathbf{f}_V(\mathbf{x}, t) + \mathbf{div}_{\mathbf{x}}\boldsymbol{\sigma}(\mathbf{x}, t), \forall \mathbf{x} \in \Omega_t, \forall t$$

on which we will focus here a little more, in the context of the infinitesimal deformation hypothesis. By definition, the acceleration is that of the particle located in  $\mathbf{x}$  at time  $t$ , i.e., using the results of

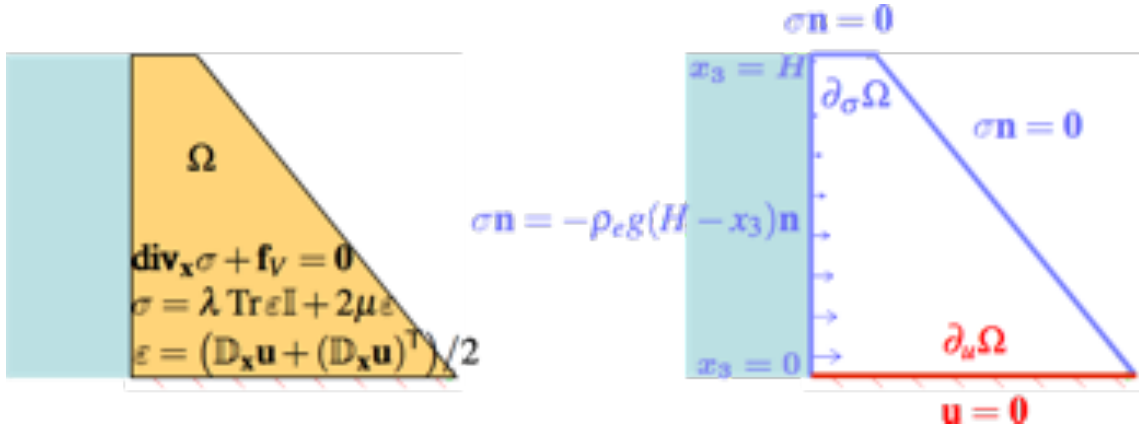


Figure 5.1: Review of all the equations and boundary conditions for an elasticity problem.

Paragraph 1.1.2:

$$\mathbf{a}(\mathbf{x}, t) = \mathbf{a}(\mathbf{f}(\mathbf{p}, t), t) = \frac{\partial^2 \mathbf{f}}{\partial t^2}(\mathbf{p}, t) = \frac{\partial^2 (\mathbf{p} + \mathbf{u}(\mathbf{p}, t))}{\partial t^2} = \frac{\partial^2 \mathbf{u}}{\partial t^2}(\mathbf{p}, t) = \ddot{\mathbf{u}}(\mathbf{p}, t)$$

In addition, the conservation of mass, obtained in Paragraph 1.4.2, makes it possible to establish, for the density, that:

$$\rho(\mathbf{x}, t) = \frac{\rho_0(\mathbf{p})}{\det \mathbb{F}(\mathbf{p}, t)} \approx \rho_0(\mathbf{p})(1 - \operatorname{div}_{\mathbf{p}} \mathbf{u}(\mathbf{p}, t))$$

and, since  $\|\mathbf{u}(\mathbf{p}, t)\| \ll \mathcal{L}$ ,  $\forall \mathbf{p} \in \Omega_0$  (where  $\mathcal{L}$  is the characteristic size of the domain), one can neglect  $|\operatorname{div}_{\mathbf{p}} \mathbf{u}(\mathbf{p}, t)| \ll 1$ , which finally results in:

$$\rho(\mathbf{x}, t) \mathbf{a}(\mathbf{x}, t) \approx \rho_0(\mathbf{x}) \ddot{\mathbf{u}}(\mathbf{x}, t)$$

by considering  $\mathbf{p} \approx \mathbf{x}$  because of the framework of the infinitesimal deformation hypothesis, and finally keeping  $\mathbf{x}$  as the spatial variable. This results in:

$$\rho_0(\mathbf{x}) \ddot{\mathbf{u}}(\mathbf{x}, t) = \operatorname{div}_{\mathbf{x}} \boldsymbol{\sigma}(\mathbf{x}, t) + \mathbf{f}_V(\mathbf{x}, t), \quad \forall \mathbf{x} \in \Omega, \quad \forall t$$

Besides, the equation expressing the infinitesimal strain tensor as the symmetrical part of the deformation gradient tensor is verified at any point in the domain, and at any time, on the one hand:

$$\boldsymbol{\varepsilon}(\mathbf{x}, t) = \frac{1}{2} \left( \mathbb{D}_{\mathbf{x}} \mathbf{u}(\mathbf{x}, t) + (\mathbb{D}_{\mathbf{x}} \mathbf{u}(\mathbf{x}, t))^T \right), \quad \forall \mathbf{x} \in \Omega, \quad \forall t$$

and, on the other hand, the constitutive relation (linear elastic and isotropic) between the stress and infinitesimal strain tensors, expressed in stiffness:

$$\boldsymbol{\sigma}(\mathbf{x}, t) = \mathbf{C}(\mathbf{x}) \boldsymbol{\varepsilon}(\mathbf{x}, t) = \lambda(\mathbf{x}) (\operatorname{tr} \boldsymbol{\varepsilon}(\mathbf{x}, t)) \mathbb{I} + 2\mu(\mathbf{x}) \boldsymbol{\varepsilon}(\mathbf{x}, t), \quad \forall \mathbf{x} \in \Omega, \quad \forall t$$

or in compliance:

$$\mathbf{e}(\mathbf{x}, t) = \mathbf{C}^{-1}(\mathbf{x}) \boldsymbol{\sigma}(\mathbf{x}, t) = \frac{1 + v(\mathbf{x})}{E(\mathbf{x})} \boldsymbol{\sigma}(\mathbf{x}, t) - \frac{v(\mathbf{x})}{E(\mathbf{x})} (\operatorname{tr} \boldsymbol{\sigma}(\mathbf{x}, t)) \mathbb{I}, \quad \forall \mathbf{x} \in \Omega, \quad \forall t$$

If the values of the material parameters can depend on the point under study, in practice we will rather try to split the material domain  $\Omega$  into several distinct sub-domains  $\Omega_k$ , on which they can be considered constant:

$$\lambda(\mathbf{x}) = \lambda_k, \mu(\mathbf{x}) = \mu_k, \quad \forall \mathbf{x} \in \Omega_k \text{ or else } E(\mathbf{x}) = E_k, \quad v(\mathbf{x}) = v_k, \quad \forall \mathbf{x} \in \Omega_k$$

It will then be important to express the conditions required at the interfaces between these different sub-domains, as we specify below.

- R** Considering the second derivative with respect to time, it is also necessary to know the initial displacements and velocities of all the points in the domain:

$$\mathbf{u}(\mathbf{x}, 0) = \mathbf{u}_0(\mathbf{x}), \text{ and } \dot{\mathbf{u}}(\mathbf{x}, 0) = \mathbf{v}_0(\mathbf{x}), \forall \mathbf{x} \in \Omega$$

In the case where the loadings exerted on the material domain are independent of time, the problem is static, and its solution is independent of time; there is therefore no longer any need to specify initial conditions.

In the case where the acceleration term ( $\rho_0 \ddot{\mathbf{u}}$ ) can be neglected at any time in the local equilibrium equation, but if some quantities are still functions of time in the equations, we speak of a “quasi-static” problem, which consists in considering that the solution is a sequence of static solutions, parameterized by time. Once again, no initial conditions are required in this case.

### 5.1.2 Boundary conditions

As we have already seen in the previous chapters, the boundary conditions expressed on the different boundaries of the domain allow us to determine the integration constants necessary to solve the partial differential equations of the previous paragraph.

#### Conditions on the external boundary

The basic hypothesis is that we have a known condition, either in displacement or in surface forces, at any point on the external boundary of the domain, and along each direction of space. By noting this partition  $\partial\Omega = \partial_u\Omega \cup \partial_\sigma\Omega$ , with  $\partial_u\Omega \cap \partial_\sigma\Omega = \emptyset$ , where  $\partial_u\Omega$  and  $\partial_\sigma\Omega$  refer to what concerns the known displacements  $\mathbf{u}_d(\mathbf{x}, t)$  and known surface forces  $\mathbf{f}_S(\mathbf{x}, t)$  respectively:

$$\mathbf{u}(\mathbf{x}, t) = \mathbf{u}_d(\mathbf{x}, t) \quad \forall \mathbf{x} \in \partial_u\Omega, \forall t, \text{ and } \boldsymbol{\sigma}(\mathbf{x}, t)\mathbf{n}(\mathbf{x}) = \mathbf{f}_S(\mathbf{x}, t), \forall \mathbf{x} \in \partial_\sigma\Omega, \forall t$$

where  $\mathbf{n}(\mathbf{x})$  is the outer unit normal vector to the domain, at point  $\mathbf{x}$ .

- ⚠️** It is essential to understand that the boundary partition that has just been established is to be interpreted in terms of components as well: thus, it is possible at a given point to constrain only one or two components of the displacement, while the component(s) of the stress vector, depending on the direction(s) left “free” in displacement, must be imposed. This is also the case for frictionless contact conditions, as mentioned below.

In the case of a part of the boundary in contact with an perfectly rigid body, supposedly fixed, several situations may occur:

- if there is adhesion at the contact surface  $\Sigma_c$ , the points of this surface remain fixed:

$$\mathbf{u}(\mathbf{x}, t) = \mathbf{0}, \forall \mathbf{x} \in \Sigma_c, \forall t$$

- if the contact allows relative movements, and if the associated slips are made without friction, then it must be expressed that there are no tangential components of the contact surface forces; if  $\mathbf{n}(\mathbf{x})$  is the local (outward) normal vector at the contact, we impose thus:

$$\langle \mathbf{u}(\mathbf{x}, t), \mathbf{n}(\mathbf{x}) \rangle = 0, \text{ and } \langle \boldsymbol{\sigma}(\mathbf{x}, t)\mathbf{n}(\mathbf{x}), \mathbf{t} \rangle = 0, \forall \mathbf{t} \perp \mathbf{n}(\mathbf{x}), \forall \mathbf{x} \in \Sigma_c, \forall t$$

where the first condition reflects that the contact is maintained from the kinematic point of view.

**R** It is of course possible to generalize the above conditions to the case of a rigid body in motion; the movement of this latter can then be a translation, or a small rotation (or the combination of these two “rigid body movements”), as for example:

$$\mathbf{u}(\mathbf{x}, t) = \varphi(t)\mathbf{e} \wedge (\mathbf{x} - \mathbf{x}_O)$$

in the case of a (small) rotation of angle  $\varphi(t)$  around the axis  $\mathbf{e}$  and of center  $\mathbf{x}_O$ , as mentioned in Appendix A.2.6.

In some cases, local surface forces are not known precisely on the surface  $\Sigma_d$  where they are applied, and it is only possible to impose the expressions  $\mathbf{R}^d(t)$  and  $\mathbf{M}_{\mathbf{x}_O}^d(t)$  respectively of the resultant force and the moment (expressed at point  $\mathbf{x}_O$ ) of these forces:

$$\int_{\Sigma_d} \boldsymbol{\sigma}(\mathbf{x}, t) \mathbf{n}(\mathbf{x}) dS_x = \mathbf{R}^d(t), \quad \forall t$$

$$\int_{\Sigma_d} (\mathbf{x} - \mathbf{x}_O) \wedge (\boldsymbol{\sigma}(\mathbf{x}, t) \mathbf{n}(\mathbf{x})) dS_x = \mathbf{M}_{\mathbf{x}_O}^d(t), \quad \forall t$$

**■ Example 5.1 — Torsion of a cylindrical shaft of arbitrary cross-section: equations review.** We are interested here in the torsion of a cylindrical shaft, of axis  $\mathbf{e}$  and height  $H$ , and whose cross-section can be of arbitrary shape. We assume that the loadings are applied in a sufficiently progressive manner so that it is possible to consider a quasi-static framework. Besides, we consider that the action of gravity can be neglected. Finally, we assume that the constitutive material is isotropic homogeneous, in the linear elasticity region, and that we can adopt the infinitesimal deformation hypothesis. The equations within the domain are therefore as follows:

$$\begin{aligned} \mathbf{0} &= \operatorname{div}_{\mathbf{x}} \boldsymbol{\sigma} \\ \boldsymbol{\varepsilon} &= \frac{1}{2} (\mathbb{D}_{\mathbf{x}} \mathbf{u} + (\mathbb{D}_{\mathbf{x}} \mathbf{u})^T) \\ \boldsymbol{\sigma} &= \lambda (\operatorname{tr} \boldsymbol{\varepsilon}) \mathbb{I} + 2\mu \boldsymbol{\varepsilon} \end{aligned}$$

In terms of boundary conditions, the purpose of the test machine is to apply a moment around the axis  $\mathbf{e}$  to each end of the specimen so that the two end cross-sections rotate relative to each other by a certain angle around  $\mathbf{e}$ . However, it is not possible to know precisely the local distribution of the surface forces exerted on the end surfaces  $\Sigma_0$  (in  $x_3 = 0$ ) and  $\Sigma_H$  (in  $x_3 = H$ ), which implies that we will only try to verify that:

$$\begin{aligned} \int_{\Sigma_H} (\mathbf{x} - \mathbf{x}_H) \wedge (\boldsymbol{\sigma} \mathbf{e}) dS_x &= M_d^H \mathbf{e} \\ \int_{\Sigma_O} (\mathbf{x} - \mathbf{x}_O) \wedge (\boldsymbol{\sigma}(-\mathbf{e})) dS_x &= M_d^O \mathbf{e} \end{aligned}$$

where the moments can be calculated at the centers of the end cross-sections for example (respectively  $\mathbf{x}_O$  and  $\mathbf{x}_H$ ). In both cases, these moments are actually “couples”, because the resultant forces of the machine’s actions on both ends of the shaft are equal to zero:

$$\begin{aligned} \int_{\Sigma_H} \boldsymbol{\sigma} \mathbf{e} dS_x &= \mathbf{0} \\ \int_{\Sigma_O} \boldsymbol{\sigma}(-\mathbf{e}) dS_x &= \mathbf{0} \end{aligned}$$

Finally, the lateral surfaces are free of forces. ■

### Conditions on an internal interface

Additional conditions are required when the studied material domain is split into several sub-domains with different (generally homogeneous) properties: in this case, on these interfaces  $\Sigma_i$  between the sub-domains, it is necessary to specify conditions for the displacement and the stress vector simultaneously, since nothing is known *a priori*.

Thus, in the typical case of a perfect adhesion interface between two sub-domains  $\Omega_k$  and  $\Omega_l$ , we must write, on the one hand, the continuity of the displacement vector (since the glueing

constrains the interface points to satisfy simultaneously the expressions of the displacements  $\mathbf{u}^{\mathcal{K}}$  and  $\mathbf{u}^{\mathcal{D}}$  respectively associated with  $\Omega_k$  and  $\Omega_l$ ):

$$\mathbf{u}^{\mathcal{K}}(\mathbf{x}, t) = \mathbf{u}^{\mathcal{D}}(\mathbf{x}, t), \forall \mathbf{x} \in \Sigma_i, \forall t$$

and, on the other hand, the continuity of the stress vector that had been established in Paragraph 2.3.2:

$$\boldsymbol{\sigma}^{\mathcal{K}}(\mathbf{x}, t)\mathbf{n}(\mathbf{x}) = \boldsymbol{\sigma}^{\mathcal{D}}(\mathbf{x}, t)\mathbf{n}(\mathbf{x}), \forall \mathbf{x} \in \Sigma_i, \forall t$$

where  $\mathbf{n}(\mathbf{x})$  is the local normal vector to  $\Sigma_i$ , of arbitrarily fixed sense.

**R** Other interface conditions are of course possible. If, for example, the two deformable media can slide without friction, only the normal components are bound:

$$\langle \mathbf{u}^{\mathcal{K}}(\mathbf{x}, t), \mathbf{n}(\mathbf{x}) \rangle = \langle \mathbf{u}^{\mathcal{D}}(\mathbf{x}, t), \mathbf{n}(\mathbf{x}) \rangle, \text{ and } \langle \boldsymbol{\sigma}^{\mathcal{K}}(\mathbf{x}, t)\mathbf{n}(\mathbf{x}), \mathbf{n}(\mathbf{x}) \rangle = \langle \boldsymbol{\sigma}^{\mathcal{D}}(\mathbf{x}, t)\mathbf{n}(\mathbf{x}), \mathbf{n}(\mathbf{x}) \rangle, \forall \mathbf{x} \in \Sigma_i, \forall t$$

knowing that we also have:

$$\langle \boldsymbol{\sigma}^{\mathcal{K}}(\mathbf{x}, t)\mathbf{n}(\mathbf{x}), \mathbf{t} \rangle = 0 = \langle \boldsymbol{\sigma}^{\mathcal{D}}(\mathbf{x}, t)\mathbf{n}(\mathbf{x}), \mathbf{t} \rangle, \forall \mathbf{t} \perp \mathbf{n}(\mathbf{x}), \forall \mathbf{x} \in \Sigma_i, \forall t$$

### Summary 5.1 — Generic formulation of an elasticity problem.

- Knowing:
- the volume force density  $\mathbf{f}_V$  exerted at any point inside the material domain  $\Omega$ ;
  - the surface force density  $\mathbf{f}_S$  exerted at any point of the part  $\partial_\sigma\Omega_t$  of the external boundary  $\partial\Omega$  of the domain;
  - the displacement  $\mathbf{u}_d$  constrained at any point of the complementary part  $\partial_u\Omega$  of the external boundary  $\partial\Omega$ ;

the problem is to find the fields  $(\mathbf{u}, \boldsymbol{\epsilon}, \boldsymbol{\sigma})$  satisfying the following equations and conditions:

- kinematic equations and conditions:

$$\boldsymbol{\epsilon}(\mathbf{x}, t) = \frac{1}{2} \left( \mathbb{D}_{\mathbf{x}}\mathbf{u}(\mathbf{x}, t) + (\mathbb{D}_{\mathbf{x}}\mathbf{u}(\mathbf{x}, t))^T \right), \forall \mathbf{x} \in \Omega, \forall t$$

$$\mathbf{u}(\mathbf{x}, t) = \mathbf{u}_d(\mathbf{x}, t) \quad \forall \mathbf{x} \in \partial_u\Omega, \forall t$$

- stress equations and conditions:

$$\rho_0(\mathbf{x})\ddot{\mathbf{u}}(\mathbf{x}, t) = \mathbf{div}_{\mathbf{x}}\boldsymbol{\sigma}(\mathbf{x}, t) + \mathbf{f}_V(\mathbf{x}, t), \forall \mathbf{x} \in \Omega, \forall t$$

$$\boldsymbol{\sigma}(\mathbf{x}, t)\mathbf{n}(\mathbf{x}) = \mathbf{f}_S(\mathbf{x}, t), \forall \mathbf{x} \in \partial_\sigma\Omega, \forall t$$

- constitutive relation:

$$\boldsymbol{\sigma}(\mathbf{x}, t) = \mathbf{C}(\mathbf{x})\boldsymbol{\epsilon}(\mathbf{x}, t) = \lambda(\mathbf{x})(\text{tr}\boldsymbol{\epsilon}(\mathbf{x}, t))\mathbb{I} + 2\mu(\mathbf{x})\boldsymbol{\epsilon}(\mathbf{x}, t), \forall \mathbf{x} \in \Omega, \forall t$$

$$\boldsymbol{\epsilon}(\mathbf{x}, t) = \mathbf{C}^{-1}(\mathbf{x})\boldsymbol{\sigma}(\mathbf{x}, t) = \frac{1 + \nu(\mathbf{x})}{E(\mathbf{x})}\boldsymbol{\sigma}(\mathbf{x}, t) - \frac{\nu(\mathbf{x})}{E(\mathbf{x})}(\text{tr}\boldsymbol{\sigma}(\mathbf{x}, t))\mathbb{I}, \forall \mathbf{x} \in \Omega, \forall t$$

- initial conditions:

$$\mathbf{u}(\mathbf{x}, 0) = \mathbf{u}_0(\mathbf{x}), \text{ et } \dot{\mathbf{u}}(\mathbf{x}, 0) = \mathbf{v}_0(\mathbf{x}), \forall \mathbf{x} \in \Omega$$

In the case where several material (sub)domains are studied, additional conditions on displacements and stress vectors are to be expressed on the associated interfaces.

### 5.1.3 Solution properties

Once all the boundary conditions detailed in the previous paragraph have been imposed, it is possible to prove mathematically that there is a solution to the problem. However, a particular case is to be studied; in the static case, if no kinematic conditions are imposed ( $\partial_u \Omega = \emptyset$ ), there can only be a solution if the material domain under study is actually in static equilibrium, i.e. if:

$$\int_{\Omega} \mathbf{f}_V dV_x + \int_{\partial\Omega} \mathbf{f}_S dS_x = \mathbf{0}$$

$$\int_{\Omega} (\mathbf{x} - \mathbf{x}_O) \wedge \mathbf{f}_V dV_x + \int_{\partial\Omega} (\mathbf{x} - \mathbf{x}_O) \wedge \mathbf{f}_S dS_x = \mathbf{0}$$

at a given fixed point  $O$ .

Another mathematical property, which we will study here, is the uniqueness of the solution, which will allow specific solution strategies to be implemented, as detailed in Paragraph 5.2.

#### Unicity in the static framework

Suppose that we are able to obtain two displacement solutions  $\mathbf{u}_1$  and  $\mathbf{u}_2$  of the same problem on the domain under study; they then both ( $k = 1$  or  $k = 2$ ) satisfy within this domain all the equations in the static framework:

$$\mathbf{0} = \mathbf{div}_x \boldsymbol{\sigma}_k + \mathbf{f}_V$$

$$\boldsymbol{\sigma}_k = \mathbf{C} \boldsymbol{\epsilon}_k$$

$$\boldsymbol{\epsilon}_k = \frac{1}{2} \left( \mathbb{D}_x \mathbf{u}_k + (\mathbb{D}_x \mathbf{u}_k)^T \right)$$

as well as the following boundary conditions:

$$\mathbf{u}_k = \mathbf{u}_d \text{ on } \partial_u \Omega, \text{ and } \boldsymbol{\sigma}_k \mathbf{n} = \mathbf{f}_S \text{ on } \partial_\sigma \Omega$$

Subtracting two by two all these equations, we see that the difference  $\mathbf{w} = \mathbf{u}_1 - \mathbf{u}_2$  between the two solutions is itself a solution to an elasticity problem with zero volume forces:

$$\mathbf{0} = \mathbf{div}_x \boldsymbol{\sigma}_1 - \mathbf{div}_x \boldsymbol{\sigma}_2 = \mathbf{div}_x \boldsymbol{\sigma}_w$$

$$\boldsymbol{\sigma}_w = \boldsymbol{\sigma}_1 - \boldsymbol{\sigma}_2 = \mathbf{C} \boldsymbol{\epsilon}_1 - \mathbf{C} \boldsymbol{\epsilon}_2 = \mathbf{C} \boldsymbol{\epsilon}_w$$

$$\boldsymbol{\epsilon}_w = \boldsymbol{\epsilon}_1 - \boldsymbol{\epsilon}_2 = \frac{1}{2} \left( \mathbb{D}_x \mathbf{u}_1 + (\mathbb{D}_x \mathbf{u}_1)^T \right) - \frac{1}{2} \left( \mathbb{D}_x \mathbf{u}_2 + (\mathbb{D}_x \mathbf{u}_2)^T \right) = \frac{1}{2} \left( \mathbb{D}_x \mathbf{w} + (\mathbb{D}_x \mathbf{w})^T \right)$$

and whose boundary conditions are also zero:

$$\mathbf{w} = \mathbf{0} \text{ on } \partial_u \Omega, \text{ and } \boldsymbol{\sigma}_w \mathbf{n} = \mathbf{0} \text{ on } \partial_\sigma \Omega$$

By calculating the scalar product of the local equilibrium equation by  $\mathbf{w}$ , then integrating on the domain, we find that:

$$\int_{\Omega} \langle \mathbf{div}_x \boldsymbol{\sigma}_w, \mathbf{w} \rangle dV_x = 0$$

Then using the formula  $\mathbf{div}_x(\mathbb{A}^T \mathbf{a}) = \langle \mathbf{div}_x \mathbb{A}, \mathbf{a} \rangle + \text{tr}(\mathbb{A}(\mathbb{D}_x \mathbf{a})^T)$  set out in Appendix B.1.1, we then obtain:

$$-\int_{\Omega} \text{tr}(\boldsymbol{\sigma}_w (\mathbb{D}_x \mathbf{w})^T) dV_x + \int_{\Omega} \mathbf{div}_x(\boldsymbol{\sigma}_w^T \mathbf{w}) dV_x = 0$$

By using the divergence formula (detailed in Appendix B.2.2), we now transform the second integral to get:

$$\int_{\Omega} \text{tr}(\boldsymbol{\sigma}_w (\mathbb{D}_x \mathbf{w})^T) dV_x = \int_{\Omega} \mathbf{div}_x(\boldsymbol{\sigma}_w^T \mathbf{w}) dV_x = \int_{\partial\Omega} \langle \boldsymbol{\sigma}_w^T \mathbf{w}, \mathbf{n} \rangle dS_x = \int_{\partial\Omega} \langle \boldsymbol{\sigma}_w \mathbf{n}, \mathbf{w} \rangle dS_x = 0$$

since, on the boundary, we have either  $\mathbf{w} = \mathbf{0}$ , or  $\boldsymbol{\sigma}_w \mathbf{n} = \mathbf{0}$ . Since  $\boldsymbol{\sigma}_w$  is symmetrical, we can write that:

$$0 = \int_{\Omega} \text{tr}(\boldsymbol{\sigma}_w (\mathbb{D}_{\mathbf{x}} \mathbf{w})^T) dV_x = \int_{\Omega} \text{tr}(\boldsymbol{\sigma}_w \mathbb{D}_{\mathbf{x}} \mathbf{w}) dV_x = \int_{\Omega} \text{tr}(\boldsymbol{\sigma}_w \boldsymbol{\epsilon}_w) dV_x$$

and, by expressing the constitutive relation using Lamé's parameters, it is finally established that:

$$\int_{\Omega} (\lambda (\text{tr} \boldsymbol{\epsilon}_w)^2 + 2\mu \text{tr}(\boldsymbol{\epsilon}_w^2)) dV_x = 0$$

Since  $\lambda > 0$  and  $\mu > 0$ , we deduce that  $\text{tr}(\boldsymbol{\epsilon}_w^2) = \|\boldsymbol{\epsilon}_w\|^2 = 0$ , and therefore, necessarily, that:

$$\boldsymbol{\epsilon}_w = 0$$

To go back to the displacement  $\mathbf{w}$ , we can write the equations verified by the components  $w_k(x_1, x_2, x_3)$  of  $\mathbf{w}$  in a Cartesian vector basis  $(\mathbf{i}_1, \mathbf{i}_2, \mathbf{i}_3)$ :

$$\frac{\partial w_1}{\partial x_1} = 0, \frac{\partial w_2}{\partial x_2} = 0, \frac{\partial w_3}{\partial x_3} = 0$$

$$\frac{\partial w_1}{\partial x_2} + \frac{\partial w_2}{\partial x_1} = 0, \frac{\partial w_1}{\partial x_3} + \frac{\partial w_3}{\partial x_1} = 0, \frac{\partial w_2}{\partial x_3} + \frac{\partial w_3}{\partial x_2} = 0$$

Differentiating the first equation of the second line with respect to  $x_1$ , we establish that:

$$0 = \frac{\partial}{\partial x_1} \left( \frac{\partial w_1}{\partial x_2} + \frac{\partial w_2}{\partial x_1} \right) = \frac{\partial^2 w_1}{\partial x_1 \partial x_2} + \frac{\partial^2 w_2}{\partial x_1^2} = \frac{\partial^2 w_2}{\partial x_1^2}$$

since  $w_1$  does not depend on  $x_1$  (considering the first equation of the first line). By doing the same for  $x_3$ , then with the other components, we can establish that:

$$\frac{\partial^2 w_k}{\partial x_l^2} = 0, 1 \leq k \leq 3, 1 \leq l \neq k \leq 3$$

which implies that:

$$w_k = a_k + b_{kl}x_l + c_{km}x_m, \quad 1 \leq k \leq 3, 1 \leq l \neq k \leq 3, 1 \leq m \neq k, m \neq l \leq 3$$

where the coefficients  $a_k$ ,  $b_{kl}$  and  $c_{km}$  are constant. By injecting these forms into the equations involving cross-derivatives:

$$\frac{\partial w_1}{\partial x_2} + \frac{\partial w_2}{\partial x_1} = 0, \frac{\partial w_1}{\partial x_3} + \frac{\partial w_3}{\partial x_1} = 0, \frac{\partial w_2}{\partial x_3} + \frac{\partial w_3}{\partial x_2} = 0$$

we conclude that the different coefficients  $b_{kl}$  and  $c_{km}$  are opposite two by two, and that  $\mathbf{w}$  is an rigid body displacement (with the infinitesimal deformation hypothesis):

$$\mathbf{w} = \mathbf{a} + \mathbf{b} \wedge (\mathbf{x} - \mathbf{x}_O)$$

consisting in the sum of an arbitrary translation and an arbitrary (small) rotation.

Finally, we know that  $\mathbf{w}$  vanishes on  $\partial_u \Omega$ ; if it is actually a surface, then this implies that  $\mathbf{w} = \mathbf{0}$  everywhere, and therefore that the solution is unique; on the other hand, if there is no constrained displacement condition ( $\partial_u \Omega = \emptyset$ ), or if  $\partial_u \Omega$  is reduced to a point or a line, the solution is not unique, resulting in an arbitrary (infinitesimal) rigid body movement.

 *The conclusions are the same in the quasi-static framework: indeed, since we can consider that it is a sequence of equilibrium states, it is sufficient to apply the previous reasoning at each time.*

■ **Example 5.2 — Torsion of a cylindrical shaft of arbitrary cross-section: existence and uniqueness of the solution.** We go on with Example 5.1 by analyzing the expected properties for the solution.

On the one hand, it is a problem where no constrained displacement condition is specified ( $\partial_u \Omega = \emptyset$ ); as we consider (quasi)static equilibrium, it is necessary, for the solution to exist, that the actions exerted on the specimen compensate each other, which implies that the two applied couples must be opposed to each other, at each time  $t$ :

$$M_d^H(t) = -M_d^O(t) = C(t)$$

On the other hand, since we have only imposed global conditions in terms of resultant forces and moments rather than local force densities, there can be no uniqueness of the solution. We will see in Example 5.6 how to affirm that we can find a solution in terms of stress field that makes sense concerning our problem. Moreover, since  $\partial_u \Omega = \emptyset$ , the displacement associated with the stress field is theoretically defined by an arbitrary (small) rigid body movement, but we can take this latter as zero because it is not relevant in the studied problem. Indeed, we will only need to know the angular difference between the two extreme cross-sections to determine the torsional stiffness of the specimen. ■

### Unicity in the dynamic framework

The approach is similar when we take into account the dynamic terms; by defining  $\mathbf{w} = \mathbf{u}_1 - \mathbf{u}_2$  as the difference between two solution displacement fields, we see that  $\mathbf{w}$  satisfies exactly the same equations as in the static framework, except the local equilibrium equation which keeps the acceleration term:

$$\rho_0 \ddot{\mathbf{w}} = \mathbf{div}_x \boldsymbol{\sigma}_w$$

and zero initial conditions on the domain  $\Omega$ :

$$\mathbf{w} = \mathbf{0}, \text{ and } \dot{\mathbf{w}} = \mathbf{0}, \text{ for } t = 0$$

Calculating the scalar product of the equilibrium equation by  $\dot{\mathbf{w}}$ , and integrating it spatially on the domain, between the initial time  $\tau = 0$  and the current time  $\tau = t$ , we obtain:

$$\int_0^t \int_{\Omega} \langle \rho_0 \ddot{\mathbf{w}}, \dot{\mathbf{w}} \rangle dV_x d\tau = \int_0^t \int_{\Omega} \langle \mathbf{div}_x \boldsymbol{\sigma}_w, \dot{\mathbf{w}} \rangle dV_x d\tau$$

The left-hand side can be simplified, by seeing that  $\langle \rho_0 \ddot{\mathbf{w}}, \dot{\mathbf{w}} \rangle = \rho_0 \overline{\langle \dot{\mathbf{w}}, \dot{\mathbf{w}} \rangle}$ , while the right-hand side can be transformed in the same way as in the static case, to finally get:

$$\int_{\Omega} \rho_0 \|\dot{\mathbf{w}}\|^2 dV_x = - \int_0^t \int_{\Omega} \text{tr}(\boldsymbol{\sigma}_w \dot{\boldsymbol{\epsilon}}_w) dV_x d\tau = - \int_0^t \int_{\Omega} \text{tr}(\mathbf{C} \boldsymbol{\epsilon}_w \dot{\boldsymbol{\epsilon}}_w) dV_x d\tau = - \int_{\Omega} \text{tr}(\mathbf{C} \boldsymbol{\epsilon}_w^2) dV_x$$

because  $\text{tr}(\mathbf{C} \boldsymbol{\epsilon}_w \dot{\boldsymbol{\epsilon}}_w) = \overline{\text{tr}(\mathbf{C} \boldsymbol{\epsilon}_w^2)}$ , and the initial conditions are equal to zero; this results in:

$$\int_{\Omega} \left( \rho_0 \|\dot{\mathbf{w}}\|^2 + \lambda (\text{tr} \boldsymbol{\epsilon}_w)^2 + 2\mu \text{tr}(\boldsymbol{\epsilon}_w^2) \right) dV_x = 0$$

Since  $\rho_0 > 0$ , we conclude that  $\dot{\mathbf{w}}(\mathbf{x}, t) = \mathbf{0}, \forall \mathbf{x} \in \Omega, \forall t$ , and therefore that  $\mathbf{w}$  is independent of time, hence, finally, since the initial conditions are equal to zero:

$$\mathbf{w}(\mathbf{x}, t) = \mathbf{0}, \forall \mathbf{x} \in \Omega, \forall t$$

In the dynamic framework, there is therefore systematically uniqueness of the solution.

## 5.2 Methods for solving an elasticity problem

Now that we have specified all the equations and boundary conditions, it remains to study here from what angle to approach the problem in order to solve it effectively. In practice, apart from the constitutive relation, each equation (or condition) concerns either the kinematic aspect (through the displacement field  $\mathbf{u}$  or the infinitesimal strain tensor  $\boldsymbol{\epsilon}$ , as well as through the imposed boundary conditions), or the force aspect (through the stress tensor  $\boldsymbol{\sigma}$  and the surface forces applied to the domain); it therefore seems wise to choose with which strategy we therefore wish to deal with the problem.

### 5.2.1 Displacement approach

A first possibility is to favour the kinematic aspect: indeed, it is often simpler to make hypotheses about displacements, which are closer to the mechanical intuition that one can have of the problem, than about the stress field, often more complex, and which presents *a priori* twice as many unknown components.

#### Displacement solution strategy

The starting point is to give oneself an *a priori* form  $\mathbf{u}_{fd}$  for the displacement you are looking for: this can consist in:

- eliminating components that are suspected to be equal to zero;
- eliminate dependencies on certain spatial variables, knowing that the question of time dependence can be decided whether we can assume that the problem can be solved in a (quasi-)static framework, or not;
- propose forms that make sense mechanically: translation, small rigid body rotation, elongation, shear strain, ...

If nothing can be proposed, we remain with the most general form for the displacement field, which then presents three components that each depend on the three variables of space. On the other hand, the choice of the vector basis for expressing the components should be as judicious as possible: for example, if the domain is cylindrical, a cylindrical vector basis associated with this geometry is quite naturally adapted.

The strategy then consists in successively verifying the different equations and boundary conditions to be able to conclude whether the proposed form is the solution to the problem; indeed, if everything is verified, the uniqueness property (except for a possibly arbitrary rigid body movement, in some cases) established in Paragraph 5.1.3 guarantees that we have the “true” solution. The steps are, therefore, as follows:

1. we start by expressing the boundary conditions in displacement using the form proposed for this latter, which possibly allow us to specify it a little more:

$$\mathbf{u}_{fd} = \mathbf{u}_d \text{ on } \partial_u \Omega$$

2. the infinitesimal strain tensor is calculated, then the stress tensor using the elastic constitutive relation:

$$\begin{aligned}\boldsymbol{\epsilon}_{fd} &= \frac{1}{2} \left( \mathbb{D}_{\mathbf{x}} \mathbf{u}_{fd} + (\mathbb{D}_{\mathbf{x}} \mathbf{u}_{fd})^T \right) \\ \boldsymbol{\sigma}_{fd} &= \mathbf{C} \boldsymbol{\epsilon}_{fd}\end{aligned}$$

3. the local equilibrium equation is introduced, either to check that the stress tensor satisfies it, or to deduce from it (a) differential equation(s) that must be verified by the functions that have yet to be determined:

$$\mathbf{div}_{\mathbf{x}} \boldsymbol{\sigma}_{fd} + \mathbf{f}_V = \rho_0 \ddot{\mathbf{u}}_{fd}$$

4. the boundary conditions are specified in terms of applied (surface) force densities, either to verify that the stress tensor satisfies them, or to deduce from them integration constants in order to solve the previous differential equation(s):

$$\boldsymbol{\sigma}_{fd} \mathbf{n} = \mathbf{f}_S \text{ on } \partial_{\sigma} \Omega$$

Once these steps have been completed, several situations are possible:

- either we have verified all the equations and boundary conditions: we can then say that we have determined the “true” solution to the problem, consisting of  $\mathbf{u} = \mathbf{u}_{fd}$ , and, consequently,  $\boldsymbol{\sigma} = \boldsymbol{\sigma}_{fd}$  and  $\boldsymbol{\epsilon} = \boldsymbol{\epsilon}_{fd}$ ;
- either a boundary condition (or even an equation) is not verified exactly: it may be possible, with the considerations of Paragraph 5.2.3, to conclude that the form adopted for the displacement is actually an approximate solution;
- or we have arrived at (a) differential equation(s) with associated boundary condition(s): if we can solve it (them) analytically, we then hold the “true” solution of the problem; otherwise, it may be possible to establish an approximate solution, as proposed in Paragraph 5.2.3.

**■ Example 5.3 — Torsion of a cylindrical shaft of arbitrary cross-section: displacement approach.**

We propose here to solve by a displacement approach the torsion problem of a shaft of arbitrary cross-section, in the framework of the infinitesimal deformation hypothesis, whose equations and boundary conditions have been specified in Example 5.1.

It is now necessary to propose a “reasonable” form for the sought displacement field; we know that, in the case of the torsion of a cylindrical shaft of revolution, the different cross-sections rotate, around the axis  $\mathbf{e}$  of the shaft, as rigid bodies with respect to each other. On the other hand, experiments show that, for other shapes, the cross-sections do not remain plane because a heterogeneous axial displacement is visible on them: we speak then of “warping”. We are therefore led to choose as a displacement field, in a Cartesian vector basis  $(\mathbf{i}_1, \mathbf{i}_2, \mathbf{i}_3 = \mathbf{e})$ , of associated coordinates  $(x_1, x_2, x_3)$  centered on the cylinder axis, the association of a small rigid body rotation (of angle a function of the cross-section coordinate) around  $\mathbf{e}$  and a heterogeneous displacement field along  $\mathbf{e}$ :

$$\boxed{\mathbf{u}_{fd}(x_1, x_2, x_3) = \alpha(x_3 \mathbf{e} \wedge \mathbf{x}_{\Sigma} + \varphi(x_1, x_2) \mathbf{e})}$$

where  $\mathbf{x}_{\Sigma} = x_1 \mathbf{i}_1 + x_2 \mathbf{i}_2$  stands for the position vector of the points of the cross-section  $\Sigma$ , and where  $\alpha$  is called the angle of twist per unit length, or “rate of twist”, which is the relative rotation angle between the two end cross-sections divided by the height of the shaft. The quantity  $\alpha\varphi$  then represents the warping, which is assumed to be identical in each cross-section.

Since there are no displacement conditions to be verified, the next step is to calculate the infinitesimal strain tensor as:

$$\boldsymbol{\epsilon}_{fd} = \frac{1}{2} (\mathbb{D}_{\mathbf{x}} \mathbf{u}_{fd} + (\mathbb{D}_{\mathbf{x}} \mathbf{u}_{fd})^T)$$

with:

$$\mathbb{D}_{\mathbf{x}} \mathbf{u}_{fd} = \sum_{k=1}^3 \frac{\partial \mathbf{u}_{fd}}{\partial x_k} \otimes \mathbf{i}_k = \sum_{k=1}^2 \alpha \left( x_3 \mathbf{e} \wedge \mathbf{i}_k + \frac{\partial \varphi}{\partial x_k} \mathbf{e} \right) \otimes \mathbf{i}_k + \alpha (\mathbf{e} \wedge \mathbf{x}_{\Sigma}) \otimes \mathbf{e}$$

hence:

$$\boldsymbol{\epsilon}_{fd} = \alpha (\nabla_{\mathbf{x}_{\Sigma}} \varphi + \mathbf{e} \wedge \mathbf{x}_{\Sigma}) \otimes_S \mathbf{e}$$

because  $\sum_{k=1}^2 ((\mathbf{e} \wedge \mathbf{i}_k) \otimes \mathbf{i}_k)^T = - \sum_{k=1}^2 (\mathbf{e} \wedge \mathbf{i}_k) \otimes \mathbf{i}_k$ , and  $\frac{\partial \varphi}{\partial x_1} \mathbf{i}_1 + \frac{\partial \varphi}{\partial x_2} \mathbf{i}_2 = \nabla_{\mathbf{x}_{\Sigma}} \varphi$ .

Since  $\text{tr} \boldsymbol{\epsilon} = 0$ , we deduce from this that the stress tensor is expressed directly as:

$$\boldsymbol{\sigma}_{fd} = 2\mu \boldsymbol{\epsilon}_{fd} = 2\mu \alpha (\nabla_{\mathbf{x}_{\Sigma}} \varphi + \mathbf{e} \wedge \mathbf{x}_{\Sigma}) \otimes_S \mathbf{e}$$

This latter must then satisfy the local equilibrium equation, i.e.:

$$\mathbf{0} = \mathbf{div}_{\mathbf{x}} \boldsymbol{\sigma} = \sum_{k=1}^3 \frac{\partial \boldsymbol{\sigma}}{\partial x_k} \mathbf{i}_k = \mu \alpha \left( \frac{\partial^2 \varphi}{\partial x_1^2} + \frac{\partial^2 \varphi}{\partial x_2^2} \right) \mathbf{e}$$

which shows, on the one hand, that the torsion kinematics induces a stress field that is compatible with the local equilibrium equation, and, on the other hand, that the warping has to satisfy:

$$\boxed{\Delta_{\mathbf{x}_\Sigma} \varphi = 0}$$

In addition, the applied surface force conditions must be taken into account; first, the lateral surfaces  $\Sigma_l$  must be free of forces, i.e.:

$$\mathbf{0} = \sigma_{fd} \mathbf{n}_l = 2\mu\alpha((\nabla_{\mathbf{x}_\Sigma} \varphi + \mathbf{e} \wedge \mathbf{x}_\Sigma) \otimes_S \mathbf{e}) \mathbf{n}_l = \mu\alpha \langle \nabla_{\mathbf{x}_\Sigma} \varphi + \mathbf{e} \wedge \mathbf{x}_\Sigma, \mathbf{n}_l \rangle \mathbf{e}$$

at every point of  $\Sigma_l$ , with outer unit normal vector  $\mathbf{n}_l \perp \mathbf{e}$ . By defining  $\mathbf{t}_l = \mathbf{e} \wedge \mathbf{n}_l$  as the vector (perpendicular to the axis  $\mathbf{e}$ ) tangent to the surface, we then obtain that the normal derivative of the warping has to satisfy:

$$\boxed{\frac{\partial \varphi}{\partial n} = \langle \nabla_{\mathbf{x}_\Sigma} \varphi, \mathbf{n}_l \rangle = \langle \mathbf{x}_\Sigma, \mathbf{t}_l \rangle}$$

at any point on the lateral surfaces  $\Sigma_l$ . Since the condition is independent of  $x_3$ , it is sufficient to verify this condition on the edge of a cross-section of arbitrary coordinate.

Finally, we must find the global conditions imposed by the test machine on the two end surfaces in  $x_3 = 0$  and  $x_3 = H$ , i.e. zero resultant forces, and moments along  $\mathbf{e}$ . As regards the calculation of the resultant force of the machine's action on the surface  $\Sigma_H$ , we find then:

$$\mathbf{R}^H = \int_{\Sigma_H} \sigma_{fd} \mathbf{e} dS_x = \int_{\Sigma_H} \alpha\mu(\nabla_{\mathbf{x}_\Sigma} \varphi + \mathbf{e} \wedge \mathbf{x}_\Sigma) dS_x$$

Using the divergence properties set out in Appendix B.1.1, we can rewrite that:

$$\begin{aligned} \nabla_{\mathbf{x}_\Sigma} \varphi + \mathbf{e} \wedge \mathbf{x}_\Sigma &= (\mathbb{D}_{\mathbf{x}_\Sigma} \mathbf{x}_\Sigma)(\nabla_{\mathbf{x}_\Sigma} \varphi + \mathbf{e} \wedge \mathbf{x}_\Sigma) \\ &= \operatorname{div}_{\mathbf{x}_\Sigma}(\mathbf{x}_\Sigma \otimes (\nabla_{\mathbf{x}_\Sigma} \varphi + \mathbf{e} \wedge \mathbf{x}_\Sigma)) - \operatorname{div}_{\mathbf{x}_\Sigma}(\nabla_{\mathbf{x}_\Sigma} \varphi + \mathbf{e} \wedge \mathbf{x}_\Sigma) \mathbf{x}_\Sigma \\ &= \operatorname{div}_{\mathbf{x}_\Sigma}(\mathbf{x}_\Sigma \otimes (\nabla_{\mathbf{x}_\Sigma} \varphi + \mathbf{e} \wedge \mathbf{x}_\Sigma)) - \operatorname{div}_{\mathbf{x}_\Sigma}(\nabla_{\mathbf{x}_\Sigma} \varphi) \mathbf{x}_\Sigma \\ &= \operatorname{div}_{\mathbf{x}_\Sigma}(\mathbf{x}_\Sigma \otimes (\nabla_{\mathbf{x}_\Sigma} \varphi + \mathbf{e} \wedge \mathbf{x}_\Sigma)) \end{aligned}$$

considering  $\operatorname{div}_{\mathbf{x}_\Sigma}(\nabla_{\mathbf{x}_\Sigma} \varphi) = \Delta_{\mathbf{x}_\Sigma} \varphi = 0$  by virtue of the equation determined above. Thus, using Stokes' formula, we find that:

$$\begin{aligned} \mathbf{R}^H &= \alpha\mu \int_{\Sigma_H} \operatorname{div}_{\mathbf{x}_\Sigma}(\mathbf{x}_\Sigma \otimes (\nabla_{\mathbf{x}_\Sigma} \varphi + \mathbf{e} \wedge \mathbf{x}_\Sigma)) dS_x \\ &= \alpha\mu \int_{\partial\Sigma_H} (\mathbf{x}_\Sigma \otimes (\nabla_{\mathbf{x}_\Sigma} \varphi + \mathbf{e} \wedge \mathbf{x}_\Sigma)) \mathbf{n}_l dl_x \\ &= \alpha\mu \int_{\partial\Sigma_H} \langle \nabla_{\mathbf{x}_\Sigma} \varphi + \mathbf{e} \wedge \mathbf{x}_\Sigma, \mathbf{n}_l \rangle \mathbf{x}_\Sigma dl_x = \mathbf{0} \end{aligned}$$

which vanishes because of the condition to be verified on the boundary of a cross-section. The calculation of the resultant force  $\mathbf{R}^O$  is identical (but for the sign).

As far as the moment is concerned, we can simply show that it is indeed along the direction  $\mathbf{e}$ , by noting that:

$$\begin{aligned} \langle \mathbf{M}^H, \mathbf{i}_1 \rangle &= \int_{\Sigma_H} \langle \mathbf{x}_\Sigma \wedge (\sigma_{fd} \mathbf{e}), \mathbf{i}_1 \rangle dS_x = \int_{\Sigma_H} \alpha\mu \langle \mathbf{x}_\Sigma \wedge (\nabla_{\mathbf{x}_\Sigma} \varphi + \mathbf{e} \wedge \mathbf{x}_\Sigma), \mathbf{i}_1 \rangle dS_x \\ &= \int_{\Sigma_H} \alpha\mu \langle \nabla_{\mathbf{x}_\Sigma} \varphi + \mathbf{e} \wedge \mathbf{x}_\Sigma, \mathbf{i}_1 \wedge \mathbf{x}_\Sigma \rangle dS_x = 0 \end{aligned}$$

since  $(\mathbf{i}_1 \wedge \mathbf{x}_\Sigma) // \mathbf{e}$ . Of course, the same result is obtained with regard to  $\mathbf{i}_2$ .

In order to deal with a practical case, let us consider a solid cross-section of elliptical shape, with semi-axes  $a$  and  $b$  along  $\mathbf{i}_1$  and  $\mathbf{i}_2$  respectively. The warping function is then searched for in the form:

$$\boxed{\varphi(x_1, x_2) = kx_1 x_2}$$

where  $k$  is a constant. We immediately verify that  $\Delta_{\mathbf{x}_\Sigma} \varphi = 0$  in the cross-section. In addition, the lateral edge conditions should be as follows:

$$\boxed{\frac{\partial \varphi}{\partial n} = \langle \mathbf{x}_\Sigma, \mathbf{e} \wedge \mathbf{n}_l \rangle}$$

where  $\mathbf{n}_l$  is the outer normal vector on the edge of the elliptical cross-section, which is of equation  $x_1^2/a^2 + x_2^2/b^2 = 1$ , hence:

$$\left\langle \mathbf{n}_l, \frac{2x_1}{a^2} \mathbf{i}_1 + \frac{2x_2}{b^2} \mathbf{i}_2 \right\rangle = 0$$

We then obtain:

$$\left\langle kx_2 \mathbf{i}_1 + kx_1 \mathbf{i}_2, \frac{2x_1}{a^2} \mathbf{i}_1 + \frac{2x_2}{b^2} \mathbf{i}_2 \right\rangle = \left\langle x_1 \mathbf{i}_1 + x_2 \mathbf{i}_2, \frac{2x_1}{a^2} \mathbf{e} \wedge \mathbf{i}_1 + \frac{2x_2}{b^2} \mathbf{e} \wedge \mathbf{i}_2 \right\rangle$$

that is:

$$\frac{2kx_1x_2}{a^2} + \frac{2kx_1x_2}{b^2} = \frac{2x_1x_2}{a^2} - \frac{2x_2x_2}{b^2}$$

which finally gives that:

$$k = \frac{b^2 - a^2}{a^2 + b^2}$$

In the case of a circular cross-section ( $a = b$ ), we naturally find that torsion occurs without warping ( $\varphi = 0$ ). ■

### Navier's equation

In the case where no hypothesis is made about the desired displacement field, the previous approach provides a set of differential equations (and associated boundary conditions) that involve the displacement field only. Indeed, by injecting the constitutive relation expressed in stiffness into the local equilibrium equation, we obtain:

$$\rho_0 \ddot{\mathbf{u}} = \mathbf{div}_x \boldsymbol{\sigma} + \mathbf{f}_V = \mathbf{div}_x (\lambda (\text{tr} \boldsymbol{\varepsilon}) \mathbb{I} + 2\mu \boldsymbol{\varepsilon}) + \mathbf{f}_V = \lambda \mathbf{div}_x ((\text{tr} \boldsymbol{\varepsilon}) \mathbb{I}) + \mu \mathbf{div}_x (\mathbb{D}_x \mathbf{u}) + \mu \mathbf{div}_x ((\mathbb{D}_x \mathbf{u})^\top) + \mathbf{f}_V$$

if we assume here that Lamé parameters ( $\lambda, \mu$ ) are homogeneous in the domain. By using some of the formulas of Appendix B.1.2, we can transform the divergences from the previous equation respectively as:

- $\mathbf{div}_x ((\text{tr} \boldsymbol{\varepsilon}) \mathbb{I}) = \nabla_x (\text{tr} \boldsymbol{\varepsilon}) = \nabla_x (\mathbf{div}_x \mathbf{u})$ , where  $\nabla_x$  refers to the space gradient;
- $\langle \mathbf{div}_x (\mathbb{D}_x \mathbf{u}), \mathbf{c} \rangle = \mathbf{div}_x ((\mathbb{D}_x \mathbf{u})^\top \mathbf{c}) = \mathbf{div}_x (\nabla_x \langle \mathbf{u}, \mathbf{c} \rangle) = \Delta_x \langle \mathbf{u}, \mathbf{c} \rangle = \langle \Delta_x \mathbf{u}, \mathbf{c} \rangle$ ,  $\forall \mathbf{c}$  constant, where  $\Delta_x$  is the (vector) Laplacian, defined in Appendix B.1.1, and:
- $\langle \mathbf{div}_x ((\mathbb{D}_x \mathbf{u})^\top), \mathbf{c} \rangle = \mathbf{div}_x ((\mathbb{D}_x \mathbf{u}) \mathbf{c}) = \langle \nabla_x (\mathbf{div}_x \mathbf{u}), \mathbf{c} \rangle$ ,  $\forall \mathbf{c}$  constant, using an arbitrary constant vector  $\mathbf{c}$ .

The following result is classically called Navier's equation.

**Navier's equation.** The formulation in terms of displacement of a homogeneous isotropic linear elasticity problem consists in solving the so-called Navier's equation:

$$(\lambda + \mu) \nabla_x (\mathbf{div}_x \mathbf{u}(\mathbf{x}, t)) + \mu \Delta_x \mathbf{u}(\mathbf{x}, t) + \mathbf{f}_V(\mathbf{x}, t) = \rho_0(\mathbf{x}) \ddot{\mathbf{u}}(\mathbf{x}, t), \quad \forall \mathbf{x} \in \Omega, \quad \forall t$$

whose scalar projections on a Cartesian vector basis ( $\mathbf{i}_1, \mathbf{i}_2, \mathbf{i}_3$ ) are established as:

$$(\lambda + \mu) \sum_{l=1}^3 \frac{\partial^2 u_l}{\partial x_k \partial x_l} + \mu \sum_{l=1}^3 \frac{\partial^2 u_k}{\partial x_l^2} + \langle \mathbf{f}_V, \mathbf{i}_k \rangle = \rho_0 \frac{\partial^2 u_k}{\partial t^2}, \quad 1 \leq k \leq 3$$

In addition, in order to determine the integration constants related to the solution of these three scalar second-order differential equations, we use the following conditions on the external boundary of the domain:

$$\mathbf{u}(\mathbf{x}, t) = \mathbf{u}_d(\mathbf{x}, t) \quad \forall \mathbf{x} \in \partial_u \Omega, \quad \forall t, \text{ and } \lambda (\text{tr} \boldsymbol{\varepsilon}(\mathbf{x}, t)) \mathbf{n}(\mathbf{x}) + 2\mu \boldsymbol{\varepsilon}(\mathbf{x}, t) \mathbf{n}(\mathbf{x}) = \mathbf{f}_S(\mathbf{x}, t), \quad \forall \mathbf{x} \in \partial_\sigma \Omega, \quad \forall t$$

where  $\boldsymbol{\varepsilon}$  is the symmetrical part of the displacement gradient tensor, and initial conditions of

displacement and velocity (except in the static and quasi-static frameworks) are given as:

$$\mathbf{u}(\mathbf{x}, 0) = \mathbf{u}_0(\mathbf{x}), \text{ and } \dot{\mathbf{u}}(\mathbf{x}, 0) = \mathbf{v}_0(\mathbf{x}), \forall \mathbf{x} \in \Omega$$

**Summary 5.2 — Displacement formulation of an elasticity problem.** Knowing:

- the volume force density  $\mathbf{f}_V$  exerted at any point inside the material domain  $\Omega$ ;
- the surface force density  $\mathbf{f}_S$  exerted at any point of the part  $\partial_\sigma\Omega$  of the external boundary  $\partial\Omega$  of the domain;
- the displacement  $\mathbf{u}_d$  constrained at any point of the complementary part  $\partial_u\Omega$  of the external boundary  $\partial\Omega$ ;

the problem for a homogeneous material consists in finding the displacement field  $\mathbf{u}$  verifying the following equation (called Navier's equation):

$$(\lambda + \mu) \nabla_{\mathbf{x}} (\operatorname{div}_{\mathbf{x}} \mathbf{u}(\mathbf{x}, t)) + \mu \Delta_{\mathbf{x}} \mathbf{u}(\mathbf{x}, t) + \mathbf{f}_V(\mathbf{x}, t) = \rho_0(\mathbf{x}) \ddot{\mathbf{u}}(\mathbf{x}, t), \forall \mathbf{x} \in \Omega, \forall t$$

and the following boundary conditions:

$$\mathbf{u}(\mathbf{x}, t) = \mathbf{u}_d(\mathbf{x}, t), \forall \mathbf{x} \in \partial_u\Omega, \forall t, \text{ and } \lambda (\operatorname{tr} \boldsymbol{\epsilon}(\mathbf{x}, t)) \mathbf{n}(\mathbf{x}) + 2\mu \boldsymbol{\epsilon}(\mathbf{x}, t) \mathbf{n}(\mathbf{x}) = \mathbf{f}_S(\mathbf{x}, t), \forall \mathbf{x} \in \partial_\sigma\Omega, \forall t$$

as well as the initial conditions:

$$\mathbf{u}(\mathbf{x}, 0) = \mathbf{u}_0(\mathbf{x}), \text{ and } \dot{\mathbf{u}}(\mathbf{x}, 0) = \mathbf{v}_0(\mathbf{x}), \forall \mathbf{x} \in \Omega$$



If the material is heterogeneous, two cases are to be studied:

- if the domain can be divided into several sub-domains, which are each of homogeneous properties, then Navier's equation can be applied separately to each sub-domain; in this case, the conditions at the interfaces between sub-domains must also be taken into account, for example for  $\Omega_k$  and  $\Omega_l$  (with obvious notations):

$$\mathbf{u}^{(k)}(\mathbf{x}, t) = \mathbf{u}^{(l)}(\mathbf{x}, t), \text{ and } \mathbf{C}^{(k)} \boldsymbol{\epsilon}^{(k)}(\mathbf{x}, t) \mathbf{n}(\mathbf{x}) = \mathbf{C}^{(l)} \boldsymbol{\epsilon}^{(l)}(\mathbf{x}, t) \mathbf{n}(\mathbf{x}), \forall \mathbf{x} \in \Sigma_i, \forall t$$

where  $\mathbf{n}(\mathbf{x})$  is the local normal vector to  $\Sigma_i$ , of arbitrarily fixed sense;

- if this is not possible, then the spatial dependencies of Lamé's parameters  $(\lambda(\mathbf{x}), \mu(\mathbf{x}))$  must be taken into account, hence the appearance of additional terms associated with the spatial gradients of these parameters.

## 5.2.2 Stress approach

The alternate possibility is to favour the static aspect; indeed, in some cases, it is possible to propose directly stress fields, for example when one believes that they should be homogeneous, or evolve linearly in the domain.

### Stress solution strategy

The starting point is thus to give oneself an *a priori* form for the stress tensor one is looking for, for example:

- by eliminating components that are suspected to be equal to zero;
- by eliminating dependencies on certain spatial variables, knowing that the question of time dependence can be decided according to the chosen framework: dynamic, or (quasi-)static;
- by proposing forms that make sense mechanically, especially those that are likely to verify the local equilibrium equation.

If nothing can be proposed, then we remain with the most general form for the stress tensor, which is equivalent to search, in a vector basis that must be judicious concerning the geometry of the domain, for six scalar components that are functions of the three variables of space.

The strategy then consists in successively verifying the different equations and boundary conditions to be able to conclude whether the proposed form is the solution to the problem (again thanks to the uniqueness property of the solution). The steps are, therefore, as follows:

1. we start by expressing the boundary conditions in terms of surface forces using the form proposed for the stress tensor, which possibly allow us to specify it a little more:

$$\sigma_{fc} \mathbf{n} = \mathbf{f}_S \text{ on } \partial_\sigma \Omega$$

2. the local equilibrium equation is introduced, either to verify it, or to deduce from it (a) differential equation(s) that the functions that have yet to be determined must verify; for example, in the static case, we must verify:

$$\operatorname{div}_{\mathbf{x}} \sigma_{fc} + \mathbf{f}_V = \mathbf{0}$$

3. the infinitesimal strain tensor is then calculated using the constitutive relation in compliance:

$$\epsilon_{fc} = \mathbf{C}^{-1} \sigma_{fc}$$

4. the displacement field is determined, possibly by means of integration constants not yet used, by solving the relation between the infinitesimal strain tensor and the displacement field:

$$\mathbf{u}_{fc} \text{ such that } \frac{1}{2} \left( \mathbb{D}_{\mathbf{x}} \mathbf{u}_{fc} + (\mathbb{D}_{\mathbf{x}} \mathbf{u}_{fc})^T \right) = \epsilon_{fc}$$

5. the boundary conditions in displacement are specified, thus making it possible to determine any integration constants of the previous step:

$$\mathbf{u}_{fc} = \mathbf{u}_d \text{ on } \partial_u \Omega$$

Once these steps have been completed, the same situations as in the case of the displacement approach are possible:

- either we have verified all the equations and boundary conditions: we can then say that we have determined the “true” solution to the problem, consisting of:  $\sigma = \sigma_{fc}$ , and, consequently,  $\mathbf{u} = \mathbf{u}_{fc}$  and  $\epsilon = \epsilon_{fc}$ ;
- either a boundary condition (or even an equation) is not verified exactly: it may be possible, with the considerations of Paragraph 5.2.3, to conclude that the form adopted for the stress is an approximate solution;
- or we have arrived at (a) differential equation(s) with associated boundary condition(s): if we can solve it (them) analytically, we then hold the “true” solution of the problem; otherwise, it may be possible to establish an approximate solution, as proposed in Paragraph 5.2.3.

■ **Example 5.4 — Torsion of a cylindrical shaft of arbitrary cross-section: stress approach.** We propose here to solve by a stress approach the torsion problem of a shaft of arbitrary cross-section, whose equations and boundary conditions have been specified in Example 5.1.

For this purpose, a “reasonable” form for the stress tensor is to assume that it has only shear components with respect to the cylinder axis; we then look for:

$$\sigma_{fc} = -2\alpha\mu(\mathbf{e} \wedge \nabla_{\mathbf{x}_\Sigma} \psi) \otimes_S \mathbf{e}$$

where  $\alpha$  is, as before, the “rate of twist”, and  $\psi(\mathbf{x}_\Sigma) = \psi(x_1, x_2)$  is a function of the coordinates in the cross-section.

With this form, the function  $\psi$  automatically satisfies the local equilibrium equation; indeed:

$$\mathbf{div}_x \boldsymbol{\sigma}_{fc} = \left( \alpha \mu \frac{\partial \psi}{\partial x \partial y} - \alpha \mu \frac{\partial \psi}{\partial y \partial x} \right) \mathbf{e} = \mathbf{0}$$

In addition, the stress tensor must satisfy free boundary conditions on the lateral surfaces  $\Sigma_l$  of the shaft, i.e.:

$$\mathbf{0} = \boldsymbol{\sigma}_{fc} \mathbf{n}_l = -\alpha \mu \langle \mathbf{e} \wedge \nabla_{x_\Sigma} \psi, \mathbf{n}_l \rangle \mathbf{e}$$

By setting  $\mathbf{t}_l = \mathbf{e} \wedge \mathbf{n}_l$  the tangent vector at any point on the lateral surfaces  $\Sigma_l$ , we obtain that:

$$\langle \nabla_{x_\Sigma} \psi, \mathbf{t}_l \rangle = 0$$

or, in other words,  $\psi$  must be constant on the boundary of the cross-section.

Finally, it is now essential to verify that we can associate to the infinitesimal strain tensor  $\boldsymbol{\varepsilon}_{fc}$  (related to the stress tensor) a displacement field  $\mathbf{u}_{fc}$ ; since  $\text{tr} \boldsymbol{\sigma}_{fc} = 0$ , we get:

$$\boldsymbol{\varepsilon}_{fc} = \frac{1}{2\mu} \boldsymbol{\sigma}_{fc} = -\alpha (\mathbf{e} \wedge \nabla_{x_\Sigma} \psi) \otimes_S \mathbf{e}$$

hence, by noting  $u_k$  the components of  $\mathbf{u}_{fc}$  in the vector basis  $(\mathbf{i}_1, \mathbf{i}_2, \mathbf{i}_3 = \mathbf{e})$ :

$$\begin{aligned} 0 &= \varepsilon_{11} = \frac{\partial u_1}{\partial x_1} \\ 0 &= \varepsilon_{22} = \frac{\partial u_2}{\partial x_2} \\ 0 &= \varepsilon_{33} = \frac{\partial u_3}{\partial x_3} \\ \alpha \frac{\partial \psi}{\partial x_2} &= 2\varepsilon_{13} = \frac{\partial u_1}{\partial x_3} + \frac{\partial u_3}{\partial x_1} \\ -\alpha \frac{\partial \psi}{\partial x_1} &= 2\varepsilon_{23} = \frac{\partial u_2}{\partial x_3} + \frac{\partial u_3}{\partial x_2} \\ 0 &= 2\varepsilon_{12} = \frac{\partial u_1}{\partial x_2} + \frac{\partial u_2}{\partial x_1} \end{aligned}$$

The last equation allows us to establish that:

$$\begin{aligned} 0 &= 2 \frac{\partial \varepsilon_{12}}{\partial x_1} = \frac{\partial^2 u_1}{\partial x_1 \partial x_2} + \frac{\partial^2 u_2}{\partial x_1^2} = \frac{\partial^2 u_2}{\partial x_1^2} \\ 0 &= 2 \frac{\partial \varepsilon_{12}}{\partial x_2} = \frac{\partial^2 u_1}{\partial x_2^2} + \frac{\partial^2 u_2}{\partial x_1 \partial x_2} = \frac{\partial^2 u_1}{\partial x_2^2} \end{aligned}$$

using the first two equations of the system. In addition, since  $u_3$  and  $\psi$  do not depend on  $x_3$ , we deduce from this that:

$$\begin{aligned} \frac{\partial^2 u_1}{\partial x_3^2} &= \frac{\partial^2 u_3}{\partial x_1 \partial x_3} - \alpha \frac{\partial^2 \psi}{\partial x_2 \partial x_3} = 0 \\ \frac{\partial^2 u_2}{\partial x_3^2} &= \frac{\partial^2 u_3}{\partial x_2 \partial x_3} + \alpha \frac{\partial^2 \psi}{\partial x_1 \partial x_3} = 0 \end{aligned}$$

which implies that the first two components of displacement are written as:

$$\begin{aligned} u_1(x_2, x_3) &= a_1 x_2 x_3 + b_1 x_2 + c_1 x_3 + d_1 \\ u_2(x_1, x_3) &= a_2 x_1 x_3 + b_2 x_1 + c_2 x_3 + d_2 \end{aligned}$$

and by reusing the last equation of the system, it is then established that:

$$0 = \frac{\partial u_1}{\partial x_2} + \frac{\partial u_2}{\partial x_1} = (a_1 + a_2)x_3 + b_1 + b_2$$

hence:  $a_1 = -a_2$  and  $b_1 = -b_2$ .

From this form, we deduce a necessary condition on the function  $\psi$ , namely:

$$-\alpha \left( \frac{\partial^2 \psi}{\partial x_1^2} + \frac{\partial^2 \psi}{\partial x_2^2} \right) = 2 \frac{\partial \varepsilon_{23}}{\partial x_1} - 2 \frac{\partial \varepsilon_{13}}{\partial x_2} = a_2 - a_1 = 2a_2$$

or by identifying  $a_2 = \alpha$  (rate of twist):

$$\Delta_{\Sigma} \psi = -2$$

With this necessary condition, it is then possible to show that it is also possible to determine the  $u_3$  component of the displacement field.

In order to treat a practical case, let us consider once again, as in Example 5.3, a solid cross-section of elliptical shape, of semi-axes  $a$  and  $b$  along  $\mathbf{i}_1$  and  $\mathbf{i}_2$  respectively. It can then be established that the function:

$$\psi(x_1, x_2) = -\frac{b^2 x_1^2 + a^2 x_2^2}{a^2 + b^2}$$

satisfies  $\Delta_{\Sigma} \psi = -2$  in the cross-section, and  $\psi$  constant on the edge of the section. ■



Unlike the displacement approach, the approach proposed above may fail in step 4, when calculating the displacement field from the infinitesimal strain tensor. Indeed, this is the tricky point of this approach, because, even if no boundary conditions are applied to the domain, it is necessary to verify that the infinitesimal strain tensor, which results from the proposed stress tensor, can be expressed as the symmetrical part of the displacement gradient tensor: this is the objective of the next paragraph, which establishes the so-called “compatibility equations”.

### Compatibility equations

The question of whether, from a given symmetrical tensor  $\boldsymbol{\varepsilon}_{fc}$ , it is possible, or not, to determine a displacement field such that this tensor is the symmetrical part of the displacement gradient tensor, is fundamental in the stress approach. It is possible to determine in the general case what are the requirements for the components of the tensor  $\boldsymbol{\varepsilon}_{fc}$ .

To do this, we start from the decomposition, presented in Paragraph 1.3.3, of the solution displacement gradient tensor as the sum of its symmetrical and antisymmetrical parts:

$$\mathbb{D}_{\mathbf{x}} \mathbf{u} = \frac{1}{2} \left( \mathbb{D}_{\mathbf{x}} \mathbf{u} + (\mathbb{D}_{\mathbf{x}} \mathbf{u})^T \right) + \frac{1}{2} \left( \mathbb{D}_{\mathbf{x}} \mathbf{u} - (\mathbb{D}_{\mathbf{x}} \mathbf{u})^T \right) = \boldsymbol{\varepsilon} + \mathbf{r}$$

or, in terms of components in a Cartesian vector basis  $(\mathbf{i}_1, \mathbf{i}_2, \mathbf{i}_3)$ , with associated coordinates  $(x_1, x_2, x_3)$ :

$$\frac{\partial u_k}{\partial x_l} = \varepsilon_{kl} + r_{kl} = \frac{1}{2} \left( \frac{\partial u_k}{\partial x_l} + \frac{\partial u_l}{\partial x_k} \right) + \frac{1}{2} \left( \frac{\partial u_k}{\partial x_l} - \frac{\partial u_l}{\partial x_k} \right), \quad 1 \leq k, l \leq 3$$

We will focus on the antisymmetrical part  $\mathbf{r}$ : indeed, if we establish the conditions necessary for its existence, in this case we could say that  $\boldsymbol{\varepsilon}$  is indeed the symmetrical part of the displacement gradient tensor. We start by expressing the partial derivatives of this antisymmetric part as a function of the derivatives of the components of  $\boldsymbol{\varepsilon}$ :

$$\begin{aligned} 2 \frac{\partial r_{kl}}{\partial x_m} &= \frac{\partial^2 u_k}{\partial x_l \partial x_m} - \frac{\partial^2 u_l}{\partial x_k \partial x_m} \\ &= \frac{\partial^2 u_k}{\partial x_l \partial x_m} + \left( \frac{\partial^2 u_m}{\partial x_k \partial x_l} - \frac{\partial^2 u_m}{\partial x_k \partial x_l} \right) - \frac{\partial^2 u_l}{\partial x_k \partial x_m} \\ &= \left( \frac{\partial^2 u_k}{\partial x_m \partial x_l} + \frac{\partial^2 u_m}{\partial x_k \partial x_l} \right) - \left( \frac{\partial^2 u_m}{\partial x_l \partial x_k} - \frac{\partial^2 u_l}{\partial x_m \partial x_k} \right) \\ &= 2 \frac{\partial \varepsilon_{km}}{\partial x_l} - 2 \frac{\partial \varepsilon_{lm}}{\partial x_k} \end{aligned}$$

since the cross second derivatives of the components of  $\mathbf{u}$  must be equal according to Schwarz's theorem. For being able to trace back to the components  $r_{kl}$  of  $\mathbf{r}$ , it is necessary (and sufficient) that its second derivatives verify Schwarz's theorem as well:

$$\frac{\partial^2 r_{kl}}{\partial x_m \partial x_n} = \frac{\partial^2 r_{kl}}{\partial x_n \partial x_m}, \quad 1 \leq k, l, m, n \leq 3$$

hence, finally:

$$\frac{\partial^2 \epsilon_{km}}{\partial x_l \partial x_n} - \frac{\partial^2 \epsilon_{lm}}{\partial x_k \partial x_n} = \frac{\partial^2 \epsilon_{kn}}{\partial x_l \partial x_m} - \frac{\partial^2 \epsilon_{ln}}{\partial x_k \partial x_m}, \quad 1 \leq k, l, m, n \leq 3$$

which constitute six independent scalar equations, called “compatibility equations”; these equations guarantee the possibility of finding a displacement field associated with the tensor  $\boldsymbol{\epsilon}$ : indeed, in this case, now that we have determined  $\mathbf{r}$ , it is enough to write that:

$$\mathbb{D}_{\mathbf{x}} \mathbf{u} = \boldsymbol{\epsilon} + \mathbf{r}$$

equation which is integrable taking into account Schwarz's theorem. Besides, the approach we have just described here has the advantage of being constructive, since it gives all the steps to go back to the displacement field from the tensor  $\boldsymbol{\epsilon}$ .

**R** Another way to establish these equations is to use the notion of the curl  $\text{rot}_{\mathbf{x}} \mathbb{A}$  of a tensor, specified in Appendix B.1.1, and which is the linear application that, to a constant vector  $\mathbf{c}$ , associates:

$$(\text{rot}_{\mathbf{x}} \mathbb{A}) \mathbf{c} = \text{rot}_{\mathbf{x}} (\mathbb{A}^T \mathbf{c})$$

where  $\text{rot}_{\mathbf{x}} \mathbf{v}$  is the curl of a vector  $\mathbf{v}$ .

Indeed, by taking the curl of the definition of the infinitesimal strain tensor, we obtain:

$$2\text{rot}_{\mathbf{x}} \boldsymbol{\epsilon} = \text{rot}_{\mathbf{x}} (\mathbb{D}_{\mathbf{x}} \mathbf{u}) + \text{rot}_{\mathbf{x}} ((\mathbb{D}_{\mathbf{x}} \mathbf{u})^T) = \mathbf{0} + \mathbb{D}_{\mathbf{x}} (\text{rot}_{\mathbf{x}} \mathbf{u})$$

hence, by applying the curl a second time:

$$\boxed{\text{rot}_{\mathbf{x}} (\text{rot}_{\mathbf{x}} \boldsymbol{\epsilon}) = \mathbf{0}}$$

Since this tensor is symmetric, six independent scalar relations can be obtained by writing its components in a vector basis, which are the compatibility equations that we have determined above.

It is interesting to see the parallel between this result, and a similar one, concerning vectors: a given vector field  $\mathbf{z}$  can be written as the gradient of a scalar function (to be determined) if and only if its curl is zero:  $\text{rot}_{\mathbf{x}} \mathbf{z} = \mathbf{0}$ .

■ **Example 5.5 — Compatibility of a thermal strain field.** We would like to study here for which conditions on the temperature variation field  $\Delta T = \Theta(\mathbf{x})$  the associated strain field ( $\boldsymbol{\epsilon}^h = \alpha \Theta(\mathbf{x}) \mathbb{I}$ ) is compatible (where the coefficient of thermal expansion  $\alpha$  is assumed uniform); we then use the approach presented above.

By using a Cartesian vector basis  $(\mathbf{i}_1, \mathbf{i}_2, \mathbf{i}_3)$ , with associated coordinates  $(x_1, x_2, x_3)$ , one can express the nine compatibility scalar equations as:

$$\begin{aligned} \alpha \frac{\partial^2 \Theta}{\partial x_2^2} &= \frac{\partial^2 \epsilon_{11}}{\partial x_2 \partial x_2} - \frac{\partial^2 \epsilon_{21}}{\partial x_1 \partial x_2} = \frac{\partial^2 \epsilon_{12}}{\partial x_2 \partial x_1} - \frac{\partial^2 \epsilon_{22}}{\partial x_1 \partial x_1} = -\alpha \frac{\partial^2 \Theta}{\partial x_1^2} \\ -\alpha \frac{\partial^2 \Theta}{\partial x_1 \partial x_3} &= \frac{\partial^2 \epsilon_{12}}{\partial x_2 \partial x_3} - \frac{\partial^2 \epsilon_{22}}{\partial x_1 \partial x_3} = \frac{\partial^2 \epsilon_{13}}{\partial x_2 \partial x_2} - \frac{\partial^2 \epsilon_{23}}{\partial x_1 \partial x_2} = 0 \\ \alpha \frac{\partial^2 \Theta}{\partial x_2 \partial x_3} &= \frac{\partial^2 \epsilon_{11}}{\partial x_2 \partial x_3} - \frac{\partial^2 \epsilon_{21}}{\partial x_1 \partial x_3} = \frac{\partial^2 \epsilon_{13}}{\partial x_2 \partial x_1} - \frac{\partial^2 \epsilon_{23}}{\partial x_1 \partial x_1} = 0 \\ 0 &= \frac{\partial^2 \epsilon_{23}}{\partial x_1 \partial x_2} - \frac{\partial^2 \epsilon_{13}}{\partial x_2 \partial x_2} = \frac{\partial^2 \epsilon_{22}}{\partial x_1 \partial x_3} - \frac{\partial^2 \epsilon_{12}}{\partial x_2 \partial x_3} = \alpha \frac{\partial^2 \Theta}{\partial x_1 \partial x_3} \\ \alpha \frac{\partial^2 \Theta}{\partial x_3^2} &= \frac{\partial^2 \epsilon_{22}}{\partial x_3 \partial x_3} - \frac{\partial^2 \epsilon_{32}}{\partial x_2 \partial x_3} = \frac{\partial^2 \epsilon_{23}}{\partial x_3 \partial x_2} - \frac{\partial^2 \epsilon_{33}}{\partial x_2 \partial x_2} = -\alpha \frac{\partial^2 \Theta}{\partial x_2^2} \end{aligned}$$

$$\begin{aligned}
-\alpha \frac{\partial^2 \Theta}{\partial x_2 \partial x_1} &= \frac{\partial^2 \varepsilon_{23}}{\partial x_3 \partial x_1} - \frac{\partial^2 \varepsilon_{33}}{\partial x_2 \partial x_1} = \frac{\partial^2 \varepsilon_{21}}{\partial x_3 \partial x_3} - \frac{\partial^2 \varepsilon_{31}}{\partial x_2 \partial x_3} = 0 \\
-\alpha \frac{\partial^3 \Theta}{\partial x_3 \partial x_2} &= \frac{\partial^2 \varepsilon_{31}}{\partial x_1 \partial x_2} - \frac{\partial^2 \varepsilon_{11}}{\partial x_3 \partial x_2} = \frac{\partial^2 \varepsilon_{32}}{\partial x_1 \partial x_1} - \frac{\partial^2 \varepsilon_{12}}{\partial x_3 \partial x_1} = 0 \\
0 &= \frac{\partial^2 \varepsilon_{32}}{\partial x_1 \partial x_3} - \frac{\partial^2 \varepsilon_{12}}{\partial x_3 \partial x_3} = \frac{\partial^2 \varepsilon_{33}}{\partial x_1 \partial x_2} - \frac{\partial^2 \varepsilon_{13}}{\partial x_3 \partial x_2} = \alpha \frac{\partial^2 \Theta}{\partial x_1 \partial x_2} \\
\alpha \frac{\partial^2 \Theta}{\partial x_1^2} &= \frac{\partial^2 \varepsilon_{33}}{\partial x_1 \partial x_1} - \frac{\partial^2 \varepsilon_{13}}{\partial x_3 \partial x_1} = \frac{\partial^2 \varepsilon_{31}}{\partial x_1 \partial x_3} - \frac{\partial^2 \varepsilon_{11}}{\partial x_3 \partial x_3} = -\alpha \frac{\partial^2 \Theta}{\partial x_3^2}
\end{aligned}$$

six of which are truly independent. From equations (1), (5) and (9) we can deduce that:

$$\frac{\partial^2 \Theta}{\partial x_1^2} = \frac{\partial^2 \Theta}{\partial x_2^2} = \frac{\partial^2 \Theta}{\partial x_3^2} = 0$$

then, using the other equations:

$$\frac{\partial \Theta}{\partial x_1} = C_1, \quad \frac{\partial \Theta}{\partial x_2} = C_2, \quad \frac{\partial \Theta}{\partial x_3} = C_3$$

where  $C_1, C_2$  and  $C_3$  are constants. It is then concluded that the temperature variation field must satisfy:

$$\Theta(\mathbf{x}) = \langle \mathbf{C}, \mathbf{x} \rangle + D$$

where  $\mathbf{C}$  is the constant vector of components  $(C_1, C_2, C_3)$  and  $D$  is a constant.

If this condition is met for the temperature variation field, the displacement field is determined by following the steps of the procedure:

1. the partial derivatives of the components of  $\mathbf{r}$  are calculated, and expressed as functions of the derivatives of the components of  $\boldsymbol{\varepsilon}$ :

$$\frac{\partial r_{kl}}{\partial x_m} = \frac{\partial \varepsilon_{km}}{\partial x_l} - \frac{\partial \varepsilon_{lm}}{\partial x_k}, \quad 1 \leq k, l, m \leq 3$$

2. we integrate the previous relations to determine the components of  $\mathbf{r}$ ;
3. we deduce from the components of  $\mathbf{r}$  the expressions of the partial derivatives of the displacement field:

$$\frac{\partial u_k}{\partial x_l} = \varepsilon_{kl} + r_{kl}, \quad 1 \leq k, l \leq 3$$

4. we integrate the previous relations to determine the displacement field, for which we finally find as components in  $(\mathbf{i}_1, \mathbf{i}_2, \mathbf{i}_3)$ :

$$\begin{aligned}
u_1(x_1, x_2, x_3) &= \frac{C_1}{2} (x_1^2 - x_2^2 - x_3^2) + C_2 x_1 x_2 + C_3 x_1 x_3 + D x_1 + a_1 - b_3 x_2 + b_2 x_3 \\
u_2(x_1, x_2, x_3) &= \frac{C_2}{2} (x_2^2 - x_1^2 - x_3^2) + C_1 x_1 x_2 + C_3 x_2 x_3 + D x_2 + a_2 - b_1 x_3 + b_3 x_1 \\
u_3(x_1, x_2, x_3) &= \frac{C_3}{2} (x_3^2 - x_1^2 - x_2^2) + C_2 x_2 x_3 + C_1 x_1 x_3 + D x_3 + a_3 - b_2 x_1 + b_1 x_2
\end{aligned}$$

where  $(a_1, a_2, a_3)$  and  $(b_1, b_2, b_3)$  are the components of two constant vectors  $\mathbf{a}$  and  $\mathbf{b}$ , which correspond to an arbitrary rigid body movement, consisting of a translation and a (small) rotation  $(\mathbf{a} + \mathbf{b} \wedge \mathbf{x})$ .

Therefore, if the temperature variation field is linear, it is possible to associate a displacement field (the one we have just calculated) with it, which means that, if there is no constraint for this displacement, the associated deformations can occur freely, and no stress is created in the domain, since we have:

$$\frac{1}{2} (\mathbb{D}_{\mathbf{x}} \mathbf{u} + (\mathbb{D}_{\mathbf{x}} \mathbf{u})^T) = \boldsymbol{\varepsilon}^t = \boldsymbol{\varepsilon}^{th}$$

On the other hand, if the temperature variation does not have this property, stresses appear together with elastic deformations so that there may actually be an associated displacement field such that:

$$\frac{1}{2} (\mathbb{D}_{\mathbf{x}} \mathbf{u} + (\mathbb{D}_{\mathbf{x}} \mathbf{u})^T) = \boldsymbol{\varepsilon}^t = \boldsymbol{\varepsilon}^e + \boldsymbol{\varepsilon}^{th}$$

■

**Summary 5.3 — Compatibility equations.** The necessary conditions for a tensor  $\epsilon(\mathbf{x}, t)$  to be effectively the symmetrical part of the displacement gradient tensor are written as the following six scalar equations:

$$\frac{\partial^2 \epsilon_{km}}{\partial x_l \partial x_n} - \frac{\partial^2 \epsilon_{lm}}{\partial x_k \partial x_n} = \frac{\partial^2 \epsilon_{kn}}{\partial x_l \partial x_m} - \frac{\partial^2 \epsilon_{ln}}{\partial x_k \partial x_m}, \quad 1 \leq k, l, m, n \leq 3$$

which are expressed in a Cartesian vector basis  $(\mathbf{i}_1, \mathbf{i}_2, \mathbf{i}_3)$ , with associated coordinates  $(x_1, x_2, x_3)$ .

**R** In the case where no hypothesis is made about the sought stress field, the compatibility equations, in which the constitutive relation expressed in compliance is injected, and which are combined with the local equilibrium equation, allow for finding relations that must be verified by the stress tensor so that it can be the true solution; these are the so-called “Beltrami’s equations”, which, in the static framework, and in the presence of a homogeneous material, are written as:

$$\frac{1}{1+v} \mathbb{D}_{\mathbf{x}} (\nabla_{\mathbf{x}} (\text{tr} \boldsymbol{\sigma})) + \Delta_{\mathbf{x}} \boldsymbol{\sigma} + \frac{v}{1-v} (\text{div}_{\mathbf{x}} \mathbf{f}_V) \mathbb{I} + \mathbb{D}_{\mathbf{x}} \mathbf{f}_V + (\mathbb{D}_{\mathbf{x}} \mathbf{f}_V)^T = 0$$

where  $\Delta_{\mathbf{x}}$  is the (tensor) Laplacian, which, in a Cartesian vector basis, is the tensor whose components are equal to the Laplacians of the original tensor components.

Since this equation corresponds to a symmetrical tensor, it can give six independent scalar relations; in the usual case of uniform volume force densities, we establish that the stress tensor must then verify:

$$\Delta_{\mathbf{x}} \Delta_{\mathbf{x}} \boldsymbol{\sigma} = 0$$

In practice, these equations are rarely used.

### 5.2.3 Approximate solutions

In most of the cases encountered, it is not possible to find fields that verify all the equations of the problem: there are indeed few analytical solutions, and these are often associated with elementary load cases and geometries. It is then necessary to find alternatives to obtain approximate solutions.

#### Saint-Venant’s principle

We have already had the opportunity to see the implications of this principle in Paragraph 3.1.1, which presented the details of a simple tensile test: whatever the way the specimen is loaded at both ends, the hypothesis of uniaxial and homogeneous stress can be adopted as long as one is “far enough” away from these ends, provided that these surface forces give, on each end, a resultant force of direction the axis  $\mathbf{e}$  of the specimen, and a zero moment at a point on the axis of symmetry of the specimen. In practice, we can see, using the numerical simulations presented in Figure 3.3 (on page 69) for example, that the entire gauge section of the specimen actually presents such a stress:  $\boldsymbol{\sigma} = \sigma_{ee} \mathbf{e} \otimes \mathbf{e}$ .

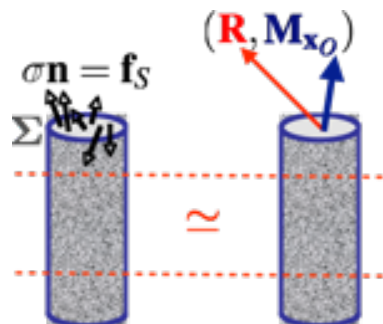


Figure 5.2: Illustration of Saint-Venant’s principle.

**Saint-Venant's principle.** This principle can be qualitatively stated as follows.

If we replace, on a boundary of “small” area, the surface force conditions by locally different conditions, but which have identical resultant force and moment, the two solutions in terms of stresses differ little, “far away” from this boundary.

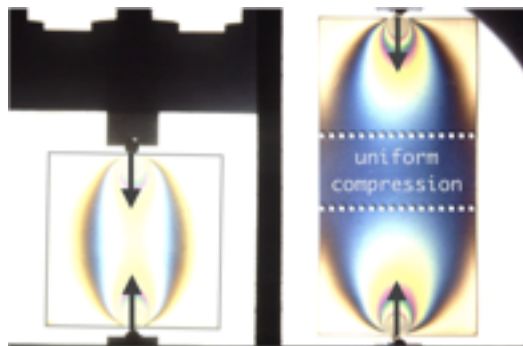
Everything happens as if the material domain under study only reacts to the global loading corresponding to the resultant force and to the moment of the action on the surface, as represented schematically in Figure 5.2 where we have defined:

$$\mathbf{R} = \int_{\Sigma} \mathbf{f}_S dS_x, \text{ and } \mathbf{M}_{x_O} = \int_{\Sigma} (\mathbf{x} - \mathbf{x}_O) \wedge \mathbf{f}_S dS_x$$

This result is useful when seeking approximate solutions to the problem being addressed since it exempts from locally verifying all the boundary conditions: thus, we have a practical means to “simplify” specific data of the problem, and to find valid analytical solutions over an extensive area of the domain.



We have deliberately limited ourselves to a qualitative statement of Saint-Venant's principle. It is, of course, possible to have a more precise mathematical version, which describes the two solutions as asymptotically equivalent, and therefore specifies the meaning of the words “small” and “far” in the previous statement. The figure below shows the size of the zone of influence in the case of a compression test, where two specimens are compared by photoelasticity.



The uniform compression zone in the right-hand specimen is easily distinguished, while the left-hand specimen is too short for Saint-Venant's principle to be applied.

■ **Example 5.6 — Torsion of a cylindrical shaft of arbitrary cross-section: Saint-Venant's principle.** This case actually corresponds to the historical origin of the principle, which was stated by Saint-Venant following his *Mémoire sur la torsion des prismes*, dans le *Résumé des leçons données à l'École des ponts et chaussées sur l'application de la mécanique à l'établissement des constructions* (1864):

*Mais cette double et longue attente n'est pas nécessaire avant de résoudre les questions de pratique, qui n'exigent que des approximations. Nous l'avons souvent dit : des faits suffisamment nombreux montrent le peu d'influence du mode de répartition et d'application, et permettent d'employer les formules soit anciennes soit nouvelles d'extension, torsion, flexion, pour des forces quelconques agissant aux extrémités de prismes très-longs par rapport à leurs dimensions transversales en n'ayant égard qu'aux grandeurs de leurs résultantes et de leurs moments résultants. D'où il suit qu'il suffit de donner des démonstrations exactes des formules relativement à un cas ou à un mode particulier d'action des forces aux extrémités, pour que la théorie soit établie et qu'on puisse faire l'application de ses résultats aux divers autres cas qui peuvent s'offrir.*

These observations allow us to justify why, in Example 5.1, the “pragmatic” choice was made to impose, as boundary conditions on the shaft ends, only the resultant forces and moments exerted by the test machine. Indeed, except in the vicinity of the ends, how the machine applies the torsion couple does not influence the solution fields of the torsion problem, provided that the resultant force and the other two components of the moment, associated with the grip forces, are effectively zero.

Thus, if we use the displacement approach proposed in Example 5.3, the solution obtained is valid as soon as we look away from the ends of the shaft, because:

$$\mathbf{R}^O = \mathbf{0} = \mathbf{R}^H$$

and:

$$\langle \mathbf{M}^O, \mathbf{i}_1 \rangle = 0 = \langle \mathbf{M}^O, \mathbf{i}_2 \rangle, \text{ et } \langle \mathbf{M}^H, \mathbf{i}_1 \rangle = 0 = \langle \mathbf{M}^H, \mathbf{i}_2 \rangle$$

The torsion couple is then expressed as:

$$\begin{aligned} \langle \mathbf{M}^H, \mathbf{e} \rangle &= \int_{\Sigma_H} \langle \mathbf{x}_\Sigma \wedge (\sigma \mathbf{e}), \mathbf{e} \rangle dS_x = \int_{\Sigma_H} \alpha \mu \langle \nabla_{\mathbf{x}_\Sigma} \varphi + \mathbf{e} \wedge \mathbf{x}_\Sigma, \mathbf{e} \wedge \mathbf{x}_\Sigma \rangle dS_x \\ &= \int_{\Sigma_H} \alpha \mu \|\mathbf{e} \wedge \mathbf{x}_\Sigma\|^2 dS_x + \int_{\Sigma_H} \alpha \mu \langle \nabla_{\mathbf{x}_\Sigma} \varphi, \mathbf{e} \wedge \mathbf{x}_\Sigma \rangle dS_x \\ &= \alpha \mu \int_{\Sigma_H} \|\mathbf{x}_\Sigma\|^2 dS_x + \alpha \mu \left\langle \mathbf{e}, \int_{\Sigma_H} \mathbf{x}_\Sigma \wedge \nabla_{\mathbf{x}_\Sigma} \varphi dS_x \right\rangle \\ &= \alpha \mu I_e + \alpha \mu \left\langle \mathbf{e}, \int_{\Sigma_H} \mathbf{x}_\Sigma \wedge \nabla_{\mathbf{x}_\Sigma} \varphi dS_x \right\rangle \end{aligned}$$

where  $I_e = \int_{\Sigma_H} \|\mathbf{x}_\Sigma\|^2 dS_x$  is the “polar moment of inertia”, which will be discussed in beam mechanics in Paragraph 6.3.3.

It is then possible to show that, whatever the geometry of the cross-section, the second integral is always negative, which leads to the conclusion that:

$$\frac{\langle \mathbf{M}^H, \mathbf{e} \rangle}{\alpha} = \mu J < \mu I_e$$

i.e. the warping phenomenon reduces the torsional stiffness of the shaft. ■

### Towards numerical solutions...

Another possibility to obtain approximate solutions is to search for them on small (functional) bases; indeed, let us imagine that, in the case of a one-dimensional problem, we use as an approximate form for the displacement its representation in the basis of the monomials of the space variable, up to a certain rank  $N$ :

$$u_h(x) = \sum_{k=1}^{\infty} U_k x^k \approx \sum_{k=1}^N U_k x^k$$

The problem has thus been discretized spatially, making it possible to consider a numerical solution: the method classically used in mechanics (as in any discipline searching for the solutions of partial differential equations) is the finite element method, whose framework is beyond this course, but some elements of which are given in the following example.

■ **Example 5.7 — Illustration of the finite element method.** To illustrate the main principles of the method, we take the example of a gravity dam subjected to the hydrostatic pressure of water, whose equations are summarized in Figure 5.1. The simplified geometry of this dam consists, with a hypothesis of a planar problem, of an isosceles right triangle with a side  $L$ .

The basis of the finite element method consists in discretizing the geometry: a certain number of points, or “nodes”, are introduced which allow us to realize a partition of the geometry into various triangles, which we call “elements” (it would also be possible to have quadrilaterals). On each element, a polynomial interpolation of the displacement field is proposed, which is thus sought for in an approximate form.

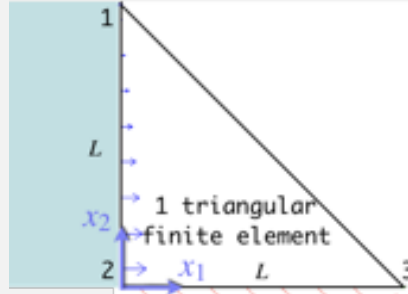
In order to simplify the presentation, let us imagine that the geometry of the dam is discretized using only three nodes, which are the vertices of the triangle; there is therefore only one associated element: the dam itself. We then choose to interpolate the approximate displacement linearly on this triangle, by choosing a Cartesian coordinate system  $(x_1, x_2)$  whose origin is taken at the vertex at the bottom left of the dam, and by writing that:

$$\boxed{\mathbf{u}_h(x_1, x_2) = \sum_{k=1}^3 N_k(x_1, x_2) \mathbf{U}_k}$$

where the functions  $N_k$  are called “shape functions”, in this case linear:

$$N_1(x_1, x_2) = \frac{x_2}{L}, N_2(x_1, x_2) = 1 - \frac{x_1}{L} - \frac{x_2}{L}, N_3(x_1, x_2) = \frac{x_1}{L}$$

and the vectors  $\mathbf{U}_k$  contain the components of the displacements of nodes 1, 2 and 3, mentioned below. We then note  $\mathbf{U}$  the vector of dimension  $6 \times 1$  containing all these components.



With this interpolation, it is possible to express the infinitesimal strain and stress tensors in matrix form, using the Voigt notation introduced in Paragraph 4.1.3:

$$\tilde{\boldsymbol{\epsilon}} = \mathbb{B}\mathbf{U}, \text{ and } \tilde{\boldsymbol{\sigma}} = \mathbb{C}\mathbb{B}\mathbf{U}$$

which allows for estimating the elastic strain energy as:

$$\mathcal{E} = \frac{1}{2} \int_{\Omega} \langle \tilde{\boldsymbol{\sigma}}, \tilde{\boldsymbol{\epsilon}} \rangle dV_x = \frac{1}{2} \int_{\Omega} \mathbf{U}^T \mathbb{B}^T \mathbb{C} \mathbb{B} \mathbf{U} dV_x$$

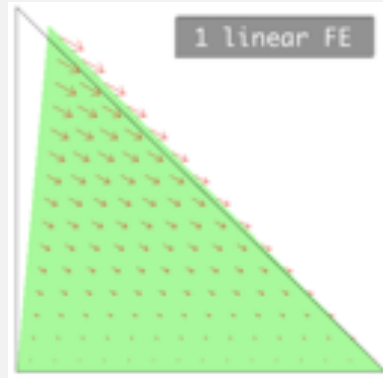
Similarly, we can estimate the work of the force densities as:

$$\mathcal{W} = \int_{\Omega} \langle \mathbf{f}_V, \mathbf{u}_h \rangle dV_x + \int_{\Sigma} \langle \mathbf{f}_S, \mathbf{u}_h \rangle dS_x = \int_{\Omega} \mathbf{U}^T \mathbf{F}_V dV_x + \int_{\Sigma} \mathbf{U}^T \mathbf{F}_S dS_x$$

where  $\Sigma$  is the area subjected to water pressure. Considering the boundary conditions in displacement, nodes 2 and 3 are fixed, and it is then possible to show that the finite element solution consists in solving the following matrix system:

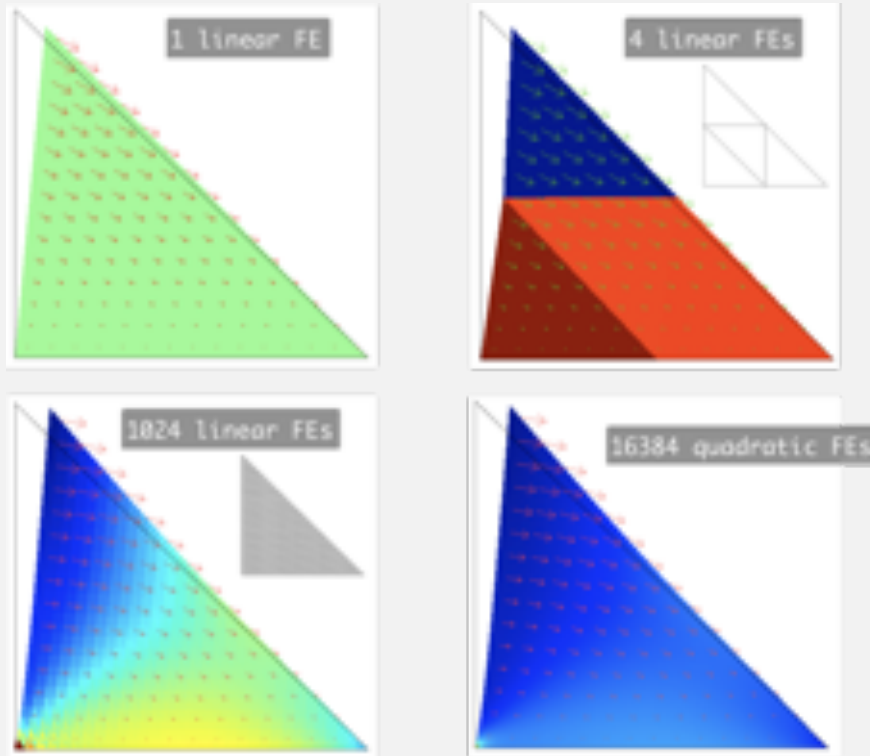
$$\left( \int_{\Omega} \mathbb{B}^T \mathbb{C} \mathbb{B} dV_x \right) \begin{pmatrix} \langle \mathbf{u}_1, \mathbf{i}_1 \rangle \\ \langle \mathbf{u}_1, \mathbf{i}_2 \rangle \end{pmatrix} = \int_{\Omega} \mathbf{F}_V dV_x + \int_{\Sigma} \mathbf{F}_S dS_x$$

where the different matrices are reduced to the indices corresponding to the two components of the displacement of node 1, resulting in the solution below (the arrows represent the displacement, while the colors refer to the first principal stress).



It is easy to see that the displacement evolves linearly in the element, while the stress is constant.

A fundamental property of the finite element method is that it converges towards the exact solution of the problem when the number of elements approaches infinity; for this purpose, it is then necessary to “assemble” the matrices presented above in order to consider a larger matrix system. This convergence phenomenon can be observed in the figures below.



It is also possible to increase the order of the proposed interpolation for the displacement, as illustrated by the last figure with 16 384 elements, and where the interpolation is quadratic. ■

## 5.3 Simplification of an elasticity problem

In some cases, it is possible to simplify the equations and/or boundary conditions established in Paragraphs 5.1.1 and 5.1.2, in order to study a simpler problem, but still close (or even equivalent) to the initial problem. These simplifications can be done in different ways.

### 5.3.1 Principle of superposition

A first possibility consists in breaking down the initial problem into several simpler problems: indeed, given the linearity of all the equations that we have detailed in Paragraphs 5.1.1 and 5.1.2, it is possible to determine the solution as a linear combination of the elementary problem solutions.

If we consider, as an illustration, the case (shown in Figure 5.3) of a building subjected to the combined action of wind and snow on its roof, it is possible to break down the problem as follows:

1. a problem where the building is only subjected to the action of the wind, and for which we determine as a solution a displacement field  $\mathbf{u}^v$ , and a stress tensor  $\boldsymbol{\sigma}^v$ ;
2. a problem where the building is only subjected to the action of snow, and for which we determine as a solution a displacement field  $\mathbf{u}^n$ , and a stress tensor  $\boldsymbol{\sigma}^n$ .

The solution of the initial problem is then written as the sum of the solutions of the two elementary problems:

$$\mathbf{u} = \mathbf{u}^v + \mathbf{u}^n, \text{ and } \boldsymbol{\sigma} = \boldsymbol{\sigma}^v + \boldsymbol{\sigma}^n$$

It is also possible to consider other scenarios once the basic solutions are known: for example, if

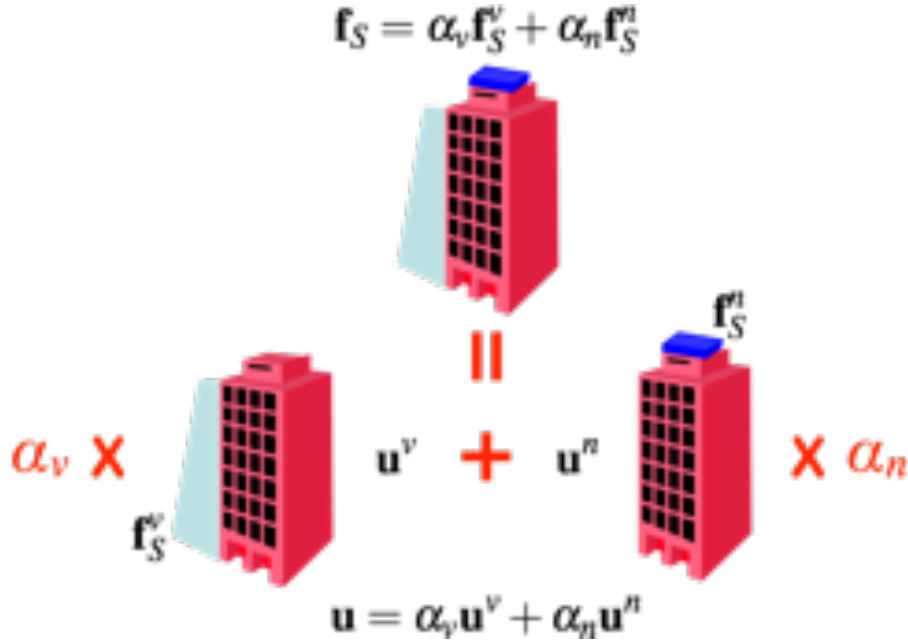


Figure 5.3: Illustration of the principle of superposition.

we now look at the building subjected to twice as much snow and half as much wind, the associated solution is simply written as:

$$\mathbf{u} = \frac{\mathbf{u}^v}{2} + 2\mathbf{u}^n, \text{ and } \boldsymbol{\sigma} = \frac{\boldsymbol{\sigma}^v}{2} + 2\boldsymbol{\sigma}^n$$

The principle of superposition thus concerns any linear combination of simple problems, as summarized in Figure 5.3.

The interest of this principle of superposition concerns above all analytical solutions, since the knowledge of solutions to elementary problems, possibly listed, allows us to solve problems with complex loads and boundary conditions. Thanks to this principle, we can also verify whether the action of gravity can be neglected, or not, since we can directly compare the solution associated with it with the one that does not take it into account.

**R** Thermoelasticity problems can also benefit from this principle: it is indeed possible to treat the mechanical loading separately from the thermal loading, considering, for example, with regard to the local equilibrium equation into which the constitutive relation has been injected, on the one hand:

$$\mathbf{div}_{\mathbf{x}}(\mathbf{C}\boldsymbol{\epsilon}^m) + \mathbf{f}_V = \rho_0 \ddot{\mathbf{u}}^m, \text{ with } \boldsymbol{\epsilon}^m = \frac{1}{2} (\mathbb{D}_{\mathbf{x}} \mathbf{u}^m + (\mathbb{D}_{\mathbf{x}} \mathbf{u}^m)^T)$$

and on the other hand:

$$\mathbf{div}_{\mathbf{x}}(\mathbf{C}(\boldsymbol{\epsilon}^e - \alpha \Delta T \mathbb{I})) = \rho_0 \ddot{\mathbf{u}}^{th}, \text{ with } \boldsymbol{\epsilon}^e = \frac{1}{2} (\mathbb{D}_{\mathbf{x}} \mathbf{u}^{th} + (\mathbb{D}_{\mathbf{x}} \mathbf{u}^{th})^T)$$

The solution to the thermoelastic problem is therefore written simply as:  $\mathbf{u} = \mathbf{u}^m + \mathbf{u}^{th}$ .

Thus, the displacement field obtained during the hindered thermal expansion of a bar, studied in the second part of Example 4.2, can be obtained as the sum of the displacement corresponding to the free expansion of this bar, developed in the first part of the same example:

$$\mathbf{u}^{th}(\mathbf{x}) = (\alpha \Delta T)(r_i(\theta) + z_i)$$

and of the displacement obtained for the compression of a bar subjected to a pressure  $p_0$ , studied in Example 4.1:

$$\mathbf{u}^m(\mathbf{x}) = \frac{p_0}{E} (v r_i(\theta) - z_i)$$

Besides, this pressure  $p_0$  is determined expressing the impossibility for the bar to lengthen:

$$\langle \mathbf{u}^m(z=H) + \mathbf{u}^{th}(z=H), \mathbf{i}_z \rangle = 0$$

which implies that  $p_0 = E(\alpha\Delta T)$ , and then that the sought displacement field is finally:

$$\mathbf{u}(\mathbf{x}) = (1+\nu)(\alpha\Delta T)r\mathbf{i}_r(\theta)$$

### 5.3.2 Plane elasticity

In some specific cases that we will describe here, it is possible to reduce the initially three-dimensional problem to a study in a particular plane, thus reducing the number of unknown components and variables to take into account.

#### Plane strain

This hypothesis is commonly applied when studying a domain whose geometry is invariant in a specific direction (according to which it is, moreover, of large dimension), and which is only loaded in the plane perpendicular to this direction (plane which will then be called a cross-section). This hypothesis is all the more valid if the out-of-plane displacement is constrained to be zero on the two end cross-sections (as in the case of a domain between two fixed, rigid bodies); otherwise, adopting this hypothesis is like considering that the out-of-plane displacement can still be ignored and that the study can limit itself to an arbitrarily chosen cross-section of the domain.

**Plane strain hypothesis.** This hypothesis implies that, with respect to a plane ( $\Pi$ ), with associated Cartesian vector basis  $(\mathbf{i}_1, \mathbf{i}_2)$ , we assume that the displacement field is in the plane ( $\Pi$ ), and depends only on the two coordinates  $(x_1, x_2)$  associated with the basis:

$$\mathbf{u}(x_1, x_2) = u_1(x_1, x_2)\mathbf{i}_1 + u_2(x_1, x_2)\mathbf{i}_2$$

It is therefore independent of the  $x_3$ -coordinate associated with  $\mathbf{i}_3 = \mathbf{i}_1 \wedge \mathbf{i}_2$ .

Therefore, the infinitesimal strain tensor is also independent of  $x_3$ , and, given the form of the displacement field, verifies  $\mathbf{\epsilon i}_3 = \mathbf{0}$ , as can be seen by using its expression in the basis  $(\mathbf{i}_1, \mathbf{i}_2, \mathbf{i}_1 \wedge \mathbf{i}_2)$ :

$$\mathbf{\epsilon}(x_1, x_2) = \begin{pmatrix} \frac{\partial u_1}{\partial x_1}(x_1, x_2) & \frac{1}{2} \left( \frac{\partial u_1}{\partial x_2}(x_1, x_2) + \frac{\partial u_2}{\partial x_1}(x_1, x_2) \right) & 0 \\ \frac{1}{2} \left( \frac{\partial u_1}{\partial x_2}(x_1, x_2) + \frac{\partial u_2}{\partial x_1}(x_1, x_2) \right) & \frac{\partial u_2}{\partial x_2}(x_1, x_2) & 0 \\ 0 & 0 & 0 \end{pmatrix}_{(\mathbf{i}_1, \mathbf{i}_2, \mathbf{i}_1 \wedge \mathbf{i}_2)}$$

The associated stress tensor is then obtained by applying the constitutive relation in stiffness:

$$\boldsymbol{\sigma} = \lambda(\text{tr } \mathbf{\epsilon})\mathbb{I} + 2\mu\mathbf{\epsilon}$$

where the Lamé parameters  $\lambda$  and  $\mu$  can depend on  $x_1$  and  $x_2$ , and are expressed as functions of the Young's modulus and Poisson's ratio just as in the three-dimensional case:

$$\lambda = \frac{\nu E}{(1+\nu)(1-2\nu)}, \text{ and } \mu = \frac{E}{2(1+\nu)}$$

In the vector basis  $(\mathbf{i}_1, \mathbf{i}_2, \mathbf{i}_1 \wedge \mathbf{i}_2)$ , the stress tensor is therefore written as:

$$\boldsymbol{\sigma} = \begin{pmatrix} (\lambda + 2\mu) \frac{\partial u_1}{\partial x_1} + \lambda \frac{\partial u_2}{\partial x_2} & \mu \left( \frac{\partial u_1}{\partial x_2} + \frac{\partial u_2}{\partial x_1} \right) & 0 \\ \mu \left( \frac{\partial u_1}{\partial x_2} + \frac{\partial u_2}{\partial x_1} \right) & \lambda \frac{\partial u_1}{\partial x_1} + (\lambda + 2\mu) \frac{\partial u_2}{\partial x_2} & 0 \\ 0 & 0 & \lambda \left( \frac{\partial u_1}{\partial x_1} + \frac{\partial u_2}{\partial x_2} \right) \end{pmatrix}_{(\mathbf{i}_1, \mathbf{i}_2, \mathbf{i}_1 \wedge \mathbf{i}_2)}$$

The local equilibrium equation then becomes a two-component vector equation, since we remain in the plane ( $\Pi$ ); in Cartesian coordinates, we must then verify that:

$$\begin{aligned} \frac{\partial \sigma_{11}}{\partial x_1} + \frac{\partial \sigma_{12}}{\partial x_2} + \langle \mathbf{f}_V, \mathbf{i}_1 \rangle &= \rho_0 \ddot{u}_1 \\ \frac{\partial \sigma_{12}}{\partial x_1} + \frac{\partial \sigma_{22}}{\partial x_2} + \langle \mathbf{f}_V, \mathbf{i}_2 \rangle &= \rho_0 \ddot{u}_2 \end{aligned}$$



As expected, the stress tensor depends only on  $(x_1, x_2)$ ; on the other hand, it is not “plane”, since there is *a priori* a non-zero non-planar component:

$$\boxed{\sigma_{33}(x_1, x_2) = \lambda (\varepsilon_{11}(x_1, x_2) + \varepsilon_{22}(x_1, x_2)) = \lambda \left( \frac{\partial u_1}{\partial x_1}(x_1, x_2) + \frac{\partial u_2}{\partial x_2}(x_1, x_2) \right) \neq 0}$$



*Even if the plane strain hypothesis is, by nature, kinematic, it is possible to adopt a stress approach to solve the problem. In this case, the stress tensor must satisfy several *a priori* conditions.*

*First, as above, he must satisfy  $\mathbf{i}_3 \wedge \boldsymbol{\sigma} \mathbf{i}_3 = \mathbf{0}$ . In addition,  $\sigma_{33}$  cannot be arbitrary, since it has been established that, necessarily:*

$$\sigma_{33} = \lambda (\varepsilon_{11} + \varepsilon_{22}) = \frac{\lambda}{2(\lambda + \mu)} (\sigma_{11} + \sigma_{22}) = v(\sigma_{11} + \sigma_{22})$$

*Finally, to be able to be the solution, it must satisfy Beltrami's equations, mentioned in Paragraph 5.2.2, and which, in the static framework, and for a homogeneous material, are simply reduced here to the following scalar relation:*

$$(1 - v) \Delta_{\mathbf{x}} (\sigma_{11} + \sigma_{22}) + \operatorname{div}_{\mathbf{x}} \mathbf{f}_V = 0$$

*Besides, the constitutive relation in compliance is written, in terms of components, as:*

$$\begin{aligned} \varepsilon_{11} &= \frac{1-v^2}{E} \left( \sigma_{11} - \frac{v}{1-v} \sigma_{22} \right) \\ \varepsilon_{22} &= \frac{1-v^2}{E} \left( \sigma_{22} - \frac{v}{1-v} \sigma_{11} \right) \\ \varepsilon_{12} &= \frac{1+v}{E} \sigma_{12} \end{aligned}$$

### Plane stress

This assumption is commonly adopted when studying a domain whose geometry is invariant in a specific direction in which it is thin, and if it is only loaded in the plane perpendicular to that direction. It is all the more valid if the two end cross-sections are free of forces; otherwise, adopting this hypothesis means that the cross-section is thin enough to neglect the stress vector across that plane and that the study can be limited to an arbitrarily chosen cross-section of the domain.

**Plane stress hypothesis.** This hypothesis implies that, with respect to a plane ( $\Pi$ ), with associated Cartesian vector basis  $(\mathbf{i}_1, \mathbf{i}_2)$ , we assume that the stress tensor is “plane” (it satisfies  $\sigma_{i3} = 0$ ) and only depends on the two coordinates  $(x_1, x_2)$  associated with the basis:

$$\boldsymbol{\sigma}(x_1, x_2) = \sigma_{11}(x_1, x_2)\mathbf{i}_1 \otimes \mathbf{i}_1 + \sigma_{22}(x_1, x_2)\mathbf{i}_2 \otimes \mathbf{i}_2 + 2\sigma_{12}(x_1, x_2)\mathbf{i}_1 \otimes_S \mathbf{i}_2$$

It is therefore independent of the  $x_3$ -coordinate associated with  $\mathbf{i}_3 = \mathbf{i}_1 \wedge \mathbf{i}_2$ .

The local equilibrium equation then becomes a two-component vector equation, since we remain in the plane ( $\Pi$ ); in Cartesian coordinates, and in the static framework, we must verify:

$$\begin{aligned}\frac{\partial \sigma_{11}}{\partial x_1} + \frac{\partial \sigma_{12}}{\partial x_2} + \langle \mathbf{f}_V, \mathbf{i}_1 \rangle &= 0 \\ \frac{\partial \sigma_{12}}{\partial x_1} + \frac{\partial \sigma_{22}}{\partial x_2} + \langle \mathbf{f}_V, \mathbf{i}_2 \rangle &= 0\end{aligned}$$

The associated infinitesimal strain tensor is then obtained by applying the constitutive relation in compliance:

$$\boldsymbol{\varepsilon} = \frac{1+\nu}{E} \boldsymbol{\sigma} - \frac{\nu}{E} (\operatorname{tr} \boldsymbol{\sigma}) \mathbb{I}$$

hence, in the vector basis  $(\mathbf{i}_1, \mathbf{i}_2, \mathbf{i}_1 \wedge \mathbf{i}_2)$ :

$$\boldsymbol{\varepsilon} = \begin{pmatrix} \frac{\sigma_{11}}{E} - \frac{\nu}{E} \sigma_{22} & \frac{1+\nu}{E} \sigma_{12} & 0 \\ \frac{1+\nu}{E} \sigma_{12} & \frac{\sigma_{22}}{E} - \frac{\nu}{E} \sigma_{11} & 0 \\ 0 & 0 & -\frac{\nu}{E} (\sigma_{11} + \sigma_{22}) \end{pmatrix}_{(\mathbf{i}_1, \mathbf{i}_2, \mathbf{i}_1 \wedge \mathbf{i}_2)}$$



As expected, the infinitesimal strain tensor depends only on  $(x_1, x_2)$ ; on the other hand, it is not “plane”, since there is *a priori* a non-zero non-planar component:

$$\varepsilon_{33}(x_1, x_2) = -\frac{\nu}{E} (\sigma_{11}(x_1, x_2) + \sigma_{22}(x_1, x_2)) = -\frac{\nu}{1-\nu} (\varepsilon_{11}(x_1, x_2) + \varepsilon_{22}(x_1, x_2)) \neq 0$$

The compliance constitutive relation can naturally be inverted, to imply that, in terms of components:

$$\begin{aligned}\sigma_{11} &= \frac{E}{1-\nu^2} (\varepsilon_{11} + \nu \varepsilon_{22}) \\ \sigma_{22} &= \frac{E}{1-\nu^2} (\varepsilon_{22} + \nu \varepsilon_{11}) \\ \sigma_{12} &= \frac{E}{1+\nu} \varepsilon_{12}\end{aligned}$$

or, directly, for the plane parts  $\tilde{\boldsymbol{\sigma}}$  and  $\tilde{\boldsymbol{\varepsilon}}$  of the stress and strain tensors:

$$\tilde{\boldsymbol{\sigma}} = \frac{\nu E}{1-\nu^2} (\operatorname{tr} \tilde{\boldsymbol{\varepsilon}}) \mathbb{I} + \frac{E}{1+\nu} \tilde{\boldsymbol{\varepsilon}}$$



The previous form is very close to the three-dimensional Hooke’s law, except that the parameter  $\lambda$  must be replaced by:

$$\lambda_{CP} = \frac{\nu E}{1-\nu^2} \neq \frac{\nu E}{(1+\nu)(1-2\nu)} = \lambda$$

Given the form of the infinitesimal strain tensor, the compatibility equations, discussed in Paragraph 5.2.2, necessarily imply that:

$$\varepsilon_{33}(x_1, x_2) = c_1 x_1 + c_2 x_2 + c_3$$

where  $c_1$ ,  $c_2$  and  $c_3$  are constants. In addition, Beltrami's equations, giving the necessary conditions for  $\sigma$  to be the solution, imply that we must have, in the static framework:

$$\Delta_{\mathbf{x}}(\sigma_{11} + \sigma_{22}) + (1 + v) \operatorname{div}_{\mathbf{x}} \mathbf{f}_V = 0$$

**R** In the case where the volume force density is uniform over the domain, the equations can be solved by introducing what is called an "Airy stress function"  $\Phi$ , such that, in Cartesian coordinates:

$$\begin{aligned}\sigma_{11} &= \frac{\partial^2 \Phi}{\partial x_2^2} - \langle \mathbf{f}_V, \mathbf{i}_1 \rangle x_1 \\ \sigma_{22} &= \frac{\partial^2 \Phi}{\partial x_1^2} - \langle \mathbf{f}_V, \mathbf{i}_2 \rangle x_2 \\ \sigma_{12} &= -\frac{\partial^2 \Phi}{\partial x_1 \partial x_2}\end{aligned}$$

Indeed, with this choice, the local equilibrium equation is automatically verified. In addition, Beltrami's equations imply that, necessarily:

$$0 = \Delta_{\mathbf{x}}(\sigma_{11} + \sigma_{22}) = \Delta_{\mathbf{x}} \Delta_{\mathbf{x}} \Phi$$

### Axisymmetry

In the case of geometries of revolution, it is possible to consider some simplifications; if we use the cylindrical coordinates  $(r, \theta, z)$  and the vector basis  $(\mathbf{i}_r(\theta), \mathbf{i}_\theta(\theta), \mathbf{i}_z)$  associated with the studied geometry, two situations can occur:

- if the loading and the displacement boundary conditions are axisymmetric, i.e. independent of the angle  $\theta$ , and, in addition, without orthoradial component, the components of the displacement vector and of the stress tensor do not depend on  $\theta$ , and the solution can be written as:

$$\begin{aligned}\mathbf{u}(\mathbf{x}) &= u_r(r, z) \mathbf{i}_r(\theta) + u_z(r, z) \mathbf{i}_z \\ \boldsymbol{\sigma}(\mathbf{x}) &= \sigma_{rr}(r, z) \mathbf{i}_r(\theta) \otimes \mathbf{i}_r(\theta) + \sigma_{\theta\theta}(r, z) \mathbf{i}_\theta(\theta) \otimes \mathbf{i}_\theta(\theta) + \sigma_{zz}(r, z) \mathbf{i}_z \otimes \mathbf{i}_z + 2\sigma_{rz}(r, z) \mathbf{i}_r(\theta) \otimes_S \mathbf{i}_z\end{aligned}$$

which means that the problem can be solved in a plane passing through the cylinder axis, with coordinates  $(r, z)$ :

**⚠** We will be careful that, even without explicit dependence in  $\theta$ , an orthoradial component remains *a priori* in the infinitesimal strain tensor, expressed as:

$$\varepsilon_{\theta\theta}(r, z) = \frac{u_r(r, z)}{r}$$

and, consequently, in the stress tensor:

$$\sigma_{\theta\theta}(r, z) = (\lambda + 2\mu) \frac{u_r(r, z)}{r} + \lambda \left( \frac{\partial u_r}{\partial r}(r, z) + \frac{\partial u_z}{\partial z}(r, z) \right)$$

- if the loading and the displacement boundary conditions are independent of  $z$ , and perpendicular to the axis of axisymmetry, in this case, a plane strain hypothesis, or a plane stress hypothesis, can be adopted in the plane of coordinates  $(r, \theta)$ .

**R** In the case of a spherically symmetrical domain, if the loading and displacement boundary conditions are radial, and independent of the angles  $\vartheta$  and  $\phi$  associated with the spherical vector basis  $(\mathbf{e}_r(\vartheta, \phi), \mathbf{e}_\vartheta(\vartheta, \phi), \mathbf{e}_\phi(\phi))$ , we can then search for a displacement vector and a stress tensor independent of  $\vartheta$  and  $\phi$ :

$$\mathbf{u}(\mathbf{x}) = u_r(r)\mathbf{e}_r(\vartheta, \phi)$$

$$\boldsymbol{\sigma}(\mathbf{x}) = \sigma_{rr}(r)\mathbf{e}_r(\vartheta, \phi) \otimes \mathbf{e}_r(\vartheta, \phi) + \sigma_{\vartheta\vartheta}(r)\mathbf{e}_\vartheta(\vartheta, \phi) \otimes \mathbf{e}_\vartheta(\vartheta, \phi) + \sigma_{\phi\phi}(r)\mathbf{e}_\phi(\phi) \otimes \mathbf{e}_\phi(\phi)$$

which means that the problem is solved along a radius of the geometry. Moreover, we should note that, even without explicit dependence in  $\vartheta$  and  $\phi$ , there remain a priori non-radial components in the infinitesimal strain tensor:

$$\varepsilon_{\vartheta\vartheta}(r) = \frac{u_r(r)}{r} = \varepsilon_{\phi\phi}(r)$$

**Summary 5.4 — Plane elasticity.** Three frameworks allow us to replace the initial three-dimensional problem by a two-dimensional problem only.

1. plane strain hypothesis in a plane of coordinates  $(x_1, x_2)$  associated with a Cartesian vector basis  $(\mathbf{i}_1, \mathbf{i}_2)$ :

$$\mathbf{u}(x_1, x_2, t) = u_1(x_1, x_2, t)\mathbf{i}_1 + u_2(x_1, x_2, t)\mathbf{i}_2$$

$$\boldsymbol{\varepsilon}(x_1, x_2, t)(\mathbf{i}_1 \wedge \mathbf{i}_2) = \mathbf{0}$$

$$\boldsymbol{\sigma}(x_1, x_2, t) = \lambda (\text{tr} \boldsymbol{\varepsilon}(x_1, x_2, t))\mathbb{I} + 2\mu \boldsymbol{\varepsilon}(x_1, x_2, t)$$

$$\sigma_{33}(x_1, x_2, t) = \lambda (\varepsilon_{11}(x_1, x_2, t) + \varepsilon_{22}(x_1, x_2, t)) = \lambda \left( \frac{\partial u_1}{\partial x_1}(x_1, x_2, t) + \frac{\partial u_2}{\partial x_2}(x_1, x_2, t) \right) \neq 0$$

2. plane stress hypothesis in a plane of coordinates  $(x_1, x_2)$  associated with a Cartesian vector basis  $(\mathbf{i}_1, \mathbf{i}_2)$ :

$$\boldsymbol{\sigma}(x_1, x_2, t)(\mathbf{i}_1 \wedge \mathbf{i}_2) = \mathbf{0}$$

$$\boldsymbol{\varepsilon}(x_1, x_2, t) = \frac{1+\nu}{E}\boldsymbol{\sigma}(x_1, x_2, t) - \frac{\nu}{E}(\text{tr} \boldsymbol{\sigma}(x_1, x_2, t))\mathbb{I}$$

$$\varepsilon_{33}(x_1, x_2, t) = -\frac{\nu}{E}(\sigma_{11}(x_1, x_2, t) + \sigma_{22}(x_1, x_2, t)) = -\frac{\nu}{1-\nu}(\varepsilon_{11}(x_1, x_2, t) + \varepsilon_{22}(x_1, x_2, t)) \neq 0$$

3. axisymmetry hypothesis around the axis  $\mathbf{i}_z$ : no component depends on the angle  $\theta$  associated with the cylindrical vector basis  $(\mathbf{i}_r(\theta), \mathbf{i}_\theta(\theta), \mathbf{i}_z)$ .

### 5.3.3 Taking into account symmetry planes

Another possibility of simplifying the problem concerns the case of geometries that present a symmetry plane; indeed, if the loadings and the displacement boundary conditions are also symmetrical with respect to this plane, it is possible to study only one half of the problem, provided that the symmetry plane is associated with particular conditions that we will specify in this section. While, from an analytical point of view, this may make it easier to solve the problem, it is mainly in the context of a numerical simulation that symmetry is of interest, since it reduces the numerical cost associated with the calculation.

The symmetry plane is associated with a Cartesian vector basis  $(\mathbf{i}_1, \mathbf{i}_2, \mathbf{i}_3)$  so that  $\mathbf{i}_3$  is normal to the plane; this latter is therefore of equation  $x_3 = 0$ . For two symmetrical points, with coordinates  $(x_1, x_2, x_3)$  and  $(x_1, x_2, -x_3)$  respectively, the displacements must also be symmetrical with respect to the plane  $x_3 = 0$ , so that their components  $(u_1, u_2, u_3)$  in  $(\mathbf{i}_1, \mathbf{i}_2, \mathbf{i}_3)$  verify:

$$u_1(x_1, x_2, -x_3) = u_1(x_1, x_2, x_3), u_2(x_1, x_2, -x_3) = u_2(x_1, x_2, x_3), \text{ and } u_3(x_1, x_2, -x_3) = -u_3(x_1, x_2, x_3)$$

as shown in Figure 5.4. When  $x_3$  approaches zero, we obtain, by continuity, that the displacements

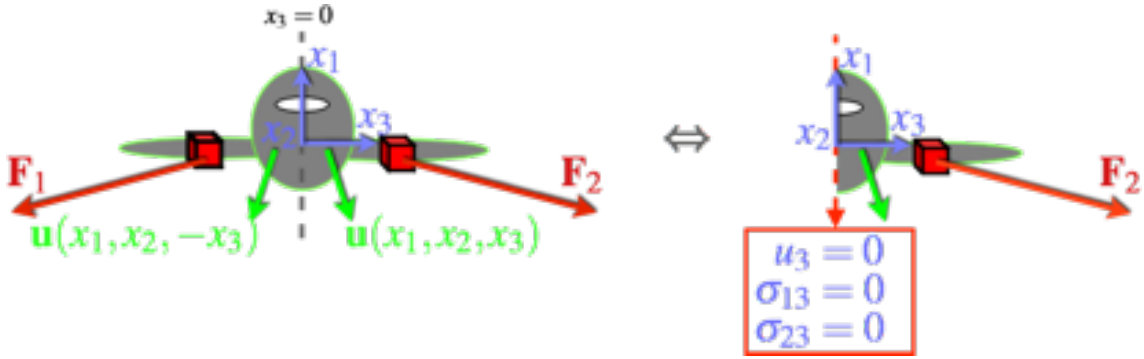


Figure 5.4: Taking into account a symmetry plane

of the points of the symmetry plane should verify:

$$u_3(x_1, x_2, 0) = 0, \forall x_1, x_2$$

which is physically interpreted by the fact that a point of the plane of symmetry must remain in this plane because, otherwise, at this point, we would have either interpenetration or creation of a void.

Moreover, since nothing can be said about the two other components of the displacement field on the symmetry plane, it is necessary, for the problem to be properly addressed, to express also conditions on the surface forces. We begin by analyzing the derivatives of the displacement components, for two symmetrical points, of coordinates  $(x_1, x_2, x_3)$  and  $(x_1, x_2, -x_3)$  respectively:

$$\begin{aligned} \frac{\partial u_3}{\partial x_1}(x_1, x_2, -x_3) &= -\frac{\partial u_3}{\partial x_1}(x_1, x_2, x_3), \text{ and } -\frac{\partial u_1}{\partial x_3}(x_1, x_2, -x_3) = \frac{\partial u_1}{\partial x_3}(x_1, x_2, x_3) \\ \frac{\partial u_3}{\partial x_2}(x_1, x_2, -x_3) &= -\frac{\partial u_3}{\partial x_2}(x_1, x_2, x_3), \text{ and } -\frac{\partial u_2}{\partial x_3}(x_1, x_2, -x_3) = \frac{\partial u_2}{\partial x_3}(x_1, x_2, x_3) \end{aligned}$$

which results in the associated shear strains:

$$\begin{aligned} 2\epsilon_{13}(x_1, x_2, -x_3) &= \frac{\partial u_3}{\partial x_1}(x_1, x_2, -x_3) + \frac{\partial u_1}{\partial x_3}(x_1, x_2, -x_3) \\ &= -\frac{\partial u_3}{\partial x_1}(x_1, x_2, x_3) - \frac{\partial u_1}{\partial x_3}(x_1, x_2, x_3) = -2\epsilon_{13}(x_1, x_2, x_3) \\ 2\epsilon_{23}(x_1, x_2, -x_3) &= \frac{\partial u_3}{\partial x_2}(x_1, x_2, -x_3) + \frac{\partial u_2}{\partial x_3}(x_1, x_2, -x_3) \\ &= -\frac{\partial u_3}{\partial x_2}(x_1, x_2, x_3) - \frac{\partial u_2}{\partial x_3}(x_1, x_2, x_3) = -2\epsilon_{23}(x_1, x_2, x_3) \end{aligned}$$

and, consequently, the shears:

$$\begin{aligned} \sigma_{13}(x_1, x_2, -x_3) &= 2\mu\epsilon_{13}(x_1, x_2, -x_3) = -2\mu\epsilon_{13}(x_1, x_2, x_3) = -\sigma_{13}(x_1, x_2, -x_3) \\ \sigma_{23}(x_1, x_2, -x_3) &= 2\mu\epsilon_{23}(x_1, x_2, -x_3) = -2\mu\epsilon_{23}(x_1, x_2, x_3) = -\sigma_{23}(x_1, x_2, -x_3) \end{aligned}$$

These last results allow us to deduce, by continuity when  $x_3$  approaches zero, that there is no shear on the plane of symmetry:

$$\sigma_{13}(x_1, x_2, 0) = 0 = \sigma_{23}(x_1, x_2, 0), \forall x_1, x_2$$

These conditions are actually equivalent to those, presented in Paragraph 5.1.2, concerning a frictionless contact condition on a fixed plane.

Once the problem is solved on the half-domain, with the addition of these frictionless contact conditions on the symmetry plane, it is sufficient to extend, by symmetry, the solution over the whole domain.

**Summary 5.5 — Taking into account symmetry planes.** In the case of a problem with a symmetry plane  $\Sigma_s$  of normal vector  $\mathbf{i}_3$ , it is sufficient to only treat the problem corresponding to one of the two halves of the material domain, by introducing, on the symmetry plane, frictionless contact conditions along the plane:

$$\langle \mathbf{u}(\mathbf{x}, t), \mathbf{i}_3 \rangle = 0, \forall \mathbf{x} \in \Sigma_s, \forall t$$

$$\boldsymbol{\sigma}(\mathbf{x}, t) \mathbf{i}_3 - \langle \boldsymbol{\sigma}(\mathbf{x}, t) \mathbf{i}_3, \mathbf{i}_3 \rangle \mathbf{i}_3 = \mathbf{0}, \forall \mathbf{x} \in \Sigma_s, \forall t$$

R

It is in fact possible to solve in a similar way a problem whose imposed surface forces and/or constrained displacements are not symmetrical with respect to the plane of symmetry of the geometry. Indeed, by using the principle of superposition, presented in Paragraph 5.3.1, we can decompose the sought solution as the sum of the solution of a symmetrical problem and the solution of an antisymmetrical problem.

If we assume e.g. that the volume force densities  $\mathbf{f}_V$  do not respect this symmetry, we can study the following two problems, to be solved over a half domain:

1. a symmetrical problem, for which we consider as loading:

$$\mathbf{f}_V^s(x_1, x_2, x_3) = \frac{1}{2} (\mathbf{f}_V(x_1, x_2, x_3) + \mathbf{f}_V(x_1, x_2, -x_3)), \forall x_1, x_2, x_3$$

and conditions of symmetry on the plane  $x_3 = 0$ :

$$u_3^s(x_1, x_2, 0) = 0, \text{ and } \sigma_{13}^s(x_1, x_2, 0) = 0 = \sigma_{23}^s(x_1, x_2, 0), \forall x_1, x_2$$

2. an antisymmetrical problem, for which we consider as loading:

$$\mathbf{f}_V^a(x_1, x_2, x_3) = \frac{1}{2} (\mathbf{f}_V(x_1, x_2, x_3) - \mathbf{f}_V(x_1, x_2, -x_3)), \forall x_1, x_2, x_3$$

and antisymmetry conditions on the plane  $x_3 = 0$ , for which it is easy to show that they are written as:

$$u_1^a(x_1, x_2, 0) = 0 = u_2^a(x_1, x_2, 0), \text{ and } \sigma_{33}^a(x_1, x_2, 0) = 0, \forall x_1, x_2$$

The solution is therefore obtained as  $\mathbf{u} = \mathbf{u}^s + \mathbf{u}^a$  and  $\boldsymbol{\sigma} = \boldsymbol{\sigma}^s + \boldsymbol{\sigma}^a$ . Even if two calculations have to be made on half a geometry, this may be more interesting, in terms of computational cost when using a numerical simulation (typically finite elements), than solving the initial problem on the whole problem.

## 5.4 Summary of important formulas

**Generic formulation of an elasticity problem** – Summary 5.1 page 121

$$\boldsymbol{\epsilon} = \frac{1}{2} \left( \mathbb{D}_{\mathbf{x}} \mathbf{u} + (\mathbb{D}_{\mathbf{x}} \mathbf{u})^T \right) \text{ in } \Omega$$

$$\mathbf{u} = \mathbf{u}_d \text{ on } \partial_u \Omega$$

$$\rho_0 \ddot{\mathbf{u}} = \mathbf{div}_{\mathbf{x}} \boldsymbol{\sigma} + \mathbf{f}_V \text{ in } \Omega$$

$$\boldsymbol{\sigma} \mathbf{n} = \mathbf{f}_S \text{ on } \partial_{\sigma} \Omega$$

$$\boldsymbol{\sigma} = \mathbf{C} \boldsymbol{\epsilon} = \lambda (\text{tr} \boldsymbol{\epsilon}) \mathbb{I} + 2\mu \boldsymbol{\epsilon} \text{ in } \Omega$$

$$\boldsymbol{\epsilon} = \mathbf{C}^{-1} \boldsymbol{\sigma} = \frac{1+\nu}{E} \boldsymbol{\sigma} - \frac{\nu}{E} (\text{tr} \boldsymbol{\sigma}) \mathbb{I} \text{ in } \Omega$$

$$\mathbf{u} = \mathbf{u}_0 \text{ and } \dot{\mathbf{u}} = \mathbf{v}_0 \text{ at } t = 0$$

**Displacement formulation of an elasticity problem** – Summary 5.2 page 129

$$(\lambda + \mu) \nabla_{\mathbf{x}} (\mathbf{div}_{\mathbf{x}} \mathbf{u}) + \mu \Delta_{\mathbf{x}} \mathbf{u} + \mathbf{f}_V = \rho_0 \ddot{\mathbf{u}} \text{ in } \Omega$$

$$\mathbf{u} = \mathbf{u}_d \text{ on } \partial_u \Omega$$

$$\lambda(\operatorname{tr}\boldsymbol{\varepsilon})\mathbf{n} + 2\mu\boldsymbol{\varepsilon}\mathbf{n} = \mathbf{f}_S \text{ on } \partial_\sigma\Omega$$

$$\mathbf{u} = \mathbf{u}_0 \text{ and } \dot{\mathbf{u}} = \mathbf{v}_0 \text{ at } t = 0$$

**Compatibility equations** – Summary 5.3 page 135

$$\frac{\partial^2 \varepsilon_{km}}{\partial x_l \partial x_n} - \frac{\partial^2 \varepsilon_{lm}}{\partial x_k \partial x_n} = \frac{\partial^2 \varepsilon_{kn}}{\partial x_l \partial x_m} - \frac{\partial^2 \varepsilon_{ln}}{\partial x_k \partial x_m}$$

**Plane strain** – Summary 5.4 page 145

$$\mathbf{u}(x_1, x_2) = u_1(x_1, x_2)\mathbf{i}_1 + u_2(x_1, x_2)\mathbf{i}_2$$

$$\boldsymbol{\varepsilon}(x_1, x_2)(\mathbf{i}_1 \wedge \mathbf{i}_2) = \mathbf{0}$$

$$\boldsymbol{\sigma}(x_1, x_2) = \lambda(\operatorname{tr}\boldsymbol{\varepsilon}(x_1, x_2))\mathbb{I} + 2\mu\boldsymbol{\varepsilon}(x_1, x_2)$$

$$\sigma_{33}(x_1, x_2) = \lambda(\varepsilon_{11}(x_1, x_2) + \varepsilon_{22}(x_1, x_2)) = \lambda\left(\frac{\partial u_1}{\partial x_1}(x_1, x_2) + \frac{\partial u_2}{\partial x_2}(x_1, x_2)\right) \neq 0$$

**Plane stress** – Summary 5.4 page 145

$$\boldsymbol{\sigma}(x_1, x_2)(\mathbf{i}_1 \wedge \mathbf{i}_2) = \mathbf{0}$$

$$\boldsymbol{\varepsilon}(x_1, x_2) = \frac{1+\nu}{E}\boldsymbol{\sigma}(x_1, x_2) - \frac{\nu}{E}(\operatorname{tr}\boldsymbol{\sigma}(x_1, x_2))\mathbb{I}$$

$$\varepsilon_{33}(x_1, x_2) = -\frac{\nu}{E}(\sigma_{11}(x_1, x_2) + \sigma_{22}(x_1, x_2)) = -\frac{\nu}{1-\nu}(\varepsilon_{11}(x_1, x_2) + \varepsilon_{22}(x_1, x_2)) \neq 0$$

**Taking into account symmetry planes (plane  $\Sigma_s$  of normal vector  $\mathbf{i}_3$ )** – Summary 5.5  
page 147

$$\langle \mathbf{u}, \mathbf{i}_3 \rangle = 0 \text{ on } \Sigma_s$$

$$\boldsymbol{\sigma}\mathbf{i}_3 - \langle \boldsymbol{\sigma}\mathbf{i}_3, \mathbf{i}_3 \rangle \mathbf{i}_3 = \mathbf{0} \text{ on } \Sigma_s$$



## 6. Beam approximation

Beam models are simplifications of models derived from continuum mechanics, in the case of so-called “slender” structures; hypotheses on kinematics and stress state allow for considering these structures as intermediate cases between deformable solids and perfectly rigid bodies, and thus for obtaining equations whose easier solution makes these calculations popular in preliminary design studies.

---

### WHY STUDY BEAMS?

#### 6.1 Kinematics of a beam

The first ingredient of a beam model consists in making kinematic assumptions in order to define an approximate displacement field, simpler than the one we would seek in the framework of three-dimensional continuum mechanics, in the case of a deformable solid of arbitrary shape.

##### 6.1.1 Geometry and parameterization

A beam is a deformable solid for which one of the characteristic dimensions is very large when compared to the other two: this dimension is then associated with what is called the “neutral axis” of the beam, which is not necessarily straight. The other two dimensions are associated with what is called “cross-section”, which, by definition, is flat and perpendicular to the tangent vector  $\mathbf{e}$  to the neutral axis of the beam when considering this latter in its initial configuration (i.e. not deformed). Thus, a beam can be seen as a (deformable) line around which the different cross-sections are positioned. Generally, in order to facilitate the description of the kinematics of the beam, one specific point for each cross-section is chosen: the geometric centre, noted  $G$ , of this latter.

In terms of parameterization, one associates to a point  $G$  of the neutral axis in the reference configuration an arc length  $s$ , which then allows for specifying a given cross-section  $\Sigma$ . In addition, a point in this cross-section  $\Sigma(s)$  is positioned relative to the centre  $G$  by its coordinates  $(\chi_1, \chi_2)$  in a given orthonormal Cartesian vector basis  $(\mathbf{e}_{\chi_1}(s), \mathbf{e}_{\chi_2}(s))$  of the plane associated with the cross-section  $\Sigma$ . Thus, a point  $M$  of the beam is located in the initial configuration by the position

vector  $\mathbf{p}$ , which can be decomposed as follows:

$$\mathbf{p}(s, \chi_1, \chi_2) = \mathbf{p}_G(s) + \mathbf{p}_\Sigma(\chi_1, \chi_2) = \int_0^s \mathbf{e}(\xi) d\xi + \chi_1 \mathbf{e}_{\chi_1}(s) + \chi_2 \mathbf{e}_{\chi_2}(s)$$

where  $\mathbf{p}_G$  is the position vector of the centre  $G$  of the cross-section, and  $\mathbf{p}_\Sigma$  refers to the position vector of point  $M$  in the cross-section (relative to the centre  $G$ ).

In this course, we will limit ourselves to the particular case of a straight neutral axis, which then defines what we call a “straight beam” (in its initial configuration): thus, the tangent vector  $\mathbf{e}$  is independent of the arc length  $s$ , and is called “axis” of the straight beam. In this case, as shown in Figure 6.1, a point  $M$  of the beam is positioned in the initial configuration as:

$$\mathbf{p}(s, \chi_1, \chi_2) = \mathbf{p}_G(s) + \mathbf{p}_\Sigma(\chi_1, \chi_2) = s\mathbf{e} + \chi_1 \mathbf{e}_{\chi_1} + \chi_2 \mathbf{e}_{\chi_2}$$

the two vectors  $(\mathbf{e}_{\chi_1}, \mathbf{e}_{\chi_2})$  being in this case independent of  $s$ , since the cross-section is perpendicular to  $\mathbf{e}$  in the initial configuration. We will come back in Paragraph 6.3.3 on the relevant choice of these two basis vectors; for the moment, we will simply specify that the basis  $(\mathbf{e}, \mathbf{e}_{\chi_1}, \mathbf{e}_{\chi_2})$  is orthonormal and right-handed.

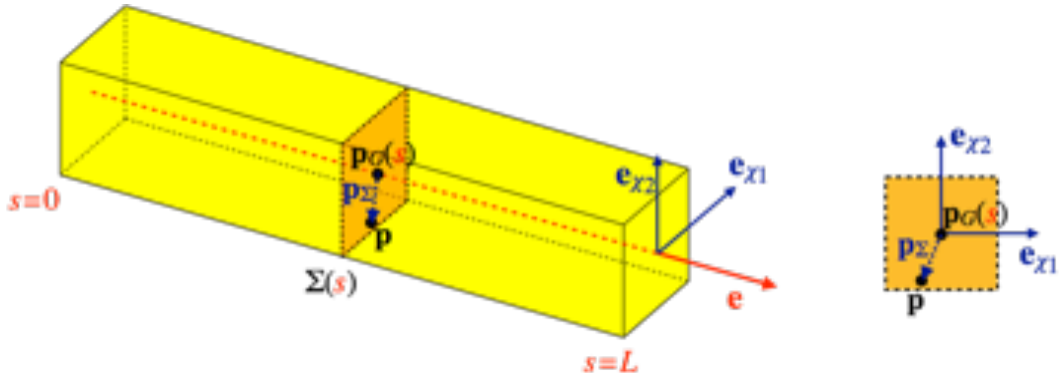


Figure 6.1: Parameterization associated with a straight beam.

### 6.1.2 Perfectly rigid cross-section hypothesis

As we have just seen, the geometry of a beam suggests that we can consider separately the cross-sections  $\Sigma(s)$  from the axis  $\mathbf{e}$  of the beam, which connects all the geometric centres  $G(s)$  of these cross-sections. Figure 6.2 shows a first result from a three-point bending test of a straight beam: this test consists of setting a straight beam on two fixed supports, spaced at a distance  $L$ , which is subjected, at the median plane between the two supports, to a downward vertical force exerted by a movable cylindrical roller. The image on the right then shows, in superimposition, the deformed beam (the deformation is strongly amplified). The initially flat cross-sections (which are then of horizontal normal vector) remain flat after deformation of the beam, as can be seen on the deformed grid where the points belonging to the same cross-section remain approximately aligned along a segment, whose length does not change (it remains equal to  $H$ ).

#### Displacement expression

Given this experimental result, a first kinematic hypothesis is to assume that the cross-sections do not deform. In this case, the placement vectors of all the points of a given cross-section  $\Sigma$  of coordinate  $s$  satisfy the placement formula of the points of a perfectly rigid body, as explained in Example 1.3 on page 5, i.e.:

$$\mathbf{x}(t) = \mathbf{x}_G(t) + \mathbb{R}(t)(\mathbf{p} - \mathbf{p}_G) = \mathbf{x}_G(t) + \mathbf{x}_\Sigma(t), \quad \forall \mathbf{p} \in \Sigma, \quad \forall t$$

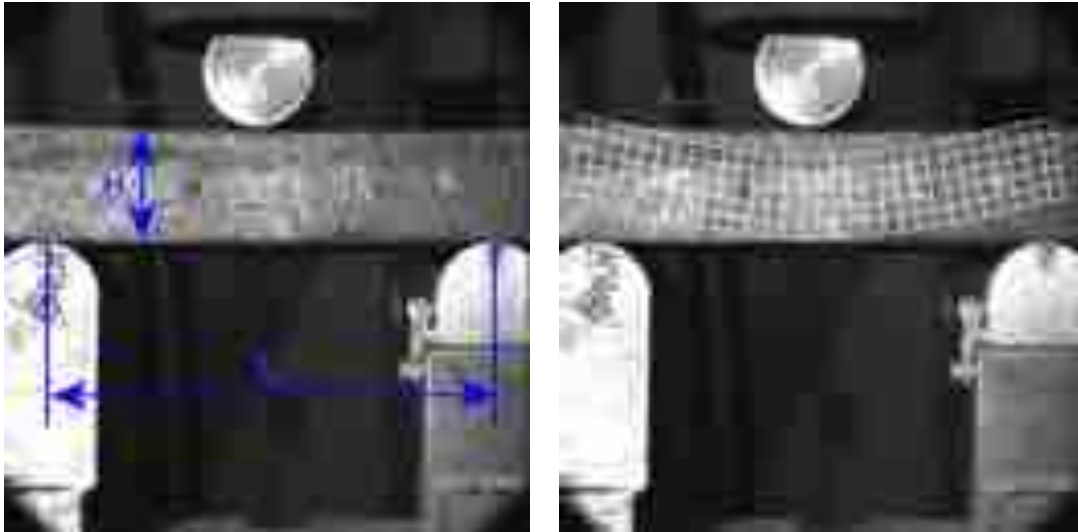


Figure 6.2: Straight beam subjected to a three-point bending test (left) and deformed beam: amplified deformation estimated by digital image correlation (right).

where  $\mathbb{R}$  is the rotation tensor of the cross-section  $\Sigma$  of coordinate  $s$ , assumed to be of axis  $\mathbf{a}$  and angle  $\theta$ .

As in the more general case of weakly deformable solids in continuum mechanics, we will adopt here the infinitesimal deformation hypothesis, which is equivalent to assume that the rotation of each cross-section is “small”, which implies, as detailed in Appendix A.2.6, that:

$$\mathbb{R} \approx \mathbb{I} + \theta \mathbf{a}^\wedge$$

up to order one in  $\theta$ , where  $\mathbf{a}^\wedge$  is an antisymmetrical tensor such that  $\mathbf{a}^\wedge \mathbf{c} = \mathbf{a} \wedge \mathbf{c}$ ,  $\forall \mathbf{c}$ . Moreover, rather than expressing the placement vectors of the points of the beam, we prefer, as in 3D continuum mechanics, to be interested in the displacement field  $\mathbf{u} = \mathbf{x} - \mathbf{p}$ , which is assumed to be “small” under the infinitesimal deformation hypothesis:

$$\mathbf{u} = \mathbf{u}_G + \theta \mathbf{a} \wedge (\mathbf{p} - \mathbf{p}_G)$$

where  $\mathbf{u}_G = \mathbf{x}_G - \mathbf{p}_G$  refers to the displacement of the centre  $G$  of the cross-section  $\Sigma$  of coordinate  $s$ . By noting  $\boldsymbol{\theta} = \theta \mathbf{a}$  the vector associated with the small cross-section rotation, and using  $\mathbf{p}_\Sigma = \mathbf{p} - \mathbf{p}_G$ , the displacement field is rewritten, for any point in the cross-section  $\Sigma$  under study, as:

$$\mathbf{u} = \mathbf{u}_G + \boldsymbol{\theta} \wedge \mathbf{p}_\Sigma$$

Finally, given the small displacement hypothesis, we can consider the initial and deformed configurations as one, and thus express the displacement field at time  $t$  using the variables  $s$  and  $(\chi_1, \chi_2)$ , which are assumed to refer indifferently to the two configurations, respectively as the arc length associated with the centres of the cross-sections  $\Sigma$  on the one hand, and the local coordinates of a point in a cross-section of coordinate  $s$  on the other hand:

$$\mathbf{u}(s, \chi_1, \chi_2, t) = \mathbf{u}_G(s, t) + \boldsymbol{\theta}(s, t) \wedge \mathbf{x}_\Sigma(\chi_1, \chi_2), \forall t$$

for any point  $M$  of the beam, of coordinates  $(s, \chi_1, \chi_2)$ . In other words, the deformation of a beam can be interpreted as the deformation of the neutral axis along which the perfectly rigid cross-sections are placed; Figure 6.3 illustrates this idea and shows how the beam, composed of small elemental volumes (initially cubic in the reference configuration), is deformed: we can see in particular that the (transverse) geometry of the cross-sections remains unchanged.

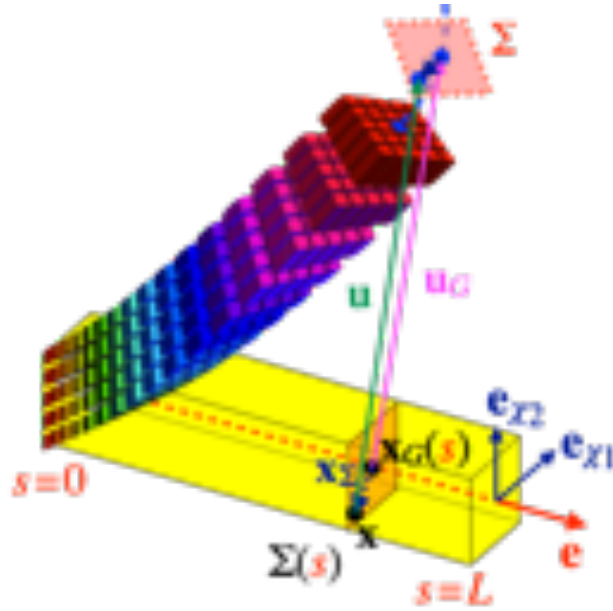


Figure 6.3: Example of beam deformation in the context of the infinitesimal deformation hypothesis: the elemental parallelepipeds, initially cubic, allow for visualizing the local deformations (here, the deformations are strongly amplified in order to gain in visibility).

**Beam kinematics.** The motion of each cross-section can be characterized by six scalar functions of the arc length  $s$ :

- three functions associated with the translation of the centre  $G$  of the cross-section  $\Sigma(s)$ , which are the three components in a given vector basis of the displacement  $\mathbf{u}_G$ : while the projection  $u_{Ge} = \langle \mathbf{u}_G, \mathbf{e} \rangle$  on the beam axis is called “longitudinal” displacement, and reflects the elongation (or shortening) of the beam, the other two projections on  $\mathbf{e}_{\chi_1}$  and  $\mathbf{e}_{\chi_2}$  constitute the “transverse” displacement  $\mathbf{u}_{G\Sigma} = \mathbf{u} - u_e \mathbf{e}$  of the beam, associated with the distortion and/or the bending of this latter:

$$\mathbf{u}_G = u_{Ge} \mathbf{e} + \mathbf{u}_{G\Sigma} = u_{Ge} \mathbf{e} + u_{G\chi_1} \mathbf{e}_{\chi_1} + u_{G\chi_2} \mathbf{e}_{\chi_2} = \langle \mathbf{u}_G, \mathbf{e} \rangle \mathbf{e} + \langle \mathbf{u}_G, \mathbf{e}_{\chi_1} \rangle \mathbf{e}_{\chi_1} + \langle \mathbf{u}_G, \mathbf{e}_{\chi_2} \rangle \mathbf{e}_{\chi_2}$$

- three functions associated with the small rotation of the cross-section  $\Sigma(s)$ , which are the three components in a given vector basis of the vector  $\boldsymbol{\theta}$ : while the projection  $\theta_e = \langle \boldsymbol{\theta}, \mathbf{e} \rangle$  on the beam axis is the angle of twist (the cross-section rotates around its normal vector), the other two projections on  $\mathbf{e}_{\chi_1}$  and  $\mathbf{e}_{\chi_2}$  constitute the bending rotation  $\boldsymbol{\theta}_{\Sigma} = \boldsymbol{\theta} - \theta_e \mathbf{e}$  of the cross-section, which then rotates around an axis contained in its plane:

$$\boldsymbol{\theta} = \theta_e \mathbf{e} + \boldsymbol{\theta}_{\Sigma} = \theta_e \mathbf{e} + \theta_{\chi_1} \mathbf{e}_{\chi_1} + \theta_{\chi_2} \mathbf{e}_{\chi_2} = \langle \boldsymbol{\theta}, \mathbf{e} \rangle \mathbf{e} + \langle \boldsymbol{\theta}, \mathbf{e}_{\chi_1} \rangle \mathbf{e}_{\chi_1} + \langle \boldsymbol{\theta}, \mathbf{e}_{\chi_2} \rangle \mathbf{e}_{\chi_2}$$

These different motions, which correspond to the Timoshenko beam model, are shown in Figure 6.4.

### Infinitesimal strain tensor

The infinitesimal strain tensor is, as in 3D continuum mechanics, the symmetrical part of the displacement gradient tensor (see Paragraph 1.3.2); this latter is calculated from the previous expressions, in the Cartesian vector basis  $(\mathbf{e}, \mathbf{e}_{\chi_1}, \mathbf{e}_{\chi_2})$ , as:

$$\mathbb{D}_{\mathbf{x}} \mathbf{u} = \frac{\partial \mathbf{u}}{\partial s} \otimes \mathbf{e} + \frac{\partial \mathbf{u}}{\partial \chi_1} \otimes \mathbf{e}_{\chi_1} + \frac{\partial \mathbf{u}}{\partial \chi_2} \otimes \mathbf{e}_{\chi_2}$$

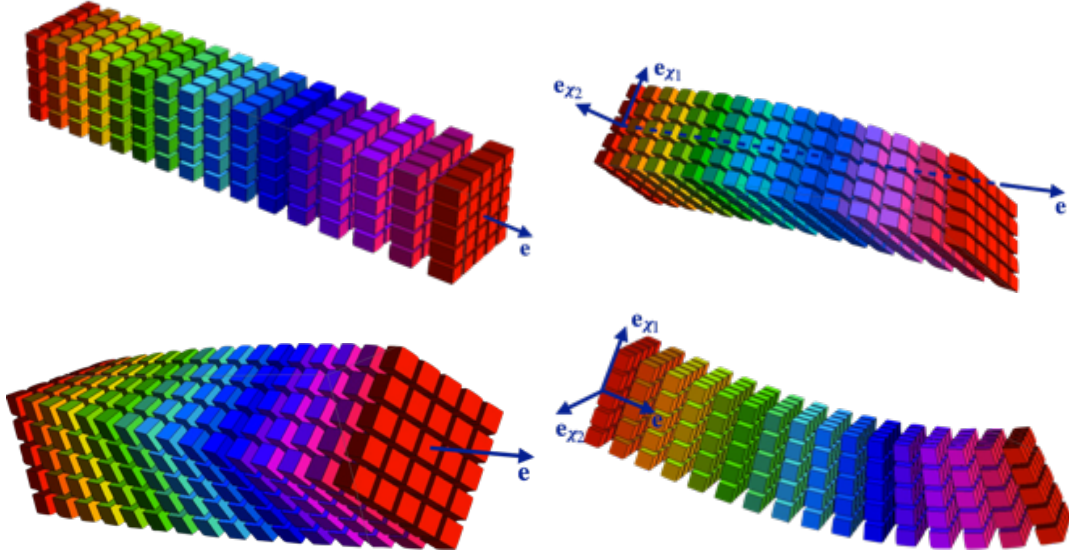


Figure 6.4: Elongation (top left), distortion (top right), torsion (bottom left) and bending (bottom right) of a beam.

and by rewriting that  $\Theta \wedge \mathbf{x}_\Sigma = \theta \mathbf{a}^\wedge \mathbf{x}_\Sigma = \theta \mathbf{a}^\wedge (\chi_1 \mathbf{e}_{\chi_1} + \chi_2 \mathbf{e}_{\chi_2})$ , we then obtain, by noting  $\bullet' = \frac{d\bullet}{ds}$ :

$$\mathbb{D}_x \mathbf{u} = (\mathbf{u}'_G + (\theta \mathbf{a}^\wedge)' \mathbf{x}_\Sigma) \otimes \mathbf{e} + (\theta \mathbf{a}^\wedge \mathbf{e}_{\chi_1}) \otimes \mathbf{e}_{\chi_1} + (\theta \mathbf{a}^\wedge \mathbf{e}_{\chi_2}) \otimes \mathbf{e}_{\chi_2}$$

In the case of a straight beam, by introducing the projections  $\bullet_e = \langle \bullet, \mathbf{e} \rangle$  on the axis  $\mathbf{e}$  on the one hand, and  $\bullet_\Sigma = \bullet - \langle \bullet, \mathbf{e} \rangle \mathbf{e}$  on the plane associated with the cross-section  $\Sigma(s)$  on the other hand, we can reorganize terms as:

$$\mathbb{D}_x \mathbf{u} = (\mathbf{u}'_{Ge} + \langle (\theta \mathbf{a}^\wedge)' \mathbf{x}_\Sigma, \mathbf{e} \rangle) \mathbf{e} \otimes \mathbf{e} + (\mathbf{u}'_{GS} + ((\theta \mathbf{a}^\wedge)' \mathbf{x}_\Sigma)_\Sigma) \otimes \mathbf{e} + \theta \mathbf{a}^\wedge (\mathbb{I} - \mathbf{e} \otimes \mathbf{e})$$

and, noting that  $\langle \theta \mathbf{a}^\wedge \mathbf{e}, \mathbf{e} \rangle = \langle \theta \mathbf{a} \wedge \mathbf{e}, \mathbf{e} \rangle = 0$ , the displacement gradient tensor is finally written as:

$$\mathbb{D}_x \mathbf{u} = (\mathbf{u}'_{Ge} + \langle (\theta \mathbf{a}^\wedge)' \mathbf{x}_\Sigma, \mathbf{e} \rangle) \mathbf{e} \otimes \mathbf{e} + (\mathbf{u}'_{GS} - \theta \mathbf{a}^\wedge \mathbf{e} + ((\theta \mathbf{a}^\wedge)' \mathbf{x}_\Sigma)_\Sigma) \otimes \mathbf{e} + \theta \mathbf{a}^\wedge$$

Taking the symmetrical part of this tensor, since  $\mathbf{a}^\wedge$  is antisymmetrical, we arrive at the following expression of the infinitesimal strain tensor:

$$\boldsymbol{\varepsilon} = (\mathbf{u}'_{Ge} + \langle \Theta' \wedge \mathbf{x}_\Sigma, \mathbf{e} \rangle) \mathbf{e} \otimes \mathbf{e} + (\mathbf{u}'_{GS} - \Theta \wedge \mathbf{e}) \otimes_S \mathbf{e} + (\Theta' \wedge \mathbf{x}_\Sigma)_\Sigma \otimes_S \mathbf{e}$$

writing  $\mathbf{c}_1 \otimes_S \mathbf{c}_2 = (\mathbf{c}_1 \otimes \mathbf{c}_2 + \mathbf{c}_2 \otimes \mathbf{c}_1)/2$  for the symmetrical part of the tensor product  $\mathbf{c}_1 \otimes \mathbf{c}_2$ , and replacing  $\theta \mathbf{a}^\wedge$  with the corresponding small rotation vector  $\Theta$ .

We then see that the infinitesimal strain tensor is antiplane, i.e. that its plane part (in the plane of the cross-section) is equal to zero: indeed, the expression we have just established does not include terms along  $\mathbf{e}_{\chi_1} \otimes \mathbf{e}_{\chi_1}$ ,  $\mathbf{e}_{\chi_2} \otimes \mathbf{e}_{\chi_2}$ , or  $\mathbf{e}_{\chi_1} \otimes \mathbf{e}_{\chi_2}$ , but only terms related to the axis  $\mathbf{e}$  of the beam:

- the first term, of the form  $\varepsilon_{ee} \mathbf{e} \otimes \mathbf{e}$ , consists of a longitudinal strain along the beam, and combines two effects:

1. a term  $\mathbf{u}'_{Ge}$  which corresponds to the rate of variation, along the beam, of the longitudinal displacements of the (centres of) cross-sections, and therefore directly translates, in terms of strain, the elongation (which is homogeneous in the cross-section) of the beam; Figure 6.5 presents the particular case where this strain is also homogeneous along the beam;

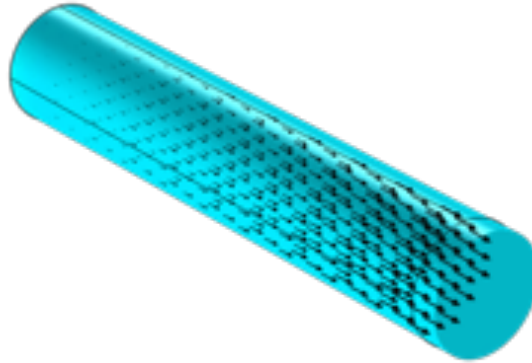


Figure 6.5: Longitudinal strain field in the case of a beam in elongation (the arrows representing the associated displacement field).

2. a term  $\langle \boldsymbol{\theta}' \wedge \mathbf{x}_\Sigma, \mathbf{e} \rangle = \langle (\boldsymbol{\theta}'_e \mathbf{e} + \boldsymbol{\theta}'_\Sigma) \wedge \mathbf{x}_\Sigma, \mathbf{e} \rangle = \langle \boldsymbol{\theta}'_\Sigma \wedge \mathbf{x}_\Sigma, \mathbf{e} \rangle$  which corresponds to the rate of variation, along the beam, of the bending rotation of the cross-sections, which, by turning about an axis contained in their plane, tend to stretch or squeeze small segments initially taken parallel to the neutral axis, in a linear way across the cross-section; Figure 6.6 allows us to notice this linear evolution according to the height of the beam, in the particular case where the bending is achieved around a horizontal axis;

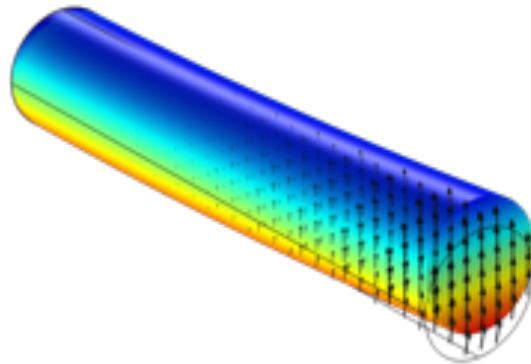


Figure 6.6: Longitudinal strain field in the case of a bending beam (the arrows representing the associated displacement field).

- the second and third terms, of the form  $\boldsymbol{\gamma}_\Sigma \otimes_S \mathbf{e} = 2\boldsymbol{\varepsilon}_{\chi_1 e} \mathbf{e}_{\chi_1} \otimes_S \mathbf{e} + 2\boldsymbol{\varepsilon}_{\chi_2 e} \mathbf{e}_{\chi_2} \otimes_S \mathbf{e}$ , reflect a distortion along the beam, with two distinct effects:
  1. the first one, associated with the term  $(\mathbf{u}'_{G\Sigma} - \boldsymbol{\theta} \wedge \mathbf{e}) = (\mathbf{u}'_{G\Sigma} - \boldsymbol{\theta}_\Sigma \wedge \mathbf{e})$ , reflects a distortion associated with the bending rotation of the cross-sections, which means that these latter do not remain perpendicular to the deformed neutral axis: this term, often referred to as “transverse shear”, will be analysed more precisely in Paragraph 6.1.3;
  2. the second one, linked to  $(\boldsymbol{\theta}' \wedge \mathbf{x}_\Sigma)_\Sigma = \boldsymbol{\theta}' \wedge \mathbf{x}_\Sigma - \langle \boldsymbol{\theta}' \wedge \mathbf{x}_\Sigma, \mathbf{e} \rangle \mathbf{e} = \boldsymbol{\theta}' \wedge \mathbf{x}_\Sigma - \boldsymbol{\theta}'_\Sigma \wedge \mathbf{x}_\Sigma = \boldsymbol{\theta}'_e \mathbf{e} \wedge \mathbf{x}_\Sigma$  reflects the rate of variation along the beam of the angle of twist of the cross-sections, thus reflecting the torsion of the beam where the cross-sections rotate around the axis  $\mathbf{e}$ ; Figure 6.7 shows the evolution, which is linear according to the two directions of the cross-section plane, of the shear strain.

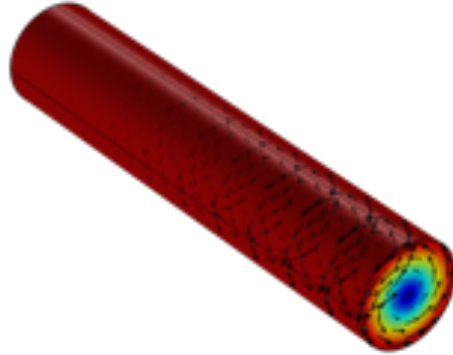


Figure 6.7: Shear strain field in the case of a beam in torsion (the arrows representing the associated displacement field).

**■ Example 6.1 — Expression of the kinematics of a beam in a Cartesian vector basis.** We detail here the kinematics that we have just established in the case of a straight beam, after projection of these relations on the vectors  $(\mathbf{i}_x, \mathbf{i}_y, \mathbf{i}_z)$  of a Cartesian basis, where  $\mathbf{i}_x$  is the beam axis. In this case, the arc length is simply  $s = x \in [0, L]$ , where  $L$  is the length of the beam, and the other two coordinates are  $(\chi_1, \chi_2) = (y, z)$ .

The displacement field at time  $t$  of a point  $M$  of coordinates  $(x, y, z)$  in the vector basis  $(\mathbf{i}_x, \mathbf{i}_y, \mathbf{i}_z)$  can then be written as:

$$\boxed{\mathbf{u}(x, y, z, t) = \mathbf{u}_G(x, t) + \boldsymbol{\theta}(x, t) \wedge (\mathbf{y}\mathbf{i}_y + \mathbf{z}\mathbf{i}_z)}$$

hence the following projections of the displacement in the vector basis  $(\mathbf{i}_x, \mathbf{i}_y, \mathbf{i}_z)$ :

$$\begin{aligned} u_x(x, y, z, t) &= u_{Gx}(x, t) + \theta_y(x, t)z - \theta_z(x, t)y \\ u_y(x, y, z, t) &= u_{Gy}(x, t) - \theta_x(x, t)z \\ u_z(x, y, z, t) &= u_{Gz}(x, t) + \theta_x(x, t)y \end{aligned}$$

where  $(u_{Gx}, u_{Gy}, u_{Gz})$  and  $(\theta_x, \theta_y, \theta_z)$  are respectively the components of  $\mathbf{u}_G$  and  $\boldsymbol{\theta}$  in the basis  $(\mathbf{i}_x, \mathbf{i}_y, \mathbf{i}_z)$ .

After differentiating the displacement components with respect to the spatial coordinates, the infinitesimal strain tensor at point  $M$  and time  $t$  can then be expressed in the vector basis  $(\mathbf{i}_x, \mathbf{i}_y, \mathbf{i}_z)$  as:

$$\boldsymbol{\varepsilon}(x, y, z, t) = \begin{pmatrix} \varepsilon_{xx}(x, y, z, t) & \varepsilon_{xy}(x, y, z, t) & \varepsilon_{xz}(x, y, z, t) \\ \varepsilon_{xy}(x, y, z, t) & 0 & 0 \\ \varepsilon_{xz}(x, y, z, t) & 0 & 0 \end{pmatrix}_{(\mathbf{i}_x, \mathbf{i}_y, \mathbf{i}_z)}$$

with, introducing  $\bullet' = \frac{d\bullet}{dx}$ :

- on the one hand, the longitudinal strain (i.e. along the axis  $\mathbf{i}_x$  of the beam), expressed as:

$$\boxed{\varepsilon_{xx}(x, y, z, t) = \frac{\partial u_x}{\partial x}(x, y, z, t) = u'_{Gx}(x, t) + \theta'_y(x, t)z - \theta'_z(x, t)y}$$

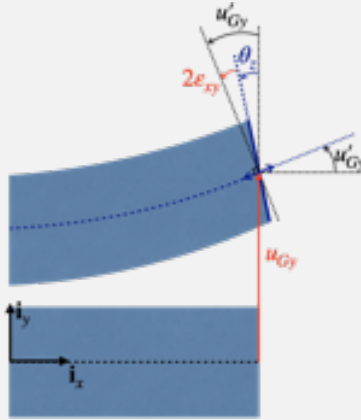
whose terms correspond, for the first one, to the elongation of the beam along  $\mathbf{i}_x$  (uniaxial strain associated with tensile stresses) and, for the other two, to the elongation caused by the bending rotation  $\boldsymbol{\theta} = \theta_y\mathbf{i}_y + \theta_z\mathbf{i}_z$  of the cross-sections, which results in a heterogeneous elongation or shortening of small segments taken parallel to the beam axis;

- and, on the other hand, the distortion  $\gamma_\Sigma$  resulting in:

$$\boxed{\varepsilon_{xy}(x, y, z, t) = \frac{1}{2} \left( \frac{\partial u_x}{\partial y}(x, y, z, t) + \frac{\partial u_y}{\partial x}(x, y, z, t) \right) = \frac{1}{2} (u'_{Gy}(x, t) - \theta_z(x, t)) - \frac{1}{2} \theta'_x(x, t)z}$$

$$\boxed{\varepsilon_{xz}(x, y, z, t) = \frac{1}{2} \left( \frac{\partial u_x}{\partial z}(x, y, z, t) + \frac{\partial u_z}{\partial x}(x, y, z, t) \right) = \frac{1}{2} (u'_{Gz}(x, t) + \theta_y(x, t)) + \frac{1}{2} \theta'_x(x, t)y}$$

the sum of the first two terms of each expression corresponding to the shear strain caused by bending, illustrated in the figure below (for  $\varepsilon_{xy}$  in the case where  $\theta_x = 0$ ), and which will be detailed in Paragraph 6.1.3, and the last term being associated with the angle of twist  $\theta_x$  of the cross-sections around their normal vector, which is the axis  $\mathbf{i}_x$  of the beam.



We also verify that the plane part of the infinitesimal strain tensor (in the plane of the cross-sections) is equal to zero:  $\varepsilon_{yy} = \varepsilon_{zz} = \varepsilon_{yz} = 0$ , since the cross-sections are assumed to be perfectly rigid.

These results effectively correspond to the generic expression determined above:

$$\boldsymbol{\varepsilon} = (u'_{Ge} + \langle \boldsymbol{\theta}'_\Sigma \wedge \mathbf{x}_\Sigma, \mathbf{e} \rangle) \mathbf{e} \otimes \mathbf{e} + (\mathbf{u}'_{G\Sigma} - \boldsymbol{\theta}_\Sigma \wedge \mathbf{e}) \otimes_S \mathbf{e} + (\boldsymbol{\theta}'_e \mathbf{e} \wedge \mathbf{x}_\Sigma) \otimes_S \mathbf{e}$$

which leads to:

$$\begin{aligned} \boldsymbol{\varepsilon} = & (u'_{Gx} + \langle (\boldsymbol{\theta}'_y \mathbf{i}_y + \boldsymbol{\theta}'_z \mathbf{i}_z) \wedge (y \mathbf{i}_y + z \mathbf{i}_z), \mathbf{i}_x \rangle) \mathbf{i}_x \otimes \mathbf{i}_x \\ & + (u'_{Gy} \mathbf{i}_y + u'_{Gz} \mathbf{i}_z - (\boldsymbol{\theta}_y \mathbf{i}_y + \boldsymbol{\theta}_z \mathbf{i}_z) \wedge \mathbf{i}_x) \otimes_S \mathbf{i}_x + (\boldsymbol{\theta}'_x \mathbf{i}_x \wedge (y \mathbf{i}_y + z \mathbf{i}_z)) \otimes_S \mathbf{i}_x \end{aligned}$$

when we express  $\mathbf{e} = \mathbf{i}_x$ ,  $\mathbf{e}_{\chi_1} = \mathbf{i}_y$ ,  $\mathbf{e}_{\chi_2} = \mathbf{i}_z$ , and  $\mathbf{x}_\Sigma = y \mathbf{i}_y + z \mathbf{i}_z$ . ■

**Summary 6.1 — Kinematics of a (Timoshenko) beam .** The basic kinematic assumption for a beam is to consider that the cross-sections are perfectly rigid, which implies a displacement field of the form:

$$\mathbf{u}(s, \chi_1, \chi_2, t) = \mathbf{u}_G(s, t) + \boldsymbol{\theta}(s, t) \wedge \mathbf{x}_\Sigma(\chi_1, \chi_2), \forall t$$

for any point  $M$  of coordinates  $(s, \chi_1, \chi_2)$  in the vector basis  $(\mathbf{e}, \mathbf{e}_{\chi_1}, \mathbf{e}_{\chi_2})$  associated with the beam.  $\mathbf{u}_G$  and  $\boldsymbol{\theta}$  refer respectively to the displacement of the cross-section centre  $G$  and the (small) rotation vector of the cross-section  $\Sigma$  of coordinate  $s$ , while  $\mathbf{x}_\Sigma$  is the placement vector in the cross-section of the point under study.

The infinitesimal strain tensor is expressed, in the case of a straight beam, and by noting  $\bullet' = \frac{d\bullet}{ds}$ , as:

$$\boldsymbol{\varepsilon} = \varepsilon_{ee} \mathbf{e} \otimes \mathbf{e} + \boldsymbol{\gamma}_\Sigma \otimes_S \mathbf{e} = (u'_{Ge} + \langle \boldsymbol{\theta}'_\Sigma \wedge \mathbf{x}_\Sigma, \mathbf{e} \rangle) \mathbf{e} \otimes \mathbf{e} + (\mathbf{u}'_{G\Sigma} - \boldsymbol{\theta}_\Sigma \wedge \mathbf{e}) \otimes_S \mathbf{e} + (\boldsymbol{\theta}'_e \mathbf{e} \wedge \mathbf{x}_\Sigma) \otimes_S \mathbf{e}$$

with the projections  $\bullet_e = \langle \bullet, \mathbf{e} \rangle$  on the axis  $\mathbf{e}$  and  $\bullet_\Sigma = \bullet - \langle \bullet, \mathbf{e} \rangle \mathbf{e}$  in the plane of the cross-section  $\Sigma$ . This corresponds to Timoshenko beam model.



The assumption of a perfectly rigid cross-section is only an approximation: thus, in the case of a tensile load along the beam axis, we expect in reality to have a reduction in the transverse dimensions of the beam due to Poisson's effect. In fact, this approximation is not prejudicial to the problems that will be solved, by virtue of the antiplane form of the stress tensor, which will be adopted in Paragraph 6.2.1.

Besides, the hypothesis of a perfectly rigid cross-section is also undermined in the case of the torsion of beams of non-circular cross-sections: indeed, we saw in Example 5.3 on page 126 that, in this case, the so-called phenomenon of “warping” appeared, consisting in an out-of-plane deformation of the different cross-sections, which also rotate around their normal vector. Here again, this is not prejudicial to the solution of a beam problem, provided one takes into account the modification, caused by the warping, of the torsional rigidity of the beam, as highlighted in Example 5.6 on page 136: this correction then requires solving the associated continuum mechanics problem.

### 6.1.3 Euler-Bernoulli hypothesis

When the beams are “thin”, i.e. when the ratio between the transverse dimensions and the length of the beam is very small (e. g.  $H/L \ll 1$  in the case of a three-point bending test), it is possible to introduce an additional kinematic assumption, called Euler-Bernoulli hypothesis, consisting in assuming that the cross-sections, which are initially perpendicular to the beam axis, remain perpendicular to the deformed neutral axis. Figure 6.8 proposes an experimental illustration of this assumption in the case of a three-point bending test analyzed by digital image correlation: it is clear that the different cross-sections of the deformed beam are perpendicular to the deformed neutral axis represented in blue, whose placement vector is given by  $\mathbf{x}_G(s) = s\mathbf{e} + \mathbf{u}_G(s)$ , at a given time.

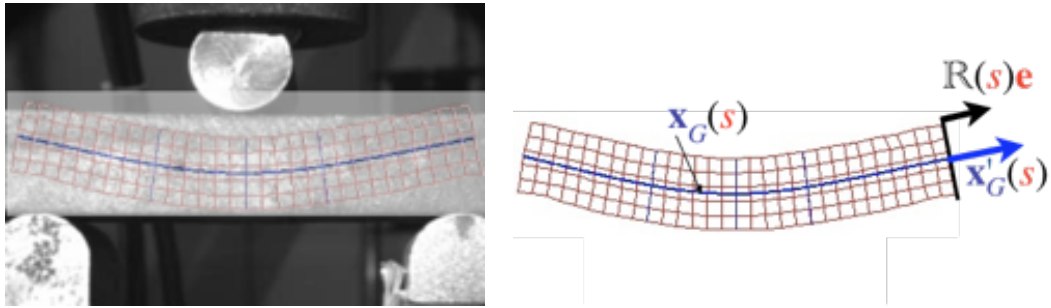


Figure 6.8: Experimental illustration of Euler-Bernoulli hypothesis in the case of a three-point bending test (digital image correlation measurements).

#### Displacement expression

Let us study the consequence of this hypothesis on the displacement field and strain tensor for a beam. More precisely, we must express that each cross-section remains perpendicular to the vector tangent to the neutral axis: by definition, this tangent vector is collinear to the vector  $\mathbf{x}'_G(s) = (s\mathbf{e} + \mathbf{u}_G(s))' = \mathbf{e} + \mathbf{u}'_G(s)$ . In addition, since each cross-section is perpendicular to the axis  $\mathbf{e}$  in the reference configuration, the normal vector to this cross-section in the current configuration can be expressed as  $\mathbb{R}\mathbf{e} = (\mathbb{I} + \theta\mathbf{a}^\wedge)\mathbf{e} = \mathbf{e} + \boldsymbol{\theta} \wedge \mathbf{e}$ . Euler-Bernoulli hypothesis then consists in expressing that these last two vectors are collinear to each other:

$$(\mathbf{e} + \mathbf{u}'_G) \wedge (\mathbf{e} + \boldsymbol{\theta} \wedge \mathbf{e}) = \mathbf{0}$$

or, up to order one, after expanding this vector product:

$$\mathbf{0} = \mathbf{u}'_G \wedge \mathbf{e} + \mathbf{e} \wedge (\boldsymbol{\theta} \wedge \mathbf{e}) = -\mathbf{e} \wedge \mathbf{u}'_{G\Sigma} + \boldsymbol{\theta} - \langle \boldsymbol{\theta}, \mathbf{e} \rangle \mathbf{e} = -\mathbf{e} \wedge \mathbf{u}'_{G\Sigma} + \boldsymbol{\theta}_\Sigma$$

where, finally:

$$\boldsymbol{\theta}_\Sigma = \mathbf{e} \wedge \mathbf{u}'_{G\Sigma}$$

or else:

$$\mathbf{u}'_{G\Sigma} = \boldsymbol{\theta}_\Sigma \wedge \mathbf{e}$$

Euler-Bernoulli hypothesis thus makes it possible to link the bending rotation of each cross-section to the derivative of the transverse displacement of the neutral axis.

By introducing this relation into the expression of the displacement determined in the previous paragraph, we finally obtain that the displacement of any point  $M$  of the beam, of coordinates  $(s, \chi_1, \chi_2)$ , is written as:

$$\mathbf{u}(s, \chi_1, \chi_2, t) = \mathbf{u}_G(s, t) + (\theta_e(s, t)\mathbf{e} + \mathbf{e} \wedge \mathbf{u}'_{G\Sigma}(s, t)) \wedge \mathbf{x}_\Sigma(\chi_1, \chi_2), \forall t$$

Thus, taking into account Euler-Bernoulli hypothesis allows us to reduce to four (instead of six) the number of scalar functions required to describe the displacement of all the points of a beam:

- the three components of the displacement  $\mathbf{u}_G$  of the neutral axis;
- the angle of twist  $\theta_e$  of each cross-section, knowing that the two components of  $\boldsymbol{\theta}_\Sigma$  are related to  $\mathbf{u}_{G\Sigma}$  because of Euler-Bernoulli hypothesis.

### Infinitesimal strain tensor

When Euler-Bernoulli hypothesis is taken into account, the expression of the infinitesimal strain tensor becomes, in the case of a straight beam:

$$\boldsymbol{\epsilon} = (u'_{Ge} + \langle (\mathbf{e} \wedge \mathbf{u}'_{G\Sigma})' \wedge \mathbf{x}_\Sigma, \mathbf{e} \rangle) \mathbf{e} \otimes \mathbf{e} + (\mathbf{u}'_{G\Sigma} - (\mathbf{e} \wedge \mathbf{u}'_{G\Sigma}) \wedge \mathbf{e}) \otimes_S \mathbf{e} + (\theta'_e \mathbf{e} \wedge \mathbf{x}_\Sigma) \otimes_S \mathbf{e}$$

or, finally, after the development of all the vector triple products:

$$\boldsymbol{\epsilon} = (u'_{Ge} - \langle \mathbf{u}''_{G\Sigma}, \mathbf{x}_\Sigma \rangle) \mathbf{e} \otimes \mathbf{e} + (\theta'_e \mathbf{e} \wedge \mathbf{x}_\Sigma) \otimes_S \mathbf{e}$$

Thus, the main effect of this hypothesis is the cancellation of the “transverse shear” term, i.e. the distortion associated with the bending rotation of the cross-sections: indeed, since we assumed that these latter remained perpendicular to the deformed neutral axis, the initially right angles remain right, and there is, therefore, no distortion associated with the bending of the beam.

Figure 6.9 allows for experimentally verifying the validity of this hypothesis in the case of a three-point bending test: the values of the shear strain field, obtained by digital image correlation, are much lower than those of the longitudinal strain field, except in the vicinity of the supports where higher values are measured. This effect would be more pronounced if the beam had an even smaller  $H/L$  ratio: in this respect, the beam model based on Euler-Bernoulli hypothesis is an approximation of Timoshenko beam model.

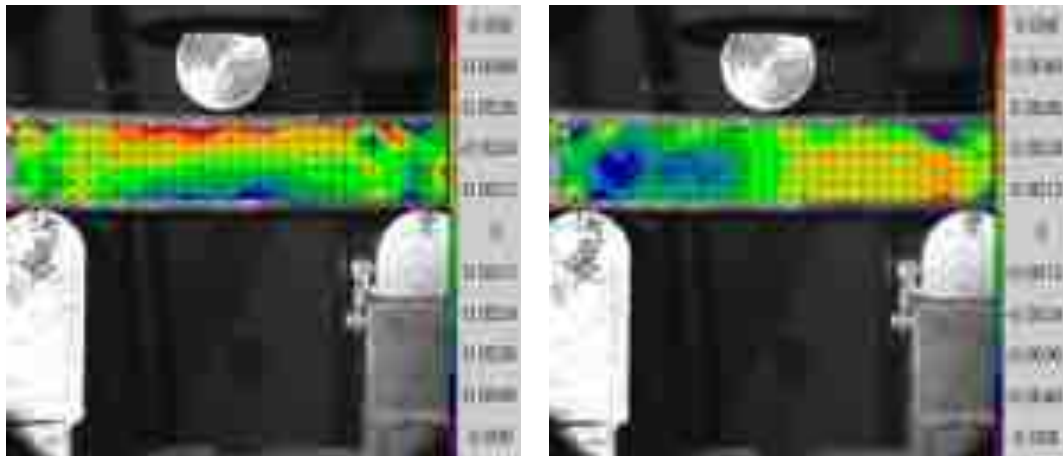


Figure 6.9: Longitudinal strain (left) and shear strain (right) fields measured by digital image correlation in the case of a three-point bending test.

In addition, it is also verified that experimentally, the longitudinal strain field evolves in a substantially linear manner in the thickness except, once again, in the vicinity of the supports; according to Saint-Venant's principle, this allows for verifying the validity of the longitudinal strain for the proposed beam model:

$$\varepsilon_{ee} = u'_{Ge} - \langle \mathbf{u}_{G\Sigma}'', \mathbf{x}_\Sigma \rangle$$

showing that the effects of elongation and bending simply add up.

**■ Example 6.2 — Expression of the kinematics of an Euler-Bernoulli beam in a Cartesian vector basis.** Here we use the case of Example 6.1, where the straight beam is of axis  $\mathbf{i}_x$ , with cross-sections initially in the plane  $(\mathbf{i}_y, \mathbf{i}_z)$ .

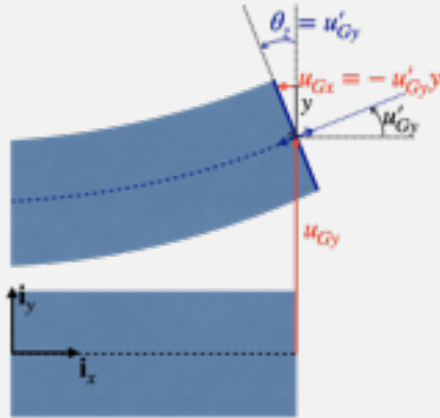
Taking into account Euler-Bernoulli hypothesis then allows us to write the displacement at time  $t$  of a point  $M$  of coordinates  $(x, y, z)$  in the vector basis  $(\mathbf{i}_x, \mathbf{i}_y, \mathbf{i}_z)$  as:

$$\mathbf{u}(x, y, z, t) = \mathbf{u}_G(x, t) + (\theta_x(x, t)\mathbf{i}_x + \mathbf{i}_x \wedge \mathbf{u}'_{G\Sigma}(x, t)) \wedge (y\mathbf{i}_y + z\mathbf{i}_z)$$

hence the following projections of the displacement field in the vector basis  $(\mathbf{i}_x, \mathbf{i}_y, \mathbf{i}_z)$ :

$$\begin{aligned} u_x(x, y, z, t) &= u_{Gx}(x, t) - u'_{Gy}(x, t)y - u'_{Gz}(x, t)z \\ u_y(x, y, z, t) &= u_{Gy}(x, t) - \theta_x(x, t)z \\ u_z(x, y, z, t) &= u_{Gz}(x, t) + \theta_x(x, t)y \end{aligned}$$

as shown, in the case of the component  $u_x$  and a bending angle  $\theta_z < 0$  around the axis  $\mathbf{i}_z$ , in the figure below (where  $u'_{Gz} = 0$  and  $\theta_x = 0$ ).



After differentiation, the infinitesimal strain tensor at point  $M$  can then be expressed, at time  $t$  and in the vector basis  $(\mathbf{i}_x, \mathbf{i}_y, \mathbf{i}_z)$ , as:

$$\boldsymbol{\varepsilon}(x, y, z) = \begin{pmatrix} \varepsilon_{xx}(x, y, z, t) & \varepsilon_{xy}(x, y, z, t) & \varepsilon_{xz}(x, y, z, t) \\ \varepsilon_{xy}(x, y, z, t) & 0 & 0 \\ \varepsilon_{xz}(x, y, z, t) & 0 & 0 \end{pmatrix}_{(\mathbf{i}_x, \mathbf{i}_y, \mathbf{i}_z)}$$

with:

- on the one hand, the longitudinal strain being expressed as:

$$\varepsilon_{xx}(x, y, z, t) = \frac{\partial u_x}{\partial x}(x, y, z, t) = u'_{Gx}(x, t) - u''_{Gy}(x, t)y - u''_{Gz}(x, t)z$$

whose terms reflect, as before, for the first one, the elongation of the beam along  $\mathbf{i}_x$  and, for the other two, the elongation caused by the bending of the beam, which is now directly related to the "curvature" of this latter, associated with the second derivatives  $u''_{Gy}$  and  $u''_{Gz}$  of the transverse displacement of the neutral axis;

- and, on the other hand, the shear strain resulting in:

$$\varepsilon_{xy}(x, y, z, t) = \frac{1}{2} \left( \frac{\partial u_x}{\partial y}(x, y, z, t) + \frac{\partial u_y}{\partial x}(x, y, z, t) \right) = -\frac{1}{2} \theta'_x(x, t) z$$

$$\varepsilon_{xz}(x, y, z, t) = \frac{1}{2} \left( \frac{\partial u_x}{\partial z}(x, y, z, t) + \frac{\partial u_z}{\partial x}(x, y, z, t) \right) = \frac{1}{2} \theta'_x(x, t) y$$

for which only remains the effect related to the torsion of the beam, associated with the rotation of the cross-sections around the axis of the beam.

This result is of course based on the generic expression of the infinitesimal strain tensor:

$$\boldsymbol{\varepsilon} = (u'_{Ge} - \langle \mathbf{u}_{G\Sigma}'', \mathbf{x}_\Sigma \rangle) \mathbf{e} \otimes \mathbf{e} + (\theta'_e \mathbf{e} \wedge \mathbf{x}_\Sigma) \otimes_S \mathbf{e}$$

expressing  $\mathbf{e} = \mathbf{i}_x$ ,  $\mathbf{e}_{\chi_1} = \mathbf{i}_y$ ,  $\mathbf{e}_{\chi_2} = \mathbf{i}_z$ , and  $\mathbf{x}_\Sigma = y\mathbf{i}_y + z\mathbf{i}_z$ . ■

**Summary 6.2 — Kinematics of a (Euler-Bernoulli) beam.** In the case of thin beams, we can add to the kinematics of a Timoshenko beam Euler-Bernoulli hypothesis, which consists in expressing that the cross-sections remain perpendicular to the deformed neutral axis:

$$\boldsymbol{\Theta}_\Sigma(s, t) = \mathbf{e} \wedge \mathbf{u}'_{G\Sigma}(s, t), \forall s, \forall t$$

where  $\mathbf{u}'_{G\Sigma} = \mathbf{u}'_G - \langle \mathbf{u}'_G, \mathbf{e} \rangle \mathbf{e}$ , which finally implies a displacement field of the form:

$$\mathbf{u}(s, \chi_1, \chi_2, t) = \mathbf{u}_G(s, t) + (\theta_e(s, t) \mathbf{e} + \mathbf{e} \wedge \mathbf{u}'_{G\Sigma}(s, t)) \wedge \mathbf{x}_\Sigma(\chi_1, \chi_2), \forall t$$

for any point  $M$  of coordinates  $(s, \chi_1, \chi_2)$  in the vector basis  $(\mathbf{e}, \mathbf{e}_{\chi_1}, \mathbf{e}_{\chi_2})$  associated with the beam.  $\mathbf{u}_G$  and  $\theta_e$  refer respectively to the displacement of the cross-section centre  $G$  and the (small) angle of twist (i.e. around the  $\mathbf{e}$  axis) of the cross-section  $\Sigma$  of coordinate  $s$ , while  $\mathbf{x}_\Sigma$  is the placement vector in the cross-section of the point under study.

The infinitesimal strain tensor is then expressed, in the case of a straight beam, as:

$$\boldsymbol{\varepsilon} = \varepsilon_{ee} \mathbf{e} \otimes \mathbf{e} + \boldsymbol{\gamma}_\Sigma \otimes_S \mathbf{e} = (u'_{Ge} - \langle \mathbf{u}_{G\Sigma}'', \mathbf{x}_\Sigma \rangle) \mathbf{e} \otimes \mathbf{e} + (\theta'_e \mathbf{e} \wedge \mathbf{x}_\Sigma) \otimes_S \mathbf{e}$$

This corresponds to Euler-Bernoulli beam model.

**R** In the case of a curved beam, the expression of the displacement field remains the same as in Summaries 6.1 and 6.2. However, when calculating the infinitesimal strain tensor, it is necessary to take into account the dependence of the vectors  $\mathbf{e}$ ,  $\mathbf{e}_{\chi_1}$  and  $\mathbf{e}_{\chi_2}$  on the arc length  $s$ .

So, since  $\mathbf{e}$  is a unit vector, we know that  $(\|\mathbf{e}(s)\|^2)' = 2\langle \mathbf{e}'(s), \mathbf{e}(s) \rangle = 0, \forall s$ , and we then define the normal vector as:

$$\mathbf{n}(s) = \rho(s) \mathbf{e}'(s), \forall s$$

where  $\rho$  is called “radius of curvature” of the neutral axis, and is such that the normal vector  $\mathbf{n}$  is unitary.

In addition, the “binormal” vector is defined as:

$$\mathbf{b}(s) = \mathbf{e}(s) \wedge \mathbf{n}(s), \forall s$$

which provides a natural orthonormal vector basis associated with the geometry of the beam, the vectors  $\mathbf{n}(s)$  and  $\mathbf{b}(s)$  being in the plane of the cross-section of arc length  $s$ . In particular, we can show the following relations, which are useful when differentiating kinematic expressions with respect to  $s$ :

$$\mathbf{n}'(s) = -\frac{1}{\rho(s)} \mathbf{e}(s) - \frac{1}{\tau(s)} \mathbf{b}(s), \forall s$$

where  $\tau$  is called the “radius of torsion” of the neutral axis, and:

$$\mathbf{b}'(s) = \frac{1}{\tau(s)} \mathbf{n}(s), \forall s$$

## 6.2 Internal loads in a beam

In addition to the above, the second ingredient of a beam model is to make assumptions about the internal forces (or “internal loads”) within a beam so as to assume a simplified form of the stress tensor, and to arrive at a condensed representation of these internal forces.

### 6.2.1 Assumption on the stresses

Here we take the example of a beam clamped at one end on a fixed support, and subjected to a uniform pressure on its upper surface. Since the internal forces associated with this case of study are not directly measurable, an alternative may be to rely on numerical simulation to determine the stress field within the beam by addressing the general problem of continuum mechanics. We will then focus on the stress tensor that we develop as follows:

$$\boldsymbol{\sigma} = \boldsymbol{\sigma}^\Sigma + \boldsymbol{\tau}_\Sigma \otimes \mathbf{e} + \mathbf{e} \otimes \boldsymbol{\tau}_\Sigma + \sigma_{ee} \mathbf{e} \otimes \mathbf{e}$$

or, in matrix form in the vector basis  $(\mathbf{e}, \mathbf{e}_{\chi_1}, \mathbf{e}_{\chi_2})$ :

$$\boldsymbol{\sigma} = \begin{pmatrix} \sigma_{ee} & \boldsymbol{\tau}_\Sigma^\top \\ \boldsymbol{\tau}_\Sigma & \boldsymbol{\sigma}^\Sigma \end{pmatrix}$$

decomposed into blocks to distinguish between what is relative to the axis  $\mathbf{e}$  of the beam, and to the plane  $\Sigma$  of the cross-section. In particular,  $\boldsymbol{\sigma}^\Sigma$  refers to the plane part of the stress tensor  $\boldsymbol{\sigma}$  in the plane of the cross-section, while the quantities  $\sigma_{ee}$  and  $\boldsymbol{\tau}_\Sigma = (\boldsymbol{\sigma}\mathbf{e})_\Sigma = \boldsymbol{\sigma}\mathbf{e} - \langle \boldsymbol{\sigma}\mathbf{e}, \mathbf{e} \rangle \mathbf{e}$  refer respectively to the normal stress, and the shear stress in the plane of the cross-section.

Figure 6.10 then represents a certain number of components of the stress tensor  $\boldsymbol{\sigma}$  in a cross-section located “far enough away” from the fixed support condition (in the sense of Saint-Venant’s principle). It thus shows that the orders of magnitude of each component are very different: the predominant component is the normal stress  $\sigma_{ee}$  along the beam axis, which is much stronger than the shear stress  $\boldsymbol{\tau}_\Sigma$  in the cross-section, this latter being much larger than the components of the plane part of the stress tensor  $\boldsymbol{\sigma}^\Sigma$ .

Besides, an asymptotic study, the detail of which is beyond the scope of this course, would establish that, generally speaking, in a beam, we have:

$$\frac{\|\boldsymbol{\sigma}^\Sigma\|}{|\sigma_{ee}|} = O\left(\frac{H^2}{L^2}\right)$$

where  $H$  is an order of magnitude of the transverse dimensions of the beam and  $L$  is its length.

In conclusion, the hypothesis systematically adopted in beam models is to assume that the plane part of the stress tensor is equal to zero:

$$\boldsymbol{\sigma}^\Sigma = 0$$

which is to say that the stress tensor is antiplane. This is consistent with the kinematic assumption of a perfectly rigid cross-section, seen above: indeed, this implies that the components of the internal forces in the plane of the cross-section are not accessible since this latter does not deform. We will therefore not attempt to estimate them here since they can be neglected.

Consequently, the knowledge of the internal forces in a beam is limited to that of the stress vector that is considered when performing a cut according to a cross-section of the beam:

$$\boldsymbol{\sigma}\mathbf{e} = \sigma_{ee}\mathbf{e} + \boldsymbol{\tau}_\Sigma = \sigma_{ee}\mathbf{e} + \sigma_{\chi_1 e}\mathbf{e}_{\chi_1} + \sigma_{\chi_2 e}\mathbf{e}_{\chi_2}$$

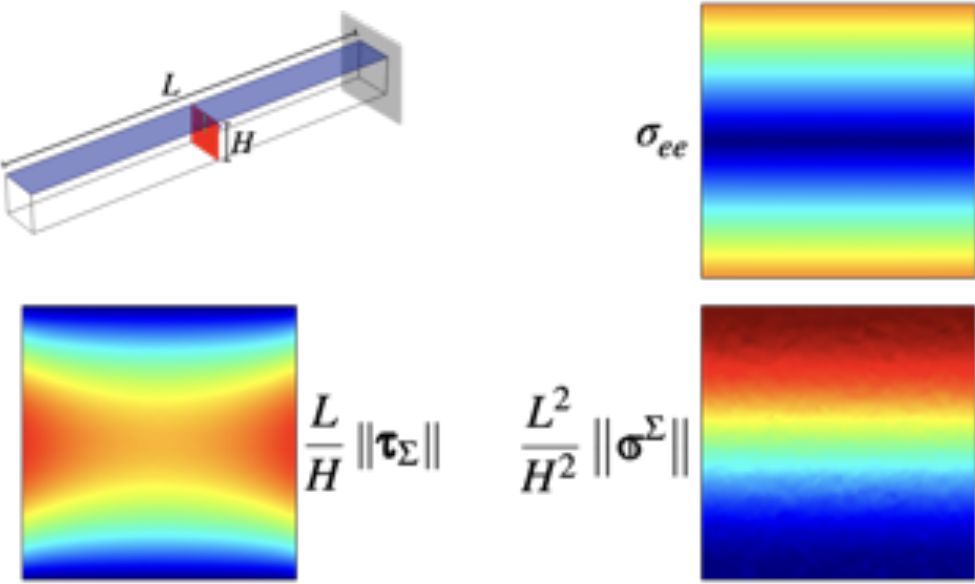


Figure 6.10: Champ des contraintes obtenu par simulation numérique dans une section de poutre soumise à de la flexion.

which is a cut with normal vector the axis  $\mathbf{e}$  of the beam. In order to simplify the calculations associated with the solution of a beam model, we will then limit ourselves to describing the internal forces in terms of the resultant force and moment of these loadings on each cross-section, which, again, is consistent with assuming that these cross-sections are perfectly rigid. This is the purpose of the following two paragraphs.

### 6.2.2 Resultant force of the internal loads and associated equilibrium equation

Thus, we study a beam of axis  $\mathbf{e}$  that we cut according to the cross-section  $\Sigma$  of coordinate  $s$ , in order to get, at time  $t$  and at any point  $M$  of coordinates  $(\chi_1, \chi_2)$  in the cross-section, the stress vector:

$$\boldsymbol{\sigma}(s, \chi_1, \chi_2, t) \mathbf{e} = \sigma_{ee}(s, \chi_1, \chi_2, t) \mathbf{e} + \boldsymbol{\tau}_\Sigma(s, \chi_1, \chi_2, t)$$

where  $\sigma_{ee} = \langle \boldsymbol{\sigma} \mathbf{e}, \mathbf{e} \rangle$  is the normal stress in the cross-section, and  $\boldsymbol{\tau}_\Sigma = (\boldsymbol{\sigma} \mathbf{e})_\Sigma = \boldsymbol{\sigma} \mathbf{e} - \langle \boldsymbol{\sigma} \mathbf{e}, \mathbf{e} \rangle \mathbf{e}$  is the shear stress in the plane of the cross-section.

**Resultant force of the internal loads.** The resultant force  $\mathbf{R}$  of the internal loads in the cross-section of coordinate  $s$  is defined in a classical way as the resultant force associated with the stress vector in the cross-section:

$$\mathbf{R}(s, t) = \int_{\Sigma(s)} \boldsymbol{\sigma}(s, \chi_1, \chi_2, t) \mathbf{e} dS, \quad \forall s \in [0, L], \quad \forall t$$

This definition is then equivalent to expressing the local forces exerted by the “downstream” segment of the beam (i.e. the beam segment of coordinates strictly greater than  $s$ ) on the “upstream” segment (i.e. the beam segment of coordinates strictly smaller than  $s$ ), since we have chosen, to express the stress vector,  $\mathbf{n} = \mathbf{e}$  as the outer unit normal vector.

The following components of the resultant force of the internal loads, represented in Figure 6.11, are then defined as follows:

- the component  $R_e = \langle \mathbf{R}, \mathbf{e} \rangle$ , called “axial force”, or “normal force” (also noted as  $N$ );

- the vector  $\mathbf{R}_\Sigma = \mathbf{R} - \langle \mathbf{R}, \mathbf{e} \rangle \mathbf{e}$ , called “shear force”, with components  $R_{\chi_1}$  and  $R_{\chi_2}$  in the vector basis  $(\mathbf{e}_{\chi_1}, \mathbf{e}_{\chi_2})$  (also noted as  $T_{\chi_1}$  and  $T_{\chi_2}$ ).

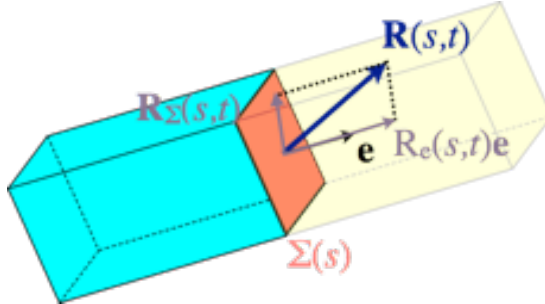


Figure 6.11: Definition of the components of the resultant force of the internal loads.



The choice of orientation in the definition of the resultant force of internal loads is purely conventional. This latter could also have been defined as the resultant force of the action of the “upstream” segment on the “downstream” segment of the beam, considering an outer unit normal vector  $\mathbf{n} = -\mathbf{e}$ :

$$\tilde{\mathbf{R}} = \int_{\Sigma(s)} \sigma(-\mathbf{e}) dS$$

a convention that is also found in Anglo-Saxon countries. It is therefore essential to specify the sign convention adopted before solving a beam problem.

#### Equilibrium equation for the resultant force: global approach

We will now determine the equilibrium equation that this resultant force, in the static or quasi-static framework, must satisfy. First of all, we assume that, like any continuous medium, the beam is subjected to volume force densities  $\mathbf{f}_V$  in its domain  $\Omega$ , and surface force densities  $\mathbf{f}_S$  on the boundary  $\partial\Omega$  of its domain.

If we isolate, as shown in Figure 6.12, a segment  $\omega$  of beam from the cut of the beam into two parts at the cross-section  $\Sigma$  of coordinate  $s$ , we can establish that this segment is subjected:

- at 0 to the resultant force  $\mathbf{R}_0$  of the external actions on this cross-section;
- at  $s$  to the resultant force of the internal loads on this cross-section;
- to external actions represented by volume force densities  $\mathbf{f}_V$  and surface force densities  $\mathbf{f}_S$ .

The static equilibrium equation of this segment  $\omega$  is then written as:

$$\int_{\omega} \mathbf{f}_V dV + \int_{\partial_l \omega} \mathbf{f}_S dS + \int_{\Sigma(0)} \mathbf{f}_S dS + \int_{\Sigma(s)} \sigma \mathbf{e} dS = \mathbf{0}$$

where the surface integrals are distinguished according to whether they concern the two cross-sections of coordinates 0 and  $s$  respectively, or the lateral surface  $\partial_l \omega$  of the segment. By introducing the resultant force of the internal loads at  $s$  and the resultant force associated with the external actions at 0, then by decomposing the integrals, we obtain:

$$\int_0^s \int_{\Sigma} \mathbf{f}_V dS ds + \int_0^s \int_{\partial\Sigma} \mathbf{f}_S dl ds + \mathbf{R}_0 + \mathbf{R}(s) = \mathbf{0}$$

where  $\partial\Sigma$  refers to the boundary of the cross-section  $\Sigma$ .

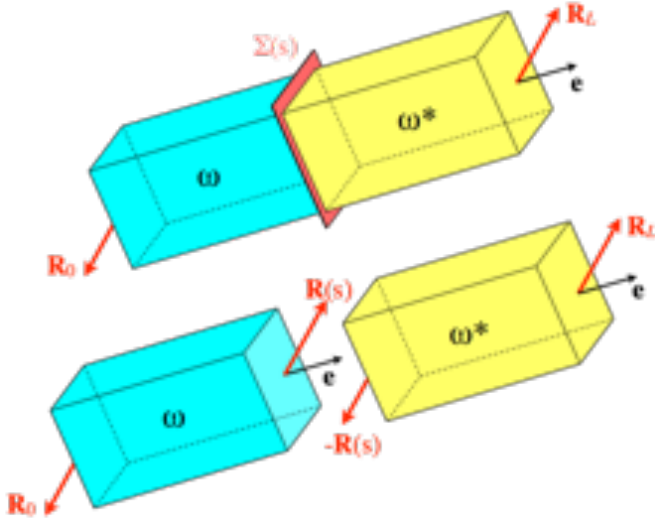


Figure 6.12: Equilibrium for the resultant force: the beam is cut into two segments at the cross-section  $\Sigma(s)$ .

**Line force density.** Knowing the volume and surface force densities exerted on the beam, we define an equivalent line force density  $\mathbf{f}_L$  as:

$$\mathbf{f}_L(s) = \int_{\Sigma(s)} \mathbf{f}_V(s, \chi_1, \chi_2) dS + \int_{\partial\Sigma(s)} \mathbf{f}_S(s, \chi_1, \chi_2) dl$$

for any cross-section  $\Sigma$  of coordinate  $s$  distinct from the ends of the beam. Considering the dimensions of the volume force densities  $\mathbf{f}_V$  (in  $N/m^3$ ) on the one hand, and surface force densities  $\mathbf{f}_S$  (in  $N/m^2$ ) on the other hand, the density  $\mathbf{f}_L$  has as units  $N/m$ , and is therefore effectively homogeneous to a line force density.

With this definition, the force equilibrium equation becomes:

$$\int_0^s \mathbf{f}_L(\xi) d\xi + \mathbf{R}_0 + \mathbf{R}(s) = \mathbf{0}, \quad \forall s \in (0, L)$$

which allows for determining the expression of the resultant force  $\mathbf{R}$  along the neutral axis of the beam. This static equilibrium equation is also valid in the quasi-static case since it amounts to neglecting the terms of inertia in the equilibrium equation of the segment  $\omega$ ; on the other hand, the different quantities can then depend on time  $t$ .

Similarly, the isolation of the other segment  $\omega^*$  implies to take into account:

- at  $L$  the resultant force  $\mathbf{R}_L$  of the external actions on this cross-section;
- at  $s$  the resultant force of the internal loads on this cross-section, which is then expressed as  $-\mathbf{R}(s)$  since it is the action of the “upstream” part of the beam on the “downstream” part;
- external actions represented by volume force densities  $\mathbf{f}_V$  and surface force densities  $\mathbf{f}_S$ .

By doing the same as before, we obtain, in terms of resultant forces:

$$\int_s^L \mathbf{f}_L(\xi) d\xi + \mathbf{R}_L - \mathbf{R}(s) = \mathbf{0}, \quad \forall s \in (0, L)$$

**R** If the choice of the isolated segment to express the resultant force of the internal loads is arbitrary, the two expressions naturally lead to the same result. Indeed, if we add the two equilibrium equations, we find:

$$\int_0^L \mathbf{f}_L(\xi) d\xi + \mathbf{R}_0 + \mathbf{R}_L = \mathbf{0}$$

which corresponds to the global force equilibrium of the entire beam.

**Summary 6.3 — Equilibrium equation for the resultant force of the internal loads (global approach).** The force equilibrium equation of a beam subjected to volume force densities  $\mathbf{f}_V$  and surface force densities  $\mathbf{f}_S$  is written, in the static case and for the global approach, as:

$$\int_0^s \mathbf{f}_L(\xi) d\xi + \mathbf{R}_0 + \mathbf{R}(s) = \mathbf{0}, \forall s \in (0, L)$$

or as:

$$\int_s^L \mathbf{f}_L(\xi) d\xi + \mathbf{R}_L - \mathbf{R}(s) = \mathbf{0}, \forall s \in (0, L)$$

where  $\mathbf{f}_L$  is the line force density equivalent to the densities  $\mathbf{f}_V$  and  $\mathbf{f}_S$ :

$$\mathbf{f}_L(s) = \int_{\Sigma(s)} \mathbf{f}_V(s, \chi_1, \chi_2) dS + \int_{\partial\Sigma(s)} \mathbf{f}_S(s, \chi_1, \chi_2) dl$$

and  $\mathbf{R}_0$  and  $\mathbf{R}_L$  are the resultant forces of the external actions exerted on the cross-sections of respective coordinates  $s = 0$  and  $s = L$ .



Strictly speaking, the previous relations do not allow for determining the expression of the resultant force of the internal loads on the extreme cross-sections of the beam, at  $s = 0$  and  $s = L$ . For these latter, it is sufficient to consider the external surface forces exerted on the corresponding cross-section to make the link with the definition of the resultant force  $\mathbf{R}$ .

Thus, if  $\mathbf{R}_0$  and  $\mathbf{R}_L$  are the resultant forces of the external actions exerted on the cross-sections of coordinates  $s = 0$  and  $s = L$  respectively, we obtain, by definition:

$$\mathbf{R}_0 = \int_{\Sigma(0)} \mathbf{f}_S dS = \int_{\Sigma(0)} \sigma(-\mathbf{e}) dS = -\mathbf{R}(0)$$

since the outer unit normal vector for the beam at  $s = 0$  is  $\mathbf{n} = -\mathbf{e}$ , and:

$$\mathbf{R}_L = \int_{\Sigma(L)} \mathbf{f}_S dS = \int_{\Sigma(L)} \sigma\mathbf{e} dS = \mathbf{R}(L)$$

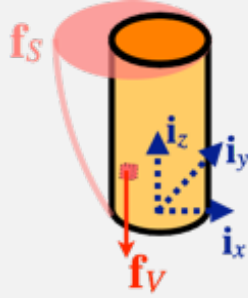
since the outer unit normal vector for the beam at  $s = L$  is  $\mathbf{n} = \mathbf{e}$ .

These differences in signs, depending on whether we are in  $s = 0$  or  $s = L$ , can also be interpreted with the sign convention established above, when approaching the end of the beam. Thus, the action from the outside on the cross-section of coordinate  $L$  is indeed an action of the “downstream” part on the “upstream” part (even if there is no beam strictly speaking beyond  $s = L$ ), which justifies the sign “+”:  $\mathbf{R}(L) = \mathbf{R}_L$ .

Conversely, the action from the outside on the cross-section of coordinate 0 can be seen as an action from the “upstream” part of the beam on the “downstream” part (even if there is no beam strictly speaking before  $s = 0$ ), hence the need to change the sign to remain consistent with the definition of the resultant force of the internal loads:  $\mathbf{R}(0) = -\mathbf{R}_0$ .

Of course, these expressions must be modified if the opposite sign convention is adopted for defining the resultant force of the internal loads.

■ **Example 6.3 — Resultant force of the internal loads for a chimney exposed to wind: global approach.** A chimney is considered as a straight beam with a vertical axis  $\mathbf{i}_z$  (going upwards) and an annular cross-section of inner radius  $r_i$  and outer radius  $r_e$ .



This latter is associated with the vector basis  $(\mathbf{i}_r(\theta), \mathbf{i}_\theta(\theta))$  such that  $(O, \mathbf{i}_r(\theta), \mathbf{i}_\theta(\theta), \mathbf{i}_z)$  defines a cylindrical coordinate system where  $O$  is the centre of the cross-section in contact with the ground. A point  $M$  of the chimney is therefore positioned by its coordinates  $(r, \theta, z)$  in this system:

$$\mathbf{p} \approx \mathbf{x} = \mathbf{x}_G(z) + \mathbf{x}_\Sigma = z\mathbf{i}_z + r\mathbf{i}_r(\theta), \forall r \in [r_i, r_e], \forall \theta \in [0, 2\pi], \forall z \in [0, H]$$

by adopting, as before, the infinitesimal deformation hypothesis. It is also assumed that the problem is static and does not depend on time.

In addition, this chimney is subjected to two actions:

- the action of gravity at any point of its volume:  $\mathbf{f}_V = -\rho g \mathbf{i}_z$ , where the density  $\rho$  is assumed to be uniform;
- the action of the wind at any point on its outer lateral surface  $\partial/\Omega$ :  $\mathbf{f}_S = -Kz^2 \sin^2(\theta/2) \mathbf{i}_r(\theta)$ , where  $K$  is a supposedly known constant.

If the chimney is cut at a cross-section of arbitrary altitude  $z$ , the isolation of the “downstream” segment  $\omega^*$  (i.e. above the  $z$  cut) allows us to write, in statics, that:

$$\int_z^H \mathbf{f}_L(\xi) d\xi + \mathbf{R}_H - \mathbf{R}(z) = \mathbf{0}$$

where  $\mathbf{R}_H = \mathbf{0}$  since the upper surface of the chimney is free of forces, and where the line force density is calculated as:

$$\begin{aligned} \mathbf{f}_L(z) &= - \int_{\Sigma(z)} \rho g \mathbf{i}_z dS - \int_{\partial\Sigma(z)} Kz^2 \sin^2(\theta/2) \mathbf{i}_r(\theta) dl \\ &= -\rho g \pi (r_e^2 - r_i^2) \mathbf{i}_z - Kz^2 \int_0^{2\pi} \sin^2(\theta/2) \mathbf{i}_r(\theta) r_e d\theta \\ &= -\rho g \pi (r_e^2 - r_i^2) \mathbf{i}_z - \frac{K r_e}{2} z^2 \int_0^{2\pi} (1 - \cos \theta) (\cos \theta \mathbf{i}_x + \sin \theta \mathbf{i}_y) d\theta \\ &= -\rho g \pi (r_e^2 - r_i^2) \mathbf{i}_z + \frac{K \pi r_e}{2} z^2 \mathbf{i}_x \end{aligned}$$

where it is assumed that  $\mathbf{i}_r(\theta)$  is defined as  $\mathbf{i}_r(\theta) = \cos \theta \mathbf{i}_x + \sin \theta \mathbf{i}_y$  in a Cartesian vector basis  $(\mathbf{i}_x, \mathbf{i}_y)$ . This results in:

$$\mathbf{R}(z) = \int_z^H \left( -\rho g \pi (r_e^2 - r_i^2) \mathbf{i}_z + \frac{K \pi r_e}{2} \xi^2 \mathbf{i}_x \right) d\xi = -\rho g \pi (r_e^2 - r_i^2) \left[ \xi \right]_z^H \mathbf{i}_z + \frac{K \pi r_e}{2} \left[ \frac{\xi^3}{3} \right]_z^H \mathbf{i}_x$$

hence, finally:

$$\boxed{\mathbf{R}(z) = -\rho g \pi (r_e^2 - r_i^2) (H - z) \mathbf{i}_z + \frac{K \pi r_e}{6} (H^3 - z^3) \mathbf{i}_x, \forall z \in (0, L)}$$

Thus the resultant force of the internal loads in the chimney consists of two components:

- the component  $R_z$  along  $\mathbf{i}_z$  is the axial force, which is a compression force since it is negative, and results from the action of gravity;
- the component  $R_x$  along  $\mathbf{i}_x$  is the shear force, also noted  $T_x$ , and results from wind action.

The isolation of the “upstream” part  $\omega$  (i.e. below the cut in  $z$ ) gives the same result, but requires first writing the global equilibrium equation of the entire chimney to determine the resultant force  $\mathbf{R}_0$  of the ground action on the chimney:

$$\mathbf{R}_0 - mg\mathbf{i}_z + \int_{\partial\Omega} \mathbf{f}_S dS = \mathbf{0}$$

where  $m = \rho g \pi (r_e^2 - r_i^2) H$  is the mass of the chimney. In particular, we can see that we have:

$$\boxed{\mathbf{R}_0 = \rho g \pi (r_e^2 - r_i^2) H \mathbf{i}_z - \frac{K\pi}{6} r_e H^3 \mathbf{i}_x = -\mathbf{R}(0)}$$

■

**R** Even if we have limited ourselves here to the (quasi-)static framework, the transition to the dynamic framework is easy: taking into account the acceleration in the isolation of the segment  $\omega$  allows us to establish that:

$$\int_{\omega} \rho \ddot{\mathbf{x}} dV = \int_0^s \int_{\Sigma} \rho \ddot{\mathbf{x}} dS d\xi$$

where we can write that:

$$\ddot{\mathbf{x}} = \ddot{\mathbf{u}} = \ddot{\mathbf{u}}_G + \ddot{\boldsymbol{\theta}} \wedge \mathbf{x}_{\Sigma}$$

and since  $G$  refers to the centre of the associated cross-section  $\Sigma$ , we have, by definition, that  $\int_{\Sigma} \mathbf{x}_{\Sigma} dS = \mathbf{0}$ , and therefore that:

$$\int_{\omega} \rho \ddot{\mathbf{x}} dV = \int_0^s \rho A \ddot{\mathbf{u}}_G d\xi$$

which finally results in:

$$\boxed{\int_0^s \mathbf{f}_L(\xi, t) d\xi + \mathbf{R}_0(t) + \mathbf{R}(s, t) = \int_0^s \rho A \ddot{\mathbf{u}}_G(\xi, t) d\xi, \forall t}$$

The isolation of the other segment  $\omega^*$  allows us to find that:

$$\boxed{\int_s^L \mathbf{f}_L(\xi, t) d\xi + \mathbf{R}_L(t) - \mathbf{R}(s, t) = \int_s^L \rho A \ddot{\mathbf{u}}_G(\xi, t) d\xi, \forall t}$$

### Equilibrium equation for the resultant force: local approach

Instead of writing the equilibrium equation of a beam segment after cutting at a cross-section of coordinate  $s$ , it is possible to establish a local relation verified by the resultant force of the inner loads at any point on the neutral axis. For this, we start from the equilibrium equation established above for a segment  $\omega$ , where we express that the resultant force of the external actions on the cross-section of coordinate 0 is  $\mathbf{R}_0 = -\mathbf{R}(0)$ :

$$\int_0^s \mathbf{f}_L(\xi) d\xi + \mathbf{R}(s) - \mathbf{R}(0) = \mathbf{0}$$

Since this expression is valid regardless of the coordinate  $s$ , it can be interpreted as the integration of a relation, which is valid regardless of  $s$  as well:

$$\int_0^s (\mathbf{f}_L(\xi) + \mathbf{R}'(\xi)) d\xi = \mathbf{0}$$

where we note  $\bullet' = \frac{d\bullet}{ds}$ , which finally gives us:

$$\mathbf{f}_L(s) + \mathbf{R}'(s) = \mathbf{0}, \forall s \in (0, L)$$

Here again, this static equilibrium equation is also valid in the quasi-static framework; in this case, the different quantities can then depend on time  $t$ .

The (quasi-)static local equilibrium of the beam is thus written as a first-order differential equation in terms of the resultant force of the internal loads. To solve it, it is therefore necessary to add a boundary condition, either at  $s = 0$ , or at  $s = L$ . As before, depending on whether we study the cross-section of coordinate  $s = 0$  or  $s = L$ , we obtain, by definition:

$$\mathbf{R}_0 = \int_{\Sigma(0)} \mathbf{f}_S dS = \int_{\Sigma(0)} \boldsymbol{\sigma}(-\mathbf{e}) dS = -\mathbf{R}(0)$$

since the outer unit normal vector at  $s = 0$  is  $\mathbf{n} = -\mathbf{e}$ , and:

$$\mathbf{R}_L = \int_{\Sigma(L)} \mathbf{f}_S dS = \int_{\Sigma(L)} \boldsymbol{\sigma} \mathbf{e} dS = \mathbf{R}(L)$$

since the outer unit normal vector at  $s = L$  is  $\mathbf{n} = \mathbf{e}$ .

**Summary 6.4 — Equilibrium equation for the resultant force of the internal loads: local approach.** The local force equilibrium of a beam subjected to volume force densities  $\mathbf{f}_V$  and surface force densities  $\mathbf{f}_S$  is written, in the static case, as:

$$\mathbf{f}_L(s) + \mathbf{R}'(s) = \mathbf{0}, \quad \forall s \in (0, L)$$

where  $\mathbf{f}_L$  is the line force density equivalent to the densities  $\mathbf{f}_V$  and  $\mathbf{f}_S$ :

$$\mathbf{f}_L(s) = \int_{\Sigma(s)} \mathbf{f}_V(s, \chi_1, \chi_2) dS + \int_{\partial\Sigma(s)} \mathbf{f}_S(s, \chi_1, \chi_2) dl$$

This differential equation is solved using a boundary condition to be written at  $s = 0$  or  $s = L$ , namely:

$$\mathbf{R}(0) = -\mathbf{R}_0, \text{ or } \mathbf{R}(L) = \mathbf{R}_L$$

where  $\mathbf{R}_0$  and  $\mathbf{R}_L$  are the resultant forces of the external actions exerted on the cross-sections of coordinates  $s = 0$  and  $s = L$  respectively.

**R** Instead of starting from the force equilibrium equation for a beam segment, we could also have directly considered the local equilibrium equation established in continuum mechanics (in Paragraph 2.3.1), namely:

$$\mathbf{div}_x \boldsymbol{\sigma} + \mathbf{f}_V = \rho \ddot{\mathbf{u}}$$

where the divergence of the stress tensor can be rewritten as:

$$\mathbf{div}_x \boldsymbol{\sigma} = \frac{\partial \sigma}{\partial s} \mathbf{e} + \frac{\partial \sigma}{\partial \chi_1} \mathbf{e}_{\chi_1} + \frac{\partial \sigma}{\partial \chi_2} \mathbf{e}_{\chi_2} = \frac{\partial \sigma}{\partial s} \mathbf{e} + \mathbf{div}_{x_\Sigma} \boldsymbol{\sigma}$$

By integrating the first equation on a cross-section  $\Sigma$  of coordinate  $s$ , we then obtain, in the case of a straight beam (i.e. when  $\mathbf{e}$  is constant):

$$\int_{\Sigma} \left( \frac{\partial \sigma}{\partial s} \mathbf{e} + \mathbf{div}_{x_\Sigma} \boldsymbol{\sigma} \right) dS + \int_{\Sigma} \mathbf{f}_V dS = \frac{\partial}{\partial s} \left( \int_{\Sigma} \boldsymbol{\sigma} \mathbf{e} dS \right) + \int_{\partial\Sigma} \boldsymbol{\sigma} \mathbf{n}_l dl + \int_{\Sigma} \mathbf{f}_V dS = \int_{\Sigma} \rho \ddot{\mathbf{u}} dS$$

by applying the divergence formula, with  $\mathbf{n}_l$  the outer unit normal vector to the contour  $\partial\Sigma$  of the cross-section  $\Sigma$ , that is, finally:

$$\mathbf{R}' + \int_{\partial\Sigma} \mathbf{f}_S dl + \int_{\Sigma} \mathbf{f}_V dS = \int_{\Sigma} \rho \ddot{\mathbf{u}} dS$$

or:

$$\boxed{\mathbf{R}' + \mathbf{f}_L = \rho A \ddot{\mathbf{u}}_G}$$

This proof shows that the local force equilibrium equation is what is obtained when we average, on each cross-section, the three-dimensional equations of continuum mechanics, which is equivalent, in a way, to “reducing” the equations on the neutral axis of the beam.

■ **Example 6.4 — Resultant force of the internal loads for a chimney exposed to wind: local approach.** Here we use Example 6.3 to highlight the local approach. The resultant force of the internal loads then satisfies:

$$\mathbf{R}'(z) + \mathbf{f}_L(z) = \mathbf{0}, \forall z \in (0, L)$$

where  $\bullet' = \frac{d\bullet}{dz}$ , and where the line force density is expressed as:

$$\mathbf{f}_L(z) = -\rho g \pi (r_e^2 - r_i^2) \mathbf{i}_z + \frac{K\pi r_e}{2} z^2 \mathbf{i}_x$$

after assuming that  $\mathbf{i}_r(\theta)$  is defined as  $\mathbf{i}_r(\theta) = \cos \theta \mathbf{i}_x + \sin \theta \mathbf{i}_y$  in a Cartesian vector basis  $(\mathbf{i}_x, \mathbf{i}_y)$ . We then find by integration that the resultant force is:

$$\mathbf{R}(z) = \rho g \pi (r_e^2 - r_i^2) z \mathbf{i}_z - \frac{K\pi r_e}{6} z^3 \mathbf{i}_x + C$$

The constant  $C$  is determined using a boundary condition; here, the most natural is the one at  $z = H$ : if we assume that no forces are exerted on the associated cross-section (free boundary), we can write that  $\mathbf{R}(H) = \mathbf{0}$ , hence, finally:

$$\boxed{\mathbf{R}(z) = \rho g \pi (r_e^2 - r_i^2) (z - H) \mathbf{i}_z - \frac{K\pi r_e}{6} (z^3 - H^3) \mathbf{i}_x}$$

as before. ■

### 6.2.3 Moment of the internal loads and associated equilibrium equation

Similarly, and to be complete in terms of equations, it is necessary to define the moment associated with the stress vector  $\sigma \mathbf{e}$  when cutting the beam at the cross-section of coordinate  $s$ .

**Moment of the internal loads.** The moment  $\mathbf{M}$  of the internal loads for a cross-section of coordinate  $s$  is defined in a classical way as the moment, expressed at the centre  $G$  of the cross-section, associated with the stress vector in the cross-section:

$$\mathbf{M}(s, t) = \int_{\Sigma(s)} \mathbf{x}_{\Sigma}(\chi_1, \chi_2) \wedge (\sigma(s, \chi_1, \chi_2, t) \mathbf{e}) dS, \forall s \in [0, L], \forall t$$

where  $\mathbf{x}_{\Sigma} = \mathbf{x} - \mathbf{x}_G$  is the placement vector in the cross-section of a point of the beam. As before, this definition expresses the integration of the local moments exerted by the “downstream” part of the beam on the “upstream” part, since we have chosen  $\mathbf{n} = \mathbf{e}$  to express the stress vector. The following components of the moment of the internal loads, represented in Figure 6.13, are then defined as follows:

- the component  $M_e = \langle \mathbf{M}, \mathbf{e} \rangle$  is called the “moment of torsion”, often noted  $M_t$ ;
- the vector  $\mathbf{M}_{\Sigma} = \mathbf{M} - \langle \mathbf{M}, \mathbf{e} \rangle \mathbf{e}$  is called the “bending moment”, of components  $M_{\chi_1}$  and  $M_{\chi_2}$  in the vector basis  $(\mathbf{e}_{\chi_1}, \mathbf{e}_{\chi_2})$ , often noted  $M_{f\chi_1}$  and  $M_{f\chi_2}$ .

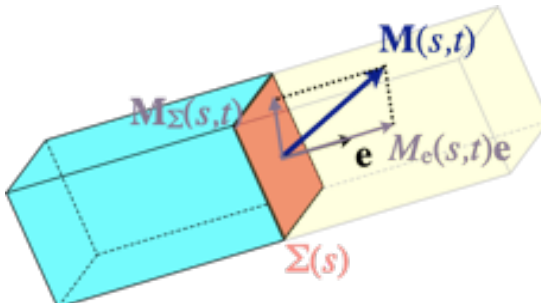


Figure 6.13: Definition of the components of the moment of the internal loads.

**⚠** As for the resultant force, it is possible to define the moment with the other sign convention:

$$\tilde{\mathbf{M}} = \int_{\Sigma(s)} \mathbf{x}_\Sigma \wedge (\sigma(-\mathbf{e})) dS$$

which is the choice adopted in Anglo-Saxon countries. Thus, once again, it is essential to specify the sign convention adopted before solving a beam problem.

### Equilibrium equation for the moment: global approach

To determine the equilibrium equation verified by the moment of the internal loads, we proceed as for the resultant force, by isolating a segment resulting from the cut into two parts of the beam at the cross-section  $\Sigma$  of coordinate  $s$ , as illustrated in Figure 6.14. So, if we study the segment  $\omega$ , it is subjected:

- at 0 to the resultant force  $\mathbf{R}_0$  and the moment  $\mathbf{M}_0$  (expressed at the centre of this cross-section) of the external actions on this latter;
- at  $s$  to the resultant force and the moment (expressed at the centre of this cross-section) of the internal loads on this latter;
- to external actions represented by volume force densities  $\mathbf{f}_V$  and surface force densities  $\mathbf{f}_S$ .

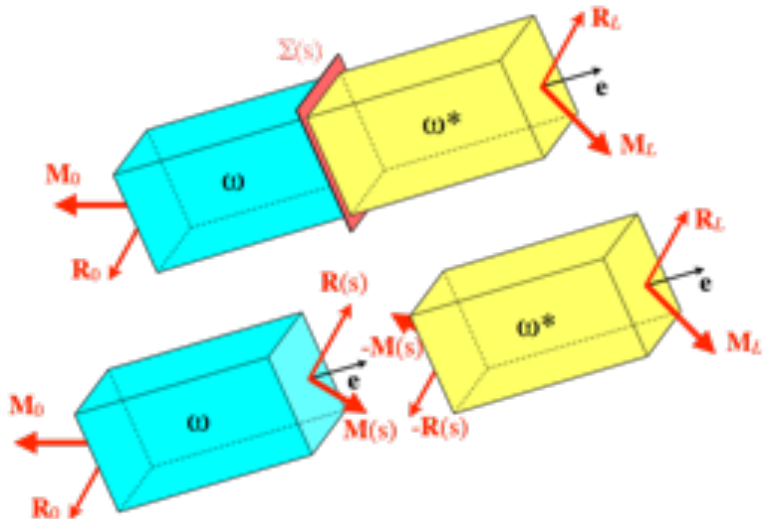


Figure 6.14: Moment equilibrium: the beam is cut into two segments at the cross-section  $\Sigma(s)$ .

We can then write the moment equilibrium of this segment, expressed at the centre  $G$  of the cross-section of coordinate  $s$  where the cut was made:

$$\int_{\omega} (\mathbf{x} - \mathbf{x}_G) \wedge \mathbf{f}_V dV + \int_{\partial_l \omega} (\mathbf{x} - \mathbf{x}_G) \wedge \mathbf{f}_S dS + \int_{\Sigma(0)} (\mathbf{x} - \mathbf{x}_G) \wedge \mathbf{f}_S dS + \int_{\Sigma(s)} (\mathbf{x} - \mathbf{x}_G) \wedge \sigma \mathbf{e} dS = \mathbf{0}$$

where  $\partial_l \omega$  is the lateral surface of the beam segment. Since, for a straight beam, the placement vector of a point  $M$  in a cross-section of coordinate  $\xi$  can be decomposed as  $\mathbf{x} = \xi \mathbf{e} + \mathbf{x}_\Sigma$ , we obtain the relation:

$$\int_{\omega} ((\xi - s)\mathbf{e} + \mathbf{x}_\Sigma) \wedge \mathbf{f}_V dV + \int_{\partial_l \omega} ((\xi - s)\mathbf{e} + \mathbf{x}_\Sigma) \wedge \mathbf{f}_S dS + \int_{\Sigma(0)} (-s\mathbf{e} + \mathbf{x}_\Sigma) \wedge \mathbf{f}_S dS + \int_{\Sigma(s)} \mathbf{x}_\Sigma \wedge \sigma \mathbf{e} dS = \mathbf{0}$$

or by introducing the moment of the internal loads at  $s$  as well as the resultant force and moment of the external actions, then by decomposing the integrals:

$$\int_0^s \int_{\Sigma} ((\xi - s)\mathbf{e} + \mathbf{x}_\Sigma) \wedge \mathbf{f}_V dS d\xi + \int_0^s \int_{\partial \Sigma} ((\xi - s)\mathbf{e} + \mathbf{x}_\Sigma) \wedge \mathbf{f}_S dl d\xi + \mathbf{M}_0 - s\mathbf{e} \wedge \mathbf{R}_0 + \mathbf{M}(s) = \mathbf{0}$$

where  $\partial \Sigma$  refers to the boundary of the cross-section  $\Sigma$ .

**Line moment density.** Knowing all the volume and surface force densities exerted on the beam, we define an equivalent line moment density  $\mathbf{c}_L$ , expressed at the centre  $G$  of each cross-section  $\Sigma$  of coordinate  $s$  as:

$$\mathbf{c}_L(s) = \int_{\Sigma(s)} \mathbf{x}_\Sigma \wedge \mathbf{f}_V(s, \chi_1, \chi_2) dS + \int_{\partial\Sigma(s)} \mathbf{x}_\Sigma \wedge \mathbf{f}_S(s, \chi_1, \chi_2) dl$$

Considering the dimensions of the densities  $\mathbf{f}_V$  (in  $N/m^3$ ) and  $\mathbf{f}_S$  (in  $N/m^2$ ), the new density  $\mathbf{c}_L$  has as units N, and is therefore effectively homogeneous to a line moment density.

By introducing the line force densities  $\mathbf{f}_L$  and line moment densities  $\mathbf{c}_L$ , we can then write that:

$$\int_0^s (\xi - s) \mathbf{e} \wedge \mathbf{f}_L(\xi) d\xi + \int_0^s \mathbf{c}_L(\xi) d\xi + \mathbf{M}_0 - s \mathbf{e} \wedge \mathbf{R}_0 + \mathbf{M}(s) = \mathbf{0}$$

Similarly, isolating the other segment  $\omega^*$ , considering the moment equilibrium expressed at the centre of the cross-section of coordinate  $s$ , simply leads to:

$$\int_s^L (\xi - s) \mathbf{e} \wedge \mathbf{f}_L(\xi) d\xi + \int_s^L \mathbf{c}_L(\xi) d\xi + \mathbf{M}_L + (L - s) \mathbf{e} \wedge \mathbf{R}_L - \mathbf{M}(s) = \mathbf{0}$$

where the moment of the internal loads is expressed as  $-\mathbf{M}(s)$ , since it is the action of the “upstream” part of the beam on the “downstream” part.

**R** As in the case of the resultant force, the sum of the two previous relations allows for finding the global moment equilibrium of the entire beam:

$$\int_0^L (\xi - s) \mathbf{e} \wedge \mathbf{f}_L(\xi) d\xi + \int_0^L \mathbf{c}_L(\xi) d\xi + \mathbf{M}_0 - s \mathbf{e} \wedge \mathbf{R}_0 + \mathbf{M}_L + (L - s) \mathbf{e} \wedge \mathbf{R}_L = \mathbf{0}$$

Noticing then that:

$$\int_0^L -s \mathbf{e} \wedge \mathbf{f}_L(\xi) d\xi = -s \mathbf{e} \wedge \left( \int_0^L \mathbf{f}_L(\xi) d\xi \right) = s \mathbf{e} \wedge (\mathbf{R}_0 + \mathbf{R}_L)$$

by virtue of the global force equilibrium equation for the entire beam, it is then possible to write that:

$$\int_0^L \xi \mathbf{e} \wedge \mathbf{f}_L(\xi) d\xi + \int_0^L \mathbf{c}_L(\xi) d\xi + \mathbf{M}_0 + \mathbf{M}_L + L \mathbf{e} \wedge \mathbf{R}_L = \mathbf{0}$$

which corresponds to the global moment equilibrium of the entire beam, expressed at the centre of the cross-section of coordinate  $s = 0$ .

**Summary 6.5 — Equilibrium equation for the moment of the internal loads (global approach).** The moment equilibrium equation of a beam subjected to volume force densities  $\mathbf{f}_V$  and surface force densities  $\mathbf{f}_S$  is written, in the static case and for the global approach, as:

$$\int_0^s (\xi - s) \mathbf{e} \wedge \mathbf{f}_L(\xi) d\xi + \int_0^s \mathbf{c}_L(\xi) d\xi + \mathbf{M}_0 - s \mathbf{e} \wedge \mathbf{R}_0 + \mathbf{M}(s) = \mathbf{0}, \forall s \in (0, L)$$

or as:

$$\int_s^L (\xi - s) \mathbf{e} \wedge \mathbf{f}_L(\xi) d\xi + \int_s^L \mathbf{c}_L(\xi) d\xi + \mathbf{M}_L + (L - s) \mathbf{e} \wedge \mathbf{R}_L - \mathbf{M}(s) = \mathbf{0}, \forall s \in (0, L)$$

where  $\mathbf{c}_L$  is the line moment density equivalent to the densities  $\mathbf{f}_V$  and  $\mathbf{f}_S$ :

$$\mathbf{c}_L(s) = \int_{\Sigma(s)} \mathbf{x}_\Sigma(\chi_1, \chi_2) \wedge \mathbf{f}_V(s, \chi_1, \chi_2) dS + \int_{\partial\Sigma(s)} \mathbf{x}_\Sigma(\chi_1, \chi_2) \wedge \mathbf{f}_S(s, \chi_1, \chi_2) dl$$

and  $\mathbf{M}_0$  and  $\mathbf{M}_L$  are the moments (expressed at the centres of the corresponding cross-sections) of the external actions exerted on the cross-sections of respective coordinates  $s = 0$  and  $s = L$ .



Strictly speaking, the previous relations do not allow us to determine the expression of the moment of the internal loads on the extreme cross-sections of the beam, at  $s = 0$  and  $s = L$ . As in the case of the resultant force, in this case, it is sufficient to consider the external surface forces exerted on the corresponding cross-section to make the link with the definition of the moment  $\mathbf{M}$ .

Thus, if  $\mathbf{M}_0$  and  $\mathbf{M}_L$  are the moments of external actions on the cross-sections of coordinates  $s = 0$  and  $s = L$  respectively, we establish that:

$$\mathbf{M}_0 = \int_{\Sigma(0)} \mathbf{x}_\Sigma \wedge \mathbf{f}_S dS = \int_{\Sigma(0)} \mathbf{x}_\Sigma \wedge \sigma(-\mathbf{e}) dS = -\mathbf{M}(0)$$

since the outer unit normal vector for the beam at  $s = 0$  is  $\mathbf{n} = -\mathbf{e}$ , and:

$$\mathbf{M}_L = \int_{\Sigma(L)} \mathbf{x}_\Sigma \wedge \mathbf{f}_S dS = \int_{\Sigma(L)} \mathbf{x}_\Sigma \wedge \sigma \mathbf{e} dS = \mathbf{M}(L)$$

since the outer unit normal vector for the beam at  $s = L$  is  $\mathbf{n} = \mathbf{e}$ .

Of course, these terms must be modified if the opposite sign convention is adopted for defining the moment of the internal loads.

#### ■ Example 6.5 — Moment of the internal loads in a chimney exposed to wind: global approach.

We use Example 6.3 of the chimney subjected to wind, in order to determine this time the evolution of the moment of the internal loads along the beam modelling this chimney. It should be remembered that this latter is subjected to:

- the action of gravity at any point of its volume:  $\mathbf{f}_V = -\rho g \mathbf{i}_z$ ;
- the action of the wind on its outer lateral surface  $\partial\Omega$ :  $\mathbf{f}_S = -Kz^2 \sin^2(\theta/2) \mathbf{i}_r(\theta)$ ;

where a cylindrical coordinate system  $(O, \mathbf{i}_r(\theta), \mathbf{i}_\theta(\theta), \mathbf{i}_z)$  has been associated with the beam.

If the chimney is cut at a cross-section of given altitude  $z$ , the isolation of the “downstream” segment  $\omega^*$  (i.e. above the  $z$  cut) allows for obtaining, in statics, when expressing the moment equilibrium equation at the centre of  $\Sigma(z)$ :

$$\int_z^H \mathbf{c}_L(\xi) d\xi + \int_z^H (\xi - z) \mathbf{i}_z \wedge \mathbf{f}_L(\xi) d\xi + \mathbf{M}_H + (L - z) \mathbf{i}_z \wedge \mathbf{R}_H - \mathbf{M}(z) = \mathbf{0}$$

where  $\mathbf{R}_H$  and  $\mathbf{M}_H$ , which characterize the action of the external forces on the cross-section of altitude  $z = H$ , are zero, since the surface is free of forces.

In addition, the line moment density along the chimney is calculated as:

$$\begin{aligned} \mathbf{c}_L(z) &= - \int_{\Sigma} \mathbf{x}_\Sigma \wedge \rho g \mathbf{i}_z dS - \int_{\partial\Sigma} \mathbf{x}_\Sigma \wedge Kz^2 \sin^2(\theta/2) \mathbf{i}_r(\theta) dl \\ &= - \int_{\Sigma} r \mathbf{i}_r(\theta) \wedge \rho g \mathbf{i}_z dS - \int_{\partial\Sigma} r \mathbf{i}_r(\theta) \wedge Kz^2 \sin^2(\theta/2) \mathbf{i}_r(\theta) dl \\ &= \rho g \int_{r_i}^{r_e} r^2 dr \int_0^{2\pi} \mathbf{i}_\theta(\theta) d\theta \\ &= \mathbf{0} \end{aligned}$$

knowing that the line force density is expressed as:

$$\mathbf{f}_L(z) = -\rho g \pi (r_e^2 - r_i^2) \mathbf{i}_z + \frac{K\pi r_e}{2} z^2 \mathbf{i}_x$$

All the above results finally show that:

$$\mathbf{M}(z) = \int_z^H \frac{K\pi r_e}{2} (\xi - z) \xi^2 \mathbf{i}_y d\xi = \frac{K\pi r_e}{2} \left[ \frac{\xi^4}{4} - z \frac{\xi^3}{3} \right]_z^H \mathbf{i}_y = \frac{K\pi r_e}{24} (z^4 - 4H^3 z + 3H^4) \mathbf{i}_y$$

which is a bending moment around the axis  $\mathbf{i}_y$ , related to wind action only. We can therefore see that the action of gravity has no effect on the beam, because this latter is vertical.

The isolation of the “upstream” part  $\omega$  (i.e. below the  $z$  cut) gives the same result, but requires first writing the global equilibrium equation of the entire chimney in order to determine the moment  $\mathbf{M}_0$  (expressed at the centre of the cross-section of altitude  $z = 0$ ) of the ground’s action on the chimney:

$$\mathbf{M}_0 + \int_{\Omega} \mathbf{x} \wedge \mathbf{f}_V dV + \int_{\partial_l \Omega} \mathbf{x} \wedge \mathbf{f}_S dS = \mathbf{0}$$

where the moment of gravity’s action here is zero. In particular, we can see that we have:

$$\boxed{\mathbf{M}_0 = -\frac{K\pi r_e}{8} H^4 \mathbf{i}_y = -\mathbf{M}(0)}$$

■

**R** The extension to the dynamic framework involves taking into account the time derivative of the angular momentum (expressed at the centre  $G$  of the cut cross-section):

$$\int_{\omega} (\mathbf{x} - \mathbf{x}_G) \wedge \rho \ddot{\mathbf{x}} dV = \int_0^s \int_{\Sigma} ((\xi - s)\mathbf{e} + \mathbf{x}_{\Sigma}) \wedge \rho \ddot{\mathbf{x}} dS d\xi$$

By transforming, as in Paragraph 6.2.2, the following inertia term as:

$$\int_{\Sigma} \mathbf{x}_{\Sigma} \wedge \rho \ddot{\mathbf{x}} dS = \int_{\Sigma} \mathbf{x}_{\Sigma} \wedge \rho \ddot{\mathbf{u}}_G dS + \int_{\Sigma} \mathbf{x}_{\Sigma} \wedge (\rho \ddot{\boldsymbol{\theta}} \wedge \mathbf{x}_{\Sigma}) dS = \int_{\Sigma} \mathbf{x}_{\Sigma} \wedge (\rho \ddot{\boldsymbol{\theta}} \wedge \mathbf{x}_{\Sigma}) dS$$

since  $\int_{\Sigma} \mathbf{x}_{\Sigma} dS = \mathbf{0}$ , we then obtain:

$$\int_{\Sigma(s)} \mathbf{x}_{\Sigma} \wedge (\rho \ddot{\boldsymbol{\theta}} \wedge \mathbf{x}_{\Sigma}) dS = \rho \mathbb{J} \ddot{\boldsymbol{\theta}}$$

assuming  $\rho$  is homogeneous in the cross-section, and posing:

$$\mathbb{J} = \int_{\Sigma} (\|\mathbf{x}_{\Sigma}\|^2 \mathbb{I} - \mathbf{x}_{\Sigma} \otimes \mathbf{x}_{\Sigma}) dS$$

called “area inertia tensor”, which will be studied in Paragraph 6.3.3.

Finally, in the dynamic framework, taking into account the inertia terms, makes it possible to obtain as an equilibrium equation for the moments:

$$\boxed{\int_0^s (\xi - s)\mathbf{e} \wedge \rho A \ddot{\mathbf{u}}_G(\xi, t) d\xi + \int_0^s \rho \mathbb{J} \ddot{\boldsymbol{\theta}}(\xi, t) d\xi = \int_0^s (\xi - s)\mathbf{e} \wedge \mathbf{f}_L(\xi, t) d\xi + \int_0^s \mathbf{c}_L(\xi, t) d\xi \\ + \mathbf{M}_0(t) - s\mathbf{e} \wedge \mathbf{R}_0(t) + \mathbf{M}(s, t), \forall t}$$

The isolation of the other beam segment  $\omega^*$  allows us to find that:

$$\boxed{\int_s^L (\xi - s)\mathbf{e} \wedge \rho A \ddot{\mathbf{u}}_G(\xi, t) d\xi + \int_s^L \rho \mathbb{J} \ddot{\boldsymbol{\theta}}(\xi, t) d\xi = \int_s^L (\xi - s)\mathbf{e} \wedge \mathbf{f}_L(\xi, t) d\xi + \int_s^L \mathbf{c}_L(\xi, t) d\xi \\ + \mathbf{M}_L(t) + (L - s)\mathbf{e} \wedge \mathbf{R}_L(t) - \mathbf{M}(s, t), \forall t}$$

### Equilibrium equation for the moment: local approach

As in the case of the resultant force, instead of writing the equilibrium equation of a beam segment after cutting at a cross-section of coordinate  $s$ , it is possible to establish a local relation verified by the moment of the inner loads at any point on the neutral axis. Thus, if we take the equilibrium equation previously established for a segment  $\omega$ , and introduce the internal loads on the cross-section of coordinate 0 ( $\mathbf{R}_0 = -\mathbf{R}(0)$  and  $\mathbf{M}_0 = -\mathbf{M}(0)$ ), we obtain:

$$\int_0^s (\xi - s)\mathbf{e} \wedge \mathbf{f}_L(\xi) d\xi + \int_0^s \mathbf{c}_L(\xi) d\xi - \mathbf{M}(0) + s\mathbf{e} \wedge \mathbf{R}(0) + \mathbf{M}(s) = \mathbf{0}, \forall s \in (0, L)$$

and, using the local force equilibrium equation ( $\mathbf{f}_L + \mathbf{R}' = \mathbf{0}$ ), we find that:

$$\begin{aligned} \int_0^s (\xi - s) \mathbf{e} \wedge \mathbf{f}_L(\xi) d\xi &= - \int_0^s (\xi - s) \mathbf{e} \wedge \mathbf{R}'(\xi) d\xi \\ &= - \left[ (\xi - s) \mathbf{e} \wedge \mathbf{R}(\xi) \right]_0^s + \int_0^s \mathbf{e} \wedge \mathbf{R}(\xi) d\xi \\ &= -s \mathbf{e} \wedge \mathbf{R}(0) + \int_0^s \mathbf{e} \wedge \mathbf{R}(\xi) d\xi \end{aligned}$$

which finally allows us to rewrite the moment equilibrium as:

$$\int_0^s \mathbf{c}_L(\xi) d\xi + \int_0^s \mathbf{e} \wedge \mathbf{R}(\xi) d\xi + \mathbf{M}(s) - \mathbf{M}(0) = \mathbf{0}$$

Since this expression is valid regardless of the coordinate  $s$ , it can be interpreted as the integration of a relation, which is valid regardless of  $s$  as well:

$$\int_0^s (\mathbf{c}_L(\xi) + \mathbf{M}'(\xi) + \mathbf{e} \wedge \mathbf{R}(\xi)) d\xi = \mathbf{0}$$

where we note  $\bullet' = \frac{d\bullet}{ds}$ , which finally gives us:

$$\mathbf{c}_L(s) + \mathbf{M}'(s) + \mathbf{e} \wedge \mathbf{R}(s) = \mathbf{0}, \forall s \in (0, L)$$

which is a first-order differential equation, requiring then to know a boundary condition to be solved:

- either at  $s = 0$ :  $\mathbf{M}(0) = -\mathbf{M}_0$ ;
- or at  $s = L$ :  $\mathbf{M}(L) = \mathbf{M}_L$ .

This static equilibrium equation is also valid in the quasi-static framework.

**Summary 6.6 — Equilibrium equation for the moment of the internal loads (local approach).** The local moment equilibrium of a beam subjected to volume force densities  $\mathbf{f}_V$  and surface force densities  $\mathbf{f}_S$  is written, in the static case, as:

$$\mathbf{c}_L(s) + \mathbf{M}'(s) + \mathbf{e} \wedge \mathbf{R}(s) = \mathbf{0}, \forall s \in (0, L)$$

where  $\mathbf{c}_L$  is the line moment density equivalent to the densities  $\mathbf{f}_V$  and  $\mathbf{f}_S$ :

$$\mathbf{c}_L(s) = \int_{\Sigma(s)} \mathbf{x}_{\Sigma}(\chi_1, \chi_2) \wedge \mathbf{f}_V(s, \chi_1, \chi_2) dS + \int_{\partial\Sigma(s)} \mathbf{x}_{\Sigma}(\chi_1, \chi_2) \wedge \mathbf{f}_S(s, \chi_1, \chi_2) dl$$

This differential equation is solved using a boundary condition to be written at  $s = 0$  or  $s = L$ , namely:

$$\mathbf{M}(0) = -\mathbf{M}_0, \text{ or } \mathbf{M}(L) = \mathbf{M}_L$$

where  $\mathbf{M}_0$  and  $\mathbf{M}_L$  are the moments (expressed at the centres of the corresponding cross-sections) of the external actions exerted on the cross-sections of coordinates  $s = 0$  and  $s = L$  respectively.



As for the local force equilibrium equation, it is also possible to use the equations of continuum mechanics to determine the result established in the case of beams for the local moment equilibrium. In the dynamic framework, we find in particular that:

$$\mathbf{c}_L(s, t) + \mathbf{M}'(s, t) + \mathbf{e} \wedge \mathbf{R}(s, t) = \int_{\Sigma(s)} \mathbf{x}_{\Sigma}(\chi_1, \chi_2) \wedge (\rho \ddot{\boldsymbol{\theta}}(s, t) \wedge \mathbf{x}_{\Sigma}(\chi_1, \chi_2)) dS = \rho \mathbb{J} \ddot{\boldsymbol{\theta}}(s, t), \forall s \in (0, L), \forall t$$

■ **Example 6.6 — Moment of the internal loads in a chimney exposed to wind: local approach.**

We use Example 6.5 of the chimney subjected to wind, in order to highlight the local approach. Since we had seen that the line moment density  $\mathbf{c}_L$  was zero at any point on the neutral axis, we then establish the (static) local moment equilibrium as:

$$\mathbf{M}'(z) + \mathbf{i}_z \wedge \mathbf{R}(z) = \mathbf{0}, \forall z \in (0, L)$$

knowing that it had previously been determined that the resultant force of the internal loads was:

$$\mathbf{R}(z) = \rho g \pi \left( r_e^2 - r_i^2 \right) (z - H) \mathbf{i}_z - \frac{K\pi r_e}{6} \left( z^3 - H^3 \right) \mathbf{i}_x$$

we then obtain that:

$$\mathbf{M}(z) = \frac{K\pi r_e}{6} \left( \frac{z^4}{4} - H^3 z \right) \mathbf{i}_y + \mathbf{C}$$

where  $\mathbf{C}$  is a constant vector to be determined using boundary conditions. Again, the easiest way is to use the free boundary condition at  $z = H$ :

$$\mathbf{M}(H) = \mathbf{0}$$

which leads to the conclusion that:

$$\boxed{\mathbf{M}(z) = \frac{K\pi r_e}{24} \left( z^4 - 4H^3 z + 3H^4 \right) \mathbf{i}_y}$$

which corresponds to the result found previously. ■

Besides, it is possible to eliminate the resultant force from the moment equilibrium equation in order to use only this latter and the different force densities applied to the beam; for this, it is sufficient to differentiate this equilibrium equation to obtain, in the case of a straight beam:

$$\mathbf{c}'_L + \mathbf{M}'' + \mathbf{e} \wedge \mathbf{R}' = \mathbf{0}$$

and use the local force equilibrium equation ( $\mathbf{f}_L + \mathbf{R}' = \mathbf{0}$ ) to establish another moment equilibrium equation:

$$\boxed{\mathbf{c}'_L(s) + \mathbf{M}''(s) - \mathbf{e} \wedge \mathbf{f}_L(s) = \mathbf{0}, \forall s \in (0, L)}$$

Finally, it is possible to determine the shear force  $\mathbf{R}_\Sigma$  from the bending moment, by taking the vector product of the local moment equilibrium equation by vector  $\mathbf{e}$ :

$$\mathbf{e} \wedge \mathbf{c}_L + \mathbf{e} \wedge \mathbf{M}' + \mathbf{e} \wedge (\mathbf{e} \wedge \mathbf{R}) = \mathbf{0}$$

which gives, after development of the vector triple product, and since  $\mathbf{e} \wedge \mathbf{M}' = \mathbf{e} \wedge \mathbf{M}'_\Sigma$ :

$$\boxed{\mathbf{R}_\Sigma(s) = \mathbf{e} \wedge (\mathbf{c}_L(s) + \mathbf{M}'_\Sigma(s)), \forall s \in (0, L)}$$



*The generalization to the dynamic framework of these relations is straightforward; indeed, we have:*

$$\mathbf{c}'_L + \mathbf{M}'' + \mathbf{e} \wedge \mathbf{R}' = \int_{\Sigma} \mathbf{x}_\Sigma \wedge (\rho \ddot{\theta}' \wedge \mathbf{x}_\Sigma) dS = \rho J \ddot{\theta}'$$

where we can use the force equilibrium equation:

$$\rho A \ddot{\mathbf{u}}_G = \mathbf{f}_L + \mathbf{R}'$$

to obtain another moment equilibrium equation:

$$\boxed{\mathbf{c}'_L + \mathbf{M}'' + \mathbf{e} \wedge (\rho A \ddot{\mathbf{u}}_G - \mathbf{f}_L) = \int_{\Sigma} \mathbf{x}_\Sigma \wedge (\rho \ddot{\theta}' \wedge \mathbf{x}_\Sigma) dS = \rho J \ddot{\theta}'}$$

Similarly, the shear force  $\mathbf{R}_\Sigma$  is expressed, in the dynamic framework, using the bending moment, as:

$$\boxed{\mathbf{R}_\Sigma = \mathbf{e} \wedge \left( \mathbf{c}_L + \mathbf{M}' - \int_{\Sigma} \mathbf{x}_\Sigma \wedge (\rho \dot{\theta} \wedge \mathbf{x}_\Sigma) dS \right) = \mathbf{e} \wedge \left( \mathbf{c}_L + \mathbf{M}' - \rho J \dot{\theta} \right)}$$

### 6.3 Beam constitutive relations

Now that we have defined all the ingredients of a beam model, both from the kinematic point of view and that of internal loads, it remains, as in continuum mechanics, to link these quantities by one or more constitutive relations. The local relations between the different components of the stress and infinitesimal strain tensors are then determined, before establishing the relations regarding the resultant force and moment of the internal loads.

#### 6.3.1 Stress-strain relations

The difficulty here lies in the fact that we are in the presence of a mixed model, in the sense that we have assumed approximations concerning both the displacement field and the stress tensor:

- the hypothesis of a perfectly rigid cross-section results in obtaining an antiplane infinitesimal strain tensor, with respect to the plane of the cross-sections;
- the hypothesis made on the stress tensor is that it is also antiplane with respect to the cross-section plane.

However, strictly speaking, this is contradictory with the constitutive relation of an isotropic linear elastic material, determined in Paragraph 4.2, and of Lamé parameters ( $\lambda, \mu$ ):

$$\boldsymbol{\sigma} = \lambda(\operatorname{tr} \boldsymbol{\epsilon})\mathbb{I} + 2\mu\boldsymbol{\epsilon}$$

since, as long as the longitudinal strain  $\epsilon_{ee}$  in the beam is not zero, the plane part  $\boldsymbol{\sigma}^\Sigma$  of the stress tensor is not zero either:

$$\boldsymbol{\sigma}^\Sigma = \lambda\epsilon_{ee}\mathbb{I}^\Sigma$$

where  $\mathbb{I}^\Sigma$  is the identity tensor in the cross-section plane. For similar reasons, of course, we obtain the same contradiction with the constitutive relation in compliance, expressed using the Young's modulus  $E$  and the Poisson's ratio  $\nu$ :

$$\boldsymbol{\epsilon} = \frac{1+\nu}{E}\boldsymbol{\sigma} - \frac{\nu}{E}(\operatorname{tr} \boldsymbol{\sigma})\mathbb{I}$$

as long as the normal stress  $\sigma_{ee}$  is not zero in the beam.

Finally, we can show, by methods that go beyond the scope of this course, that the best mixed model consists in assuming an antiplane stress tensor:

$$\boldsymbol{\sigma} = \sigma_{ee}\mathbf{e} \otimes \mathbf{e} + \boldsymbol{\tau}_\Sigma \otimes \mathbf{e} + \mathbf{e} \otimes \boldsymbol{\tau}_\Sigma$$

and using the compliance constitutive relation to determine the stress-strain relations of the beam model. In this case, the infinitesimal strain tensor is written as:

$$\boldsymbol{\epsilon} = \frac{1+\nu}{E}(\sigma_{ee}\mathbf{e} \otimes \mathbf{e} + \boldsymbol{\tau}_\Sigma \otimes \mathbf{e} + \mathbf{e} \otimes \boldsymbol{\tau}_\Sigma) - \frac{\nu}{E}\sigma_{ee}\mathbb{I}$$

In addition, the hypothesis of a perfectly rigid cross-section had led, by differentiation, to an infinitesimal strain tensor of the form:

$$\boldsymbol{\epsilon} = \epsilon_{ee}\mathbf{e} \otimes \mathbf{e} + \frac{1}{2}\boldsymbol{\gamma}_\Sigma \otimes \mathbf{e} + \frac{1}{2}\mathbf{e} \otimes \boldsymbol{\gamma}_\Sigma$$

with  $\epsilon_{ee} = u'_{Ge} + \langle \boldsymbol{\theta}'_\Sigma \wedge \mathbf{x}_\Sigma, \mathbf{e} \rangle$  and  $\boldsymbol{\gamma}_\Sigma = \mathbf{u}'_{G\Sigma} - \boldsymbol{\theta}_\Sigma \wedge \mathbf{e} + \theta'_e \mathbf{e} \wedge \mathbf{x}_\Sigma$  if we do not take into account for the time being Euler-Bernoulli hypothesis.

By identification, it is therefore determined that:

$$\epsilon_{ee} = \frac{\sigma_{ee}}{E}, \text{ and } \boldsymbol{\gamma}_\Sigma = \frac{2(1+\nu)}{E}\boldsymbol{\tau}_\Sigma = \frac{1}{\mu}\boldsymbol{\tau}_\Sigma$$

or, conversely:

$$\sigma_{ee} = E\varepsilon_{ee}, \text{ and } \tau_\Sigma = \frac{E}{2(1+\nu)}\gamma_\Sigma = \mu\gamma_\Sigma$$

The antiplane parts of the infinitesimal strain tensor  $\varepsilon$  and stress tensor  $\sigma$  are therefore connected, locally and reciprocally, which will allow, in what follows, the characteristics of the beam kinematics (displacement of the cross-section centre and cross-section rotation) to be linked to the internal loads (resultant force and moment).

- R** The previous model also allows us to determine, using the compliance constitutive relation, that the plane part of the infinitesimal strain tensor is written as:

$$\varepsilon^\Sigma = -\frac{\nu}{E}\sigma_{ee}\mathbb{I}^\Sigma$$

where  $\mathbb{I}^\Sigma$  is the identity tensor in the cross-section plane. Thus, we find the Poisson effect usually observed in the case of a tensile test on an elongated specimen (the transverse strains are  $\varepsilon_T = -\nu\varepsilon_{ee}$ , as seen in Paragraph 4.2.2), even though this effect had been neglected in the approximation of the displacement, with the assumption of a perfectly rigid cross-section.

This is not necessarily contradictory, because the error made with this approximate displacement is amplified when calculating the infinitesimal strain tensor by the fact that the plane part of this latter depends on partial derivatives with respect to the transverse coordinates  $\chi_1$  and  $\chi_2$ , which are "small" when compared to  $L$ : one thus expects to obtain a plane part of the infinitesimal strain tensor that is unrepresentative of reality.

### 6.3.2 Constitutive relation for the resultant force of the internal loads

Starting from the definition of the resultant force of the internal loads, and using the two stress-strain relations just determined, we obtain, for a cross-section  $\Sigma$  of given coordinate  $s$ , that:

$$\mathbf{R} = \int_\Sigma \sigma \mathbf{e} dS = \int_\Sigma (\sigma_{ee} \mathbf{e} + \boldsymbol{\tau}_\Sigma) dS = \int_\Sigma (E\varepsilon_{ee} \mathbf{e} + \mu\boldsymbol{\gamma}_\Sigma) dS = \left( \int_\Sigma E\varepsilon_{ee} dS \right) \mathbf{e} + \int_\Sigma \mu\boldsymbol{\gamma}_\Sigma dS$$

Since, by definition,  $\langle \boldsymbol{\gamma}_\Sigma, \mathbf{e} \rangle = 0$ , we can consider the cases of normal force and shear force separately:

- the normal force  $N = R_e$  then satisfies:

$$R_e = \langle \mathbf{R}, \mathbf{e} \rangle = \int_\Sigma E\varepsilon_{ee} dS = \int_\Sigma E(u'_{Ge} + \langle \boldsymbol{\theta}'_\Sigma \wedge \mathbf{x}_\Sigma, \mathbf{e} \rangle) dS$$

Since  $u'_{Ge}$  and  $\boldsymbol{\theta}'_\Sigma$  depend only on  $s$ , and since  $\int_\Sigma \mathbf{x}_\Sigma dS = \mathbf{0}$  by definition of the cross-section centre  $G$ , the relation is then reduced to:

$$R_e = EAu'_{Ge}$$

if we assume that the Young's modulus  $E$  is homogeneous in the cross-section of area  $A$ ;

- the shear force  $\mathbf{T} = \mathbf{R}_\Sigma$  satisfies:

$$\mathbf{R}_\Sigma = \int_\Sigma \mu (u'_{G\Sigma} - \boldsymbol{\theta}_\Sigma \wedge \mathbf{e} + \theta'_e \mathbf{e} \wedge \mathbf{x}_\Sigma) dS$$

and, since  $\mathbf{u}'_{G\Sigma}$ ,  $\boldsymbol{\theta}_\Sigma$  and  $\theta'_e$  only depend on  $s$ , and since  $\int_\Sigma \mathbf{x}_\Sigma dS = \mathbf{0}$ , the relation is then reduced to:

$$\mathbf{R}_\Sigma = \mu A (u'_{G\Sigma} - \boldsymbol{\theta}_\Sigma \wedge \mathbf{e})$$

if we assume that the shear modulus  $\mu$  is homogeneous in the cross-section of area  $A$ .

**Summary 6.7 — Constitutive relation for the resultant force in the case of a Timoshenko beam.** For a beam with parameters  $(E, \mu)$  constant in each cross-section, the resultant force of the internal loads satisfies (where  $A$  is the area of the cross-section):

$$\mathbf{R}(s, t) = R_e(s, t)\mathbf{e} + \mathbf{R}_\Sigma(s, t) = EAu'_{Ge}(s, t)\mathbf{e} + \mu A (\mathbf{u}'_{G\Sigma}(s, t) - \boldsymbol{\theta}_\Sigma(s, t) \wedge \mathbf{e}), \forall s \in [0, L], \forall t$$

If we also assume that Euler-Bernoulli hypothesis can be adopted, i.e. that the cross-sections remain orthogonal to the deformed neutral axis, this means that:

$$\mathbf{u}'_{G\Sigma} - \boldsymbol{\theta}_\Sigma \wedge \mathbf{e} = \mathbf{0}$$

as we saw in Paragraph 6.1.3. However, since this is an approximation on which a particular error is made, it is not possible to state that the integral of this quantity, calculated on the cross-section, is also zero. We can only conclude that the shear force can no longer be linked to the kinematics by a constitutive relation: its knowledge can therefore only be possible by using the equilibrium equations in terms of resultant force and moment. For example, if we know the moment  $\mathbf{M}$  of the internal loads at any point, we can use the local moment equilibrium equation, as we saw in Paragraph 6.2.3, to obtain that:

$$\mathbf{R}_\Sigma(s) = \mathbf{e} \wedge (\mathbf{c}_L(s) + \mathbf{M}'(s)), \forall s \in (0, L)$$

**Summary 6.8 — Constitutive relation for the resultant force in the case of an Euler-Bernoulli beam.** For a beam with Young's modulus  $E$  constant in each cross-section, which verifies Euler-Bernoulli hypothesis, the resultant force of the internal loads is such that:

$$\mathbf{R}(s, t) = R_e(s, t)\mathbf{e} + \mathbf{R}_\Sigma(s, t) = EAu'_{Ge}(s, t)\mathbf{e} + \mathbf{R}_\Sigma(s, t), \forall s \in [0, L], \forall t$$

where  $A$  is the area of the cross-section. The shear force  $\mathbf{R}_\Sigma$  must be determined, in this case, using the resultant and moment equilibrium equations.

### 6.3.3 Constitutive relation for the moment of the internal loads

As for the resultant force, we start here from the equation defining the moment of the internal loads, in which we use the two stress-strain relations for  $\sigma_{ee}$  and  $\tau_\Sigma$ , and we then obtain, for a cross-section  $\Sigma$  of given coordinate  $s$ :

$$\mathbf{M} = \int_\Sigma \mathbf{x}_\Sigma \wedge (\sigma \mathbf{e}) dS = \int_\Sigma \mathbf{x}_\Sigma \wedge (\sigma_{ee}\mathbf{e} + \boldsymbol{\tau}_\Sigma) dS = \int_\Sigma \mathbf{x}_\Sigma \wedge (E\varepsilon_{ee}\mathbf{e}) dS + \int_\Sigma \mathbf{x}_\Sigma \wedge (\mu\boldsymbol{\gamma}_\Sigma) dS$$

with  $\varepsilon_{ee} = u'_{Ge} + \langle \boldsymbol{\theta}'_\Sigma \wedge \mathbf{x}_\Sigma, \mathbf{e} \rangle$  and  $\boldsymbol{\gamma}_\Sigma = \mathbf{u}'_{G\Sigma} - \boldsymbol{\theta}_\Sigma \wedge \mathbf{e} + \theta'_e \mathbf{e} \wedge \mathbf{x}_\Sigma$  if we do not take into account for the time being Euler-Bernoulli hypothesis. Let us analyze separately the two previous integrals:

- the first one is perpendicular to  $\mathbf{e}$ , and therefore concerns the bending component  $\mathbf{M}_f = \mathbf{M}_\Sigma$  of the moment:

$$\mathbf{M}_\Sigma = \int_\Sigma E\mathbf{x}_\Sigma \wedge u'_{Ge}\mathbf{e} dS + \int_\Sigma E\mathbf{x}_\Sigma \wedge (\boldsymbol{\theta}'_\Sigma \wedge \mathbf{x}_\Sigma) dS$$

since  $\boldsymbol{\theta}'_\Sigma \wedge \mathbf{x}_\Sigma$  is collinear to the axis  $\mathbf{e}$ ; since  $u'_{Ge}$  and  $\boldsymbol{\theta}'_\Sigma$  only depend on the coordinate  $s$ , and since  $\int_\Sigma \mathbf{x}_\Sigma dS = \mathbf{0}$ , the relation is then reduced to:

$$\mathbf{M}_\Sigma = E \int_\Sigma \mathbf{x}_\Sigma \wedge (\boldsymbol{\theta}'_\Sigma \wedge \mathbf{x}_\Sigma) dS = E \left( \int_\Sigma (\|\mathbf{x}_\Sigma\|^2 \mathbb{I} - \mathbf{x}_\Sigma \otimes \mathbf{x}_\Sigma) dS \right) \boldsymbol{\theta}'_\Sigma = E \mathbb{J} \boldsymbol{\theta}'_\Sigma$$

if we assume that the Young's modulus  $E$  is homogeneous in the cross-section; we then note  $\mathbb{J}$  what is called “area inertia tensor”, on which we will come back a little further;

- the second integral is collinear to the axis  $\mathbf{e}$ , and therefore concerns the torsion component  $M_t = M_e$  of the moment:

$$M_e = \langle \mathbf{M}, \mathbf{e} \rangle = \left\langle \int_{\Sigma} \mu \mathbf{x}_{\Sigma} \wedge (\mathbf{u}'_{G\Sigma} - \boldsymbol{\theta}_{\Sigma} \wedge \mathbf{e}) dS, \mathbf{e} \right\rangle + \left\langle \int_{\Sigma} \mu \mathbf{x}_{\Sigma} \wedge (\boldsymbol{\theta}'_e \mathbf{e} \wedge \mathbf{x}_{\Sigma}) dS, \mathbf{e} \right\rangle$$

and since  $\mathbf{u}'_{G\Sigma}$ ,  $\boldsymbol{\theta}_{\Sigma}$  and  $\boldsymbol{\theta}'_e$  only depend on  $s$ , and since  $\int_{\Sigma} \mathbf{x}_{\Sigma} dS = \mathbf{0}$ , the relation is then reduced to:

$$M_e = \left\langle \mu \int_{\Sigma} \mathbf{x}_{\Sigma} \wedge (\boldsymbol{\theta}'_e \mathbf{e} \wedge \mathbf{x}_{\Sigma}) dS, \mathbf{e} \right\rangle = \left\langle \mu \int_{\Sigma} \|\mathbf{x}_{\Sigma}\|^2 \boldsymbol{\theta}'_e \mathbf{e} dS, \mathbf{e} \right\rangle = \mu I_e \boldsymbol{\theta}'_e$$

with  $I_e = \int_{\Sigma} \|\mathbf{x}_{\Sigma}\|^2 dS = \langle \mathbb{J} \mathbf{e}, \mathbf{e} \rangle$ , called “polar moment of inertia”, and in the case where it is assumed that the shear modulus  $\mu$  is uniform in the cross-section  $\Sigma$ .

**Summary 6.9 — Constitutive relation for the moment in the case of a Timoshenko beam.**

For a beam with parameters  $(E, \mu)$  constant in each cross-section, the moment of the internal loads satisfies:

$$\mathbf{M}(s, t) = M_e(s, t) \mathbf{e} + \mathbf{M}_{\Sigma}(s, t) = \mu I_e \boldsymbol{\theta}'_e(s, t) \mathbf{e} + E \mathbb{J} \boldsymbol{\theta}'_{\Sigma}(s, t), \quad \forall s \in [0, L], \forall t$$

where  $\mathbb{J} = \int_{\Sigma} (\|\mathbf{x}_{\Sigma}\|^2 \mathbb{I} - \mathbf{x}_{\Sigma} \otimes \mathbf{x}_{\Sigma}) dS$  is the area inertia tensor, and  $I_e = \langle \mathbb{J} \mathbf{e}, \mathbf{e} \rangle$  is the polar moment of inertia of the cross-section, both detailed below.

If we assume, moreover, that Euler-Bernoulli hypothesis can be adopted, i.e. that the cross-sections remain orthogonal to the deformed neutral axis, we have seen in Paragraph 6.1.3 that this means that, in this case:

$$\boldsymbol{\theta}_{\Sigma} = \mathbf{e} \wedge \mathbf{u}'_{G\Sigma}$$

expression that can be introduced in the above relations. Since, in addition, the beam is straight, the axis  $\mathbf{e}$  is constant, and we then have:

$$\boldsymbol{\theta}'_{\Sigma} = \mathbf{e} \wedge \mathbf{u}''_{G\Sigma}$$

**Summary 6.10 — Constitutive relation for the moment in the case of an Euler-Bernoulli beam.** For a straight beam with parameters  $(E, \mu)$  constant in each cross-section, and which satisfies Euler-Bernoulli hypothesis, the moment of the internal loads is such that:

$$\mathbf{M}(s, t) = M_e(s, t) \mathbf{e} + \mathbf{M}_{\Sigma}(s, t) = \mu I_e \boldsymbol{\theta}'_e(s, t) \mathbf{e} + E \mathbb{J} (\mathbf{e} \wedge \mathbf{u}''_{G\Sigma}(s, t)), \quad \forall s \in [0, L], \forall t$$

where  $\mathbb{J} = \int_{\Sigma} (\|\mathbf{x}_{\Sigma}\|^2 \mathbb{I} - \mathbf{x}_{\Sigma} \otimes \mathbf{x}_{\Sigma}) dS$  is the area inertia tensor, and  $I_e = \langle \mathbb{J} \mathbf{e}, \mathbf{e} \rangle$  is the polar moment of inertia of the cross-section, detailed below.

**R** The constitutive relations just established for the resultant force and moment of the internal loads remain valid in the case of curved beams, provided that the dependence of the vectors  $\mathbf{e}$ ,  $\mathbf{e}_{\chi_1}$  and  $\mathbf{e}_{\chi_2}$  on the arc length  $s$  is taken into account.

### Tensor $\mathbb{J}$ : properties and practical calculation

Now let us detail a little more the tensor  $\mathbb{J}$  that was introduced in the previous relations.

**Area inertia tensor.** We call “area inertia tensor”, associated with the cross-section  $\Sigma$  of coordinate  $s$ , the tensor:

$$\mathbb{J} = \int_{\Sigma} (\|\mathbf{x}_{\Sigma}\|^2 \mathbb{I} - \mathbf{x}_{\Sigma} \otimes \mathbf{x}_{\Sigma}) dS$$

The area inertia tensor  $\mathbb{J}$  thus characterizes how “matter” in this cross-section is spatially distributed around its centre  $G$ ; however, here the integral concerns a surface domain and does not involve density, the components being expressed in  $m^4$ .

With respect to this tensor, the  $\mathbf{e}$  axis of the beam is a “principal axis of inertia”; indeed, we have:

$$\mathbb{J}\mathbf{e} = \int_{\Sigma} (\|\mathbf{x}_{\Sigma}\|^2 \mathbb{I} - \mathbf{x}_{\Sigma} \otimes \mathbf{x}_{\Sigma}) \mathbf{e} dS = \int_{\Sigma} \|\mathbf{x}_{\Sigma}\|^2 \mathbf{e} dS = I_e \mathbf{e}$$

where  $I_e = \int_{\Sigma} \|\mathbf{x}_{\Sigma}\|^2 dS$  is called “polar moment of inertia” of the cross-section  $\Sigma$ .

If we want to calculate the components of this tensor in the Cartesian vector basis  $(\mathbf{e}, \mathbf{e}_{\chi_1}, \mathbf{e}_{\chi_2})$  associated with the beam, we have:

$$\mathbb{J} = \int_{\Sigma} ((\chi_1^2 + \chi_2^2) \mathbb{I} - (\chi_1 \mathbf{e}_{\chi_1} + \chi_2 \mathbf{e}_{\chi_2}) \otimes (\chi_1 \mathbf{e}_{\chi_1} + \chi_2 \mathbf{e}_{\chi_2})) dS$$

where  $(s, \chi_1, \chi_2)$  are the coordinates of a point of the beam in the vector basis  $(\mathbf{e}, \mathbf{e}_{\chi_1}, \mathbf{e}_{\chi_2})$ : in other words,  $\mathbf{x} = \mathbf{x}_G + \mathbf{x}_{\Sigma} = s\mathbf{e} + \chi_1 \mathbf{e}_{\chi_1} + \chi_2 \mathbf{e}_{\chi_2}$ . Thus, in this basis, we can write:

$$\mathbb{J} = \begin{pmatrix} \int_{\Sigma} (\chi_1^2 + \chi_2^2) dS & 0 & 0 \\ 0 & \int_{\Sigma} \chi_2^2 dS & -\int_{\Sigma} \chi_1 \chi_2 dS \\ 0 & -\int_{\Sigma} \chi_1 \chi_2 dS & \int_{\Sigma} \chi_1^2 dS \end{pmatrix}_{(\mathbf{e}, \mathbf{e}_{\chi_1}, \mathbf{e}_{\chi_2})}$$

Here again, we can see that the axis  $\mathbf{e}$  of the beam is a principal axis of inertia of the tensor  $\mathbb{J}$ , of associated principal moment of inertia  $I_e = \int_{\Sigma} (\chi_1^2 + \chi_2^2) dS$ , which we have called polar moment of inertia of the cross-section.

With regard to the cross-section plane, since the tensor  $\mathbb{J}$  is symmetrical, we know that it is possible to find two perpendicular directions  $\mathbf{e}_{\chi_1}$  and  $\mathbf{e}_{\chi_2}$  which are two principal axes of inertia of  $\mathbb{J}$ , i.e. which are the two other eigenvectors of the tensor  $\mathbb{J}$ . In particular, we can show that the axes of symmetry of the cross-section are principal axes of inertia.

Thus, in the following, we will systematically choose as vectors  $\mathbf{e}_{\chi_1}$  and  $\mathbf{e}_{\chi_2}$  the principal axes of inertia of the cross-section, and we will note  $I_{\chi_1}$  and  $I_{\chi_2}$  the principal moments of inertia respectively associated. The tensor  $\mathbb{J}$  is therefore diagonal in the vector basis  $(\mathbf{e}, \mathbf{e}_{\chi_1}, \mathbf{e}_{\chi_2})$ :

$$\begin{aligned} \mathbb{J} &= I_e \mathbf{e} \otimes \mathbf{e} + I_{\chi_1} \mathbf{e}_{\chi_1} \otimes \mathbf{e}_{\chi_1} + I_{\chi_2} \mathbf{e}_{\chi_2} \otimes \mathbf{e}_{\chi_2} \\ &= \left( \int_{\Sigma} (\chi_1^2 + \chi_2^2) dS \right) \mathbf{e} \otimes \mathbf{e} + \left( \int_{\Sigma} \chi_2^2 dS \right) \mathbf{e}_{\chi_1} \otimes \mathbf{e}_{\chi_1} + \left( \int_{\Sigma} \chi_1^2 dS \right) \mathbf{e}_{\chi_2} \otimes \mathbf{e}_{\chi_2} \end{aligned}$$

where we note that the different principal moments of inertia systematically satisfy the following property:

$$I_e = I_{\chi_1} + I_{\chi_2}$$

It is thus possible to project the constitutive relation for the moment in such a way as to link each of its components to the associated kinematic quantities. Thus, for a Timoshenko beam model, we

obtain:

$$\begin{aligned} M_e &= \mu I_e \theta'_e \\ M_{\chi_1} &= EI_{\chi_1} \theta'_{\chi_1} \\ M_{\chi_2} &= EI_{\chi_2} \theta'_{\chi_2} \end{aligned}$$

and if, in addition, we adopt Euler-Bernoulli hypothesis, we can establish for a straight beam that:

$$\begin{aligned} M_e &= \mu I_e \theta'_e \\ M_{\chi_1} &= -EI_{\chi_1} u''_{G\chi_2} \\ M_{\chi_2} &= EI_{\chi_2} u''_{G\chi_1} \end{aligned}$$

It is thus possible to decouple the different constitutive relations: torsion around  $\mathbf{e}$ , bending around  $\mathbf{e}_{\chi_1}$ , and bending around  $\mathbf{e}_{\chi_2}$ .

**R** As mentioned above, in the case of a static Euler-Bernoulli beam, the shear force is determined from the moment equilibrium equation:

$$\mathbf{R}_\Sigma = \mathbf{e} \wedge (\mathbf{c}_L + \mathbf{M}')$$

With the constitutive relation that has just been specified for the bending moment, we can therefore establish, for a straight beam, that:

$$\mathbf{R}_\Sigma = \mathbf{e} \wedge (\mathbf{c}_L + E \mathbb{J}(\mathbf{e} \wedge \mathbf{u}'''_{G\Sigma}))$$

or, in the vector basis  $(\mathbf{e}_{\chi_1}, \mathbf{e}_{\chi_2})$  associated with the cross-section:

$$T_{\chi_1} = -EI_{\chi_1} u'''_{G\chi_1} - c_{L\chi_2}$$

$$T_{\chi_2} = -EI_{\chi_2} u'''_{G\chi_2} + c_{L\chi_1}$$

which can be rewritten in a more compact form:

$$\boxed{\mathbf{R}_\Sigma = -E \mathbb{P} \mathbb{J} \mathbb{P} \mathbf{u}'''_{G\Sigma} + \mathbf{e} \wedge \mathbf{c}_L}$$

where  $\mathbb{P} = \mathbf{e} \otimes \mathbf{e} + \mathbf{e}_{\chi_1} \otimes \mathbf{e}_{\chi_2} + \mathbf{e}_{\chi_2} \otimes \mathbf{e}_{\chi_1}$  allows for swapping the axes  $\mathbf{e}_{\chi_1}$  and  $\mathbf{e}_{\chi_2}$ , so that one has:

$$\mathbb{P} \mathbb{J} \mathbb{P} = I_c \mathbf{e} \otimes \mathbf{e} + I_{\chi_2} \mathbf{e}_{\chi_1} \otimes \mathbf{e}_{\chi_1} + I_{\chi_1} \mathbf{e}_{\chi_2} \otimes \mathbf{e}_{\chi_2}$$

In the dynamic framework, it is necessary to take into account the inertia terms associated with the bending rotation, i.e., since  $\ddot{\theta}_\Sigma = \mathbf{e} \wedge \ddot{\mathbf{u}}'_{G\Sigma}$ :

$$\mathbf{R}_\Sigma = -E \mathbb{P} \mathbb{J} \mathbb{P} \mathbf{u}'''_{G\Sigma} + \mathbf{e} \wedge (\mathbf{c}_L - \rho \mathbb{J}(\mathbf{e} \wedge \ddot{\mathbf{u}}'_{G\Sigma}))$$

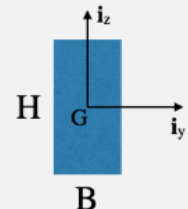
■ **Example 6.7 — Area inertia tensor for some classical cross-sections.** We study here a beam of axis  $\mathbf{i}_x$ , for which we detail the calculation of the area inertia tensor for various examples of cross-section geometries that we frequently encounter in practice.

### Rectangular cross-section

It is assumed here that the cross-section is rectangular, with dimensions  $B$  and  $H$  respectively along the axes  $\mathbf{i}_y$  and  $\mathbf{i}_z$ , which form a Cartesian vector basis of the cross-section. Since these latter are axes of symmetry of the cross-section geometry, the area inertia tensor is then diagonal in this vector basis, and can be written as:

$$\mathbb{J} = I_x \mathbf{i}_x \otimes \mathbf{i}_x + I_y \mathbf{i}_y \otimes \mathbf{i}_y + I_z \mathbf{i}_z \otimes \mathbf{i}_z$$

with:



$$I_y = \int_{\Sigma} z^2 dS = \int_{-B/2}^{B/2} \int_{-H/2}^{H/2} z^2 dz dy = B \left[ \frac{z^3}{3} \right]_{-H/2}^{H/2} = \frac{BH^3}{12}$$

and:

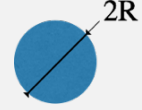
$$I_z = \int_{\Sigma} y^2 dS = \int_{-H/2}^{H/2} \int_{-B/2}^{B/2} y^2 dy dz = H \left[ \frac{y^3}{3} \right]_{-B/2}^{B/2} = \frac{HB^3}{12}$$

Therefore, the polar moment of inertia of the cross-section is:

$$I_x = I_y + I_z = \frac{BH^3}{12} + \frac{HB^3}{12} = \frac{BH}{12}(H^2 + B^2)$$

### Circular cross-section

We now assume that the cross-section is circular with radius  $R$ ; we can then use any cylindrical coordinate system  $(G, \mathbf{i}_r(\theta), \mathbf{i}_\theta(\theta), \mathbf{i}_x)$ , centred in the cross-section, to calculate the area inertia tensor, which here is such that:



$$\mathbb{J} = \int_{\Sigma} (\|\mathbf{x}_{\Sigma}\|^2 \mathbb{I} - \mathbf{x}_{\Sigma} \otimes \mathbf{x}_{\Sigma}) dS = \int_0^{2\pi} \int_0^R (\|r\mathbf{i}_r(\theta)\|^2 \mathbb{I} - r\mathbf{i}_r(\theta) \otimes r\mathbf{i}_r(\theta)) r dr d\theta$$

since  $\mathbf{x}_{\Sigma} = r\mathbf{i}_r(\theta)$ . We then obtain:

$$\mathbb{J} = 2\pi \int_0^R r^3 dr \mathbf{i}_x \otimes \mathbf{i}_x + \int_0^R r^3 dr \int_0^{2\pi} \mathbf{i}_{\theta}(\theta) \otimes \mathbf{i}_{\theta}(\theta) d\theta$$

If the cylindrical vector basis is such that  $(\mathbf{i}_r(\theta), \mathbf{i}_{\theta}(\theta), \mathbf{i}_x) = (\mathbb{R}\mathbf{i}_y, \mathbb{R}\mathbf{i}_z, \mathbf{i}_x)$ , where  $\mathbb{R}$  is the rotation tensor around axis  $\mathbf{i}_x$  and of angle  $\theta$ , and with  $(\mathbf{i}_y, \mathbf{i}_z, \mathbf{i}_x)$  a Cartesian vector basis, we easily verify that:

$$\int_0^{2\pi} \mathbf{i}_{\theta}(\theta) \otimes \mathbf{i}_{\theta}(\theta) d\theta = \pi(\mathbf{i}_y \otimes \mathbf{i}_y + \mathbf{i}_z \otimes \mathbf{i}_z)$$

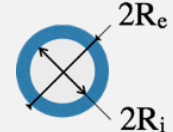
which finally implies that:

$$\mathbb{J} = \pi \frac{R^4}{2} \mathbf{i}_x \otimes \mathbf{i}_x + \pi \frac{R^4}{4} \mathbf{i}_y \otimes \mathbf{i}_y + \pi \frac{R^4}{4} \mathbf{i}_z \otimes \mathbf{i}_z$$

where we find in particular that  $I_x = I_y + I_z$ .

### Annular cross-section

We now study an annular hollow cross-section, with inner radius  $R_i$  and outer radius  $R_e$ . A simple way to calculate the associated area inertia tensor is to consider that the cross-section is obtained as the “difference” between a circular cross-section  $\Sigma_e$  of radius  $R_e$  and a circular cross-section  $\Sigma_i$  of radius  $R_i$ :



$$\mathbb{J} = \int_{\Sigma_e \setminus \Sigma_i} (\|\mathbf{x}_{\Sigma}\|^2 \mathbb{I} - \mathbf{x}_{\Sigma} \otimes \mathbf{x}_{\Sigma}) dS = \int_{\Sigma_e} (\|\mathbf{x}_{\Sigma}\|^2 \mathbb{I} - \mathbf{x}_{\Sigma} \otimes \mathbf{x}_{\Sigma}) dS - \int_{\Sigma_i} (\|\mathbf{x}_{\Sigma}\|^2 \mathbb{I} - \mathbf{x}_{\Sigma} \otimes \mathbf{x}_{\Sigma}) dS$$

which makes it possible to obtain directly:

$$\mathbb{J} = \pi \frac{R_e^4 - R_i^4}{2} \mathbf{i}_x \otimes \mathbf{i}_x + \pi \frac{R_e^4 - R_i^4}{4} \mathbf{i}_y \otimes \mathbf{i}_y + \pi \frac{R_e^4 - R_i^4}{4} \mathbf{i}_z \otimes \mathbf{i}_z$$

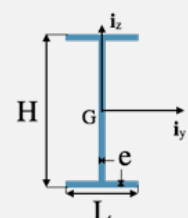
In addition, if the thickness  $e = R_e - R_i$  is very small when compared to  $R_i \approx R_e \approx R$ , we obtain, up to order one in  $e/R$ :

$$\mathbb{J} = 2\pi e R^3 \mathbf{i}_x \otimes \mathbf{i}_x + \pi e R^3 \mathbf{i}_y \otimes \mathbf{i}_y + \pi e R^3 \mathbf{i}_z \otimes \mathbf{i}_z$$

### “I”-shaped cross-section

We study here a cross-section profile very widespread in the field of construction, namely an “I-profile” (or “universal profile”), which consists of two horizontal and symmetrical elements (“flanges”), of width  $L$  and thickness  $e$ , connected by a vertical element (“web”), of height  $H$  and thickness  $e$ . This profile can then be decomposed into three cross-sections of elementary shapes:

- a rectangular cross-section  $\Sigma_1$  of width  $L$  along  $\mathbf{i}_y$  and height  $H$  along  $\mathbf{i}_z$ ;
- a rectangular cross-section  $\Sigma_2$  of width  $L$  along  $\mathbf{i}_y$  and height  $H - 2e$  along  $\mathbf{i}_z$ ;
- a rectangular cross-section  $\Sigma_3$  of thickness  $e$  along  $\mathbf{i}_y$  and height  $H - 2e$  along  $\mathbf{i}_z$ .



The “I-profile” studied here therefore corresponds to  $\Sigma = (\Sigma_1 \setminus \Sigma_2) \cup \Sigma_3$ , and the associated area inertia tensor is then simply:

$$\mathbb{J} = I_x \mathbf{i}_x \otimes \mathbf{i}_x + I_y \mathbf{i}_y \otimes \mathbf{i}_y + I_z \mathbf{i}_z \otimes \mathbf{i}_z$$

with:

$$I_y = \frac{LH^3}{12} - \frac{L(H-2e)^3}{12} + \frac{e(H-2e)^3}{12} \approx \frac{eH^2}{12}(H+6L)$$

if we assume that the thickness  $e$  is small when compared to the transverse dimensions  $H$  and  $L$ , and, similarly:

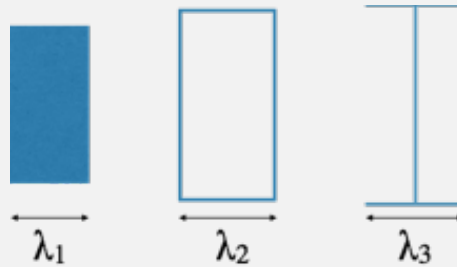
$$I_z = \frac{HL^3}{12} - \frac{(H-2e)L^3}{12} + \frac{(H-2e)e^3}{12} \approx \frac{eL^3}{6}$$

as well as, finally:

$$I_x = I_y + I_z \approx \frac{e}{12} (H^3 + 6H^2L + 2L^3)$$

This cross-section profile is widely used in the case of beams subjected to bending stresses: indeed, a beam is all the more rigid against such stresses when the associated area moment of inertia is large. Let us compare the geometry of three cross-sections of different shapes, but with the same moment of inertia  $I_y$ :

1. a beam of rectangular cross-section, of dimensions  $\lambda_1$  along  $\mathbf{i}_y$  and  $2\lambda_1$  along  $\mathbf{i}_z$ ;
2. a beam with a hollow rectangular cross-section, of external dimensions  $\lambda_2$  along  $\mathbf{i}_y$  and  $2\lambda_2$  along  $\mathbf{i}_z$ , and thickness  $\lambda_2/10$ ;
3. a beam with a “I-profile” cross-section, with dimensions  $L = \lambda_3$ ,  $H = 2\lambda_3$  and  $e = \lambda_3/10$ .



The table below lists for these three cross-section geometries the dimensions allowing us to obtain a moment of inertia  $I_y$  identical in the three cases (equal to  $100 \text{ cm}^4$ ), as well as the associated areas: we can see that the “I”-shaped cross-section has the minimum area, which means it is the best of the three in terms of bending stiffness / required mass ratio, which explains why it is very widespread.

	Solid cross-section	Hollow cross-section	“I”-shaped cross-section
Size	$\lambda_1 = 3.5 \text{ cm}$	$\lambda_2 = 4.2 \text{ cm}$	$\lambda_3 = 4.4 \text{ cm}$
Area	$A_1 = 2\lambda_1^2 = 24.5 \text{ cm}^2$	$A_2 = \frac{3}{5}\lambda_2^2 = 10.4 \text{ cm}^2$	$A_3 = \frac{2}{5}\lambda_3^2 = 7.7 \text{ cm}^2$
Moment of inertia	$I_{y1} = \frac{2}{3}\lambda_1^4 = 100 \text{ cm}^4$	$I_{y2} = \frac{\lambda_2^4}{3} = 100 \text{ cm}^4$	$I_{y3} = \frac{4}{15}\lambda_3^4 = 100 \text{ cm}^4$

### “L”-shaped cross-section

Finally, we study a last cross-section profile, very used in the construction field, namely a “L-profile” (or “angle profile”) composed of two perpendicular “legs”, of respective directions  $\mathbf{i}_y$  and  $\mathbf{i}_z$ , of length  $L$  and thickness  $e$ . The very shape of this profile implies a number of precautions, which are detailed below.

The first step is to determine the centre of the cross-section; the associated calculation leads to:

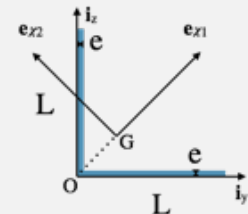
$$y_G = z_G = \frac{L^2 + Le - e^2}{4L - 2e}$$

if the origin  $O$  of the coordinate system  $(O, \mathbf{i}_y, \mathbf{i}_z)$  has been placed at the vertex of the angle. If, as is the case in practice, we assume that  $e \ll L$ , we find the following position:

$$y_G = z_G \approx \frac{L}{4}$$

The second step is the calculation of the area inertia tensor of the cross-section expressed at point  $G$ ; this results in:

$$\mathbb{J} = I_x \mathbf{i}_x \otimes \mathbf{i}_x + I_y \mathbf{i}_y \otimes \mathbf{i}_y + I_z \mathbf{i}_z \otimes \mathbf{i}_z - I_{yz} (\mathbf{i}_y \otimes \mathbf{i}_z + \mathbf{i}_z \otimes \mathbf{i}_y)$$



with:

$$I_y = I_z = \frac{e}{12} \frac{(5L^2 - 5Le + e^2)(L^2 - Le + e^2)}{2L - e} \approx \frac{5}{24} eL^3$$

and:

$$I_x = I_y + I_z = \frac{e}{6} \frac{(5L^2 - 5Le + e^2)(L^2 - Le + e^2)}{2L - e} \approx \frac{5}{12} eL^3$$

and:

$$I_{yz} = \frac{e}{4} \frac{L^2(L-e)^2}{2L-e} \approx \frac{eL^3}{8}$$

when  $e \ll L$ . Thus, the product of inertia  $I_{yz}$  is not zero, which means that the axes  $\mathbf{i}_y$  and  $\mathbf{i}_z$  are not principal axes of inertia.

In order to facilitate bending calculations, it is interesting to work with the principal directions of the area inertia tensor; for this purpose, we can see that the bisector of  $(\mathbf{i}_y, \mathbf{i}_z)$  is an axis of symmetry of the cross-section geometry, and, consequently, a principal axis of inertia, noted  $\mathbf{e}_{\chi_1}$ . The second principal direction is then given by  $\mathbf{e}_{\chi_2} = \mathbf{i}_x \wedge \mathbf{e}_{\chi_1}$ . In this vector basis, the area inertia tensor is now expressed as a diagonal tensor:

$$\mathbb{J} = I_x \mathbf{i}_x \otimes \mathbf{i}_x + I_{\chi_1} \mathbf{e}_{\chi_1} \otimes \mathbf{e}_{\chi_1} + I_{\chi_2} \mathbf{e}_{\chi_2} \otimes \mathbf{e}_{\chi_2}$$

with:

$$I_{\chi_1} = \frac{e}{12} (2L - e)(2L^2 - 2Le + e^2) \approx \frac{eL^3}{3}$$

and:

$$I_{\chi_2} = \frac{e}{12} \frac{2L^4 - 4L^3e + 8L^2e^2 - 6Le^3 + e^4}{2L - e} \approx \frac{eL^3}{12}$$

when  $e \ll L$ , and:

$$I_x = I_{\chi_1} + I_{\chi_2} = \frac{e}{6} \frac{(5L^2 - 5Le + e^2)(L^2 - Le + e^2)}{2L - e} \approx \frac{5}{12} eL^3$$

■



*In the case where the cross-section is not circular, we have seen in Example 5.3 (on page 126) that the cross-sections did not remain planar when subjected to torsion, and that this warping phenomenon reduced the torsional stiffness of the beam under study. To take this into account, the polar moment of inertia of the cross-section “without warping”  $I_e$  is replaced by its counterpart  $J$  defined in Example 5.6 (on page 136) as:*

$$J = I_e + \left\langle \mathbf{e}, \int_{\Sigma} \mathbf{x}_{\Sigma} \wedge \nabla_{\mathbf{x}_{\Sigma}} \varphi dS_x \right\rangle$$

where  $\varphi(\mathbf{x}_{\Sigma})$  is the warping function, obtained by solving on the cross-section:

$$\Delta_{\mathbf{x}_{\Sigma}} \varphi = 0$$

with, as a boundary condition on the contour of the cross-section:

$$\frac{\partial \varphi}{\partial n} = \langle \mathbf{x}_{\Sigma}, \mathbf{t}_l \rangle$$

where  $\mathbf{t}_l$  is the vector tangent to the contour.

■ **Example 6.8 — Deformation of a chimney subjected to wind.** The goal is to determine here the displacements of the points of the chimney, starting from the knowledge of the resultant force and the moment of the internal loads along the neutral axis.

The first constitutive relation allows us to link the axial force to the longitudinal displacement of the cross-section centres, and can be written as:

$$EAu'_{Gz}(z) = R_z(z) = \rho g \pi (r_e^2 - r_i^2)(z - H), \forall z \in [0, H]$$

with  $A = \pi (r_e^2 - r_i^2)$ , which implies that:

$$u_{Gz}(z) = \frac{\rho g}{2E} (z^2 - 2Hz)$$

since the integration constant is zero using the boundary condition at  $z = 0$ :

$$u_{Gz}(0) = 0$$

the cross section of altitude  $z = 0$  being placed on the ground, assumed fixed and perfectly rigid, with no possibility of relative movement. The settlement of the chimney (since  $u_{Gz} \leq 0, \forall z$ ) therefore evolves as a quadratic function of the altitude.

The second constitutive relation connects the moment of torsion to the angle of twist of the cross-sections, and is written here as:

$$\mu I_z \theta'_z(z) = M_z(z) = 0, \forall z \in [0, H]$$

which leads to the conclusion that:

$$\boxed{\theta_z(z) = C = 0}$$

as, since the cross-section of altitude  $z = 0$  is fixed, its rotation is zero. So there is no torsion of the chimney.

The third constitutive relation links, according to Euler-Bernoulli hypothesis, the bending moment to the transverse displacement of the neutral axis:

$$EI_y \mathbf{i}_z \wedge \mathbf{u}_{G\Sigma}''(z) = M_y(z) \mathbf{i}_y = \frac{K\pi r_e}{24} (z^4 - 4H^3 z + 3H^4) \mathbf{i}_y$$

If we take the vector product of this equation with  $\mathbf{i}_z$ , we get:

$$EI_y \mathbf{u}_{G\Sigma}''(z) = \frac{K\pi r_e}{24} (z^4 - 4H^3 z + 3H^4) \mathbf{i}_x$$

which gives, after two successive integrations:

$$\mathbf{u}_{G\Sigma}(z) = \frac{K\pi r_e}{720EI_y} (z^6 - 20H^3 z^3 + 45H^4 z^2) \mathbf{i}_x + \mathbf{C}_1 z + \mathbf{C}_2$$

where  $\mathbf{C}_1$  and  $\mathbf{C}_2$  are two constant vectors to be determined using the boundary conditions at  $z = 0$ : the fact that the chimney is fixed to the ground with no possibility of relative movement means that the transverse displacement is zero:

$$\mathbf{u}_{G\Sigma}(0) = \mathbf{0}, \text{ hence } \mathbf{C}_2 = \mathbf{0}$$

and that the rotation of the cross-section is also equal to zero, which implies, using Euler-Bernoulli hypothesis, that the derivative of the transverse displacement is zero at  $z = 0$ :

$$\mathbf{u}'_{G\Sigma}(0) = \mathbf{0}, \text{ hence } \mathbf{C}_1 = \mathbf{0}$$

hence, the neutral axis satisfies the following transverse displacement:

$$\mathbf{u}_{G\Sigma}(z) = \frac{K\pi r_e}{720EI_y} (z^6 - 20H^3 z^3 + 45H^4 z^2) \mathbf{i}_x$$

Thus, the displacement of the neutral axis is finally:

$$\boxed{\mathbf{u}_G(z) = \frac{K\pi r_e}{720EI_y} (z^6 - 20H^3 z^3 + 45H^4 z^2) \mathbf{i}_x + \frac{\rho g}{2E} (z^2 - 2Hz) \mathbf{i}_z}$$

which allows us to determine the displacements of all the points of the beam, since the cross-sections remain perpendicular to the deformed neutral axis according to Euler-Bernoulli hypothesis, which is expressed as:

$$\boldsymbol{\theta}_\Sigma(z) = \mathbf{i}_z \wedge \mathbf{u}'_{G\Sigma}(z) = u'_{Gx}(z) \mathbf{i}_y = \frac{K\pi r_e}{120EI_y} (z^5 - 10H^3 z^2 + 15H^4 z) \mathbf{i}_y$$

In conclusion, a point  $M$  of coordinates  $(x, y, z)$  in the Cartesian vector basis  $(\mathbf{i}_x, \mathbf{i}_y, \mathbf{i}_z)$  satisfies the following displacement:

$$\boxed{\begin{aligned} \mathbf{u}(x, y, z) &= \mathbf{u}_G(z) + \boldsymbol{\theta}(z) \wedge (x\mathbf{i}_x + y\mathbf{i}_y) \\ &= u_{Gx}(z) \mathbf{i}_x + u_{Gz}(z) \mathbf{i}_z - yu'_{Gx}(z) \mathbf{i}_z \\ &= \frac{K\pi r_e}{720EI_y} (z^6 - 20H^3 z^3 + 45H^4 z^2 - y(6z^5 - 60H^3 z^2 + 90H^4 z)) \mathbf{i}_x \\ &\quad + \frac{\rho g}{2E} (z^2 - 2Hz) \mathbf{i}_z \end{aligned}}$$

■

**R** The characteristics of the cross-section (area and area inertia tensor) can evolve along the neutral axis without questioning the validity of the constitutive relations that we established for the resultant force and the moment of the internal loads. In this case, these characteristics then become functions of the arc length  $s$ .

### 6.3.4 Stresses within a cross-section

We have just seen how to link the internal loads to the kinematics of a beam, using the local stress-strain relations; conversely, it is possible to use these relations in order to make a link between the local stresses in the cross-section, and the internal loads represented by the resultant force and the moment of the actions on a cross-section.

Indeed, we can establish using the relations of Paragraph 6.3.1 that the stress vector in the cross-section  $\Sigma$  of coordinate  $s$  can be written as:

$$\sigma \mathbf{e} = \sigma_{ee} \mathbf{e} + \tau_\Sigma = E \varepsilon_{ee} \mathbf{e} + \mu \gamma_\Sigma$$

with  $\varepsilon_{ee} = u'_{Ge} + \langle \boldsymbol{\theta}'_\Sigma \wedge \mathbf{x}_\Sigma, \mathbf{e} \rangle$  and  $\gamma_\Sigma = \mathbf{u}'_{G\Sigma} - \boldsymbol{\theta}_\Sigma \wedge \mathbf{e} + \theta'_e \mathbf{e} \wedge \mathbf{x}_\Sigma$  if we do not take into account for the time being Euler-Bernoulli hypothesis.

It is then sufficient to replace each kinematic quantity by the associated components of the resultant force and moment of the internal loads, using the relations established in Paragraphs 6.3.2 and 6.3.3. Thus, the normal stress  $\sigma_{ee}$  is such that:

$$\sigma_{ee} = E(u'_{Ge} + \langle \boldsymbol{\theta}'_\Sigma \wedge \mathbf{x}_\Sigma, \mathbf{e} \rangle)$$

and we can use in this equation the relations:

$$R_e = EAu'_{Ge}, \text{ and } \mathbf{M}_\Sigma = E\mathbb{J}\boldsymbol{\theta}'_\Sigma$$

after inverting them (since, in particular, the area inertia tensor  $\mathbb{J}$  is invertible), to obtain that:

$$\sigma_{ee} = E \left( \frac{R_e}{EA} + \left\langle \frac{1}{E} \mathbb{J}^{-1} \mathbf{M}_\Sigma \wedge \mathbf{x}_\Sigma, \mathbf{e} \right\rangle \right)$$

which finally leads to:

$$\sigma_{ee} = \frac{R_e}{A} + \langle \mathbf{x}_\Sigma, \mathbf{e} \wedge \mathbb{J}^{-1} \mathbf{M}_\Sigma \rangle$$

The normal stress  $\sigma_{ee}$  is therefore expressed as the sum of two terms:

- the first one, which is constant in the cross-section, results from the tensile (or compression) axial force  $N = R_e$  applied along the beam axis;
- the second one, linear along both directions  $\mathbf{e}_{\chi_1}$  and  $\mathbf{e}_{\chi_2}$  of the cross-section, is related to the two components of the bending moment  $\mathbf{M}_f = \mathbf{M}_\Sigma$  around these two axes.

Thus, we see that the normal stress is linear in the cross-section, as shown in Figure 6.15, where only bending in the vertical plane is taken into account, in addition to tension.

Similarly, the shear stress  $\tau_\Sigma$  can be expressed as:

$$\tau_\Sigma = \mu (\mathbf{u}'_{G\Sigma} - \boldsymbol{\theta}_\Sigma \wedge \mathbf{e} + \theta'_e \mathbf{e} \wedge \mathbf{x}_\Sigma)$$

and by using in this equation the following relations, once inverted:

$$\mathbf{R}_\Sigma = \mu A (\mathbf{u}'_{G\Sigma} - \boldsymbol{\theta}_\Sigma \wedge \mathbf{e}), \text{ and } M_e = \mu I_e \theta'_e$$

we finally end up with:

$$\tau_\Sigma = \frac{1}{A} \mathbf{R}_\Sigma + \frac{M_e}{I_e} \mathbf{e} \wedge \mathbf{x}_\Sigma$$

Thus, the shear stress is expressed as the conjunction of two effects:

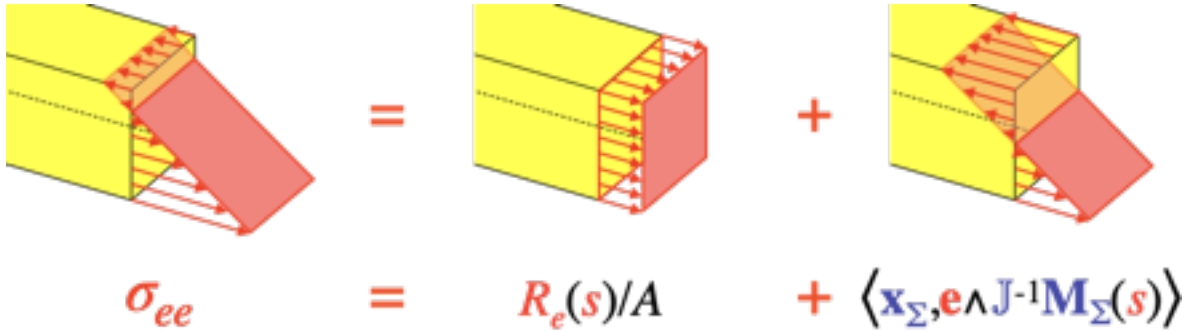


Figure 6.15: Variation of the normal stress  $\sigma_{ee}$  in a given cross-section: cumulative effects of tension and bending.

- the first one, associated with bending, corresponds to the transverse shear, homogeneous in the cross-section, and which reflects the fact that this latter does not remain perpendicular to the deformed neutral axis;
- the second one, which evolves as a linear function of the distance from the centre of the cross-section, is associated with torsion, as shown in Figure 6.16.

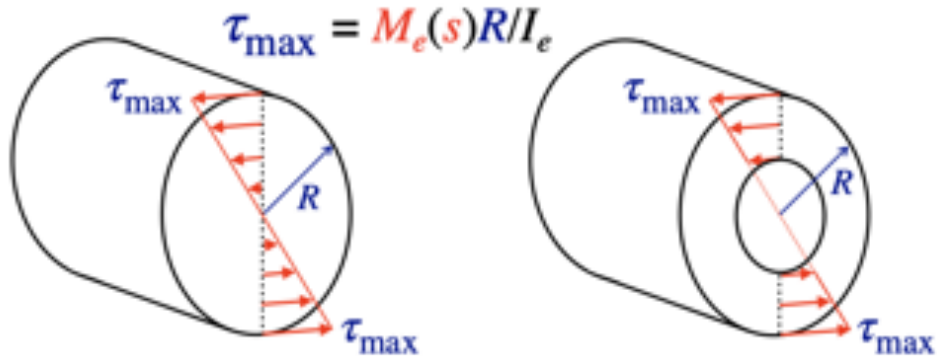


Figure 6.16: Variation of the shear stress  $\tau_\Sigma$  associated with torsion, in the case of a circular cross-section.

**Summary 6.11 — Stress vector in a cross-section.** In the general case, the stress vector in a cross-section  $\Sigma$  of coordinate  $s$  can be expressed, as a function of the components of the resultant force and moment of the internal loads:

$$\sigma \mathbf{e} = \sigma_{ee}(s, t) \mathbf{e} + \tau_\Sigma(s, t) = \left( \frac{R_e(s, t)}{A} + \langle \mathbf{x}_\Sigma, \mathbf{e} \wedge \mathbb{J}^{-1} \mathbf{M}_\Sigma(s, t) \rangle \right) \mathbf{e} + \frac{1}{A} \mathbf{R}_\Sigma(s, t) + \frac{M_e(s, t)}{I_e} \mathbf{e} \wedge \mathbf{x}_\Sigma, \forall t$$

where  $A$  is the cross-section area, and  $I_e$  the polar moment of inertia of the cross-section.

(R) It can be shown that, in the case of bending (without torsion):

$$\frac{\|\tau_\Sigma\|}{|\sigma_{ee}|} = O\left(\frac{H}{L}\right)$$

where  $H$  is an order of magnitude of the transverse dimensions of the beam. The shear stress is therefore all the more negligible when compared to the normal stress that the beam is “thin” and it is therefore often neglected when adopting Euler-Bernoulli hypothesis.

■ **Example 6.9 — Stresses in a chimney exposed to wind.** From the resultant force and moment of the internal loads determined in Examples 6.4 and 6.6, we can estimate the normal stress at each point of coordinates  $(x, y, z)$  as:

$$\sigma_{zz}(x, y, z) = \frac{R_z(z)}{A} + \langle x\mathbf{i}_x + y\mathbf{i}_y, \mathbf{i}_z \wedge \mathbb{J}^{-1}\mathbf{M}_{\Sigma}(z) \rangle$$

with:

$$A = \pi(r_e^2 - r_i^2), \text{ and } \mathbb{J} = \pi \frac{r_e^4 - r_i^4}{4} (\mathbf{i}_x \otimes \mathbf{i}_x + \mathbf{i}_y \otimes \mathbf{i}_y + 2\mathbf{i}_z \otimes \mathbf{i}_z)$$

and:

$$R_z(z) = -\rho g \pi (r_e^2 - r_i^2) (H - z)$$

$$\mathbf{M}_{\Sigma}(z) = \frac{K\pi r_e}{24} (z^4 - 4H^3 z + 3H^4) \mathbf{i}_y$$

which leads to:

$$\sigma_{zz}(x, y, z) = -\rho g(H - z) - \frac{Kr_e}{6(r_e^4 - r_i^4)} (z^4 - 4H^3 z + 3H^4) x$$

Thus, for a cross-section of given altitude  $z$ , the axial stress evolves linearly between the two following extreme values:

$$\sigma_{zz\min/\max} = -\rho g(H - z) \mp \frac{Kr_e^2}{6(r_e^4 - r_i^4)} (z^4 - 4H^3 z + 3H^4)$$

and the most loaded cross-section is the one in contact with the ground, at  $z = 0$ , for which the maximum stress is, in absolute value:

$$|\sigma_{zz}|_{\max} = \rho g H + \frac{Kr_e^2 H^4}{2(r_e^4 - r_i^4)}$$

which is located at  $x = r_e$ . The shear stress is then:

$$\tau_{\Sigma}(z) = \frac{1}{A} \mathbf{R}_{\Sigma}(z) = \frac{Kr_e}{6(r_e^2 - r_i^2)} (H^3 - z^3) \mathbf{i}_x$$

and is negligible when compared to the normal stress when  $r_e \ll H$ .

■

## 6.4 Connections between beams

In order to be able to address problems where multiple beams are assembled, a first step is to describe the connections that can be proposed for these assemblies, particularly in terms of kinematics and transmissible actions.

### 6.4.1 Kinematics associated with a connection

Any connection between a beam  $\Omega$  and another body  $\Omega^*$  (a fixed support, a rigid body, or another beam) allows, for the concerned cross-section  $\Sigma$  of  $\Omega$ , a certain number of relative movements with respect to the other body, namely, since the cross-section  $\Sigma$  is perfectly rigid:

- three elementary translational movements of the centre  $G$  of the cross-section  $\Sigma$ ;
- three elementary rotational movements of the cross-section  $\Sigma$ .

In what follows, we will assume that these elementary movements remain “small”, which allows us to adopt the framework of the infinitesimal deformation hypothesis, and, in particular, to consider the initial and current configurations as one.

Thus, it is assumed that the placement vector of the points of the body  $\Omega^*$  (or a subpart, such as one of its cross-sections if it is a beam) verifies:

$$\mathbf{x}^* = \mathbf{x}_A + \mathbf{r}(\mathbf{p} - \mathbf{p}_A)$$

where  $A$  is a given point of  $\Omega^*$ , and  $\mathbf{r} = \mathbb{I} + \alpha \wedge$  is the “small” rotation associated with  $\Omega^*$ , as defined in Appendix A.2.6. Usually, we will focus on the displacements of the points of  $\Omega^*$  (or a subpart),

by adopting the infinitesimal deformation hypothesis allowing us to consider the initial and current configurations as one:

$$\mathbf{u}^* = \mathbf{u}_A + \boldsymbol{\alpha} \wedge (\mathbf{x} - \mathbf{x}_A)$$

where  $\mathbf{u}_A$  is the displacement of point  $A$ , and  $\boldsymbol{\alpha}$  is the vector of “small” rotation associated with the antisymmetrical tensor  $\boldsymbol{\alpha}^\wedge$ .

Four types of connections are commonly found in the case of beams: they are detailed in the following.

### Rigid connection

The first connection studied here is a perfectly rigid connection, or a “clamped end”, that does not allow any relative movement between  $\Omega$  and  $\Omega^*$ . Thus, the displacements  $\mathbf{u}$  of the points of the (perfectly rigid) cross-section  $\Sigma$  of  $\Omega$  which is clamped are entirely determined by the expression of the displacement field of the points of  $\Omega^*$ :

$$\mathbf{u}_G + \boldsymbol{\theta} \wedge \mathbf{x}_\Sigma = \mathbf{u} = \mathbf{u}^* = \mathbf{u}_A + \boldsymbol{\alpha} \wedge (\mathbf{x}_G - \mathbf{x}_A) + \boldsymbol{\alpha} \wedge \mathbf{x}_\Sigma$$

or, by term-to-term identification:

$$\mathbf{u}_G = \mathbf{u}_A + \boldsymbol{\alpha} \wedge (\mathbf{x}_G - \mathbf{x}_A), \text{ and } \boldsymbol{\theta} = \boldsymbol{\alpha}$$

In the particular case where  $\Omega^*$  is a perfectly rigid and fixed support, the movements of all the points of the cross-section  $\Sigma$  are then zero, i.e., more precisely:

$$\mathbf{u}_G = \mathbf{0}, \text{ and } \boldsymbol{\theta} = \mathbf{0}$$

If we also adopt Euler-Bernoulli hypothesis, which is equivalent to assuming that  $\mathbf{u}'_{G\Sigma} = \boldsymbol{\theta}_\Sigma \wedge \mathbf{e}$ , this implies that:

$$\mathbf{u}'_{G\Sigma} = \mathbf{0}$$

In the common case where  $\Omega^*$  is another beam (where the cross-section  $\Sigma^*$  is concerned by the connection), the rigid connection between the two beams implies that the movements of the centres of the two cross-sections, on the one hand, and the rotations of the two cross-sections, on the other hand, are the same. Moreover, if an intermediate part does not constitute the rigid connection, this is equivalent to assuming that the two neutral axes intersect at a point  $G$  common to both beams, implying then, with evident notations to distinguish the expressions relating to the two beams, that:

$$\mathbf{u}_G = \mathbf{u}_G^*, \text{ and } \boldsymbol{\theta} = \boldsymbol{\theta}^*$$

This is, of course, a schematization of reality, since such a connection between the two beams can only be made according to a particular volume domain (a cube, for example, for two perpendicular beams of square cross-sections of the same transverse dimensions), which has no reason to verify the kinematic assumptions of beams rigorously. If the dimensions of the cross-sections are small when compared to the lengths of the beams, this approximation is still considered to be correct.

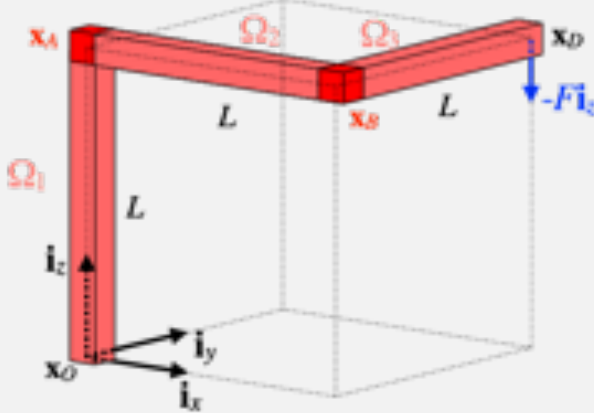
If, moreover, we adopt for the two beams Euler-Bernoulli hypothesis, which is equivalent to assuming that  $\boldsymbol{\theta}_\Sigma = \mathbf{e} \wedge \mathbf{u}'_{G\Sigma}$  and  $\boldsymbol{\theta}_\Sigma^* = \mathbf{e}^* \wedge \mathbf{u}_{G\Sigma^*}'$ , we can then write that:

$$\theta_e \mathbf{e} + \mathbf{e} \wedge \mathbf{u}'_{G\Sigma} = \theta_{e^*} \mathbf{e}^* + \mathbf{e}^* \wedge \mathbf{u}_{G\Sigma^*}'$$

where  $\mathbf{e}$  and  $\mathbf{e}^*$  are the respective axes of the beams  $\Omega$  and  $\Omega^*$ .

■ **Example 6.10 — Kinematic conditions for connections in a portal frame.** We study here a portal frame made of three beams  $\Omega_1$ ,  $\Omega_2$  and  $\Omega_3$  of same length, and oriented respectively along the three directions of a Cartesian vector basis ( $\mathbf{i}_z, \mathbf{i}_x, \mathbf{i}_y$ ):

- the coordinate along the beam  $\Omega_1$  goes from  $z = 0$  at point  $O$  to  $z = L$  at point  $A$ ;
- the coordinate along the beam  $\Omega_2$  goes from  $x = 0$  at point  $A$  to  $x = L$  at point  $B$ ;
- the coordinate along the beam  $\Omega_3$  goes from  $y = 0$  at point  $B$  to  $y = L$  at point  $D$ .



The first beam  $\Omega_1$  is clamped at the cross-section of centre  $O$  on a rigid and fixed support, which allows us to write at  $z = 0$  that:

$$\mathbf{u}_G^{\mathcal{Q}}(0) = \mathbf{0}, \text{ and } \boldsymbol{\theta}^{\mathcal{Q}}(0) = \mathbf{0}$$

In addition, if we adopt Euler-Bernoulli hypothesis, the condition on the rotation at  $z = 0$  becomes:

$$\boldsymbol{\theta}_z^{\mathcal{Q}}(0)\mathbf{i}_z + \mathbf{i}_z \wedge \mathbf{u}_{G\Sigma}^{\mathcal{Q}}(0) = \mathbf{0}$$

The second beam  $\Omega_2$  is clamped on the previous one at the point  $A$  common to the neutral axes of the two beams, i.e. at  $z = L$  for the beam  $\Omega_1$  and at  $x = 0$  for the beam  $\Omega_2$ :

$$\mathbf{u}_G^{\mathcal{Q}}(L) = \mathbf{u}_G^{\mathcal{Q}}(0), \text{ and } \boldsymbol{\theta}^{\mathcal{Q}}(L) = \boldsymbol{\theta}^{\mathcal{Q}}(0)$$

In addition, if we adopt Euler-Bernoulli hypothesis, the condition on rotations at  $z = L$  and  $x = 0$  becomes:

$$\boldsymbol{\theta}_z^{\mathcal{Q}}(L)\mathbf{i}_z + \mathbf{i}_z \wedge \mathbf{u}_{G\Sigma}^{\mathcal{Q}}(L) = \boldsymbol{\theta}_x^{\mathcal{Q}}(0)\mathbf{i}_x + \mathbf{i}_x \wedge \mathbf{u}_{G\Sigma}^{\mathcal{Q}}(0)$$

which leads to the following scalar relations:

$$\begin{aligned} -u_{Gy}^{\mathcal{Q}}(L) &= \theta_x^{\mathcal{Q}}(0) \\ u_{Gx}^{\mathcal{Q}}(L) &= -u_{Gz}^{\mathcal{Q}}(0) \\ \theta_z^{\mathcal{Q}}(L) &= u_{Gy}^{\mathcal{Q}}(0) \end{aligned}$$

Finally, the third beam  $\Omega_3$  is clamped on the previous one at the point  $B$  common to the neutral axes of the two beams, i.e. at  $x = L$  for the beam  $\Omega_2$  and at  $y = 0$  for the beam  $\Omega_3$ :

$$\mathbf{u}_G^{\mathcal{Q}}(L) = \mathbf{u}_G^{\mathcal{Q}}(0), \text{ and } \boldsymbol{\theta}^{\mathcal{Q}}(L) = \boldsymbol{\theta}^{\mathcal{Q}}(0)$$

In addition, if we adopt Euler-Bernoulli hypothesis, the condition on rotations at  $x = L$  and  $y = 0$  becomes:

$$\boldsymbol{\theta}_x^{\mathcal{Q}}(L)\mathbf{i}_x + \mathbf{i}_x \wedge \mathbf{u}_{G\Sigma}^{\mathcal{Q}}(L) = \boldsymbol{\theta}_y^{\mathcal{Q}}(0)\mathbf{i}_y + \mathbf{i}_y \wedge \mathbf{u}_{G\Sigma}^{\mathcal{Q}}(0)$$

leading to scalar relations similar to those written in  $A$ . ■

### Spherical joint

A “spherical joint” (or “ball joint”) between  $\Omega$  and  $\Omega^*$  allows no relative translation, and any relative rotation between the two bodies: it is generally a “pin joint”, such as those visible in Figure 6.17, and whose clearance allows a rotation of arbitrary axis. Thus, only the displacement of the centre  $G$  of the cross-section  $\Sigma$  of the beam  $\Omega$ , located at the centre of the spherical joint, is related to the displacement of the body  $\Omega^*$  at the same point:

$$\mathbf{u}_G = \mathbf{u}_G^* = \mathbf{u}_A + \boldsymbol{\alpha} \wedge (\mathbf{x}_G - \mathbf{x}_A)$$

and the beam  $\Theta$  of the cross-section  $\Sigma$  remains free.



Figure 6.17: Examples of spherical joints.

In the case of a fixed and perfectly rigid support  $\Omega^*$ , this means that the centre  $G$  of the cross-section  $\Sigma$  concerned by the linkage is fixed:

$$\mathbf{u}_G = \mathbf{0}$$

In the case where two beams  $\Omega^*$  and  $\Omega$  are connected by a spherical joint, the point  $G$  of intersection between the two neutral axes remains common to both beams, i.e., with evident notations:

$$\mathbf{u}_G = \mathbf{u}_G^*$$

### Pin joint

Compared to the previous case, for a “pin joint” (or “hinged joint”) the relative rotation allowed between  $\Omega$  and  $\Omega^*$  is done around an axis  $\mathbf{a}$ , as it is visible in Figure 6.18. The axis is assumed to be linked to  $\Omega^*$ , which implies that, in addition to the displacement of the cross-section centre, the two components of the rotation vector of the cross-section  $\Sigma$  of  $\Omega$  which are perpendicular to  $\mathbf{a}$  (i.e. along  $\boldsymbol{\theta} - \langle \boldsymbol{\theta}, \mathbf{a} \rangle \mathbf{a}$ ) are also related to the expression of the displacement field of the body  $\Omega^*$ :

$$\mathbf{u}_G = \mathbf{u}_A + \boldsymbol{\alpha} \wedge (\mathbf{x}_G - \mathbf{x}_A), \text{ and } \boldsymbol{\theta} - \langle \boldsymbol{\theta}, \mathbf{a} \rangle \mathbf{a} = \boldsymbol{\alpha} - \langle \boldsymbol{\alpha}, \mathbf{a} \rangle \mathbf{a}$$

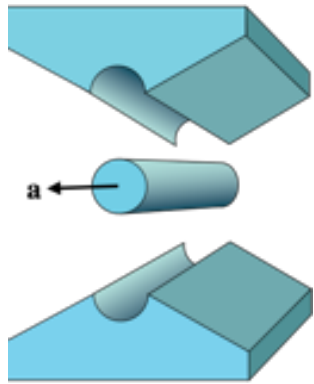
So we can write the displacement of a point of the cross-section  $\Sigma$  as:

$$\mathbf{u} = \mathbf{u}_G + \boldsymbol{\theta} \wedge \mathbf{x}_\Sigma = \mathbf{u}_A + \boldsymbol{\alpha} \wedge (\mathbf{x}_G - \mathbf{x}_A) + (\boldsymbol{\alpha} + \langle \boldsymbol{\theta} - \boldsymbol{\alpha}, \mathbf{a} \rangle \mathbf{a}) \wedge \mathbf{x}_\Sigma$$

which shows that the rotation around the axis  $\mathbf{a}$  remains free.

If  $\Omega^*$  is a fixed and perfectly rigid support (“pinned support” or “hinged support”), in this case, all components other than the cross-section rotation around the axis  $\mathbf{a}$  are zero:

$$\mathbf{u}_G = \mathbf{0}, \text{ and } \boldsymbol{\theta} - \langle \boldsymbol{\theta}, \mathbf{a} \rangle \mathbf{a} = \mathbf{0}$$



(a) Realization.



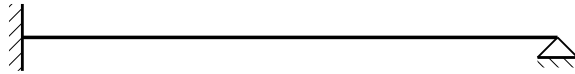
(b) Illustration from Henrius bridge.

Figure 6.18: Pin joint (or “pinned support”).

Finally, in the case where the pin joint connects two beams  $\Omega^*$  and  $\Omega$  at the same cross-section centre  $G$ , we can write that:

$$\mathbf{u}_G = \mathbf{u}_G^*, \text{ and } \boldsymbol{\theta} - \langle \boldsymbol{\theta}, \mathbf{a} \rangle = \boldsymbol{\theta}^* - \langle \boldsymbol{\theta}^*, \mathbf{a} \rangle$$

**R** In the case where the problem treated is planar, of normal vector the axis of the pin joint, we only speak of “pinned support” to designate such a connection, which is then symbolized by a triangle; we obtain for example the following graphic representation for a beam clamped at one end and supported at the other:



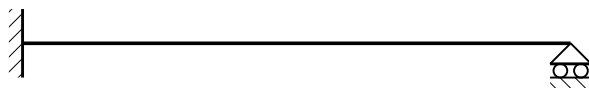
It should also be noted that a spherical joint is equivalent to a pinned support if the problem under study is planar.

### Roller support

This connection, which is found almost exclusively between a beam  $\Omega$  and a fixed and perfectly rigid support  $\Omega^*$ , is illustrated in Figure 6.19: the elastomer “cushion” is deformable (and flexible enough so that the associated forces can be neglected), and therefore allows any relative rotation. We find ourselves in the case of a spherical joint, but this time with a possible relative translation of the centre of the cross-section  $\Sigma$ , allowed by the guiding device along the axis  $\mathbf{e}$  of the beam  $\Omega$ . Thus, in the case of a fixed and perfectly rigid support  $\Omega^*$ :

$$\mathbf{u}_G - \langle \mathbf{u}_G, \mathbf{e} \rangle \mathbf{e} = \mathbf{0}$$

**R** In the case where the problem treated is planar, we also speak of roller support to designate such a connection, which is symbolized by a triangle on two rollers; we obtain for example the following graphic representation for a beam clamped at one end and with a roller support at the other:



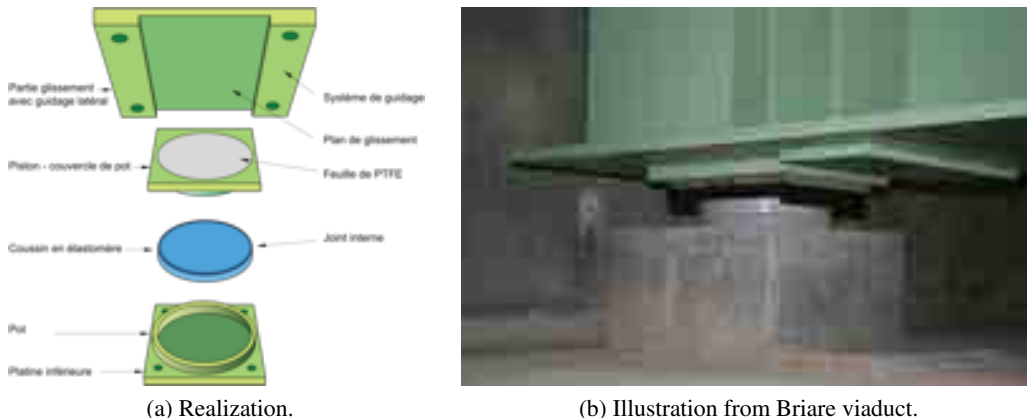


Figure 6.19: Roller support.

**Summary 6.12 — Kinematic parameters of the cross-section of a beam  $\Omega$  in connection with a body  $\Omega^*$ .**

Connection ( $\Omega/\Omega^*$ )	Case of a fixed support $\Omega^*$	Case of a beam $\Omega^*$
Pinned support (2D)	$\mathbf{u}_G = \mathbf{0}$	$\mathbf{u}_G = \mathbf{u}_G^*$ (in plane)
Roller support (2D)	$\mathbf{u}_G - \langle \mathbf{u}_G, \mathbf{e} \rangle \mathbf{e} = \mathbf{0}$	not encountered in reality
Rigid connection	$\mathbf{u}_G = \mathbf{0}$ , and $\boldsymbol{\theta} = \mathbf{0}$	$\mathbf{u}_G = \mathbf{u}_G^*$ , and $\boldsymbol{\theta} = \boldsymbol{\theta}^*$
Pin joint (of axis $\mathbf{a}$ )	$\mathbf{u}_G = \mathbf{0}$ , $\boldsymbol{\theta} - \langle \boldsymbol{\theta}, \mathbf{a} \rangle \mathbf{a} = \mathbf{0}$	$\mathbf{u}_G = \mathbf{u}_G^*$ , $\boldsymbol{\theta} - \langle \boldsymbol{\theta}, \mathbf{a} \rangle = \boldsymbol{\theta}^* - \langle \boldsymbol{\theta}^*, \mathbf{a} \rangle$
Roller support	$\mathbf{u}_G - \langle \mathbf{u}_G, \mathbf{e} \rangle \mathbf{e} = \mathbf{0}$	not encountered in reality
Spherical joint	$\mathbf{u}_G = \mathbf{0}$	$\mathbf{u}_G = \mathbf{u}_G^*$

#### 6.4.2 Connection actions

In addition to the kinematic aspect, which we have just seen, a description of the connection actions between the two bodies  $\Omega$  and  $\Omega^*$  must be proposed. In the following, we assume that the connections are perfect, i.e. such that:

- the geometries of the contact surfaces are perfect (of canonical forms, and perfectly rigid);
- the contact is made without friction, which means that the forces are only along the normal vector to the contact surface (contact pressure).

The issue is then to determine, for a given connection, which components of the resultant force and/or moment are necessarily zero under this assumption of perfect connection. The following example shows the approach in the case of a spherical joint.

■ **Example 6.11 — Transmissible action through a perfect spherical joint.** In order to allow a rotation of arbitrary axis between  $\Omega$  and  $\Omega^*$ , this connection is obtained by the perfect association of two spherical surfaces with same centre  $O$  and radius  $R$ . We then naturally introduce the associated spherical vector basis  $(\mathbf{e}_r(\vartheta, \phi), \mathbf{e}_\vartheta(\vartheta, \phi), \mathbf{e}_\phi(\phi))$ , of coordinates  $(r, \vartheta, \phi)$ .

Since it is assumed that the contact is frictionless, the stress vector at each point of the contact surface  $\Sigma_c$  is normal to the contact surface:

$$\sigma(\mathbf{x}, t)\mathbf{n}(\mathbf{x}) = -p(\mathbf{x}, t)\mathbf{n}(\mathbf{x}), \forall t$$

where  $\mathbf{n}(\mathbf{x})$  is the outer unit normal vector at a point  $M$  of  $\Sigma_c$  (considering the actions of  $\Omega^*$  on  $\Omega$ ); however, the local distribution of contact pressure  $p(\mathbf{x}, t)$  is not known, and this is even less accessible because the concerned cross-section  $\Sigma$  of  $\Omega$  is perfectly rigid, and therefore the stress field cannot be determined.

Thus, if we describe a point  $M$  of the contact surface by its spherical coordinates:

$$\mathbf{x} = R\mathbf{e}_r(\vartheta, \phi), \forall \vartheta \in [0, \pi], \forall \phi \in [0, 2\pi)$$

the stress vector is written as:

$$\sigma(\mathbf{x}, t)\mathbf{n}(\mathbf{x}) = p(\vartheta, \phi, t)\mathbf{e}_r(\vartheta, \phi)$$

if the outer unit normal vector is  $\mathbf{n}(\mathbf{x}) = -\mathbf{e}_r(\vartheta, \phi)$ . Then we can calculate the resultant force and moment in  $O$  of the connection actions from  $\Omega^*$  on  $\Omega$  respectively as:

$$\begin{aligned}\mathbf{R}^l(t) &= \int_{\Sigma_c} \sigma(\mathbf{x}, t)\mathbf{n}(\mathbf{x}) dS_x = \int_0^\pi \int_0^{2\pi} p(\vartheta, \phi, t)\mathbf{e}_r(\vartheta, \phi)R \sin \vartheta d\phi d\vartheta \\ \mathbf{M}_{\mathbf{x}_O}^l(t) &= \int_{\Sigma_c} \mathbf{x} \wedge \sigma(\mathbf{x}, t)\mathbf{n}(\mathbf{x}) dS_x = \int_0^\pi \int_0^{2\pi} R\mathbf{e}_r(\vartheta, \phi) \wedge p(\vartheta, \phi, t)\mathbf{e}_r(\vartheta, \phi)R \sin \vartheta d\phi d\vartheta = \mathbf{0}\end{aligned}$$

since  $\mathbf{x}_O = \mathbf{0}$  in our spherical vector basis.

The perfect connection hypothesis therefore allows us to conclude that the moment (expressed at the centre of the spherical joint) of the connection actions is zero, regardless of the distribution of the contact pressure between  $\Omega$  and  $\Omega^*$ . On the other hand, nothing can be said for the associated resultant force. ■

Rather than studying the connections one by one, it is possible to adopt a systematic criterion to determine which components of the resultant force and/or moment are necessarily zero for a given perfect connection. For this reason, in the case of a connection with a fixed and perfectly rigid support  $\Omega^*$ , it can be shown that such a connection must verify that:

$$\langle \mathbf{R}, \mathbf{u}_G \rangle = 0, \text{ and } \langle \mathbf{M}, \boldsymbol{\theta} \rangle = 0$$

for any arbitrary movement allowed by the connection. This makes it possible to determine which components of the resultant force or moment of the actions of  $\Omega^*$  on  $\Omega$  can be assumed to be zero. A similar result is obtained in the case of a connection with another beam  $\Omega^*$ .



*A justification of the previous result can be made by introducing the work of linkage connection such that:*

$$\mathcal{T}(\Omega^* \leftrightarrow \Omega) = \int_{\Sigma} \langle \sigma \mathbf{n}, \mathbf{u} - \mathbf{u}^* \rangle dS$$

*where it has been systematically assumed that the connection action of  $\Omega^*$  on the beam  $\Omega$  is directly exerted on the cross-section  $\Sigma$  of  $\Omega$  concerned by the connection with  $\Omega^*$ . Thus, depending on where the cross-section in question is located, the outer normal vector  $\mathbf{n}$  is equal either to  $\mathbf{e}$  or  $-\mathbf{e}$ .*

*It is then established that a perfect connection is neither driving nor resistant, and is therefore characterized by a zero work:*

$$\mathcal{T}(\Omega^* \leftrightarrow \Omega) = 0$$

*which allows us to consider, one by one, the connections introduced above. In the case of a connection with a fixed and perfectly rigid support  $\Omega^*$  ( $\mathbf{u}^* = \mathbf{0}$ ), we can rewrite the work of the connection actions as:*

$$\begin{aligned}\mathcal{T}(\Omega^* \leftrightarrow \Omega) &= \int_{\Sigma} \langle \sigma(\pm \mathbf{e}), \mathbf{u}_G + \boldsymbol{\theta} \wedge \mathbf{x}_{\Sigma} \rangle dS \\ &= \int_{\Sigma} \langle \sigma(\pm \mathbf{e}), \mathbf{u}_G \rangle dS + \int_{\Sigma} \langle \mathbf{x}_{\Sigma} \wedge \sigma(\pm \mathbf{e}), \boldsymbol{\theta} \rangle dS \\ &= \pm \langle \mathbf{R}, \mathbf{u}_G \rangle \pm \langle \mathbf{M}, \boldsymbol{\theta} \rangle\end{aligned}$$

*Thus, for a connection to be perfect, it must therefore satisfy:*

$$\langle \mathbf{R}, \mathbf{u}_G \rangle = 0, \text{ and } \langle \mathbf{M}, \boldsymbol{\theta} \rangle = 0$$

*regardless of the movement allowed by the connection. In the case of the spherical joint studied in Example 6.11, this condition is reduced to  $\langle \mathbf{M}, \boldsymbol{\theta} \rangle = 0$  since the centre of the concerned cross-section remains fixed ( $\mathbf{u}_G = \mathbf{0}$ ); since the cross-section rotation  $\boldsymbol{\theta}$  is arbitrary, the moment of the connection action  $\mathbf{M}$  must be equal to zero to be able to satisfy this condition.*

**Summary 6.13 — Connection action of the body  $\Omega^*$  on the beam  $\Omega$  on the cross-section  $\Sigma$ , for a perfect connection..**

Connection ( $\Omega/\Omega^*$ )	Resultant force and moment of the connection action of $\Omega^*$ on $\Omega$
Pinned support (2D)	arbitrary $\mathbf{R}$ (in the plane), and $\mathbf{M} = \mathbf{0}$
Roller support (2D)	$\langle \mathbf{R}, \mathbf{e} \rangle = 0$ , and $\mathbf{M} = \mathbf{0}$
Rigid connection	arbitrary $\mathbf{R}$ and $\mathbf{M}$
Pin joint (of axis $\mathbf{a}$ )	arbitrary $\mathbf{R}$ , and $\langle \mathbf{M}, \mathbf{a} \rangle = 0$
Roller support	$\langle \mathbf{R}, \mathbf{e} \rangle = 0$ , and $\mathbf{M} = \mathbf{0}$
Spherical joint	arbitrary $\mathbf{R}$ , and $\mathbf{M} = \mathbf{0}$



The case of a rigid connection has not been mentioned here. In this case, no relative movement is possible between the two solids, which means that no information is available on the components of the resultant force and moment of the connection actions.

### 6.4.3 Complete solution of a beam problem

We saw in the previous paragraph that, for each perfect connection studied, a certain number of components of the resultant force and/or moment of the connection actions could be assumed to be equal to zero; the others, on the other hand, are not fixed *a priori*, and we then speak of “connection unknowns”. As these latter are involved in the equilibrium equations specified in Paragraphs 6.2.2 and 6.2.3, they must be determined if we wish to be able to evaluate these internal loads in the different beams.

To do this, we need to compare the number of independent equations with these connection unknowns. In the static case, it is a question of writing the global equilibrium equations in terms of resultant force and moment of the entire beam (or each of the entire beams in the case of an assembly), which allows, at each time, for establishing six scalar relations (three in force, three in moment) between the different connection unknowns.

#### Statically determinate beams

If we have as many scalar relations as we have connection unknowns, we call the problem “statically determinate” (or “isostatic”): it is then possible to determine the resultant force and moment of the internal loads within each beam of the assembly under study.

■ **Example 6.12 — Determination of the internal loads in a portal frame.** The study of the portal frame of Example 6.10 is repeated here in order to calculate, at any point, the resultant force and moment of the internal loads using the equilibrium equations.

To do this, it is useful first to make a list of the unknowns of the problem, as well as the equations that can be established:

- each rigid connection is equivalent to six scalar connection unknowns (three components for the resultant force, and three components for the moment), bringing the total to 18 connection unknowns;
- for each beam, it is possible to write three scalar relations for the global force equilibrium of the entire beam, and three scalar relations for the global moment equilibrium, which finally allows for obtaining, for the treated problem, 18 independent scalar equations.

The problem is thus statically determinate: it is possible to determine the resultant force and moment of the internal loads at any point of the three beams of the portal frame.

We begin with the local approach. Concerning the resultant force, the (static) local equilibrium allows us to

write for the three beams that:

$$\mathbf{R}^{\mathcal{D}\prime} = \mathbf{0}, \mathbf{R}^{\mathcal{Q}\prime} = \mathbf{0}, \text{ and } \mathbf{R}^{\mathcal{S}\prime} = \mathbf{0}$$

The resultant force of the internal loads is then constant on each beam. Besides, we have at the rigid connections:

$$\mathbf{R}^{\mathcal{D}}(L) = \mathbf{R}^{\mathcal{Q}}(0), \text{ and } \mathbf{R}^{\mathcal{Q}}(L) = \mathbf{R}^{\mathcal{S}}(0)$$

since no external action is applied on them. We also know, by definition of the resultant force, that:

$$\mathbf{R}^{\mathcal{S}}(L) = -F\mathbf{i}_z$$

which implies:

$$\boxed{\mathbf{R}^{\mathcal{D}}(z) = -F\mathbf{i}_z, \forall z \in [0, L], \mathbf{R}^{\mathcal{Q}}(x) = -F\mathbf{i}_z, \forall x \in [0, L], \text{ and } \mathbf{R}^{\mathcal{S}}(y) = -F\mathbf{i}_z, \forall y \in [0, L]}$$

which, notably, allows for finding the resultant force of the action of the fixed support on the portal frame as:  $\mathbf{R}_0 = -\mathbf{R}^{\mathcal{D}}(0) = F\mathbf{i}_z$ .

Secondly, the local moment equilibrium for each beam allows for writing that:

$$\mathbf{M}^{\mathcal{D}\prime} + \mathbf{i}_z \wedge \mathbf{R}^{\mathcal{D}} = \mathbf{0}, \mathbf{M}^{\mathcal{Q}\prime} + \mathbf{i}_x \wedge \mathbf{R}^{\mathcal{Q}} = \mathbf{0}, \text{ et } \mathbf{M}^{\mathcal{S}\prime} + \mathbf{i}_y \wedge \mathbf{R}^{\mathcal{S}} = \mathbf{0}$$

Thus, the moment along beam  $\Omega_3$  verifies:

$$\mathbf{M}^{\mathcal{S}}(y) = (\mathbf{i}_y \wedge F\mathbf{i}_z)y + C_3$$

where constant  $C_3$  is determined using the loading conditions at the cross-section of coordinate  $y = L$  (moment equal to zero:  $\mathbf{M}^{\mathcal{S}}(L) = \mathbf{0}$ ), hence, finally:

$$\boxed{\mathbf{M}^{\mathcal{S}}(y) = -F(L-y)\mathbf{i}_x, \forall y \in [0, L]}$$

Then the moment along beam  $\Omega_2$  is such that:

$$\mathbf{M}^{\mathcal{Q}}(x) = (\mathbf{i}_x \wedge F\mathbf{i}_z)x + C_2$$

hence, expressing the equilibrium of the rigid joint between  $\Omega_2$  and  $\Omega_3$  ( $\mathbf{M}^{\mathcal{Q}}(L) = \mathbf{M}^{\mathcal{S}}(0)$ ):

$$\boxed{\mathbf{M}^{\mathcal{Q}}(x) = F(L-x)\mathbf{i}_y - FL\mathbf{i}_x, \forall x \in [0, L]}$$

Finally, the moment along beam  $\Omega_1$  verifies:

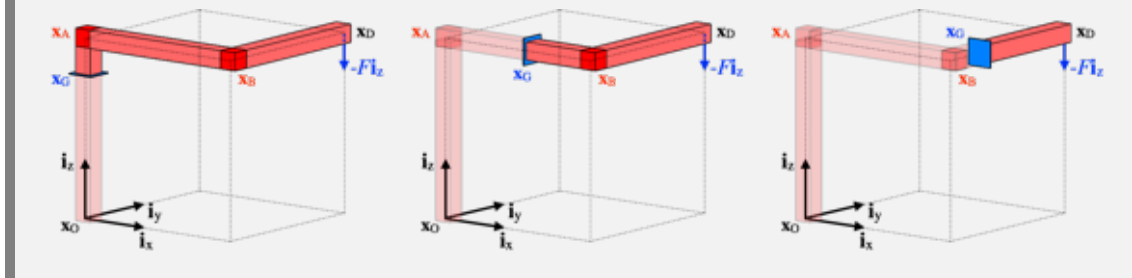
$$\mathbf{M}^{\mathcal{D}}(z) = (\mathbf{i}_z \wedge F\mathbf{i}_z)z + C_1 = C_1$$

where  $C_1$  is determined using the equilibrium of the rigid joint between  $\Omega_1$  and  $\Omega_2$  ( $\mathbf{M}^{\mathcal{D}}(L) = \mathbf{M}^{\mathcal{Q}}(0)$ ):

$$\boxed{\mathbf{M}^{\mathcal{D}}(z) = FL\mathbf{i}_y - FL\mathbf{i}_x, \forall z \in [0, L]}$$

which allows for finding the moment (expressed at point  $O$ ) of the action of the fixed support on the portal frame as:  $\mathbf{M}_0 = -\mathbf{M}^{\mathcal{D}}(0) = FL\mathbf{i}_x - FL\mathbf{i}_y$ .

Equivalently, we can apply the global approach. For different locations of the cut within the three beams of the portal frame, we can write the equilibrium equations of the “downstream” segment.



Whether we cut at a cross-section of the beam  $\Omega_1$ ,  $\Omega_2$  or  $\Omega_3$ , the equilibrium equation of the “downstream” segment then allows us to directly establish that:

$$-\mathbf{R} - F\mathbf{i}_z = \mathbf{0}$$

and therefore that:

$$\boxed{\mathbf{R}^{\circledcirc}(z) = -F\mathbf{i}_z, \forall z \in [0, L], \mathbf{R}^{\circledcirc}(x) = -F\mathbf{i}_z, \forall x \in [0, L], \text{ and } \mathbf{R}^{\circledcirc}(y) = -F\mathbf{i}_z, \forall y \in [0, L]}$$

We therefore find, by this global reasoning, that the resultant force is constant regardless of the beam studied. However, whereas the beam  $\Omega_1$  is subjected to a compressive load (negative axial force), the resultant forces in the beams  $\Omega_2$  and  $\Omega_3$  correspond to shear forces.

In addition, we obtain for the expression of the moment, by considering the cuts according to the beams where they are located:

- for the beam  $\Omega_1$ :

$$-\mathbf{M}^{\circledcirc}(z) + ((L-z)\mathbf{i}_z + L\mathbf{i}_x + L\mathbf{i}_y) \wedge (-F\mathbf{i}_z) = \mathbf{0}$$

at the centre of the cut cross-section, which finally results in:

$$\boxed{\mathbf{M}^{\circledcirc}(z) = FL\mathbf{i}_y - FL\mathbf{i}_x, \forall z \in [0, L]}$$

which shows that the beam  $\Omega_1$  is loaded in bending (as well as in tension, here);

- for the beam  $\Omega_2$ , we establish that, at the centre of the cut cross-section, we have:

$$-\mathbf{M}^{\circledcirc}(x) + ((L-x)\mathbf{i}_x + L\mathbf{i}_y) \wedge (-F\mathbf{i}_z) = \mathbf{0}$$

or, finally:

$$\boxed{\mathbf{M}^{\circledcirc}(x) = F(L-x)\mathbf{i}_y - FL\mathbf{i}_x, \forall x \in [0, L]}$$

which shows that the beam  $\Omega_2$  is loaded in bending-torsion;

- finally, for the beam  $\Omega_3$ , we have:

$$-\mathbf{M}^{\circledcirc}(y) + (L-y)\mathbf{i}_y \wedge (-F\mathbf{i}_z) = \mathbf{0}$$

or, directly:

$$\boxed{\mathbf{M}^{\circledcirc}(y) = -F(L-y)\mathbf{i}_x, \forall y \in [0, L]}$$

which corresponds to a simple bending loading.

■

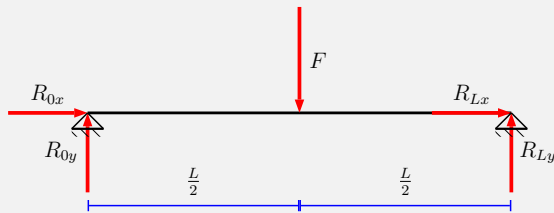


If we are interested in the deformation of the portal frame, the approach consists in using the beam constitutive relations obtained in Paragraph 6.3, and the kinematic connection conditions, detailed in Example 6.10. In the case of a straight beam, the differential equations corresponding to each loading (tension, bending, torsion) are then decoupled from each other.

### Statically indeterminate problems

If there are more connection unknowns than scalar relations coming from the equilibrium equations of the entire beams, the problem is said to be “statically indeterminate” (or “hyperstatic”), and the “hyperstaticity degree” is the difference between these two quantities. In this case, the resultant force and moment of the internal loads in each beam must be expressed as a function of so-called “hyperstatic connection unknowns”, which cannot be determined using the equilibrium equations of the entire beams alone, and whose number is equal to the hyperstaticity degree of the problem.

■ **Example 6.13 — Determination of the internal loads in a three-point bending test.** We come back here to the study of a three-point bending test, as presented in Figure 6.2 on page 151: the beam, of axis  $\mathbf{i}_x$ , is placed at  $x = 0$  and  $x = L$  on two supports which, if we assume a plane problem (in the vertical plane associated with  $(\mathbf{i}_x, \mathbf{i}_y)$ ), can be modelled by pinned supports, as shown in the figure below.



We can therefore identify four connection unknowns, namely the two components along  $\mathbf{i}_x$  and  $\mathbf{i}_y$  of the resultant force  $\mathbf{R}_0$ , and the same for  $\mathbf{R}_L$ , of the connection actions at each support (since the associated moment is zero):  $R_{0x}$  and  $R_{0y}$  at  $x = 0$ , and  $R_{Lx}$  and  $R_{Ly}$  at  $x = L$ . To determine them, it is possible to write three scalar equations corresponding to the static equilibrium of the entire beam, knowing that the action applied by the upper roller of the test machine is characterized by a resultant force  $\mathbf{R}^{ext} = -F\mathbf{i}_y$ , and a moment  $\mathbf{M}^{ext}$  equal to zero at the centre of the cross-section located midway along the beam:

- the two projections in the plane of the (static) global force equilibrium equation of the complete beam:

$$R_{0x} + R_{Lx} = 0$$

$$R_{0y} + R_{Ly} - F = 0$$

- the projection along the normal vector  $\mathbf{i}_z$  of the (static) global moment equilibrium equation of the entire beam, expressed in  $x = 0$ :

$$\left\langle \frac{L}{2}\mathbf{i}_x \wedge (-F\mathbf{i}_y) + L\mathbf{i}_x \wedge (R_{Lx}\mathbf{i}_x + R_{Ly}\mathbf{i}_y), \mathbf{i}_z \right\rangle = -F\frac{L}{2} + R_{Ly}L = 0$$

It is then easily determined that:

$$R_{0y} = R_{Ly} = \frac{F}{2}$$

while the horizontal components  $R_{0x}$  and  $R_{Lx}$  remain undetermined. The problem treated is therefore statically indeterminate (hyperstaticity degree of one): the resultant force and the moment of the internal loads along the beam can only be determined as functions of a hyperstatic connection unknown, to be chosen between  $R_{0x}$  and  $R_{Lx}$ .

Thus, if we apply for example the global approach for the resultant force and the moment, we must first distinguish two cases:

1. if the beam is cut at a cross-section of abscissa  $x < L/2$ , then we obtain, by isolating for example the “upstream” segment:

$$\mathbf{R}(x) + \mathbf{R}_0 = \mathbf{0}$$

as well as, at the centre of the cross-section of abscissa  $x$ :

$$\mathbf{M}(x) - x\mathbf{i}_x \wedge \mathbf{R}_0 = \mathbf{0}$$

hence, finally, the scalar components of the resultant force  $\mathbf{R}$  and the moment  $\mathbf{M}$  such that:

$$\boxed{\begin{aligned} R_x(x) &= -R_{0x}, \forall x \in [0, \frac{L}{2}] \\ R_y(x) &= -\frac{F}{2}, \forall x \in [0, \frac{L}{2}] \\ M_z(x) &= \frac{F}{2}x, \forall x \in [0, \frac{L}{2}] \end{aligned}}$$

2. if the beam is cut at a cross-section of abscissa  $x > L/2$ , the resultant force is, by isolating, for example, the “downstream” segment:

$$-\mathbf{R}(x) + \mathbf{R}_L = \mathbf{0}$$

as well as, at the centre of the cross-section of abscissa  $x$ :

$$-\mathbf{M}(x) + (L-x)\mathbf{i}_x \wedge \mathbf{R}_L = \mathbf{0}$$

hence, finally, the scalar components of the resultant force  $\mathbf{R}$  and the moment  $\mathbf{M}$  such that:

$$\boxed{\begin{aligned} R_x(x) &= R_{Lx} = -R_{0x}, \forall x \in (\frac{L}{2}, L] \\ R_y(x) &= \frac{F}{2}, \forall x \in (\frac{L}{2}, L] \\ M_z(x) &= \frac{F}{2}(L-x), \forall x \in (\frac{L}{2}, L] \end{aligned}}$$

if  $R_{0x}$  is chosen as the hyperstatic unknown.

Of course, we could also have used the local equilibrium equations for the resultant force and moment, taking into account that the beam should be actually considered as two half beams clamped one with the other at the cross-section in contact with the mobile part of the test machine. Hence the local force equilibrium equation allows for determining that:

$$\mathbf{R}'(x) = \mathbf{0}, \forall x \in \left[0, \frac{L}{2}\right] \cup \left[\frac{L}{2}, L\right]$$

and, then, that the resultant force is constant on each half beam, hence:

$$\boxed{\mathbf{R}(x) = \begin{cases} -\mathbf{R}_0 = -R_{0x}\mathbf{i}_x - \frac{F}{2}\mathbf{i}_y, & \forall x \in \left[0, \frac{L}{2}\right] \\ +\mathbf{R}_L = R_{Lx}\mathbf{i}_x + \frac{F}{2}\mathbf{i}_y, & \forall x \in \left[\frac{L}{2}, L\right] \end{cases}}$$

Besides, the local moment equilibrium should be expressed on each half beam separately:

$$\begin{cases} \mathbf{M}'(x) + \mathbf{i}_x \wedge (-R_{0x}\mathbf{i}_x - \frac{F}{2}\mathbf{i}_y) = \mathbf{0}, & \forall x \in \left[0, \frac{L}{2}\right] \\ \mathbf{M}'(x) + \mathbf{i}_x \wedge (R_{Lx}\mathbf{i}_x + \frac{F}{2}\mathbf{i}_y) = \mathbf{0} & \forall x \in \left[\frac{L}{2}, L\right] \end{cases}$$

to find:

$$\boxed{\mathbf{M}(x) = \begin{cases} \frac{F}{2}x\mathbf{i}_z, & \forall x \in \left[0, \frac{L}{2}\right] \\ -\frac{F}{2}x\mathbf{i}_z + \frac{F}{2}L\mathbf{i}_z, & \forall x \in \left[\frac{L}{2}, L\right] \end{cases}}$$

using the zero moment conditions at  $x = 0$  and  $x = L$ . Therefore, whereas the shear force and the bending moment are completely determined, the axial force should be expressed using a hyperstatic unknown.

Whatever the approach used, we can see that the resultant force of the internal loads is discontinuous at  $x = L/2$ ; this is explained by the force  $F$  applied at this point: indeed, if we write the force equilibrium equation for the infinitesimal cross-section of abscissa  $L/2$ , by distinguishing the resultant forces of the actions of the “downstream” and “upstream” segments, we find that:

$$\boxed{\mathbf{R}\left(\frac{L}{2}^+\right) - \mathbf{R}\left(\frac{L}{2}^-\right) + \mathbf{R}^{ext} = \mathbf{0}}$$

since  $\mathbf{R}^{ext} = -F\mathbf{i}_y$  is defined as the resultant force of the action of the roller on the beam at  $x = L/2$ ; in addition, care has been taken to distinguish:

- the resultant force  $\mathbf{R}\left(\frac{L}{2}^+\right)$  of the action of the “downstream” segment on the cross-section of abscissa  $L/2$ ;
  - the resultant force  $-\mathbf{R}\left(\frac{L}{2}^-\right)$  of the action of the “upstream” segment on the cross-section of abscissa  $L/2$ ;
- which is equivalent to considering that the beam is in fact composed of two half beams in rigid connection at the point of application of the resultant force of the roller’s action. As far as the moment is concerned, the equilibrium of the infinitesimal cross-section of abscissa  $L/2$ , expressed at its centre, allows us to establish, with the same notations and sign convention, that:

$$\boxed{\mathbf{M}\left(\frac{L}{2}^+\right) - \mathbf{M}\left(\frac{L}{2}^-\right) = \mathbf{0}}$$

since the moment of the roller’s action on the beam is zero at this point. This therefore confirms that the moment of the internal loads is continuous at  $x = L/2$ , and is:

$$M_z\left(\frac{L}{2}\right) = \frac{FL}{4}$$

■

If we wish to determine the hyperstatic unknowns of the problem, it is, in this case, necessary to calculate the deformation of the beams of the assembly, by introducing the constitutive relations obtained in Paragraph 6.3; the differential equations obtained are then solved using the conditions imposed on kinematics, which allows us, by the way, to determine the hyperstatic unknowns.

■ **Example 6.14 — Three-point bending test: full solution.** Here we continue to solve the problem of the three-point bending test, started in Example 6.13, for which there was still a hyperstatic connection unknown. As this latter concerned the axial component of the resultant force, we will use the constitutive relation between the axial force and the longitudinal displacement, then the associated kinematic boundary conditions to fully determine the tension-compression solution. So, since we have:

$$R_x(x) = EAu'_{Gx}(x), \forall x \in [0, L]$$

the longitudinal displacements of the cross-section centres therefore satisfy, on each half beam:

$$EAu'_{Gx}(x) = \begin{cases} -R_{0x}, & \forall x \in (0, \frac{L}{2}) \\ +R_{Lx} = -R_{0x}, & \forall x \in (\frac{L}{2}, L) \end{cases}$$

Knowing that, at the supports, the longitudinal displacement is zero ( $u_{Gx}(0) = 0 = u_{Gx}(L)$ ), we arrive at:

$$EAu_{Gx}(x) = \begin{cases} -R_{0x}x, & \forall x \in (0, \frac{L}{2}) \\ -R_{0x}(x-L), & \forall x \in (\frac{L}{2}, L) \end{cases}$$

and, since it is a single beam, the longitudinal displacement must be continuous at  $x = L/2$ , i.e.:

$$-R_{0x}\frac{L}{2} = R_{0x}\frac{L}{2}$$

which directly implies that the hyperstatic unknown is actually zero:

$$\boxed{R_{0x} = 0}$$

As a result, the axial force is zero along the beam, as are the longitudinal displacements of the cross-section centres. The use of the constitutive relation has thus allowed us to use additional boundary conditions (i. e., those coming from kinematics constraints) to determine both the hyperstatic unknown and the associated kinematics.

In addition, now that we know the resultant force and moment of the internal loads along the beam, we can determine the normal stress as:

$$\sigma_{xx}(x, y) = -y \frac{M_z(x)}{I_z}$$

which is then maximum for  $x = L/2$  and  $y = -h/2$  (where  $h$  is the height of the beam):

$$\sigma_{xxmax} = \frac{FLh}{8I_z}$$

If, in addition, we are interested in the bending deformation of the beam, and we adopt Euler-Bernoulli hypothesis, we only need to use the constitutive relations between the bending moment and the transverse displacement:

$$\mathbf{M}_\Sigma(x) = E\mathbb{J}(\mathbf{i}_x \wedge \mathbf{u}_{G\Sigma}''(x)), \forall x \in [0, L]$$

which gives, along the normal vector to the plane of the problem:

$$M_z(x) = EI_z u_{Gy}''(x), \forall x \in [0, L]$$

The transverse displacement of the neutral axis therefore satisfies, on each half beam:

$$EI_z u_{Gy}''(x) = \begin{cases} \frac{F}{2}x, & \forall x \in (0, \frac{L}{2}) \\ \frac{F}{2}(L-x), & \forall x \in (\frac{L}{2}, L) \end{cases}$$

and, knowing that, at the supports, the transverse displacement is zero ( $u_{Gy}(0) = 0 = u_{Gy}(L)$ ), we arrive at:

$$EI_z u_{Gy}(x) = \begin{cases} \frac{F}{12}x^3 + C_1x, & \forall x \in (0, \frac{L}{2}) \\ \frac{F}{12}(3Lx^2 - x^3 - 2L^3) + C_2(x-L), & \forall x \in (\frac{L}{2}, L) \end{cases}$$

where  $C_1$  and  $C_2$  are constants to be determined. Since it is the case of a single beam, the transverse displacement and cross-section rotation (and therefore the derivative of the transverse displacement taking into account Euler-Bernoulli hypothesis) must be continuous at  $x = L/2$ , i.e.:

$$\frac{FL^3}{96} + C_1 \frac{L}{2} = -\frac{11FL^3}{96} - C_2 \frac{L}{2}, \text{ and } \frac{FL^2}{16} + C_1 = \frac{3FL^2}{16} + C_2$$

which allows us to determine the two constants as follows:

$$C_1 = -\frac{FL^2}{16}, \text{ and } C_2 = -\frac{3FL^2}{16}$$

The deformed neutral axis is therefore:

$$u_{Gy}(x) = \begin{cases} \frac{Fx}{2EI_z} \left( \frac{x^2}{6} - \frac{L^2}{8} \right), & \forall x \in [0, \frac{L}{2}] \\ -\frac{F}{2EI_z} \left( \frac{x^3}{6} - \frac{L}{2}x^2 + \frac{3L^2}{8}x - \frac{L^3}{24} \right), & \forall x \in [\frac{L}{2}, L] \end{cases}$$

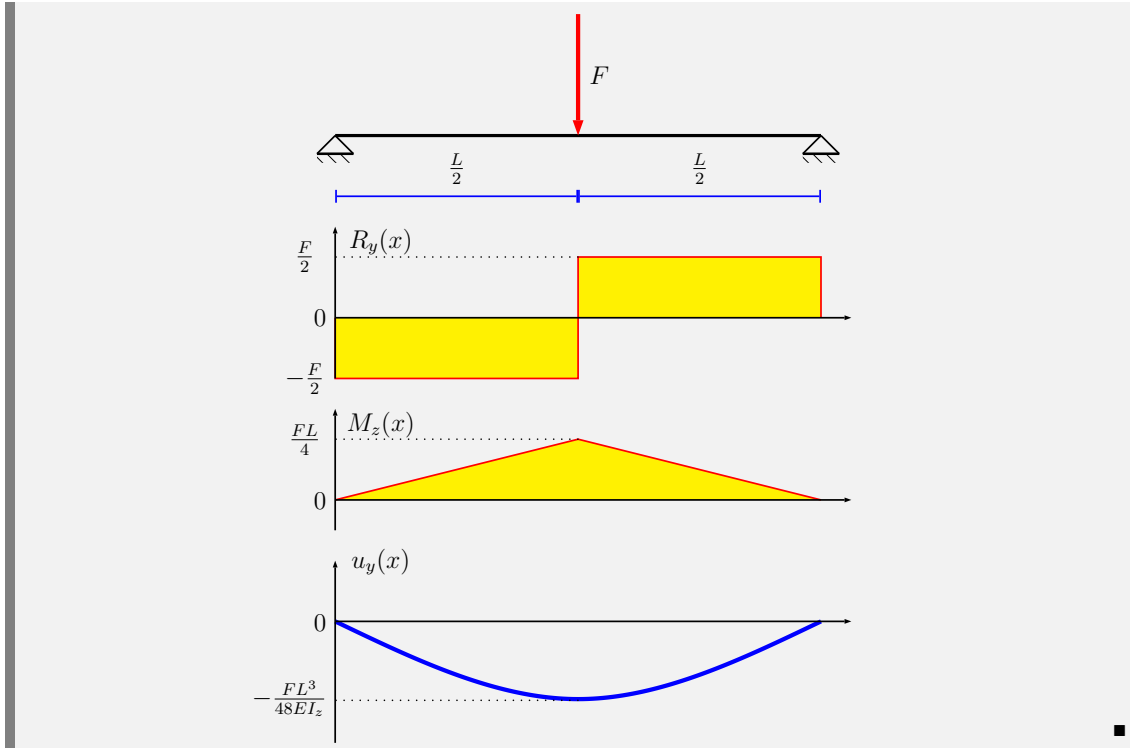
and is maximum (in absolute value) at  $x = L/2$ , being:

$$|u_{Gy}|_{max} = \frac{FL^3}{48EI_z}$$

which makes it possible, for example, to determine the Young's modulus of the constitutive material if the force exerted by the machine and the displacement of the middle of the beam are measured simultaneously.

The graphs below (called "shear and moment diagram") summarize the evolution of the resultant force and moment of the internal loads, as well as the deformation of the beam, and make it possible to verify in particular that the shear force and the bending moment are connected by the local moment equilibrium equation, which here is written as:

$$R_y(x) = -M'_z(x), \forall x \in (0, \frac{L}{2}) \cup (\frac{L}{2}, L)$$



## 6.5 Buckling of straight beams

We will study here the phenomenon of buckling, which corresponds to the sudden appearance of a bending solution in a beam subjected to mechanical actions that we would “classically” associate with compression. Figure 6.20 illustrates this phenomenon in the case of a railway rail: when the temperature increases, if the free expansion of the rail is not allowed, it is possible that the resulting normal stress reaches a level sufficient for buckling to occur.



Figure 6.20: Rail buckling.

This is an unstable phenomenon, which appears as soon as the compression load reaches a particular value, called the critical load: at that moment, the problem loses its property of uniqueness in solution, due to geometric nonlinearities. To describe these latter, it is therefore necessary to modify the local moment equilibrium equation we determined in Paragraph 6.2.3.

### 6.5.1 Local moment equilibrium equation in the deformed configuration

We take again for that purpose the case of the isolation of a segment  $\omega$  of infinitesimal length, between the coordinates  $s^-$  and  $s^+ = s^- + ds$  distinct from the ends of the beam. We had then determined in Paragraph 6.2.3 the moment equilibrium of this segment, expressed in the centre  $G^-$  of the cross-section of coordinate  $s^-$ , as:

$$\begin{aligned} \mathbf{0} &= \int_{\omega} (\mathbf{x}_G(s) - \mathbf{x}_{G^-}(s^-) + \mathbf{x}_{\Sigma}) \wedge \mathbf{f}_V dV + \int_{\partial\omega \cap \partial\Omega} (\mathbf{x}_G(s) - \mathbf{x}_{G^-}(s^-) + \mathbf{x}_{\Sigma}) \wedge \mathbf{f}_S dS \\ &\quad - \mathbf{M}(s^-) + (\mathbf{x}_G(s) - \mathbf{x}_{G^-}(s^-)) \wedge \mathbf{R}(s^+) + \mathbf{M}(s^+) \end{aligned}$$

Instead of writing that  $\mathbf{x}_G(s) - \mathbf{x}_{G^-}(s^-) = (s - s^-)\mathbf{e}$  under the infinitesimal deformation hypothesis, we keep the expression unchanged, so that we obtain, assuming  $ds \rightarrow 0$ :

$$\mathbf{c}_L(s) + \mathbf{M}'(s) + \mathbf{x}'_G(s) \wedge \mathbf{R}(s) = \mathbf{0}, \forall s \in ]0, L[$$

We then assume that it is sufficient to express the placement of the neutral axis as  $\mathbf{x}_G = s\mathbf{e} + \mathbf{u}_{G\Sigma}$  to finally obtain that:

$$\mathbf{c}_L(s) + \mathbf{M}'(s) + (\mathbf{e} + \mathbf{u}'_{G\Sigma}(s)) \wedge \mathbf{R}(s) = \mathbf{0}, \forall s \in ]0, L[$$

Thus, even if the initial and deformed configurations remain close to each other, the cross-section rotations associated with bending are no longer neglected, since we explicitly keep the derivative  $\mathbf{u}'_{G\Sigma}$  of the transverse displacement, which, in accordance with Euler-Bernoulli hypothesis, is associated with  $\Theta_{\Sigma}$ .

Finally, in order to obtain an equation formally close to that previously obtained in bending, the equation established above is differentiated, then the local force equilibrium equation is injected to finally obtain:

$$\mathbf{c}'_L(s) + \mathbf{M}''(s) + \mathbf{u}''_{G\Sigma}(s) \wedge \mathbf{R}(s) - (\mathbf{e} + \mathbf{u}'_{G\Sigma}(s)) \wedge \mathbf{f}_L(s) = \mathbf{0}, \forall s \in ]0, L[$$

This is the only equation that needs to be modified: all the other relations remain within the infinitesimal deformation hypothesis. We can see that a normal (compressive) load can now be found in this moment equilibrium equation, through the two terms that have been added, whereas the tension-compression and bending behaviours were decoupled until now in the case of a straight beam.

**R** Even though buckling is a nonlinear phenomenon, with the above assumptions we get a linear equation, which corresponds to a model known as “linear buckling”. As we will see in the following paragraph, this theory will allow us to describe buckling in a partial way, by specifying how the phenomenon starts to establish itself.

### 6.5.2 Linear buckling

For the sake of illustration, we are now moving into a slightly more specific framework:

- the beam is not subjected to any line force or moment density;
- the beam is only subjected to compression: therefore, all boundary conditions in a direction perpendicular to the beam's axis  $\mathbf{e}$  are equal to zero, and normal stress is constant, being equal to  $R_e = -P, P > 0$ ;
- we adopt Euler-Bernoulli hypothesis, which makes it possible in particular to link the bending moment to the transverse displacement directly.

In this case, the moment equilibrium established in the previous paragraph can be rewritten as:

$$\mathbf{M}_\Sigma''(s) + \mathbf{u}_{G\Sigma}''(s) \wedge (-P\mathbf{e}) = \mathbf{0}, \forall s \in ]0, L[$$

where  $\mathbf{M}_\Sigma = E\mathbb{J}(\mathbf{e} \wedge \mathbf{u}_{G\Sigma}'')$ , which allows us to finally obtain:

$$E\mathbb{J}(\mathbf{e} \wedge \mathbf{u}_{G\Sigma}''') (s) - \mathbf{u}_{G\Sigma}''(s) \wedge P\mathbf{e} = \mathbf{0}, \forall s \in ]0, L[$$

which implies, by projection on the principal axes of inertia  $\mathbf{e}_{\chi_1}$  and  $\mathbf{e}_{\chi_2}$ , that:

$$\begin{aligned} EI_{\chi_2} u_{G\chi_1}'''(s) + Pu_{G\chi_1}''(s) &= 0, \forall s \in ]0, L[ \\ EI_{\chi_1} u_{G\chi_2}'''(s) + Pu_{G\chi_2}''(s) &= 0, \forall s \in ]0, L[ \end{aligned}$$

Since these two scalar equations are similar, we will limit ourselves in what follows to the first one.

We can then write the general solution to this equation as:

$$u_{G\chi_1}(s) = A \cos(ks) + B \sin(ks) + Cs + D, \forall s \in [0, L], \text{ with } k = \sqrt{\frac{P}{EI_{\chi_2}}}$$

where  $A, B, C$  and  $D$  are four constants to be determined using four boundary conditions, as in the case of a “classical” bending problem. Since we assumed that the beam was only subjected to compression, all the boundary conditions that can be written are homogeneous, and we then have to solve a problem of the form:

$$\left( \begin{array}{c} \\ \mathbb{L} \\ \end{array} \right) \begin{pmatrix} A \\ B \\ C \\ D \end{pmatrix} = \begin{pmatrix} 0 \\ 0 \\ 0 \\ 0 \end{pmatrix}$$

where the components of the matrix  $\mathbb{L}$  are functions of  $k$  and  $L$ . Since we are looking here for a non-trivial solution ( $\mathbf{u}_{G\Sigma} \neq \mathbf{0}$ ), it is necessary that the matrix  $\mathbb{L}$  is not invertible, hence:

$$\det \mathbb{L} = 0$$

which allows us to write a scalar equation giving a condition that  $k$  must verify in order for the bending solution to be established. We then find a family of possible values  $k_i, i \in \mathbb{N}^*$  corresponding to given loads  $P_i$ .

The smallest of these loads is called “critical load” (or “Euler’s critical load”) and corresponds to the occurrence of the phenomenon. We then determine the displacement associated with this load, but the expression of this displacement remains indeterminate up to an arbitrary multiplicative constant, given the singularity of the matrix  $\mathbb{L}$ : we speak of “buckling mode shape”.



*The problem solved here is in fact a generalized eigenvalue problem, where the eigenvalues are the different buckling loads, and the eigenmodes are the different buckling modes, whose amplitudes are therefore not known. This can be explained by the model used, which is a linearized approach that cannot fully account for the phenomenon, which is non-linear by nature.*

*The buckling modes therefore give the deformation of the beam at the beginning of buckling, but cannot describe its geometry in the current configuration: for this, we need a model that is not based on the infinitesimal deformation hypothesis. However, the model is sufficient to determine the critical load satisfactorily, which explains why it is widely used for designing beams under compression.*

■ **Example 6.15 — Buckling of a beam supported at each end.** We consider a straight beam of axis  $\mathbf{i}_x$  and length  $L$ , supported at its two ends, and subjected to a compressive loading at  $x = L$  (resultant force  $-P\mathbf{i}_x$  and moment equal to zero). The buckling problem is then written as:

$$EI_z u_{Gy}''''(x) + Pu_{Gy}''(x) = 0, \forall x \in ]0, L[$$

whose general solution is:

$$u_{Gy}(x) = A \cos(kx) + B \sin(kx) + Cx + D, \forall x \in [0, L], \text{ with } k = \sqrt{\frac{P}{EI_z}}$$

The four constants then verify the following boundary conditions:

- the transverse displacement is equal to zero at each support:

$$u_{Gy}(0) = 0, \text{ and } u_{Gy}(L) = 0$$

- the moment is equal to zero at each support:

$$EI_z u_{Gy}''(0) = 0, \text{ and } EI_z u_{Gy}''(L) = 0$$

which can be rewritten in matrix form as:

$$\begin{pmatrix} 1 & 0 & 0 & 1 \\ \cos kL & \sin kL & L & 1 \\ 1 & 0 & 0 & 0 \\ \cos kL & \sin kL & 0 & 0 \end{pmatrix} \begin{pmatrix} A \\ B \\ C \\ D \end{pmatrix} = \begin{pmatrix} 0 \\ 0 \\ 0 \\ 0 \end{pmatrix}$$

In order to obtain a non-zero solution, it is necessary that the previous matrix is not invertible, and therefore that its determinant is zero, which implies that:

$$0 = \det \mathbb{L} = \sin kL$$

which is possible for  $k_i = i\pi/L$ ,  $i \in \mathbb{N}^*$  ( $i \neq 0$  in order to avoid the trivial solution once again), hence:

$$P_i = \frac{i\pi^2 EI_z}{L^2}, i \in \mathbb{N}^*$$

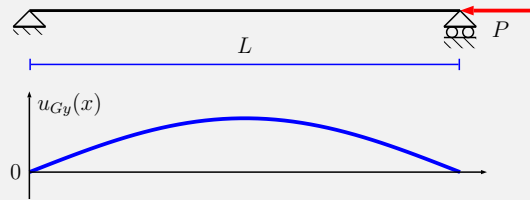
The critical load then corresponds to the first of these values, i.e.:

$$P_c = \frac{\pi^2 EI_z}{L^2}$$

the associated displacement being:

$$u_{Gy}(x) = B_c \sin\left(\frac{\pi x}{L}\right), \forall x \in [0, L]$$

where the constant  $B_c$  remains indeterminate. Thus, buckling occurs all the more easily the longer the beam is, and the lower the cross-section moment of inertia.



The other buckling modes, associated with critical loads  $P_i$ , are then:

$$u_{Gy}(x) = B_i \sin\left(\frac{i\pi x}{L}\right), \forall x \in [0, L]$$

where each constant  $B_i$  remains, once again, indeterminate. ■

The expression of the critical load is strongly influenced by the boundary conditions at the ends of the beam, as can be seen in Figure 6.21. Indeed, the scalar equation associated with  $\det \mathbb{L} = 0$  is modified each time, and leads logically to different expressions of the parameter  $k$  and of the critical load, which are summarized in Figure 6.22: we notice nevertheless that all the expressions are of similar form:

$$P_c = \frac{\pi^2 EI_z}{L_{eq}^2}$$

where  $L_{eq}$  is an equivalent length, from the point of view of buckling, which depends on the conditions at the ends of the beam:

- for a beam clamped at its two ends (from the point of view of bending), the equivalent length is twice the length of the beam;
- for a cantilever beam, the equivalent length is half the length of the beam;
- for a beam clamped at one end and supported at the other, the equivalent length is about 70% of the length of the beam (the exact value is associated with solving the buckling equation  $\tan kL = kL$ ).

This shows that the fewer degrees of freedom the beam has at its ends (rotation or even transverse displacement), the higher the load required for buckling. It is therefore in one's interest to favour this type of configuration in order to avoid the phenomenon. Similarly, it is also possible to add intermediate supports in order to "shorten" the beam, that is, to reduce the value of  $L_{eq}$ .



Figure 6.21: Illustration of the influence of boundary conditions on the value of the critical load.



*In the case of beams where the shear stiffness is much lower than the bending stiffness, as in the case of sandwich beams (where a layer made of a very compliant material is between two layers of a very rigid material) for example, the previous formulas are no longer valid, as it is necessary to take into account the influence of shear. In this case, the critical load verifies:*

$$P_c = \frac{\pi^2 \langle EI_z \rangle}{L_{eq}^2} \frac{1}{1 + \frac{\pi^2 \langle EI_z \rangle}{L_{eq}^2 \langle \mu A \rangle}} \approx \langle \mu A \rangle$$

when  $L_{eq}^2 \langle \mu A \rangle \ll \langle EI_z \rangle$ , where  $\langle \bullet \rangle$  stands for the average of  $\bullet$  on a cross-section.

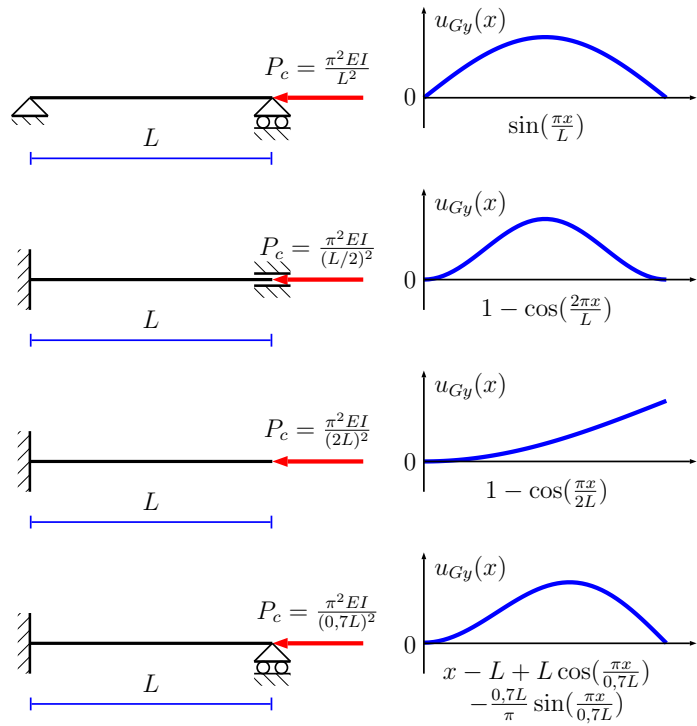


Figure 6.22: Critical loads and buckling modes for different boundary conditions.

## 6.6 Summary of important formulas

**Kinematics of a (Timoshenko) beam – Summary 6.1 page 156**

$$\begin{aligned}\mathbf{u} &= \mathbf{u}_G + \boldsymbol{\theta} \wedge \mathbf{x}_\Sigma \\ \boldsymbol{\varepsilon} &= (u'_{Ge} + \langle \boldsymbol{\theta}'_\Sigma \wedge \mathbf{x}_\Sigma, \mathbf{e} \rangle) \mathbf{e} \otimes \mathbf{e} + (\mathbf{u}'_{G\Sigma} - \boldsymbol{\theta}_\Sigma \wedge \mathbf{e}) \otimes_S \mathbf{e} + (\boldsymbol{\theta}'_e \mathbf{e} \wedge \mathbf{x}_\Sigma) \otimes_S \mathbf{e}\end{aligned}$$

**Kinematics of a (Euler-Bernoulli) beam – Summary 6.2 page 160**

$$\begin{aligned}\boldsymbol{\theta}_\Sigma &= \mathbf{e} \wedge \mathbf{u}'_{G\Sigma} \\ \mathbf{u} &= \mathbf{u}_G + (\boldsymbol{\theta}_e \mathbf{e} + \mathbf{e} \wedge \mathbf{u}'_{G\Sigma}) \wedge \mathbf{x}_\Sigma \\ \boldsymbol{\varepsilon} &= (u'_{Ge} - \langle \mathbf{u}''_{G\Sigma}, \mathbf{x}_\Sigma \rangle) \mathbf{e} \otimes \mathbf{e} + (\boldsymbol{\theta}'_e \mathbf{e} \wedge \mathbf{x}_\Sigma) \otimes_S \mathbf{e}\end{aligned}$$

**Equilibrium equation for the resultant force of the internal loads (global approach) – Summary 6.3 page 165**

$$\begin{aligned}\int_0^s \mathbf{f}_L d\xi + \mathbf{R}_0 + \mathbf{R}(s) &= \mathbf{0} \\ \int_s^L \mathbf{f}_L d\xi + \mathbf{R}_L - \mathbf{R}(s) &= \mathbf{0} \\ \mathbf{f}_L &= \int_\Sigma \mathbf{f}_V dS + \int_{\partial\Sigma} \mathbf{f}_S dl\end{aligned}$$

**Equilibrium equation for the resultant force of the internal loads (local approach) – Summary 6.4 page 168**

$$\mathbf{f}_L + \mathbf{R}' = \mathbf{0}$$

$$\mathbf{R}(0) = \int_{\Sigma(0)} \sigma \mathbf{e} dS = -\mathbf{R}_0, \text{ and } \mathbf{R}(L) = \int_{\Sigma(L)} \sigma \mathbf{e} dS = \mathbf{R}_L$$

**Equilibrium equation for the moment of the internal loads (global approach) – Summary 6.5 page 171**

$$\begin{aligned} & \int_0^s (\xi - s) \mathbf{e} \wedge \mathbf{f}_L d\xi + \int_0^s \mathbf{c}_L d\xi + \mathbf{M}_0 - s \mathbf{e} \wedge \mathbf{R}_0 + \mathbf{M}(s) = \mathbf{0} \\ & \int_s^L (\xi - s) \mathbf{e} \wedge \mathbf{f}_L d\xi + \int_s^L \mathbf{c}_L d\xi + \mathbf{M}_L + (L - s) \mathbf{e} \wedge \mathbf{R}_L - \mathbf{M}(s) = \mathbf{0} \\ & \mathbf{c}_L = \int_{\Sigma} \mathbf{x}_{\Sigma} \wedge \mathbf{f}_V dS + \int_{\partial\Sigma} \mathbf{x}_{\Sigma} \wedge \mathbf{f}_S dl \end{aligned}$$

**Equilibrium equation for the moment of the internal loads (local approach) – Summary 6.6 page 174**

$$\begin{aligned} & \mathbf{c}_L + \mathbf{M}' + \mathbf{e} \wedge \mathbf{R} = \mathbf{0} \\ & \mathbf{M}(0) = \int_{\Sigma(0)} \mathbf{x}_{\Sigma} \wedge \sigma \mathbf{e} dS = -\mathbf{M}_0, \text{ and } \mathbf{M}(L) = \int_{\Sigma(L)} \mathbf{x}_{\Sigma} \wedge \sigma \mathbf{e} dS = \mathbf{M}_L \\ & \mathbf{R}_{\Sigma} = \mathbf{e} \wedge (\mathbf{c}_L + \mathbf{M}') \end{aligned}$$

**Constitutive relation for the resultant force in the case of a Timoshenko beam – Summary 6.7 page 178**

$$\mathbf{R} = R_e \mathbf{e} + \mathbf{R}_{\Sigma} = EA u'_{Ge} \mathbf{e} + \mu A (\mathbf{u}'_{G\Sigma} - \boldsymbol{\theta}_{\Sigma} \wedge \mathbf{e})$$

**Constitutive relation for the resultant force in the case of an Euler-Bernoulli beam – Summary 6.8 page 178**

$$\begin{aligned} \mathbf{R} &= R_e \mathbf{e} + \mathbf{R}_{\Sigma} = EA u'_{Ge} \mathbf{e} - E (I_{\chi_2} \mathbf{e}_{\chi_1} \otimes \mathbf{e}_{\chi_1} + I_{\chi_1} \mathbf{e}_{\chi_2} \otimes \mathbf{e}_{\chi_2}) \mathbf{u}'''_{G\Sigma} + \mathbf{e} \wedge \mathbf{c}_L \\ R_{\chi_1} &= -EI_{\chi_2} u'''_{G\chi_1} - c_{L\chi_2} \\ R_{\chi_2} &= -EI_{\chi_1} u'''_{G\chi_2} + c_{L\chi_1} \end{aligned}$$

**Area inertia tensor (principal basis)**

$$\begin{aligned} \mathbb{J} &= \int_{\Sigma} (\|\mathbf{x}_{\Sigma}\|^2 \mathbb{I} - \mathbf{x}_{\Sigma} \otimes \mathbf{x}_{\Sigma}) dS \\ \mathbb{J} &= I_e \mathbf{e} \otimes \mathbf{e} + I_{\chi_1} \mathbf{e}_{\chi_1} \otimes \mathbf{e}_{\chi_1} + I_{\chi_2} \mathbf{e}_{\chi_2} \otimes \mathbf{e}_{\chi_2} \\ I_{\chi_1} &= \int_{\Sigma} \chi_2^2 dS \\ I_{\chi_2} &= \int_{\Sigma} \chi_1^2 dS \\ I_e &= I_{\chi_1} + I_{\chi_2} = \int_{\Sigma} (\chi_1^2 + \chi_2^2) dS \end{aligned}$$

**Constitutive relation for the moment in the case of a Timoshenko beam – Summary 6.9 page 179**

$$\begin{aligned} \mathbf{M} &= M_e \mathbf{e} + \mathbf{M}_{\Sigma} = \mu I_e \theta'_e \mathbf{e} + E \mathbb{J} \boldsymbol{\theta}'_{\Sigma} \\ M_e &= \mu I_e \theta'_e \\ M_{\chi_1} &= EI_{\chi_1} \theta'_{\chi_1} \end{aligned}$$

$$M_{\chi_2} = EI_{\chi_2} \theta'_{\chi_2}$$

**Constitutive relation for the moment in the case of an Euler-Bernoulli beam – Summary 6.10 page 179**

$$\begin{aligned}\mathbf{M} &= M_e \mathbf{e} + \mathbf{M}_\Sigma = \mu I_e \theta'_e \mathbf{e} + E \mathbb{J} (\mathbf{e} \wedge \mathbf{u}_{G\Sigma}'') \\ M_e &= \mu I_e \theta'_e \\ M_{\chi_1} &= -EI_{\chi_1} u''_{G\chi_2} \\ M_{\chi_2} &= EI_{\chi_2} u''_{G\chi_1}\end{aligned}$$

**Stress vector in a cross-section – Summary 6.11 page 187**

$$\boldsymbol{\sigma} \mathbf{e} = \sigma_{ee} \mathbf{e} + \boldsymbol{\tau}_\Sigma = \left( \frac{R_e}{A} + \langle \mathbf{x}_\Sigma, \mathbf{e} \wedge \mathbb{J}^{-1} \mathbf{M}_\Sigma \rangle \right) \mathbf{e} + \frac{1}{A} \mathbf{R}_\Sigma + \frac{M_e}{I_e} \mathbf{e} \wedge \mathbf{x}_\Sigma$$

**Kinematic parameters of the cross-section of a beam  $\Omega$  in connection with a body  $\Omega^*$  – Summary 6.12 page 193**

Connection ( $\Omega/\Omega^*$ )	Case of a fixed support $\Omega^*$	Case of a beam $\Omega^*$
Pinned support (2D)	$\mathbf{u}_G = \mathbf{0}$	$\mathbf{u}_G = \mathbf{u}_G^*$ (in plane)
Roller support (2D)	$\mathbf{u}_G - \langle \mathbf{u}_G, \mathbf{e} \rangle \mathbf{e} = \mathbf{0}$	not encountered in reality
Rigid connection	$\mathbf{u}_G = \mathbf{0}$ , and $\boldsymbol{\theta} = \mathbf{0}$	$\mathbf{u}_G = \mathbf{u}_G^*$ , and $\boldsymbol{\theta} = \boldsymbol{\theta}^*$
Pin joint (of axis $\mathbf{a}$ )	$\mathbf{u}_G = \mathbf{0}$ , $\boldsymbol{\theta} - \langle \boldsymbol{\theta}, \mathbf{a} \rangle \mathbf{a} = \mathbf{0}$	$\mathbf{u}_G = \mathbf{u}_G^*$ , $\boldsymbol{\theta} - \langle \boldsymbol{\theta}, \mathbf{a} \rangle = \boldsymbol{\theta}^* - \langle \boldsymbol{\theta}^*, \mathbf{a} \rangle$
Roller support	$\mathbf{u}_G - \langle \mathbf{u}_G, \mathbf{e} \rangle \mathbf{e} = \mathbf{0}$	not encountered in reality
Spherical joint	$\mathbf{u}_G = \mathbf{0}$	$\mathbf{u}_G = \mathbf{u}_G^*$

**Connection action of the body  $\Omega^*$  on the beam  $\Omega$  on the cross-section  $\Sigma$ , for a perfect connection. – Summary 6.13 page 195**

Connection ( $\Omega/\Omega^*$ )	Resultant force and moment of the connection action of $\Omega^*$ on $\Omega$
Pinned support (2D)	arbitrary $\mathbf{R}$ (in the plane), and $\mathbf{M} = \mathbf{0}$
Roller support (2D)	$\langle \mathbf{R}, \mathbf{e} \rangle = 0$ , and $\mathbf{M} = \mathbf{0}$
Rigid connection	arbitrary $\mathbf{R}$ and $\mathbf{M}$
Pin joint (of axis $\mathbf{a}$ )	arbitrary $\mathbf{R}$ , and $\langle \mathbf{M}, \mathbf{a} \rangle = 0$
Roller support	$\langle \mathbf{R}, \mathbf{e} \rangle = 0$ , and $\mathbf{M} = \mathbf{0}$
Spherical joint	arbitrary $\mathbf{R}$ , and $\mathbf{M} = \mathbf{0}$



## A. Tensor algebra

### A.1 Vectors

#### A.1.1 Definitions and notations

Briefly and generally, the three-dimensional space to which we will refer is an affine space  $\mathcal{E}$ , whose points are the elements. The underlying vector space  $\mathcal{V}$  then includes the three-dimensional vectors, which we will write in boldface:  $\mathbf{v} \in \mathcal{V}$ .

To keep a unified formalism, we will represent the points of the space  $\mathcal{E}$  in the form of the position vectors associated with them: considering the point  $A \in \mathcal{E}$  is equivalent to take into account the position vector  $\mathbf{x}_A \in \mathcal{V}$ . Thus, the vectors of the underlying vector space  $\mathcal{V}$  can also be represented as differences of points of  $\mathcal{E}$ : the vector connecting two points  $A$  and  $B$  of  $\mathcal{E}$  will naturally be written as  $\mathbf{x}_B - \mathbf{x}_A$ , where  $\mathbf{x}_A$  and  $\mathbf{x}_B$  are the position vectors respectively associated with the points  $A$  and  $B$ , while the middle point  $I$  of the segment  $[AB]$  is such that  $\mathbf{x}_I = (\mathbf{x}_A + \mathbf{x}_B)/2$ , as shown in Figure A.1.

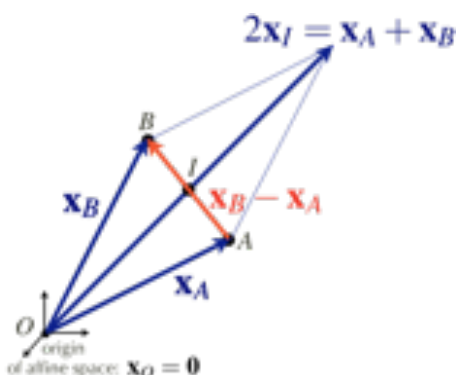


Figure A.1: Points and vectors.

A vector basis of  $\mathcal{V}$  is a family of three vectors  $(\mathbf{i}_1, \mathbf{i}_2, \mathbf{i}_3)$  which are free and span the vector space  $\mathcal{V}$ . In other words, any vector  $\mathbf{v} \in \mathcal{V}$  can be written in a unique way as a linear combination

of these three vectors:

$$\mathbf{v} = \sum_{n=1}^3 v_n \mathbf{i}_n$$

where  $v_n$  are the components of the vector  $\mathbf{v}$  in the basis  $(\mathbf{i}_1, \mathbf{i}_2, \mathbf{i}_3)$ .

As we will see in Paragraph A.1.2, orthonormal bases, i.e. those whose vectors are orthogonal to each other, and of unit norm, are chosen in a privileged way. In this context, we define the scalar product between two vectors  $\mathbf{a}$  and  $\mathbf{b}$  as the bilinear form  $\langle \bullet, \bullet \rangle$ , symmetric and positive definite, which is expressed as:

$$\langle \mathbf{a}, \mathbf{b} \rangle = \sum_{n=1}^3 a_n b_n$$

where  $a_n$  and  $b_n$  are respectively the components of  $\mathbf{a}$  and  $\mathbf{b}$  in the orthonormal basis  $(\mathbf{i}_1, \mathbf{i}_2, \mathbf{i}_3)$ . We then define the norm  $\|\mathbf{a}\|$  of a vector  $\mathbf{a}$  as:

$$\|\mathbf{a}\| = \sqrt{\langle \mathbf{a}, \mathbf{a} \rangle}$$

Finally, we will note the vector product of two vectors  $\mathbf{a}$  and  $\mathbf{b}$  as  $\mathbf{c} = \mathbf{a} \wedge \mathbf{b}$ , whose components  $c_n$  in an orthonormal basis  $(\mathbf{i}_1, \mathbf{i}_2, \mathbf{i}_3)$  verify:

$$c_1 = a_2 b_3 - a_3 b_2, \quad c_2 = a_3 b_1 - a_1 b_3, \quad c_3 = a_1 b_2 - a_2 b_1$$

We also recall some classic formulas about the vector product:

$$\mathbf{a} \wedge (\mathbf{b} \wedge \mathbf{c}) = \langle \mathbf{a}, \mathbf{c} \rangle \mathbf{b} - \langle \mathbf{a}, \mathbf{b} \rangle \mathbf{c}, \quad \forall \mathbf{a}, \forall \mathbf{b}, \forall \mathbf{c}$$

$$\langle \mathbf{a} \wedge \mathbf{d}, \mathbf{b} \wedge \mathbf{c} \rangle = \langle \mathbf{a}, \mathbf{b} \rangle \langle \mathbf{d}, \mathbf{c} \rangle - \langle \mathbf{a}, \mathbf{c} \rangle \langle \mathbf{b}, \mathbf{d} \rangle, \quad \forall \mathbf{a}, \forall \mathbf{b}, \forall \mathbf{c}, \forall \mathbf{d}$$

including Jacobi identity formula:

$$\mathbf{a} \wedge (\mathbf{b} \wedge \mathbf{c}) + \mathbf{b} \wedge (\mathbf{c} \wedge \mathbf{a}) + \mathbf{c} \wedge (\mathbf{a} \wedge \mathbf{b}) = \mathbf{0}, \quad \forall \mathbf{a}, \forall \mathbf{b}, \forall \mathbf{c}$$

and the permutation property of the mixed product:

$$\langle \mathbf{a}, \mathbf{b} \wedge \mathbf{c} \rangle = \langle \mathbf{b}, \mathbf{c} \wedge \mathbf{a} \rangle = \langle \mathbf{c}, \mathbf{a} \wedge \mathbf{b} \rangle, \quad \forall \mathbf{a}, \forall \mathbf{b}, \forall \mathbf{c}$$

### A.1.2 Classical vector bases

In the following, we present three orthonormal vector bases commonly used in mechanics, because they are associated with basic geometries that can be found in most of the problems considered.

#### Cartesian vector basis

A Cartesian vector basis consists of three vectors  $(\mathbf{i}_1, \mathbf{i}_2, \mathbf{i}_3)$ , of unit norm and orthogonal to each other, which do not depend on any parameter. It is then associated with the Cartesian coordinates  $(x_1, x_2, x_3)$ , so that a point in space satisfies the following position vector:

$$\mathbf{x} = x_1 \mathbf{i}_1 + x_2 \mathbf{i}_2 + x_3 \mathbf{i}_3$$

as represented in Figure A.2.

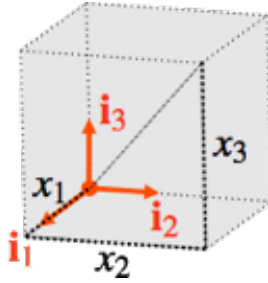


Figure A.2: Cartesian vector basis and associated coordinates.

### Cylindrical vector basis

In the case of a geometry in the shape of a cylinder of revolution, a cylindrical vector basis can be used, which consists of three vectors ( $\mathbf{i}_r(\theta), \mathbf{i}_\theta(\theta), \mathbf{i}_z$ ), of unit norm and orthogonal to each other, where:

- the vector  $\mathbf{i}_z$  corresponds to the axis of the cylinder to which the base is associated;
- the other two vectors can be deduced from a given Cartesian vector basis ( $\mathbf{i}_1, \mathbf{i}_2$ ) of the circular section of the cylinder as:

$$\begin{aligned}\mathbf{i}_r(\theta) &= \cos \theta \mathbf{i}_1 + \sin \theta \mathbf{i}_2, \quad \forall \theta \in [0, 2\pi) \\ \mathbf{i}_\theta(\theta) &= -\sin \theta \mathbf{i}_1 + \cos \theta \mathbf{i}_2, \quad \forall \theta \in [0, 2\pi)\end{aligned}$$

This vector basis is associated with the cylindrical coordinates  $(r, \theta, z)$ , so that a point in space satisfies the following position vector:

$$\mathbf{x} = r\mathbf{i}_r(\theta) + z\mathbf{i}_z$$

as represented in Figure A.3.

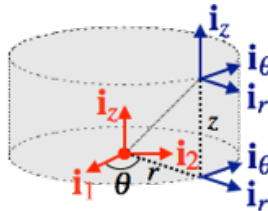


Figure A.3: Cylindrical vector basis and associated coordinates.

### Spherical vector basis

In the case of a spherical geometry, a spherical vector basis can be used, which consists of three vectors ( $\mathbf{e}_r(\vartheta, \phi), \mathbf{e}_\theta(\vartheta, \phi), \mathbf{e}_\phi(\phi)$ ), of unit norm and orthogonal to each other, which can be deduced from a given Cartesian vector basis ( $\mathbf{i}_1, \mathbf{i}_2, \mathbf{i}_3$ ) as:

$$\begin{aligned}\mathbf{e}_r(\vartheta, \phi) &= \sin \vartheta \cos \phi \mathbf{i}_1 + \sin \vartheta \sin \phi \mathbf{i}_2 + \cos \vartheta \mathbf{i}_3, \quad \forall \vartheta \in [0, \pi], \forall \phi \in [0, 2\pi) \\ \mathbf{e}_\theta(\vartheta, \phi) &= \cos \vartheta \cos \phi \mathbf{i}_1 + \cos \vartheta \sin \phi \mathbf{i}_2 - \sin \vartheta \mathbf{i}_3, \quad \forall \vartheta \in [0, \pi], \forall \phi \in [0, 2\pi) \\ \mathbf{e}_\phi(\phi) &= -\sin \phi \mathbf{i}_1 + \cos \phi \mathbf{i}_2, \quad \forall \phi \in [0, 2\pi)\end{aligned}$$

This basis is associated with the spherical coordinates  $(r, \vartheta, \phi)$ , so that a point in space satisfies the following position vector:

$$\mathbf{x} = r\mathbf{e}_r(\vartheta, \phi)$$

as represented in Figure A.4.

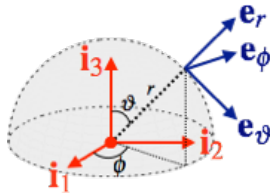


Figure A.4: Spherical vector basis and associated coordinates.

## A.2 Second-order tensors

### A.2.1 Definitions and properties

A second-order tensor (noted with a blackboard bold letter:  $\mathbb{A}$ ) is a linear application of a vector space in itself, which, to any vector  $\mathbf{a}$ , associates the vector  $\mathbf{b} = \mathbb{A}(\mathbf{a})$  of components:

$$b_m = \sum_{n=1}^3 A_{mn} a_n$$

where  $a_p$  and  $b_p$  ( $1 \leq p \leq 3$ ) are respectively the components of  $\mathbf{a}$  and  $\mathbf{b}$  in a given orthonormal vector basis  $(\mathbf{i}_1, \mathbf{i}_2, \mathbf{i}_3)$ , and the components of  $\mathbb{A}$  are defined as:

$$A_{mn} = \langle \mathbf{i}_m, \mathbb{A}(\mathbf{i}_n) \rangle, \quad 1 \leq m, n \leq 3$$

It is therefore a multiplication  $\mathbf{b} = \mathbb{A}\mathbf{a}$  in the sense of the matrix-vector product, which is a notation that is used preferentially in this textbook. In this context, we note  $\mathbb{I}$  the identity tensor, which is such that  $\mathbb{I}\mathbf{a} = \mathbf{a}$ ,  $\forall \mathbf{a}$ , and whose components are therefore written as:

$$I_{mn} = \langle \mathbf{i}_m, \mathbf{i}_n \rangle = \delta_{mn}, \quad 1 \leq m, n \leq 3$$

where  $\delta_{mn}$  stands for the “Kronecker delta”, defined as:

$$\delta_{mn} = \begin{cases} 0 & \text{if } m \neq n \\ 1 & \text{if } m = n \end{cases}$$

Besides, the (non-commutative) tensor multiplication structure, which corresponds to the composition of linear applications, is used; thus, the product  $\mathbb{C} = \mathbb{A}\mathbb{B}$  is defined by its effect on a vector  $\mathbf{a}$ :

$$\mathbf{b} = \mathbb{C}\mathbf{a} = (\mathbb{A}\mathbb{B})\mathbf{a} = \mathbb{A}(\mathbb{B}(\mathbf{a}))$$

whose components thus verify:

$$b_m = \sum_{n=1}^3 A_{mn} \sum_{p=1}^3 B_{np} a_p$$

which is equivalent to write that the components of the product  $\mathbb{C}$  verify:

$$C_{mp} = \sum_{n=1}^3 A_{mn} B_{np}, \quad 1 \leq m, p \leq 3$$

which is actually the multiplication of two matrices. In the particular case of the identity tensor ( $\mathbb{C} = \mathbb{I}$ ), we call inverse of  $\mathbb{A}$  the tensor  $\mathbb{A}^{-1}$  verifying:

$$\mathbb{A}\mathbb{A}^{-1} = \mathbb{I} = \mathbb{A}^{-1}\mathbb{A}$$

and therefore corresponding to the inverse application of the one associated with the tensor  $\mathbb{A}$ .

Finally,  $\mathbb{A}^T$  stands for the transpose tensor of  $\mathbb{A}$ , in the sense of the scalar product:

$$\langle \mathbb{A}^T \mathbf{a}, \mathbf{b} \rangle = \langle \mathbf{a}, \mathbb{A} \mathbf{b} \rangle, \forall \mathbf{a}, \forall \mathbf{b}$$

which allows to find that, in an orthonormal vector basis:

$$(\mathbb{A}^T)_{mn} = \mathbb{A}_{nm}, 1 \leq m, n \leq 3$$

Besides, when the tensor  $\mathbb{A}$  is invertible, the inverse of the transpose is defined as the transpose of the inverse, noted  $\mathbb{A}^{-T}$ :  $(\mathbb{A}^T)^{-1} = \mathbb{A}^{-T} = (\mathbb{A}^{-1})^T$ .

In another orthonormal vector basis  $(\mathbf{i}_1^*, \mathbf{i}_2^*, \mathbf{i}_3^*) = (\mathbb{R}\mathbf{i}_1, \mathbb{R}\mathbf{i}_2, \mathbb{R}\mathbf{i}_3)$ , linked to the previous one by a rotation  $\mathbb{R}$  of components  $R_{mn}$  in the vector basis  $(\mathbf{i}_1, \mathbf{i}_2, \mathbf{i}_3)$  (as defined in Paragraph A.2.6), the components of  $\mathbb{A}$  are transformed according to:

$$A_{mn}^* = \langle \mathbf{i}_m^*, \mathbb{A} \mathbf{i}_n^* \rangle = \langle \mathbb{R}\mathbf{i}_m, \mathbb{A} \mathbb{R}\mathbf{i}_n \rangle = \langle \mathbf{i}_m, \mathbb{R}^T \mathbb{A} \mathbb{R} \mathbf{i}_n \rangle = \sum_{1 \leq p, q \leq 3} R_{pm} A_{pq} R_{qn}, 1 \leq m, n \leq 3$$

which corresponds to the classical formula of change of basis for the components of a matrix.

### Tensor product of two vectors

We note  $\mathbf{a} \otimes \mathbf{b}$  the tensor product of two vectors  $\mathbf{a}$  and  $\mathbf{b}$ , which is a particular tensor with the following property:

$$(\mathbf{a} \otimes \mathbf{b}) \mathbf{c} = \langle \mathbf{b}, \mathbf{c} \rangle \mathbf{a}, \forall \mathbf{c}$$

which can be interpreted in terms of matrix calculus as  $\mathbf{a} \otimes \mathbf{b} = \mathbf{a} \mathbf{b}^T$  (where the transpose of a “column vector”  $\mathbf{b}$  is the “row vector”  $\mathbf{b}^T$ ). Geometrically, if  $\mathbf{e}$  is a unit vector,  $\mathbf{e} \otimes \mathbf{e}$  represents the projection along the direction  $\mathbf{e}$ , and, therefore,  $\mathbb{I} - \mathbf{e} \otimes \mathbf{e}$  is interpreted as the projection on the plane of normal  $\mathbf{e}$ .

Besides, the following relations should be noted, which are valid regardless of  $\mathbf{a}, \mathbf{b}, \mathbf{c}, \mathbf{d}$  and  $\mathbb{A}$ , and can facilitate calculations:

$$(\mathbf{a} \otimes \mathbf{b})^T = \mathbf{b} \otimes \mathbf{a}, \text{ and } (\mathbf{a} \otimes \mathbf{b})(\mathbf{c} \otimes \mathbf{d}) = \langle \mathbf{b}, \mathbf{c} \rangle \mathbf{a} \otimes \mathbf{d}$$

$$\mathbb{A}(\mathbf{a} \otimes \mathbf{b}) = (\mathbb{A}\mathbf{a}) \otimes \mathbf{b}, \forall \mathbb{A}, \text{ and } (\mathbf{a} \otimes \mathbf{b})\mathbb{A} = \mathbf{a} \otimes (\mathbb{A}^T \mathbf{b})$$

Finally, it is easy to see that the identity tensor can be written as:

$$\mathbb{I} = \sum_{n=1}^3 \mathbf{i}_n \otimes \mathbf{i}_n$$

where  $(\mathbf{i}_1, \mathbf{i}_2, \mathbf{i}_3)$  is a given orthonormal vector basis; this result allows to obtain the expression of a tensor  $\mathbb{A}$  with all the tensor products of the vectors of the considered vector basis:

$$\mathbb{A} = \sum_{n=1}^3 (\mathbb{A} \mathbf{i}_n) \otimes \mathbf{i}_n = \sum_{m=1}^3 \sum_{n=1}^3 A_{mn} \mathbf{i}_m \otimes \mathbf{i}_n$$

where we naturally find the components  $A_{mn}$  of  $\mathbb{A}$ .

### Symmetrical and antisymmetrical parts

Any tensor  $\mathbb{A}$  can be decomposed as the sum of a symmetrical part  $(\mathbb{A})_S$  and an antisymmetrical part  $(\mathbb{A})_A$ :

$$\mathbb{A} = (\mathbb{A})_S + (\mathbb{A})_A = \frac{1}{2}(\mathbb{A} + \mathbb{A}^T) + \frac{1}{2}(\mathbb{A} - \mathbb{A}^T)$$

where it is easily verified that  $(\mathbb{A})_S^T = (\mathbb{A})_S$  and  $(\mathbb{A})_A^T = -(\mathbb{A})_A$ .

Moreover, since antisymmetry implies that  $\langle (\mathbb{A})_A \mathbf{a}, \mathbf{a} \rangle = -\langle (\mathbb{A})_A \mathbf{a}, \mathbf{a} \rangle$ ,  $\forall \mathbb{A}$ ,  $\forall \mathbf{a}$ , we deduce that this scalar product is equal to zero, which allows to associate to the antisymmetrical part of  $\mathbb{A}$  a vector  $\mathbf{w}$  such that we have:

$$(\mathbb{A})_A \mathbf{a} = \mathbf{w} \wedge \mathbf{a}, \quad \forall \mathbf{a}$$

which is then the vector of components:

$$\langle \mathbf{w}, \mathbf{i}_n \rangle = \sum_{m=1}^3 \langle (\mathbb{A})_A \mathbf{i}_m, \mathbf{i}_n \wedge \mathbf{i}_m \rangle$$

Conversely, knowing the vector  $\mathbf{w}$ , we can build the antisymmetrical tensor  $\mathbf{w}^\wedge$ , of components:

$$\mathbf{w}_{mn}^\wedge = \langle \mathbf{w}, \mathbf{i}_n \wedge \mathbf{i}_m \rangle$$

Similarly, it is also possible to express the vector triple product using the product of antisymmetrical tensors:

$$\mathbf{w}_1 \wedge (\mathbf{w}_2 \wedge \mathbf{a}) = \mathbf{w}_1^\wedge \mathbf{w}_2^\wedge \mathbf{a}, \quad \forall \mathbf{a}$$

or, using Jacobi identity formula presented in Paragraph A.1.1:

$$(\mathbf{w}_1 \wedge \mathbf{w}_2) \wedge \mathbf{a} = (\mathbf{w}_1^\wedge \mathbf{w}_2^\wedge - \mathbf{w}_2^\wedge \mathbf{w}_1^\wedge) \mathbf{a}, \quad \forall \mathbf{a}$$

Finally, the previous definitions can naturally be applied to the tensor product of two vectors, by writing:

$$\mathbf{a} \otimes \mathbf{b} = \mathbf{a} \otimes_S \mathbf{b} + \mathbf{a} \otimes_A \mathbf{b} = \frac{1}{2}(\mathbf{a} \otimes \mathbf{b} + \mathbf{b} \otimes \mathbf{a}) + \frac{1}{2}(\mathbf{a} \otimes \mathbf{b} - \mathbf{b} \otimes \mathbf{a})$$

where  $\mathbf{a} \otimes_S \mathbf{b} = (\mathbf{a} \otimes \mathbf{b})_S$  and  $\mathbf{a} \otimes_A \mathbf{b} = (\mathbf{a} \otimes \mathbf{b})_A$  respectively stand for the symmetrical and antisymmetrical parts of the tensor product  $\mathbf{a} \otimes \mathbf{b}$ . The antisymmetrical part therefore corresponds to a vector associated with the vector product, which is simply  $\mathbf{w} = -(\mathbf{a} \wedge \mathbf{b})/2$  since we have:

$$2(\mathbf{a} \otimes_A \mathbf{b}) \mathbf{c} = \langle \mathbf{b}, \mathbf{c} \rangle \mathbf{a} - \langle \mathbf{a}, \mathbf{c} \rangle \mathbf{b} = -(\mathbf{a} \wedge \mathbf{b}) \wedge \mathbf{c}, \quad \forall \mathbf{c}$$

## A.2.2 Scalar product and tensor norm

### Trace of a tensor

In order to be able to define a scalar product and a tensor norm, we start by defining the trace of a tensor, which is a linear form noted  $\text{tr}$ , which we can define on the space of second-order tensors as:

$$\text{tr}(\mathbf{a} \otimes \mathbf{b}) = \langle \mathbf{a}, \mathbf{b} \rangle = \text{tr}(\mathbf{b} \otimes \mathbf{a}), \quad \forall \mathbf{a}, \forall \mathbf{b}$$

which allows to deduce, by linearity, the classical expression:

$$\text{tr} \mathbb{A} = \sum_{n=1}^3 \text{tr}(\mathbb{A}(\mathbf{i}_n \otimes \mathbf{i}_n)) = \sum_{n=1}^3 \text{tr}((\mathbb{A}\mathbf{i}_n) \otimes \mathbf{i}_n) = \sum_{n=1}^3 \langle \mathbb{A}\mathbf{i}_n, \mathbf{i}_n \rangle = \sum_{n=1}^3 A_{nn}$$

We then conclude that the trace  $\text{tr} \mathbb{A}$  is an “invariant” of the tensor  $\mathbb{A}$ : its value does not depend on the vector basis chosen to express the components  $A_{mn}$  of the considered tensor.

### Properties

The following product, sometimes called “contracted product” (and noted  $\mathbb{A} : \mathbb{B}$ ), is a scalar product defined in the second-order tensor space:

$$\langle \mathbb{A}, \mathbb{B} \rangle = \text{tr}(\mathbb{A}\mathbb{B}^T) = \sum_{m=1}^3 \sum_{n=1}^3 A_{mn}B_{mn}$$

considering the components  $A_{mn}$  and  $B_{mn}$  of  $\mathbb{A}$  and  $\mathbb{B}$  in a given vector basis. Indeed, this form is clearly bilinear and symmetrical, as well as positive definite, since  $\text{tr}(\mathbb{A}\mathbb{A}^T) \geq 0$  and since, if  $\text{tr}(\mathbb{A}\mathbb{A}^T) = 0$ , then  $\mathbb{A} = 0$  necessarily.

This scalar product then allows to define a tensor norm as:

$$\|\mathbb{A}\| = \sqrt{\text{tr}(\mathbb{A}\mathbb{A}^T)}$$

and obtain Cauchy-Schwarz inequality:

$$\left( \text{tr}(\mathbb{A}\mathbb{B}^T) \right)^2 = \langle \mathbb{A}, \mathbb{B} \rangle^2 \leq \|\mathbb{A}\|^2 \|\mathbb{B}\|^2 = \text{tr}(\mathbb{A}\mathbb{A}^T) \text{tr}(\mathbb{B}\mathbb{B}^T), \forall \mathbb{A}, \forall \mathbb{B}$$

Finally, we can see that a symmetrical tensor and an antisymmetrical tensor are orthogonal to each other in the sense of this scalar product; indeed, on the one hand, we have:

$$\langle (\mathbb{A})_S, \mathbb{B} \rangle = \frac{\langle \mathbb{A} + \mathbb{A}^T, \mathbb{B} \rangle}{2} = \frac{\langle \mathbb{A}, \mathbb{B} + \mathbb{B}^T \rangle}{2} = \langle \mathbb{A}, (\mathbb{B})_S \rangle, \forall \mathbb{A}, \forall \mathbb{B}$$

and, on the other hand:

$$\langle (\mathbb{A})_A, \mathbb{B} \rangle = \frac{\langle \mathbb{A} - \mathbb{A}^T, \mathbb{B} \rangle}{2} = \frac{\langle \mathbb{A}, \mathbb{B} - \mathbb{B}^T \rangle}{2} = \langle \mathbb{A}, (\mathbb{B})_A \rangle, \forall \mathbb{A}, \forall \mathbb{B}$$

which implies that:

$$\langle (\mathbb{A})_S, (\mathbb{B})_A \rangle = \text{tr}((\mathbb{A})_S(\mathbb{B})_A^T) = 0, \forall \mathbb{A}, \forall \mathbb{B}$$

### A.2.3 Determinant of a tensor and remarkable relations

#### Definition and properties

A pragmatic definition of the determinant  $\det \mathbb{A}$  of a tensor  $\mathbb{A}$  is to consider the mixed product of the images of three vectors by the linear application associated with  $\mathbb{A}$ , by writing that:

$$\langle \mathbb{A}\mathbf{a}, (\mathbb{A}\mathbf{b}) \wedge (\mathbb{A}\mathbf{c}) \rangle = \det \mathbb{A} \langle \mathbf{a}, \mathbf{b} \wedge \mathbf{c} \rangle, \forall \mathbf{a}, \forall \mathbf{b}, \forall \mathbf{c}$$

It is then easy to show that the determinant can be expressed as a function of the components  $A_{mn}$  of the tensor  $\mathbb{A}$  in a given orthonormal vector basis  $(\mathbf{i}_1, \mathbf{i}_2, \mathbf{i}_3)$ :

$$\det \mathbb{A} = A_{11}A_{22}A_{33} + A_{12}A_{23}A_{31} + A_{13}A_{21}A_{32} - A_{31}A_{22}A_{13} - A_{21}A_{12}A_{33} - A_{11}A_{32}A_{23}$$

where we recognize Sarrus' rule of calculation of the determinant of a  $3 \times 3$  matrix; however, the determinant  $\det \mathbb{A}$  is an invariant of the tensor  $\mathbb{A}$ , insofar as its value does not depend on the vector basis chosen to express the components  $A_{mn}$  of the considered tensor.

We can then show that the determinant of a product of tensors is the product of the determinants:

$$\det(\mathbb{A}\mathbb{B}) = (\det \mathbb{A})(\det \mathbb{B}), \forall \mathbb{A}, \forall \mathbb{B}$$

and therefore that the determinant of the inverse of a tensor is the inverse of the determinant:

$$\det(\mathbb{A}^{-1}) = \frac{1}{\det \mathbb{A}}, \forall \mathbb{A} \text{ invertible}$$

and that a tensor is invertible if and only if its determinant is not zero.

### Piola's formula

Using the previous definition, it is possible to write, for three arbitrary vectors and an invertible tensor  $\mathbb{A}$ , that:

$$\det \mathbb{A} \langle \mathbf{c}, \mathbf{a} \wedge \mathbf{b} \rangle = \langle \mathbb{A}\mathbf{c}, (\mathbb{A}\mathbf{a}) \wedge (\mathbb{A}\mathbf{b}) \rangle = \langle \mathbf{c}, \mathbb{A}^T((\mathbb{A}\mathbf{a}) \wedge (\mathbb{A}\mathbf{b})) \rangle, \forall \mathbf{c}$$

hence, finally:

$$(\mathbb{A}\mathbf{b}) \wedge (\mathbb{A}\mathbf{b}) = (\det \mathbb{A}) \mathbb{A}^{-T}(\mathbf{a} \wedge \mathbf{b}), \forall \mathbf{a}, \forall \mathbf{b}$$

In the case of a rotation tensor (as defined in Paragraph A.2.6), which then satisfies  $\mathbb{R}^T \mathbb{R} = \mathbb{I}$  and  $\det \mathbb{R} = 1$ , Piola's formula allows to establish the distributive property of the rotation tensor over the vector product:

$$\mathbb{R}(\mathbf{a} \wedge \mathbf{b}) = (\mathbb{R}\mathbf{a}) \wedge (\mathbb{R}\mathbf{b}), \forall \mathbf{a}, \forall \mathbf{b}$$

## A.2.4 Invariants of a tensor

### Spectral decomposition of a tensor

The eigenvectors  $\phi_k$  and eigenvalues  $\lambda_k$  of a tensor  $\mathbb{A}$  are intrinsic quantities related to it, and which satisfy:

$$\mathbb{A}\phi_k = \lambda_k\phi_k, 1 \leq k \leq 3$$

These quantities do not depend on the vector basis chosen to express the components of the tensor  $\mathbb{A}$ .

We can show that, if  $\mathbb{A}$  is symmetrical, it admits three real eigenvalues, to which we can associate an orthonormal basis of eigenvectors, which in Mechanics are often called “principal directions”. The latter then have a particular physical meaning depending on the nature of the considered tensor  $\mathbb{A}$ ; mathematically, the tensor  $\mathbb{A}$  is diagonal in the basis of its principal directions.

### Invariants

We can show that the eigenvalues of a tensor  $\mathbb{A}$  are the roots of the characteristic polynomial  $\mathcal{P}(\lambda)$  which is expressed as:

$$\mathcal{P}(\lambda) = \det(\mathbb{A} - \lambda \mathbb{I}) = -\lambda^3 + i_1(\mathbb{A})\lambda^2 - i_2(\mathbb{A})\lambda + i_3(\mathbb{A})$$

where the scalars  $i_k(\mathbb{A})$  are the “principal invariants” of the tensor  $\mathbb{A}$ :

$$\begin{aligned} i_1(\mathbb{A}) &= \text{tr } \mathbb{A} \\ i_2(\mathbb{A}) &= \frac{(\text{tr } \mathbb{A})^2 - \text{tr}(\mathbb{A}^2)}{2} \\ i_3(\mathbb{A}) &= \det \mathbb{A} \end{aligned}$$

hence, as functions of the eigenvalues  $\lambda_k$ :

$$\begin{aligned} i_1(\mathbb{A}) &= \lambda_1 + \lambda_2 + \lambda_3 \\ i_2(\mathbb{A}) &= \lambda_1\lambda_2 + \lambda_2\lambda_3 + \lambda_3\lambda_1 \\ i_3(\mathbb{A}) &= \lambda_1\lambda_2\lambda_3 \end{aligned}$$

These quantities are therefore invariant in the sense that they are not affected by a change of basis when expressing the components of the tensor  $\mathbb{A}$ .

### A.2.5 Square root of a tensor

#### Definition and properties

A symmetrical tensor  $\mathbb{A}$  is said to be positive semi-definite if its eigenvalues are all non-negative; in this case, by expressing it on the associated basis of its eigenvectors, it is possible to define the square root  $\mathbb{U}$  of  $\mathbb{A}$  as the diagonal tensor in this same basis, whose diagonal components are the square roots of the eigenvalues of  $\mathbb{A}$ . Then we have clearly that  $\mathbb{U}^2 = \mathbb{A}$ .

By definition, the square root  $\mathbb{U}$  is also a positive semi-definite and symmetrical tensor; moreover, if  $\mathbb{A}$  is positive definite, so is  $\mathbb{U}$ . Therefore, the square root  $\mathbb{U}$  is invertible if and only if  $\mathbb{A}$  is invertible.

#### Polar decomposition of a tensor

If  $\mathbb{A}$  is a tensor such that  $\det \mathbb{A} > 0$ , it admits the following unique decomposition, called “polar decomposition”:

$$\mathbb{A} = \mathbb{R}\mathbb{U} = \mathbb{V}\mathbb{R}$$

where  $\mathbb{R}$  is a rotation tensor (as defined in Paragraph A.2.6), and where  $\mathbb{U}$  and  $\mathbb{V}$  are the square roots of  $\mathbb{A}^T\mathbb{A}$  and  $\mathbb{A}\mathbb{A}^T$  respectively:

$$\mathbb{U}^2 = \mathbb{A}^T\mathbb{A}, \text{ and } \mathbb{V}^2 = \mathbb{A}\mathbb{A}^T$$

Indeed, once one has built  $\mathbb{U}$ , it is easy to verify that  $\mathbb{A}\mathbb{U}^{-1}$  is an orthogonal tensor, i.e. a rotation tensor:

$$(\mathbb{A}\mathbb{U}^{-1})^T(\mathbb{A}\mathbb{U}^{-1}) = \mathbb{U}^{-T}\mathbb{A}^T\mathbb{A}\mathbb{U}^{-1} = \mathbb{U}^{-1}\mathbb{U}^2\mathbb{U}^{-1} = \mathbb{I}$$

and, similarly, with  $\mathbb{V}$ . Eventually, we easily verify that  $\mathbb{V} = \mathbb{R}\mathbb{U}\mathbb{R}^T$ .

### A.2.6 Rotation tensors

In what follows, we present a tensor that plays an important role in describing the movement of a material medium. In particular, it allows to express a movement occurring with no deformation, such as the one presented in Example 1.3 on page 5.

#### Definition and properties

A rotation tensor  $\mathbb{R}$  is an orthogonal tensor, i.e. it satisfies the following property:

$$\mathbb{R}^T\mathbb{R} = \mathbb{I}$$

Thus, when expressed in a given orthonormal vector basis  $(\mathbf{i}_1, \mathbf{i}_2, \mathbf{i}_3)$ , the column vectors of the associated matrix are of unit norm and must be orthogonal to each other:

$$\langle \mathbb{R}\mathbf{i}_m, \mathbb{R}\mathbf{i}_n \rangle = \langle \mathbb{R}^T\mathbb{R}\mathbf{i}_m, \mathbf{i}_n \rangle = \langle \mathbf{i}_m, \mathbf{i}_n \rangle = \delta_{mn}, \forall m, n$$

hence the name of “orthogonal” matrix. These six scalar relations are independent and relate the nine scalar components of the matrix  $\mathbb{R}$ , which means that a rotation tensor can be characterized by three independent scalar quantities.

Besides, the orthogonality property implies that  $\mathbb{R}^T = \mathbb{R}^{-1}$ , and, therefore, that we also have the relation  $\mathbb{R}\mathbb{R}^T = \mathbb{I}$ . In addition, since  $\mathbb{R}^T\mathbb{R} = \mathbb{I}$ , we have  $(\det \mathbb{R})^2 = (\det \mathbb{R}^T)(\det \mathbb{R}) = \det(\mathbb{R}^T\mathbb{R}) = \det \mathbb{I} = 1$ , hence:

$$\det \mathbb{R} = 1$$

considering that rotations do not change the orientation of space (contrary to reflections whose determinant is equal to  $-1$ ).

Mathematically as well as physically, a rotation tensor is an isometry, because the associated application is a distance-preserving transformation, as can be seen with an arbitrary vector  $\mathbf{c}$ :

$$\|\mathbb{R}\mathbf{c}\|^2 = \langle \mathbb{R}\mathbf{c}, \mathbb{R}\mathbf{c} \rangle = \langle \mathbb{R}^T \mathbb{R}\mathbf{c}, \mathbf{c} \rangle = \langle \mathbf{c}, \mathbf{c} \rangle = \|\mathbf{c}\|^2, \forall \mathbf{c}$$

which explains why it can express the movement of a medium with no deformation.

Besides, the search for eigenvalues  $\lambda_k$  and eigenvectors  $\phi_k$  of the tensor  $\mathbb{R}$  is equivalent to solve:

$$\mathbb{R}\phi_k = \lambda_k\phi_k, 1 \leq k \leq 3$$

The orthogonality property of  $\mathbb{R}$  then implies that  $\|\phi_k\|^2 = \langle \mathbb{R}\phi_k, \mathbb{R}\phi_k \rangle = |\lambda_k|^2 \|\phi_k\|^2$ , hence:

$$|\lambda_k| = 1$$

knowing that we also have  $\det \mathbb{R} = \lambda_1 \lambda_2 \lambda_3 = 1$ . Since these eigenvalues are the roots of the characteristic polynomial  $\mathcal{P}(\lambda) = \det(\mathbb{R} - \lambda \mathbb{I})$  which is of odd degree, at least one of these eigenvalues is real, and therefore, necessarily, we have:

$$\lambda_1 = 1, \lambda_2 = e^{i\varphi}, \lambda_3 = e^{-i\varphi} = \bar{\lambda}_2$$

The eigenvector  $\phi_1$  associated with  $\lambda_1 = 1$  is therefore real and can be interpreted geometrically as the axis of the rotation, since  $\mathbb{R}\phi_1 = \phi_1$ : any vector collinear to  $\phi_1$  is unchanged by the rotation  $\mathbb{R}$ .

### Axis and angle of a rotation

We have just seen that it is possible to associate to any rotation tensor  $\mathbb{R}$  a direction that characterizes it, that we will note  $\mathbf{e}$ , which is a unit vector verifying  $\mathbb{R}\mathbf{e} = \mathbf{e}$ . Similarly, we will see in the following how to define the angle of the rotation around the axis  $\mathbf{e}$  from the tensor  $\mathbb{R}$ .

Let us consider an arbitrary vector  $\mathbf{c}$  and its image  $\mathbb{R}\mathbf{c}$  by the rotation. Since this latter is an isometry, these two vectors have the same norm, and it is therefore possible to place them as shown in Figure A.5 : the two ends of these vectors are therefore in the same plane perpendicular to the axis  $\mathbf{e}$ , and form in this plane an angle  $\varphi$ . We can then decompose  $\mathbb{R}\mathbf{c}$  as:

$$\mathbb{R}\mathbf{c} = \langle \mathbb{R}\mathbf{c}, \mathbf{e} \rangle \mathbf{e} + (\mathbb{R}\mathbf{c})_{\perp} = \langle \mathbf{c}, \mathbb{R}^T \mathbf{e} \rangle \mathbf{e} + (\mathbb{R}\mathbf{c})_{\perp} = \langle \mathbf{c}, \mathbf{e} \rangle \mathbf{e} + (\mathbb{R}\mathbf{c})_{\perp}$$

where  $(\mathbb{R}\mathbf{c})_{\perp}$  stands for the component of  $\mathbb{R}\mathbf{c}$  which is contained in the plane perpendicular to  $\mathbf{e}$ . This component can then be expressed using two orthogonal vectors  $\mathbf{e} \wedge \mathbf{c}$  and  $\mathbf{e} \wedge (\mathbf{e} \wedge \mathbf{c})$  constituting a basis of this particular plane:

$$(\mathbb{R}\mathbf{c})_{\perp} = \sin \varphi \mathbf{e} \wedge \mathbf{c} - \cos \varphi \mathbf{e} \wedge (\mathbf{e} \wedge \mathbf{c})$$

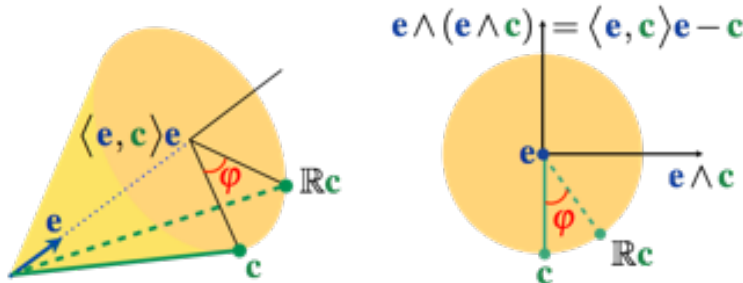


Figure A.5: Axio-angular parametrization of a rotation of axis  $\mathbf{e}$  and angle  $\varphi$ .

By expanding the vector triple product as  $\mathbf{e} \wedge (\mathbf{e} \wedge \mathbf{c}) = \langle \mathbf{e}, \mathbf{c} \rangle \mathbf{e} - \langle \mathbf{e}, \mathbf{e} \rangle \mathbf{c}$ , and by knowing that  $\langle \mathbf{e}, \mathbf{e} \rangle = 1$ , we finally get:

$$\mathbb{R}\mathbf{c} = \langle \mathbf{c}, \mathbf{e} \rangle \mathbf{e} + \sin \varphi \mathbf{e} \wedge \mathbf{c} - \cos \varphi \langle \mathbf{c}, \mathbf{e} \rangle \mathbf{e} + \cos \varphi \mathbf{c}$$

or, by noting  $\mathbb{e}^\wedge$  the antisymmetrical tensor, defined in Appendix A.2.1, and defined as  $\mathbb{e}^\wedge \mathbf{c} = \mathbf{e} \wedge \mathbf{c}$ ,  $\forall \mathbf{c}$ , the following expression:

$$\mathbb{R} = \cos \varphi \mathbb{I} + (1 - \cos \varphi) \mathbf{e} \otimes \mathbf{e} + \sin \varphi \mathbb{e}^\wedge = \mathbb{Q}(\mathbf{e}, \varphi)$$

With this parametrization, described as “axio-angular”, we find that for a given rotation there are three independent parameters: two that define the direction of the axis (since  $\mathbf{e}$  is a unit vector), and one that is the angle.

It remains to be seen now if the reciprocal is possible, i.e. if we can find  $\mathbf{e}$  and  $\varphi$  from a given rotation matrix  $\mathbb{R}$ . For that, we already know that  $\mathbb{R} = 1 + 2 \cos \varphi$ , and therefore that:

$$\varphi = \pm \arccos \left( \frac{\text{tr} \mathbb{R} - 1}{2} \right)$$

then, to determine the axis, we can simply write that, if  $\sin \varphi \neq 0$ :

$$\mathbb{e}^\wedge = \frac{1}{2 \sin \varphi} (\mathbb{R} - \mathbb{R}^T)$$

hence the expression of the components of  $\mathbf{e}$  in a given vector basis. The choice of the sign of  $\varphi$  does not matter, since changing the sign of the angle is the same as changing the sense of the unit vector of the rotation axis.

In the particular case where  $\sin \varphi = 0$ , i.e. if  $\varphi \equiv 0 \pmod{\pi}$ , since  $\text{tr} \mathbb{R} = 1 + 2 \cos \varphi$ , we get two possibilities:

- if  $\text{tr} \mathbb{R} = 3$ , then  $\varphi \equiv 0 \pmod{2\pi}$ : the rotation is actually the identity tensor  $\mathbb{I}$ , and  $\mathbf{e}$  is then arbitrary;
- if  $\text{tr} \mathbb{R} = -1$ , then  $\varphi \equiv \pi \pmod{2\pi}$ : the rotation is actually  $\mathbb{R} = -\mathbb{I} + 2\mathbf{e} \otimes \mathbf{e}$  and  $\mathbf{e}$  comes directly from the relation  $\mathbf{e} \otimes \mathbf{e} = (\mathbb{I} + \mathbb{R})/2$ .

Apart from the latter cases, for which the singularity can still be removed, the axio-angular parametrization of a rotation is therefore invertible.

### Case of an infinitesimal rotation

In the case where the rotation angle  $\varphi$  is very small when compared to 1, we can simplify the expression of the axio-angular parametrization of the infinitesimal rotation as:

$$\mathbb{R} = \mathbb{I} + \varphi \mathbb{e}^\wedge + O(\varphi^2)$$

If this rotation occurs to express the position of a point, this implies that the associated movement  $\mathbf{u} = \mathbf{x} - \mathbf{p}$  satisfies:

$$\mathbf{u} = (\mathbb{R} - \mathbb{I})(\mathbf{p} - \mathbf{p}_O) = \varphi \mathbf{e} \wedge (\mathbf{p} - \mathbf{p}_O)$$

where  $O$  is a point on the axis of rotation. This expression is used in continuum mechanics to specify rotation boundary conditions in the framework of the infinitesimal deformation hypothesis. It is also used in beam mechanics, in Paragraph 6.1.2, to express the approximate kinematics of a beam.

### A.3 Fourth-order tensors

#### A.3.1 Definition and properties

A fourth-order tensor  $\mathbf{T}$  is a linear application of the second-order tensor space in itself, which, to any tensor  $\mathbb{A}$  associates the tensor  $\mathbb{B} = \mathbf{T}(\mathbb{A})$  of components:

$$B_{mn} = \sum_{p=1}^3 \sum_{q=1}^3 T_{mnpq} A_{pq}, \quad 1 \leq m, n \leq 3$$

where  $A_{pq}$  and  $B_{mn}$  ( $1 \leq m, n, p, q \leq 3$ ) are the respective components of  $\mathbb{A}$  and  $\mathbb{B}$  in a given orthonormal vector basis  $(\mathbf{i}_1, \mathbf{i}_2, \mathbf{i}_3)$ , and the components of  $\mathbf{T}$  can be expressed as:

$$T_{mnpq} = \text{tr} \left( (\mathbf{T}(\mathbf{i}_p \otimes \mathbf{i}_q))(\mathbf{i}_m \otimes \mathbf{i}_n) \right)$$

It is therefore a multiplication  $\mathbb{B} = \mathbf{T}\mathbb{A}$  in the sense of a matrix-vector product if we adopt Voigt notation, defined in Paragraph 4.1.3, in the case of symmetrical tensors  $\mathbb{A}$  and  $\mathbb{B}$ , and of a tensor  $\mathbf{T}$  satisfying the major symmetry property:

$$\begin{pmatrix} \tilde{B}_1 = B_{11} \\ \tilde{B}_2 = B_{22} \\ \tilde{B}_3 = B_{33} \\ \tilde{B}_4 = B_{23} \\ \tilde{B}_5 = B_{13} \\ \tilde{B}_6 = B_{12} \end{pmatrix} = \begin{pmatrix} \tilde{T}_{11} & \tilde{T}_{12} & \tilde{T}_{13} & \tilde{T}_{14} & \tilde{T}_{15} & \tilde{T}_{16} \\ \tilde{T}_{12} & \tilde{T}_{22} & \tilde{T}_{23} & \tilde{T}_{24} & \tilde{T}_{25} & \tilde{T}_{26} \\ \tilde{T}_{13} & \tilde{T}_{23} & \tilde{T}_{33} & \tilde{T}_{34} & \tilde{T}_{35} & \tilde{T}_{36} \\ \tilde{T}_{14} & \tilde{T}_{24} & \tilde{T}_{34} & \tilde{T}_{44} & \tilde{T}_{45} & \tilde{T}_{46} \\ \tilde{T}_{15} & \tilde{T}_{25} & \tilde{T}_{35} & \tilde{T}_{45} & \tilde{T}_{55} & \tilde{T}_{56} \\ \tilde{T}_{16} & \tilde{T}_{26} & \tilde{T}_{36} & \tilde{T}_{46} & \tilde{T}_{56} & \tilde{T}_{66} \end{pmatrix} \begin{pmatrix} \tilde{A}_1 = A_{11} \\ \tilde{A}_2 = A_{22} \\ \tilde{A}_3 = A_{33} \\ \tilde{A}_4 = 2A_{23} \\ \tilde{A}_5 = 2A_{13} \\ \tilde{A}_6 = 2A_{12} \end{pmatrix}$$

Besides, we can also define the tensor product  $\mathbb{A} \otimes \mathbb{B}$  of two second-order tensors  $\mathbb{A}$  and  $\mathbb{B}$ , which is a fourth-order tensor such that:

$$(\mathbb{A} \otimes \mathbb{B})\mathbb{C} = \langle \mathbb{B}, \mathbb{C} \rangle \mathbb{A} = \text{tr}(\mathbb{B}\mathbb{C}^T)\mathbb{A}, \forall \mathbb{C}$$

of components  $(\mathbb{A} \otimes \mathbb{B})_{mnpq} = A_{mn}B_{pq}$  in an orthonormal vector basis  $(\mathbf{i}_1, \mathbf{i}_2, \mathbf{i}_3)$ .

#### A.3.2 Particular forms

In the case of fourth-order tensors acting in symmetrical tensor spaces, and having the major symmetry property, Voigt notation used above shows that 21 out of the 36 components are independent. It is possible to reduce this number if the fourth-order tensor is invariant when specific symmetry transformations are applied to it.

##### Orthotropy

If the tensor  $\mathbf{T}$  is invariant to three reflection symmetries of mutual orthogonal planes, whose normal vectors are assumed oriented along the three vectors of a basis  $(\mathbf{i}_1, \mathbf{i}_2, \mathbf{i}_3)$ , some components of  $\mathbf{T}$  vanish, and this latter can then be written, using Voigt notation, as:

$$\begin{pmatrix} \tilde{B}_1 = B_{11} \\ \tilde{B}_2 = B_{22} \\ \tilde{B}_3 = B_{33} \\ \tilde{B}_4 = B_{23} \\ \tilde{B}_5 = B_{13} \\ \tilde{B}_6 = B_{12} \end{pmatrix} = \begin{pmatrix} \tilde{T}_{11} & \tilde{T}_{12} & \tilde{T}_{13} & 0 & 0 & 0 \\ \tilde{T}_{12} & \tilde{T}_{22} & \tilde{T}_{23} & 0 & 0 & 0 \\ \tilde{T}_{13} & \tilde{T}_{23} & \tilde{T}_{33} & 0 & 0 & 0 \\ 0 & 0 & 0 & \tilde{T}_{44} & 0 & 0 \\ 0 & 0 & 0 & 0 & \tilde{T}_{55} & 0 \\ 0 & 0 & 0 & 0 & 0 & \tilde{T}_{66} \end{pmatrix} \begin{pmatrix} \tilde{A}_1 = A_{11} \\ \tilde{A}_2 = A_{22} \\ \tilde{A}_3 = A_{33} \\ \tilde{A}_4 = 2A_{23} \\ \tilde{A}_5 = 2A_{13} \\ \tilde{A}_6 = 2A_{12} \end{pmatrix}$$

hence 9 independent components.

### Cubic symmetry

If, as in the previous case, the tensor  $\mathbf{T}$  is invariant to three reflection symmetries of mutual orthogonal planes, but, in addition, the directions of the three normal vectors to these planes are equivalent, then this tensor can be written, using Voigt notation, as:

$$\begin{pmatrix} \tilde{B}_1 = B_{11} \\ \tilde{B}_2 = B_{22} \\ \tilde{B}_3 = B_{33} \\ \tilde{B}_4 = B_{23} \\ \tilde{B}_5 = B_{13} \\ \tilde{B}_6 = B_{12} \end{pmatrix} = \begin{pmatrix} \tilde{T}_{11} & \tilde{T}_{12} & \tilde{T}_{12} & 0 & 0 & 0 \\ \tilde{T}_{12} & \tilde{T}_{11} & \tilde{T}_{12} & 0 & 0 & 0 \\ \tilde{T}_{12} & \tilde{T}_{12} & \tilde{T}_{11} & 0 & 0 & 0 \\ 0 & 0 & 0 & \tilde{T}_{44} & 0 & 0 \\ 0 & 0 & 0 & 0 & \tilde{T}_{44} & 0 \\ 0 & 0 & 0 & 0 & 0 & \tilde{T}_{44} \end{pmatrix} \begin{pmatrix} \tilde{A}_1 = A_{11} \\ \tilde{A}_2 = A_{22} \\ \tilde{A}_3 = A_{33} \\ \tilde{A}_4 = 2A_{23} \\ \tilde{A}_5 = 2A_{13} \\ \tilde{A}_6 = 2A_{12} \end{pmatrix}$$

hence 3 independent components.

### Transverse isotropy

If the tensor  $\mathbf{T}$  is invariant by rotation around a fixed axis  $\mathbf{i}_3$ , it can be written, using Voigt notation, as:

$$\begin{pmatrix} \tilde{B}_1 = B_{11} \\ \tilde{B}_2 = B_{22} \\ \tilde{B}_3 = B_{33} \\ \tilde{B}_4 = B_{23} \\ \tilde{B}_5 = B_{13} \\ \tilde{B}_6 = B_{12} \end{pmatrix} = \begin{pmatrix} \tilde{T}_{11} & \tilde{T}_{12} & \tilde{T}_{13} & 0 & 0 & 0 \\ \tilde{T}_{12} & \tilde{T}_{11} & \tilde{T}_{13} & 0 & 0 & 0 \\ \tilde{T}_{13} & \tilde{T}_{13} & \tilde{T}_{11} & 0 & 0 & 0 \\ 0 & 0 & 0 & \tilde{T}_{44} & 0 & 0 \\ 0 & 0 & 0 & 0 & \tilde{T}_{44} & 0 \\ 0 & 0 & 0 & 0 & 0 & \tilde{T}_{11} - \tilde{T}_{12} \end{pmatrix} \begin{pmatrix} \tilde{A}_1 = A_{11} \\ \tilde{A}_2 = A_{22} \\ \tilde{A}_3 = A_{33} \\ \tilde{A}_4 = 2A_{23} \\ \tilde{A}_5 = 2A_{13} \\ \tilde{A}_6 = 2A_{12} \end{pmatrix}$$

hence 5 independent components.

### Isotropy

If the tensor  $\mathbf{T}$  is invariant by rotation, whatever it is, it can be written simply, using Voigt notation, as:

$$\begin{pmatrix} \tilde{B}_1 = B_{11} \\ \tilde{B}_2 = B_{22} \\ \tilde{B}_3 = B_{33} \\ \tilde{B}_4 = B_{23} \\ \tilde{B}_5 = B_{13} \\ \tilde{B}_6 = B_{12} \end{pmatrix} = \begin{pmatrix} \tilde{T}_{11} & \tilde{T}_{12} & \tilde{T}_{12} & 0 & 0 & 0 \\ \tilde{T}_{12} & \tilde{T}_{11} & \tilde{T}_{12} & 0 & 0 & 0 \\ \tilde{T}_{12} & \tilde{T}_{12} & \tilde{T}_{11} & 0 & 0 & 0 \\ 0 & 0 & 0 & \tilde{T}_{11} - \tilde{T}_{12} & 0 & 0 \\ 0 & 0 & 0 & 0 & \tilde{T}_{11} - \tilde{T}_{12} & 0 \\ 0 & 0 & 0 & 0 & 0 & \tilde{T}_{11} - \tilde{T}_{12} \end{pmatrix} \begin{pmatrix} \tilde{A}_1 = A_{11} \\ \tilde{A}_2 = A_{22} \\ \tilde{A}_3 = A_{33} \\ \tilde{A}_4 = 2A_{23} \\ \tilde{A}_5 = 2A_{13} \\ \tilde{A}_6 = 2A_{12} \end{pmatrix}$$

hence 2 independent components. This result corresponds actually to the Rivlin-Ericksen theorem, in the linear case, of which the following statement is recalled.

**Rivlin-Ericksen theorem (linear case).** A fourth-order tensor  $\mathbf{T}$ , acting from the symmetrical second-order tensor space in itself, is said to be isotropic if and only if it satisfies:

$$\mathbb{R}(\mathbf{T}\mathbb{A})\mathbb{R}^T = \mathbf{T}(\mathbb{R}\mathbb{A}\mathbb{R}^T), \forall \mathbb{A} \text{ symmetrical}, \forall \mathbb{R} \text{ such that } \mathbb{R}\mathbb{R}^T = \mathbb{I}$$

Then there are two scalars  $\alpha$  and  $\beta$  such that the tensor  $\mathbf{T}$  can be expressed as:

$$\mathbf{T}\mathbb{A} = \alpha\mathbb{A} + \beta(\operatorname{tr}\mathbb{A})\mathbb{I}, \forall \mathbb{A} \text{ symmetrical}$$

A proof of this theorem is detailed below.

Let  $\mathbb{A}$  be a symmetrical second-order tensor: we can then write this tensor using the basis of the associated eigenvectors  $(\phi_1, \phi_2, \phi_3)$ :

$$\mathbb{A} = \sum_{k=1}^3 \lambda_k \phi_k \otimes \phi_k$$

where  $(\lambda_1, \lambda_2, \lambda_3)$  are the associated eigenvalues. Besides, for any tensor  $\mathbb{B}$ , we have:

$$\mathbb{B}(\phi_k \otimes \phi_k) \mathbb{B}^T = (\mathbb{B}\phi_k) \otimes (\mathbb{B}\phi_k)$$

Using this relation for  $\mathbb{B} = \mathbb{S}_k = \mathbb{I} - 2\phi_k \otimes \phi_k$  (which then corresponds to the reflection symmetry with respect to the plane of normal vector  $\phi_k$ ), we obtain that:

$$\mathbb{S}_k(\phi_k \otimes \phi_k) \mathbb{S}_k^T = (\mathbb{S}_k\phi_k) \otimes (\mathbb{S}\phi_k) = (-\phi_k) \otimes (-\phi_k) = \phi_k \otimes \phi_k$$

which implies that:

$$\mathbb{S}_k \mathbb{A} \mathbb{S}_k^T = \mathbb{A}$$

Let now  $\mathbf{T}$  be a fourth-order isotropic tensor, acting from the symmetrical second-order tensor space in itself; since the tensor  $\mathbb{S}_k$  is orthogonal ( $\mathbb{S}_k \mathbb{S}_k^T = \mathbb{I}$ ), the tensor  $\mathbf{T}$  then satisfies:

$$\mathbb{S}_k(\mathbf{T}\mathbb{A}) \mathbb{S}_k^T = \mathbf{T}(\mathbb{S}_k \mathbb{A} \mathbb{S}_k^T) = \mathbf{T}\mathbb{A}$$

which allows to establish that:

$$\mathbb{S}_k((\mathbf{T}\mathbb{A})\phi_k) = (\mathbf{T}\mathbb{A})\mathbb{S}_k\phi_k = -(\mathbf{T}\mathbb{A})\phi_k$$

which means that the symmetric of  $(\mathbf{T}\mathbb{A})\phi_k$  relatively to the plane of normal vector  $\phi_k$  is equal to its opposite, which can only happen if  $(\mathbf{T}\mathbb{A})\phi_k$  is collinear to  $\phi_k$ :

$$((\mathbf{T}\mathbb{A})\phi_k) \wedge \phi_k = \mathbf{0}$$

which is equivalent to say that  $\phi_k$  is an eigenvector of  $\mathbf{T}\mathbb{A}$ .

Let  $\mathbf{e}$  be an arbitrary unit vector; the tensor  $\mathbf{e} \otimes \mathbf{e}$  is symmetrical, and then admits as eigenvectors  $\mathbf{e}$  (of associated eigenvalue 1), and any vector perpendicular to  $\mathbf{e}$  (of associated eigenvalue 0). We then know, from the above, that  $\mathbf{T}(\mathbf{e} \otimes \mathbf{e})$  has the same eigenvectors as  $\mathbf{e} \otimes \mathbf{e}$ , and can then be written as:

$$\mathbf{T}(\mathbf{e} \otimes \mathbf{e}) = \alpha(\mathbf{e})(\mathbf{e} \otimes \mathbf{e}) + \beta(\mathbf{e})\mathbb{I}$$

where  $\alpha$  and  $\beta$  are scalar functions of  $\mathbf{e}$ .

Let now  $\mathbf{e}$  and  $\mathbf{f}$  be two arbitrary unit vectors; then we can find an orthogonal tensor  $\mathbb{R}$  such that  $\mathbb{R}\mathbf{e} = \mathbf{f}$ , hence, if  $\mathbf{T}$  is isotropic:

$$\mathbf{T}(\mathbf{f} \otimes \mathbf{f}) = \mathbf{T}((\mathbb{R}\mathbf{e}) \otimes (\mathbb{R}\mathbf{e})) = \mathbf{T}(\mathbb{R}(\mathbf{e} \otimes \mathbf{e})\mathbb{R}^T) = \mathbb{R}(\mathbf{T}(\mathbf{e} \otimes \mathbf{e}))\mathbb{R}^T$$

and by introducing the form according to the functions  $\alpha$  and  $\beta$ , we end up with:

$$(\alpha(\mathbf{e}) - \alpha(\mathbf{f}))(\mathbf{f} \otimes \mathbf{f}) + (\beta(\mathbf{e}) - \beta(\mathbf{f}))\mathbb{I} = 0$$

which implies, necessarily, that:

$$\alpha(\mathbf{e}) = \alpha(\mathbf{f}), \text{ and } \beta(\mathbf{e}) = \beta(\mathbf{f}), \forall \mathbf{e}, \forall \mathbf{f}$$

or, in other words, that the scalars  $\alpha$  and  $\beta$  are constant; so we have:

$$\mathbf{T}(\mathbf{e} \otimes \mathbf{e}) = \alpha(\mathbf{e} \otimes \mathbf{e}) + \beta\mathbb{I}$$

By writing  $\mathbb{A}$  again in the basis of its eigenvectors, we finally establish, using the linearity of  $\mathbf{T}$ , that:

$$\mathbf{T}\mathbb{A} = \sum_{k=1}^3 \lambda_k \mathbf{T}(\phi_k \otimes \phi_k) = \alpha \left( \sum_{k=1}^3 \lambda_k \phi_k \otimes \phi_k \right) + \beta \left( \sum_{k=1}^3 \lambda_k \right) \mathbb{I} = \alpha \mathbb{A} + \beta (\text{tr } \mathbb{A}) \mathbb{I}$$

i.e. the sought result.

## B. Tensor analysis

### B.1 Differentiation

#### B.1.1 Conventional space operators

In the following, we wish to characterize, through different operators, the spatial evolution of scalar or vector fields;  $\mathbf{x}$  will designate the placement vector of the current point.

##### Gradient

We define the spatial gradient of a scalar function  $\phi(\mathbf{x})$  as the vector noted  $\nabla_{\mathbf{x}}\phi$  such that:

$$\langle \nabla_{\mathbf{x}}\phi(\mathbf{x}), \mathbf{c} \rangle = \lim_{\alpha \rightarrow 0} \frac{\phi(\mathbf{x} + \alpha\mathbf{c}) - \phi(\mathbf{x})}{\alpha}, \forall \mathbf{x}$$

where  $\mathbf{c}$  is an arbitrary constant vector; by choosing a Cartesian vector basis  $(\mathbf{i}_1, \mathbf{i}_2, \mathbf{i}_3)$  of associated coordinates  $(x_1, x_2, x_3)$ , the components of the gradient are then determined as:

$$\langle \nabla_{\mathbf{x}}\phi(\mathbf{x}), \mathbf{i}_n \rangle = \lim_{\alpha \rightarrow 0} \frac{\phi(\mathbf{x} + \alpha\mathbf{i}_n) - \phi(\mathbf{x})}{\alpha} = \frac{\partial \phi}{\partial x_n}(\mathbf{x}), \forall \mathbf{x}, 1 \leq n \leq 3$$

In the case of a vector field  $\mathbf{v}(\mathbf{x})$ , the gradient  $\mathbb{D}_{\mathbf{x}}\mathbf{v}$  can be defined in a similar way as the linear application which, to any constant vector  $\mathbf{c}$ , associates the vector  $(\mathbb{D}_{\mathbf{x}}\mathbf{v})\mathbf{c}$  such that:

$$(\mathbb{D}_{\mathbf{x}}\mathbf{v}(\mathbf{x}))\mathbf{c} = \lim_{\alpha \rightarrow 0} \frac{\mathbf{v}(\mathbf{x} + \alpha\mathbf{c}) - \mathbf{v}(\mathbf{x})}{\alpha}, \forall \mathbf{x}$$

The components of this tensor, which is also called the “Jacobian matrix”, are obtained as:

$$(\mathbb{D}_{\mathbf{x}}\mathbf{v})_{mn} = \langle (\mathbb{D}_{\mathbf{x}}\mathbf{v})\mathbf{i}_n, \mathbf{i}_m \rangle = \left\langle \frac{\partial \mathbf{v}}{\partial x_n}, \mathbf{i}_m \right\rangle = \frac{\partial v_m}{\partial x_n}, 1 \leq m, n \leq 3$$

(where  $v_m$  are the components of  $\mathbf{v}$  in the Cartesian vector basis  $(\mathbf{i}_1, \mathbf{i}_2, \mathbf{i}_3)$ ), which allows the gradient tensor to be expressed in intrinsic form, using tensor products, as:

$$\mathbb{D}_{\mathbf{x}}\mathbf{v} = \sum_{n=1}^3 \frac{\partial \mathbf{v}}{\partial x_n} \otimes \mathbf{i}_n$$

### Divergence

We define the divergence of a vector field  $\mathbf{v}(\mathbf{x})$  as the trace of the gradient tensor of this field:

$$\operatorname{div}_{\mathbf{x}} \mathbf{v} = \operatorname{tr}(\mathbb{D}_{\mathbf{x}} \mathbf{v}) = \sum_{n=1}^3 \left\langle \frac{\partial \mathbf{v}}{\partial x_n}, \mathbf{i}_n \right\rangle$$

For a tensor  $\mathbb{A}(\mathbf{x})$ , we define the divergence using the divergence of a vector by posing that:

$$\langle \operatorname{div}_{\mathbf{x}} \mathbb{A}, \mathbf{c} \rangle = \operatorname{div}_{\mathbf{x}} (\mathbb{A}^T \mathbf{c})$$

for  $\mathbf{c}$  constant and arbitrary, which allows to get, by choosing a Cartesian vector basis  $(\mathbf{i}_1, \mathbf{i}_2, \mathbf{i}_3)$  of associated coordinates  $(x_1, x_2, x_3)$ :

$$\langle \operatorname{div}_{\mathbf{x}} \mathbb{A}, \mathbf{i}_m \rangle = \operatorname{div}_{\mathbf{x}} (\mathbb{A}^T \mathbf{i}_m) = \sum_{n=1}^3 \frac{\partial A_{mn}}{\partial x_n}, \quad 1 \leq m \leq 3$$

which are actually the divergences, expressed in Cartesian coordinates, of the row vectors of  $\mathbb{A}$ .

Besides, we can show the following relation, very useful to simplify the calculations:

$$\operatorname{div}_{\mathbf{x}} (\mathbf{v} \otimes \mathbf{w}) = (\mathbb{D}_{\mathbf{x}} \mathbf{v}) \mathbf{w} + (\operatorname{div}_{\mathbf{x}} \mathbf{w}) \mathbf{v}$$

(where  $\mathbf{v}(\mathbf{x})$  and  $\mathbf{w}(\mathbf{x})$  are two vector fields), as well as the following two formulas:

$$\begin{aligned} \operatorname{div}_{\mathbf{x}} (\phi \mathbb{A}) &= \phi \operatorname{div}_{\mathbf{x}} \mathbb{A} + \mathbb{A} \nabla_{\mathbf{x}} \phi \\ \operatorname{div}_{\mathbf{x}} (\mathbb{A}^T \mathbf{v}) &= \langle \operatorname{div}_{\mathbf{x}} \mathbb{A}, \mathbf{v} \rangle + \operatorname{tr} (\mathbb{A} (\mathbb{D}_{\mathbf{x}} \mathbf{v})^T) \end{aligned}$$

where  $\phi(\mathbf{x})$  is a scalar field and  $\mathbf{v}(\mathbf{x})$  is a vector field.

### Curl

The (rotational) curl of a vector field  $\mathbf{v}(\mathbf{x})$  is defined as:

$$(\operatorname{rot}_{\mathbf{x}} \mathbf{v}) \wedge \mathbf{c} = (\mathbb{D}_{\mathbf{x}} \mathbf{v} - (\mathbb{D}_{\mathbf{x}} \mathbf{v})^T) \mathbf{c}$$

where  $\mathbf{c}$  is an arbitrary constant vector; it is thus the vector corresponding to the double of the antisymmetrical part of the gradient tensor of the vector field, introduced in Paragraph A.2.1; by choosing a Cartesian vector basis  $(\mathbf{i}_1, \mathbf{i}_2, \mathbf{i}_3)$  of associated coordinates  $(x_1, x_2, x_3)$ , we can determine the components of  $\operatorname{rot}_{\mathbf{x}} \mathbf{v}$ .

We also define the curl of a second-order tensor  $\mathbb{A}(\mathbf{x})$  using the curl of a vector, by writing that:

$$(\operatorname{rot}_{\mathbf{x}} \mathbb{A}) \mathbf{c} = \operatorname{rot}_{\mathbf{x}} (\mathbb{A}^T \mathbf{c})$$

for any constant vector  $\mathbf{c}$ ; we then have in particular:

$$(\operatorname{rot}_{\mathbf{x}} \mathbb{A}) \mathbf{i}_n = \operatorname{rot}_{\mathbf{x}} (\mathbb{A}^T \mathbf{i}_n), \quad 1 \leq n \leq 3$$

which shows that the columns of the tensor in the vector basis correspond to the curls of the row vectors of  $\mathbb{A}$ .

### Laplacian

We define the Laplacian of a vector field  $\mathbf{v}(\mathbf{x})$  as follows:

$$\Delta_{\mathbf{x}} \mathbf{v} = \operatorname{div}_{\mathbf{x}} (\mathbb{D}_{\mathbf{x}} \mathbf{v})$$

which, in terms of components in a Cartesian vector basis  $(\mathbf{i}_1, \mathbf{i}_2, \mathbf{i}_3)$  of associated coordinates  $(x_1, x_2, x_3)$ , means:

$$\langle \Delta_{\mathbf{x}} \mathbf{v}, \mathbf{i}_m \rangle = \sum_{n=1}^3 \frac{\partial^2}{\partial x_n^2} \langle \mathbf{v}, \mathbf{i}_m \rangle = \Delta_{\mathbf{x}} \langle \mathbf{v}, \mathbf{i}_m \rangle, \quad 1 \leq m \leq 3$$

where  $\Delta_{\mathbf{x}}$  is the scalar Laplacian, defined as:

$$\Delta_{\mathbf{x}} f(\mathbf{x}) = \sum_{n=1}^3 \frac{\partial^2 f}{\partial x_n^2}(\mathbf{x})$$

## B.1.2 Useful formulas

First of all, we note two fundamental properties:

$$\begin{aligned}\operatorname{rot}_{\mathbf{x}}(\nabla_{\mathbf{x}} \phi) &= \mathbf{0} \\ \operatorname{div}_{\mathbf{x}}(\operatorname{rot}_{\mathbf{x}} \mathbf{v}) &= 0\end{aligned}$$

where, as in what follows,  $\mathbf{v}(\mathbf{x})$  is a vector field, and  $\phi(\mathbf{x})$  is a scalar field.

### Vector relations

We assume in the following relations that  $\mathbf{c}$  is a constant vector:

$$\begin{aligned}\nabla_{\mathbf{x}} \langle \mathbf{v}, \mathbf{c} \rangle &= (\mathbb{D}_{\mathbf{x}} \mathbf{v})^T \mathbf{c} \\ \operatorname{div}_{\mathbf{x}}(\mathbf{v} \wedge \mathbf{c}) &= \langle \operatorname{rot}_{\mathbf{x}} \mathbf{v}, \mathbf{c} \rangle \\ \operatorname{rot}_{\mathbf{x}}(\mathbf{v} \wedge \mathbf{c}) &= (\mathbb{D}_{\mathbf{x}} \mathbf{v}) \mathbf{c} - (\operatorname{div}_{\mathbf{x}} \mathbf{v}) \mathbf{c} \\ \mathbb{D}_{\mathbf{x}}(\phi \mathbf{c}) &= \mathbf{c} \otimes \nabla_{\mathbf{x}} \phi \\ \operatorname{div}_{\mathbf{x}}(\phi \mathbf{c}) &= \langle \nabla_{\mathbf{x}} \phi, \mathbf{c} \rangle \\ \operatorname{rot}_{\mathbf{x}}(\phi \mathbf{c}) &= (\nabla_{\mathbf{x}} \phi) \wedge \mathbf{c}\end{aligned}$$

### Tensor relations

In the following,  $\mathbb{A}(\mathbf{x})$  is an arbitrary second-order tensor, while  $\mathbf{v}(\mathbf{x})$  is still a vector field:

$$\begin{aligned}\operatorname{div}_{\mathbf{x}}(\mathbb{D}_{\mathbf{x}} \mathbf{v}) &= \Delta_{\mathbf{x}} \mathbf{v} = \nabla_{\mathbf{x}}(\operatorname{div}_{\mathbf{x}} \mathbf{v}) - \operatorname{rot}_{\mathbf{x}}(\operatorname{rot}_{\mathbf{x}} \mathbf{v}) \\ \operatorname{div}_{\mathbf{x}}((\mathbb{D}_{\mathbf{x}} \mathbf{v})^T) &= \nabla_{\mathbf{x}}(\operatorname{div}_{\mathbf{x}} \mathbf{v}) \\ \operatorname{rot}_{\mathbf{x}}(\mathbb{D}_{\mathbf{x}} \mathbf{v}) &= 0 \\ \operatorname{rot}_{\mathbf{x}}((\mathbb{D}_{\mathbf{x}} \mathbf{v})^T) &= \mathbb{D}_{\mathbf{x}}(\operatorname{rot}_{\mathbf{x}} \mathbf{v}) \\ \operatorname{div}_{\mathbf{x}}(\operatorname{rot}_{\mathbf{x}} \mathbb{A}) &= \operatorname{rot}_{\mathbf{x}}(\operatorname{div}_{\mathbf{x}}(\mathbb{A}^T)) \\ \operatorname{div}_{\mathbf{x}}((\operatorname{rot}_{\mathbf{x}} \mathbb{A})^T) &= 0\end{aligned}$$

Finally, if  $\mathbb{A}$  is a symmetrical second-order tensor, we have the following property:

$$\operatorname{tr}(\operatorname{rot}_{\mathbf{x}} \mathbb{A}) = 0$$

### B.1.3 Time differentiation

#### General principle

In order to define the time derivative of a vector, we can use the “basic” definition of a derivative, i.e. the expression of the vector variation between two close times (when the time difference approaches zero):

$$\dot{\mathbf{c}}(t) = \lim_{\Delta t \rightarrow 0} \frac{1}{\Delta t} (\mathbf{c}(t + \Delta t) - \mathbf{c}(t)), \forall \mathbf{c}, \forall t$$

formula which can be interpreted using the components  $(c_1, c_2, c_3)$  of vector  $\mathbf{c}$  in a given fixed vector basis  $(\mathbf{i}_1, \mathbf{i}_2, \mathbf{i}_3)$ :

$$\dot{\mathbf{c}}(t) = \dot{c}_1(t)\mathbf{i}_1 + \dot{c}_2(t)\mathbf{i}_2 + \dot{c}_3(t)\mathbf{i}_3$$

Similarly, the time derivative of a tensor can be expressed as:

$$\dot{\mathbb{A}}(t) = \lim_{\Delta t \rightarrow 0} \frac{1}{\Delta t} (\mathbb{A}(t + \Delta t) - \mathbb{A}(t)), \forall \mathbb{A}, \forall t$$

which can also be interpreted using the components  $A_{ij}$  of tensor  $\mathbb{A}$  in a given fixed vector basis  $(\mathbf{i}_1, \mathbf{i}_2, \mathbf{i}_3)$ :

$$\dot{\mathbb{A}}(t) = \sum_{m=1}^3 \sum_{n=1}^3 \dot{A}_{mn}(t) \mathbf{i}_m \otimes \mathbf{i}_n$$

This has the practical consequence that all the classical properties of differentiation can be verified:

$$\overline{(\mathbf{c}_1(t) + \mathbf{c}_2(t))} = \dot{\mathbf{c}}_1(t) + \dot{\mathbf{c}}_2(t), \forall \mathbf{c}_1, \forall \mathbf{c}_2, \forall t$$

$$\overline{(\mathbb{A}(t) + \mathbb{B}(t))} = \dot{\mathbb{A}}(t) + \dot{\mathbb{B}}(t), \forall \mathbb{A}, \forall \mathbb{B}, \forall t$$

$$\overline{\langle \mathbf{c}_1(t), \mathbf{c}_2(t) \rangle} = \langle \dot{\mathbf{c}}_1(t), \mathbf{c}_2(t) \rangle + \langle \mathbf{c}_1(t), \dot{\mathbf{c}}_2(t) \rangle, \forall \mathbf{c}_1, \forall \mathbf{c}_2, \forall t$$

$$\overline{(\mathbf{c}_1(t) \wedge \mathbf{c}_2(t))} = \dot{\mathbf{c}}_1(t) \wedge \mathbf{c}_2(t) + \mathbf{c}_1(t) \wedge \dot{\mathbf{c}}_2(t), \forall \mathbf{c}_1, \forall \mathbf{c}_2, \forall t$$

$$\overline{(\mathbb{A}(t)\mathbb{B}(t))} = \dot{\mathbb{A}}(t)\mathbb{B}(t) + \mathbb{A}(t)\dot{\mathbb{B}}(t), \forall \mathbb{A}, \forall \mathbb{B}, \forall t$$

$$\overline{(\lambda(t)\mathbf{c}(t))} = \dot{\lambda}(t)\mathbf{c}(t) + \lambda(t)\dot{\mathbf{c}}(t), \forall \lambda, \forall \mathbf{c}, \forall t$$

$$\overline{(\lambda(t)\mathbb{A}(t))} = \dot{\lambda}(t)\mathbb{A}(t) + \lambda(t)\dot{\mathbb{A}}(t), \forall \lambda, \forall \mathbb{A}, \forall t$$

The penultimate relation, assuming that  $\mathbf{c}$  is a unit vector, shows how the derivative of a vector whose norm changes over time can be calculated. In addition, it is also necessary to express the direction variation of a vector in terms of time derivative; this is what is proposed in the following.

#### Angular velocity vector

By deriving with respect to time the orthogonality property of the rotation tensor ( $\mathbb{R}\mathbb{R}^T = \mathbb{I}$ ), established in Paragraph A.2.6, we obtain:

$$\dot{\mathbb{R}}\mathbb{R}^T + \mathbb{R}\dot{\mathbb{R}}^T = 0$$

or, by posing  $\Omega_{\mathbb{R}} = \dot{\mathbb{R}}\mathbb{R}^T$ :

$$\Omega_{\mathbb{R}} = \dot{\mathbb{R}}\mathbb{R}^T = -(\dot{\mathbb{R}}\mathbb{R}^T)^T = -\Omega_{\mathbb{R}}^T$$

which means that  $\Omega_{\mathbb{R}}$  is an antisymmetrical tensor. This constitutes what is called, in fluid mechanics, the “spin tensor”; while this latter may then depend on the point considered, the tensor  $\Omega_{\mathbb{R}}$  associated with a rigid body movement is the same throughout the domain of the considered solid.

In addition, since  $\Omega_{\mathbb{R}}$  is antisymmetrical, it is possible, as mentioned in Paragraph A.2.1, to associate a vector, noted  $\omega_{\mathbb{R}}$ , called “angular velocity vector”, which therefore verifies:

$$\omega_{\mathbb{R}} \wedge \mathbf{c} = \omega_{\mathbb{R}}^{\wedge} \mathbf{c} = \Omega_{\mathbb{R}} \mathbf{c} = \dot{\mathbb{R}} \mathbb{R}^T \mathbf{c}, \forall \mathbf{c}$$

Thus, if, in a given vector basis  $(\mathbf{i}_1, \mathbf{i}_2, \mathbf{i}_3)$ , the matrix is written as:

$$\Omega_{\mathbb{R}} = \begin{pmatrix} 0 & \Omega_{12} & \Omega_{13} \\ -\Omega_{12} & 0 & \Omega_{23} \\ -\Omega_{13} & -\Omega_{23} & 0 \end{pmatrix}$$

the associated angular velocity vector  $\omega_{\mathbb{R}}$  has as components in this same basis:

$$(\omega_1 = -\Omega_{23}, \omega_2 = \Omega_{13}, \omega_3 = -\Omega_{12})$$

This makes it possible to express the time derivative of a vector: for this, let us consider a vector that can be expressed as  $\mathbf{c}(t) = \mathbb{R}(t)\mathbf{c}_0$ , where  $\mathbf{c}_0$  is assumed to be fixed. We can then write that:

$$\dot{\mathbf{c}} = \dot{\mathbb{R}} \mathbf{c}_0 = \Omega_{\mathbb{R}} \mathbb{R} \mathbf{c}_0 = \Omega_{\mathbb{R}} \mathbf{c} = \omega_{\mathbb{R}} \wedge \mathbf{c}$$

## B.2 Transformations of integrals

### B.2.1 Substitutions

The purpose of this paragraph is to make the substitution  $\mathbf{x} = \mathbf{f}(\mathbf{p}, t)$  when tracking a set of particles as they move, in order to estimate a specific quantity obtained by integration.

#### Volume integration

The volume of a parallelepiped built from three vectors  $\mathbf{a}$ ,  $\mathbf{b}$  and  $\mathbf{c}$  can be expressed using the mixed product:

$$\mathcal{V}(\mathbf{a}, \mathbf{b}, \mathbf{c}) = |\langle \mathbf{a}, \mathbf{b} \wedge \mathbf{c} \rangle|$$

Thus, if we consider an elemental volume in the vicinity of a point  $\mathbf{p}$ , represented by a parallelepiped constructed from three elemental vectors  $d\mathbf{p}_1$ ,  $d\mathbf{p}_2$  and  $d\mathbf{p}_3$ , which become  $d\mathbf{x}_1$ ,  $d\mathbf{x}_2$  and  $d\mathbf{x}_3$  at time  $t$ , the associated volume can be defined as:

$$|\langle d\mathbf{x}_1, d\mathbf{x}_2 \wedge d\mathbf{x}_3 \rangle| = |\langle \mathbb{F} d\mathbf{p}_1, (\mathbb{F} d\mathbf{p}_2) \wedge (\mathbb{F} d\mathbf{p}_3) \rangle|$$

where  $\mathbb{F}$  is the deformation gradient tensor. Using the result of Appendix A.2.3, we then establish that :

$$|\langle d\mathbf{x}_1, d\mathbf{x}_2 \wedge d\mathbf{x}_3 \rangle| = |\det \mathbb{F} \langle d\mathbf{p}_1, d\mathbf{p}_2 \wedge d\mathbf{p}_3 \rangle| = \det \mathbb{F} |\langle d\mathbf{p}_1, d\mathbf{p}_2 \wedge d\mathbf{p}_3 \rangle|$$

because  $\det \mathbb{F} > 0$ .

This result then allows to make the substitution  $\mathbf{x} = \mathbf{f}(\mathbf{p}, t)$  in a volume integral, by writing that:

$$\int_{\Omega_t} \phi(\mathbf{x}) dV_x = \int_{\Omega_0} \phi(\mathbf{f}(\mathbf{p}, t)) \det \mathbb{F}(\mathbf{p}, t) dV_p$$

where  $\phi$  is a given scalar field.

### Surface Integral

The area of a parallelogram built from two vectors  $\mathbf{a}$  and  $\mathbf{b}$  can be expressed simply as:

$$\mathcal{A}(\mathbf{a}, \mathbf{b}) = \|\mathbf{a} \wedge \mathbf{b}\|$$

Thus, if we consider an elemental surface in the vicinity of a point  $\mathbf{p}$ , and represented by a parallelogram constructed from two elemental vectors  $d\mathbf{p}_1$  and  $d\mathbf{p}_2$ , which become  $d\mathbf{x}_1$  and  $d\mathbf{x}_2$  at time  $t$ , the associated area can then be expressed as:

$$\|d\mathbf{x}_1 \wedge d\mathbf{x}_2\| = \|(\mathbb{F} d\mathbf{p}_1) \wedge (\mathbb{F} d\mathbf{p}_2)\|$$

with  $\mathbb{F}$  the deformation gradient tensor. Using Piola's formula established in Appendix A.2.3, we arrive at:

$$\|d\mathbf{x}_1 \wedge d\mathbf{x}_2\| = \|(\det \mathbb{F}) \mathbb{F}^{-T} (d\mathbf{p}_1 \wedge d\mathbf{p}_2)\| = \det \mathbb{F} \left\| \mathbb{F}^{-T} (d\mathbf{p}_1 \wedge d\mathbf{p}_2) \right\|$$

because  $\det \mathbb{F} > 0$ . In addition, by posing  $d\mathbf{p}_1 \wedge d\mathbf{p}_2 = dS_0 \mathbf{n}_p$ , where  $\mathbf{n}_p$  is the outer unit normal vector to the elemental surface in its initial configuration, we can make the substitution  $\mathbf{x} = \mathbf{f}(\mathbf{p}, t)$  in a surface integral, by writing that:

$$\int_{S_t} \phi(\mathbf{x}) dS_x = \int_{S_0} \phi(\mathbf{f}(\mathbf{p}, t)) \det \mathbb{F}(\mathbf{p}, t) \left\| \mathbb{F}^{-T} \mathbf{n}_p \right\| dS_p$$

where  $\phi$  is a given scalar field.

## B.2.2 Stokes formulas

Stokes formulas play a major role in many cases, for example when it comes to making balances between variations in specific quantities within a domain and the corresponding surface flows (or “fluxes”) through the boundaries of that domain. They are commonly used in electromagnetism, where Maxwell’s equations are often introduced from the laws of Biot and Savart. In mechanics, it is mainly the formula of divergence that is used.

### Gradient formula

We consider a domain  $\Omega_t$ , with a regular boundary  $\partial\Omega_t$ , with an outer unit normal vector  $\mathbf{n}$  at any point  $\mathbf{x}$ , as well as a scalar field  $\phi(\mathbf{x})$  which is also regular. We then have the Stokes formula, also called the “gradient formula”:

$$\int_{\partial\Omega_t} \phi \mathbf{n} dS_x = \int_{\Omega_t} \nabla_{\mathbf{x}} \phi dV_x$$

The principle of the proof consists in dividing the domain  $\Omega_t$  into small elemental cubes  $V$ , for which we can write, for example for faces parallel to the axis  $\mathbf{i}_1$  of associated Cartesian coordinate  $x_1$ :

$$\int_{S(x_1^+)} \phi dS - \int_{S(x_1^-)} \phi dS = \int_S \int_{x_1^-}^{x_1^+} \frac{\partial \phi}{\partial x_1} dx_1 dS = \int_V \frac{\partial \phi}{\partial x_1} dV$$

For two adjacent cubes that are inside the domain, the integrals on the faces cancel each other out two by two, because the normal vectors are opposite; there are only the faces of the cubes that are truncated by the boundary  $\partial\Omega_t$  of the domain, for which an adapted configuration allows to obtain the result.

Mathematically as well as physically, this gradient formula is a three-dimensional generalization of the relation between primitive function and derivative that can be written for functions of a single variable. In addition, if we consider a domain of infinitesimal size, we obtain that:

$$\nabla_{\mathbf{x}} \phi \approx \frac{1}{|\Omega_t|} \int_{\partial\Omega_t} \phi \mathbf{n} dS_t$$

### Divergence formula

We deduce from Stokes' formula the so-called “divergence formula”, which is expressed as:

$$\int_{\partial\Omega_t} \langle \mathbf{v}, \mathbf{n} \rangle dS_x = \int_{\Omega_t} \operatorname{div}_x \mathbf{v} dV_x$$

Physically, the divergence then appears as the average value of the flow through the boundary of the domain, if we consider that this latter is of infinitesimal size:

$$\operatorname{div}_x \mathbf{v} \approx \frac{1}{|\Omega_t|} \int_{\partial\Omega_t} \langle \mathbf{v}, \mathbf{n} \rangle dS_x$$

Using the definition of the divergence of a second-order tensor  $\mathbb{A}(\mathbf{x})$ , recalled in Paragraph B.1.1, we obtain a formula similar to the previous one:

$$\int_{\partial\Omega_t} \mathbb{A} \mathbf{n} dS_x = \int_{\Omega_t} \operatorname{div}_x \mathbb{A} dV_x$$

which allows, when the size of the domain is infinitesimal, to physically interpret the divergence of a tensor as:

$$\operatorname{div}_x \mathbb{A} \approx \frac{1}{|\Omega_t|} \int_{\partial\Omega_t} \mathbb{A} \mathbf{n} dS_x$$

Eventually, starting from the definition of the divergence of a symmetrical tensor  $\mathbb{A}(\mathbf{x})$ , we can establish that:

$$\operatorname{div}_x (\mathbb{A}^T(\mathbf{c} \wedge \mathbf{x})) = \langle \operatorname{div}_x \mathbb{A}, \mathbf{c} \wedge \mathbf{x} \rangle + \operatorname{tr}(\mathbb{A}(\mathbb{D}_x(\mathbf{c} \wedge \mathbf{x}))^T)$$

with  $\mathbf{x}$  the placement vector, and  $\mathbf{c}$  an arbitrary constant vector; we then obtain that:

$$\mathbb{D}_x(\mathbf{c} \wedge \mathbf{x}) = \sum_{n=1}^3 \frac{\partial(\mathbf{c} \wedge \mathbf{x})}{\partial x_n} \otimes \mathbf{i}_n = \sum_{n=1}^3 (\mathbf{c} \wedge \mathbf{i}_n) \otimes \mathbf{i}_n$$

where  $(\mathbf{i}_1, \mathbf{i}_2, \mathbf{i}_3)$  is a Cartesian vector basis of associated coordinates  $(x_1, x_2, x_3)$ . The divergence formula then allows to write that:

$$\int_{\partial\Omega_t} \langle \mathbf{c}, \mathbf{x} \wedge \mathbb{A} \mathbf{n} \rangle dS_x = \int_{\partial\Omega_t} \langle \mathbb{A}(\mathbf{c} \wedge \mathbf{x}), \mathbf{n} \rangle dS_x = \int_{\Omega_t} \operatorname{div}_x (\mathbb{A}(\mathbf{c} \wedge \mathbf{x})) dV_x$$

and using the previous results, we finally arrive at a divergence formula with a vector product:

$$\int_{\partial\Omega_t} \mathbf{x} \wedge \mathbb{A} \mathbf{n} dS_x = \int_{\Omega_t} \left( \mathbf{x} \wedge \operatorname{div}_x \mathbb{A} + \sum_{n=1}^3 \mathbf{i}_n \wedge \mathbb{A} \mathbf{i}_n \right) dV_x$$

### Derived formulas

Using the following remarkable relation, valid for any vector field  $\mathbf{v}(\mathbf{x})$  and an arbitrary constant vector  $\mathbf{c}$ :

$$\langle \operatorname{rot}_x \mathbf{v}, \mathbf{c} \rangle = \operatorname{div}_x (\mathbf{v} \wedge \mathbf{c})$$

a derived formula is established:

$$\int_{\partial\Omega_t} \mathbf{n} \wedge \mathbf{v} dS_x = \int_{\Omega_t} \operatorname{rot}_x \mathbf{v} dV_x$$

which allows to obtain an interpretation of the curl when the size of the considered domain becomes infinitesimal:

$$\operatorname{rot}_x \mathbf{v} \approx \frac{1}{|\Omega_t|} \int_{\partial\Omega_t} \mathbf{n} \wedge \mathbf{v} dS_x$$

Finally, a formula can be established for the gradient tensor of a vector field  $\mathbf{v}(\mathbf{x})$ :

$$\int_{\partial\Omega_t} \mathbf{v} \otimes \mathbf{n} dS_x = \int_{\Omega_t} \mathbb{D}_x \mathbf{v} dV_x$$

## B.3 Formulas

### B.3.1 Change of coordinates

In the case of specific geometries, it is often more interesting to have vector bases (and associated coordinates) that are naturally linked to them. In this case, all the operators introduced in the above can be expressed using these new coordinate systems; the principle then consists in making substitutions in the expressions that have been established in the case of Cartesian coordinates.

For example, if we want to calculate the gradient tensor of a vector  $\mathbf{v}$  expressed using particular curvilinear coordinates  $(\xi, \eta, \zeta)$ , we establish that:

$$\mathbb{D}_{\mathbf{x}} \mathbf{v} = \frac{\partial \mathbf{v}}{\partial \xi} \otimes \nabla_{\mathbf{x}} \xi + \frac{\partial \mathbf{v}}{\partial \eta} \otimes \nabla_{\mathbf{x}} \eta + \frac{\partial \mathbf{v}}{\partial \zeta} \otimes \nabla_{\mathbf{x}} \zeta$$

and for the divergence of a tensor  $\mathbb{A}$ :

$$\operatorname{div}_{\mathbf{x}} \mathbb{A} = \frac{\partial \mathbb{A}}{\partial \xi} \nabla_{\mathbf{x}} \xi + \frac{\partial \mathbb{A}}{\partial \eta} \nabla_{\mathbf{x}} \eta + \frac{\partial \mathbb{A}}{\partial \zeta} \nabla_{\mathbf{x}} \zeta$$

The following gives the expressions of the different operators in the cylindrical and spherical coordinate systems.

### B.3.2 Cylindrical coordinates

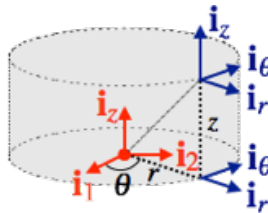


Figure B.1: Cylindrical vector basis and associated coordinates.

It is recalled that a point in space verifies the following placement vector:

$$\mathbf{x} = r \mathbf{i}_r(\theta) + z \mathbf{i}_z$$

where, in a Cartesian vector basis  $(\mathbf{i}_1, \mathbf{i}_2, \mathbf{i}_3)$ , with  $\mathbf{i}_3$  as the cylinder axis, and  $(x_1, x_2, x_3)$  as associated coordinates, the basis vectors satisfy:

$$\begin{aligned} \mathbf{i}_r(\theta) &= \cos \theta \mathbf{i}_1 + \sin \theta \mathbf{i}_2, \quad \forall \theta \in [0, 2\pi) \\ \mathbf{i}_\theta(\theta) &= -\sin \theta \mathbf{i}_1 + \cos \theta \mathbf{i}_2, \quad \forall \theta \in [0, 2\pi) \\ \mathbf{i}_z &= \mathbf{i}_3 \end{aligned}$$

which implies that:

$$x_1 = r \cos \theta, \quad x_2 = r \sin \theta, \quad x_3 = z$$

The inverse relations are then given by:

$$r = \sqrt{x_1^2 + x_2^2}, \quad \theta = \arctan \frac{x_2}{x_1}, \quad z = x_3$$

for  $x_1 \neq 0$ . The derivatives of the basis vectors then satisfy:

$$\begin{aligned} \frac{d}{d\theta} \mathbf{i}_r(\theta) &= -\sin \theta \mathbf{i}_1 + \cos \theta \mathbf{i}_2 = \mathbf{i}_\theta(\theta), \quad \forall \theta \in [0, 2\pi) \\ \frac{d}{d\theta} \mathbf{i}_\theta(\theta) &= -\cos \theta \mathbf{i}_1 - \sin \theta \mathbf{i}_2 = -\mathbf{i}_r(\theta), \quad \forall \theta \in [0, 2\pi) \end{aligned}$$

while the gradients of the coordinates are established as:

$$\nabla_{\mathbf{x}} r = \mathbf{i}_r(\theta), \nabla_{\mathbf{x}} \theta = \frac{\mathbf{i}_{\theta}(\theta)}{r}, \nabla_{\mathbf{x}} z = \mathbf{i}_z$$

Finally, an elemental volume is written as:

$$dV_x = r dr d\theta dz$$

while an elemental surface is expressed, depending on the coordinate remaining constant, as:

$$dS_x^r = r d\theta dz, dS_x^\theta = dr dz, \text{ and } dS_x^z = r dr d\theta$$

### Expressions of the conventional operators

For a scalar field  $\psi(r, \theta, z)$  and a given vector field  $\mathbf{v}(r, \theta, z) = v_r(r, \theta, z)\mathbf{i}_r + v_\theta(r, \theta, z)\mathbf{i}_\theta + v_z(r, \theta, z)\mathbf{i}_z$ , we can establish that:

$$\begin{aligned} \nabla_{\mathbf{x}} \psi &= \frac{\partial \psi}{\partial r} \mathbf{i}_r + \frac{1}{r} \frac{\partial \psi}{\partial \theta} \mathbf{i}_\theta + \frac{\partial \psi}{\partial z} \mathbf{i}_z \\ \Delta_{\mathbf{x}} \psi &= \frac{1}{r} \frac{\partial}{\partial r} \left( r \frac{\partial \psi}{\partial r} \right) + \frac{1}{r^2} \frac{\partial^2 \psi}{\partial \theta^2} + \frac{\partial^2 \psi}{\partial z^2} \\ \operatorname{div}_{\mathbf{x}} \mathbf{v} &= \frac{\partial v_r}{\partial r} + \frac{v_r}{r} + \frac{1}{r} \frac{\partial v_\theta}{\partial \theta} + \frac{\partial v_z}{\partial z} \\ \mathbf{rot}_{\mathbf{x}} \mathbf{v} &= \left( \frac{1}{r} \frac{\partial v_z}{\partial \theta} - \frac{\partial v_\theta}{\partial z} \right) \mathbf{i}_r + \left( \frac{\partial v_r}{\partial z} - \frac{\partial v_z}{\partial r} \right) \mathbf{i}_\theta + \left( \frac{\partial v_\theta}{\partial r} + \frac{v_\theta}{r} - \frac{1}{r} \frac{\partial v_r}{\partial \theta} \right) \mathbf{i}_z \\ \Delta_{\mathbf{x}} \mathbf{v} &= \left( \frac{\partial^2 v_r}{\partial r^2} + \frac{1}{r} \frac{\partial v_r}{\partial r} - \frac{v_r}{r^2} + \frac{1}{r^2} \frac{\partial^2 v_r}{\partial \theta^2} - \frac{2}{r^2} \frac{\partial v_\theta}{\partial \theta} + \frac{\partial^2 v_r}{\partial z^2} \right) \mathbf{i}_r \\ &\quad + \left( \frac{\partial^2 v_\theta}{\partial r^2} + \frac{1}{r} \frac{\partial v_\theta}{\partial r} - \frac{v_\theta}{r^2} + \frac{1}{r^2} \frac{\partial^2 v_\theta}{\partial \theta^2} + \frac{2}{r^2} \frac{\partial v_r}{\partial \theta} + \frac{\partial^2 v_\theta}{\partial z^2} \right) \mathbf{i}_\theta \\ &\quad + \left( \frac{\partial^2 v_z}{\partial r^2} + \frac{1}{r} \frac{\partial v_z}{\partial r} + \frac{1}{r^2} \frac{\partial^2 v_z}{\partial \theta^2} + \frac{\partial^2 v_z}{\partial z^2} \right) \mathbf{i}_z \end{aligned}$$

### Mechanical equations

In the case of a displacement field  $\mathbf{u}(r, \theta, z) = u_r(r, \theta, z)\mathbf{i}_r + u_\theta(r, \theta, z)\mathbf{i}_\theta + u_z(r, \theta, z)\mathbf{i}_z$ , we establish that the infinitesimal strain tensor is written as:

$$\boldsymbol{\epsilon} = \frac{\partial \mathbf{u}}{\partial r} \otimes_S \mathbf{i}_r + \frac{\partial \mathbf{u}}{\partial \theta} \otimes_S \frac{\mathbf{i}_\theta}{r} + \frac{\partial \mathbf{u}}{\partial z} \otimes_S \mathbf{i}_z$$

or, in matrix components in the cylindrical vector basis:

$$\boldsymbol{\epsilon} = \begin{pmatrix} \frac{\partial u_r}{\partial r} & \frac{1}{2} \left( \frac{1}{r} \frac{\partial u_r}{\partial \theta} + \frac{\partial u_\theta}{\partial r} - \frac{u_\theta}{r} \right) & \frac{1}{2} \left( \frac{\partial u_r}{\partial z} + \frac{\partial u_z}{\partial r} \right) \\ \text{sym.} & \frac{1}{r} \frac{\partial u_\theta}{\partial \theta} + \frac{u_r}{r} & \frac{1}{2} \left( \frac{\partial u_\theta}{\partial z} + \frac{1}{r} \frac{\partial u_z}{\partial \theta} \right) \\ \text{sym.} & \text{sym.} & \frac{\partial u_z}{\partial z} \end{pmatrix}_{(\mathbf{i}_r, \mathbf{i}_\theta, \mathbf{i}_z)}$$

In addition, in the case of a stress field written as:

$$\begin{aligned} \boldsymbol{\sigma}(\mathbf{x}) &= \sigma_{rr}(r, \theta, z)\mathbf{i}_r(\theta) \otimes \mathbf{i}_r(\theta) + \sigma_{\theta\theta}(r, \theta, z)\mathbf{i}_\theta(\theta) \otimes \mathbf{i}_\theta(\theta) + \sigma_{zz}(r, \theta, z)\mathbf{i}_z \otimes \mathbf{i}_z \\ &\quad + 2\sigma_{r\theta}(r, \theta, z)\mathbf{i}_r(\theta) \otimes_S \mathbf{i}_\theta(\theta) + 2\sigma_{rz}(r, \theta, z)\mathbf{i}_r(\theta) \otimes_S \mathbf{i}_z + 2\sigma_{\theta z}(r, \theta, z)\mathbf{i}_\theta(\theta) \otimes_S \mathbf{i}_z \end{aligned}$$

we can express the divergence of the stress tensor as:

$$\operatorname{div}_x \boldsymbol{\sigma} = \frac{\partial \sigma}{\partial r} \mathbf{i}_r + \frac{\partial \sigma}{\partial \theta} \frac{\mathbf{i}_\theta}{r} + \frac{\partial \sigma}{\partial z} \mathbf{i}_z$$

or, using the cylindrical vector basis:

$$\begin{aligned} \operatorname{div}_x \boldsymbol{\sigma} &= \left( \frac{\partial \sigma_{rr}}{\partial r} + \frac{1}{r} \frac{\partial \sigma_{r\theta}}{\partial \theta} + \frac{\partial \sigma_{rz}}{\partial z} + \frac{\sigma_{rr} - \sigma_{\theta\theta}}{r} \right) \mathbf{i}_r \\ &\quad + \left( \frac{\partial \sigma_{r\theta}}{\partial r} + \frac{1}{r} \frac{\partial \sigma_{\theta\theta}}{\partial \theta} + \frac{\partial \sigma_{\theta z}}{\partial z} + 2 \frac{\sigma_{r\theta}}{r} \right) \mathbf{i}_\theta \\ &\quad + \left( \frac{\partial \sigma_{rz}}{\partial r} + \frac{1}{r} \frac{\partial \sigma_{\theta z}}{\partial \theta} + \frac{\partial \sigma_{zz}}{\partial z} + \frac{\sigma_{rz}}{r} \right) \mathbf{i}_z \end{aligned}$$

### B.3.3 Spherical coordinates

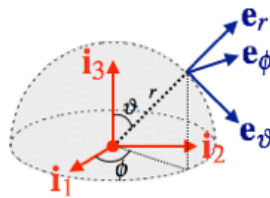


Figure B.2: Spherical vector basis and associated coordinates.

It is recalled that a point in space verifies the following placement vector:

$$\mathbf{x} = r \mathbf{e}_r(\vartheta, \phi)$$

where, in a Cartesian vector basis  $(\mathbf{i}_1, \mathbf{i}_2, \mathbf{i}_3)$ , with  $(x_1, x_2, x_3)$  as associated coordinates, the basis vectors satisfy:

$$\mathbf{e}_r(\vartheta, \phi) = \sin \vartheta \cos \phi \mathbf{i}_1 + \sin \vartheta \sin \phi \mathbf{i}_2 + \cos \vartheta \mathbf{i}_3, \quad \forall \vartheta \in [0, \pi], \quad \forall \phi \in [0, 2\pi)$$

$$\mathbf{e}_\vartheta(\vartheta, \phi) = \cos \vartheta \cos \phi \mathbf{i}_1 + \cos \vartheta \sin \phi \mathbf{i}_2 - \sin \vartheta \mathbf{i}_3, \quad \forall \vartheta \in [0, \pi], \quad \forall \phi \in [0, 2\pi)$$

$$\mathbf{e}_\phi(\phi) = -\sin \phi \mathbf{i}_1 + \cos \phi \mathbf{i}_2, \quad \forall \phi \in [0, 2\pi)$$

which implies that:

$$x_1 = r \sin \vartheta \cos \phi, \quad x_2 = r \sin \vartheta \sin \phi, \quad x_3 = r \cos \vartheta$$

The inverse relations are then given by:

$$r = \sqrt{x_1^2 + x_2^2 + x_3^2}, \quad \vartheta = \arccotan \frac{x_3}{\sqrt{x_1^2 + x_2^2}}, \quad \phi = \arctan \frac{x_2}{x_1}$$

for  $x_1 \neq 0$  and  $x_3 \neq 0$ . The derivatives of the basis vectors then satisfy:

$$\frac{\partial}{\partial \vartheta} \mathbf{e}_r(\vartheta, \phi) = \cos \vartheta \cos \phi \mathbf{i}_1 + \cos \vartheta \sin \phi \mathbf{i}_2 - \sin \vartheta \mathbf{i}_3 = \mathbf{e}_\vartheta(\vartheta, \phi), \quad \forall \vartheta \in [0, \pi], \quad \forall \phi \in [0, 2\pi)$$

$$\frac{\partial}{\partial \phi} \mathbf{e}_r(\vartheta, \phi) = -\sin \vartheta \sin \phi \mathbf{i}_1 + \sin \vartheta \cos \phi \mathbf{i}_2 + \cos \vartheta \mathbf{i}_3 = \sin \vartheta \mathbf{e}_\phi(\phi), \quad \forall \vartheta \in [0, \pi], \quad \forall \phi \in [0, 2\pi)$$

$$\frac{\partial}{\partial \vartheta} \mathbf{e}_\vartheta(\vartheta, \phi) = -\sin \vartheta \cos \phi \mathbf{i}_1 - \sin \vartheta \sin \phi \mathbf{i}_2 - \cos \vartheta \mathbf{i}_3 = -\mathbf{e}_r(\vartheta, \phi), \quad \forall \vartheta \in [0, \pi], \quad \forall \phi \in [0, 2\pi)$$

$$\frac{\partial}{\partial \phi} \mathbf{e}_\vartheta(\vartheta, \phi) = -\cos \vartheta \sin \phi \mathbf{i}_1 + \cos \vartheta \cos \phi \mathbf{i}_2 - \sin \vartheta \mathbf{i}_3 = \cos \vartheta \mathbf{e}_\phi(\phi), \quad \forall \vartheta \in [0, \pi], \quad \forall \phi \in [0, 2\pi)$$

$$\frac{d}{d\phi} \mathbf{e}_\phi(\phi) = -\cos \phi \mathbf{i}_1 - \sin \phi \mathbf{i}_2 = -\sin \vartheta \mathbf{e}_r(\vartheta, \phi) - \cos \vartheta \mathbf{e}_\vartheta(\vartheta, \phi), \quad \forall \vartheta \in [0, \pi], \quad \forall \phi \in [0, 2\pi)$$

while the gradients of the coordinates are established as:

$$\nabla_x r = \mathbf{e}_r(\vartheta, \phi), \quad \nabla_x \vartheta = \frac{\mathbf{e}_\vartheta(\vartheta, \phi)}{r}, \quad \nabla_x \phi = \frac{\mathbf{e}_\phi(\phi)}{r \sin \vartheta}$$

Finally, an elemental volume is written as:

$$dV_x = r^2 \sin \vartheta dr d\vartheta d\phi$$

while an elemental surface is expressed, depending on the coordinate remaining constant, as:

$$dS_x^r = r^2 \sin \vartheta d\vartheta d\phi, \quad dS_x^\vartheta = r \sin \vartheta dr d\phi, \quad \text{and} \quad dS_x^\phi = r dr d\vartheta$$

### Expressions of the conventional operators

For a scalar field  $\psi(r, \vartheta, \phi)$  and a given vector field  $\mathbf{v}(r, \vartheta, \phi) = v_r(r, \vartheta, \phi)\mathbf{e}_r + v_\vartheta(r, \vartheta, \phi)\mathbf{e}_\vartheta + v_\phi(r, \vartheta, \phi)\mathbf{e}_\phi$ , we can establish that:

$$\begin{aligned} \nabla_x \psi &= \frac{\partial \psi}{\partial r} \mathbf{e}_r + \frac{1}{r} \frac{\partial \psi}{\partial \vartheta} \mathbf{e}_\vartheta + \frac{1}{r \sin \vartheta} \frac{\partial \psi}{\partial \phi} \mathbf{e}_\phi \\ \Delta_x \psi &= \frac{\partial^2 \psi}{\partial r^2} + \frac{2}{r} \frac{\partial \psi}{\partial r} + \frac{1}{r^2} \frac{\partial^2 \psi}{\partial \vartheta^2} + \frac{1}{r^2 \tan^2 \vartheta} \frac{\partial \psi}{\partial \vartheta} + \frac{1}{r^2 \sin^2 \vartheta} \frac{\partial^2 \psi}{\partial \phi^2} \\ \operatorname{div}_x \mathbf{v} &= \frac{\partial v_r}{\partial r} + 2 \frac{v_r}{r} + \frac{1}{r} \frac{\partial v_\vartheta}{\partial \vartheta} + \cot \vartheta \frac{v_\vartheta}{r} + \frac{1}{r \sin \vartheta} \frac{\partial v_\phi}{\partial \phi} \\ \operatorname{rot}_x \mathbf{v} &= \frac{1}{r \sin \vartheta} \left( \frac{\partial(v_\phi \sin \vartheta)}{\partial \vartheta} - \frac{\partial v_\vartheta}{\partial \phi} \right) \mathbf{e}_r + \frac{1}{r \sin \vartheta} \left( \frac{\partial v_r}{\partial \phi} - \frac{\partial(rv_\phi \sin \vartheta)}{\partial r} \right) \mathbf{e}_\vartheta + \left( \frac{\partial v_\vartheta}{\partial r} + \frac{v_\vartheta}{r} - \frac{1}{r} \frac{\partial v_r}{\partial \vartheta} \right) \mathbf{e}_\phi \\ \Delta_x \mathbf{v} &= \left( \frac{1}{r} \frac{\partial^2(rv_r)}{\partial r^2} - \frac{2}{r^2} (v_r + v_\vartheta \cot \vartheta) + \frac{1}{r^2} \frac{\partial^2 v_r}{\partial \vartheta^2} + \frac{\cot \vartheta}{r^2} \frac{\partial v_r}{\partial \vartheta} - \frac{2}{r^2} \frac{\partial v_\vartheta}{\partial \vartheta} + \frac{1}{r^2 \sin^2 \vartheta} \frac{\partial^2 v_r}{\partial \phi^2} - \frac{2}{r^2 \sin \vartheta} \frac{\partial v_\phi}{\partial \phi} \right) \mathbf{e}_r \\ &\quad + \left( \frac{1}{r} \frac{\partial^2(rv_\vartheta)}{\partial r^2} - \frac{v_\vartheta}{r^2 \sin^2 \vartheta} + \frac{1}{r^2} \frac{\partial^2 v_\vartheta}{\partial \vartheta^2} + \frac{\cot \vartheta}{r^2} \frac{\partial v_\vartheta}{\partial \vartheta} + \frac{2}{r^2} \frac{\partial v_r}{\partial \vartheta} + \frac{1}{r^2 \sin^2 \vartheta} \frac{\partial^2 v_\vartheta}{\partial \phi^2} - \frac{2 \cot \vartheta}{r^2 \sin \vartheta} \frac{\partial v_\phi}{\partial \phi} \right) \mathbf{e}_\vartheta \\ &\quad + \left( \frac{1}{r} \frac{\partial^2(rv_\phi)}{\partial r^2} - \frac{v_\phi}{r^2 \sin^2 \vartheta} + \frac{1}{r^2} \frac{\partial^2 v_\phi}{\partial \vartheta^2} + \frac{\cot \vartheta}{r^2} \frac{\partial v_\phi}{\partial \vartheta} + \frac{1}{r^2 \sin^2 \vartheta} \frac{\partial^2 v_\phi}{\partial \phi^2} + \frac{2}{r^2 \sin \vartheta} \frac{\partial v_r}{\partial \phi} + \frac{2 \cot \vartheta}{r^2 \sin \vartheta} \frac{\partial v_\vartheta}{\partial \phi} \right) \mathbf{e}_\phi \end{aligned}$$

### Mechanical equations

In the case of a displacement field  $\mathbf{u}(r, \vartheta, \phi) = u_r(r, \vartheta, \phi)\mathbf{e}_r + u_\vartheta(r, \vartheta, \phi)\mathbf{e}_\vartheta + u_\phi(r, \vartheta, \phi)\mathbf{e}_\phi$ , we establish that the infinitesimal strain tensor is written as:

$$\boldsymbol{\epsilon} = \frac{\partial \mathbf{u}}{\partial r} \otimes_S \mathbf{e}_r + \frac{\partial \mathbf{u}}{\partial \vartheta} \otimes_S \frac{\mathbf{e}_\vartheta}{r} + \frac{\partial \mathbf{u}}{\partial \phi} \otimes_S \frac{\mathbf{e}_\phi}{r \sin \vartheta}$$

or, in matrix components in the spherical vector basis:

$$\boldsymbol{\epsilon} = \begin{pmatrix} \frac{\partial u_r}{\partial r} & \frac{1}{2} \left( \frac{1}{r} \frac{\partial u_r}{\partial \vartheta} + \frac{\partial u_\vartheta}{\partial r} - \frac{u_\vartheta}{r} \right) & \frac{1}{2} \left( \frac{1}{r \sin \vartheta} \frac{\partial u_r}{\partial \phi} + \frac{\partial u_\phi}{\partial r} - \frac{u_\phi}{r} \right) \\ \text{sym.} & \frac{1}{r} \frac{\partial u_\vartheta}{\partial \vartheta} + \frac{u_r}{r} & \frac{1}{2r} \left( \frac{\partial u_\phi}{\partial \vartheta} - (\cot \vartheta) u_\phi \right) + \frac{1}{2r \sin \vartheta} \frac{\partial u_\vartheta}{\partial \phi} \\ \text{sym.} & \text{sym.} & \frac{1}{r \sin \vartheta} \frac{\partial u_\phi}{\partial \phi} + \cot \vartheta \frac{u_\vartheta}{r} + \frac{u_r}{r} \end{pmatrix}_{(\mathbf{e}_r, \mathbf{e}_\vartheta, \mathbf{e}_\phi)}$$

In addition, in the case of a stress field written as:

$$\begin{aligned} \boldsymbol{\sigma}(r, \vartheta, \phi) &= \sigma_{rr}(r)\mathbf{e}_r(\vartheta, \phi) \otimes \mathbf{e}_r(\vartheta, \phi) + \sigma_{\vartheta\vartheta}(r)\mathbf{e}_\vartheta(\vartheta, \phi) \otimes \mathbf{e}_\vartheta(\vartheta, \phi) + \sigma_{\phi\phi}(r)\mathbf{e}_\phi(\phi) \otimes \mathbf{e}_\phi(\phi) \\ &\quad + 2\sigma_{r\vartheta}(r)\mathbf{e}_r(\vartheta, \phi) \otimes_S \mathbf{e}_\vartheta(\vartheta, \phi) + 2\sigma_{r\phi}(r)\mathbf{e}_r(\vartheta, \phi) \otimes_S \mathbf{e}_\phi(\phi) \\ &\quad + 2\sigma_{\vartheta\phi}(r)\mathbf{e}_\vartheta(\vartheta, \phi) \otimes_S \mathbf{e}_\phi(\phi) \end{aligned}$$

we can express the divergence of the stress tensor as:

$$\mathbf{div}_x \boldsymbol{\sigma} = \frac{\partial \sigma}{\partial r} \mathbf{e}_r + \frac{\partial \sigma}{\partial \vartheta} \frac{\mathbf{e}_\vartheta}{r} + \frac{\partial \sigma}{\partial \phi} \frac{\mathbf{e}_\phi}{r \sin \vartheta}$$

or, in the spherical vector basis:

$$\begin{aligned} \mathbf{div}_x \boldsymbol{\sigma} = & \left( \frac{\partial \sigma_{rr}}{\partial r} + \frac{1}{r} \frac{\partial \sigma_{r\vartheta}}{\partial \vartheta} + \frac{1}{r \sin \vartheta} \frac{\partial \sigma_{r\phi}}{\partial \phi} + \frac{2\sigma_{rr} - \sigma_{\vartheta\vartheta} - \sigma_{\phi\phi} + \sigma_{r\vartheta} \cot \vartheta}{r} \right) \mathbf{e}_r \\ & + \left( \frac{\partial \sigma_{r\vartheta}}{\partial r} + \frac{1}{r} \frac{\partial \sigma_{\vartheta\vartheta}}{\partial \vartheta} + \frac{1}{r \sin \vartheta} \frac{\partial \sigma_{\vartheta\phi}}{\partial \phi} + \frac{(\sigma_{\vartheta\vartheta} - \sigma_{\phi\phi}) \cot \vartheta + 3\sigma_{r\vartheta}}{r} \right) \mathbf{e}_\vartheta \\ & + \left( \frac{\partial \sigma_{r\phi}}{\partial r} + \frac{1}{r} \frac{\partial \sigma_{\vartheta\phi}}{\partial \vartheta} + \frac{1}{r \sin \vartheta} \frac{\partial \sigma_{\phi\phi}}{\partial \phi} + \frac{3\sigma_{r\phi} + 2\sigma_{\vartheta\phi} \cot \vartheta}{r} \right) \mathbf{e}_\phi \end{aligned}$$



## Index

### A

- Acceleration ..... 7, 117
- Accomodation ..... 100
- Action ..... 42–45, 193
- Action-reaction principle ..... 40, 48, 64
- Adaptation ..... 100
- Airy stress function ..... 144
- Angle of twist ..... 6, 152, 179, 185
- Angular velocity vector ..... 229
- Area inertia tensor ..... 173, 178, 180–184
- Axial force. 162, 166, 177, 178, 184, 186, 200
- Axisymmetry ..... 144, 145

### B

- Ball joint ..... *see* Spherical joint
- Beam
  - Euler-Bernoulli *see* Euler-Bernoulli beam
  - Timoshenko ..... *see* Timoshenko beam
- Beltrami's equations ..... 135, 142, 144
- Bending ..... 78, 152, 154, 155, 159
  - three-point ..... 157, 197, 200
- Boundary conditions ..... 62, 64, 65, 98, 119, 121, 125, 130, 165, 168, 171, 172, 174, 175, 184
- Brazilian test ..... 81

- Brittle ..... 70, 73, 80
- Buckling ..... 202
  - critical load ..... 204
  - mode ..... 204
- Bulk modulus ..... 108
- Buoyancy ..... 53, 59

### C

- Cleavage ..... 73, 80, 83
- Coefficient of thermal expansion ..... 111, 133
- Compatibility equations ..... 132, 133, 135, 144
- Compliance tensor ..... *see* Elasticity tensor
- Composite ..... 89
- Compression ..... *see* Tension
- Connection ..... 188–202
  - perfect ..... 193
  - pin ..... *see* Pin joint
  - rigid ..... *see* Rigid connection
  - roller ..... *see* Roller support
  - spherical ..... *see* Spherical joint
- Conservation
  - of angular momentum ..... 41–42
  - of mass ..... *see* Mass conservation
  - of momentum ..... 40–41, 117
- Contracted product ..... 86, 217
- Coordinates
  - cylindrical . 6, 25, 60, 108, 112, 144, 169, 175, 213, 232

spherical	55, 61, 145, 213, 234
Couple	43, 120, 127
Creep	99
Criterion	
Mohr-Coulomb	<i>see</i> Mohr-Coulomb criterion
Tresca	<i>see</i> Tresca criterion
Tsaï-Hill	<i>see</i> Tsaï-Hill criterion
von Mises	<i>see</i> von Mises criterion
Cross-section	149, 161, 186, 188
Curl	
tensor	133, 226
vector	226

## D

Damage	100
Deformation gradient tensor	9–13
Density	35, 43, 118
Determinant	33, 34, 217, 219, 229
Dislocation	71, 74
Displacement	4, 22, 27, 97, 125–129, 132, 141, 151, 152, 156, 157, 160
approach	125–129
longitudinal	152, 177, 184, 200
transverse	152, 158, 177, 185, 201
Divergence	
formula	168, 231
tensor	57, 58, 60, 226, 231
vector	33–36, 226, 231
Ductile	70, 74, 83, 87

## E

Elasticity	70, 99, 101, 176
tensor	102
Elongation	15, 25, 152, 153, 155, 159
uniform	4, 7, 10, 16, 18, 26, 34
Engineering stress	71
Equilibrium	
global	43, 47, 51, 53, 55, 122, 163–167, 170–173, 196, 198
local	56–66, 98, 117, 125, 126, 130, 131, 167–169, 173–175, 195, 199, 203
Euler-Bernoulli beam	157–160, 178, 179, 185, 187, 189, 201, 202
Euler-Bernoulli hypothesis	<i>see</i> Euler-Bernoulli beam

Extensometry	31
--------------	----

## F

Facet	47, 51, 75–82, 85, 161
Fatigue	90, 100
Finite elements	137
Fragile	<i>see</i> Brittle
Fundamental principles of dynamics	<i>see</i> Conservation

## G

Gradient	
formula	<i>see</i> Stokes' formula
tensor	9–14, 225
vector	225
Gravity	43, 51, 58, 63, 166, 169, 172, 175, 184, 188
Green-Lagrange strain tensor	15, 21

## H

Hardening	99
Hinged joint	<i>see</i> Pin joint
Hooke's law	104, 107, 118, 176

## I

Incompressibility	34–36, 108
Inertia	
polar	<i>see</i> Polar moment of inertia
product	184
tensor	<i>see</i> Area inertia tensor
Infinitesimal deformation hypothesis	22, 28, 33, 35, 36, 97, 123, 189
Infinitesimal strain tensor	22–32, 97, 117, 132, 133, 152, 156, 158, 160, 176
Infinitesimal thermal strain tensor	111, 133
Initial conditions	98, 119, 121
Isotropy	103–105, 223
transverse	223

## J

Jacobi identity formula	212
-------------------------	-----

**K**

Kronecker delta ..... 214

**L**

Lamé parameters ..... 104, 106, 107, 141

Laplacian

- scalar ..... 126, 130, 184, 227
- tensor ..... 135
- vector ..... 128, 129, 227

Line force density ..... 164, 165, 168, 169

Line moment density ..... 171, 174, 175

**M**

Mass ..... 35, 43, 53

  conservation ..... 35–36, 118

Mixed product ..... 33, 212, 229

Modulus

- bulk ..... *see* Bulk modulus
- shear ..... *see* Shear modulus
- Young ..... *see* Young's modulus

Mohr's circles ..... 78, 82

Mohr-Coulomb criterion ..... 89

Moment .42–45, 120, 127, 136, 172, 193, 194

  bending 169, 175, 178–180, 185, 186, 201

  of the internal loads .. 175, 178, 187, 195

  torsion ..... 169, 179, 180, 185, 187

**N**

Navier's equation ..... 128

Necking ..... 71, 74

Neutral axis ..... 149

Norm

  tensor ..... 87, 217

  vector ..... 6, 15, 212

Normal force ..... *see* Axial force

**P**

Photoelasticity ..... 78, 91, 93, 95, 136

Pin joint ..... 191

Piola's formula ..... 218, 230

Placement vector ..... 3, 4

Plane strain ..... 141, 145

Plane stress ..... 142, 143, 145

Plasticity ..... 70, 99

Poisson's ratio ..... 106, 107

Polar decomposition ..... 14, 219

Polar moment of inertia ... 137, 179–184, 187

Portal frame ..... 190, 195

Pressure ..... 52, 166, 169, 172, 175, 184

  hydrostatic ..... 63, 117

  tank ..... 55, 61, 65

Principal moment of inertia ..... 180, 181

Principal strain ..... 29, 105

Principal stress ..... *see* Stress...principal

Principle of superposition ..... 139

Product

  contracted ..... *see* Contracted product

  mixed ..... *see* Mixed product

  scalar ..... *see* Scalar product

  tensor ..... *see* Tensor product

  vector ..... *see* Vector product

Pure force ..... 43

Pure moment ..... *see* Couple

**R**

Ratcheting ..... 100

Relaxation ..... 99

Resultant force .. 42–45, 53, 59, 69, 120, 136,

  165, 167, 193, 194

  of the internal loads .. 162–169, 177, 178,

  187, 195

Right Cauchy-Green deformation tensor... 16

Rigid connection ..... 189, 190, 195

Rivlin-Ericksen theorem ..... 104, 223

Roller support ..... 192

Rotation ..... 5, 12, 14, 19, 24, 103, 218, 219

  bending ..... 152, 158, 177, 178

  cross-section.....151, 152

  infinitesimal .. 24, 29, 120, 123, 126, 134,

  188, 221

  torsion.....*see* Angle of twist

**O**

Orthotropy ..... 222

## S

- Saint-Venant's principle . . . . . 70, 135–137, 161  
Scalar product . . . . . 4, 17, 212  
Shakedown  
    elastic . . . . . *see* Adaptation  
    plastic . . . . . *see* Accommodation  
Shape function . . . . . 138  
Shear failure . . . . . 83, 87  
Shear force . . . . . 163, 166, 175, 177, 178, 187  
Shear modulus . . . . . 107, 176, 178, 179  
Shear strain . . . . . 17, 25, 107, 152, 154, 155, 160  
    uniform . . . . . 5, 11, 18, 26  
Shear stress . . . . . 75, 82, 84, 107, 161, 162, 176,  
    186–188  
Slip . . . . . 71, 83  
    frictionless . . . . . 119, 121, 147  
Specimen . . . . . 68  
Spherical joint . . . . . 191, 193  
Square root of a tensor . . . . . 14, 219  
Static determinacy . . . . . *see* Static indeterminacy  
Static indeterminacy . . . . . 195–202  
Stokes' formula . . . . . 57, 230  
Strength . . . . . 72, 80, 81  
Stress  
    antiplane . . . . . 161  
    approach . . . . . 129–135  
    concentrations . . . . . 90  
    deviatoric part . . . . . 86, 88  
    engineering . . . . . *see* Engineering stress  
    normal . . . . . 75, 161, 162, 176, 186–188, 200  
    plane . . . . . *see* Plane stress  
    principal . . . . . 77, 81, 84, 105  
    shear . . . . . *see* Shear stress  
    tangential . . . . . *see* Shear stress  
    tensor 48–56, 97, 117, 129–135, 176, 186  
    true . . . . . *see* True stress  
    vector . . . . . 47, 49, 54, 162, 169, 186, 187  
Surface change . . . . . 35, 230  
Symmetry . . . . . 145, 147  
    cubic . . . . . 223

## T

- Tension 52, 64, 68, 76, 77, 80, 83, 85, 87, 105,  
    136, 156  
Tensor . . . . . iv, 214

- invariants . . . . . 77, 86, 218  
    product . . . . . 10, 12, 24, 50, 60, 215  
    trace . . . . . 33, 86, 216  
    transpose . . . . . 15, 215

- Timoshenko beam . . . . . 156, 179, 180  
Torque . . . . . *see* Moment  
Torsion . . . . . 6, 8, 13, 20, 23, 29, 30, 34, 120, 124,  
    126, 130, 152, 156, 160  
Trajectory . . . . . 4  
Tresca criterion . . . . . 84, 87  
True stress . . . . . 71  
Tsaï-Hill criterion . . . . . 89

## V

- Vector product . . . . . 28, 35, 151, 212, 221  
Velocity . . . . . 7  
Viscoelasticity . . . . . 99  
Voigt notation . . . . . 102, 222  
Volume change . . . . . 32, 35, 107, 229  
von Mises criterion . . . . . 86, 88

## W

- Warping . . . . . 126, 137, 157, 184

## Y

- Yield strength . . . . . 70, 72, 85–87, 99  
Young's modulus . . . . . 105–107, 176, 178, 179